

MODIFICATION OF THE MECHANICAL  
PROPERTIES OF SYNTHETIC HYDROGELS  
BY VARIOUS TECHNIQUES

A thesis submitted to the Council for National  
Academic Admissions in partial fulfilment of  
the requirement for the degree of  
Doctor of Philosophy

by

R.J. SEARLE, B.Sc., M.Sc., CChem., MRSC

London School of Polymer Technology,  
Polytechnic of North London,  
Holloway Road,  
LONDON.  
N7 8DB.

January, 1988

Advanced Studies Undertaken in Conjunction with the Programme of  
Research in Partial Fulfilment of the Requirements of the Degree

1. A course of postgraduate lectures on the mechanical properties of elastomers.
2. A course of guided study on filler reinforcement of elastomers.
3. A symposium on hydrogels, organised by Macro Group UK/SCI.

### ACKNOWLEDGEMENTS

I would like to acknowledge the thorough and expert help and advice of Dr. D.C. Blackley (Internal Supervisor) throughout this project, and in addition, the helpful comments of Messrs. I. Atkinson \*(External Supervisor) and B. Holdstock \*(External Advisor). I would like to thank Dr. Alan Haynes for his help and encouragement, together with Mr. Percy Gayapersad and the research staff of LSPT. I am grateful to the Polytechnic of North London for the award of a Research Assistantship, and to the SERC for provision of a Research Grant. Finally, I thank my wife Diane, for her support, both moral and practical, Mr. E.J. Pearson, Mrs. E. Williams and Mr. T. Fowler of Chloride Technical Ltd., and Heather Stapleton for typing this thesis.

\* Cooper Vision Ltd.

## ABSTRACT

A study in the field of hydrogel reinforcement has been carried out, the reinforced hydrogel being a copolymer of 2-hydroxyethyl methacrylate and methacrylic acid, crosslinked with ethylene glycol dimethacrylate and having an equilibrium water content at pH 8.5 of 74% by weight. Three methods of incorporating hydrophobic groups into the polymer have been investigated, in order to compare the reinforcing effects of each, viz. reinforcement by the addition of polymeric fillers; by forming interpenetrating polymer networks (IPNs); and by preparing terpolymers of 2-hydroxyethyl methacrylate/methacrylic acid with hydrophobic monomers. The hydrogels were prepared by redox polymerisation in IMS solution. A method has been developed for producing poly(2-hydroxyethyl methacrylate/methacrylic acid)/poly(methyl methacrylate) IPNs. They were prepared by drying the gels, swelling them in a solution containing monomers, initiators, crosslinker and suitable solvents, and then exposed to ultra-violet light. Filled hydrogels were formed by adding quantities of a PMMA dispersion in IMS to the hydrogel polymerisation mixture. The properties which represent best the level of mechanical reinforcement are the tear strength or tearing energy, tensile strength and modulus of the material. The tensile strengths of the various types of reinforced gel were compared as a function of composition, and of water content. It was observed that the addition of filler to the gels gave no improvement in tensile strength compared with the terpolymers, although the tensile strength increased with increasing filler content. However, it was not possible to produce a monodispersed dispersion of PMMA in IMS, of small particle size. Using the IPN method, hydrogels of high water content and high strength have been produced. The reproducibility of the process is so far poor, due to its complex nature, but it merits much further investigation. It was found that the tensile strength did not depend on the level of crosslinker in the hydrophobic component of the IPN. Stress-strain curves of several terpolymer hydrogels showed an increase in slope at high strains, thought to be caused by the presence of hydrophobic phase domains. Tearing energies of hydrogels may be measured by the "trouser" method, which has been previously applied to dry rubbers. Terpolymers containing EHA or styrene show particularly high tearing energies at a given mol % hydrophobic monomer. The homo-IPN hydrogels were translucent.



## C O N T E N T S

	<u>PAGE</u>
CHAPTER 1 - INTRODUCTION	1
CHAPTER 2 - LITERATURE SURVEY	6
2.1 Hydrogels	6
2.1.1 Introduction to Hydrogels	6
2.1.1.1 Definition of a gel; Concept of an Infinite Network	6
2.1.1.2 Types of Crosslink	7
2.1.1.3 Methods of Effecting Covalent Crosslinking in Polymers	8
2.1.1.4 Physical Characteristics of a Gel	10
2.1.2 Classification of Hydrogels	11
2.1.2.1 Naturally-Occurring Hydrogels	11
2.1.2.2 Synthetic Hydrogels	12
2.1.3 Synthesis of Hydrogels	13
2.1.3.1 Methacrylic and Acrylic Acid and their Hydroxyethyl Esters	13
2.1.3.2 Other Monomers	20
2.1.3.3 Methods of Polymerisation	22
2.1.4 Physical Properties of Hydrogels	24
2.1.4.1 Swelling in Aqueous Media	24
2.1.4.2 Mechanical Properties	35
2.1.5 Mechanical Reinforcement of Hydrogels	44
2.1.5.1 Copolymers of Hydrophilic with Hydrophobic Monomers	44
2.1.5.2 Filled Hydrogels and Composites	45
2.1.5.3 Hydrogel IPNs	48
2.1.6 Applications of Hydrogels	51
2.2 Filler Reinforcement of Elastomers	53
2.3 Interpenetrating Polymer Networks (IPNs)	54
2.3.1 Types of IPN and IPN Nomenclature	54
2.3.1.1 Classification of IPNs	54
2.3.1.2 IPN Nomenclature and Terminology	55

	<u>PAGE</u>
2.3.2    Synthesis of IPNs	57
2.3.2.1    Sequential IPNs	57
2.3.2.2    Simultaneous IPNs	60
2.3.2.3    Latex IPNs	62
2.3.2.4    Interpenetrating Elastomeric Networks	63
2.3.3    Morphology and Physical Properties of IPNs	63
2.3.3.1    Morphology of IPNs	63
2.3.3.2    Mechanical Properties of IPNs	66
2.4    Failure Properties of Materials	71
2.4.1    Fracture of Glassy Polymers	71
2.4.1.1    The Griffith Criterion	71
2.4.1.2    Fracture Mechanics	72
2.4.2    Rupture of Rubbers	73
2.4.2.1    Energy Dissipation in Rubbers	73
2.4.2.2    Crack Initiation and Propagation	75
CHAPTER 3 - EXPERIMENTAL DETAILS	77
3.1    Materials	77
3.1.1    Sources of Materials and Purification Procedures	77
3.1.1.1    Materials and Suppliers	77
3.1.1.2    Purification Procedures	78
3.1.2    GLC Analysis of HEMA(1)	78
3.2    Terpolymers of HEMA with MAA and with Hydrophobic Monomers	80
3.2.1    Preparation of Crosslinked Poly(HEMA) Gel by Polymerisation in Solution	80
3.2.2    EWC of Crosslinked HEMA-MAA Copolymers as a Function of Composition	82
3.2.2.1    Preparation of Materials	82
3.2.2.2    Measurement of EWC	83
3.2.3    Synthesis of Terpolymers of HEMA with MMA and Hydrophobic Monomers	85
3.2.3.1    Gels Containing HEMA(1), MAA and MMA(2)	85
3.2.3.2    Gels Containing HEMA(3), MMA and MMA(2)	87
3.2.3.3    Gels Containing HEMA(3), MAA and Various Hydrophobic Monomers	87

	<u>PAGE</u>
3.2.4	Determination of Tensile Strength 89
3.2.5	Low-Extension Elastic Modulus Determination 89
3.2.5.1	Samples and Apparatus 89
3.2.5.2	Procedure 91
3.2.6	Determination of Stress-Strain Characteristics 92
3.2.7	Determination of Tearing Energy 92
3.2.7.1	Single Edge-Notch Samples 92
3.2.7.2	The "Trouser" Test Method 93
3.2.8	Determination of Viscoelastic Properties 96
3.2.9	Differential Scanning Calorimetry Experiments 97
3.3	IPNs of Poly (HEMA-MAA) 99
3.3.1	Initial Experiments on IPNs 99
3.3.2	Further Experiments on IPNs 102
3.3.2.1	Development of the Preparative Procedure 102
3.3.2.2	Calculation of Polymer II Content in IPN 104
3.3.3	Initial Experiments on Semi-IPNs 104
3.3.4	Further Work on IPNs-Poly(HEMA-MAA)/PMMA 104
3.3.5	Further Variants on the Procedure for Preparing IPNs 108
3.3.5.1	Surrounding Samples with Oil 108
3.3.5.2	Cooling of Samples whilst Exposed to UV Light (i) 108
3.3.5.3	Cooling of Samples whilst Exposed to UV Light (ii) 108
3.3.5.4	IPNs 112
3.3.5.5	Pre-Swelling of Gels in DMF Vapour 112
3.3.6	Extent of Photopolymerisation vs. Time of Reaction 113
3.3.6.1	First Experiment 113
3.3.6.2	Second Experiment 113

	<u>PAGE</u>
3.3.7 Swelling of Crosslinked Poly(HEMA-MAA) Hydrogels in Various Mixtures	114
3.3.7.1 Swelling in MMA-IMS and MMA-DMF Mixtures	114
3.3.7.2 Swelling in MMA-Ethyl Acetate-DMF Mixtures	114
3.3.8 More Systematic Study of IPNs	115
3.3.8.1 First Series: Poly(HEMA-MAA)/PMMA IPNs	115
3.3.8.2 Second Series: IPNs of Poly(HEMA- MAA) with Various Polymers and Copolymers	117
3.3.9 Methylene Blue as a Photosensitiser	121
3.3.10 Latex IPNs	124
3.3.10.1 Dispersion Polymerisation of MMA in a Hydrocarbon Medium	124
3.3.10.2 "Core-Shell" Type Polymerisation	125
3.3.10.3 Measurement of Particle Size	125
3.4 Filled Hydrogels	126
3.4.1 Attempts to make PMMA Dispersions in IMS	126
3.4.1.1 DISP 1	126
3.4.1.2 Pre-formed Dispersants	126
3.4.1.3 DISP 2	127
3.4.1.4 DISP 3	127
3.4.1.5 DISP 4	127
3.4.1.6 DISP 5	128
3.4.1.7 Synthesis of a Comb-Type Graft Copolymer for Use as a Dispersant	128
3.4.2 Filled Hydrogels	129
3.4.2.1 FIL 1 and FIL 2	129
3.4.2.2 FIL 3 - 7	129
3.4.2.3 Incorporation of Dried Aqueous Latex into Hydrogels	130
CHAPTER 4 - TERPOLYMERS OF HEMA WITH MAA AND HYDROPHOBIC MONOMERS - RESULTS AND DISCUSSION	132
4.1 GLC Analysis of HEMA (1)	132

	<u>PAGE</u>
4.2 Copolymers of HEMA with MAA	140
4.2.1 Crosslinked Poly(HEMA) Gels Prepared by Polymerisation in Solution	140
4.2.2 Equilibrium Water Contents of Crosslinked HEMA-MAA Copolymers	142
4.3 Terpolymers Containing HEMA, MAA and MMA	153
4.3.1 HEMA (1)-MAA-MMA (2) Terpolymer Hydrogels	153
4.3.2 HEMA (3)-MAA-MMA (2) Terpolymer Hydrogels	165
4.4 Gels Containing HEMA (3), MAA and Various Hydrophobic Monomers	193
CHAPTER 5 - INTERPENETRATING POLYMER NETWORKS - RESULTS AND DISCUSSION	278
5.1 Initial Experiments on IPNs	278
5.2 Further Experiments on Semi-IPNs	281
5.3 Further Exploratory Work on Semi-IPNs	285
5.4 Further Work on IPNs	287
5.5 Further Developments in the IPN Preparation Procedure	290
5.5.1 Surrounding Samples with Oil	290
5.5.2 Cooling of Samples under UV Light (i)	290
5.5.3 Cooling of Samples (ii) and Pre-Swelling	290
5.5.4 Interpenetrating Networks	291
5.6 Extent of Photopolymerisation vs. Time of Reaction	295
5.7 Swelling of Crosslinked Poly(HEMA-MAA) Hydrogels in MMA-DMF-Ethyl Acetate Mixtures	303
5.7.1 Swelling in MMA-IMS and MMA-DMF Mixtures	303
5.7.2 Swelling in MMA-DMF-Ethyl Acetate Mixtures	311
5.8 More Systematic Study of IPN Hydrogels	326
5.8.1 First Series: IPN Hydrogels of Poly(HEMA-MAA) with PMMA	326
5.8.2 Second Series: IPN Hydrogels of Poly(HEMA-MAA) with Various Polymers and Copolymers	333

	<u>PAGE</u>
5.9 Use of Methylene Blue as a Photosensitiser	387
5.10 Latex IPNs	389
CHAPTER 6 - FILLED HYDROGELS - RESULTS AND DISCUSSION	392
6.1 Introduction	392
6.2 Preparation of PMMA Dispersions in IMS	393
6.2.1 DISP 1	393
6.2.2 Pre-formed Dispersants	394
6.2.3 DISP 2	394
6.2.4 DISP 3	395
6.2.5 DISP 4	395
6.2.6 DISP 5	396
6.2.7 Use of a Comb-Type Graft Copolymer Dispersant	396
6.3 Filled Hydrogels	397
6.3.1 FIL 1 to FIL 7	397
6.3.1.1 FIL 1 and FIL 2	397
6.3.1.2 FIL 3 to FIL 7	397
6.3.2 Incorporation of Dried Latex into Hydrogels	400
6.3.2.1 Dried Latices	400
6.3.2.2 Filled Hydrogels	400
6.4 Summary	403
CHAPTER 7 - COMPARISON OF THE VARIOUS METHODS OF HYDROGEL MODIFICATION	404
7.1 Equilibrium Water Content	404
7.2 Tensile Strength	407
7.3 Strain at Break	413
7.4 Tearing Energy	416
7.5 Shear Modulus	418
7.6 Stress-Strain Curves	421
7.7 Viscoelastic Properties	423

	<u>PAGE</u>
CHAPTER 8 - CONCLUSIONS AND SUGGESTIONS FOR FURTHER WORK	427
8.1 General Conclusions	427
8.2 Particular Conclusions	428
8.3 Suggestions for Further Work	429
REFERENCES	430

## CHAPTER ONE

### INTRODUCTION



In 1959 Wichterle (1) proposed that a synthetic polymer hydrogel be used for biomedical purposes. Since then, this type of material has been exploited extensively in the biomedical field, and principally as soft contact lenses. Hydrogels are defined as water-swollen network polymers. They contain varying proportions of water, depending on the chemical nature of the polymer and the concentration of crosslinks in the polymer. The material which Wichterle proposed, crosslinked poly (2-hydroxyethyl methacrylate) (poly(HEMA)), contained approximately 40% water by weight at equilibrium. The material is transparent and extremely chemically inert. These are properties which render it suitable for contact lens applications.

However, the material has low mechanical strength and the uses to which such synthetic hydrogels may be put are therefore restricted. Mechanical strength is not well defined, but is characterised by tensile strength, tear strength, tearing energy and abrasion resistance.

The properties used as criteria for determining mechanical strength depend to some extent on the use to which the material is to be put, but in general tensile strength and tear strength are used. These quantities are more suited to laboratory measurement than is abrasion resistance. The objectives of this project were to investigate the possibility of improving the mechanical properties of synthetic hydrogels, whilst at the same time retaining a high water content. Three methods of reinforcement were to be investigated:

- (i) filling hydrogels with small, highly dispersed polymeric particles, in the same way that rubbers are filled with fillers such as carbon black; the polymers constituting the particles were to be hydrophobic;

- (ii) copolymerisation of the hydrogel monomers with hydrophobic monomers;
- (iii) formation of interpenetrating polymer networks (IPNs) of hydrogels and hydrophobic polymers.

The feasibilities and relative effectiveness of the three methods were to be compared.

The hydrogel monomer which was chosen was HEMA. It was, however, copolymerised with a small proportion of a hydrophilic monomer, methacrylic acid. This provided a material of high water content which was used as a standard gel on which reinforcement experiments were carried out. Various mechanical properties were studied, including tensile strength, tearing energy, modulus and viscoelastic properties. These properties were studied as functions of both composition and water content. It was intended that these various properties should be compared at given water contents for gels prepared using each of the three modifications listed above. Little systematic work of this kind has so far been published. Some investigations of mechanical and swelling properties of hydrogels as functions of polymer composition have been published and some claims for remarkable reinforcement of hydrogels have been made. However, in most cases the equilibrium water contents of the hydrogels have been reduced drastically, often to a few per cent. The literature survey (Chapter 2) comprises reviews of the published work on

- (i) hydrogels. This includes their synthesis; physical properties such as equilibrium water content (EWC), swelling behaviour and mechanical properties; and mechanical modification by the three methods listed above;

- (ii) filled elastomers. This includes a brief review of the effects fillers have on the mechanical properties of elastomeric materials;
- (iii) IPNs. This includes their classification; synthesis; morphology; and mechanical properties such as stress/strain relationship, tensile strength and viscoelastic properties.

Several abbreviations and symbols are used throughout this thesis.

They are listed below:

<u>Symbol or Abbreviation</u>	<u>Meaning</u>
HEMA	2-hydroxyethyl methacrylate
MMA	methyl methacrylate
AZDN	azo-bisisobutyronitrile
EGDMA	ethylene glycol dimethacrylate
DVB	divinylbenzene
EHA	2-ethylhexyl acrylate
DDA	dodecyl acrylate
MAA	methacrylic acid
PPM6	poly(propylene glycol) methacrylate - on average 6 propylene glycol units per molecule
DMPT	4, 4' - dimethyl-p-toluidine
EG	ethylene glycol
DBPO	dibenzoyl peroxide
DEA	diethyl adipate
S	styrene
DMF	dimethyl formamide
$W_D$	weight of dry gel
$W_S$	weight of swollen gel
EWC	equilibrium water content

Symbol or AbbreviationMeaning

s	swelling in solvents other than water: $s = \frac{W_S - W_D}{W_S}$
$\sigma_b$	tensile strength
$F_b$	force at break
$\epsilon_b$	strain at break
w	sample width
b	sample thickness
$\sigma$	stress
M	mass of load on sample (equation 3-5)
$\epsilon$	strain
T	tearing energy
K	sample geometry constant
l	distance between clamps
G	shear modulus
$G_{sw}$	shear modulus of swollen material
$G'$	shear storage modulus
$G''$	shear loss modulus
$\tan\delta$	loss tangent
q	swelling ratio
A	peak area
P	mole fraction of hydrophobic monomer
$\alpha$	degree of dissociation
$\chi_1$	Flory-Huggins polymer-solvent interaction parameter
$\nu$	concentration of crosslink sites in dry polymer
$\nu_1$	molar volume of swelling agent
$\nu_2$	volume fraction of polymer in swollen gel

<u>Symbol or Abbreviation</u>	<u>Meaning</u>
$c$	initial crack length
$\lambda$	extension ratio
$E$	Young's modulus
$T_g$	glass transition temperature
$C_1, C_2$	Mooney-Rivlin coefficients
$\omega$	frequency of vibration
$P_{II}$	mole fraction or percentage of polymer II in IPN
$P_{II \text{ max}}$	maximum mole percentage of polymer II (assuming 100% conversion)
$[M]$	monomer concentration
$[M]_0$	monomer concentration at time $t = 0$
$k$	first order rate constant

CHAPTER TWO

LITERATURE SURVEY

## 2.1 HYDROGELS

### 2.1.1 Introduction to Hydrogels

#### 2.1.1.1 Definition of a Gel; Concept of an Infinite Network

It is appropriate to commence by considering the definition of the term "gel". Flory (ref.2, p.347) applied the term "infinite network" to a three-dimensional macromolecular structure, the dimensions of which might be measured on a macroscopic scale. Such a network may be produced in a number of different ways. One of the physical characteristics of these structures is that they swell in suitable solvents, rather than dissolving as the corresponding linear polymer would be expected to do. An infinite network requires the presence of cross-links, which may be either physical (such as hydrogen bonds) or chemical (covalent bonds). Therefore a definition based on the structure of the material might be that a gel is a swollen, crosslinked three-dimensional polymer network. It is also possible to define the term phenomenologically, a gel being a material which is swollen, insoluble and exhibits a particular response when an oscillatory stress or strain is applied to it (3). The former definition will be adopted here, since the latter is merely one of the consequences of the molecular structure of the material.

The term "infinite" refers not only to the fact that the molecular weight of the structure is very much greater than that of the monomer units of which it is made, but also to the potential that the structure has to extend over an infinite distance. A structure of any size may be made, depending only on the size of the container. During a network polymerisation, a point is reached where one such structure is formed, and a gel is therefore produced. However, at this point there still exist polymer molecules which are not connected to the infinite network.

#### 2.1.1.2 Types of Crosslink

The majority of synthetic hydrogels are covalently crosslinked. This is most frequently achieved by the copolymerisation of hydrophilic monomers with small amounts of compounds which contain more than one carbon - carbon double bond. Other types of crosslink exist however. Hydrogen bonds especially may be important in the case of hydrogels, where polar groups present on the polymer chains may interact with each other. In the biological field, the case of protein hydrogen-bonding is a typical example. It has also been suggested (4) that hydrophobic interactions may play a large part in determining the properties of certain hydrogels. In addition, biological polymers such as polysaccharides form ionic crosslinks by bridging through divalent cations such as  $\text{Ca}^{2+}$  (Fig. 2-1). An example of this is the

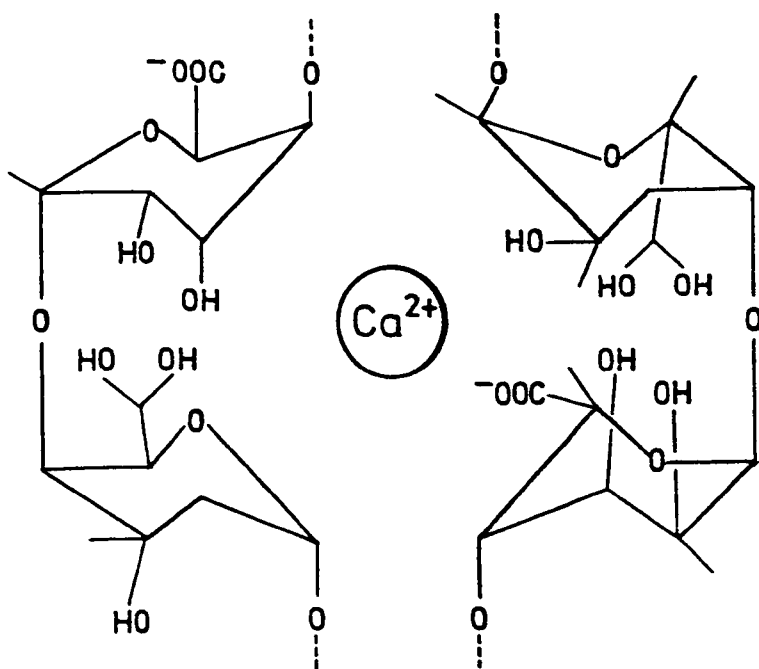


Fig. 2-1: "Egg-box" model for  $\text{Ca}^{2+}$  induced dimerisation of polysaccharides (5)

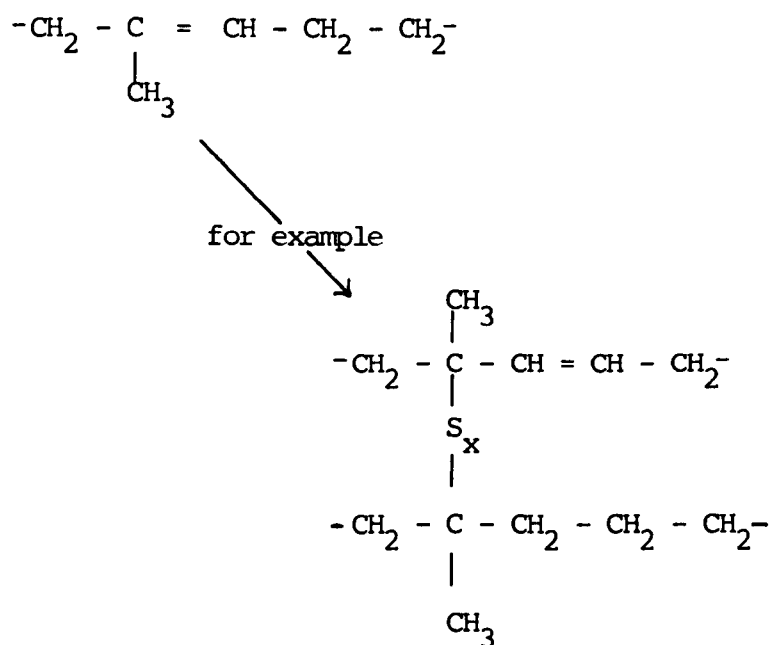


crosslinking of alginate gels by calcium ions. Ionic interactions also play a part in the crosslinking of those polymers which contain ionisable groups. Many of these types of interactions may be applicable to hydrogels, and may serve to increase the effective crosslink concentration of the material.

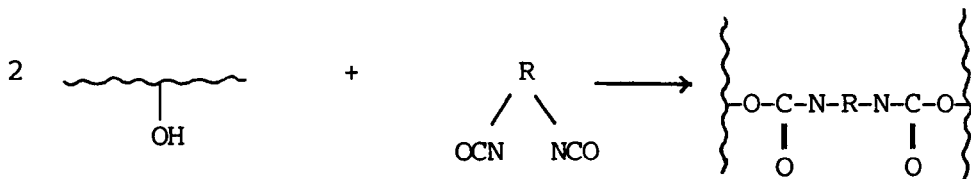
### 2.1.1.3 Methods of Effecting Covalent Crosslinking in Polymers

#### (i) Crosslinking through Functional Groups on the Polymer Chains

A typical example of this type of crosslinking is the vulcanisation of rubber. The C=C bond in the polymer chain furnishes an allylic hydrogen atom available for attack by free radicals, to provide a site for reaction with sulphur. Mono or polysulphidic crosslinks are formed:



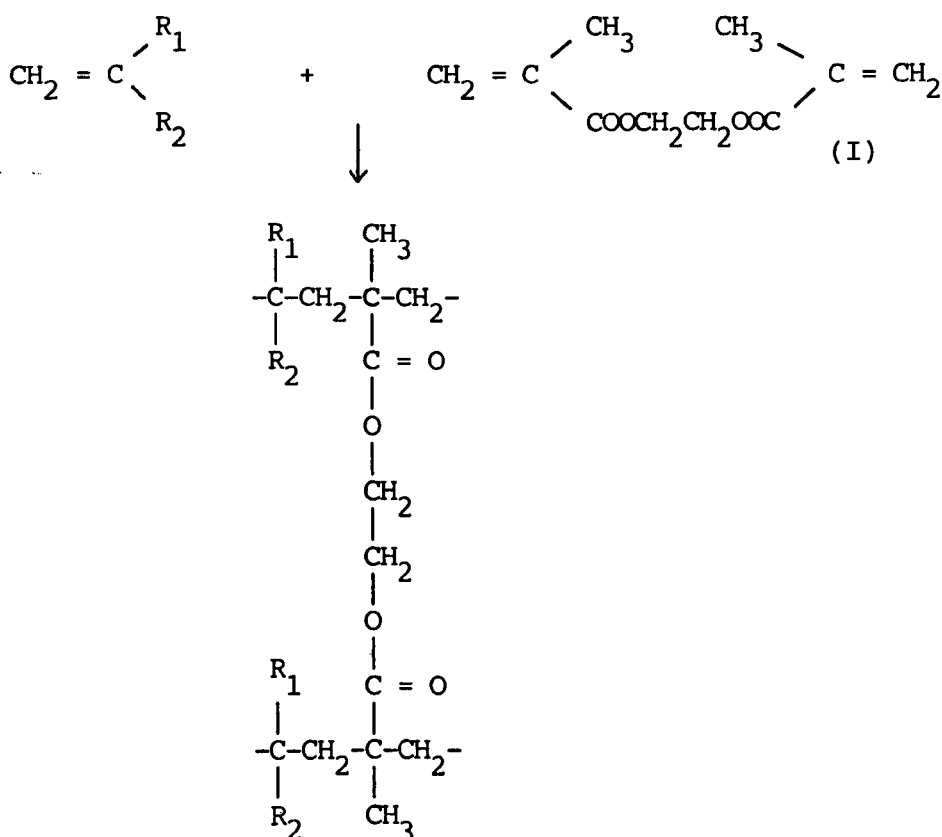
Polymers containing hydroxyl groups may be crosslinked by, for example, diisocyanates (6):



This type of reaction may be used where it is necessary to crosslink the polymer after the linear polymer has been synthesised. There are other possibilities for reactions of this kind, including the reaction of hydroxyl groups with diacid chlorides.

(ii) Crosslinking of Addition Polymers by Copolymerisation with Monomers  
Containing More Than One Carbon-Carbon Double Bond

The copolymerisation of compounds such as ethylene glycol dimethacrylate (I) with monovinyl monomers yields crosslinked products, if more than one of the C=C bonds of the former can participate in the polymerisation, thus linking two polymer chains:



#### 2.1.1.4 Physical Characteristics of a Gel (7)

The physical properties of hydrogels will be dealt with in greater detail in section 2.1.4.

##### (i) Swelling (ref.2, p.576; ref.7, p.64)

Gels swell in fluids which are good solvents for the primary polymer chains. This implies that there is a strong thermodynamic tendency for the polymer repeat units to mix with the molecules of the solvent.

Two factors control this swelling:

- (a) the increase in conformational entropy of the chains as they are diluted by the swelling fluid;
- (b) the solvent-segment interactions which either aid or hinder the tendency of the polymer and swelling liquid to mix.

Opposing the swelling action is the elastic retractive force which the polymer chains exert as the entropy decreases. Ultimately, the swelling reaches an equilibrium level, when the swelling force tending to increase the volume of the gel is balanced by the elastic retractive force. The equilibrium swelling of a given network is therefore controlled in part by the affinity of the solvent for the polymer chains, and this is quantified by the so-called "polymer-solvent interaction parameter",  $\chi$ .

##### (ii) Mechanical Properties

Gels are elastomers because the polymer chains between crosslinks develop an elastic retractive force when the entropy is decreased, either by swelling or by an externally applied force. When subjected to an oscillatory deformation, for example in shear, the in-phase component of the complex modulus (in this case  $G'$ ) is large compared to the quadrature component  $G''$ .  $G'$  is fairly constant over a range of frequencies.

Indeed, an ideal gel should behave as a Hookean spring, for which  $G''$  is zero. In practice, however,  $G''$  is non-zero, its magnitude depending on the material.

## 2.1.2 Classification of Hydrogels

### 2.1.2.1 Naturally-Occurring Hydrogels

#### (i) Proteins

Most naturally-occurring hydrogels contain either polysaccharide or protein structures. Probably the best known hydrogel-forming protein is gelatin, a water-soluble material which is a hydrolysis product of its parent protein, collagen. On chilling an aqueous solution, a gel forms. Gelation is thermally reversible, i.e. on warming, the solution is reformed. This indicates the presence of physical crosslinks. The primary reactive groups available for interaction in the gelatin structure are hydroxyl (from hydroxyproline), carboxyl (from glutamic acid), amino (from arginine and lysine) and imino (from arginine and proline). On cooling, hydrogen bonding and hydrophobic interactions cause the gelatin molecules to form a three-dimensional structure. When the gel is warmed, the physical crosslinks are broken, and a solution is formed (8).

Much of the organic material found in the animal and plant kingdoms is proteinaceous. A large proportion of it is water-swollen. It is therefore not surprising that proteinaceous hydrogels occur widely.

#### (ii) Polysaccharides

The second major category of hydrogel which occurs in biological systems is that based upon polysaccharides. Crosslinking in this case may occur by virtue of "junction zones" of ordered chain conformation, which together with disordered regions provide networks which swell

in aqueous media (5). Substituted polysaccharides, such as the galactomannans, form hydrogels because the monosaccharide sidechains interfere with close-packing to provide regions of disorder, where hydrogen bonding between polysaccharide hydroxyl groups and water may occur. Unsubstituted polysaccharides, such as cellulose, often do not form hydrogels. Some polysaccharides, alginates for example, will gel in the presence of divalent cations (particularly calcium ions). It has been proposed that the formation of bridged structures by the siting of calcium ions in cavities between two polysaccharide chains causes ordering and therefore acts as a physical crosslink. Such hydrogels are important in the food industry for thickening and gelation. Both in nature and in industry, polysaccharide hydrogels are used for various purposes.

#### 2.1.2.2 Synthetic Hydrogels (9, 10)

Synthetic hydrogels have emerged in recent years as a new class of materials of interest to polymer scientists and technologists and also to biologists and to some workers in certain areas of medicine. They were first produced by Wichterle and Lim in 1959, and proposed for application as contact lenses (1). These materials can be prepared either by polymerisation of their constituent monomers, which is usually the case, or by conversion from previously synthesised polymers. Their uses are diverse, ranging from soft contact lenses (11 to 13), artificial implants (14) and synthetic tendons (15) to drug release systems (16) and artificial caviar (17). One of the most useful properties of synthetic hydrogels is their ability to mimic human body tissue. This has led to their being used in a variety of ways as biomedical materials, although there are differences in biocompatibility and physical properties between the different polymers.

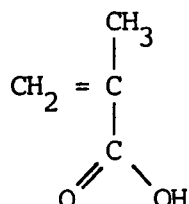
Undoubtedly the most commonly used monomer for preparing synthetic hydrogels is 2-hydroxyethyl methacrylate (HEMA). Others include acrylamide and N-vinyl pyrrolidone, which is often copolymerised with hydrophobic monomers such as methyl methacrylate. Synthetic hydrogels are usually crosslinked by copolymerisation with acrylic or methacrylic diesters. The most widely used is ethylene glycol dimethacrylate (EGDMA). The synthesis of hydrogels is dealt with in more detail in Section 2.1.3.

### 2.1.3 Synthesis of Hydrogels

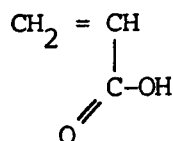
#### 2.1.3.1 Methacrylic and Acrylic Acid and their Hydroxyalkyl Esters

Some of the monomers of this type which have been used are:

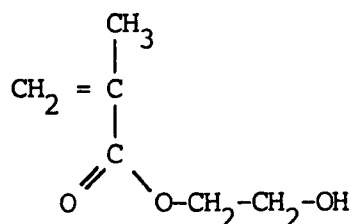
II methacrylic acid (MAA):



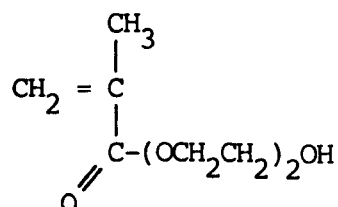
III acrylic acid (AA):



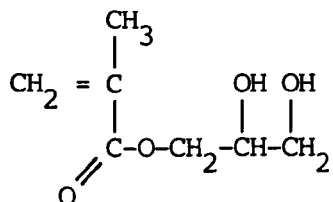
IV 2-hydroxyethyl methacrylate (HEMA):



V hydroxy ethoxyethyl methacrylate (HEEMA):

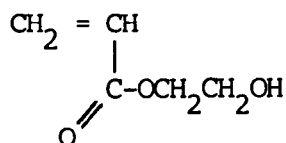


VI 2,3-dihydroxypropyl methacrylate (DHPMA):



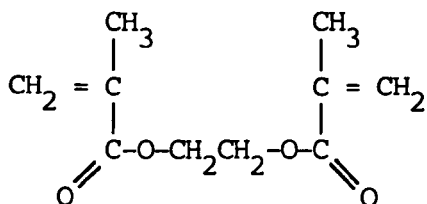
(also known as glyceryl methacrylate)

VII 2-hydroxyethyl acrylate (HEA):

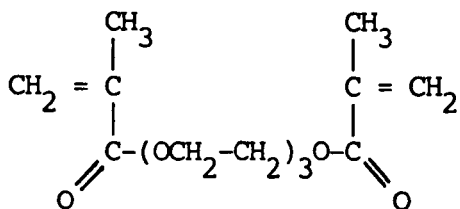


The most frequently used crosslinking agents copolymerised with these and other monomers are:

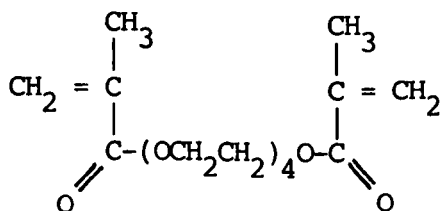
I ethylene glycol dimethacrylate (EGDMA):



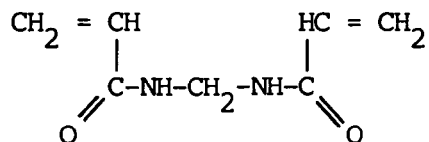
VIII triethylene glycol dimethacrylate (TEGDMA):



IX tetraethylene glycol dimethacrylate:



and X methylenebis-acrylamide:



The first synthesis of a poly (HEMA) hydrogel in the presence of cross-linking agent was carried out by Wichterle and Lim (1, 18). Since then, poly (HEMA) gels have been the most widely investigated of all the hydrogel materials. Poly (HEMA) gels were originally proposed for soft contact lenses, and still are the most important materials in this field. They have become the typical hydrogels with which the physical properties and behaviour of other similar materials are often compared.

HEMA has been copolymerised with both hydrophobic and hydrophilic comonomers in attempts to increase on the one hand the strength and rigidity of the gel and on the other the equilibrium water content. The latter is perhaps the single most important quantity pertaining to a hydrogel, especially in the contact lens field, where the high oxygen permeability necessary for extended-wear lenses requires a high water content ( > 70%) (19).

A large number of research papers and patents concerning HEMA-containing hydrogels has been published. A selection is listed in Table 2-1. The amount of published work using other hydrophilic acrylate and methacrylate monomers is much smaller. A review outlining the synthesis and properties of polymers containing various hydrophilic methacrylate esters including HEMA, DHPMA and HEEMA was published by Gregonis, Chen and Andrade (75). At the present time, the use of monomers other than HEMA, DHPMA and the like is limited by commercial availability. Even the use of DHPMA is restricted by the high price and high toxicity



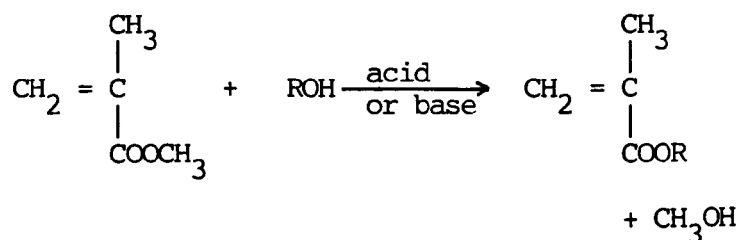
of its precursor, glycidyl methacrylate (76).

DHPMA hydrogels were investigated by Refojo in 1965 (77) and Yasuda, Gochin and Stone in 1966 (78). More recently, copolymers of DHPMA and MMA have been synthesised (79). Macret and Hild (80) have studied the kinetics of copolymerisation of HEMA and DHPMA. Sung et al investigated HEMA/DHPMA copolymers from the point of view of swelling as a function of water activity (81).

Methacrylic acid has not been extensively used in hydrogel synthesis, although it is used in small proportions as a comonomer with HEMA to increase the water content of the resulting hydrogel (35, 36). Lightly crosslinked poly(methacrylic acid) is too fragile to be useful in the contact lens industry.

There are three main methods of producing HEMA and other hydroxyalkyl esters of MAA (9, 75):

- (i) transesterification of methyl methacrylate with an appropriate alcohol:



- (ii) reaction of methacrylic acid with ethylene oxide:

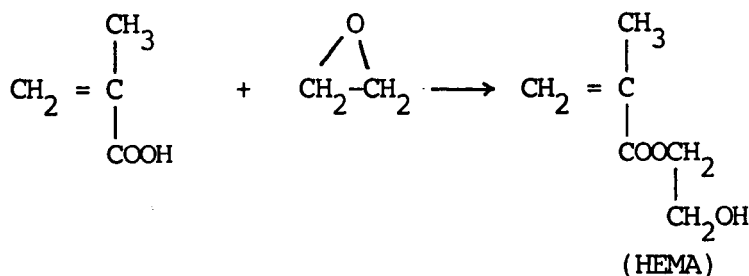
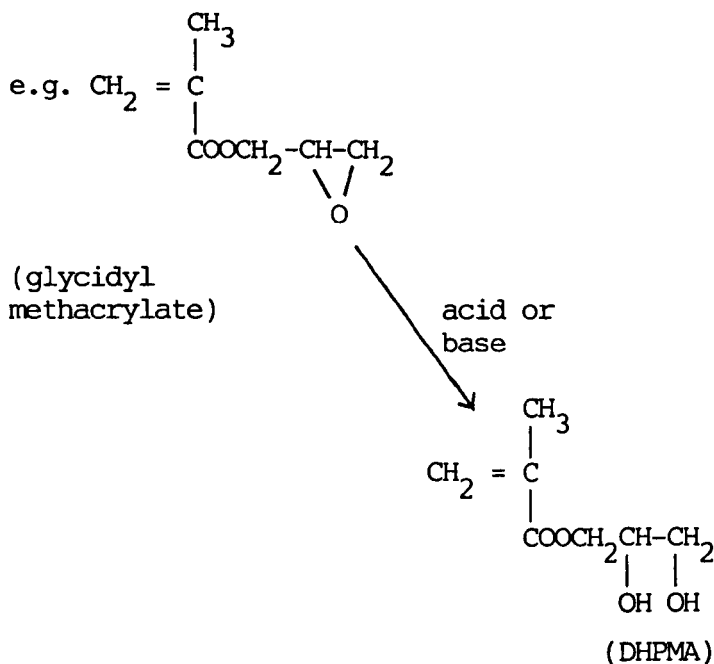


Table 2-1 : A Selection of Publications Concerning Hydrogels

Derived from HEMA

comonomer(s)	references
MMA	20 to 26
styrene	27 to 31
MAA	29, 30, 31, 32 to 36
NVP	32, 33, 21, 37, 38
methacrylamide	39
propylene glycol monoacrylate	40
2-ethoxyethyl methacrylate	28
ethyl methacrylate/butyl methacrylate	41
methoxyethyl methacrylate	42
amyl methacrylate	43
fluorine-containing monomers	44
isobutyl methacrylate	45
methoxytriethylene glycol methacrylate	46
diethylene glycol methacrylate	29
ethyl acrylate	47
n-butyl acrylate	47
dodecyl methacrylate	47
none	44, 48 to 74

(iii) hydrolysis of esters containing an epoxy group:



The main impurities found in the hydroxyalkyl methacrylates are the corresponding diesters; in HEMA, small amounts of ethylene glycol, methacrylic acid and higher homologues of the series  $\text{CH}_2 = \text{C}(\text{CH}_3)\text{CO}(\text{OCH}_2\text{CH}_2)_n\text{OH}$  are also found. The diester content of HEMA is typically 2 - 5% (w/w) and sometimes lower. Proportions as low as 0.5% (w/w) are, under many reaction conditions, sufficient to crosslink the polymer, resulting in the formation of a gel. The diester is sometimes removed from the monomer by extraction of an aqueous solution of HEMA with hydrocarbons such as hexane, followed by salting out and drying. Macret and Hild however (80) suggested that this process removes little of the diester. They compared conventionally distilled HEMA with the extracted monomer by means of g.l.c. analysis. The distillation of HEMA is usually carried out under reduced pressure, its boiling point at 0.5mm Hg being 64°C (80). (Gregonis et al (75) give a value of 69°C at 0.1mm Hg). Suitable arrangements need to be made to prevent polymerisation of the monomer in the flask, for example using an air or oxygen bleed, or distilling

over copper (I) chloride (82). Lower distillation temperatures clearly discourage polymerisation. Distillation in this way is suitable for removing more volatile impurities such as water and methacrylic acid, but is not an efficient method for the removal of the diester, for two reasons:

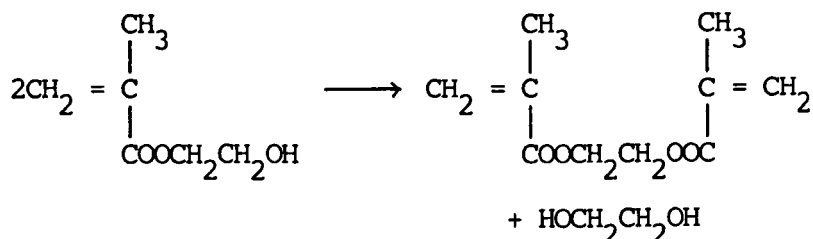
- (i) the boiling points of EGDMA and HEMA are similar:

HEMA 64°C at 0.5mm Hg (80)

69°C at 0.1mm Hg (75)

EGDMA 68°C at 0.2mm Hg (83)

- (ii) the occurrence of the disproportionation ("dismutation") reaction leading to an increase in the EGDMA concentration:



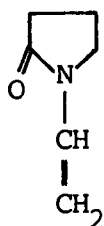
The rate of the disproportionation reaction increases faster than that of the reverse reaction as the temperature increases. At lower temperatures, the rate is still appreciable, however. Thus the EGDMA content of HEMA stored in a refrigerator may gradually increase.

Pinchuk, Eckstein and Van de Mark (36) maintained that, using a reduced pressure of 50 - 80  $\mu^m$  Hg during the HEMA distillation (at which the boiling point of HEMA is 38 - 42°C), HEMA with an EGDMA content as low as 0.001% (mol/mol) can be produced. Their analyses were carried out using HPLC equipment, which obviates the necessity for the high injection temperatures used in GLC analysis. A much more elaborate distillation system has been suggested, in which a spray-cooling apparatus was introduced (84). Macret and Hild, however, found that the most effective method for removing the diester from both HEMA and DHPMA is by preparative adsorption chromatography using a silica

column, followed by elution with a mixture of benzene and ethyl acetate or benzene and acetone. Further methods, other than distillation, which have been proposed for the removal of methacrylic acid include treatment with copper (I) oxide (85) and conversion of the acid to the insoluble N-acyl urea (86).

#### 2.1.3.2 Other Monomers

Uncrosslinked homopolymers of N-vinyl pyrrolidone (NVP) are water-soluble.



The crosslinked polymers swell in water to produce hydrogels of high equilibrium water content, but high levels of crosslinker are required to give gels with good mechanical properties (10). NVP is more often used as a comonomer with hydrophobic monomers, to provide mechanical strength. A selection of publications describing the use of NVP in hydrogels is listed in Table 2-2.

NVP is usually purified by distillation under reduced pressure (87); literature boiling point values are 92 - 95°C at 11mm Hg (83) and 94 - 96°C at 13 - 14mm (177). Acrylamide, methacrylamide and related monomers have been used to produce hydrogels, notably by the Tanaka group in their recent investigations of gel phase transitions (178, 179, 180).

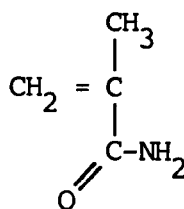
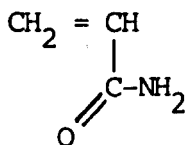


Table 2-2: A Selection of Publications Concerning Hydrogels

Derived from NVP

polymer	references
poly (NVP)	88 to 90
poly (NVP - HEMA)	37, 38, 41, 91
poly (NVP - HEMA - MAA)	32, 33
poly (MMA - NVP - methyl substituted DHPMA)	92
poly (NVP - HEMA - MMA)	21
poly (NVP - MMA)	93 to 97, 90, 26

The crosslinking monomer usually used is methylenebis-acrylamide. The proportion of crosslinker is a factor controlling the equilibrium water content.

One method of synthesising hydrogels is by polymerising acrylonitrile in aqueous zinc (II) solution (181, 182). The resulting polymer can then be partly hydrolysed to produce methacrylic acid groups. This type of procedure has been found to give gels which are stronger than poly (HEMA) materials (183). The copolymerisation of acrylamide with acrylic acid salts has been studied (184); the product is an insoluble polyelectrolyte.

Crosslinked poly (vinyl alcohol), usually prepared by saponification of poly (vinyl acetate), has also been used as a hydrogel (185, 186). An interesting method of producing reinforced gels has been developed, whereby an annealing process is used to form crystallites within the polymer (98, 97). More recently, similar experiments have been carried out by Japanese researchers, on the formation of hydrogels by repeated freeze-thawing of aqueous PVA solution (99 to 101).

#### 2.1.3.3 Methods of Polymerisation

Hydrogels which are crosslinked by using monomers such as EGDMA are usually synthesised by polymerisation either in bulk or in solution. Polymerisation of bulk monomer (e.g. 56, 102, 87) necessitates subsequent hydration of the crosslinked xerogel. The polymerisation may be carried out in polypropylene moulds or in glass ampoules (87). Polymerisation in solution has advantages over bulk polymerisation, particularly when redox initiator systems at room temperature are used. The monomers and initiators are dissolved in a suitable solvent, poured into moulds, which may be for example glass or PTFE plates separated by a gasket (e.g. 78, 58, 103) or polypropylene or glass syringes or tubes

(e.g. 36, 179), and kept at the required temperature until polymerisation has occurred. The gel is then removed either by separating the plates or applying pressure to the material in the syringe or tube. One commercial advantage of bulk and solution methods is that the article to be produced may be shaped during the polymerisation, therefore obviating the need for any machining. Refojo and Yasuda (40), experimenting with poly (HEMA) hydrogels, found that heterogeneous, spongy gels resulted if, when the monomers were polymerised in water, the percentage (w/w) of water in the polymerisation mixture was more than 40. However, the addition of polar solvents such as ethylene glycol to the polymerisation mixture enabled homogeneous transparent gels to be made even when the proportion of HEMA in the mixture was as low as 10% w/w.

The most common diluent used for solution polymerisation of HEMA and crosslinking agents is water. However, a polar solvent such as ethanol, IMS or DMF can be used. The more hydrophilic the diluent, the greater the proportion which can be used in the initial monomer/diluent/initiator mixture.

Thermal initiation may be provided by initiators such as azodiisobutyronitrile (AZDN), azobiscyanovaleric acid or its water-soluble sodium salt, or peroxides such as benzoyl peroxide or cumyl peroxide. A problem which may be encountered when polymerisation is initiated thermally is that, if more volatile diluents such as ethanol are used, excessive evaporation may occur. This problem is largely eliminated when redox initiation systems are used, since polymerisations can then be carried out at lower temperatures. Water-soluble redox free-radical initiator systems include persulphate/bisulphite, persulphate/iron (II) and hydrogen peroxide/iron (II) (104). In this project,



[illegible]

- 24 -

$$\text{EWC} = \frac{\text{weight or volume of swollen gel} - \text{weight or volume of dry gel}}{\text{weight or volume of swollen gel}}$$

The swelling in water is only slightly dependent on the concentration of crosslinks in the poly (HEMA) gel. This aspect was investigated by Refojo and Yasuda in 1965 (40). They carried out experiments whereby the concentration of crosslinks and the initial dilution of the monomer were varied. Homogeneous hydrogels were produced by redox polymerisation in mixtures of water and ethylene glycol. It was found that increasing the weight percentage of TEGDMA crosslinker from zero to 3.0% did not alter the EWC. These gels were transparent, and were produced when the percentage of water in the initial polymerisation mixture was low. When higher initial dilutions were used, heterogeneous, "spongy" gels were produced, the EWC of which increased with increasing initial dilution. A wide range of experiments was carried out using mixtures of ethylene glycol and water in the polymerisation mixture and varying the initiator concentration. For homogeneous gels, the EWC depended neither on the initiator concentration nor on the initial dilution.

These observations were explained in the following way. Uncrosslinked poly (HEMA) is not water-soluble. Hence water is not a good solvent for it. This factor dominates others which control swelling, such as initial dilution and crosslink density. The authors state that "in order to obtain homogeneous network polymers it is necessary to add to the polymerisation mixture an organic solvent which is miscible with both water and monomer".

From the work of Yasuda, Gochin and Stone (78), it is clear that this is not the case. They carried out a detailed study of the swelling behaviour of poly (HEMA), and also of poly (DHPMA) and HEMA-DHPMA

copolymers, polymerised in ethylene glycol/water mixtures.

Fig. 2-2 shows that homogeneous gels can indeed be prepared in pure

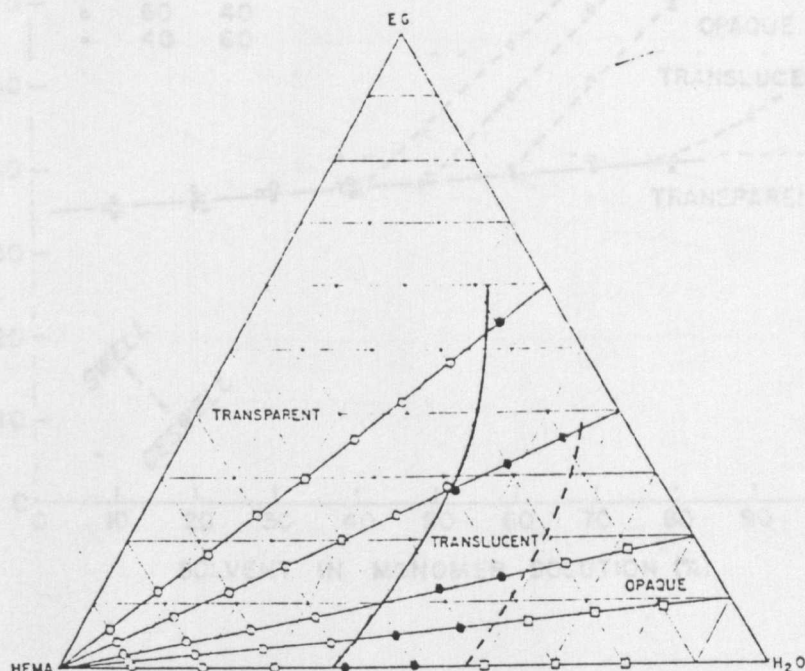


Fig. 2-3: Effect of the Initial Dilution of Monomer Solution and the

Fig. 2-2: Transparency of poly (HEMA) Hydrogels in HEMA-Water-Ethylene Glycol System (78): (O) transparent gels; (●) translucent gels; (□) opaque gels.

"isovolumic" gels, the volume swelling of which is unchanged after water, with the proviso that the initial water content is below the critical level of approximately 40%. This critical level increases as the proportion of ethylene glycol in the dilution mixture increases.

Three types of gel were observed: transparent gels which had an EWC below 41%; translucent gels which had an EWC between 41 and 54%; and opaque gels which had an EWC above 54%. Fig. 2-3 shows that, for translucent and opaque gels, there is a marked dependence of EWC on initial dilution.

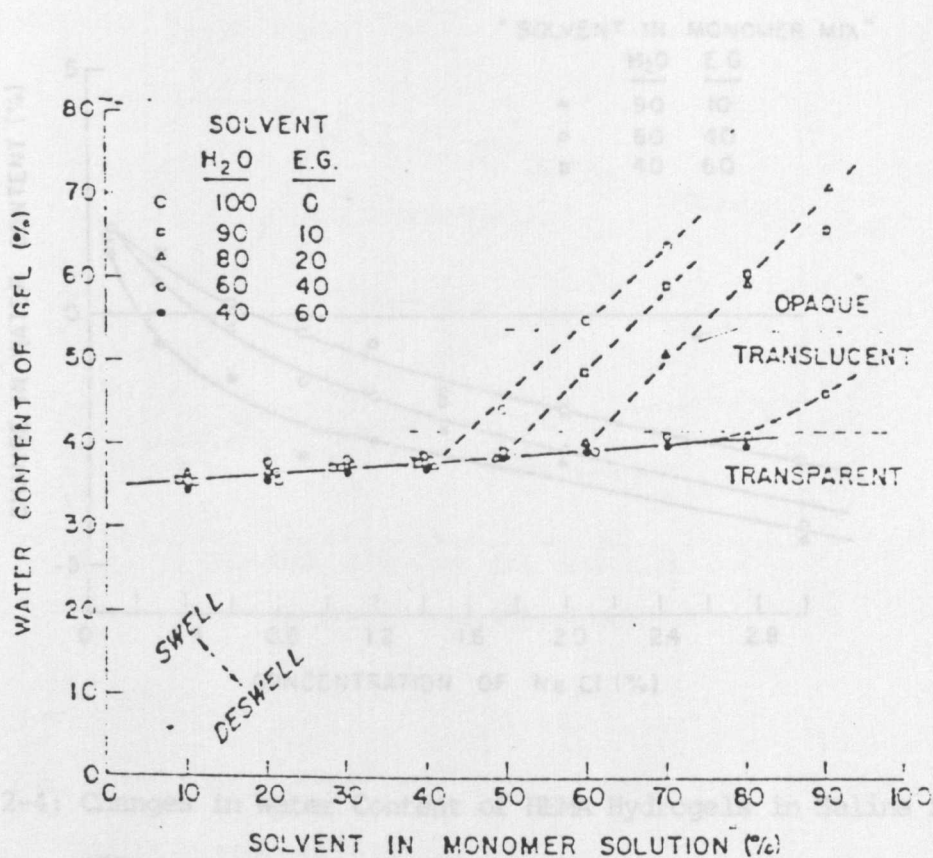


Fig. 2-3: Effect of the Initial Dilution of Monomer Solution and the Composition of the Solvent on the Water Content of HEMA Hydrogels (78).

Similar results were obtained by Refojo (4), who also found that swelling "Isovolumic" gels, the volume swelling of which is unchanged after equilibration in water, can be obtained by polymerisation in a mixture which contains approximately 35% diluent, regardless of the diluent composition. The effect of the immersion of these gels in aqueous solutions of sodium chloride was investigated. It was found that, as the concentration of salt increased, so the EWC decreased (Fig. 2-4).



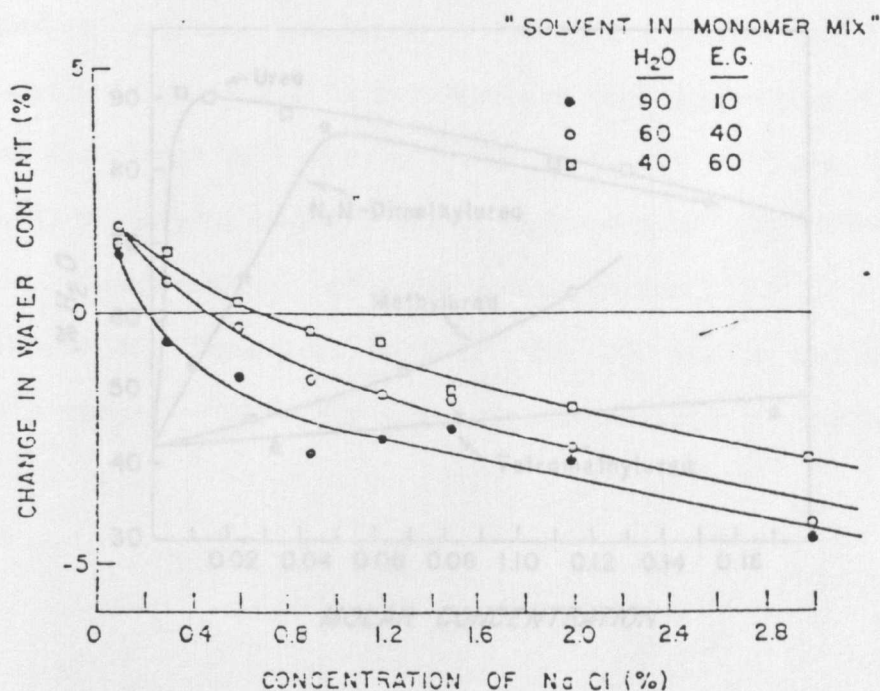


Fig. 2-4: Changes in Water Content of HEMA Hydrogels in Saline Solutions (78).

Similar results were obtained by Refojo (4), who also found that swelling in solutions of alkali metal iodides increased the EWC of poly (HEMA) gels. Refojo also studied the effects of urea and some of its derivatives, cetylpyridinium chloride solutions, acetone, ethanol and solutions of several salts, on the swelling properties (106) (Fig. 2-5). It was concluded that hydrophobic bonding between polymer segments plays a very important role in the swelling behaviour of poly (HEMA) hydrogels, since extensive polymer-polymer hydrogen bonding is unlikely. The effect of hydrophobic bonding is to create a network of non-covalent hydrophobic crosslinks. The addition of solutes which decrease the solubility of poly (HEMA) segments in the medium, such as chlorides and sulphates, causes a strengthening of the hydrophobic bonding, and therefore a decrease in swelling. Solutes such as urea, acetone and ethanol have the opposite effect, causing an increase in swelling.

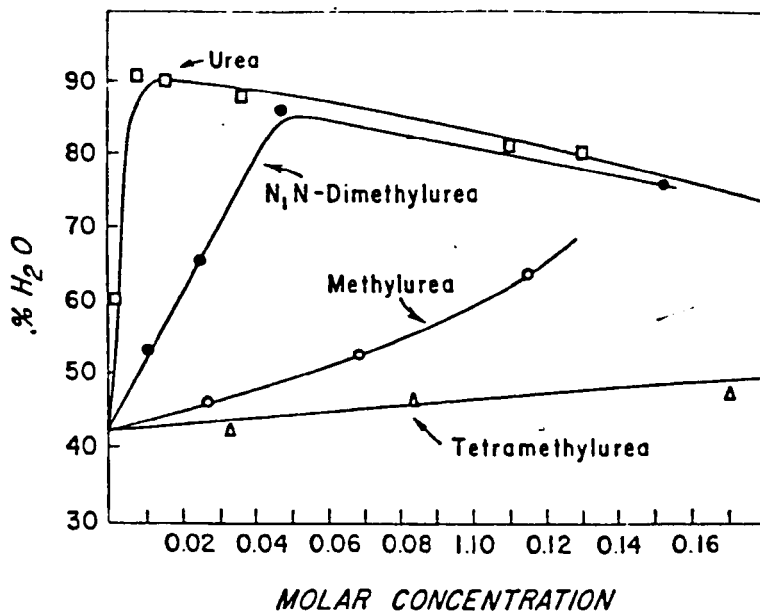


Fig. 2-5: Water Content of Poly (HEMA) Hydrogel in Low Concentrations of Urea and Methylureas (106).

This theory has been contested by Ratner and Miller (107). They investigated poly (HEMA), poly (HPMA) and poly (MAA) gels swollen in urea solutions, by means of IR spectroscopy and fluorescence quenching spectroscopy. They concluded that the secondary structure existing in poly (HEMA) hydrogels involves hydrogen bonding, rather than hydrophobic interactions. They suggested that, since polymer-polymer hydrogen bonds would seem unfavourable in a water-swollen gel, there may be regions of hydrogen bonding between pendant hydroxyl groups, from which water molecules are excluded.

As might be expected, copolymerisation of HEMA with more hydrophilic monomers such as 2,3-dihydroxypropyl methacrylate (DHPMA, glyceryl (methacrylate) increases the dependence of equilibrium water content on composition. Fig. 2-6 shows that, for homogeneous materials, the slope of the graph of EWC against initial percentage of solvent in

the monomer solution increases as the proportion of DHPMA increases. The isovolumic initial dilution increases with increasing DHPMA content, so that isovolumic gels with an EWC of up to 60% (v/v) can be prepared. Refojo (102) showed that the EWC of hydrogels of poly (DHPMA) exhibits a marked dependence on crosslink concentration. Refojo also studied the effect of temperature on EWC. The EWC varies approximately 2% over the range 0 - 100°C for a gel crosslinked with 5% TEGDMA.

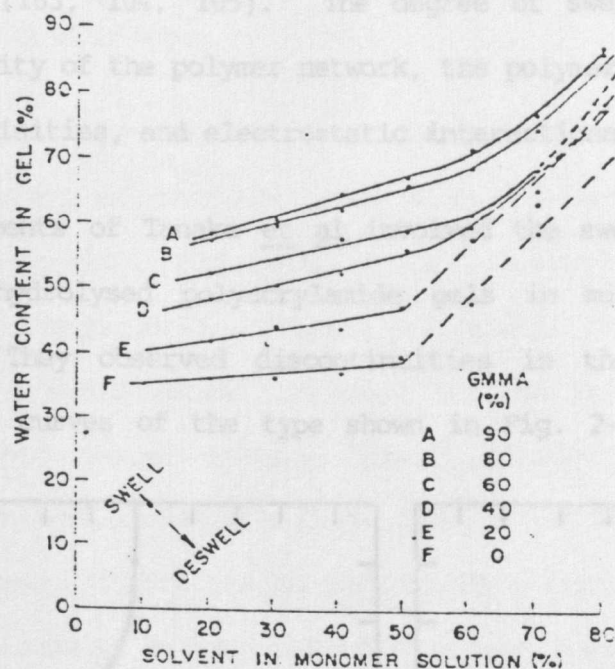


Fig. 2-6: Effect of the Composition of Copolymers and the Initial Dilution on the Water Content of HEMA-GMA Hydrogels.

High values of EWC may be attained, particularly in alkaline aqueous media, when HEMA is copolymerised with methacrylic acid (MAA). With increasing degree of neutralisation, the EWC decreases (35), so that the swelling of these gels may be controlled by the pH of the medium in which they are immersed. At low degrees of ionisation, the Flory-Huggins interaction parameter  $\chi_1$  and the modulus of the gel  $G$  are

determined by the EWC. Low levels of MAA copolymerised with HEMA can lead to pronounced increases in EWC (36). Pinchuk and coworkers (36) found that the effects of the addition of MAA are most marked at low levels of crosslinker. For gels containing less than 2% MAA and less than 0.06% crosslinking agent, dissolution occurred. Similar results were obtained by Gregonis et al (75). The explanation by Pinchuk et al (36) of the large changes in volume which occur when the gels are immersed in different environments is similar to that of Tanaka (103, 104, 105). The degree of swelling is governed by the elasticity of the polymer network, the polymer-polymer and polymer-solvent affinities, and electrostatic interactions.

The experiments of Tanaka et al involved the swelling of crosslinked partially hydrolysed polyacrylamide gels in mixtures of water and acetone. They observed discontinuities in the swelling/solvent composition curves of the type shown in Fig. 2-7. To explain these

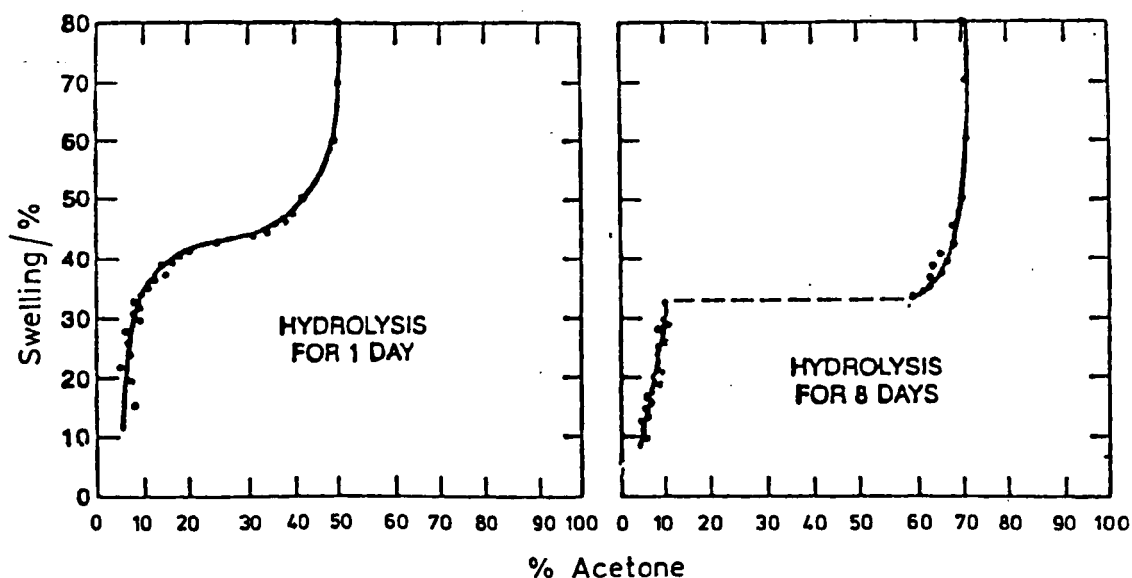


Fig. 2-7: Swelling against Solvent Composition for Partially Hydrolysed Polyacrylamide Gels



very interesting results, Tanaka considered the total osmotic pressure to be the sum of three components arising from respectively (a) rubber elasticity, (b) polymer-polymer interactions and (c) what he termed the "hydrogen ion pressure", i.e. the pressure caused by the hydrogen ions released into the gel by ionisation of the carboxyl groups. Certain conditions other than changes in solvent composition may cause the collapse of a gel, such as the application of an electric field, and the addition of water-soluble electrolytes such as sodium chloride or magnesium chloride.

As might be expected, the copolymerisation of hydrophobic monomers such as methyl methacrylate (MMA) with HEMA decreases the equilibrium water content (24). Migliaresi et al (23) examined the water absorption and desorption properties of such copolymers. One of their conclusions was that a small amount of water remains trapped in the gel after drying. This water differs from the "bound" water which has been observed by other workers (e.g. 108, 109, 110). Rather than being bound to particular sites on the polymer network, it is trapped inside a polymer matrix in which it has a very low diffusion coefficient.

Several papers have appeared in the literature concerning the nature of water in hydrogels. In general, three structural forms of water are found in these materials. These forms are often categorised by means of their response to differential scanning calorimetry (DSC) (108 to 111, 71, 99). The three categories are (108 to 110):

- (i) ordinary, or "bulk" water;
- (ii) intermediate, or "interfacial" water;
- (iii) "bound" water.

Ahad (108) found, in experiments on guar and xanthan gums and poly-

acrylamide, that types (i) and (iii) occurred in all the gels investigated, whereas type (ii) occurred only in those gels which contained more than a certain equilibrium water content. Type (iii) water, which is considered to be bound to specific sites on the polymer, is sometimes called "non-freezing water". Pedley and Tighe prepared copolymers of styrene, methacrylic acid and acrylamide which had a high non-freezing water content of 29%, the total equilibrium water content being 30% (111). Several methods other than DSC have been used to analyse the nature of the water present in hydrogels, for example dilatometry (109), specific conductivity (109), thermal expansivity (71) and pulse NMR (99).

Refojo (112) carried out experiments on the swelling pressure of poly (HEMA) and higher EWC hydrogels. It was found to be more difficult to expel water by applying mechanical pressure to gels of low water content, than to gels of high water content, such as the type used for extended-wear contact lenses. By measuring the equilibrium relative humidity of gels at a given temperature, it was concluded that approximately 30% of the water contained in the hydrogels was of type (iii), i.e. "bound" water. This result agrees with those of Lee, Jhon and Andrade (109).

An important property of hydrogels used for the manufacture of soft contact lenses is permeability to dissolved oxygen. This is a particular requirement for extended wear lenses. The permeability to dissolved oxygen,  $P_d$ , depends strongly on the EWC of the gel (27, 113) and the temperature. It was found that, for a number of gels, the value of  $P_d$  approximately doubled on increasing the temperature from 25°C to 34°C. The importance of high EWC has been emphasised (114, 115, 27) for both contact lens applications and applications as drug release

materials (115, 24). In the latter case, the permeation of pharmaceuticals through a hydrogel depends on the water content of the hydrogel.

The role which conformation of the polymer repeat unit plays in the swelling of poly (HEMA) in aqueous media has been studied. It has been found that the isotactic polymer has a larger EWC than the tactic polymer (61, 81). Gregonis (60) found this to be the case at temperatures below 30°C. Syndiotactic polymers were prepared by UV irradiation; tactic polymers by anionic polymerisation.

Finally, it has been shown (75) that when poly (HEMA) xerogels are swollen in water, the curves of percent equilibrium hydration and percent linear swelling as a function of time are different (see Fig. 2-8). This is said to indicate the presence of free volume within the xerogel, which must be occupied by water molecules before the gel is forced to swell by osmotic pressure.

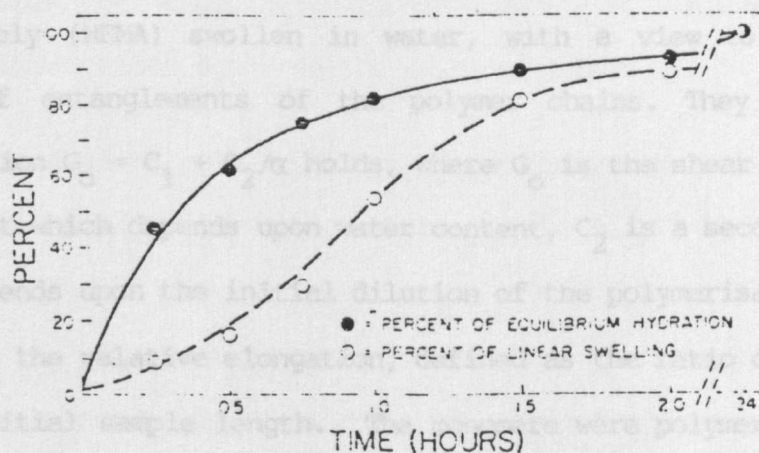


Fig. 2-8: Percent Equilibrium Hydration (100% = 40% EWC) and Percent Equilibrium Linear Swelling (100% = 1.165 =  $1_s$ ) Plotted vs Time for Poly (HEMA) Gel (75).

#### 2.1.4.2 Mechanical Properties of Hydrogels

Little systematic work has been published concerning the stress/strain and rupture properties of swollen synthetic hydrogels. Perhaps the most important mechanical property is the tearing energy. This gives information concerning the inherent strength of a material. No information concerning the tearing properties of hydrogels has apparently been published so far, although the results of tensile strength and elongation at break measurements for gels have been published (47, 91). The viscoelastic properties of hydrogels have been investigated in a little more detail, much of the work being concerned with poly (HEMA). Little published information is available concerning the fundamental aspect of the variation of such properties with water content. Some of the publications which contain information concerning the mechanical properties of hydrogels are summarised below.

##### (i) Tensile Stress/Strain Properties

Hasa and Janacek (116) studied the deformational behaviour of cross-linked poly (HEMA) swollen in water, with a view to examining the nature of entanglements of the polymer chains. They observed that the equation  $G_0 = C_1 + C_2/\alpha$  holds, where  $G_0$  is the shear modulus,  $C_1$  is a constant which depends upon water content,  $C_2$  is a second constant which depends upon the initial dilution of the polymerisation mixture, and  $\alpha$  is the relative elongation, defined as the ratio deformed sample length/initial sample length. The monomers were polymerised in water, the proportion of which was varied. It was found that  $C_2$  decreased with increasing concentration of water in the initial mixture, although it was almost independent of the level of crosslinker. These observations were interpreted as implying a decrease in the number of entanglements as the initial dilution is increased.

Tensile stress-strain measurements for poly (HEMA) and copolymers of HEMA with hydrophobic monomers have been made by Kolarik and Migliaresi (47). Their results are shown in Fig. 2-9. The curves for poly (HEMA-ethyl acrylate) and poly (HEMA-butyl acrylate) (Fig. 2-9 a and b) resemble those for gum elastomers. The modulus of the HEMA-butyl acrylate copolymers passed through a minimum as the ratio BA/HEMA increased, while that of HEMA-ethyl acrylate copolymers remained approximately constant. This was explained as possibly due to the effect of varying crosslinking efficiency. The effects caused by the copolymerisation with dodecyl methacrylate (Fig. 2-9c) differed markedly from those caused by copolymerisation with ethyl acrylate and butyl acrylate, even though their water contents were similar (Fig. 2-10). Those copolymers which contained less than 20% (w/w) of dodecyl methacrylate displayed rubber-like behaviour, while those which contained more than 30% of dodecyl methacrylate showed distinctly different stress-strain characteristics. The stress rose rapidly at low strains to a maximum, at which yielding occurred. It then decreased to a minimum and increased again to the point of rupture.

The tensile stress-strain behaviour of copolymers of HEMA with hydrophilic monomers was studied by Starodubtsev et al (91). It was found that the results for a range of copolymers all fell on the straight line predicted by the kinetic theory of rubber elasticity when  $\sigma / G_0$  was plotted against  $(\lambda - \lambda^{-2})$ , where  $\sigma$  is the tensile stress,  $G_0$  is the initial slope of the Gaussian curve and  $\lambda$  is the deformation ratio. Fig. 2-11 shows the results that were obtained. In view of these results, it was concluded that these hydrogels could be "described by an ideal network model", and that the effective number of moles of polymer chains per unit volume of unswollen polymer,  $n_0$ , could be calculated.

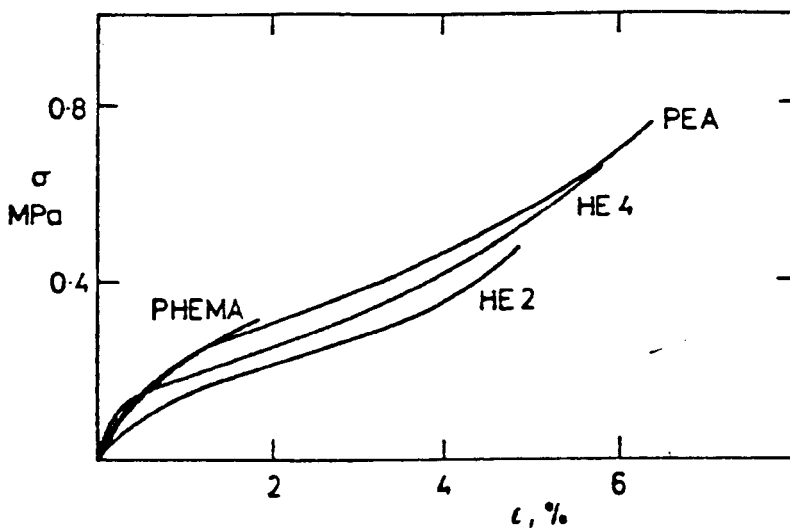


Fig. 2-9a: Tensile Stress-Strain Behaviour of Copolymers HEMA-Ethyl Acrylate Swollen in Water to Equilibrium (47).

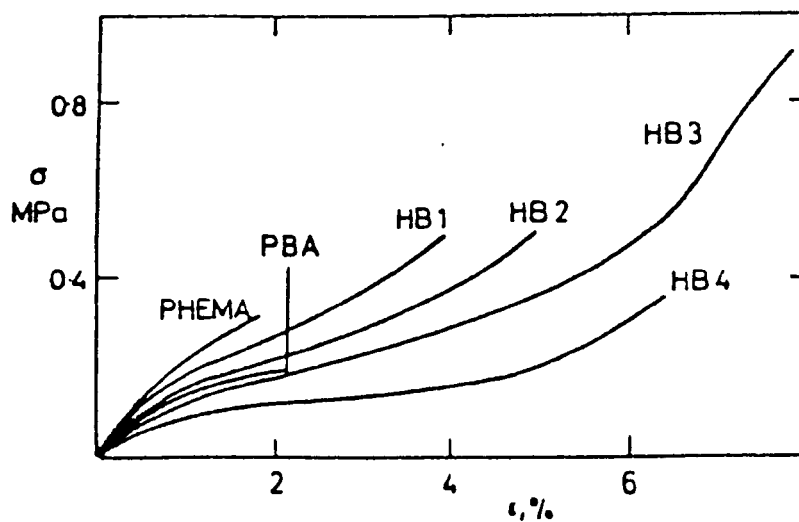


Fig. 2-9b: Tensile Stress-Strain Behaviour of Copolymers HEMA-Butyl Acrylate Swollen in Water to Equilibrium (47).

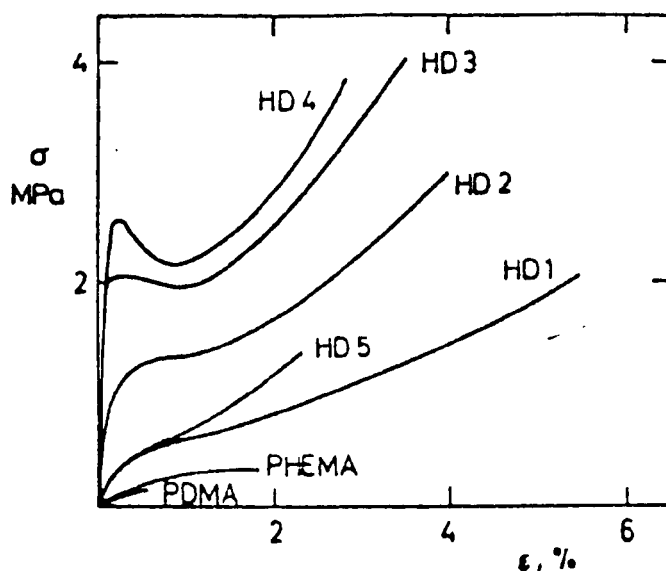


Fig. 2-9c: Tensile Stress-Strain Behaviour of Copolymers HEMA-Dodecyl Methacrylate Swollen in Water to Equilibrium (47).

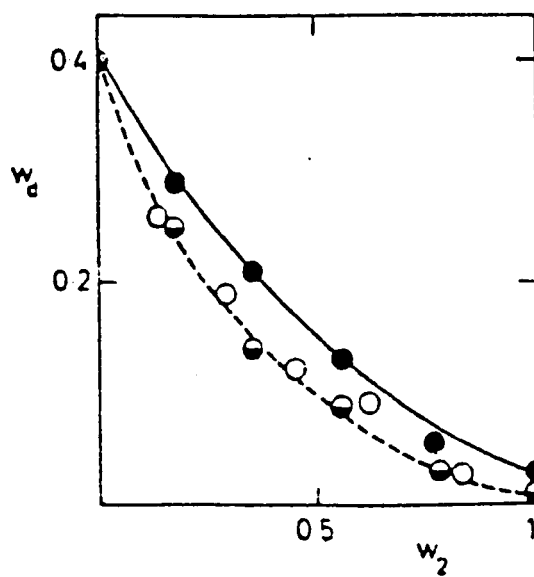


Fig. 2-10: Effect of the Weight Fraction of Ethyl Acrylate (●), n-Butyl Acrylate (◐), and Dodecyl Methacrylate (○) on the Equilibrium Weight Fraction of Water of Copolymers with HEMA (47).

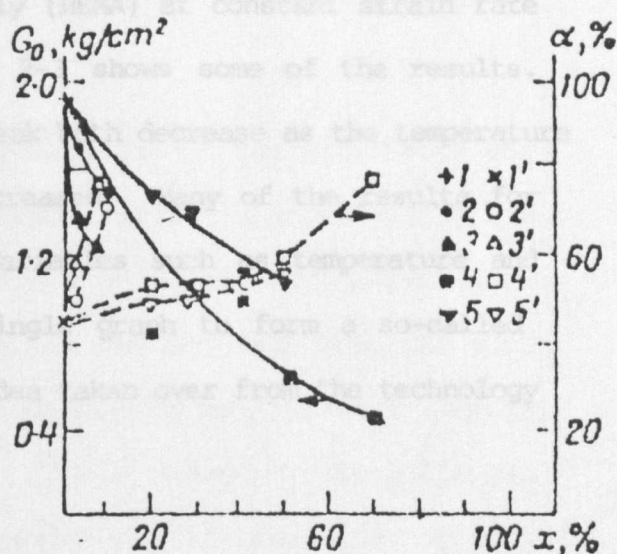
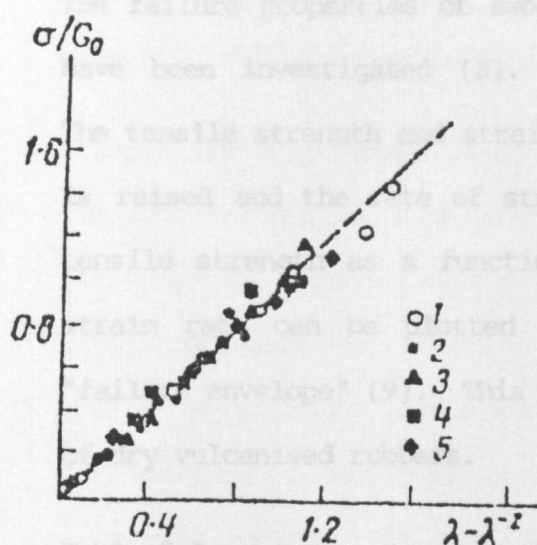


Fig. 2-11a:  $\sigma / G_0$  vs  $\lambda - \lambda^{-2}$  plot for Hydrogels of Varying Chemical

Composition: 1-PHEMA; 2-10% Dimethylaminoethyl Methacrylate/90% HEMA (pH 4.4); 3-8% MAA/92% HEMA (pH7); 4-70% NVP/30% HEMA; 5-50% PVP/50% PHEMA (91).

Fig. 2-11b: Modulus  $G_0$  (1-5) and EWC (1'-5') vs Amount of Hydrophilising Additives in Hydrogels: 1,1' - PHEMA; 2,2' - Dimethylaminoethyl Methacrylate/HEMA (pH4.4); 3,3' - MAA/HEMA (pH7); 4,4' - NVP/HEMA; 5,5' - PVP/PHEMA (91).

It is clear therefore that the tensile stress-strain properties of poly (HEMA) can be modified by copolymerisation with other monomers. The initial modulus may be greatly increased by copolymerising with hydrophobic monomers, although the equilibrium water content is thereby reduced. According to Kolarik and Migliaresi (47), an eightfold increase in initial modulus, achieved by copolymerisation with dodecyl methacrylate (14% w/w) is accompanied by a decrease in EWC from 40% to 26%. Thus the modulus increases by significantly more than would be expected on a basis of water content alone.



(ii) Ultimate Tensile Properties

The failure properties of swollen poly (HEMA) at constant strain rate have been investigated (8). Table 2-3 shows some of the results. The tensile strength and strain at break both decrease as the temperature is raised and the rate of strain decreased. Many of the results for tensile strength as a function of variables such as temperature and strain rate can be plotted on a single graph to form a so-called "failure envelope" (9). This is an idea taken over from the technology of dry vulcanised rubbers.

Table 2-3:

Effect of Crosslinker Concentration  $c$  During Crosslinking  
Copolymerisation of PHEMA upon Tensile Strength and Strain-at-Break  
( $\sigma_b$  and  $\epsilon_b$  respectively)

$c \times 10^4$ (mole $\text{cm}^{-3}$ )	$v_2$	$\sigma_b (\text{kg cm}^{-2})$		$\epsilon_b (\%)$	
		A	B	A	B
0.0855	0.525	7.4	3.4	480	480
0.225	0.528	6.6	4.1	390	300
0.435	0.533	7.8	2.8	305	130
0.845	0.544	10.3	4.1	225	110
1.570	0.559	12.0	3.2	160	50
3.000	0.583	35.5	7.4	120	60
5.650	0.696	49.0	18.6	55	50

Volume fraction of the polymer during polymerisation,  $v_0 = 0.6$ .

Temperature of measurement: A,  $5^\circ\text{C}$ ; B,  $25^\circ\text{C}$ . Rate of strain: A,  $10\text{mm sec}^{-1}$ ;  
B,  $1\text{mm sec}^{-1}$ .

Janacek and Raab (117) measured the strain and stress at break (tensile strength) over a range of strain rates,  $\dot{\epsilon}$ , and superimposed the results by empirical shifts,  $a_r$ , along the  $\log \dot{\epsilon}$  axis. These shifts obeyed

the WLF equation. They found that there were two regions in the graph of tensile strength ( $\sigma_b$ ) against  $\log \dot{\epsilon} a_T$ ; the slope of this graph increases with increasing strain rate.

Kolarik and Migliaresi (47), in their studies of the effects of the copolymerisation of HEMA with hydrophobic monomers, investigated the variation of tensile strength and strain at break with composition. Large increases in tensile strength can be achieved compared with that of poly (HEMA), but always at the expense of reduced water content. For example, a copolymer containing 62% w/w dodecyl methacrylate had a tensile strength of 32.6 MPa, approximately 90 times that of poly (HEMA), but the equilibrium water content was only 9.3% w/w. For copolymers of HEMA with butyl acrylate, both  $\sigma_b$  and  $\epsilon_b$  increased with increasing BA/HEMA ratio to a maximum value, and then decreased. Starodubtsev et al (91) found significantly lower values of tensile strength (approximately  $300 \pm 50$  kPa) and elongation at break ( $106 \pm 42\%$ ) for poly (HEMA) hydrogels than did Kolarik and Migliaresi ( $\sigma_b = 392$  kPa;  $\epsilon_b = 181\%$  : ref. 47). They studied the effect of copolymerisation with hydrophilic monomers on the tensile properties, and found that increasing the proportion of hydrophilic monomer decreased both  $\sigma_b$  and  $\epsilon_b$ .

Janacek, Stoy and Stoy (103) were able to produce hydrogels of high water content and high tensile strength and elongation at break compared with poly (HEMA) gels by the partial hydrolysis of polyacrylonitrile networks. For example, a gel containing 52.4% v/v water had a tensile strength of 3530 kPa and an elongation at break of 840%. Thus their materials appear to have had very good tensile properties, as a function of water content, in comparison with poly (HEMA) gels.

The variation in mechanical properties as a function of the number of oxyethylene units for methoxypolyethylene glycol methacrylate polymers has been investigated (118). It was found that tensile strength and tear strength, along with equilibrium water content, decreased as the number of oxyethylene units increased. The elongation at break increased to a maximum and then decreased. Copolymers of methoxypolyethylene glycol methacrylate (MPEGMA) with HEMA are materials possessing improved mechanical properties in comparison with poly (HEMA) gels. Copolymerising HEMA with a MPEGMA for which the number of oxyethylene units is greater than three produced gels of greater tensile strength than that of the MPEGMA copolymers.

### (iii) Viscoelastic Properties

A survey of the viscoelastic behaviour of poly (HEMA) was included in the review of the mechanical properties of hydroxyalkyl methacrylate polymers published by Janacek (69). Janacek and Ferry (119) measured the dynamic mechanical spectrum for poly (HEMA) swollen in diethylene glycol. The same workers investigated the variation of the storage modulus  $G'$  with temperature for the same system (120). The variation of  $G'$  and  $G''$  with temperature for poly (HEMA) swollen in ethylene glycol has been investigated (121). Again using diethylene glycol as the swelling agent, Janacek and Ferry (58) studied the effect of crosslink density on viscoelastic behaviour. Water-swollen samples have been investigated (122), using various crosslinker concentrations and initial dilutions.

Kolarik and Migliaresi (47) reported the temperature-dependence of both  $G'$  and  $G''$  for crosslinked copolymers of HEMA with ethyl acrylate (EA), butyl acrylate (BA) and dodecyl methacrylate (DDMA) swollen in water. They investigated the effect of copolymerisation on the main glass-rubber transition temperature  $T_g$ . Fig. 2-12 shows the

effects which were observed. The variation of  $T_g$  with weight fraction of comonomer  $W_2$  could be represented by the equation:

$$T = \frac{T_{\alpha 1} + (kT_{\alpha 2} - T_{\alpha 1})W_2}{1 + (k-1)W_2} \quad (2-8)$$

where  $T_{\alpha 1}$  and  $T_{\alpha 2}$  are the glass-transition temperatures for the homopolymers, and  $k$  is an empirical coefficient. Reference 69 gives an extensive bibliography and survey of work carried out in this field up to the year 1972.

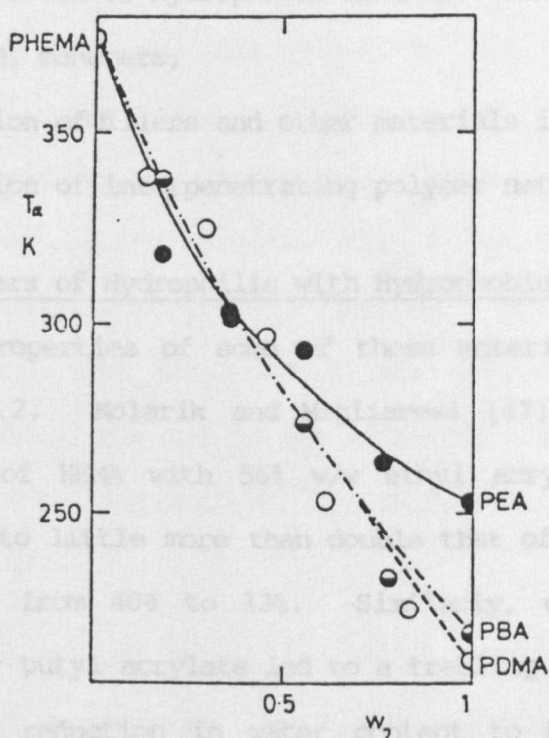


Fig. 2-12: Effect of the Weight Fraction of Ethyl Acrylate (●), n-Butyl Acrylate (◐), and Dodecyl Methacrylate (○) on the Main Transition Temperature  $T_g$  (1Hz) of Copolymers with HEMA (47).

The mechanical properties of hydrogels reinforced by various methods will be dealt with in section 2.1.5.

### 2.1.5 Mechanical Reinforcement of Hydrogels

The fundamental problem which has restricted the wider use of hydrogels, particularly for biomedical applications, has been their poor mechanical strength, especially at high water contents. In general, for a given system, properties such as tensile strength and tear strength decrease with increasing water content. This has led to several attempts to increase the tensile strength and tear strength of hydrogels as a function of EWC. These attempts fall into three categories:

- (i) copolymerisation of hydrophilic monomers with other, usually more hydrophobic, monomers;
- (ii) incorporation of fillers and other materials in hydrogels;
- (iii) incorporation of interpenetrating polymer networks into hydrogels.

#### 2.1.5.1 Copolymers of Hydrophilic with Hydrophobic Monomers

The mechanical properties of some of these materials were discussed in section 2.1.4.2. Kolarik and Migliaresi (47) reported that the copolymerisation of HEMA with 56% w/w ethyl acrylate increased the tensile strength to little more than double that of poly (HEMA), while reducing the EWC from 40% to 13%. Similarly, copolymerisation of HEMA with 56% w/w butyl acrylate led to a trebling of tensile strength accompanied by a reduction in water content to 8%. In cases such as these, it is questionable whether there was any reinforcement. Rather, the increase in tensile strength may be caused merely by the reduction in EWC.

Boiko et al (97) produced gels with higher tensile strength compared to those of poly (HEMA/MAA) by copolymerising MMA, MAA and NVP. For example, a gel with the same water content had more than ten times the tensile strength and twice the modulus compared to a gel from poly (HEMA/MAA).

#### 2.1.5.2 Filled Hydrogels and Hydrogel Composites

Attempts to reinforce poly (HEMA) hydrogels by the incorporation of filler particles were made by Raab and Janacek (123) and by Janacek et al. It is claimed (124) that when HEMA is polymerised in the presence of fillers such as silica, the tensile strength, tear resistance and modulus of the resulting polymer are improved. The tensile strength, compared with poly (HEMA), could be increased four-fold for filled samples with the elongation at break remaining approximately constant.

Reinforcement with inorganic fillers was investigated by Rejda, de Groot and de Visser (125) for hydrogels to be used for tissue implants. Because of their good biocompatibility, poly (HEMA) hydrogels are ideal materials for use as implants for soft tissue replacement. Hard tissue however, such as bones and teeth, is much superior to poly (HEMA) in tensile strength. It was found that the incorporation of alumina fillers into poly (HEMA) gels increased the strength, rigidity and hardness, but not to the extent that they were comparable with bone. The water contents of the resulting materials were low, ranging from 6 to 15%.

The mechanical behaviour of swollen poly (HEMA) has been modified by the addition of crosslinked poly (HEMA) particles as fillers (126, 127). These particles can be prepared by the polymerisation of HEMA with crosslinking agent in water at high dilutions. Various concentrations of EGDMA crosslinker were used in both the filler particles and the polymer matrix. The strengthening effect decreased as the temperature of measurement was raised (126). Stress-strain curves for swollen samples are shown in Fig. 2-13. Materials prepared using an uncross-linked poly (HEMA) matrix showed a definite yield point (Fig. 2-13b). The authors suggested that the particles swell when mixed with the

monomer during the preparation of the filled material. Subsequently, polymerisation leads to the formation of interpenetrating polymer networks, which increase the adhesion of particles to the polymer matrix. The equilibrium swelling was only slightly affected by the incorporation of filler particles, since only 10% of filler was used.

The viscoelastic behaviour of similar systems has been studied (127), together with the dependence of mechanical properties on filler content. It was found that the strengthening effect increases with increasing filler content, the tensile strength being improved up to four-fold with only small changes in EWC.

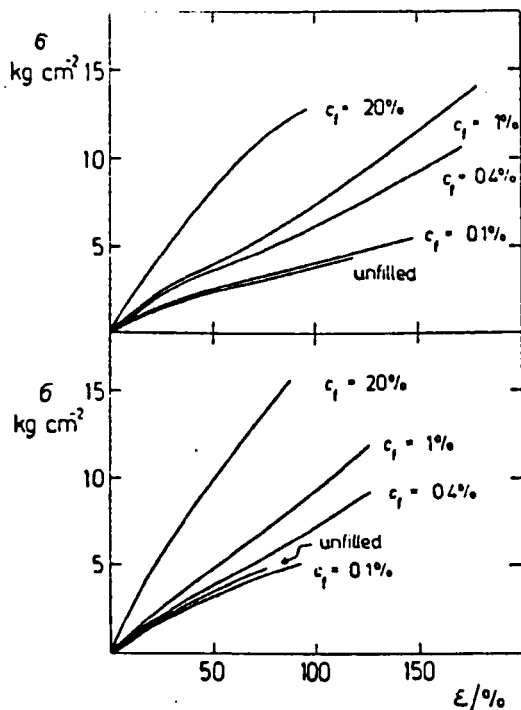


Fig. 2-13a: Stress-Strain Curves of Equilibrium Water Swollen Samples, Measured at 3°C. Concentration of the Crosslinking Agent in the Polymer Matrix : Upper Figure, 0.4%; Lower Figure, 1%.  $c_f$  denotes the Concentration of Crosslinking Agent in the Filler Particles (126).

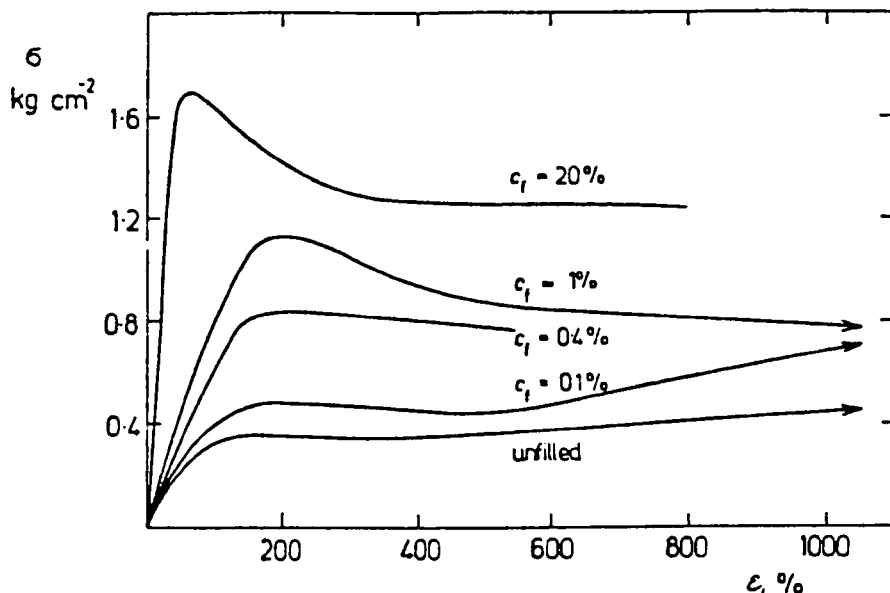


Fig. 2-13b: Stress-Strain Curves of Equilibrium Water-Swollen Samples, Measured at 25°C. Samples Prepared with an Uncrosslinked Soluble Matrix (126).

Dynamic mechanical measurements on various composite hydrogels have been made (128). The composites were poly (HEMA) filled with poly (ethylene terephthalate) (PET) fibres, PET net or polypropylene (PP) fibrillated films. The results showed that the time-temperature shift factors were independent of filler content, and the loss factor,  $\tan \delta$ , was dependent on the reinforcing agent. Equilibrium water contents were not reported.

Similar systems have been used as model synthetic tendons (15). HEMA containing 20% v/v PET pretreated fibres was polymerised inside silicone rubber tubing. At filler contents below this value, the regions of the material close to its surface had inferior mechanical properties, while above 30% v/v, problems arose concerning the orientation of the fibres. Tensile strengths of 90 - 100 MPa were achieved, compared with approximately 0.3 MPa for poly (HEMA) (91). Again, water contents were not reported.



### 2.1.5.3 Hydrogel Interpenetrating Polymer Networks

A further possible method of increasing the tensile strength of hydrogels is by forming IPNs (see Section 2.3). Two or more continuous networks are formed within the same material, although in practice phase separation often occurs, especially if the two networks are chemically dissimilar.

Starodubtsev et al (91) found that the tensile strengths of semi-IPNs of crosslinked poly (HEMA) with uncrosslinked PVP were lower than that of poly (HEMA), but the EWC was higher. As expected, the tensile strength decreased with increasing EWC. At identical EWCs, the tensile strengths of the semi-IPNs were similar to those of HEMA/VP copolymers.

Predecki (129) attempted to produce IPNs of silicone rubber and poly (HEMA) by swelling the rubber in HEMA with suitable solvents, and subsequently thermally polymerising the HEMA. It was noted that the resulting white or opaque materials swelled less in saline solution than did poly (HEMA) gels, but no values for EWC were given. The tensile strength of the IPNs was 38% of that of the silicone rubber, but greater than that of poly (HEMA). No tensile strength values were reported.

The swelling and some of the mechanical properties of gradient IPNs of poly (ether urethane)s with polyacrylamide have been investigated by Dror et al (130). They measured the dependence of EWC on variables such as composition, solvent used, and initiator concentration. The materials were in fact sequential IPNs (see section 2.3.1.1). Electron micrographs of the poly (ether urethane)s (PEUs) revealed a domain structure, the diameter of the domains being approximately 30 - 50nm. The swelling measurements indicated that the polyether component of the poly (ether urethane) swelled, while the hard polyurethane domains

preserved the rigidity of the structure. Fig. 2-14 shows the suggested model structure of the IPNs. The polyacrylamide (PAM) domains were

PAM ranged from 5 - 20%, and the materials showed good reinforcement. PAM granules were dissolved in HEMA, and the HEMA subsequently polymerised. The IPNs of the materials were very similar to those of HEMA/PAM random copolymers of corresponding composition, but their elastic modulus was much higher, especially at high poly (HEMA) contents (see Fig. 2-15).

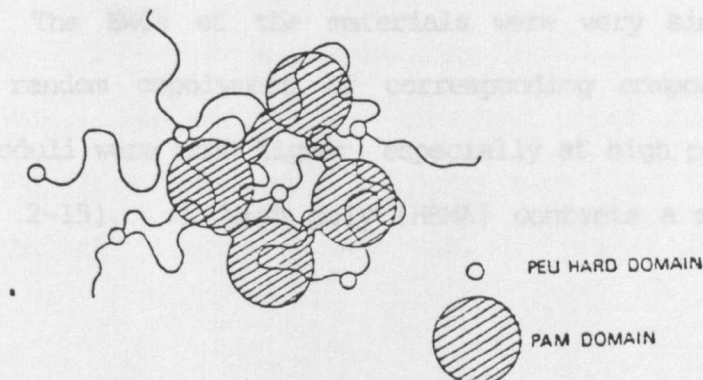


Fig. 2-14: Morphological Model of IPN of Poly (ether urethane) and Polyacrylamide.

embedded in the soft polyether matrix, amongst the hard PEU domains. The water content decreased with increasing PAM content for PAM contents below 8%. The decrease of EWC with increasing hydrogel content at low PAM contents was explained by isolation of the PAM domains, and the consequent inability of water to diffuse through from one PAM domain to another.

Highgate (131) prepared hydrogel IPNs by swelling various polymers in monomers and crosslinking agents and irradiating with  $^{60}\text{Co}$   $\gamma$ -radiation. A crosslinked copolymer of NVP and MMA produced an IPN with crosslinked MMA which, although wettable by water and having high tensile strength, contained only 2% water. At this water content it would be surprising if the tensile strength was not very high. IPNs produced by swelling crosslinked PMMA in NVP and allyl methacrylate with various concentrations of crosslinker had EWCs of up to 90%. Unfortunately no measurements of mechanical properties were reported.

The swelling behaviour and mechanical properties of blends of poly (HEMA) with PMMA have been investigated (132). The proportion of PMMA ranged from 0 - 100%, and the materials showed good reinforcement. PMMA granules were dissolved in HEMA, and the HEMA subsequently polymerised. The EWCs of the materials were very similar to those of HEMA/MMA random copolymers of corresponding composition, but their elastic moduli were much higher, especially at high poly (HEMA) contents (see Fig. 2-15). At high poly (HEMA) contents a marked increase in

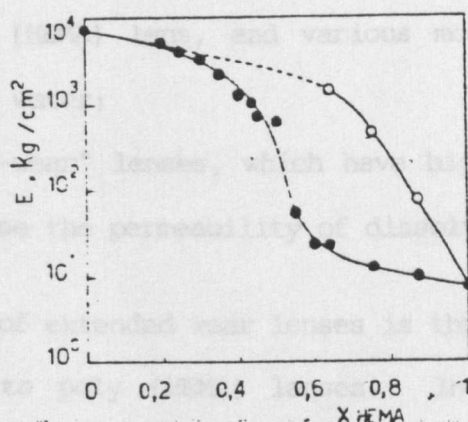


Fig. 2-15: Elastic Modulus as a Function of Mole Fraction of HEMA for Blends (o) and Copolymers (●) (132).

tensile strength was observed, compared with the corresponding copolymers. For example, a blend containing 87.4% poly (HEMA) had a tensile strength of about 110 kPa, compared with approximately 300 kPa for the copolymer of that composition. Both materials had an EWC of approximately 36%. Shah (133) prepared blends of acrylic acid/ethyl acrylate copolymers with poly (NVP). It was reported that both the tensile strength and the elongation at break were high. It has been claimed (134) that materials produced by ultrasonic treatment of blends of hydrophilic copolymers, e.g. poly (HEMA/NVP) with poly

(butyl methacrylate/hydroxypropyl methacrylate), gave materials of high water content, suitable for contact lens applications. No data concerning mechanical properties were reported.

#### 2.1.6 Applications of Hydrogels

The properties of hydrogels make them inherently suitable for various applications. Several of these have been noted already. Soft contact lenses, for which synthetic hydrogels were first developed, are still by far the most important use. Two main types of soft lens are now available:

- (i) the poly (HEMA) lens, and various modifications, which contain about 40% water;
- (ii) "extended-wear" lenses, which have higher water content in order to increase the permeability of dissolved oxygen.

A disadvantage of extended wear lenses is their low mechanical strength, when compared to poly (HEMA) lenses. In addition, they are often thinner than daily-wear lenses, again in order to increase oxygen permeability. There are several limitations on the materials which can be used for contact lenses:

- (i) they must be optically clear when hydrated;
- (ii) they must be wetted by tear solution in order for a tear film to cover the lens;
- (iii) they must have some degree of mechanical integrity;
- (iv) they must be chemically inert.

A second use of synthetic hydrogels is as drug release substrates, although this is mainly still in the development stage. Water-soluble pharmaceuticals incorporated into, or encased within, a hydrogel diffuse out into the body when the gel is imbibed or inserted into the body.

By this method, a slow controlled rate of release of the drug into the body can be achieved. This type of system has yet to be used extensively.

The compatibility of hydrogels with body tissue has led to an interest in hydrogel implants. Again, the major failing of the hydrogels is their lack of mechanical strength. This has in some instances been partly overcome by the use of composite materials.

## 2.2 FILLER REINFORCEMENT OF ELASTOMERS

The most common method of reinforcing elastomeric materials is by the incorporation of fillers such as carbon black or silica. These reinforcing agents usually affect many properties of the material, including modulus, tensile strength, and tearing energy. In consequence, the meaning which attaches to the term "reinforcement" can be rather vague. From the point of view of the technologist, an increase in failure properties such as tear resistance and tensile strength is more important than mere increase in modulus. Reinforcement is commonly measured by increase in properties such as resistance to abrasion, tearing energy, cut growth, flex cracking and tensile fracture (135). Boonstra (136) considers the best criteria for rubber reinforcement to be Wiegand's energy at rupture (137). In this work, failure properties are regarded as providing the primary criteria for rubber reinforcement. This is because these properties are particularly important for materials intended for use in the biomedical field.

The tensile strength of styrene-butadiene rubber vulcanisates can be increased up to ten-fold by the incorporation of carbon black particles as fillers (ref. 136, p.13). Carbon blacks are the most widely-used fillers in the rubber industry. Together with silicas, they account for most of the materials used for the particulate reinforcement of elastomers. The extent and type of reinforcement depends on various factors, such as the particle size of the filler, the extent of filler aggregation, and the surface properties. Carbon black is used as the main example of a reinforcing filler because more work has been carried out on this filler than on any other.

Detailed descriptions of the reinforcing effect of fillers, the properties of fillers and filled rubbers, and the proposed mechanisms of reinforcement are given in references 139, 138 and 136.

## 2.3 INTERPENETRATING POLYMER NETWORKS (IPNs) ( 140 )

### 2.3.1 Types of IPN and IPN Nomenclature

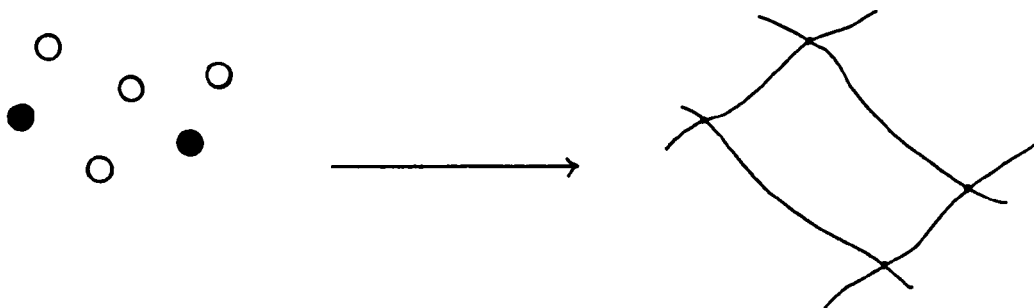
An interpenetrating polymer network is defined as an intimate mixture of two or more polymers, of which at least one is a network polymer. There are several ways in which this type of material can be produced. The resulting polymers are classified according to the mode of preparation.

#### 2.3.1.1 Classification of IPNs

##### (i) Sequential IPNs

A crosslinked polymer, I, is prepared. Monomer II, containing appropriate crosslinking agents, initiators and solvents, is swollen into polymer I, and subsequently polymerised. Fig. 2-16 illustrates this process.

STAGE (1):



STAGE (2):

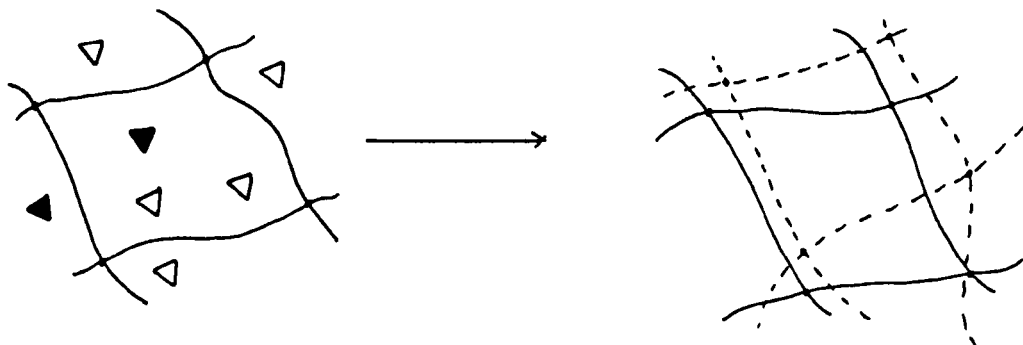


Fig. 2-16: Preparation of a Sequential IPN

Key to Fig. 2-16:    ○ monomer I :    ● crosslinker I  
                          △ monomer II :    ▲ crosslinker II  
                          — polymer I :    - - - polymer II

(ii) Simultaneous IPNs (SINs)

This type of IPN is produced when two or more monomers, with cross-linking agents and initiators, are mixed and simultaneously polymerised by separate, non-interfering reactions. Fig. 2-17 illustrates this process.

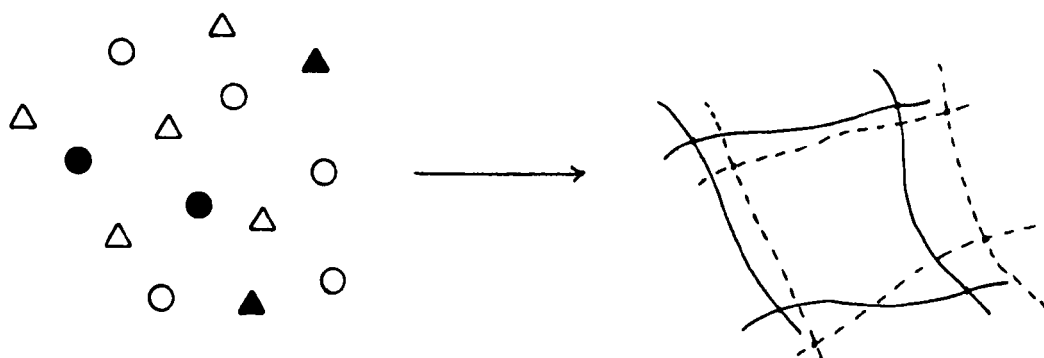


Fig. 2-17: Preparation of a Simultaneous IPN

(iii) Interpenetrating Elastomeric Networks (IENs) (Ref. 140, p.72)

Two polymer latices or solutions are mixed, together with crosslinking agents, and then co-coagulated or evaporated. The material is then heated to cause simultaneous crosslinking of the polymers. An example is a mixture of silicone latex and poly (styrene-butadiene) latex.

(iv) Latex IPNs

This type of IPN consists of latex particles. A crosslinked polymer I latex is used as the seed latex, and after addition of monomer II, crosslinking agent and initiator, and subsequent polymerisation, a polymer II shell is formed.

2.3.1.2 IPN Nomenclature and Terminology

(i) Semi-IPNs

The term "semi-IPN" refers to an IPN where one of the component polymers is uncrosslinked. At one time, this type of structure was known as a "snake cage". Semi-I IPNs have polymer I as the crosslinked component, whereas in semi-II IPNs, polymer II is crosslinked.



(ii) Homo-IPNs

Homo-IPNs are materials in which both polymer I and polymer II are the same substance.

(iii) Gradient IPNs

Gradient IPNs are IPNs of non-uniform composition, in which the concentration of one polymer in the other is gradually varied through the material.

In naming IPNs systematically, account must be taken not only of the types of polymer used and of the way in which they are combined, but also of the time sequence in which they were produced. This is the case because different morphologies, and hence different mechanical properties, can result from different polymerisation sequences.

IPNs are often denoted as poly(X)/poly(Y), where the first polymerised network is poly(X) and the second is poly(Y). However, some information is lost in this notation, for example, the type of IPN, and whether both polymers are crosslinked. Sperling (ref. 140, Chapter 3) has therefore developed a nomenclature for describing polymer blends, IPNs and similar materials, an example of which is as follows:

$P_1^O C_2$  denotes a semi-IPN, where polymer II is crosslinked,  
and I is uncrosslinked.

However, this type of notation does not distinguish between simultaneous, sequential or latex IPNs.

A further notation which is sometimes encountered is the use of the letter i such that, for example, poly(styrene-i-methyl methacrylate) denotes a polystyrene/PMMA IPN.

### 2.3.2 Synthesis of IPNs

There are two major aspects to consider concerning the synthesis of IPNs:

- (i) the chemical composition, i.e. the properties of monomers, cross-linking agents, etc. used in the reaction; and
- (ii) the sequence and type of polymerisation reaction, whether it be simultaneous or sequential, etc.

#### 2.3.2.1 Sequential IPNs

Fig. 2-18 summarises the steps involved in the synthesis of sequential IPNs.

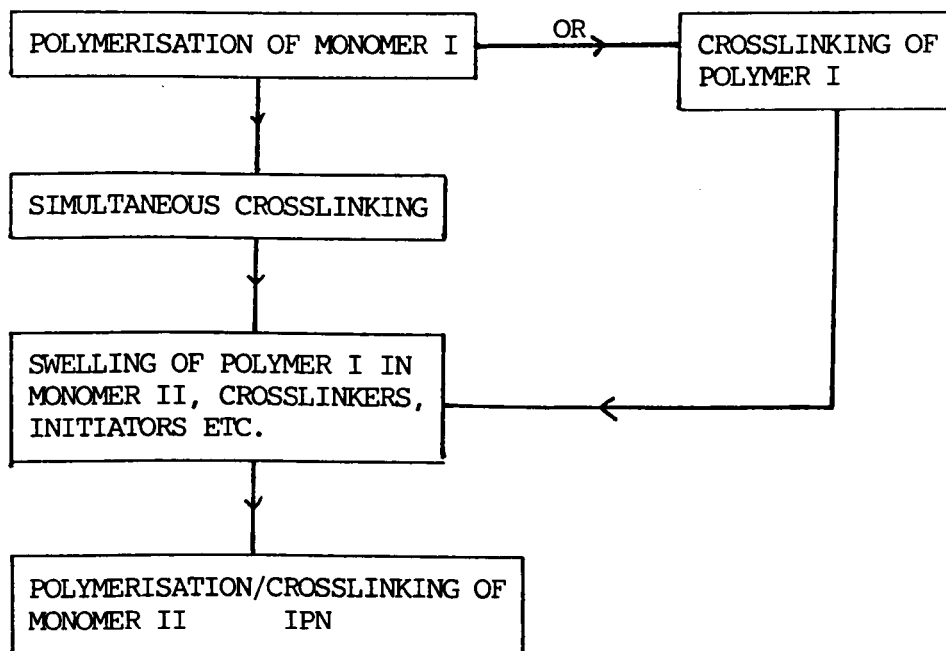


Fig. 2-18: Synthesis of Sequential IPNs

IPNs produced in this fashion typically have a plastic material as one component, and an elastomer as the other. Thus Huelck, Thomas and Sperling (141) synthesised IPNs of poly(ethyl acrylate) with PMMA and polystyrene, by swelling dry poly(ethyl acrylate), produced by photopolymerisation, in styrene or MMA with benzoin and divinyl benzene

or TEGDMA. The IPNs which were produced varied in properties from reinforced rubbers (high PEA content) and leathery materials to tough plastics (high PS or PMMA content).

Thermal initiation has been used for the synthesis of SBR/polystyrene IPNs and semi-IPNs (142). The rubber, crosslinked by compression moulding with dicumyl peroxide, was swollen in styrene, with initiator and crosslinking agent, and then placed in an environment saturated with styrene vapour to ensure uniform distribution of styrene throughout the material. The styrene was then polymerised at 50°C. Semi-IPNs were formed by dissolving uncrosslinked SBR in styrene monomer solution, followed by thermally-initiated free-radical polymerisation, using dicumyl peroxide as the initiator. The effect of varying the crosslink concentration of both components by changing the concentration of divinyl benzene in the polystyrene and the concentration of dicumyl peroxide used to vulcanise the SBR, was investigated.

Widmaier and Sperling (143, 144) crosslinked poly(n-butyl acrylate) (poly(BA)) with acrylic acid anhydride. After swelling in styrene and polymerising, poly(BA)/polystyrene IPNs were formed. They were then able to break the acrylic acid anhydride crosslinks by alkaline hydrolysis, extract the polystyrene and thus examine the resulting porous structure.

Polystyrene has been used to form IPNs with crosslinked castor oil - urethane elastomers (145). Castor oil was mixed with excess 2,4-tolylene diisocyanate, stirred, and then crosslinked by adding excess castor oil, as shown in Fig. 2-19:

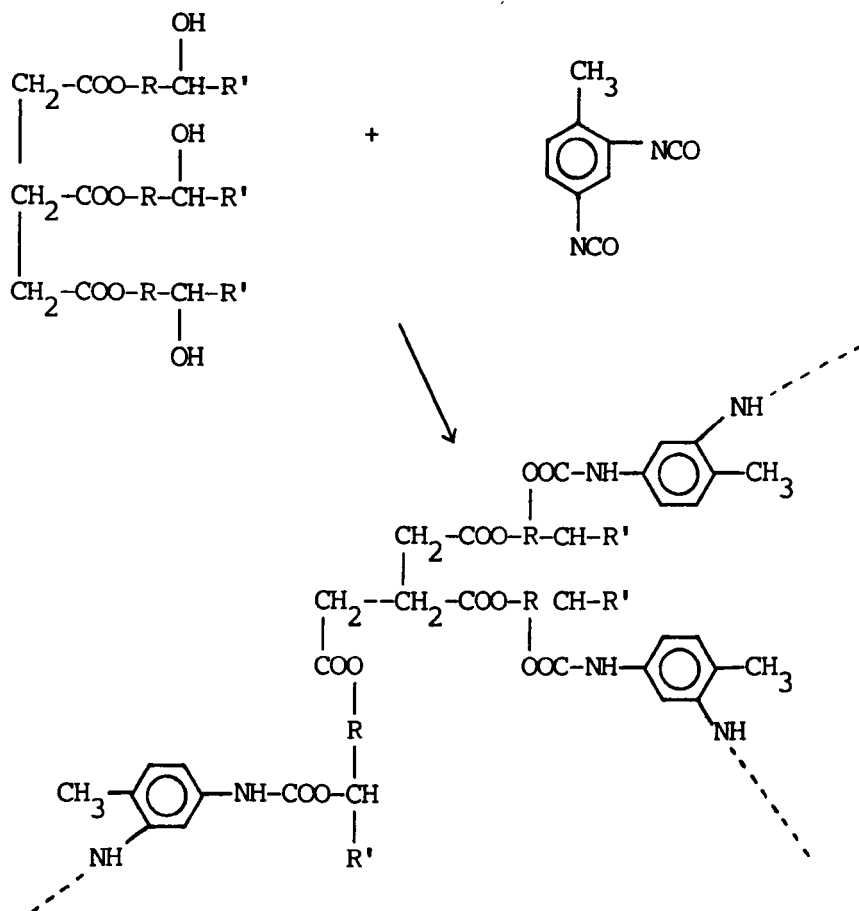


Fig. 2-19: Synthesis of PS/Castor Oil-Urethane Elastomer IPNs:

Formation of Castor Oil - Urethane Elastomer

The elastomer was swollen in styrene, DVB and benzoin, and polymerisation initiated by UV irradiation.

"Semi-compatible" sequential IPNs and semi-IPNs have been prepared by Adachi and co-workers (146, 147). These included PEA/PMMA and polyoxyethylene/poly(acrylic acid). PEA/PMMA IPNs were prepared by two different methods: firstly, by swelling crosslinked PEA for various times and polymerising; and, secondly, by swelling fully, and then polymerising for various lengths of time. It was found that the physical properties of materials of equivalent composition produced by these two methods differed.

Sperling (ref. 140, p.71) made some general remarks concerning the synthesis of IPNs:

- (i) the properties of the materials depend both on the ratio of polymer I to polymer II in the IPN, and the intimacy of mixing of the components;
- (ii) the crosslink concentration of polymer I controls the swelling in the monomer II mixture;
- (iii) polymer I is often an elastomer because of the ease of swelling and the absence of cracking.

Another remark is of interest (148): from the definition of a sequential IPN, polymer I is fully polymerised before being swollen in monomer II. In the case of simultaneous IPNs (SINs), ideally the two monomers are polymerised in separate but simultaneous reactions, but in practice the rate of each reaction may be controlled, so that sequential polymerisation may occur. Hence there is no clear distinction between the two types of IPN.

#### 2.3.2.2 Simultaneous IPNs (SINs)

SINs are formed when monomers, crosslinking agents, initiators, etc. are mixed, and the monomers simultaneously polymerised by non-interfering reactions. Many examples of this type of synthesis exist, especially involving the use of polyurethanes. A few examples will be cited here, to illustrate the method of synthesis.

One form of SIN synthesis is that in which both polymer networks reach the gel point simultaneously. An example is an epoxy/acrylic IPN (149). Polymer I was a crosslinked epoxy polymer made by adding phthalic anhydride to an epoxy resin of low molecular weight. Polymer II was poly (n-butyl acrylate) (PBA), crosslinked with diethylene glycol dimethacrylate (DEGDMA), and copolymerised with 2% isoprene to enable staining for electron microscopy to be carried out. The rate of polymerisation of polymer II was varied by changing the initiator concentration

of the polymer II initiator. Hence, the rate could be slower, faster or approximately the same as that of the epoxy polymerisation.

In another method of producing SINS, a prepolymer mixture is synthesised, and subsequently the two prepolymers are brought to the network state simultaneously. Sperling (ref. 140, p.80) gave an example of this type of synthesis. Methyl methacrylate, crosslinked with trimethylolpropane trimethacrylate, was polymerised to a conversion of 10 - 15%. The mixture was added to a polyurethane prepolymer, prepared by adding MDI to poly(caprolactone glycol), 1,4-butanediol and trimethylolpropane. After mixing in a high-torque mixer, the IPNs were cast at 80 - 100°C under 350 psi pressure for 20 hours.

Suzuki et al (151) studied different ways of producing acrylate/epoxy IPNs. The rate of the epoxy polymer reaction was controlled by heat, while that of the acrylic polymer was controlled by UV light intensity. It was found that the three types of IPN, namely (i) true SINS, (ii) those where polymer I was polymerised first, (iii) those where polymer II was polymerised first, were significantly different in their morphology and properties.

Frisch et al (151) synthesised SINS which contained a considerable amount of grafting, i.e. chemical bonding between the two components. A terpolymer of butyl acrylate (BA), styrene and HEMA, containing a small amount of MAA, was mixed with a polyurethane (PU) in solution. The acrylic polymer and the PU were simultaneously crosslinked, the former by reaction with a butylated melamine formaldehyde resin, and the latter by reaction of isocyanate groups with trimethylolpropane (TMP). Grafting occurred through reaction of pendant hydroxyl groups on the acrylic polymer with isocyanate attached to the PU. A single-phase material was obtained.

Grafting can not only be obtained by reactions such as the one described above, but also by other methods such as radiation treatment, or the addition of molecules containing groups which react with both polymers. For example, glycidyl methacrylate (152) may be used to provide grafting sites between epoxy resins and acrylic polymers.

#### 2.3.2.3 Latex IPNs

This term refers to materials produced as latex particles which are built up by an emulsion polymerisation. Monomer II mixture, containing crosslinker and initiator, but not soap, is added to a seed latex of crosslinked polymer I, and polymerised. The result is a core of polymer I surrounded by a shell of polymer II which may interpenetrate to varying extents.

In this way, plastic/rubber IPNs such as PVC/nitrile rubber have been produced (152). A crosslinked PVC latex was prepared, and fresh initiator was added. After incorporating butadiene and acrylonitrile, the reaction bottle was capped and the second polymerisation carried out at 40°C. The final latex was either cast into films by evaporation of the water, or coagulated and moulded at high temperature and pressure to give sheets.

More recently, Hourston and Satgurunathan (153) studied latex IPNs containing various acrylic and methacrylic monomers, by a similar technique. Latices of about 20% (w/w) solids content were prepared, the ratio of polymer I to polymer II being 1:1 in each case. The IPNs prepared were: poly (isobutyl acrylate)/poly(ethyl methacrylate), poly(iso-BA)/poly(t-BA), poly(n-BA)/poly(t-BA), poly(n-BA)/poly(ethyl methacrylate), poly(ethyl acrylate)/poly(ethyl methacrylate), poly(ethyl acrylate )/poly(t-BA) and poly(iso-BA)/poly(HEMA). It is stated that the IPN containing HEMA was difficult to synthesise, because

the latex tended to coagulate, but that this problem was overcome by careful control of the temperature and rate of stirring of the reaction system.

#### 2.3.2.4 Interpenetrating Elastomeric Networks

These materials are produced when two latices are mixed, co-coagulated or cast as films and the polymers subsequently crosslinked. An example of this type of synthesis is that carried out by Klemperer et al (156). Several types of latex were used, including polydimethylsiloxane, poly(urethane urea) and poly(styrene-butadiene). The resulting mixtures of latices were cast into films, and the polymers were crosslinked. In the case of two of the IENs, one of the polymer networks was hydrolysed and extracted from the material, to demonstrate the independence of the two networks. However, this does not in itself show that an IPN was formed. It is probable that the structure which forms comprises the original latex particles chemically bonded together. One of the two polymers might coalesce to form a continuous phase. However, this structure is not strictly an IPN.

#### 2.3.3 Morphology and Physical Properties of IPNs

##### 2.3.3.1 Morphology of IPNs

The sizes and shapes of phase domains in IPNs are influenced to a large extent by the mode of synthesis, the chemical compatibility of the two polymers, and factors such as their crosslink concentrations and molecular weights (ref. 140, p.105). Most IPNs, however they have been synthesised, exhibit phase separation. Their morphology largely determines their physical characteristics, and therefore the extent and type of phase separation is an important criterion in the design of IPNs. Morphology can be studied by means of transmission electron microscopy. To differentiate between the two phases, those polymers which contain C=C bonds can be stained with osmium tetroxide.



Where double bonds are not present, a small proportion of butadiene may be incorporated into addition polymers to facilitate staining.

In a 1977 review (154), Sperling compared the morphology of SBR/PS sequential IPNs and other, related materials. High-impact polystyrene prepared by polymerising styrene containing dissolved polybutadiene whilst stirring the mixture exhibits a different morphology to that obtained when the mixture is not stirred. The commercial polymer, where the mixture is stirred, has domains of polybutadiene in a polystyrene matrix, which themselves contain smaller polystyrene domains. If the mixture is not stirred, the structure is one of large polystyrene domains in an uncrosslinked SBR matrix, forming a much weaker material. The two semi-IPNs of PS and poly(butadiene) (PBD) have markedly different morphologies and therefore exhibit different mechanical properties. The material which has PS crosslinked and PBD uncrosslinked has small PS domains and the material has a higher tensile strength than the material which has PS uncrosslinked and PBD crosslinked. Both the morphology and mechanical properties of the former semi-IPN are similar to that of high impact polystyrene produced without stirring. The full sequential IPN, where both materials are crosslinked, has small phase domains and, according to Sperling (ref. 154, p.157), "suggests the possibility of two continuous phases."

Another system which has been studied is poly(ethyl acrylate)/polystyrene (PEA/PS) (141). A 1:1 sequential PEA/PS IPN had a cellular morphology, the cell diameter being  $1000\text{\AA}$ . The cell walls consisted mainly of PEA and the contents of PS. The walls of the cells had a fine structure, in that they contained PS particles of the order of  $100\text{\AA}$  in size. The PS/PEA IPN of the same overall composition also had a cellular structure, but now the cells had walls which

consisted mainly of PS and the contents were PEA. It therefore seems from this work that the first-formed network forms the continuous phase. The size of the polymer II domains is controlled by such factors as the overall composition, the crosslink concentration of polymer I and the compatibility of the two polymers. Variations in the crosslink concentration of polymer II have little effect on the size of the phase domains (155).

During the preparation of SINS both polymer networks form at the same time, although not necessarily at the same rate. In their studies of epoxy/acrylic SINS, Touhsaent et al found that the domains were smallest when the gel points occurred simultaneously (149). Klemperer et al (156) showed that the compatibility of the two polymer networks influenced the morphology of SINS. They prepared polyurethane/PMMA materials and found that the higher compatibility of the two polymers resulted in smaller phase domains, when compared with the less compatible polyurethane/PS IPNs. For polyurethane/PMMA materials, the morphology depended on the composition.

The mixing of polymers during simultaneous IPN formation was studied by Devia et al (157). During the formation of castor oil-sebacic acid polyester/PS SINS with rapid stirring, samples were taken at various times. Two layers were formed during the synthesis. In the upper layer, the polyester was the continuous phase, whereas in the lower layer PS was continuous. The upper layer gradually decreased in volume, until the material was uniform. This occurred before gelation, and in the time interval between the two, the material attained its final form.

The morphologies of latex IPNs and IENs are different. Matsuo et al (158) prepared IENs by co-coagulating polyacrylate and poly(urethane-

urea) latices, and then crosslinking. On examination of the resulting materials using transmission electron microscopy, it was found that at all compositions, poly(urethane-urea) particles were dispersed in a polyacrylate matrix, but at 30% polyacrylate/70% PUU, and higher levels of PUU, the PUU particles touched forming a continuous network.

Sionakidis et al (152) investigated the nature of the morphology of latex IPNs, prepared as indicated in section 2.3.2.3. Sequential latex IPNs of PVC/poly(butadiene-acrylonitrile) were shown to have a core-shell structure. Sperling (ref. 140, p.121) suggested several models for the detailed morphology of these IPNs, pointing out the possibility of a smooth gradient of composition between the core and the shell. Another possibility is phase separation inside the core, with formation of a cellular structure.

#### 2.3.3.2 Mechanical Properties of IPNs

For many applications, mechanical properties are important, and some IPNs might prove in the future to be successful in this respect (ref. 140, chaps. 6,7). Some of the materials have been found to exhibit a synergistic effect, i.e. to possess mechanical properties which differ from those expected on the basis of simple additivity. The mechanical characteristics of IPNs depend on such factors as the morphology, the types of polymers, their glass-transition temperatures and their mutual compatibility. The major categories of material have been listed by Sperling (ref. 140, p.167) as follows:

- (i) tough, impact-resistant plastics
- (ii) reinforced elastomers
- (iii) vibration damping materials
- (iv) vulcanised rubber/rubber blends
- (v) electrical insulators

(vi) coatings and adhesives

(vii) ion-exchange resins

Several examples are discussed below with particular reference to their mechanical properties.

Curtius et al (159) found that polybutadiene/PS IPNs were considerably stronger than polybutadiene (see Fig. 2-20). Both tensile strength and elongation at break were increased by the incorporation of polystyrene. However, this would be expected even if an IPN were not

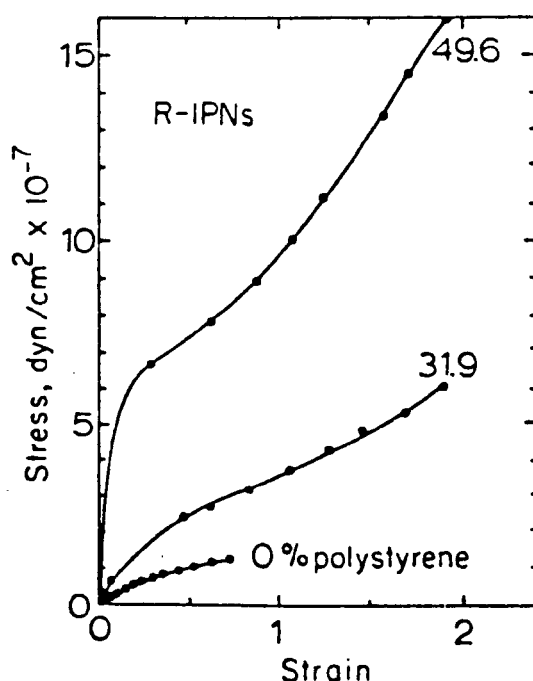


Fig. 2-20: Stress-Strain Curves of Polybutadiene/Polystyrene IPNs Containing Various Amounts of Incorporated Polystyrene (159).

formed. The stress-strain curves for two IPNs of different compositions exhibit an increase in slope at large strains compared with that at medium strains. In the case shown, the larger component of the IPN was the elastomer. Where the proportion of the non-elastomeric polymer is greater than that of the elastomeric polymer, high-impact plastic

materials are formed. In fact, the latter IPNs have impact resistance three to four times greater than that of the corresponding grafted materials, i.e. than that of the usual high-impact PS. Hence a distinct advantage is gained by assembling the materials as IPNs rather than graft copolymers. It has not been reported that such IPNs have yet been used commercially. The semi-IPNs where SBR is the uncrosslinked component are slightly weaker than the full IPNs, whereas the semi-IPNs containing uncrosslinked PS are much weaker, an illustration of the importance of polymerisation sequence in determining mechanical properties. The reinforcement is undoubtedly due to the presence of the finely-dispersed PS phase. As Manson and Sperling wrote (160): "IPNs constitute another example of the simple requirement of needing only a hard or plastic phase sufficiently finely dispersed in an elastomer to yield significant reinforcement". The crosslinking of polymer I means however that the polymer II domain diameter may be rather small in comparison with those of graft copolymers and blends, being usually less than  $1000\text{\AA}$  (ref. 140, p.172). That the continuity of polymer II is important is shown in Fig. 2-21, in which impact strength is plotted against composition for a range of SBR/PS IPNs. Where dual-phase continuity exists, reinforcement occurs.

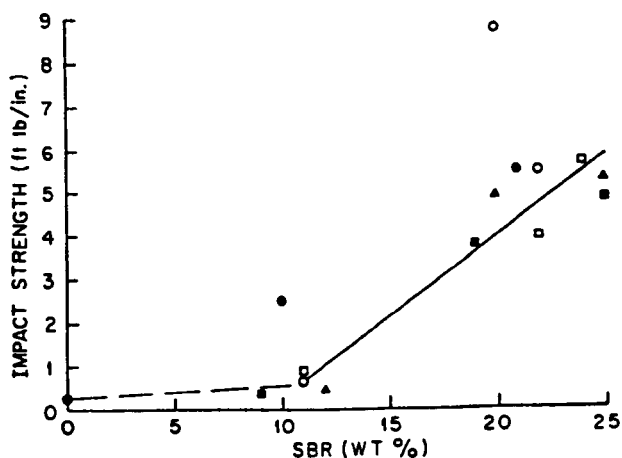


Fig. 2-21: Impact Strength vs Composition and Crosslinking in PS (140).

Touhsaent et al (161) examined the mechanical properties of simultaneous IPNs of epoxy resins with poly(n-butyl acrylate), where the initiator content of the acrylic component, the crosslinker level, and the epoxy pre-reaction time were varied. The SINS showed improved tensile strength in comparison with the epoxy resin, although their moduli were lower because of the softening effect of the incorporated plastic. The weakest materials were formed when polymerisation conditions were such that simultaneous gelation occurred. Polyurethane/PMMA SINS and semi-SINS were studied by Kim et al (162). Tensile strength was a maximum when the PU content was 85%. At this composition, the PU phase is continuous. The tear resistance reached a maximum value at a composition of 60% PU. These materials are more compatible than epoxy/poly(n-butyl acrylate) SINS. Kim et al concluded that, in their IPN system, interpenetration did not directly affect the tensile properties, although interpenetration at the phase boundaries improved adhesion between the phases.

The effect of phase continuity is evident from the discussion by Sperling (ref. 140, p.182) of results for castor-oil polyurethane/polystyrene IPNs (COPU/PS) (163, 164) (see Fig. 2-22). The two 40/60 COPU/PS

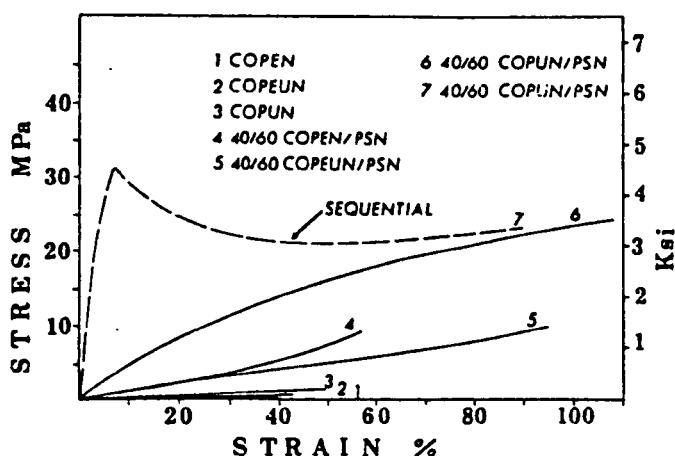


Fig. 2-22: Stress-Strain Curves for SINS Containing 40% Castor Oil Elastomer (140).

materials had the same overall composition, differing only in their methods of preparation. One was an SIN and the other a sequential IPN. A difference can be seen in their stress/strain curves. The sequential IPN possesses a yield point, whereas the SIN does not. Klemperer et al (165) discovered that the tensile strength of polyurethane/polyacrylate IENs could be either greater or less than that expected on a basis of additivity, depending on composition. At approximately 20% polyacrylate, the tensile strength was a minimum, while at about 80% polyacrylate it was a maximum. Klemperer et al (165) attributed the maximum to the presence of a large number of polymer chain entanglements.

From the examples given above, it is clear that the mechanical properties of the various types of IPN depend on their morphology. This in turn is controlled by the compatibility of the polymers, the composition, the mode of polymerisation, and the polymerisation sequence. It is therefore possible to design IPNs with various mechanical properties, for use in different applications.

## 2.4 FAILURE PROPERTIES OF MATERIALS

### 2.4.1 Fracture of Glassy Polymers

This is an extensive subject. The reader is referred to references 166 and 167 for a more detailed discussion than can be given here.

#### 2.4.1.1 The Griffith Criterion

Fracture of polymers commences at flaws and imperfections in the polymer. The analysis of stress concentrations around cracks and holes in the material is complicated. It is dealt with in detail in reference 166. One elementary analysis uses the concept of an elliptical hole in a thin sheet under constant applied stress,  $\sigma_o$ , perpendicular to the major axis of the ellipse. The stress  $\sigma_t$  at the end of the major axis is then given by

$$\sigma_t = \sigma_o (1 + 2 \sqrt{a/\rho}) \quad (2-22)$$

where  $\rho$  is the radius of curvature of the tip and  $2a$  is the length of the major axis. Griffith (168) derived the following expression for the stress required to make a crack in a plate:

$$\sigma_f = \left\{ \frac{2E\gamma}{\pi a} \right\}^{\frac{1}{2}} \quad (2-23)$$

where  $\sigma_f$  is the stress required to fracture the material,  $E$  is the Young's modulus of the material,  $\gamma$  is the surface free energy of the interface between the material and air, and  $a$  is the crack length. This equation holds for glassy polymers, although the values which are obtained from measurements of  $\sigma_f$  do not correspond to known values of surface free energy, because of energy dissipated by plastic deformation at the crack tip (166).



#### 2.4.1.2 Fracture Mechanics

It can be shown (169) that the theoretical tensile strength of a material  $\sigma_t$  approximates to  $\sqrt{E\gamma}/h$ , where  $2\gamma$  is the energy required to create two new surfaces at rupture. Using typical values for  $h$  and  $\gamma$ , the theoretical tensile strength becomes

$$\sigma_t \approx E/10 \quad (2-27)$$

The experimentally-determined tensile strengths of polymers are much lower than  $E/10$  because, in the case of ductile materials, dislocations occur, and for brittle materials flaws exist (ref. 169, p.222).

Fracture of polymers can occur not only by the breaking of covalent bonds, but also by the pulling-out of polymer molecules from the bulk of the material. This is not possible, however, for crosslinked materials such as vulcanised rubber. The experimental value of fracture energy is much greater than the energy required to break bonds, and the intrinsic fracture energy,  $G_0$ , which includes other dissipation processes has been measured for some crosslinked rubbers (170).  $G_0$  was found to be in the range  $40 - 100 \text{ Jm}^{-2}$ , in contrast to that required to break the covalent bonds (about  $0.5 \text{ Jm}^{-2}$ ). Thus for network polymers, the failure process is mainly governed by the breaking of covalent bonds, whereas for materials such as uncrosslinked thermoplastics, molecular pull-out may be important (166).

The kinetic approach has been useful in explaining the observed effects of crack initiation in polymers (171). The rupture of a bond is seen as a random activated process, requiring an activation energy. The accumulation of individual bond rupture-events eventually leads to fracture. Young (169) summed up the kinetic approach by saying that it complements fracture mechanics by being concerned with crack

initiation, whereas fracture mechanics is concerned with crack propagation.

According to Young (169), there are two main approaches to the study of fracture mechanics, viz, the energy-balance, and stress-intensity-factor approaches. It has already been noted that the measured value of  $\gamma$  is much greater than the true surface energy, because of other energy-dissipation processes. Griffith (168) explained this discrepancy in terms of flaws within the sample, and it is on this principle that fracture mechanics is based. If the term  $2\gamma$  is replaced in the Griffith equation by  $G_c$ , representing the actual energy of fracture, then it can be written

$$\sigma_f = \left\{ \frac{EG_c}{\pi a} \right\}^{\frac{1}{2}} \quad (2-28)$$

The stress-intensity factor  $K$  is defined as

$$K = \sigma_f \sqrt{\pi a} \quad (2-29)$$

Thus the condition for crack propagation is when  $K$  reaches a critical value  $K_c$ , given by

$$K_c = \sqrt{EG_c} \quad (2-30)$$

The two basic parameters used in linear elastic fracture mechanics are  $K_c$  and  $G_c$  (169). A detailed description of this subject is given in ref. 166.

#### 2.4.2 Rupture of Rubbers (ref. 166, ch.10; 172)

##### 2.4.2.1 Energy Dissipation in Rubbers

In glassy polymers, energy losses on deformation usually occur because of plastic deformation. For rubbers, however, plastic deformation does not usually occur, and there are other mechanisms which can lead

to energy dissipation. Some of these mechanisms are as follows:

- (i) internal friction, caused by polymer segments sliding past one another;
- (ii) strain-induced crystallisation, a phenomenon which some rubbers, particularly natural rubber, display at high strains, caused by orientation of polymer chains, and resulting in much higher hysteresis;
- (iii) stress softening, particularly with filled rubbers (although the effect has also been observed in unfilled rubbers), which causes increased hysteresis;
- (iv) disintegration of aggregates of carbon black or other filler particles in filled rubbers. It is clear that the chemical structure of the rubber is important, since for strain-induced crystallisation, the polymer chains must be able to align themselves. Whether or not fillers are present is another factor influencing energy losses, as also are temperature and rate of deformation. The extent of hysteresis is also dependent on the extension ratio of the material (see Fig. 2-23).

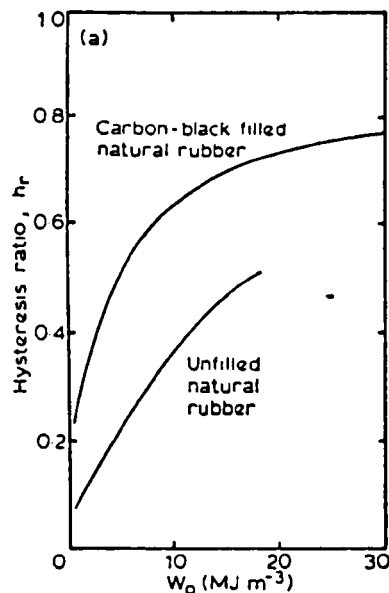


Fig. 2-23a: Hysteresis Ratio  $h_r$  vs Applied Strain-Energy Density for Filled and Unfilled Natural Rubber

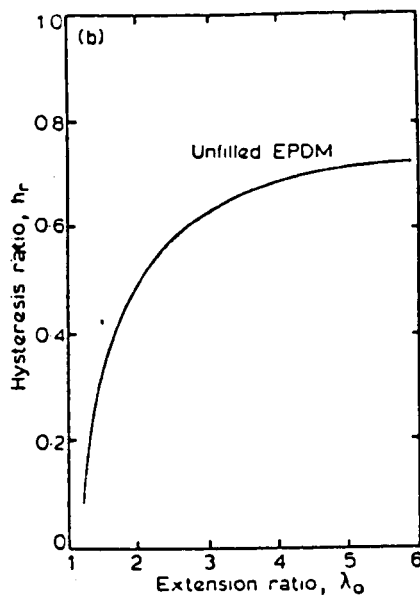


Fig. 2-23b: Hysteresis Ratio  $h_r$  vs Extension Ratio for Unfilled Ethylene-Propylene-Diene Rubber (166).

#### 2.4.2.2 Crack Initiation and Propagation

Cracks in a crosslinked rubber can arise from either

- (i) flaws and imperfections in the bulk of the material or on the surface; or
- (ii) inhomogeneities caused by local fluctuations in the crosslink concentration of the material (ref. 166, ch.10).

Rivlin and Thomas (173) derived the following equation for  $G_c$  for single edge-notch test-pieces of crosslinked rubber:

$$G_c = 2k_1 a W_c \quad (2-34)$$

where  $k_1$  is a function of the extension ratio,  $a$  is the crack length, and  $W_c$  is the strain energy density.

Using the value of the intrinsic fracture energy  $G_o$ , Kinlock and Young (ref. 166, ch.10) estimates the intrinsic flaw size to be approximately 25-30 m.

When fillers are incorporated into crosslinked rubbers, sites immediately above and below the filler particles may act as crack initiation sites.

Gent (174) considered the debonding of filler particles from the rubber matrix by spherical cavitation occurring adjacent to the particle. If the radii of the particles are small, initiation sites close to the particles are favourable for cavitation and subsequent crack growth.

Thomas (175) has proposed the following approximate equation relating the fracture energy  $G_c$  to the radius of the crack tip  $\rho_c$ :

$$G_c \approx 2\rho_c W_{tc} \quad (2-35)$$

where  $W_{tc}$  is the strain energy density at rupture.

Greensmith (176) found that values of crack tip radii of a few tenths of a millimetre fitted equation 2-35, which were consistent with sizes of irregularities found on the surface of the fracture.

Reference 166, chapter 10 gives a more detailed description of crack propagation in rubbers. Two further points are noted here:

- (i) strain-induced crystallisation may occur at the tip of a crack, where the strain is high, thereby increasing hysteresis and causing "stick-slip" crack propagation;
- (ii) filled rubbers tend to exhibit "knotty" tearing, resulting from deviations of the crack, which increases the tear resistance of the material, so that the effective tip radius, and therefore  $G_c$ , are high.

## CHAPTER THREE

### EXPERIMENTAL DETAILS

### 3.1 MATERIALS

#### 3.1.1 Sources of Materials and Purification Procedures

##### 3.1.1.1 Materials and Suppliers

Table 3-1 shows the materials used in the experimental work, and their origins.

Table 3-1: Materials Used in the Experimental Work

MATERIAL	SUPPLIER	PURIFICATION	PURITY
HEMA(1)	B.P.	-	See Section 4.1
HEMA(2)	B.P.	Extraction	Unknown
HEMA(3)	Cooper Vision	Distillation	98%
Styrene(1)	Aldrich	-	99%
Styrene(2)	Aldrich	Washing	99%
MMA(1)	Aldrich	-	99%
MMA(2)	Aldrich	Washing	99%
AZDN(1)	Aldrich	-	97%
AZDN(2)	Aldrich	Recrystallisation	97%
EGDMA	Fluka	-	98%
DVB	Aldrich	-	55-60%
EHA(1)	Fluka	-	98%
EHA(2)	Fluka	Washing	98%
DDA	Fluka	-	60-70%
PPM6	B.P.	-	Unknown
MAA	Aldrich	Distillation	99%
DMPT	Aldrich	-	99%
EG	Aldrich	-	99+%
DBPO	Aldrich	-	70%
Adipicacid	Aldrich	-	99%

### 3.1.1.2 Purification Procedures

(i) HEMA(1), used for preliminary experiments, was of unknown purity, although attempts were made to analyse it by gas-liquid chromatography.

(ii) HEMA(2) was purified in the following way:

HEMA(1) (100ml) was mixed with distilled water (100ml) and extracted twice with cyclohexane (200ml). The HEMA was salted out from the aqueous solution using sodium chloride, and then distilled under reduced pressure at a temperature of approximately 80-90°C, using an air-bleed. The resulting material was stored in a refrigerator.

(iii) MMA(2) was purified in the following way:

MMA(1) (200ml) was shaken with 5 w/v% sodium hydroxide solution (200ml) in a separating funnel. After drawing off the lower, aqueous layer, the process was repeated using the upper MMA layer. The MMA portion was washed with two 100ml volumes of distilled water, dried over anhydrous potassium carbonate, filtered and stored over 5A molecular sieves in a refrigerator.

(iv) AZDN was purified by recrystallisation, firstly from methanol and then from diethyl ether. It was then stored in a refrigerator.

### 3.1.2 GLC Analysis of HEMA(1)

The gas-liquid chromatograph which was used was a Perkin-Elmer Model F11, equipped with a flameionisation detector. The internal standard was diethyl adipate (DEA). It was synthesised by the following method: Adipic acid (15g), sulphuric acid (1ml), toluene (100ml) and IMS (50ml) were boiled for approximately 4 hours in a 500ml round-bottomed flask fitted with a Dean and Stark apparatus. After the maximum amount of water had been collected, the reaction was stopped. The product was mixed with diethyl ether, and the unreacted acid extracted with two portions of sodium bicarbonate solution (10% w/v). After washing



with water and separating, the ether phase was dried with anhydrous potassium carbonate, and the ether was evaporated. GLC analysis was carried out in the following way: 0.5  $\mu$ l of the DEA was injected by means of a microsyringe into the injection port of the apparatus. The column temperature was programmed to rise at 10°C per minute from 100°C to 150°C. The response was observed as a peak on the chart-recorder paper. The column used was 2.5% Apiezon, adsorbed on Chromosorb W. This was chosen after several preliminary experiments using an OV column. A solution of DEA in HEMA was made up as follows: 0.6135g of DEA was added to HEMA (30.0111g). The weight percentage of DEA was 2.00%. EGDMA was added to this mixture in various proportions, and 0.2-0.4  $\mu$ l of each of the resulting mixtures was injected into the GLC apparatus. The column temperature was programmed to increase at 20°C per minute from 100°C to 200°C.

The chromatogram was analysed by measuring the areas of the DEA and EGDMA peaks in the following way. The peaks were divided into triangles, and the areas of the triangles were measured. The ratio of the area of the EGDMA peak to that of the DEA peak was plotted against the percentage by weight of added EGDMA.

### 3.2 TERPOLYMERS OF HEMA WITH MAA AND WITH HYDROPHOBIC MONOMERS

#### 3.2.1 Preparation of Crosslinked Poly(HEMA) Gel by Polymerisation in Solution

The procedure used in the initial, introductory experiments was retained, with minor variations, throughout the project. The composition of the polymerisation mixture for the first experiment was as follows:

HEMA(1)	50g
DBPO	0.50g
6.25% (w/w) solution of DMPT in IMS/ ethylene glycol (50% w/w)	1.03g
EGDMA	0.19g
IMS	50g

The concentrations of the initiators and crosslinking agent, expressed as a percentage of the total monomer, were:

DBPO	0.37%
DMPT	0.12%
EGDMA	0.25%

DBPO (0.50g) was dissolved in a mixture of HEMA(1) (50g) and EGDMA (0.19g), in a 250ml conical flask using a magnetic stirrer. To this solution was added a mixture of IMS (50g) and DMPT solution (1.03g). After stirring for a few minutes, the resulting solution was fed by means of silicone rubber tubing (outside diameter 3mm, inside diameter 1.5mm, Scientific Supplies), into the mould, a diagram of which is shown in Fig. 3-1.

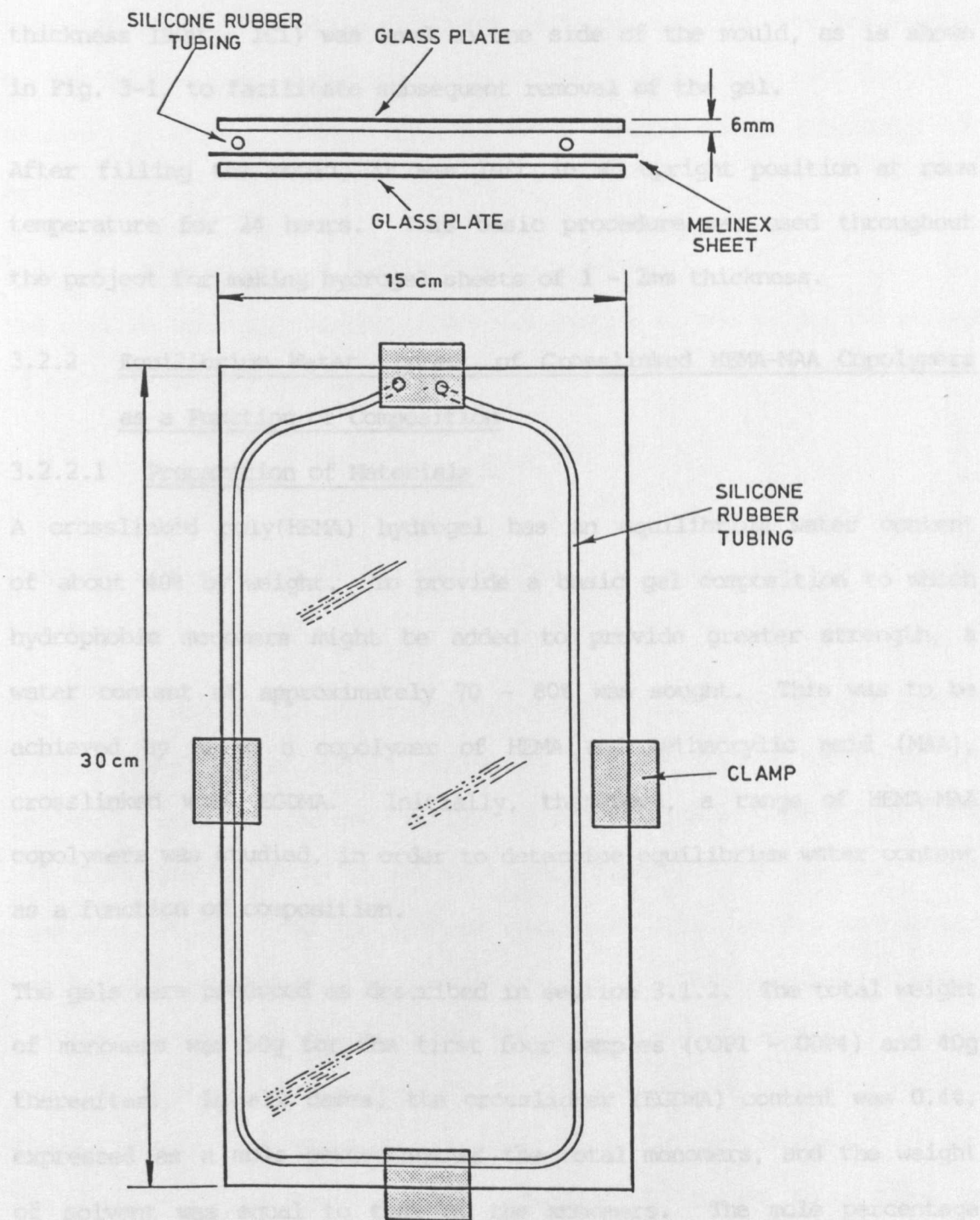


Fig. 3-1: Polymerisation Mould

Silicone rubber tubing was used as a gasket between two 6mm glass plates measuring 150 x 300mm. The mould was clamped together by four metal clips. A piece of "Melinex" (poly(ethylene terephthalate)),

thickness 190 $\mu$  , ICI) was used on one side of the mould, as is shown in Fig. 3-1, to facilitate subsequent removal of the gel.

After filling the mould, it was left in an upright position at room temperature for 24 hours. This basic procedure was used throughout the project for making hydrogel sheets of 1 - 2mm thickness.

### 3.2.2 Equilibrium Water Content of Crosslinked HEMA-MAA Copolymers as a Function of Composition

#### 3.2.2.1 Preparation of Materials

A crosslinked poly(HEMA) hydrogel has an equilibrium water content of about 40% by weight. To provide a basic gel composition to which hydrophobic monomers might be added to provide greater strength, a water content of approximately 70 - 80% was sought. This was to be achieved by using a copolymer of HEMA and methacrylic acid (MAA), crosslinked with EGDMA. Initially, therefore, a range of HEMA-MAA copolymers was studied, in order to determine equilibrium water content as a function of composition.

The gels were produced as described in section 3.1.2. The total weight of monomers was 50g for the first four samples (COP1 - COP4) and 40g thereafter. In all cases, the crosslinker (EGDMA) content was 0.4%, expressed as a mole percentage of the total monomers, and the weight of solvent was equal to that of the monomers. The mole percentage of DBPO was 0.5%, and the weight of DMPT solution was twice that of DBPO (i.e. the weight of DMPT was one-eighth that of DBPO). The solvent was IMS, except in the case of COP1 - COP3, where it was a 50:50 (w/w) mixture of IMS and ethylene glycol.

HEMA(1) was used for samples COP8 - COP21, and HEMA(2) was used for samples COP1 - COP7. Table 3-2 summarises the compositions of the

gels. After leaving in the mould for 24 hours, each gel was transferred to distilled water, and swollen for at least three days, with frequent changes of water. Water contents were determined as described in section 3.2.2.2.

#### 3.2.2.2. Measurement of Equilibrium Water Content

The equilibrium water content (EWC) was defined as the weight percentage of water in the swollen gel:

$$EWC = \frac{W_s - W_D}{W_s} \times 100 \quad \dots(3-1)$$

where  $W_s$  is the weight of the swollen gel, and  $W_D$  is the weight of the dried gel (xerogel).

The EWC was determined in the following way: Four to six capped sample bottles were weighed on an analytical balance with a precision of  $\pm 0.2\text{mg}$ . Samples of the gel, swollen to equilibrium at room temperature and approximately  $0.1\text{g}$  in weight, were placed in the bottles. The caps were replaced and the bottles reweighed. The bottles containing the gel samples were then placed uncapped in an oven in order to remove the water from the samples. For the first few experiments, a vacuum oven was used, the temperature being  $70^\circ\text{C}$  and the vacuum approximately  $1\text{mmHg}$ . Using this method, approximately 1 day was necessary to dry the samples to constant weight. Subsequently it was found that an ordinary oven at  $60 - 70^\circ\text{C}$  was equally effective in drying to constant weight, the process taking 2 - 3 days. Therefore most of the measurements were carried out using this method.

After drying, the bottles containing the dried samples were recapped and reweighed.

Table 3-2: Compositions of HEMA-MAA Copolymers

Sample	HEMA/g	MAA/g	mol %MAA	Remarks*
COP1	48.50	1.50	5.0	a, b
COP2	47.50	2.50	7.5	a, b
COP3	42.00	8.00	23.0	a, b
COP4	49.00	1.00	3.0	c, b
COP5	39.47	0.53	2.0	c, b
COP6	39.73	0.27	1.0	c, b
COP7	39.47	0.53	2.0	c, b
COP8	38.73	0.27	1.0	c, d
COP9	39.47	0.53	2.0	c, d
COP10	48.50	1.50	5.6	c, d
COP11	39.20	0.80	3.0	c, d
COP12	39.87	0.13	0.5	c, d
COP13	37.26	2.74	10.0	c, d
COP14	39.07	0.93	3.5	c, d
COP15	39.80	0.20	0.75	c, d
COP16	39.60	0.40	1.5	c, d
COP17	39.33	0.67	2.5	c, d
COP18	39.13	0.87	3.2	c, d
COP19	38.79	1.21	4.5	c, d
COP20	38.10	1.90	7.0	c, d
COP21	38.80	1.20	4.4	c, d

\* a : solvent was 50% (w/w) IMS/ethylene glycol

b : HEMA(2) was used

c : solvent was IMS

d : HEMA(1) was used

The EWC was calculated as:

$$\begin{aligned} \text{EWC} &= \frac{(W_{\text{SB}} - W_{\text{B}}) - (W_{\text{DB}} - W_{\text{B}})}{(W_{\text{SB}} - W_{\text{B}})} \times 100 \\ &= \frac{W_{\text{SB}} - W_{\text{DB}}}{W_{\text{SB}} - W_{\text{B}}} \times 100 \quad \dots(3-2) \end{aligned}$$

where  $W_{\text{SB}}$  is the weight of the capped bottle containing the swollen gel,  $W_{\text{DB}}$  is the weight of the capped bottle containing the dried gel, and  $W_{\text{B}}$  is the weight of the empty capped bottle. The arithmetic mean of the four to six EWC results was taken as the equilibrium water content.

### 3.2.3 Synthesis of Terpolymers of HEMA with MAA and Hydrophobic Monomers

#### 3.2.3.1 Gels Containing HEMA(1), MAA and MMA(2)

A stock solution of 5.0% (mol/mol) MAA in HEMA(1) was prepared by mixing MAA (12.81g) with HEMA(1) (387.19g). The gels were made in the following way: DBPO was dissolved in a mixture of EGDMA, MMA(2) and HEMA(1)/MAA stock solution. DMPT, made up as a 6.25% (w/w) solution in IMS, was mixed with IMS (40g), and this mixture was added to the monomer mixture, whilst stirring using a magnetic stirrer. After stirring for a few minutes, the solution was poured into the mould described in section 3.2.1. The EGDMA content was 0.4% (mol/mol); 0.5% (mol/mol) DBPO and 0.16% (mol/mol) DMPT were used.\* The equilibrium water content (section 3.2.2.2) and the tensile strength (section 3.2.4) were determined. Table 3-3 shows the composition of the various gels.

All the polymerisation mixtures contained 40.0g of IMS. It can be seen from Table 3-3 that samples TER1 - TER13 were made using 40.0g

\* The gels were swollen to equilibrium in 0.1M sodium bicarbonate solution.

Table 3-3: Compositions of Terpolymer Gels

Sample	(HEMA + MAA)/g	MMA/g	mol % MMA
TER1	40.0	0	0
TER2	40.0	0.50	1.6
TER3	40.0	1.50	4.8
TER4	40.0	2.00	6.9
TER5	40.0	2.50	7.4
TER6	40.0	0.77	2.4
TER7	40.0	1.25	3.9
TER8	40.0	1.75	5.4
TER9	40.0	2.25	6.8
TER10	40.0	0.25	0.8
TER11	40.0	1.50	4.8
TER12	40.0	1.75	5.4
TER13	40.0	0.50	1.6
TER14	29.26	10.00	30.5
TER15	33.46	6.54	20.0
TER16	36.80	3.20	10.0
TER17	31.73	8.27	25.0
TER18	35.22	4.78	15.0
TER19	22.61	17.39	50.0
TER20	26.28	13.72	40.0
TER21	29.96	10.04	30.0



of (HEMA + MAA + MMA). The weight of IMS was 40.0g in all cases. Hence the dilution of the monomers on a weight basis is slightly different for the first set of samples (TER1 - TER13). It is thought that this difference is negligible, since the quantity of MMA was small compared to that of HEMA.

### 3.2.3.2 Gels Containing HEMA(3), MAA and MMA(2)

Gels were prepared as described in section 3.2.3.1. They contained 5.0mol % MAA in HEMA(3), and varying amounts of MMA(2). The IMS content was equal to the total weight of monomers. As before, the EGDMA content was 0.4mol %; 0.5mol % DBPO and 0.16mol % DMPT were used. \* Table 3-4 shows the composition of these gels.

Table 3-4: Composition of Terpolymer Gels

Sample	(HEMA + MAA)/g	MMA/g	mol % MMA
TER22	13.18	1.82	15.0
TER23	29.95	10.05	30.0
TER24	31.73	8.27	25.0
TER25	29.95	10.05	30.0
TER26	36.80	3.20	10.0
TER27	33.46	6.54	20.0
TER28	26.29	13.71	40.0

### 3.2.3.3 Gels Containing HEMA(3), MAA and Various Hydrophobic Monomers

Gels were prepared as described in section 3.2.3.2. The weight of IMS was equal to the weight of monomers. The EGDMA content was again 0.4mol %; 0.5mol % DBPO and 0.16mol % DMPT were used. Various hydrophobic monomers were used. The gels were swollen to equilibrium in 0.1M

\* The gels were swollen to equilibrium in 0.1M sodium bicarbonate solution.

Table 3-5: Composition of Terpolymer Gels

Sample	(HEMA + MAA)g	X*/g	mol %X*
TER29	27.60	2.40	10% MMA
TER30	29.95	10.05	30% MMA
TER31	25.02	4.98	15% HPMA
TER32	20.22	9.78	30% HPMA
TER33	17.88	12.12	40% HPMA
TER34	14.11	15.89	50% HPMA
TER35	28.77	1.23	Ø 5% styrene
TER36	28.14	1.86	Ø 7.5% styrene
TER37	27.51	2.49	Ø 10% styrene
TER38	26.88	3.12	Ø 12.5% styrene
TER39	26.23	3.76	15% styrene
TER40	24.81	5.19	10% DDA
TER41	24.81	5.19	10% DDA
TER42	22.53	7.47	15% DDA
TER43	20.42	9.58	20% DDA
TER44	16.61	13.39	30% DDA
TER45	16.61	13.39	30% DDA
TER46	25.86	4.14	10% EHA(1)
TER47	22.06	7.94	20% EHA(1)
TER48	18.55	11.45	30% EHA(1)
TER49	25.86	4.14	10% EHA(2)
TER50	22.06	7.94	20% EHA(2)
TER51	20.98	9.02	30% BA
TER52	21.78	8.22	10% PPM6
TER53	18.76	11.24	15% PPM6
TER54	16.23	13.77	20% PPM6
TER55	14.07	15.93	25% PPM6
TER56	29.59	0.41	2% MAA
TER57	14.87	15.13	50% HEMA

Ø these gels contained 0.4% DVB as crosslinker

\* X denotes the monomer

sodium bicarbonate. The compositions of the gels are shown in Table 3-5.

### 3.2.4 Determination of Tensile Strength

The tensile strength of hydrogels was determined in the following way. The test-piece was a dumbbell cut from the material. The width at the narrowest part was 4mm. The thickness of the test-piece was measured in the central region, using a Mercer measuring gauge. The arithmetic mean of the three results was taken as the thickness. The ends of the sample were placed in the grips of an Instron testing machine. Pieces of soft polysulphide rubber were placed between the faces of the grips and the samples. The grips were tightened by hand, finger-tight but not so tight as to damage the sample. The grips were then separated at a constant rate (see below). The force at break was obtained from the chart-recorder output from the machine. The tensile strength,  $\sigma_b$  (kPa), was calculated as:

$$\sigma_b = \frac{F_b}{W \cdot t} \times 1000 \quad \dots(3-3)$$

where  $F_b$  is the force at break (N),  $W$  is the sample width (mm), and  $t$  is the sample thickness (mm). The rate of separation of the grips was usually  $5\text{mm min}^{-1}$ , but for some of the earlier tests it was  $50\text{mm min}^{-1}$ .

### 3.2.5 Low-Extension Elastic Modulus Determination

#### 3.2.5.1 Samples and Apparatus

The samples were rectangular strips cut with a scalpel from the sheet material. Their dimensions were  $30 \times 60 \times t$  mm,  $t$  being the thickness of the material. The thickness,  $t$ , was determined as the arithmetic mean of measurements in three places with a Mercer gauge. The grips for holding the sample consisted of "Bulldog" clips faced with rubber

to prevent cutting of the gel and provided with a nut and bolt through the hole in the clip, in order to allow the pressure on the gel to be controlled (see Fig. 3-2). The apparatus used for these determinations is shown in Fig. 3-3.

Fig. 3-2: Grips Used in Modulus Determination

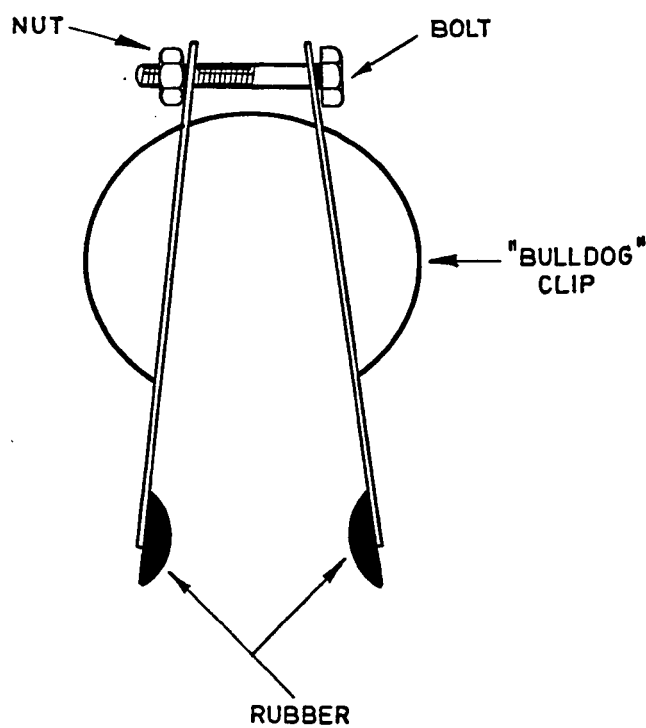
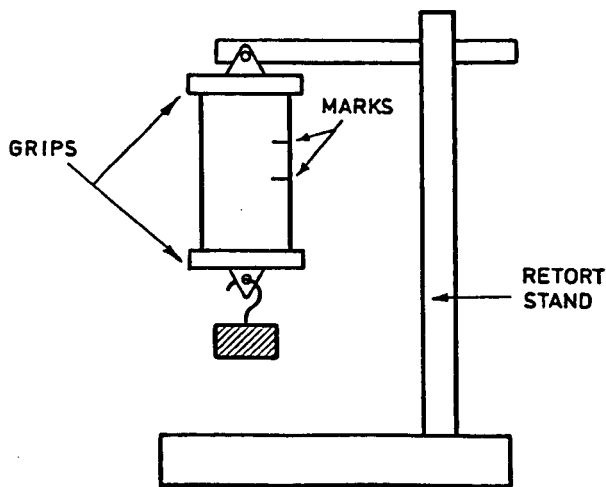


Fig. 3-3: Apparatus used for Modulus Determination



The sample was suspended from the stand by means of the upper set of grips. Weights were hung from the lower set.

### 3.2.5.2 Procedure

Two marks were drawn on the sample in its unloaded state, using an indelible marking pen. The marks were approximately 10mm apart. The sample was attached to the upper grips. The whole apparatus was placed in a closed glass-sided container which also contained an open bowl filled with water, the purpose of which was to prevent excessive evaporation from the sample by maintaining a water-saturated atmosphere. A cathetometer was focussed on each mark in turn, and the readings noted. From the difference in the two readings a precise measurement of the unstrained distance was found. To determine the stress-strain curve, the lower grips were attached to the sample, and weights hung from the lower grips. For each load, the distance between the two marks was measured as described above. The stress,  $\sigma$  (kPa), was calculated as

$$\sigma = \frac{M \cdot g}{W \cdot t} \times 1000 \quad \dots(3-5)$$

where M is the mass of the load on the sample (including the lower grips) (kg), g is the acceleration due to gravity ( $\text{ms}^{-2}$ ), W is the sample width (30mm), and t is the sample thickness (mm).

The strain  $\epsilon$  was calculated as

$$\epsilon = \frac{l_M - l_0}{l_0} \quad \dots(3-6)$$

where  $l_M$  is the distance between the marks at load Mg, and  $l_0$  is the distance between the marks when the sample is unloaded. For each sample, stress was plotted against strain, and the slope at zero strain was taken as the low-extension elastic modulus.

### 3.2.6 Determination of Stress-Strain Characteristics

Dumbbell-shaped samples were prepared, as described in Section 3.2.4 above. The Instron was again used to extend the samples, and measure the applied load. The extension of the sample was measured in the early stages of the project by the use of an extensometer. This consisted of two grips which clipped on to the narrow part of the dumbbell, and before extension occurred were 10mm apart. During the test the grips moved apart, and a strain gauge measured the distance between them. The extension was given as a percentage of the original length: every 10% extension produced a mark on the chart recorder output.

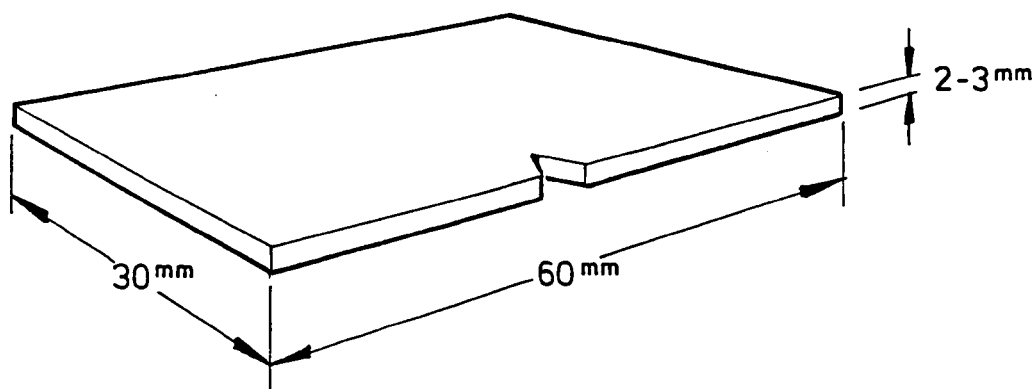
However, it was found that, especially when testing softer samples, the extensometer grips cut into the samples, which then broke at the grips, thus invalidating the test. Therefore the following alternative method was used. Two marks 10mm apart were made with an indelible marker pen on the narrowest part of the dumbbell. As the sample was extended by the Instron, the distance between the marks was periodically measured with a pair of dividers and a ruler. The percent extensions were marked at the appropriate points on the chart output of the machine. The stress was calculated as described in Section 3.2.5, and plotted against strain for each sample.

### 3.2.7 Determination of Tearing Energy

#### 3.2.7.1 Single Edge-Notch Samples

(i) Several experiments were carried out on terpolymer gels using a single edge-notch method (173). The test-pieces were identical in size to those used for the determination of low-extension elastic modulus (Section 3.2.5). A small notch was cut into one of the long edges of the sample, using a very sharp scalpel (see Fig. 3-4). The sample was held in the same way as described in Section 3.2.5, but

Fig. 3-4: Sample Used in Single Edge-Notch Tearing Experiments



the cathetometer was arranged to move horizontally in order to measure crack length. The load on the sample was constant throughout each test. The length of the crack was measured at various times, and crack length plotted against time for each sample.

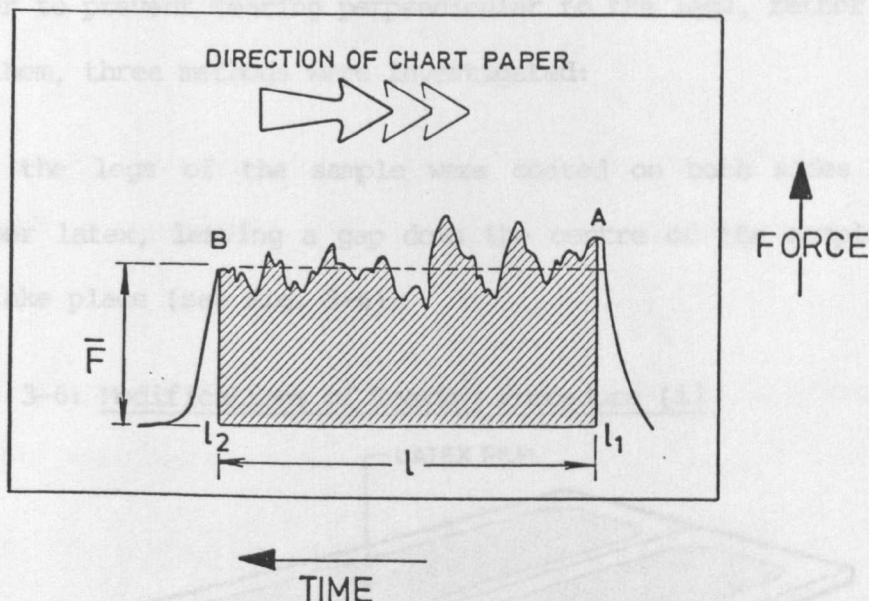
Experiments using similar test-pieces were carried out on the terpolymer containing 15 mol % MMA in the following way. The ends of the test-piece were clamped in the jaws of an Instron machine, and the sample was elongated at a constant rate of jaw separation of  $5\text{ mm min}^{-1}$  until tearing occurred. The initial jaw separation having been noted, the force on the sample was recorded at various jaw separations. The results were analysed using the method of Rivlin and Thomas ( 173).

#### 3.2.7.2 The "Trouser" Test Method

Most of the measurements of tearing energy were made using the "trouser" test-piece. The grips used to hold the test-pieces were identical to those used in the measurement of tensile strength. The Instron was used to extend the test-pieces. The legs of the test-piece were pulled in a direction parallel to the direction of tearing. The force required to propagate the tear was recorded on a chart. The method assumes that the extension of the legs of the test-piece is negligible.

The results were analysed in the following way. Because of the nature of the tearing process, the plot which is obtained shows a force which varies with time, although the underlying trend is that the force is constant. Fig. 3-5 shows an illustration of a typical chart record for tearing.

Fig. 3-5: Form of Tearing Energy Results



The area of the shaded portion of Fig. 3-5 was measured for each plot, using a planimeter. The mean force,  $\bar{F}$ , was then found by dividing this area by the length  $l$ , the latter being proportional to the time  $t$  taken for the chart pen to travel from A to B.  $\bar{F}$  is the height of a rectangle of length  $l_2 - l_1$ , which has the same area as that under the actual trace. Thus  $\bar{F}$  can be expressed as

$$\bar{F} = \frac{1}{l_2 - l_1} \int_{l_1}^{l_2} F dl \quad \dots(3-7)$$



The tearing energy,  $T$ , was then calculated as

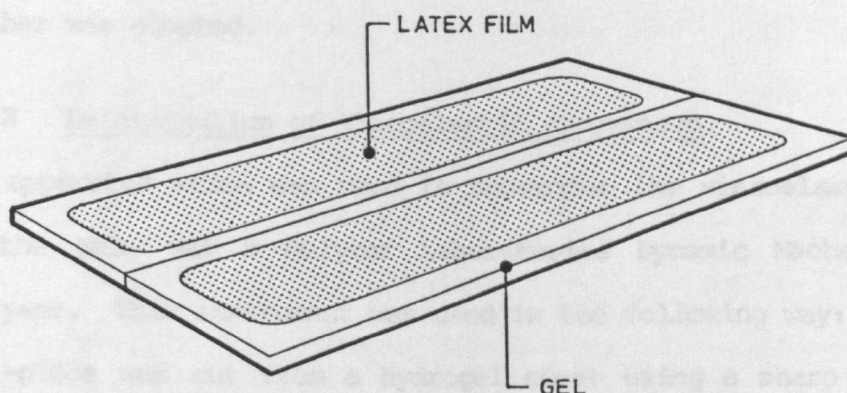
$$T = \frac{2\bar{F}}{t} \quad \dots(3-8)$$

where  $t$  is the sample thickness, measured as described in Section 3.2.5.1.

Several modifications to the tearing procedure were attempted. In order to prevent tearing perpendicular to the legs, rather than parallel to them, three methods were investigated:

(i) the legs of the sample were coated on both sides with natural rubber latex, leaving a gap down the centre of the sample for tearing to take place (see Fig. 3-6);

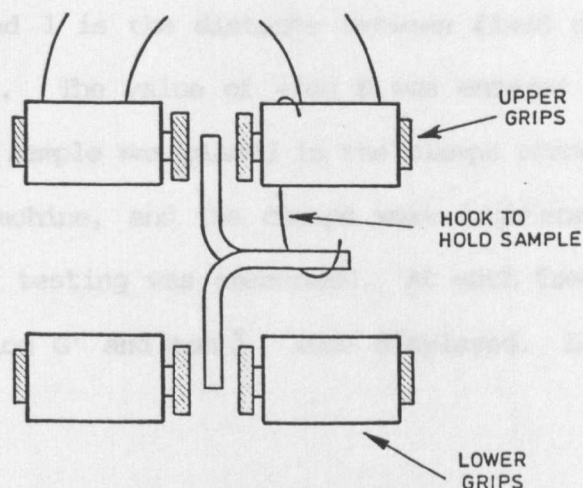
Fig. 3-6: Modifications of Tearing Procedure (i)



(ii) as (i), except PVC adhesive tape was used instead of rubber latex;

(iii) the sample was held up with a metal hook attached to the upper grips, to attempt to minimise the bending of the test-piece (see Fig. 3-7).

Fig. 3-7: Modifications of Tearing Procedure (iii)



To prevent breakage of the sample at the face of the grips, pieces of soft polysulphide rubber were placed between the grips and the sample.

Neither of the modifications described above proved effective. Hence neither was adopted.

### 3.2.8 Determination of Viscoelastic Properties

The apparatus which was used to determine the viscoelastic properties of the gels was a Polymer Laboratories Dynamic Mechanical Thermal Analyser. This instrument was used in the following way: A rectangular test-piece was cut from a hydrogel sheet using a sharp scalpel. Its dimensions were 30 x 10mm. The thickness was measured in three places using a Mercer micrometer gauge. The arithmetic mean of the three values was taken as the sample thickness. The tests were carried out in the dual cantilever bending mode, i.e., the samples were clamped at each end and vibrated in the centre. The geometry constant,  $K$ , for each sample was calculated as

$$K = 2w \left\{ \frac{t}{l} \right\}^3 \quad \text{.....(3-9)}$$

where  $w$  is the width of the sample (0.010m),  $t$  is the thickness of the sample, and  $l$  is the distance between fixed clamp and the centre clamp (0.008m). The value of  $-\log K$  was entered into the mechanical analyser. The sample was placed in the clamps connected to the vibrator head of the machine, and the clamps were tightened. After replacing the cover, the testing was commenced. At each frequency of vibration,  $w$ , values of  $\log G'$  and  $\tan \delta$  were displayed.  $\log G''$  was calculated as

$$\log G'' = \log G' + \log(\tan \delta) \quad \dots(3-10)$$

The experiments were carried out at room temperature. For each sample,  $\log G'$ ,  $\log G''$  and  $\tan \delta$  were plotted against  $\log w$ .

### 3.2.9 Differential Scanning Calorimetry (DSC) Experiments

The DSC apparatus used was a Perkin-Elmer DSC-2, equipped with a liquid nitrogen cooling system in order to enable sub-zero temperatures to be attained. The samples were discs of gel approximately 4mm in diameter. They were cut from hydrogel sheets using a circular die. They were sealed in aluminium pans by placing the sample in the pan with the aluminium lid, and crimping the assembly in a press. The pan was weighed before and after sealing the sample inside it; hence the sample weight was known. The sample holder of the instrument was contained in an air-tight glove-box purged with nitrogen. The sample was transferred into it by means of a suction-tube. The range of heating was set at 250-300 K, the heating rate being in most cases  $5 \text{ K min}^{-1}$ . A chart-recorder output was obtained from the instrument. Table 3-6 shows the conditions for the experiments which were carried out. It was hoped that the nature of the water in the hydrogels might be investigated by means of the DSC experiments.

Table 3-6: DSC Experiments

Sample	Heating rate/Kmin <sup>-1</sup>
(i) TER 27	45
(ii) TER 27	5
distilled water	5
(iii) TER 27	5

### 3.3 INTERPENETRATING NETWORKS OF POLY(HEMA-MAA) WITH HYDROPHOBIC MONOMERS

#### 3.3.1 Initial Experiments on IPNs

These experiments were intended as an introductory feasibility study of IPNs of poly (HEMA-MAA) with hydrophobic polymers. The development of a preparatory procedure was achieved, which was used for subsequent experiments.

(a) A gel was prepared as described in Section 3.2.1. The composition of the polymerisation mixture was HEMA(1) (50g), DBPO (0.50g), DMPT solution (6.25% w/w in 50% w/w IMS/ethylene glycol) (1.03g), EGDMA (0.19g) and IMS (50g). The gel was removed from the mould and was cut into eight equal-sized strips using a sharp scalpel. Their dimensions were approximately 120 x 30mm. A solution of AZDN(1) (0.01g) in styrene(1) (5g) and IMS (400g) was prepared. Four of the gel strips were immersed in this solution, and four in IMS alone. After swelling for 24 hours, one strip swollen in IMS and one strip swollen in IMS/styrene(1)/AZDN(1) were placed on glass plates in an oven at 55°C. One of each type of swollen strip was immersed in a water-bath at 55°C. After swelling for 48 hours, two more strips, one of each type, were placed in the water-bath.

(b) A gel was prepared as described in (a), but using 0.3g EGDMA instead of 0.19g. This corresponds to 0.4% of the total number of moles of monomer, as opposed to 0.25% in (a). The gel was again cut into eight strips as in (a). Four were immersed in IMS, and four in a solution of AZDN(1) (0.01g) in styrene(1) (10g) and 50% w/w IMS/ethylene glycol (400ml). After swelling for 24 hours, two strips of each type were placed between two 6mm-thick glass plates held together by clips, and exposed for 4 hours to ultraviolet (UV) light of wavelength approximately 350nm from a Philips 250W lamp. Two strips of

each type were wrapped in "Saran" clear plastic film, and placed in an oven at 55°C for 3 hours. All the strips were then placed in distilled water.

(c) A gel was prepared by the usual method (Section 3.2.1). The composition was the same as that of (a) above, except that 0.01g of AZDN(1) was added to the polymerisation mixture. The swelling procedure was followed as in (a). Four strips of gel were immersed in IMS, and four in a mixture of IMS (400ml) and styrene(1) (10g). After swelling for one day, they were exposed to UV light for 6 hours between glass plates.

(d) Two small (5 - 6 ml) glass bottles with push-on caps were filled with styrene(1) (5g) and AZDN(1) (0.01g). The first was exposed to UV light for 2 hours. The second was placed in an oven at 55°C for 2 hours.

(e)(i) A gel was prepared as in (b) above. It was cut into 8 strips. Four were immersed in IMS, and four in styrene(2) (5g), IMS (200g) and a UV polymerisation photosensitiser, Quantacure 659 (10 drops). After swelling for 24 hours, the strips were placed between glass plates and exposed to UV light for 3 hours.

(e)(ii) Two bottles were used, as in (d) above. The first was filled with styrene(2) (5g) and Quantacure 659 (10 drops), and the second with styrene(2) (5g) and AZDN (0.05g). They were exposed to UV light for 3 hours.

(f) A gel was prepared as in Section 3.2.1 and experiment (b) above. Four strips were immersed in IMS (400g), styrene(2) (5g) and AZDN(1) (0.05g); four were immersed in MMA(1) (100g) and AZDN (0.1g). After swelling for 24 hours, two of each type of swollen sheet were placed between glass plates sealed with a silicone rubber tubing gasket

(O.D. 3mm, I.D. 1.5mm); two of each type were similarly treated, except that the tubing was thicker (O.D. 3mm, I.D. 1mm). The gels were exposed to UV light for approximately 4 hours.

(g) A gel was prepared as in (b) above. Four strips were immersed in IMS only, and four in MMA(1) (5g), IMS (400g) and Quantacure 659 (10 drops). After swelling for a day, the strips were placed between glass plates, using a gasket of the thicker silicone rubber tubing (see (f)), and exposed to UV light for 4 hours, together with some of the swelling liquid (in a small stoppered glass bottle). The strips were then placed in IMS, to remove unreacted monomer.

(h) A gel prepared as in (b) was swollen as in previous experiments. Two swelling mixtures were used:

(i) IMS alone

(ii) MMA(1) (50ml) and IMS (20ml)

After swelling for 24 hours, the strips were placed between glass plates and exposed to UV light for 6 hours. After this treatment, one strip was immersed in IMS and one in water. They were swollen for 24 hours and weighed. After drying to constant weight in an oven at 60°C, the water and IMS contents of the respective swollen gels were calculated.

(i) A gel was prepared as in the previous experiments. The strips were treated in the following ways:

(i) strip A was immersed in MMA(1) containing 1.0% (w/w) AZDN; after swelling for 24 hours, it was exposed between glass plates to UV light for 4 hours, and transferred to IMS for a day. It was then swollen in distilled water;

(ii) strip B was treated as strip A, but swollen in the monomer mixture for 48 hours;

- (iii) strip C was treated as strip A, but styrene(2) was used instead of MMA(1);
- (iv) strip D was treated as strip C, but the swelling mixture included 0.5% (w/w) divinylbenzene.

### 3.3.2 Further Experiments on IPNs

#### 3.3.2.1 The Development of the Preparative Procedure

As a consequence of the experiments described in Section 3.3.1, a preparative procedure was developed which was used for a further series of experiments on the preparation of IPNs. The procedure was as follows:

- (i) a crosslinked poly(HEMA) gel was made, as described in Section 3.2.1;
- (ii) the gel was cut into strips, and immersed in IMS for 24 hours to extract excess monomer and initiators;
- (iii) the strips were dried to constant weight;
- (iv) they were immersed in swelling mixtures of various compositions, as summarised in Table 3-7;
- (v) they were sandwiched between glass plates, sealed with a silicone rubber tubing gasket, and exposed to UV light;
- (vi) they were immersed in IMS again for 24 hours;
- (vii) they were dried to constant weight in a vacuum oven at 70°C.

Experiments 1 - 10 were carried out in order that the effects on the resulting IPNs of varying the concentrations of monomer and initiator in the swelling mixture could be observed. Thus various monomer and initiator concentrations were used. Butan-2-ol is less volatile than IMS. It was used in the swelling mixture for IPN 7 to reduce evaporation from the swollen gel. This evaporation was thought to be the cause of non-uniformity in IPNs prepared using swelling mixtures containing IMS.



Table 3-7: Swelling Mixtures for IPNs 1 - 10

Sample	MMA(1)/g	IMS/g	AZDN/g	butan-2-ol/g
IPN1	50	20	0.5	0
IPN2	50	50	0.5	0
IPN3	50	200	0.5	0
IPN4	50	150	0.5	0
IPN5	50	40	0.5	0
IPN6	50	150	0.5	0
IPN7	50	0	0.25	50
IPN8	70	30	0.7	0
IPN9	70	30	0.14	0
IPN10	70	20	0.14	0

### 3.3.2.2 Calculation of Content of Polymer II in IPN

The content of polymer II,  $P_{II}$ , was expressed as a weight percentage of the total dry polymer, and was calculated using the equation

$$P_{II} = \frac{W_2 - W_1}{W_2} \quad \dots(3-11)$$

where  $W_1$  is the weight of the initial dry polymer before immersion in solution of monomer II, and  $W_2$  is the weight of dry polymer after monomer II has been polymerised.

### 3.3.3 Initial Experiments on Semi-IPNs

It was thought that it might be possible to prepare semi (II)-IPNs by an alternative, simpler, route to that described in Section 3.3.2.1. This involved copolymerising HEMA and MAA in the presence of a polymer. Hence, some attempts were made to dissolve polymers in suitable solvents (Table 3-8) and add the solutions to a polymerisation mixture which consisted of HEMA (50g), DBPO (0.5 mol %), EGDMA (0.4 mol %) and DMPT (one-eighth the weight of DBPO; added as a 1:15 solution in IMS). In each case, the DBPO was dissolved in HEMA and EGDMA, and this solution added to the solution of polymer. After stirring, the DMPT solution was added and stirring continued. The polymerisation mixture was then cast in a mould in the usual way (Section 3.2.1). Polystyrene was in granular form; the poly(vinyl alcohol) was powdered; all solvents were general-purpose reagents.

### 3.3.4 Further Work on IPNs: IPNs of poly (HEMA-MAA)/PMMA with Mole Ratio MAA:HEMA = 5:95

Since a mole ratio of 5:95 for MAA: HEMA was selected for the production of crosslinked HEMA-MAA-MMA terpolymers, this same ratio was used for the HEMA-MAA component of poly(HEMA-MAA)/PMMA IPNs. It was found that poly(HEMA) gels swell in butan-2-ol/MMA mixtures, but this is

not so for poly(HEMA-MAA) gels of this mole ratio. Hence a different swelling solvent was sought. DMF was chosen. In addition to DMF, ethyl acetate was incorporated into the swelling mixture. The objective was to keep the swelling of the gel approximately constant, whilst at the same time varying the amount of MMA taken up into the gel. Ethyl acetate is a non-polymerisable analogue of MMA, which would not be expected to affect the swelling appreciably if the ratio DMF/(MMA + ethyl acetate) is kept constant whilst the ratio MMA/(MMA + ethyl acetate) is varied. (Methyl 2-methylpropanoate would be an even better analogue, but is not readily available at reasonable cost.) More detailed experiments using this combination of solvents were subsequently carried out.

In this series of experiments, gels comprising 40g of a 95:5:0.4 mole HEMA(1)/MAA/EGDMA terpolymer, 40g IMS, 0.5 mol % DBPO, and DMPT (one-eighth the weight of DBPO) were made as described in Section 3.2.1. After immersing in IMS for a few hours, the gels were dried to constant weight in an oven at 70°C, under a partial vacuum of approximately 1mm Hg. They were then placed in the various swelling mixtures (Table 3-9) for 1 - 2 days. After this, they were sandwiched between glass plates sealed with silicone rubber tubing, and exposed to UV light. The gels were then re-immersed in IMS for a few hours, dried again to constant weight, and placed in 0.1M sodium bicarbonate buffer solution (pH 8.4) and allowed to swell to equilibrium.

Table 3-8: Compositions of Mixtures Used for Preparation of Semi-IPNs

Sample	HEMA(l)/g	(a) PS/g	(b) PVAL/g	toluene/g	ethyl acetate/g	acetone/g	cyclo- hexane/g	(c) (IMS/EG)/g	water/g	THF/g
IPN11	50	1.0		50						
IPN12	50	2.0			50					
IPN13	50	0.5		50		50				
IPN14	50	0.5		12		12				
IPN15	50	0.5				12				
IPN16	50	0.5				10	10			
IPN17	50	0.5				25	25			
IPN18	50		0.5					50		
IPN19	50		0.5						5	
IPN20	20	0.1								20
IPN21	30	0.2								20

Notes: (a) polystyrene  
 (b) poly(vinyl alcohol)  
 (c) 50:50 w/w mixture

Table 3-9: Swelling Mixtures for IPNs 22-31

Sample	MMA(2)/g	DMF/g	AZDN(1)/g	butan-2-ol/g	ethyl acetate/g
IPN22	5.0		0.05	95.0	
IPN23	1.0		0.01	99.0	
IPN24	20.0		0.20	80.0	
IPN26	60.0	20.0	0		40.0
IPN27	100.0	100.0	0.50		100.0
IPN28	100.0	40.0	0.50		100.0
IPN29	100.0	20.0	0.50		0
IPN30	100.0	20.0	1.00		0
IPN31	50.0	20.0	1.00		50.0

### 3.3.5 Further Variants of the Procedure for Preparing IPNs

#### 3.3.5.1 Surrounding Samples with Oil

Several of the IPN samples prepared as described above were visually non-uniform. It appeared that bubbles formed between the gel surface and the glass plate whilst exposed to UV light. To overcome this problem, the gels were surrounded by a non-volatile oil (oleyl alcohol). A few drops of oil were placed on one glass plate, and the gel was gently placed on top, to ensure a bubble-free oil film between the glass and the gel. A few more drops of oil were put onto the top surface of the gel. The silicone rubber tubing was then placed around the gel, leaving a ca. 1cm gap between the gel and tubing. The "Melinex" sheet was placed on top, followed by the other glass plate. The whole assembly was then clipped together, squeezing the gasket to provide a good seal with the mould in a vertical position, the gap around the edges of the gel filled with oleyl alcohol through the opening in the gasket at the top of the mould using a dropping pipette. Oleyl alcohol was added until the level was approximately 0.5cm above the top of the gel.

#### 3.3.5.2 Cooling of Samples whilst Exposed to UV Light (i)

To provide cooling whilst the samples were exposed to UV light, cold tap water was passed over the mould, which stood in a glass chromatography tank. The experimental arrangement is shown in Fig. 3-8.

#### 3.3.5.3 Cooling of Samples whilst Exposed to UV Light (ii)

In order to attain better control of the temperature of polymerisation, the moulds containing the IPNs were immersed in a glass-fronted water bath. The front glass plate of the mould was placed in the water, about 1cm away from the glass side of the water bath, and the lamp arranged so that the UV light was directed through the glass. The temperature was controlled by a Circotherm thermostat-stirrer-pump.

(a)

Table 3-10: Swelling Properties for IPN 32 - 46

Sample	Wt% (21/g)	D <sub>50</sub> /g	MOULD	Wt% (21/g)	Wt% (21/g)
IPN32	40				0.40
IPN33	40				0.40
IPN34	40				1.00
IPN35	40				1.00
IPN36	40				1.40
IPN37	40				1.40
IPN38	40				1.40
IPN39	40				1.40
IPN40	40				1.40
IPN41	40				1.40
IPN42	40				1.40
IPN43	40				1.40
IPN44	40				1.40
IPN45	40				1.40
IPN46	40				1.40

(b)

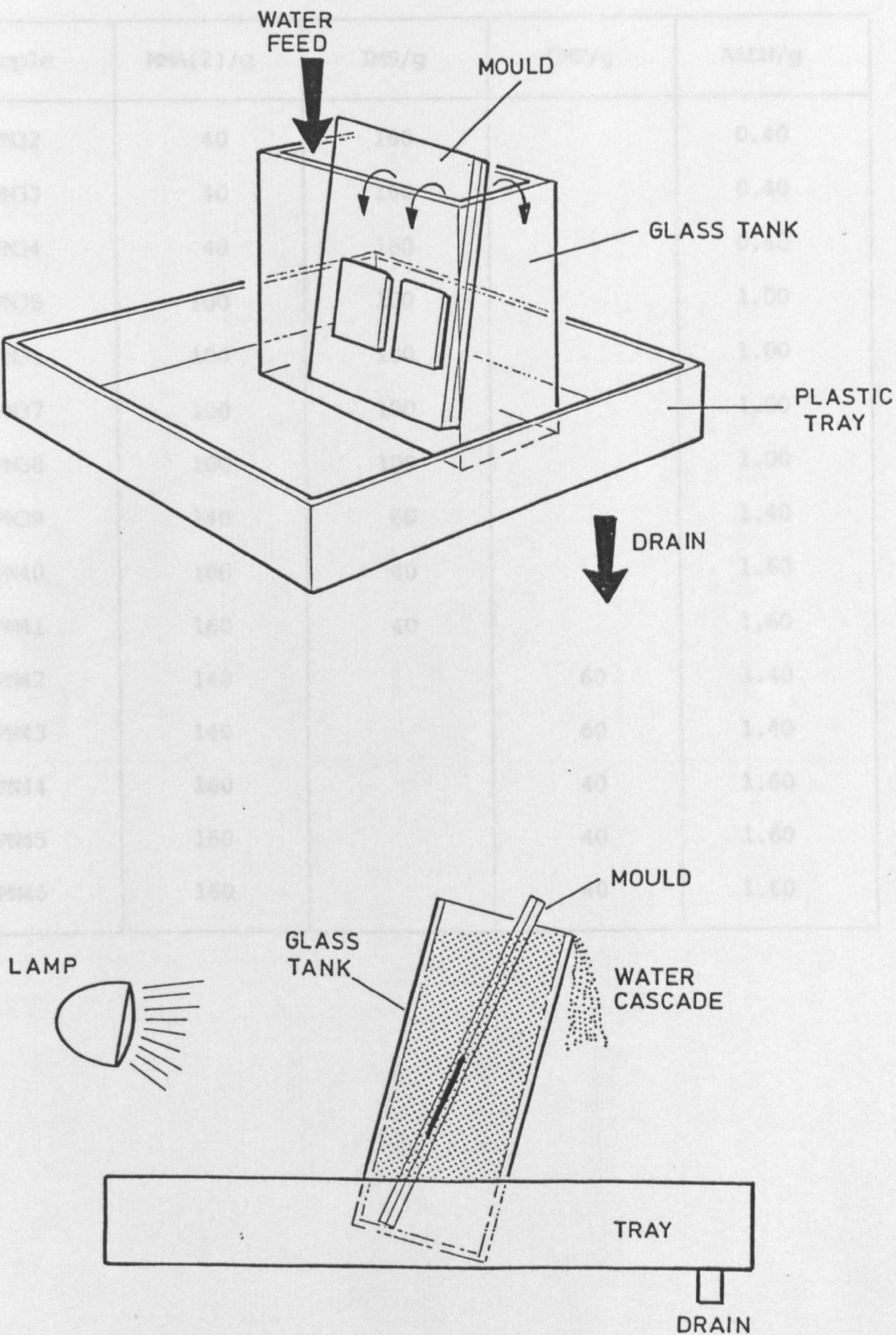


Fig. 3-8: Cooling Apparatus

Table 3-10: Swelling Mixtures for IPNs 32 - 46

Sample	MMA(2)/g	IMS/g	DMF/g	AZDN/g
IPN32	40	160		0.40
IPN33	40	160		0.40
IPN34	40	160		0.40
IPN35	100	100		1.00
IPN36	100	100		1.00
IPN37	100	100		1.00
IPN38	100	100		1.00
IPN39	140	60		1.40
IPN40	160	40		1.60
IPN41	160	40		1.60
IPN42	140		60	1.40
IPN43	140		60	1.40
IPN44	160		40	1.60
IPN45	160		40	1.60
IPN46	160		40	1.60



Table 3-11: Swelling Mixtures for IPNs 47 - 58

Sample	MMA(2)/g	DMF/g	AZDN/g
IPN47	154	46	1.54
IPN48	154	46	1.54
IPN49	154	46	1.54
IPN50	144	56	1.44
IPN51	144	56	1.44
IPN52	154	46	0.77
IPN53	160	40	0.80
IPN54	160	40	0.80
IPN55	160	40	0.80
IPN56	160	40	0.80
IPN57	160	40	0.80
IPN58	160	40	0.80

To determine the constancy of the temperature, the lamp was switched on, and the water temperature recorded after 1.5, 3 and 4 hours. The temperature increased by 1°C during 4 hours. The apparatus was used in a blacked-out area of the laboratory. This method was used for IPNs 59 onwards.

#### 3.3.5.4 IPNs

Several IPNs were made using the procedures described in Sections 3.3.4 and 3.3.5.1. IPNs 32 - 45 were not cooled during polymerisation. IPNs 46 - 58 were prepared using the cooling method described in Section 3.3.5.2. Table 3-10 shows the compositions of the swelling mixtures for these samples. The time of exposure to UV light was 6 hours.

IPNs 47 - 58 (Table 3-11) were made using the cooling method described in Section 3.3.5.2. However, in order to prevent stress-cracking of the gels when immersed in the swelling mixture, they were first swollen in mixtures deficient in DMF. The remainder of the DMF was added gradually over a period of about three days. The temperature of the water used for cooling was measured.

#### 3.3.5.5 Pre-Swelling of Gels in DMF Vapour

To prevent stress-cracking of the xerogels when they were immersed in the swelling mixture, IPNs 59 onwards were pre-swollen in DMF vapour. After the gels were dried to constant weight, they were placed in a desiccator containing about 100ml of DMF. The desiccator was left in an oven at 100°C overnight. The gels were then weighed to give the weight of DMF absorbed. They were then immersed in the swelling mixture from which DMF had been omitted. DMF was then added to give the total required amount.

### 3.3.6 Extent of Photopolymerisation vs. Time of Reaction

In order to determine the time for which the gels were required to be exposed to UV light, to achieve high conversion of monomer II to polymer II, the extent of photopolymerisation as a function of time was measured.

#### 3.3.6.1 First Experiment

Five gel strips were prepared according to the method described in Section 3.2.1. The molar composition of the polymer was 95/5/0.4 HEMA/MAA/EGDMA. The DBPO Level was 0.5mol %. The weight of DMPT was one-eighth that of DBPO. The weight of IMS used was equal to the total weight of monomers. The gels were dried and pre-swollen in DMF vapour. They were then swollen in the swelling mixture. The total weight of DMF, i.e. DMF contained in the swollen gels + DMF in the swelling mixture, was 50g. The weight of MMA(2) in the swelling mixture was 150g, and the weight of AZDN 1.50g. After swelling for 3 days, the gels were sandwiched between glass plates sealed with silicone rubber tubing. They were exposed to UV light using the cooling method described in Section 3.3.5.3. The distance of the lamp from the sample was 38cm. Four of the samples were masked from the UV light with aluminium foil after 1.5, 2.75, 4.0 and 5.25 hours respectively. The lamp was switched off after 6 hours. The gels were removed from the mould and swollen in IMS to remove unreacted monomer. After drying to constant weight in a vacuum oven at 60 - 70°C, the proportion of polymer II was calculated using the method of Section 3.3.2.2.

#### 3.3.6.2 Second Experiment

An experiment similar to that described in Section 3.3.6.1 was carried out, but with two differences:

(i) the total amount of DMF, i.e. DMF contained in the gels + DMF in the swelling mixture, was 40g. The weight of MMA(2) in the swelling mixture was 160g, and that of AZDN was 1.60g.

(ii) the distance of the lamp from the sample was reduced to 30cm.

### 3.3.7 Swelling of Crosslinked Poly(HEMA-MAA) Hydrogels in Various Mixtures

#### 3.3.7.1 Swelling in MMA-IMS and MMA-DMF Mixtures

Several small (5 - 6ml) glass bottles with push-on tops were filled with mixtures of MMA(2) and IMS (experiment A) and MMA(2) and DMF (experiment B). The compositions were determined by weighing the empty bottles, placing in them the required amount of MMA, reweighing, and repeating with IMS or DMF. Weighed samples of dry poly(HEMA(1)-MAA) xerogel(HEMA/MAA = 95/5 molar) were placed in the bottles and allowed to swell for 2 days. They were then reweighed. The equilibrium swelling  $s$  was calculated as

$$s = \frac{W_S - W_D}{W_S} \times 100 \quad \dots(3-12)$$

where  $W_S$  is the swollen weight of the gel, and  $W_D$  is the dry weight of the gel.

#### 3.3.7.2 Swelling in MMA-Ethyl Acetate-DMF Mixtures

The experiments were conducted as described in Section 3.3.7.1 above, except that HEMA(2) was used. The mixtures contained MMA(2), ethyl acetate and DMF. Table 3-12 summarises the compositions which were used. Swelling measurements were made after 2 or 5 days, except those for experiments F, which were after 3 and 56 days, and G, which were after 5 and 11 days.

### 3.3.8 More Systematic Study of IPNs

#### 3.3.8.1 First Series: Poly(HEMA-MAA)/PMMA IPNs

In these experiments, IPNs were made using the method described in Sections 3.3.2 and 3.3.5. They were pre-swollen in DMF vapour before immersing in the swelling mixture. All polymerisations of monomer II were carried out using the method of temperature control referred to in Section 3.3.5.4.

However, some mould growth was observed in some of the gels after drying in air at room temperature, prior to swelling in the swelling mixture. This problem was solved by extracting the gels before the drying stage in a 50:50 mixture of IMS and water to which a little cetyl trimethylammonium bromide had been added. The procedure was therefore:

- (i) make the 95:5 HEMA/MAA gel;
- (ii) extract in 50:50 IMS/Water containing CTAB;
- (iii) dry to constant weight;
- (iv) pre-swell in DMF vapour;
- (v) swell in swelling mixture;
- (vi) expose gel to UV light;
- (vii) extract in 50:50 (v/v) IMS/water;
- (viii) dry to constant weight;
- (ix) swell in 0.1M aqueous sodium bicarbonate solution.

Table 3-13 shows the composition of swelling mixtures used for these gels. In this table, method 1 refers to the normal method, whereas method 2 used the slightly different mould shown in Fig. 3-9. The polymerisation time was 6 hours.

Table 3-12: Compositions of Swelling Mixtures for MMA/Ethyl Acetate/  
DMF Swelling Experiments

Experiment	Weight ratio	Composition range	Swelling time
	MMA:EtOAc	%(MMA + EtOAc)	days
A	0:1	0-100	2
B	0:1	0-100	2
C	0:1	0-100	2
D	1:1	0-100	2
E	3:1	0-100	2
F	1:0	0-100	3, 56
G	1:3	50-100	5, 11
H	1:3	50-100	5
I	1:1	50-100	5
J	3:1	50-100	5
K	1:4	50-100	5
L	4:1	50-100	5

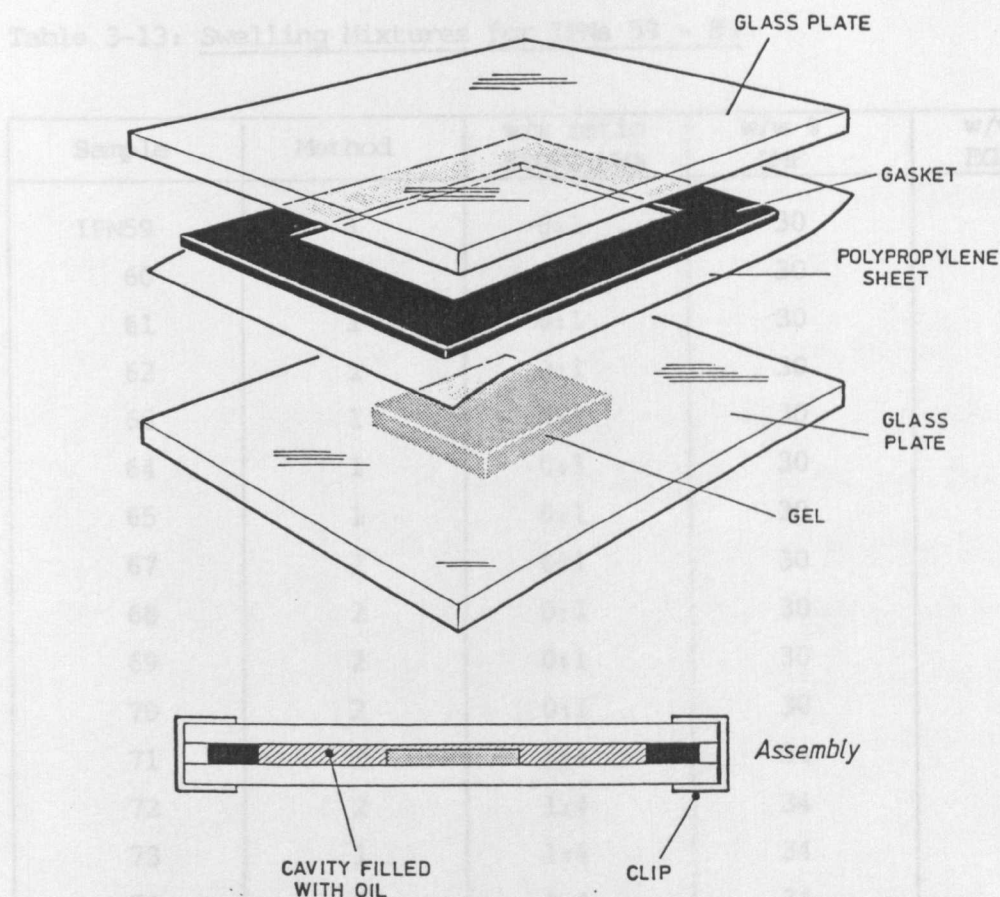


Fig. 3-9: Mould (Method 2)

### 3.3.8.2 Second Series: IPNs of Poly(HEMA-MAA) with Various Polymers and Copolymers

The procedure used for preparing this series of IPNs was similar to that described in Section 3.3.8.1, except for the following modifications:

- (i) after removing the 'Melinex' sheet from the mould, the gels were swollen off the glass plate in water containing a small amount of cetyltrimethylammonium bromide (CTAB). They were then dried, firstly in air at room temperature for 1 day, and then in a vacuum oven at 60°C under a partial vacuum of 1mm Hg, until the weight loss per hour was less than 0.1% of the total weight;
- (ii) when surrounding the samples with oil, the minimum quantity of oil was used. The silicone rubber tubing gasket was pushed with a spatula so that it came into contact with the gel; this procedure

Table 3-13: Swelling Mixtures for IPNs 59 - 89

Sample	Method	w/w ratio EtOAc:MMA	w/w % DMF	w/w % EGDMA
IPN59	1	0:1	30	0
60	1	0:1	30	0
61	1	0:1	30	0
62	1	0:1	30	0
63	1	0:1	30	0
64	1	0:1	30	0
65	1	0:1	30	0
67	2	0:1	30	0.5
68	2	0:1	30	0.5
69	2	0:1	30	0.5
70	2	0:1	30	0.5
71	2	1:4	34	0
72	2	1:4	34	0
73	1	1:4	34	0
74	2	1:4	34	0
75	1	1:4	34	2.0
76	1	1:4	34	2.0
77	1	1:4	34	2.0
78	1	1:4	34	5.0
79	1	1:4	34	5.0
80	1	1:4	34	5.0
82	1	3:1	30	0
83	1	3:1	30	0
84	1	3:1	30	0
85	1	3:1	30	0
86	1	3:1	30	0
87	1	3:1	30	5.0
88	1	3:1	30	5.0
89	1	3:1	30	5.0
90	1	3:1	30	5.0
91	1	3:1	30	5.0
92	1	3:1	30	5.0
93	1	3:1	30	5.0
94	1	3:1	30	5.0
95	1	3:1	30	5.0
96	1	3:1	30	5.0
97	1	3:1	30	5.0
98	1	3:1	30	5.0



was used for IPNs 105 onwards;

(iii) the oil which was used to surround the samples was liquid paraffin, rather than oleyl alcohol.

In attempts to control the quantity of polymer II formed in the gel, in previous experiments (Section 3.3.8.1), a saturated non-polymerisable analogue of MMA (ethyl acetate) was included in the swelling mixture. In this series of experiments, IMS was used as an analogue of HEMA/MAA, and ethylbenzene as an analogue of styrene. AZDN was again used as the photo-initiator; the level was 0.5mol % (based on total monomers), except for IPNs 99 - 104, where it was 0.1mol %. The time of exposure to UV light was either 6 or 10 hours.

Where polymer II was a copolymer, and a saturated analogue was used, the analogue consisted of a mixture of the analogues for both monomers. For example, if polymer II was a 70/30 molar MMA/(HEMA + MAA) copolymer, then the saturated analogue added to the swelling mixture was 70/30 molar ethyl acetate /IMS. The IMS was assumed to consist of 95% (w/w) ethanol and 5%(w/w) water. As usual, the weight of DMF in the swelling mixture included that pre-swollen into the gels. EGDMA was included in some of the swelling mixtures, to act as a crosslinker for polymer II. Table 3-14 shows the compositions of the swelling mixtures for these IPNs. The tank which was used to swell these sheets is shown in Fig. 3-10.

Where possible, physical testing of the IPNs was carried out. Their compositions and equilibrium water contents were determined.

Table 3-14: Swelling Mixtures for IPNs 99 - 165

Samples	Monomer II (mol %)	w/w % SAM	w/w % DMF	* mol % * EGDMA
IPN 99-104	MMA	0	30	0
105-107	S	0	30	0
108-109	S	0	40	0
110-112	50 MMA/50 MAA	0	30	0
113-114	70 MMA/30 MAA	0	30	0
115-120	95 HEMA/5 MAA	0	10	0
121-123	50 MMA/50 HEMA-*MAA	0	10	0
124-127	50 MMA/50 HEMA-*MAA	0	17	0
128-131	95 HEMA/5 MAA	0	10	0.4
132-135	70 MMA/30 HEMA-*MAA	0	20	0
136-139	5S/95 HEMA-*MAA	0	10	0
140-143	50 MMA/50 HEMA-*MAA	50	17	0
144-147	50 MMA/50 HEMA-*MAA	80	17	0
148-151	95 HEMA/5 MAA	50	10	0
152-155	95 HEMA/5 MAA	20	10	0
156-159	70 MMA/30 HEMA-*MAA	20	25	0
160-162	70 MMA/30 HEMA-*MAA	50	25	0

\* 95 mol % HEMA : 5 mol % MAA

\* denotes the level of EGDMA in polymer II

\*

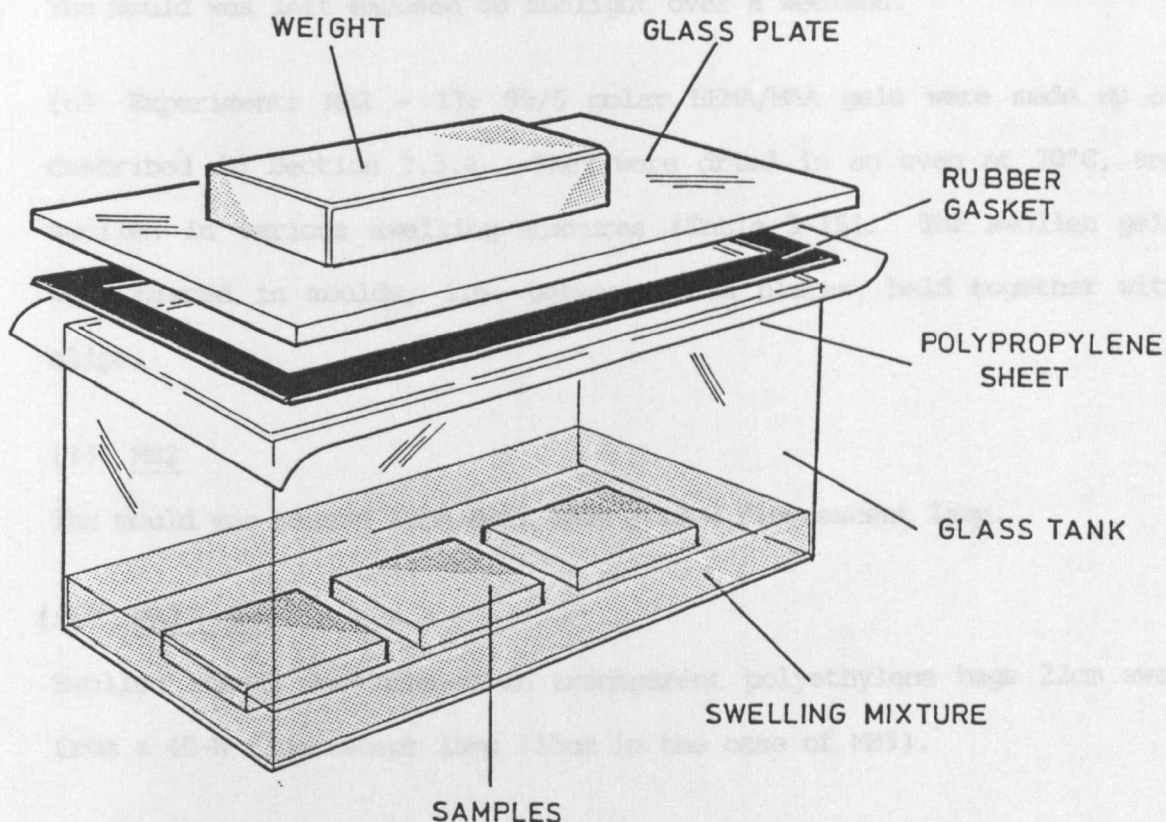


Fig. 3-10: Tank Used for Swelling IPNs 99 - 165

### 3.3.9 Methylene Blue as a Photosensitiser

Some experiments were carried out to investigate the feasibility of using methylene blue as a photosensitiser for the polymerisation of PMMA as polymer II, in conjunction with dibenzoyl peroxide.

(a) Experiment MBI: the following mixture was poured into a mould (described in Section 3.2.1):

MMA(2)	20g
IMS	20g
MB	0.02g
DBPO	0.2g

The mould was left exposed to sunlight over a weekend.

(b) Experiments MB2 - 13: 95/5 molar HEMA/MAA gels were made up as described in Section 3.3.4. They were dried in an oven at 70°C, and swollen in various swelling mixtures (Table 3-15). The swollen gels were placed in moulds, i.e. between glass plates, held together with clips.

(i) MB2

The mould was placed 22cm away from a 40-W fluorescent lamp.

(ii) MB3 - 5

Swollen sheets were placed in transparent polyethylene bags 22cm away from a 40-W fluorescent lamp (15cm in the case of MB5).

(iii) MB6 - 9

The swollen sheet was placed in a mould as described above, and surrounded by the swelling mixture. It was placed 22cm away from a 40-W fluorescent lamp.

(iv) MB10

This experiment was carried out as for MB9, but the swelling liquid surrounding the gel was masked off from the light with aluminium foil.

(v) MB11

The swollen gel was placed in the mould as in MB9 and MB10, left in sunlight for 1 hour, and then exposed to UV light using a Philips 250-W lamp.

(vi) MB12 - 13

MB12(a) and MB13 were masked as above; MB12(b) was not. Both swollen gels were exposed to UV light.

Table 3-15: Swelling Mixtures Used for Methylene Blue Experiments

Experiment	MMA(2)/g	IMS/g	DBPO/g	Methylene Blue/g
MB2	50	50	0.5	0.05
MB3	50	50	0.5	0.05
MB4	50	50	0.5	0.05
MB5	70	30	0.7	0.07
MB6	70	30	1.4	0.14
MB9	50	50	0.5	0.05
MB10	70	30	0.7	0.07
MB11	70	30	0.7	0.002
MB12a,b	70	30	0.7	0.007
MB13	70	30	0.7	0.007

### 3.3.10 Latex IPNs

The following experiments were carried out to investigate the possibility of preparing latex IPNs from polymer dispersions in hydrocarbons. Hence, attempts were made to prepare stable PMMA dispersions in hydrocarbons. An attempt was made (3.3.10.2) to prepare a poly(HEMA)/PMMA latex IPN.

#### 3.3.10.1 Dispersion Polymerisation of MMA in a Hydrocarbon Medium

##### (i) Preparation of Dispersant

A mixture of hexane (24g) and heptane (36g) was heated to reflux in a three-neck flask fitted with a condenser and thermometer. Dodecyl acrylate (32g), glycidyl methacrylate (1g), AZDN (0.4g) and ethyl acetate (5g) was fed in via a tap funnel, over several hours. The hexane was then removed by distillation, and replaced by an equal volume of heptane. Hydroquinone (0.02g), methacrylic acid (0.48g) and dimethyl-p-toluidine (DMPT, 0.16g) were added. The mixture was refluxed for 8 hours.

##### (ii) Dispersion Polymerisations

(a) A mixture of MMA (7.3g), AZDN (0.1g), the solution prepared in (i) above (6.5g), 70° - 90° petrol (39g) and 230° - 250° petrol (3.5g) was refluxed for 45 minutes in a conical flask fitted with a three-neck adaptor, and stirred using a magnetic stirrer. 0.32g of a 10% w/w solution of n-octyl mercaptan in 230° - 250° petrol was then added. A mixture of MMA (41.4g), MAA (0.8g), AZDN (0.1g) and n-octyl mercaptan was fed in over 3 hours, during reflux.

(b) This experiment was similar to (a), except that the MMA/MAA/AZDN mixture was added at the start of the experiment.

(c) Similar to (a), except that the 7.3g of MMA was replaced by 7.3g

of HEMA, and the dispersion medium was hexane (42g).

(d) Similar to (a), except that the quantity of dispersant solution was 13.0g. The dispersion medium was hexane (42g).

(e) Similar to (d) except that the quantity of dispersant solution was 3.0g.

#### 3.3.10.2 "Core-shell" Type Polymerisation

A portion of the dispersion formed in experiment (d) above (20g) was refluxed in a conical flask, whilst stirring with a magnetic stirrer. HEMA (3.0g) and AZDN (0.04g) were fed in over a period of 3 hours, via a tap-funnel.

#### 3.3.10.3 Measurement of Particle Size

Particle sizes were measured using a Coulter Nanosizer. A portion of the dispersion was diluted with hexane, and this sample was used in the instrument.

### 3.4 FILLED HYDROGELS

#### 3.4.1 Attempts to Make PMMA Dispersions in IMS

##### 3.4.1.1 DISP 1

The following mixture was stirred under reflux in a 1-litre reaction vessel equipped with a tap funnel and thermometer:

MMA(2)	10.0g
IMS	80.0g
AZDN(1)	0.20g
*PEGMM(10)	4.0g

\* PEGMM(10) is poly(ethylene glycol) monomethacrylate:

$\text{CH}_2 = \text{C}(\text{CH}_3) \text{CO} (\text{OCH}_2\text{CH}_2)_n \text{OH}$  where the average value of  $n$  is approximately 10 in this case.

After about 45 minutes, a mixture of MMA(1) (40g) and AZDM(1) (0.1g) was slowly added via the tap funnel. After 4 hours, the reaction mixture was cooled.

##### 3.4.1.2 Pre-formed Dispersants

(a) A mixture of IMS (50ml), MMA(1) (10.0g), PEGMM(10) (10.0g) and AZDN (0.50g) was refluxed for 3 hours. The resulting polymer was precipitated in water, filtered and dried in an oven at 70°C.

(b) As (a), but the composition of the mixture was:

IMS	200ml	PEGMM(10)	10g
MMA(2)	10g	AZDN	0.50g

(c) As (a), but the composition of the mixture was:



PEGMM(10)	10g
IMS	100ml
AZDN(1)	0.02g

The AZDN was introduced as a  $0.2\text{gdm}^{-3}$  solution in IMS. The polymer was left in solution after refluxing for 3 hours.

#### 3.4.1.3 DISP 2

10ml of the solution from (c) above (known as DSI) was refluxed with IMS (190ml). A solution of AZDN(1) (0.25g) in MMA(2) (30ml) was added dropwise via a tap funnel. After 3 hours, the reaction mixture was cooled. The particle size of the resulting precipitated polymer was measured by Coulter Nanosizer after dispersing a little in IMS.

#### 3.4.1.4 DISP 3

Dispersant solution DSI (10ml), IMS (190ml) and DMPT solution (1:15 w/ws in IMS, 0.5g) were stirred in a 1-litre reaction vessel at room temperature. A solution of DBPO (0.25g) in MMA(1) (20ml) was added dropwise, via a tap funnel. After 3 hours, the stirring was discontinued, and the reaction mixture cooled.

#### 3.4.1.5 DISP 4

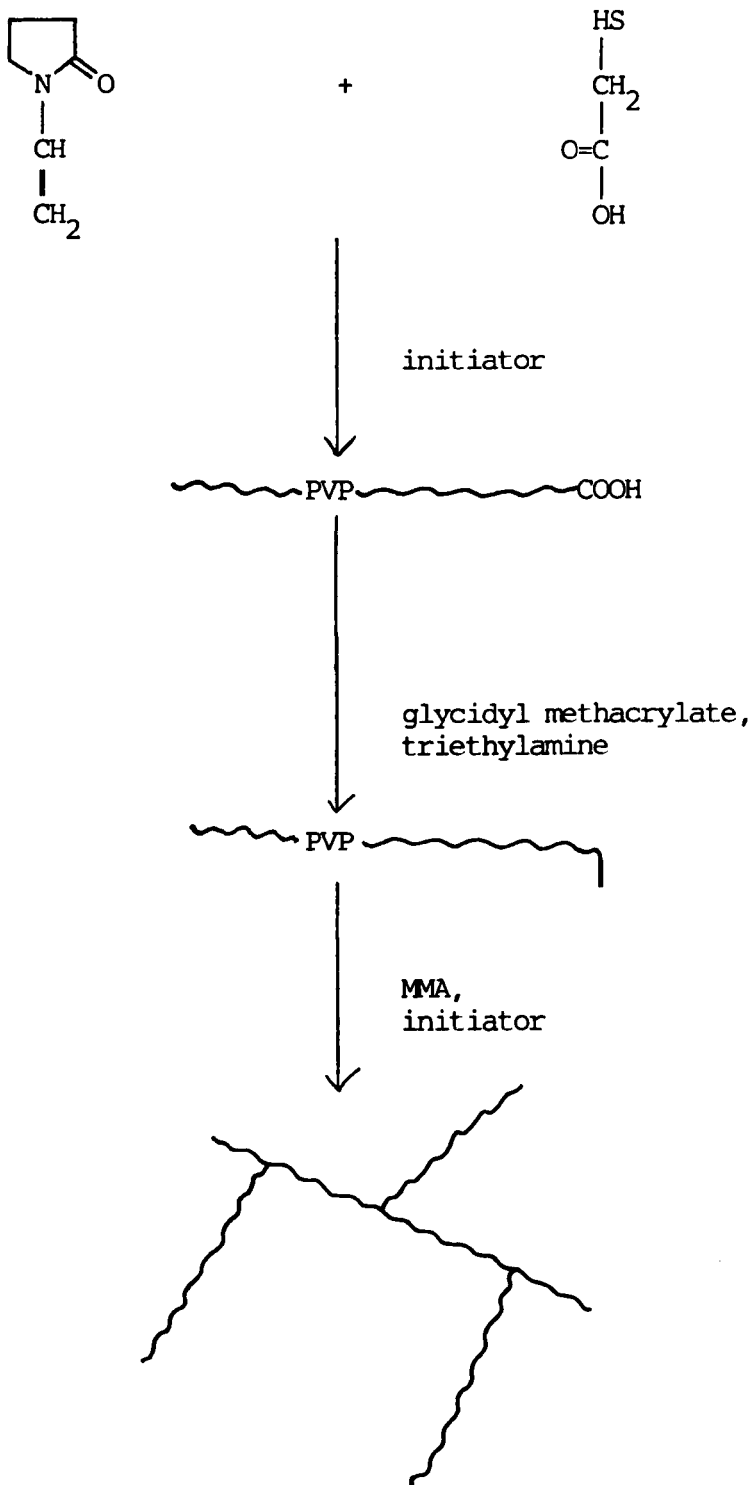
Similar to 3.4.1.4, except that the reaction vessel was purged with nitrogen, and nitrogen was passed through the solution during the reaction via a capillary bleed. The particle size of the dispersion was measured using the Coulter Nanosizer. The solids content was measured by weighing a small bottle of known weight, containing a few grammes of the dispersion, to which a few crystals of hydroquinone had been added. After drying in an oven at  $70^{\circ}\text{C}$  overnight, the sample was dried to constant weight under a vacuum of 1mm at  $70^{\circ}\text{C}$ . The procedure was repeated for several samples.

#### 3.4.1.6 DISP 5

Similar to 3.4.1.5, except that 57ml of IMS was used, and the feed solution was DBPO (0.12g) in MMA(1) (10g).

#### 3.4.1.7 Synthesis of a Comb-Type Graft Copolymer for Use as a Dispersant

The following reaction scheme was used for this experiment:



N-vinyl pyrrolidone (25ml) was refluxed in a round-bottomed flask on a heating mantle with IMS (25ml), 4,4'-azobis-(4-cyanovaleric acid) (0.25g) and thioglycolic acid (1.0g). After 4 hours, a further portion of azo-acid was added. After a further 4 hours, the reaction was stopped by cooling. The IMS was evaporated off completely and the dry polymer was dissolved in DMF (150ml). Glycidyl methacrylate (5ml) and triethylamine (0.5ml) were added. The mixture was heated to 70°C for 3 hours. MMA(2) (12.5g) and DBPO (0.13g) were added, and the mixture was left at 70°C for a further 3 hours. The solvent was evaporated on a rotary evaporator.

### 3.4.2 Filled Hydrogels

#### 3.4.2.1 FIL 1 and FIL 2

Two hydrogels were made as described in Sections 3.2.1 and 3.3.4. However, in each case, some of the IMS was replaced by DISP 4 (Section 3.4.1.5). The compositions of the polymerisation mixtures were as shown in Table 3-16.

Table 3-16: Mixtures for Preparing Filled Hydrogels

Experiment	DISP 4/g	(HEMA/MAA)/g	EGDMA/g	* DMPT/g	DBPO/g
FIL 1	45	35	0.25	0.04	0.35
FIL 2	10	40	0.25	0.04	0.35

\* added as a 1:15 w/w solution in IMS

#### 3.4.2.2 FIL 3 - 7

Using the method described in Section 3.4.2.1 above, a series of gels were made. The dispersion used in these experiments was made by A.C. Haynes. Its average particle size, measured on the Coulter Nanosizer,

was 500nm. It sedimented quickly into two fractions. The overall solids content was 12.5% by weight. The solids content of the upper layer after sedimentation was 6.5%; this is the fraction which was used in the following experiments. Table 3-17 shows the compositions of the polymerisation mixtures.

Table 3-17: Mixtures for Preparing Filled Hydrogels

Experiment	(HEMA/MAA)/g	Dispersion/g	IMS/g	* DMPT/g	DBPO/g	EGDMA/g
FIL3	34.80	45.20	0	0.05	0.39	0.26
FIL4	36.80	27.83	15.17	0.05	0.39	0.26
FIL5	38.42	13.74	27.84	0.05	0.38	0.25
FIL6	39.69	2.70	37.61	0.05	0.38	0.25
FIL7	36.12	33.57	6.43	0.05	0.38	0.25

\* added as a 1:15 w/w solution in IMS

#### 3.4.2.3 Incorporation of Dried Aqueous Latex into Hydrogels

##### (i) Preparation of Dried Latices

###### (a) Latex L1

An emulsion polymerisation was carried out by dissolving sodium dodecyl sulphate (5g) and potassium persulphate (0.5g) in water, and stirring with MMA(2) (100g) and EGDMA (0.5g) under nitrogen in a 1-litre reaction vessel for 6 hours at 70°C. The average particle size was measured on the Coulter Nanosizer, and found to be 70nm.

###### (b) Latex KAP1

A PMMA latex was prepared by K.A. Popoola, having the average particle size (by Coulter Nanosizer) of 70nm.

The latices were dried by stirring latex (100ml) in a 250ml beaker

on a hot-plate set on a low heat, placed in a fume-cupboard. When most of the liquid had evaporated, the material was placed in a vacuum oven and dried at 40°C and 1mm Hg to constant weight. The dried latices were then ground with a pestle and mortar.

A few grammes of dried latex KAP1 were mixed with IMS, and ground with a pestle and mortar. The particle size was measured using the Coulter Nanosizer. An attempt was made to redisperse the latices by mixing a few grammes with IMS in a conical flask, and placing the flask in an ultrasonic bath. The particle size was measured after 15 minutes and 2 hours, and found to be > 3000nm in both cases.

(ii) Filled Hydrogels

(a) A standard 95:5 HEMA/MAA hydrogel (Section 3.3.4) of total weight 10g was prepared. After a noticeable increase in viscosity had been observed, dried latex KAP1 (3g) was added. The resulting paste was crushed, using a pestle and mortar, and left in a small (5 - 6ml) capped glass bottle.

(b) A 95:5 HEMA/MAA hydrogel was made up, incorporating dried latex KAP1 (4g). The total weight of the mixture was 34g. The dried latex was mixed with the EGDMA, DBPO and HEMA, ground to a paste with a pestle and mortar, mixed with the other components and poured into a mould. It was left in an oven at 60°C.

(c) A hydrogel was made as in the previous section (b), but 1g of dried latex powder was used. The total weight of mixture was 31g. The reaction was carried out at room temperature.

## C H A P T E R   4

TERPOLYMERS OF HEMA WITH MAA AND HYDROPHOBIC MONOMERS -

RESULTS AND DISCUSSION

#### 4.1 GLC ANALYSIS OF HEMA(1)

Fig. 4-1 shows the gas chromatograph obtained for the diethyl adipate, used as the internal standard in the HEMA analysis. There are two maxima: a small maximum occurring at 14 mins. which is thought to be the monoester; and a large maximum occurring at 20 mins. which is thought to be the diester. A typical gas chromatograph of HEMA(1), using DEA as the internal standard and with EGDMA added, is shown in Fig. 4-2. The largest maximum, that of HEMA, occurs at approximately 1.5 mins.; those of EGDMA and DEA occur at 3.5 mins. and 5 mins. respectively. The broken lines marked on the gas chromatograph show the assumed extents of the area of each peak; the area of the EGDMA peak is marked as A, and that of the DEA peak is marked as B.

If the peak area of the EGDMA maximum  $A_{\text{EGDMA}}$  is proportional to the concentration  $C_{\text{EGDMA}}$ , then

$$A_{\text{EGDMA}} = K_{\text{EGDMA}} \cdot C_{\text{EGDMA}} \quad \dots(4-1)$$

where  $K_{\text{EGDMA}}$  is a constant. Similarly for DEA,

$$A_{\text{DEA}} = K_{\text{DEA}} \cdot C_{\text{DEA}} \quad \dots(4-2)$$

where  $K_{\text{DEA}}$  is a second constant. Hence the ratio of the peak areas is given by

$$\frac{A_{\text{EGDMA}}}{A_{\text{DEA}}} = \frac{K_{\text{EGDMA}} \cdot C_{\text{EGDMA}}}{K_{\text{DEA}} \cdot C_{\text{DEA}}} \quad \dots(4-3)$$

Table 4-1 and Fig. 4-3 show the weight percentages of added EGDMA and the ratio of peak areas which were observed. The points in Fig. 4-3 are rather scattered, and can be divided into two groups. The shaded circles represent data from similar experiments to the open circles, except that in the case of the shaded circles, the sensitivity of the flame ionisation detector was increased.

Fig. 4-1: Gas Chromatograph of Diethyl Adipate (DEA)

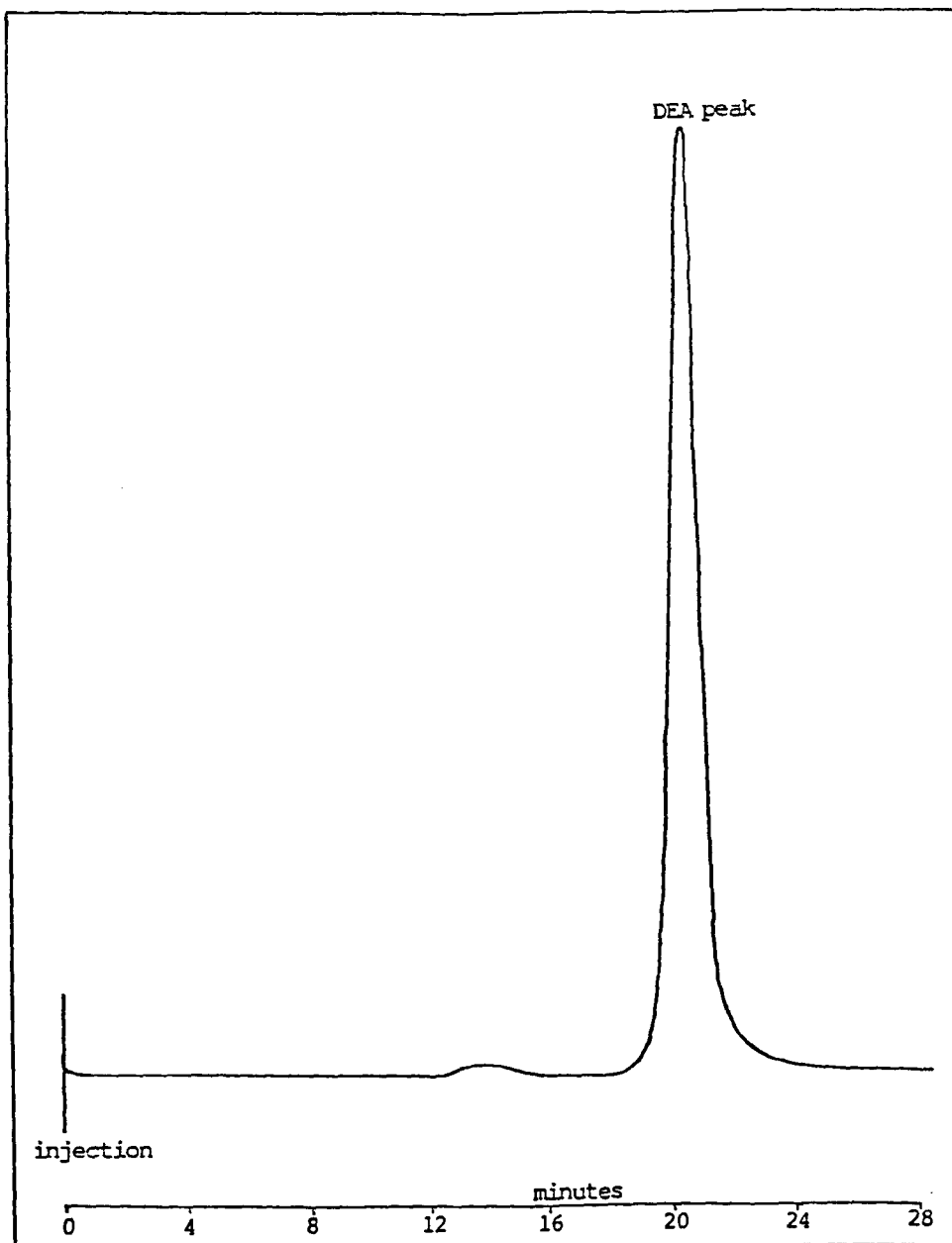




Table 4-1: Weight Percentages of Added EGDMA and Observed Ratios of Peak Areas

Weight percentage of added EGDMA	ratio $\frac{A_{\text{EGDMA}}}{A_{\text{DEA}}}$
0	0.80
0	2.65
0.27	1.68
0.40	3.07
0.40	2.24
0.40	1.39
0.40	2.14
0.50	3.52
0.53	1.81
2.00	0.83

The gas chromatograph for the diethyl adipate (Fig. 4-1) shows the purity of the material. Yields of approximately 90% are usual for this type of reaction (187). It was assumed that the relatively small proportion of monoester did not interfere with the determinations of the proportion of EGDMA using DEA as an internal standard. Indeed, Fig. 4-2 indicates that the monoester maximum is absorbed into either that of HEMA or EGDMA. It was assumed that if the latter were the case, the effect was negligible.

The DEA maximum (Fig. 4-2) appears as a shoulder on the EGDMA peak, which in turn appears as a shoulder on the HEMA peak. The retention time for EGDMA was 1.5 mins. less than that for DEA. The boiling point of EGDMA at 1 atmosphere is approximately 200°C, and that of

DEA is 138°C (ref. 187, p.422). Hence the lower boiling material, DEA, might be expected to emerge from the column first. However, the other factor which affects retention time, given that the column and conditions remain the same, is the affinity of the material for the liquid absorbed onto the packing material of the column. It may be that the order of decreasing polarity is HEMA > EGDMA > DEA, and this is reflected in the order in which these substances emerge from a non-polar column.

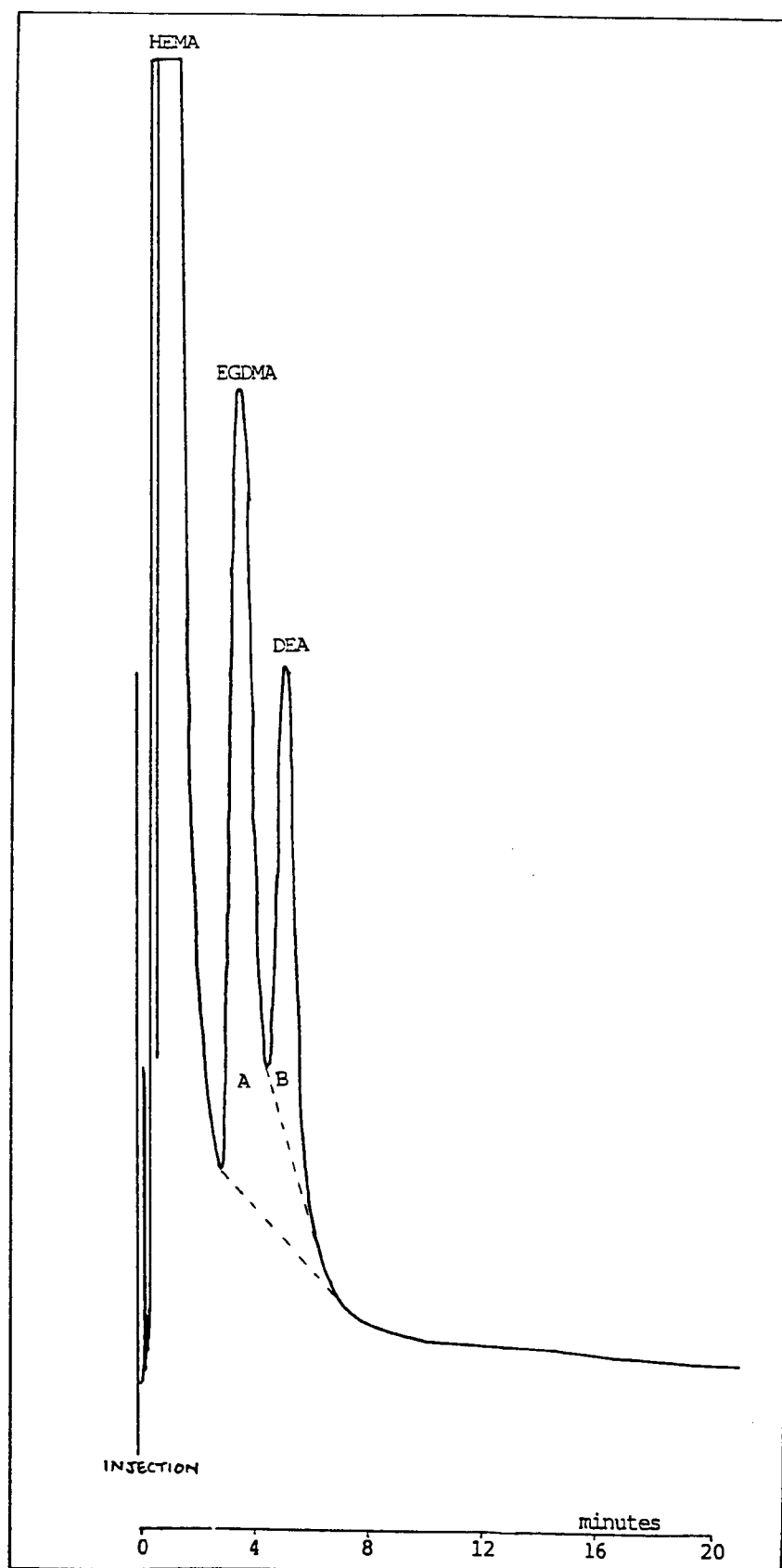
Gas liquid chromatography is often used for the analysis of HEMA and other similar monomers (e.g. refs. 62, 188, 80), but workers rarely state the conditions or types of column which were used. Macret and Hild (80) gave diagrams of some of their chromatograms, which showed good separation between HEMA and EGDMA, but unfortunately details of the chromatograph and its conditions of use are not given.

If the concentration of EGDMA already present in the HEMA is  $C_E$  and the concentration of added EGDMA is  $C'_E$ , then  $C_{\text{EGDMA}} = C_E + C'_E$ , and hence

$$\frac{A_{\text{EGDMA}}}{A_{\text{DEA}}} = K.(C_E + C'_E) \quad \dots(4-4)$$

where K is a constant. Therefore if  $A_{\text{EGDMA}}/A_{\text{DEA}}$  is plotted against  $C'_E$ , a straight line should be obtained of slope K and intercept on the %EGDMA axis  $C_E$ . The value of  $C_E$  of 0.2 - 0.4 w/w % (Fig. 4-3) is quite consistent with data given by other workers (62, 80), although according to Macret and Hild (80) it is low; they claimed that up to 4 or 5% of EGDMA may be found in commercial HEMA. The HEMA used by Wichterle and Chromacek (188) contained 1.2 - 5% EGDMA, which, it was alleged, was reduced to 0.31% after extraction and distillation. Using a lengthy process of repeated extraction and distillation, Fort and Polyzoidis

Fig. 4-2: Gas Chromatograph of HEMA(1) with 0.4% Added EGDMA, using  
DEA as Internal Standard



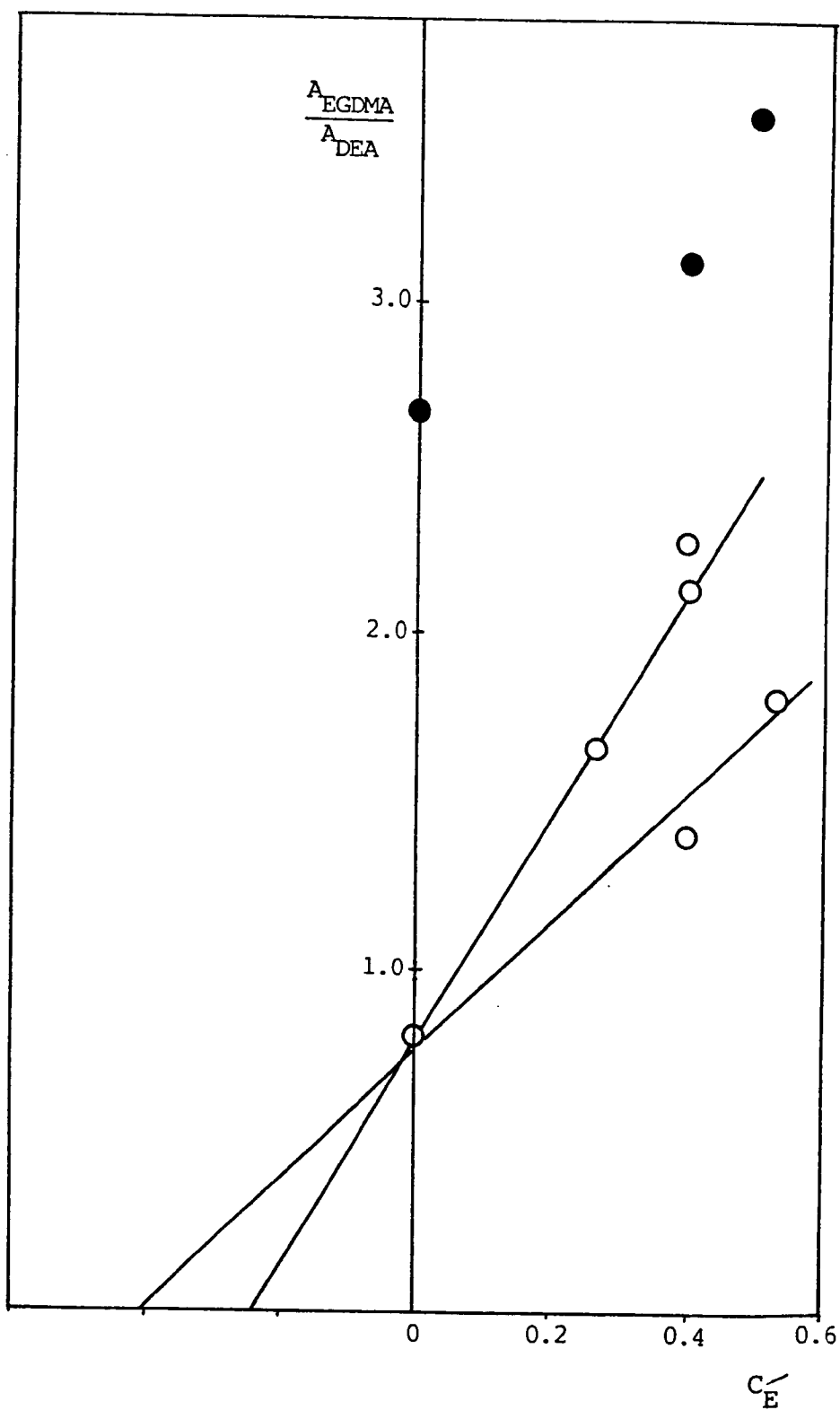


Fig. 4-3: Ratio of Peak Areas vs. Proportion of Added EGDMA

(62) claimed to have reduced the EGDMA content to 0.04%. Macret and Hild (80) state that HEMA purified by a preparative absorption chromatography method contained no detectable EGDMA.

It should be pointed out that the degree of scatter in the points of Fig. 4-3 precludes an accurate estimation of the concentration of EGDMA in HEMA(1) using these data. It is possible that the HEMA disproportionation reaction occurs during its passage through the column. This may cause variations in EGDMA content large enough to give serious scatter. Errors in estimating the peak areas may also be partly responsible. It would be possible to reduce the former errors by the use of high-performance liquid chromatography apparatus similar to that used by Pinchuk, Eckstein and van de Mark (36), and the latter errors by the use of an electronic integrator. Hence, more sophisticated analytical equipment might improve the quality of the data.

Alteration of the setting of the "Range" control of the flame ionisation detector control unit should change the peak areas in the same proportion. Therefore the ratio of the peak areas should remain constant for any given value of  $C_E^<$ . However, it was noted that the two sets of results obtained with two different range settings showed marked differences in peak area ratio for a given value of  $C_E^<$ . No explanation for this observation can be given.

It is concluded that the matters of the analysis of HEMA and methods of HEMA purification merit a more detailed investigation than has been possible in this work. On the basis of the results reported here, it is impossible to give a more accurate description of the EGDMA content of HEMA(1) than that it is "probably less than 2% w/w."

However, for subsequent experiments, it was possible to use HEMA(3) provided by Cooper Vision Optics. The EGDMA content of this material had been determined by the suppliers, and was considerably lower than that of the normal commercial material.

## 4.2 COPOLYMERS OF HEMA WITH MAA

### 4.2.1 Crosslinked Poly(HEMA) Gels Prepared by Polymerisation in Solution

The gels produced were yellowish in colour, and transparent. The "Melinex" sheet peeled off quite easily, but the hydrogels adhered a little more tenaciously to the glass plate. A strip about 5mm wide around the edges of the sheet did not gel, but formed a viscous, sticky liquid. The hydrogel was easily cut with a sharp scalpel. On swelling in water, the hydrogel became at first translucent, and subsequently transparent.

Similar gels, using the polymerisation mixture and procedure outlined in Section 3.2.1, had been previously produced by Lyskowski (189). Although the weights and percentages of initiator and crosslinker indicate approximately the amounts present in the polymerisation mixtures, they do not necessarily give the exact quantities present, for the following reasons:

- (i) the DBPO was damped with approximately 28 - 32% water, to reduce potential handling hazards;
- (ii) the HEMA contained EGDMA as an impurity.

The damping of the DBPO with water has two effects:

- (i) it reduces the concentration of DBPO in the mixture from the nominal, added concentration of 0.37% to approximately 0.26%;
- (ii) it introduces a small quantity of water into the system.

Although the first effect may have influenced the experimental results, the effect was constant, since the nominal DBPO content was constant for each set of experiments. It is assumed that the quantity of water added with the DBPO was so small that its effect upon the experimental results was small.

The yellow coloration of the gels may have been due to a reaction involving the tertiary amine part of the initiator system, dimethyl-p-toluidine. When benzoyl peroxide is used alone in polymerisations at elevated temperatures, such coloration is not observed. It is possible that an oxidation involving atmospheric oxygen is the cause, since emulsion polymerisations of other monomers under nitrogen using this initiator system yield products which do not show this yellow colouring (see Section 6.1.2). In the case of these hydrogels, the oxygen may have been dissolved in the constituents of the polymerisation mixture.

The observations concerning the transparency of the gels agree with those of Yasuda, Gochin and Stone (78). They found that poly(HEMA) gels are transparent if the proportion of solvent present in the initial polymerisation mixture is below a critical level. This critical level increases with the increasing affinity of the solvent for the polymer. IMS is likely to be a good solvent for the polymer, and therefore the critical dilution is likely to be high.

The adhesion of the hydrogel to the glass plate is caused by the hydrophilic nature of the glass surface. Hydroxyl groups on the glass surface are able to form hydrogen bonds with functional groups on the surface of the polymer, which contains both hydroxyl and carboxyl groups. On swelling, the number of groups available for hydrogen bonding on the polymer surface per unit area decreases, and hence the force of adhesion between the two materials is reduced. The gel is therefore able to be lifted more easily from the glass plate after immersion in water. The material adheres less strongly to the "Melinex" sheet because this is poly(ethylene terephthalate). It is less hydrophilic than glass, and its interaction with the hydrogel will be weaker.



It is therefore useful as a mould-release material for hydrogels.

It was reported above that a strip around the edges of the sheet showed greatly retarded polymerisation. This strip is in contact with the silicone rubber tubing gasket, and it is possible that the effect is caused by one or more substances leaching from the tubing into the polymerisation mixture, and inhibiting polymerisation in this region. Alternatively, oxygen from the atmosphere might permeate through the silicone rubber and act as an inhibitor. Silicone rubbers are particularly permeable to oxygen. The phenomenon of the intermediate translucence on swelling in water before regaining transparency has also been reported by Refojo (4). He attempted to account for the effect in the following way. The polymer segments are solvated with IMS in the initial IMS-swollen material. On exposing to water, precipitation of the polymer segments occurs, since water is a poorer solvent for the polymer than is IMS. The slow mobility of the segments results in the occurrence of phase separation before they rearrange themselves to accommodate hydration by water molecules. This rearrangement occurs at a slower rate than diffusion of the organic solvent from the gel. Refojo suggested that hydrophobic interactions bring together the hydrophobic portions of the polymer, enabling the hydrophilic portions to be hydrated. Hence the translucent state is intermediate between two stable transparent states. An alternative explanation is that IMS/water mixtures are poorer solvents for poly(HEMA) than either solvent separately.

#### 4.2.2 Equilibrium Water Contents of Crosslinked HEMA-MAA Copolymers

The gels were transparent. Fig. 4-4 shows the variation of equilibrium water content (EWC) with MAA content. As the proportion of MAA in the gel increases, the EWC increases, but the rate of increase decreases

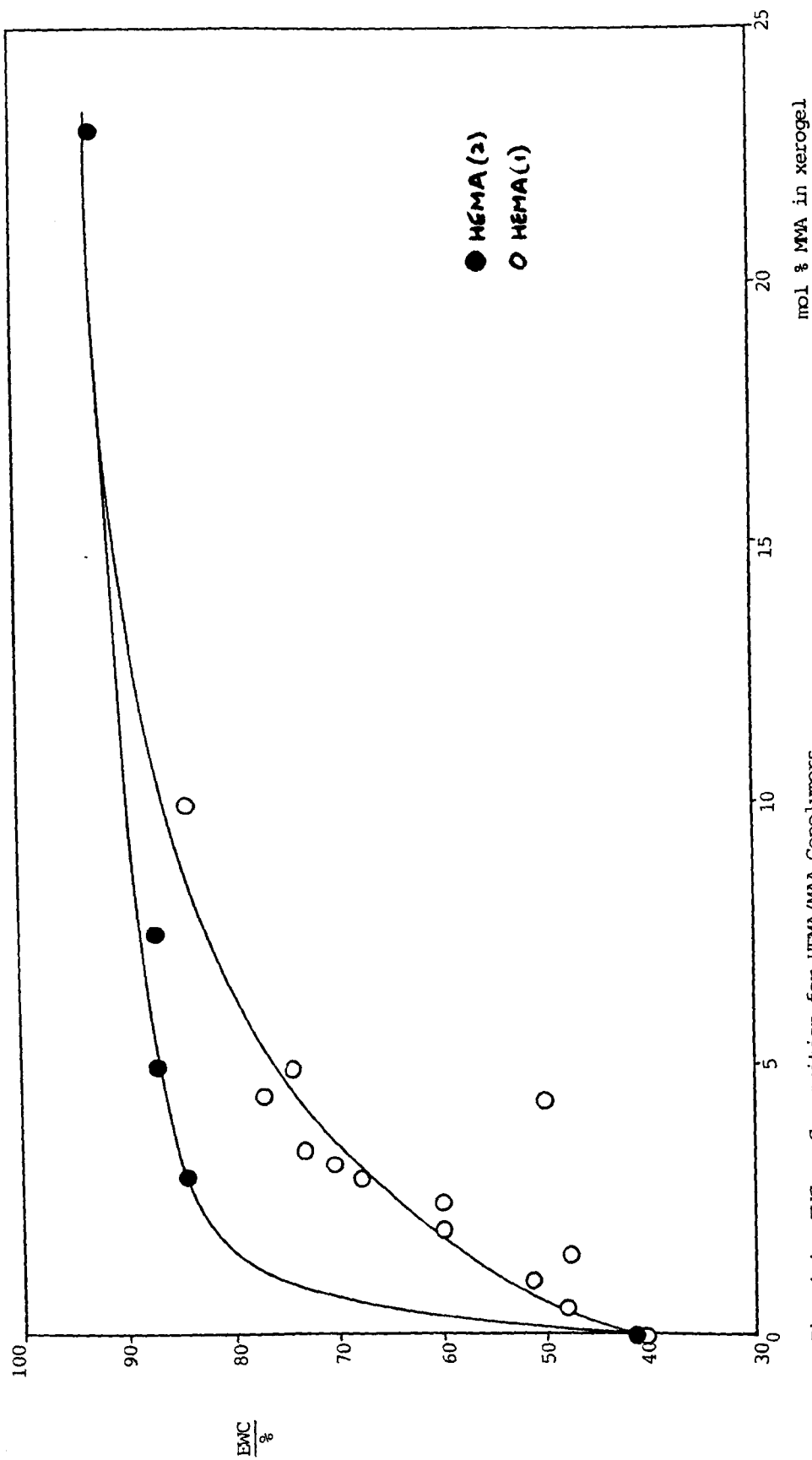


Fig. 4-4: EMC vs Composition for HEMA/MAA Copolymers

until at mole percentages of MAA above 20% a plateau is reached at an EWC of approximately 90%. Over the range 0 - 2% MAA, the slope of the curve for gels containing HEMA(2) (purified) is greater than that of the curve for gels containing HEMA(1) (unpurified). At approximately 2% MAA, the HEMA(2) curve exhibits a sharp decrease in slope. At approximately 20% MAA, the two curves merge. There is some scatter in the data for the HEMA(1) gels.

The DBPO level was 0.35 mol %, the amount of damped DBPO added being 0.5 mol %. The EGDMA content is unknown, being the proportion present as an impurity in the HEMA plus that added, i.e. 0.4 mol %. The GLC results (Section 4.1) suggest that the level of EGDMA in the HEMA was approximately 0.2 - 0.4 w/w % (i.e. 0.13 - 0.26 mol %), and thus the total EGDMA content might therefore have been 0.5 - 0.7 mol %.

Pinchuk, Eckstein and van de Mark (36) studied the swelling of similar materials in various aqueous media, including alkaline solutions. The crosslinking agent used was tetraethylene glycol dimethacrylate (TEGDMA) rather than EGDMA. These workers varied the level of crosslinker up to 0.3% and the MAA content up to 4%. The gels were swollen in 0.15M aqueous urea, which buffers at pH9.2. The authors did not make it clear whether percentages were based on weight or on the number of moles. It is assumed that mole percentages were used, since these units were used elsewhere in the paper.

For a given MAA content, the EWC values for the gels produced in this work using HEMA(1) are lower than those reported by Pinchuk et al. This is attributed to the pH of distilled water being lower (5.5) than that of 0.15M urea (9.2); hence the degree of ionisation of the gels will be greater. The pK value for the HEMA-MAA copolymer containing 5 mol % was given by Ilavsky et al (35) as approximately 7.5. Hence

the MAA units are essentially un-ionised. Flory (ref. 2, p.589) has derived equations relating the swelling behaviour of ionic gels to the degree of neutralisation. However, for complete ionisation of MAA groups the equation is much simpler, since the gel behaves in the same way as a non-ionic material.

It is interesting to note that the materials made using HEMA(2) show higher EWCs than do those made using HEMA(1), although at higher levels of MAA the curves probably converge. Two possible causes of this are:

- (i) that increased amounts of hydrophilic impurities such as MAA are formed during distillation;
- (ii) that EGDMA is removed from the HEMA during purification, thereby decreasing the level of crosslinker in the hydrogel.

There are, however, objections to both of these hypotheses:

- (i) the boiling points of HEMA and MAA are such that separation during distillation would be expected to be good, although if MAA were produced during the distillation it is possible that they might distil together;
- (ii) other workers (80) argue that purification of HEMA by the extraction and distillation method is inefficient, only a small proportion of the EGDMA being removed.

It appears that (i) is the most likely of these hypotheses. The EWCs would be expected to be more sensitive to MAA content at low MAA contents than at high MAA contents. This explains why at higher MAA contents the curves converge, where the additional MAA makes little difference.

The pH of distilled water is approximately 5.5. The Henderson equation relates the pH,  $pK_a$  and concentrations of ionised and un-ionised acid groups in the following way:

$$\text{pH} = \text{pK}_a + \log_{10} \frac{[\text{salt}]}{[\text{acid}]} \quad \text{....(4-4)}$$

where  $K_a$  is the dissociation constant of the acid,  $\text{pK}_a = -\log_{10} K_a$ ,  $[\text{salt}]$  is the concentration of  $-\text{COO}^-$  in this case, and  $[\text{acid}]$  is the concentration of  $-\text{COOH}$  in this case. The degree of dissociation,  $\alpha$ , of the acid is given by

$$\alpha = \frac{[\text{salt}]}{[\text{salt}] + [\text{acid}]} \quad \text{....(4-5)}$$

Equations 4-4 and 4-5 give

$$\frac{1}{\alpha} = \exp (\text{pK}_a - \text{pH}) + 1 \quad \text{....(4-6)}$$

Ilavsky et al (35) gave a value of approximately 7.5 for the  $\text{pK}_a$  of 5 mol % MAA HEMA-MAA copolymers. Table 4-2 shows values of  $\alpha$  calculated from equation 4-6 for various pH values using this value of  $\text{pK}_a$ . Ilavsky et al (35) showed that, in general, the  $\text{pK}_a$  increased as the MAA content of the copolymer increased. Hence for copolymers where the MAA content exceeds 5%, the  $\text{pK}_a$  is likely to be greater than 7.5. If the  $\text{pK}_a$  were 8.0, for example, at pH 5.5 the degree of dissociation would be 0.08.

swelling solution	pH	$\alpha$
Distilled water	5.5	0.12
0.1M $\text{NaHCO}_3$ (aq)	8.45	0.72
0.15M urea (aq)	9.2	0.85

Table 4-2: Degree of Dissociation vs pH, for MAA Groups in 5 mol % MAA Poly (HEMA-MAA)

If  $\alpha$  is assumed to be negligible, the relationship between swelling and crosslink concentration is greatly simplified. The "hydrogen ion pressure", which Tanaka (179) calls the osmotic pressure caused by  $H^+$  ions within the gel screened by negative charges, is negligible. For low levels of crosslinking, Flory (ref. 2, p.580) gave the equation

$$\chi_1 = -q^2 \ln(1 - 1/q) + 1/q + \frac{V_1 v_e}{V_o} (q^{-1/3} - 1/2q) \quad \dots(4-7)$$

where  $q$  is volume of swollen gel/volume of unswollen gel,  $\chi_1$  is the Flory interaction parameter,  $V_1$  is the molar volume of the swelling liquid, and  $V_o/v_e$  is  $1/2x$ , where  $x$  is the concentration of crosslinks in the material. Assuming that the densities of the swelling agent and the polymer are approximately equal, then

$$q = \frac{1}{1 - EWC} \quad \dots(4-8)$$

The level of added EGDMA was 0.4 mol % based on total monomers, and therefore, assuming that the density of the polymer is approximately unity,

$$x = \frac{0.4 \times 10^{-2}}{M} \text{ mol cm}^{-3} \quad \dots(4-9)$$

where  $M$  is the weighted average molecular weight of the monomers (HEMA and MAA). For example, for a polymer which contains 5 mol % MAA, the value of  $M$  is  $[(5 \times 86) + (95 \times 130)]/100$ , i.e.  $127.8 \text{ g mol}^{-1}$ , since the molecular weights of HEMA and MAA are  $130$  and  $86 \text{ g mol}^{-1}$  respectively. Hence, for this polymer,

$$\begin{aligned} x &= \frac{0.4 \times 10^{-2}}{127.8} \text{ mol g}^{-1} \\ &= 3.13 \times 10^{-5} \text{ mol g}^{-1} \text{ of dry polymer} \end{aligned}$$

From the swelling data, values of  $\chi_1$  as a function of composition were calculated using equation 4-7. The results are shown in Table 4-3. The decrease in  $\chi_1$  as the MAA content increases reflects the increasing polarity of the copolymer with increasing MAA content. This analysis assumes that the crosslink concentration is equal to that calculated from equation 4-9. Conversely, if a value of  $\chi_1$  is assumed, crosslink concentrations can be calculated.

Table 4-3: Values of  $\chi_1$  Calculated Using Equation 4-7

mol % MAA	q	$\chi_1$
1.0	2.04	0.76
2.0	2.49	0.69
3.0	6.37	0.55
5.0	3.82	0.60
5.0	7.58	0.49
7.5	7.63	0.49
23.0	13.70	0.48

The molar volume of the swelling agent was assumed to be that of water, i.e.  $V_1 = 18\text{cm}^3 \text{mol}^{-1}$ .

If a typical value of  $\chi_1$ , say 0.4, is assumed and inserted into equation 4-7, the effective crosslink concentration  $x$  can be calculated. Values of  $x$  obtained in this way are shown in Table 4-4, together with the crosslink concentrations calculated from equation 4-9. Table 4-4 shows that the majority of the data yield crosslink concentrations far in excess of the introduced crosslink when a value of 0.4 for  $\chi_1$  is used. The exception is the polymer which contained 23% MAA.

Table 4-4: Calculated Values of Crosslink Concentration Assuming

$\chi_1 = 0.4$

mol % MAA	q	$\frac{M}{\text{gmol}^{-1}}$	x (from 4-7)	x (from 4-11)
			$10^5 \text{ mol}$	$10^5 \text{ mol}$
1.0	2.04	129.6	84.7	3.09
2.0	2.49	129.1	60.7	3.10
3.0	6.37	128.7	12.7	3.11
5.0	3.82	127.8	29.8	3.13
5.0	7.58	127.8	9.5	3.13
7.5	7.63	126.7	9.4	3.16
23.0	13.70	119.9	3.5	3.34

Two reasons can be suggested for the discrepancies between the two sets of values of x:

- (i) equation 4-7 relating q to x and  $\chi_1$  is inapplicable in this case;
- (ii) the effective crosslink concentration is indeed significantly higher than that calculated from the level of EGDMA.

(i) It is possible that the small degree of ionisation of the carboxyl groups of the MAA significantly affects the swelling of the polymers in distilled water. Flory (ref. 2, p.587) gave the following equation for the swelling of ionic gels where the electrolyte concentration is low:

$$q^{2/3} = \frac{i}{Z \cdot V_u} \cdot \frac{V_o}{V_e} \tag{4-10}$$

$$= \frac{i}{Z \cdot V_u} \cdot \frac{1}{2x} \tag{4-11}$$



where  $i$  is the degree of ionisation,  $Z_-$  is the valency of the ionic group of the polymer, and  $V_u$  is the molar volume of the structural units of the polymer.

If it is postulated that the contributions to swelling by the HEMA and MAA parts of the copolymer,  $q_{\text{HEMA}}$  and  $q_{\text{MAA}}$  respectively, are additive, i.e. that

$$q = pq_{\text{MAA}} + (1 - p)q_{\text{HEMA}} \quad \dots(4-12)$$

where  $p$  is the mole fraction of MAA in the copolymer, then the total swelling is given by

$$q = (1 - p)q_{\text{HEMA}} + p \left\{ \frac{i}{2Z_- V_u x} \right\}^{3/2} \quad \dots(4-13)$$

from equation 4-11. Hence  $q$  should vary linearly with  $p$ , the slope of the relationship being

$$\frac{i}{2Z_- V_u x}^{3/2} - q_{\text{HEMA}}$$

The quantity  $x$  in this simple model refers to the concentration of crosslinks in the "poly(MAA)" part of the copolymer, which is assumed to be equal to that of the material as a whole. A plot of  $q$  as a function of  $p$  is shown in Fig. 4-6. The slope is 51 for polymers made using HEMA(1). Using a value of  $86 \text{ cm}^3 \text{ mol}^{-1}$  for  $V_u$  gives a value for  $x$  of  $4.97 \times 10^{-5} \text{ mol cm}^{-3}$ . This compares with an expected crosslink concentration of approximately  $3 \times 10^{-5} \text{ mol cm}^{-3}$  of dry polymer based upon the EGDMA concentration. The data therefore fit the model remarkably well.

(ii) As can be seen from the analysis given above, the crosslink concentration calculated using equation 4-13 is indeed higher than

the expected crosslink concentration based upon the EGDMA concentration.

The additional crosslinks may arise from at least two sources:

- (a) from physical crosslinks;
- (b) from EGDMA already present as an impurity in the HEMA.

If the additional crosslinks were all caused by the presence of EGDMA as an impurity, then the level of EGDMA in the HEMA would have been approximately 0.3 mol %. This value is similar to those obtained by GLC analysis. However, it is not clear to what extent physical crosslinks also occur. Refojo (4) and Ratner and Miller (107) postulated that with poly(HEMA) gels additional crosslinking is caused by hydrophobic and hydrophilic bonding respectively.

The gels synthesised using purified HEMA, HEMA(2), are shown by the shaded circles in Fig. 4-6. The value of  $q$  for the material containing 23% MAA lies on the  $q/p$  line for the HEMA(1) gels, but those containing less MAA show  $q$  values significantly greater than those for gels containing HEMA(1).

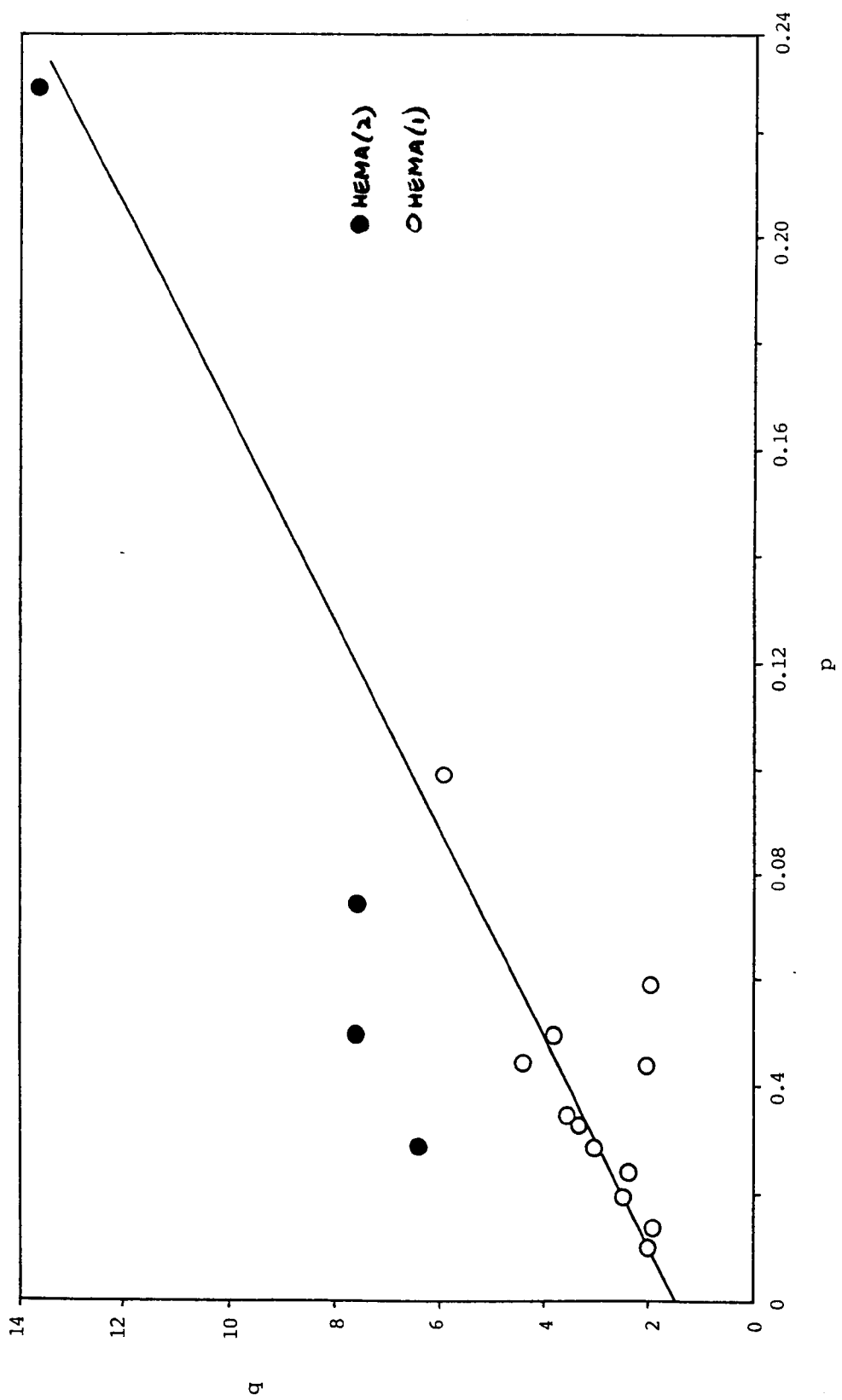


Fig. 4-6: Swelling Ratio vs Composition for HEMA/MAA Copolymers

### 4.3 TERPOLYMERS CONTAINING HEMA, MAA AND MMA

#### 4.3.1 HEMA(1)-MAA-MMA(2) Terpolymer Hydrogels

##### (a) Swelling Behaviour

The hydrogels were transparent. This suggests that, if phase separation does occur, the phase domain size is smaller than the wavelength of the incident light, i.e. below 500nm approximately. An increase in the time taken for the gel to become transparent, on exchanging the IMS from the polymerisation mixture for water was observed with increasing proportion of MMA. This is thought to be caused by the decreased permeability of the materials to aqueous media as the hydrophobicity of the material is increased. Hence as the hydrophobicity of the polymer is increased, aqueous solutions take a greater time to exchange with the IMS in which the gels were polymerised.

EWC was observed to decrease with increasing MMA content (Fig. 4-7) when the materials were swollen in 0.1M sodium bicarbonate solution (pH 8.5). Presumably this decrease in EWC is caused by an increase in hydrophobicity of the terpolymer as the level of MMA is increased, causing the free energy of mixing to become less negative, mainly because  $\Delta H$  increases.

Fig. 4-8 shows that the swelling ratio,  $q$ , decreases with increasing MMA content. The points follow a curve, the slope of which decreases as the mole fraction of hydrophobic monomer, increases. It would be expected that the volume swelling ratio would vary linearly with  $P$ , if the following assumptions are true:

- (i) that any change in  $q$  is dependent only on changes in the Flory-Huggins interaction parameter for the copolymer/solvent system;
- (ii) that the overall value of  $\chi_1$  varies linearly with the mole fraction of MMA.

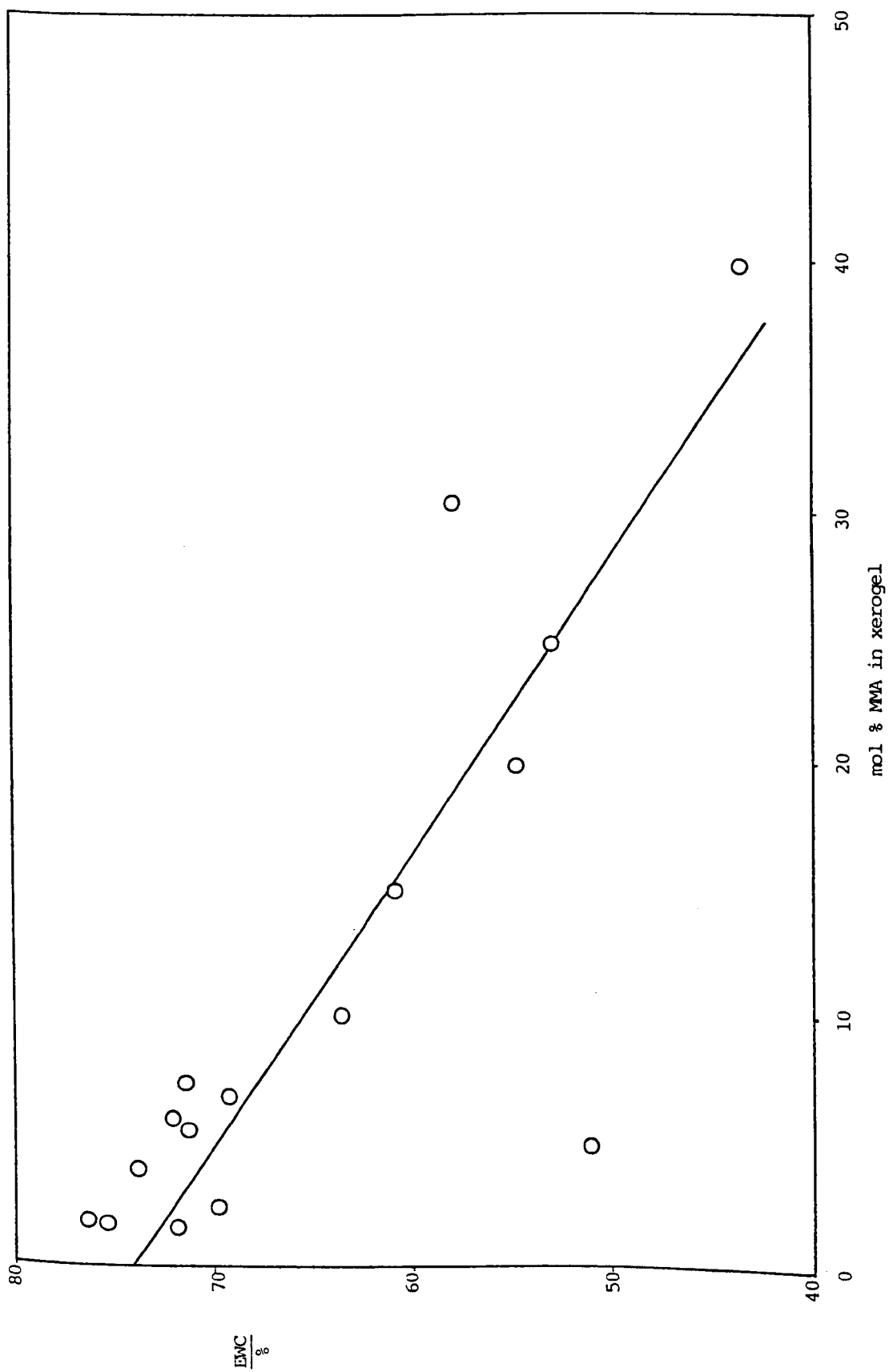


Fig. 4-7: EWC vs Composition for HEMA(1)/MAA/MMA Terpolymers (pH8.5)

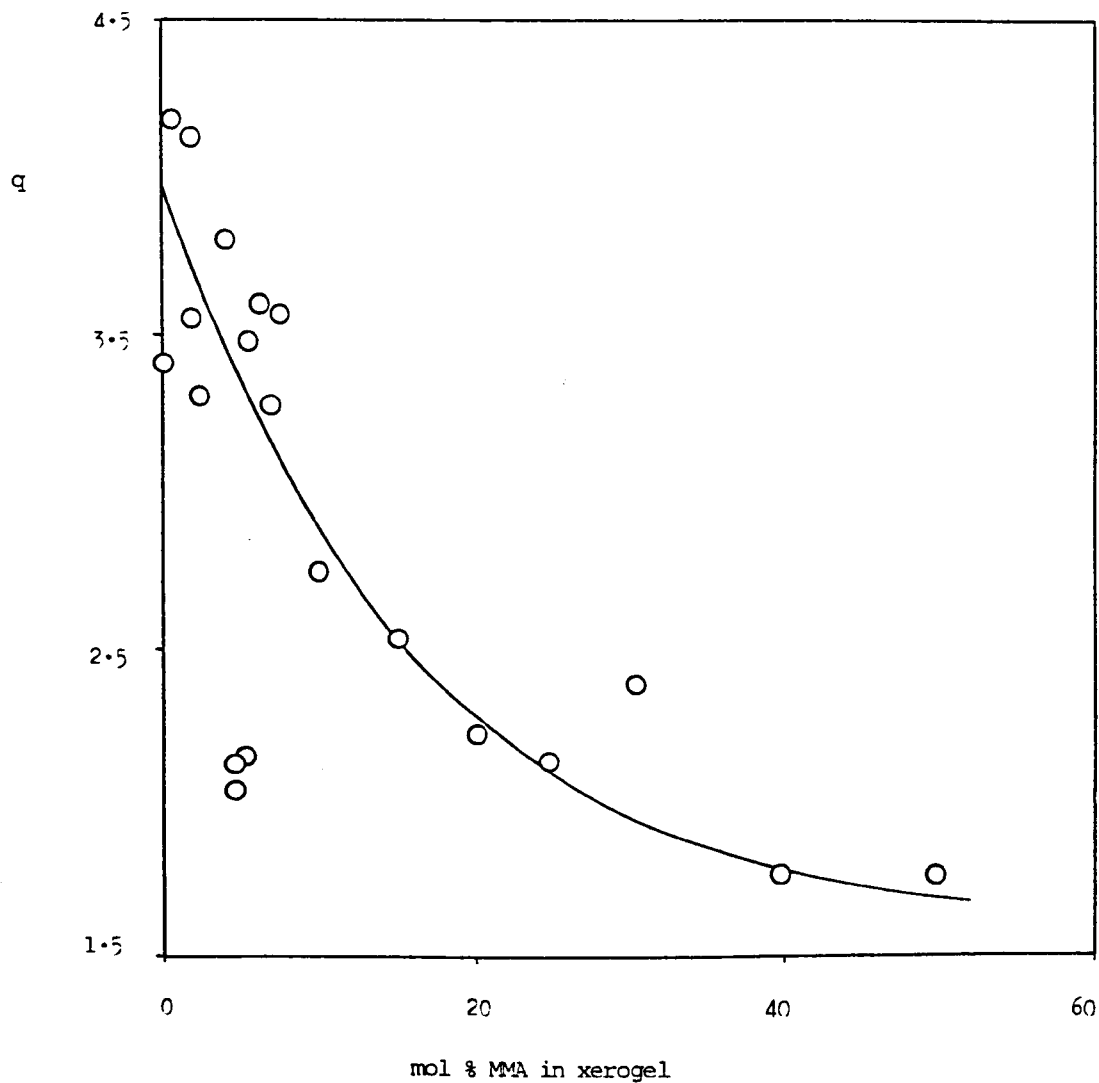


Fig. 4-8: Swelling Ratio vs Composition for HEMA(1)/MMA/MAA Terpolymers

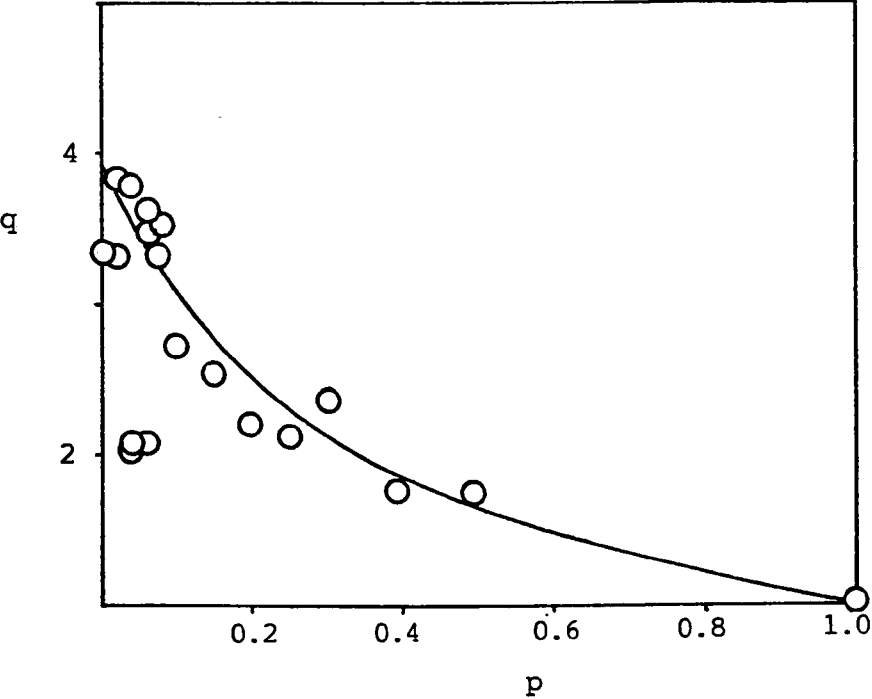
Fig. 4-9 shows  $q$  as a function of  $P$ . The assumption is made that  $q$  is equal to the volume swelling ratio, since the densities of copolymer and swelling agent are approximately equal. Included in Fig. 4-9 is the point for pure PMMA; the value of  $q$  for this polymer is approximately 1.0. Fig. 4-9 shows that the observed EWC value at a given composition is lower than that predicted on the basis of the above assumptions. Hence the assumptions are rejected. Two reasons for the observed swelling behaviour can be offered:

- (i) The effective crosslink concentration of the material increases with increasing hydrophobicity. This supposition is supported by values of crosslink concentration calculated from results for the shear moduli of hydrogels reported below (Section 4.3.2).
- (ii) As the mole fraction of MMA is increased, the proportion of MMA-rich domains increases. The rigidity of these domains limits their ability to swell to the extent that their HEMA/MAA content might suggest. Hence the overall swelling of the material is lower than would be expected from the above hypothesis.

(b) Mechanical Properties

As expected, the tensile strength of the hydrogels increased with the proportion of MMA (Fig. 4-10). Figs. 4-11 and 4-12 show tensile strength as a function of EWC. Fig. 4-12 includes results for polymers of lower water content. As the water content increases, a very sharp decrease in tensile strength occurs between 40 and 50% water. At water contents above approximately 50 to 54%, the decrease in tensile strength is more gradual. There are several factors which may influence the change in tensile strength with composition, and therefore with EWC:

Fig. 4-9: Swelling Ratio vs. Mole Fraction of Hydrophobic Monomer  
for HEMA(1)-MMA-MAA Terpolymers





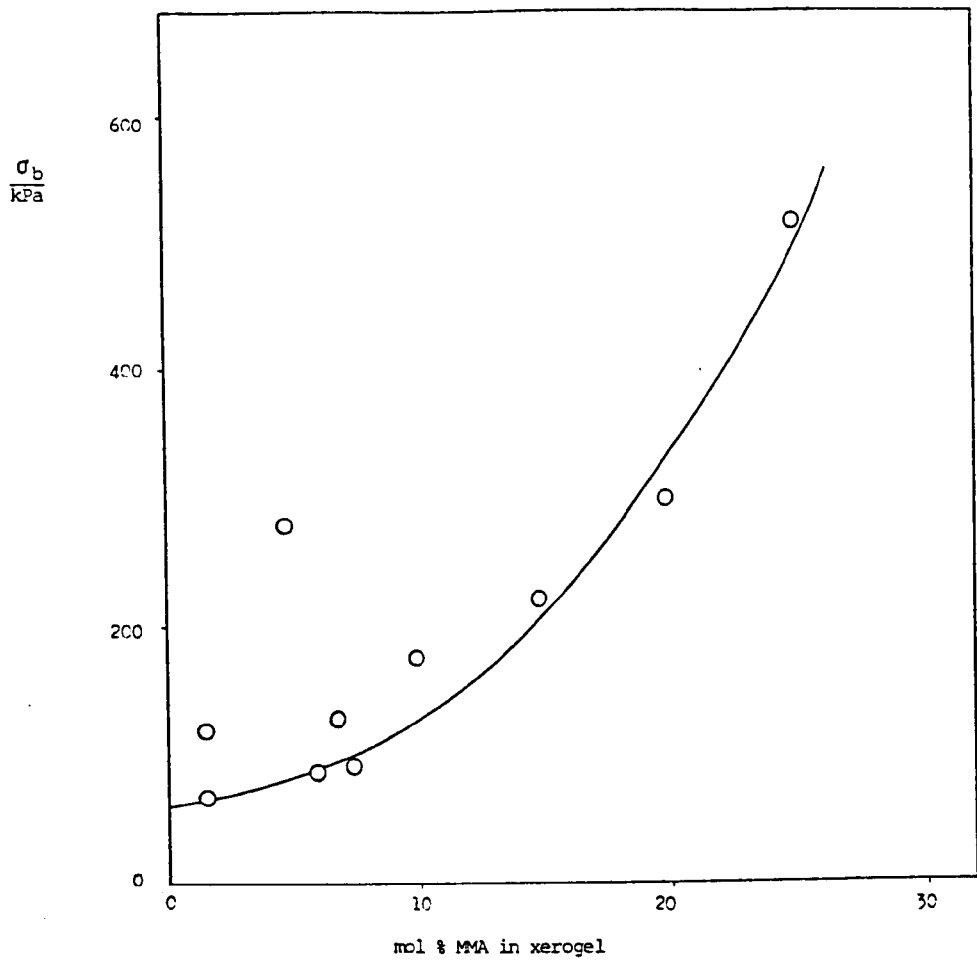


Fig. 4-10: Tensile Strength vs Composition for HEMA(1)/MAA/MMA Hydrogels

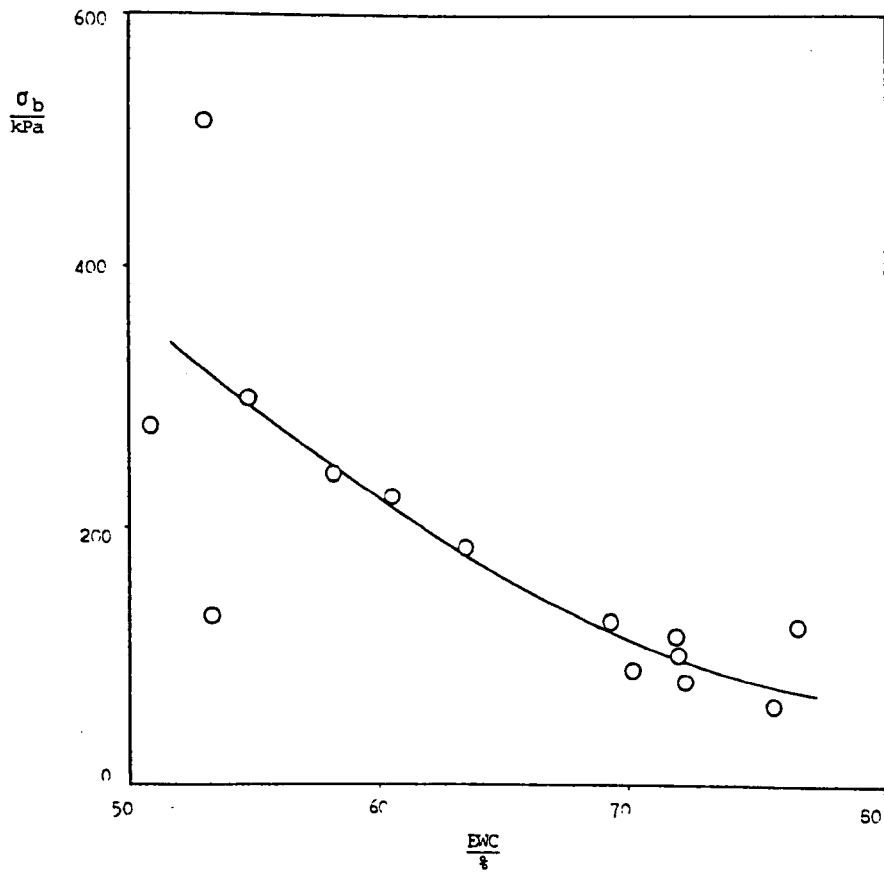


Fig. 4-11: Tensile Strength vs EWC for HEMA(1)/MAA/MMA Hydrogels

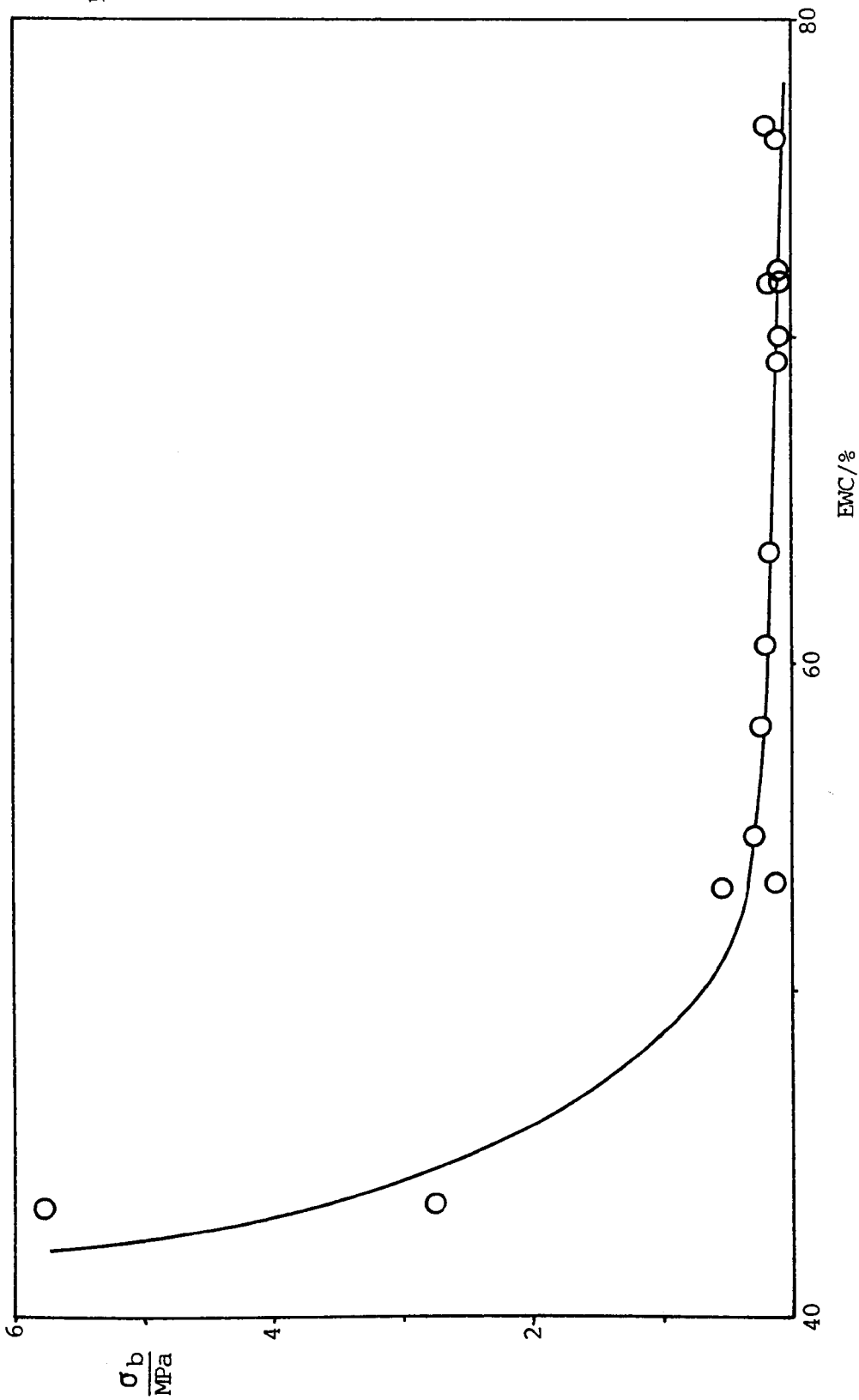


Fig. 4-12: Tensile Strength  
vs EMC for  
HEMA-MAA-MMA Hydrogels

- (i) Increasing the proportion of MMA in the hydrogel leads to a decrease in EWC, since the greater hydrophobicity of the polymer causes an increase in the free energy of mixing of polymer with solvent. Hence the number of network chains per unit volume of the swollen material increases, and the tensile strength would therefore be expected to increase.
- (ii) The effective crosslink density of the material may vary as the EWC is varied.
- (iii) As the proportion of hydrophobic monomer is increased, hydrophobic domains may separate and increase the tensile strength by acting in the same way as filler particles in a crosslinked elastomer.
- (iv) Strain-induced crystallisation at higher strains may occur. This would also tend to increase the tensile strength.

The simplest theoretical model which would describe the variation of tensile strength with water content is one in which the tensile strength  $\sigma_b$  is proportional to the number of polymer chains which have to be ruptured per unit area as the material breaks. This model gives

$$\sigma_b \propto v_2 \quad \dots(4-21)$$

where  $v_2$  is the volume fraction of polymer in the gel. Hence

$$\sigma_b \propto 100 - \text{EWC} \quad \dots(4-22)$$

At values of EWC of between 50 and 70%, the plot of  $\sigma_b$  as a function of EWC is indeed approximately linear, as shown in Fig. 4-11. At lower values of EWC however, the plot deviates from linearity. This is illustrated in Fig. 4-12. The large increase in tensile strength

as the EWC decreases between 40 and 50% EWC may be caused by several factors. One possibility is that phase separation occurs, resulting in a material which consists of domains of low water content and high modulus, dispersed in regions of higher water content which are rich in HEMA/MAA. The higher modulus domains could act in the same way as filler particles in a filler-reinforced elastomer (Section 2.2). This is a similar situation to that which occurs in certain block copolymers (e.g. 203).

However, if this were the case, some visible evidence of phase separation might be expected, in the form of translucence or opacity of the gel. Domains larger than the wavelength of visible light, i.e. larger than 400-700 nm would be expected to cause light-scattering, and therefore translucence or opacity. All the materials were transparent, and this therefore suggests that phase separation did not occur. However, it may be present, if

- (i) the domain size is very small ( $< 400\text{-}700\text{ nm}$ );
- (ii) the refractive indices of the two phases are almost identical;  
or
- (iii) the phase boundary is ill-defined.

It is unlikely that the refractive indices of water-rich and water-poor phases would be identical. Hence, if phase-separation is the cause of the rise in tensile strength, then it must be such that the domains are of small size.

Another possibility is that strain-induced crystallisation occurs in materials containing higher proportions of MMA, similar to that which is displayed by natural rubber at high strains. Hydrophobic bonding between polymer chains might help to induce crystallisation. As the proportion of MMA is increased, hydrophobic bonding between polymer chains, rather than between polymer chains and water, becomes

more favourable. The orientation of polymer chains therefore might occur to a greater extent in the higher-MMA materials. The hypothesis of crystallisation is corroborated by the stress-strain curves for similar materials, which are discussed below. The curve for the 10% MMA terpolymer exhibits a steady decrease in slope as the strain is increased (Fig. 4-54). However, that for the 20% MMA terpolymer shows a definite increase in slope above strains of approximately 100% (Fig. 4-28). Hence a stiffening of the material, or increase in modulus, occurs at high strains, which is consistent with the occurrence of strain-induced crystallisation.

Figs. 4-13 and 4-14 show the tensile strength data plotted on a different scale, to include the value for PMMA (201). Figs. 4-15 and 4-16 show  $\log (\sigma_b/\text{kPa})$  as a function of composition and EWC respectively. It is interesting that  $\log \sigma_b$  falls approximately linearly with EWC. Similar observations have not previously been published. In addition to data collected in this work, Figs. 4-15 and 4-16 include results reported by Migliaresi et al (132) for both HEMA-MMA copolymers and poly(HEMA)/PMMA blends. Fig. 4-16 shows that in general, the tensile strengths of the HEMA-MMA copolymers are higher than the terpolymers, for a given mol%MMA. At a given mol%MMA however, the water contents of the terpolymers are greater, and this fact is reflected in Fig. 4-15. For a given water content, the tensile strengths of the terpolymers are greater than those of either the HEMA/MMA copolymers or the blends. At 40 - 50% EWC, the tensile strength ratio is of the order of 10.

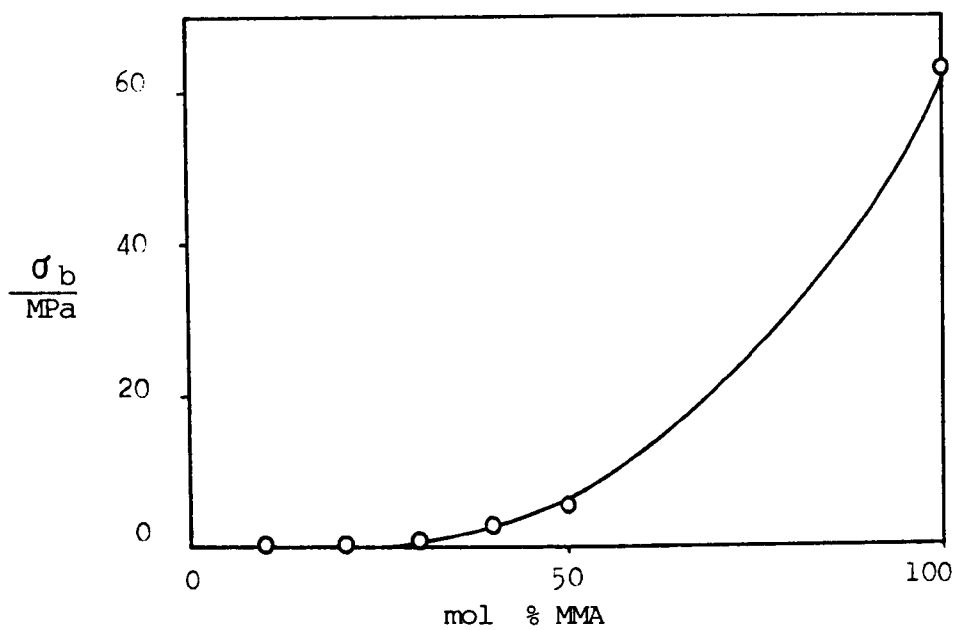


Fig. 4-13: Tensile Strength vs Composition for  
HEMA-MAA-MMA Hydrogels

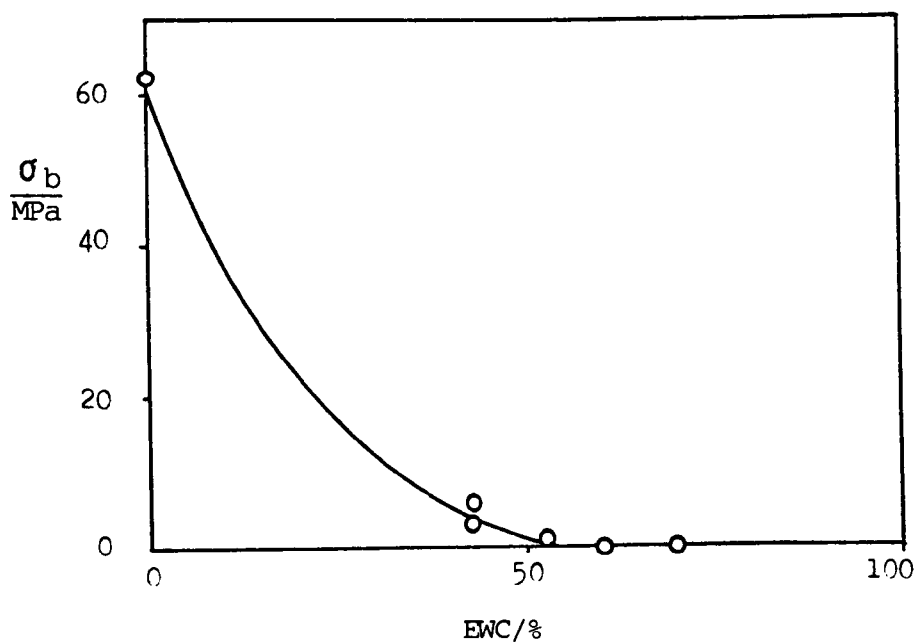


Fig. 4-14: Tensile Strength vs EWC for  
HEMA-MAA-MMA

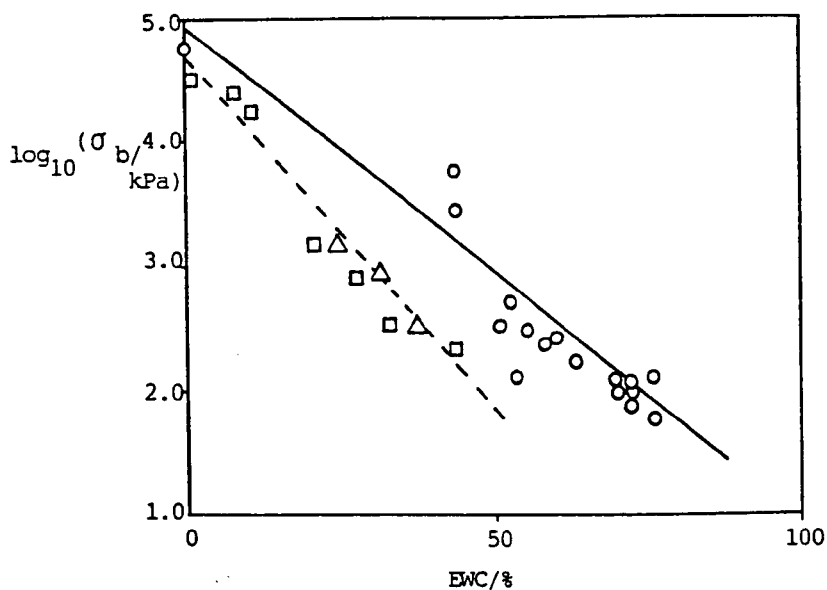


Fig. 4-16: Log (Tensile Strength) vs. EWC for HEMA/MAA/MMA Terpolymer Hydrogels, HEMA/MMA Blends and HEMA/MMA Copolymer Hydrogels

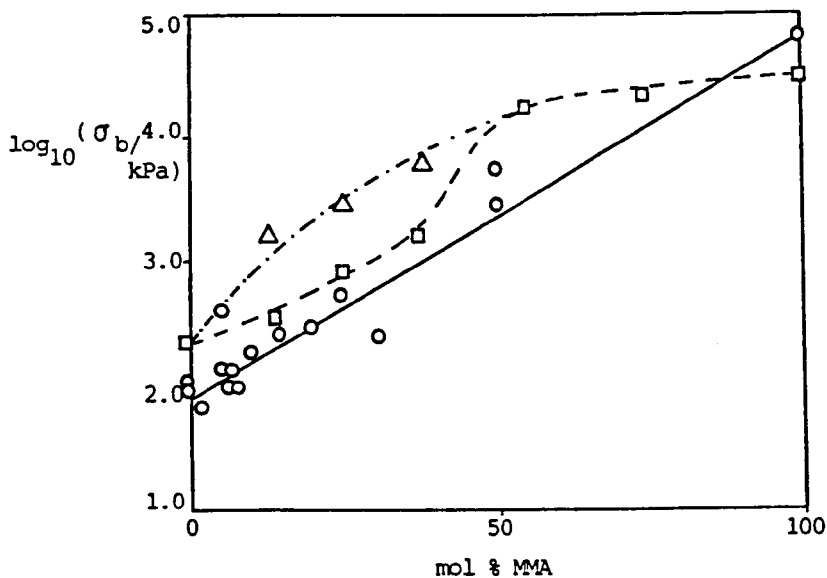


Fig. 4-15: Log (Tensile Strength) vs. Composition for HEMA/MAA/MMA Terpolymer Hydrogels, HEMA/MMA Blends and HEMA/MMA Copolymer Hydrogels

#### 4.3.2 HEMA(3)-MAA-MMA(2) Terpolymer Hydrogels

The gels were similar in appearance to those discussed in Section 4.3.1. Fig. 4-17 shows the EWC plotted against composition. From an EWC value of approximately 75% at 0 mol % MMA, the EWC decreased, with increasingly negative slope as the proportion of MMA was increased. At a mole percentage of MMA of 30%, the EWC was approximately 58%. Fig. 4-18 shows the tensile strengths of these materials as a function of composition. At a composition of 0% MMA, the tensile strength was approximately 50kPa. From this point, the tensile strength increased with increasing slope, as the proportion of MMA increased. At 25 mol % MMA, the tensile strength was 166kPa.

Figs. 4-19 to 4-21 show the results of tearing experiments conducted on single edge-notch samples cut from several HEMA-MMA-MAA terpolymer hydrogels. In the case of the 10 mol % MMA terpolymer, the crack length was constant during the first 20 minutes of the experiment, and then began to increase. After 50 minutes the slope increased sharply, until the sample broke. The 15 mol % sample behaved similarly. The crack length remained constant until 6 minutes had elapsed, and then increased sharply over a period of approximately 0.5 minutes, until the sample broke. The 30 mol % sample, however, showed slightly different behaviour. The crack length was approximately constant for the first 30 minutes of the experiment, and then began to increase. After 140 minutes, the slope increased sharply, but the sudden change in slope was not as apparent as in the two cases mentioned above. After 160 minutes, the slope became too steep to measure. For the single edge-notch experiments carried out using the Instron, the data shown in Table 4-5 were obtained for the terpolymer hydrogel containing 15 mol % MMA.



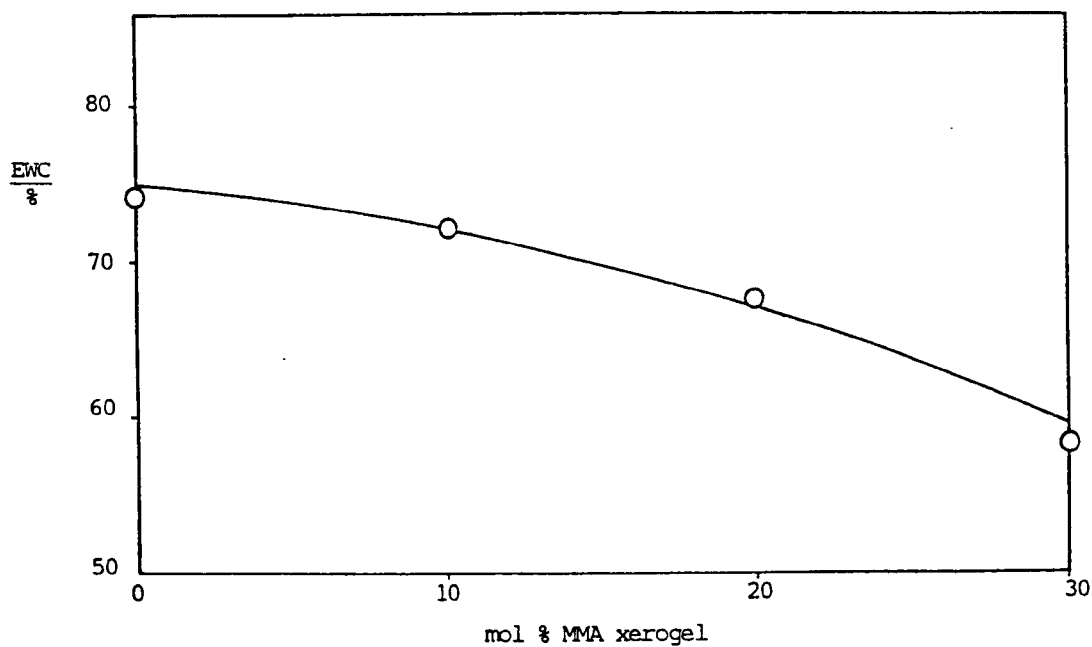


Fig. 4-17: EWC vs. Composition for HEMA(3)-MAA-MMA Terpolymer Hydrogels

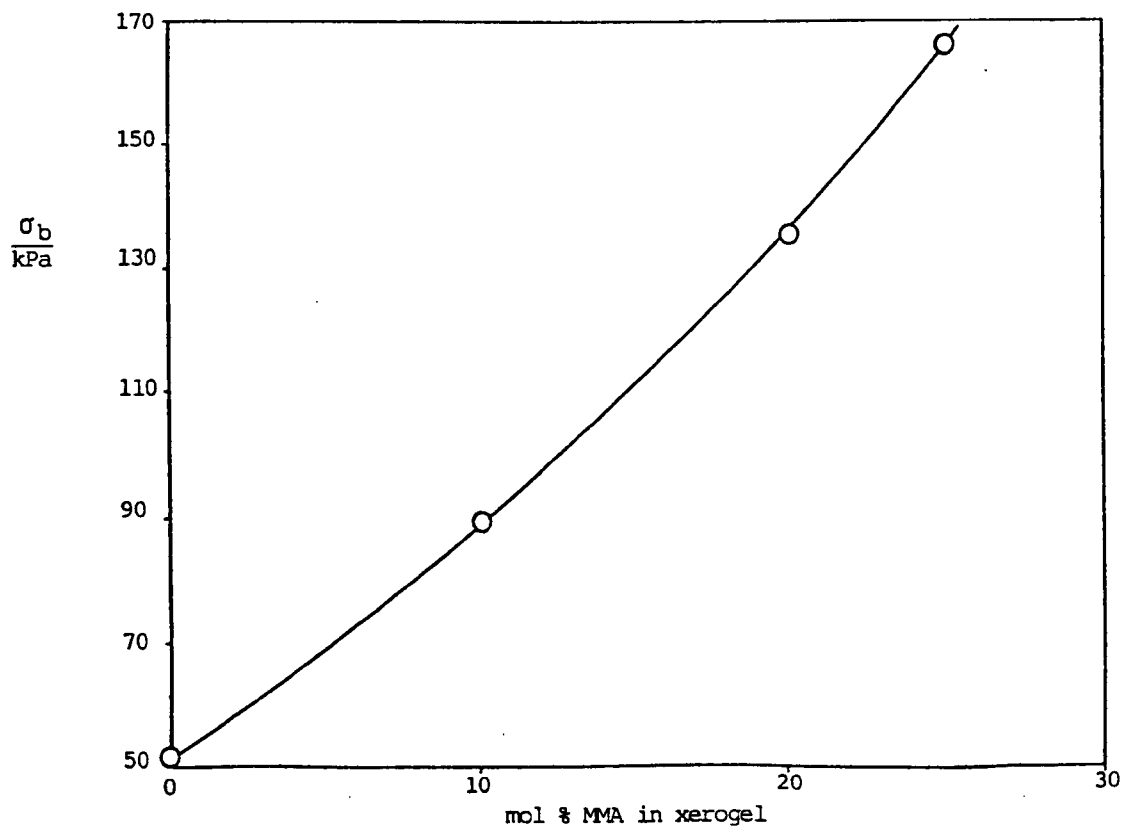


Fig. 4-18: Tensile Strength vs. Composition for HEMA(3)-MAA-MMA Terpolymer Hydrogels.

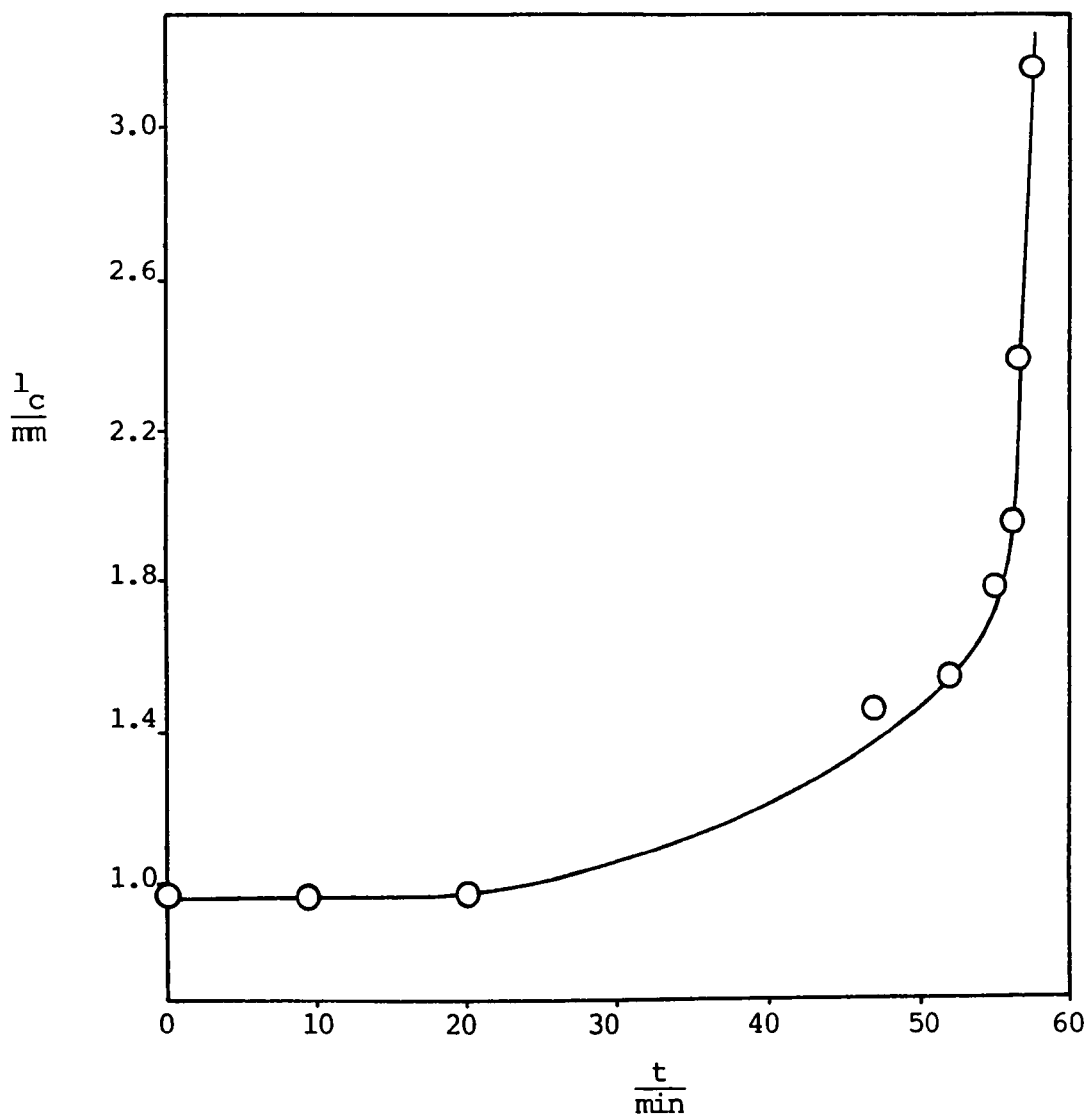


Fig. 4-19: Crack Length vs. Time for a Terpolymer Hydrogel  
Containing 10 mol % MMA

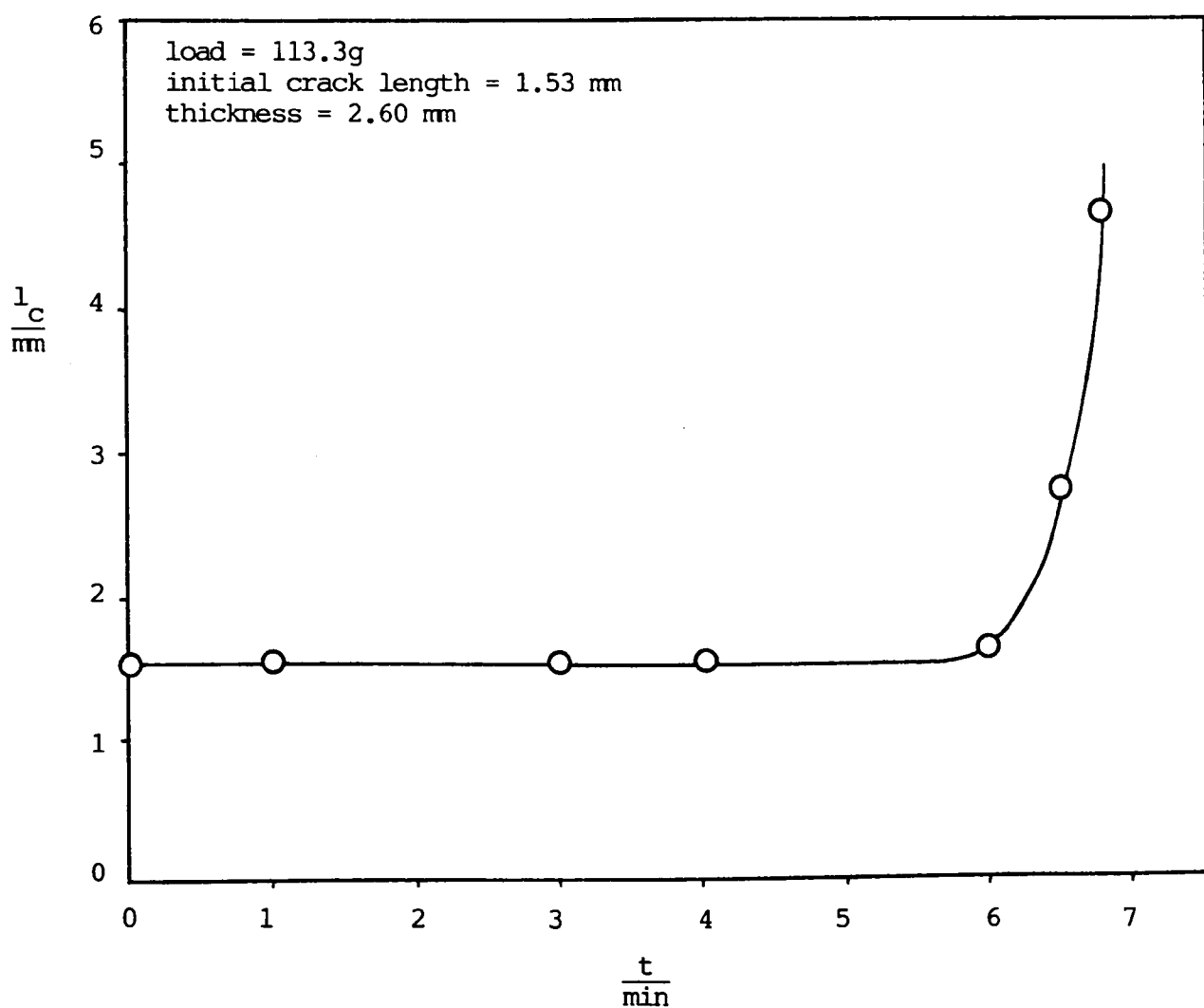


Fig. 4-20: Crack Length vs. Time for a Terpolymer Hydrogel Containing  
15 mol % MMA

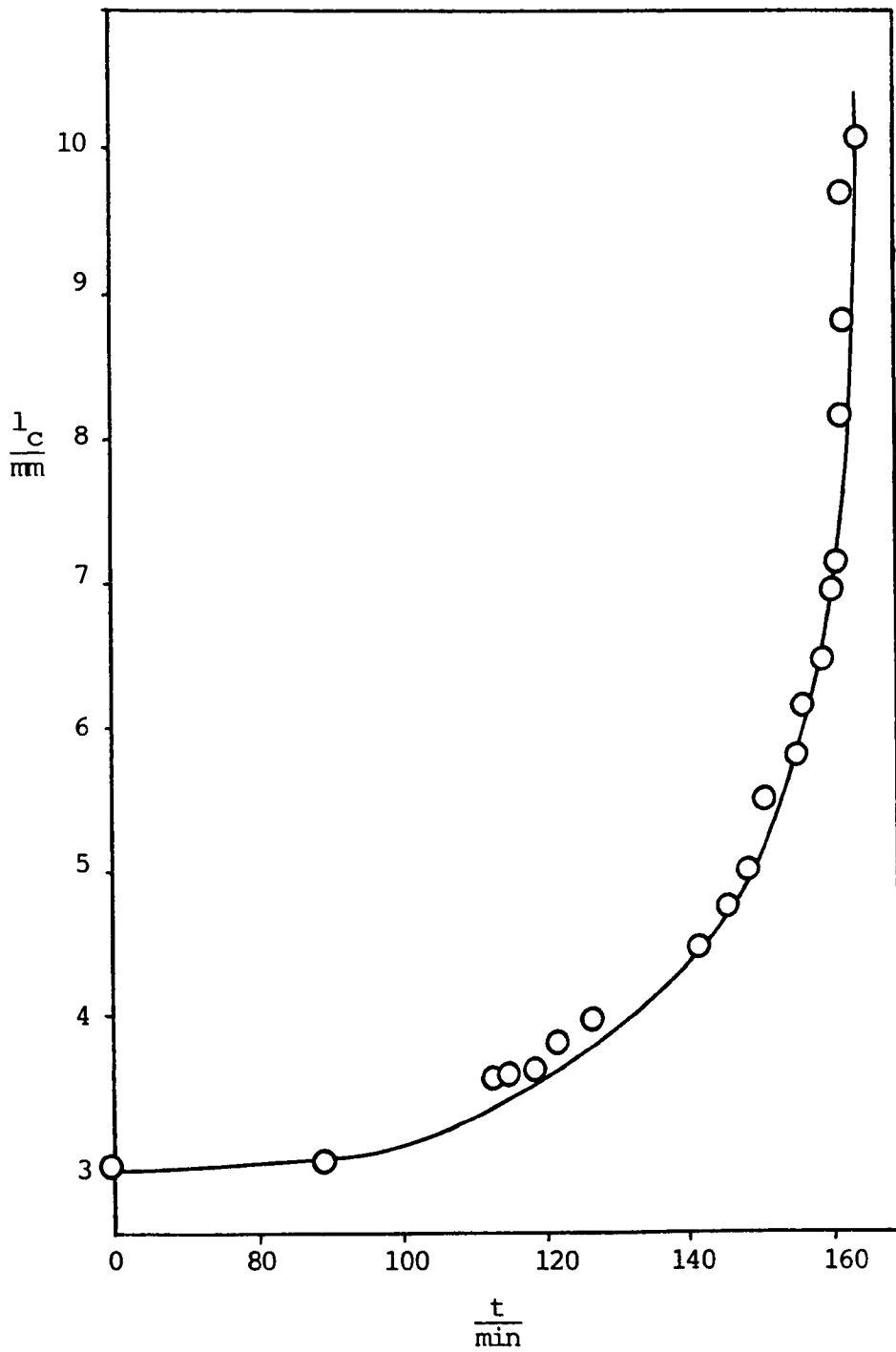


Fig. 4-21: Crack Length vs. Time for a Terpolymer Hydrogel Containing  
30 mol % MMA

Table 4-5: Tearing Data for Terpolymer Hydrogel Containing  
15 mol % MMA

Sample	c/mm	$l_o$ /mm	$l_b$ /mm	$\epsilon_b$
1	0.84	34	39.8	0.17
2	4.0	26	29.4	0.13
3	2.0	31	35.0	0.13
4	4.0	31	35.0	0.13
5	1.69	31	35.7	0.15
6	3.01	31	34.7	0.12

Notes: c is the initial crack length,  $l_o$  is the initial sample length,  $l_b$  is the sample length at break, and  $\epsilon_b$  is the strain at break, i.e.  
 $\epsilon_b = (l_b - l_o)/l_o$ .

Figs. 4-22 to 4-27 show the results of low-extension modulus experiments for several HEMA/MMA/MAA terpolymer hydrogels. The stress-strain curve for the 0 % MMA sample (Fig. 4-22) was linear, until the stress reached the value of 16kPa and the strain 12%, when the slope of the curve began to decrease. The low-extension modulus obtained from the slope of the linear portion was 121kPa. The stress-strain curve for the 10% MMA sample (Fig. 4-23) was linear until the stress reached a value of 20kPa and the strain 12%, when the slope of the curve began to decrease. The low-extension modulus was 172kPa. Curves for two different but nominally identical 15% MMA samples (Figs. 4-24 and 4-25) were linear, their low-extension moduli being 159 and 92kPa. There is therefore a degree of irreproducibility within these experiments. Fig. 4-26 shows the stress-strain curve for the 20% MMA sample. Although the stress increased with increasing strain,

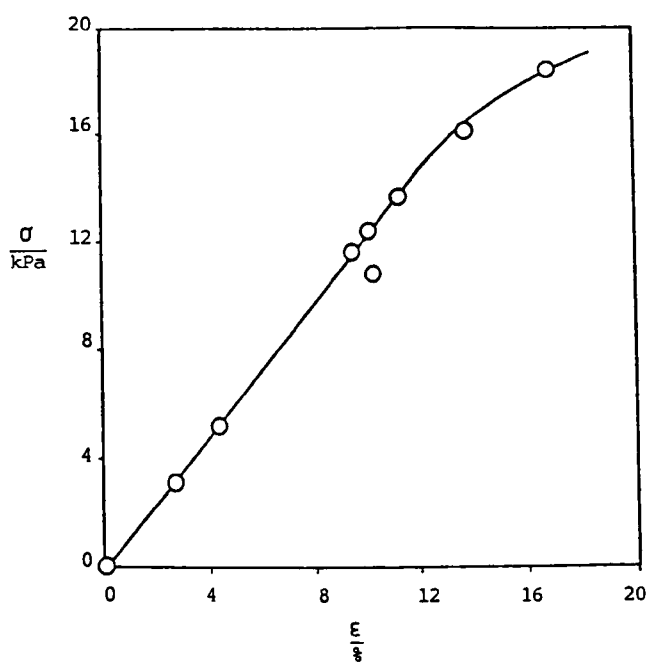


Fig. 4-22: Stress-Strain Curve for a Terpolymer Hydrogel Containing  
0 % MMA, Measured by Hanging Weights

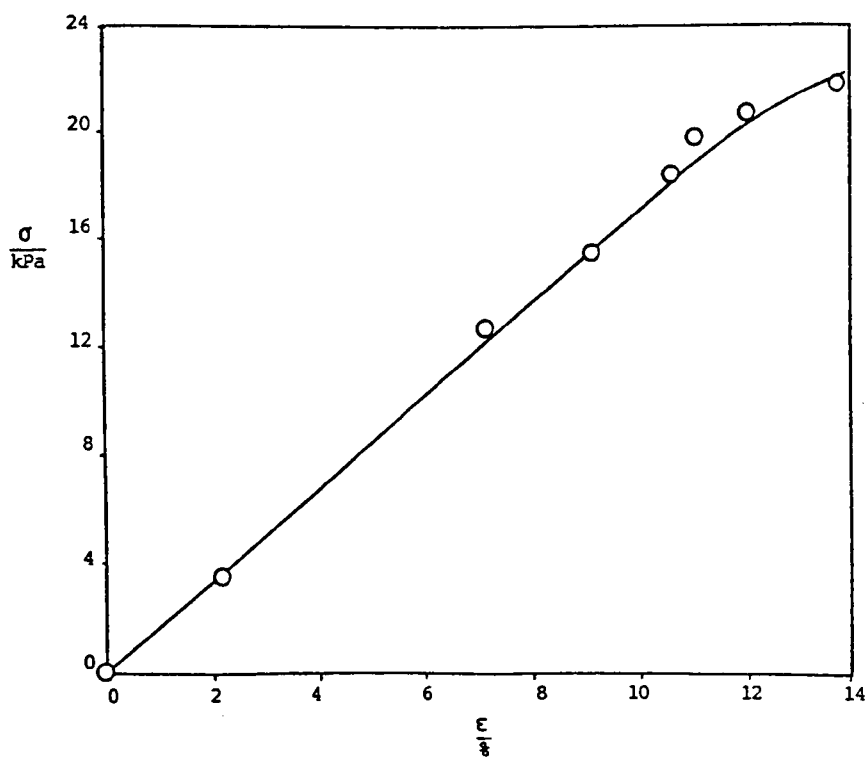


Fig. 4-23: Stress-Strain Curve for a Terpolymer Hydrogel Containing  
10 % MMA, Measured by Hanging Weights

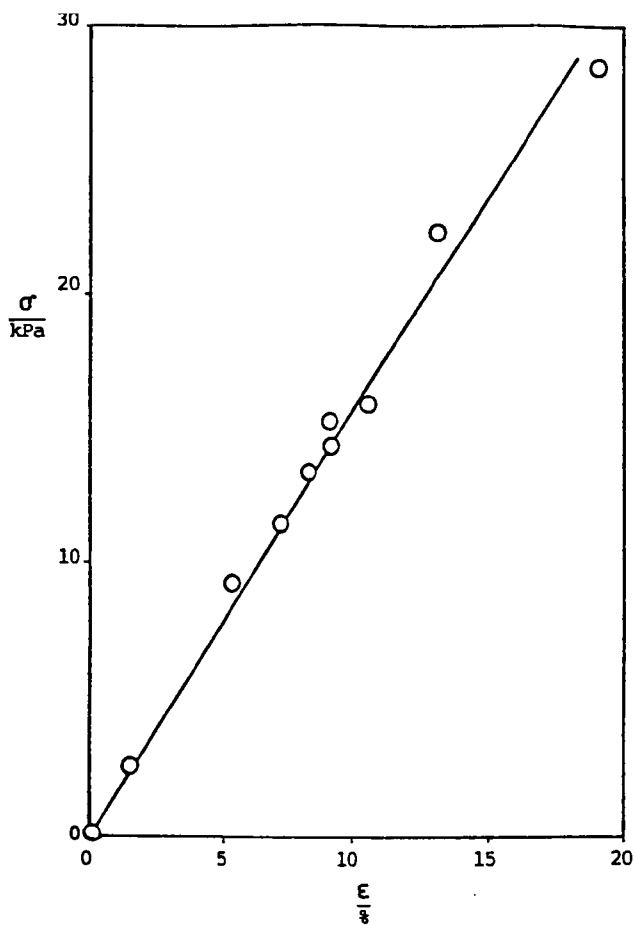


Fig. 4-24: Stress-Strain Curve for a Terpolymer Hydrogel Containing 15% MMA, Measured by Hanging Weights

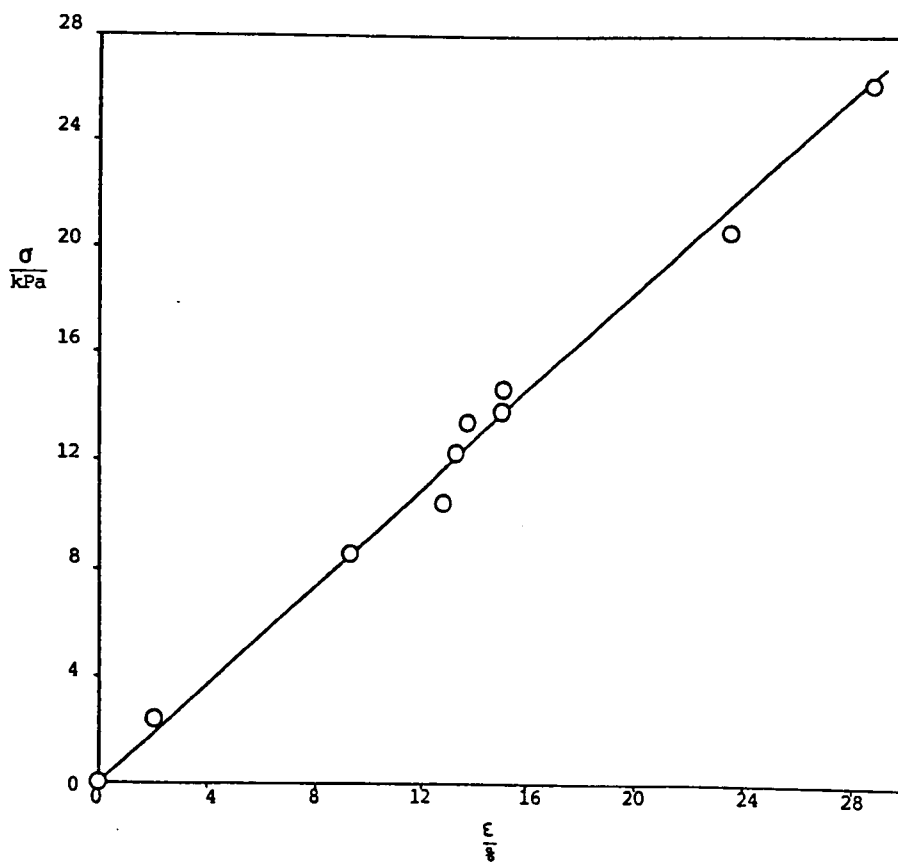


Fig. 4-25: Stress-Strain Curve for a Further Hydrogel Containing 15 mol % MMA, Measured by Hanging Weights

Fig. 4-26: Stress-Strain Curve for a Terpolymer Hydrogel Containing  
20% MMA, Measured by Hanging Weights

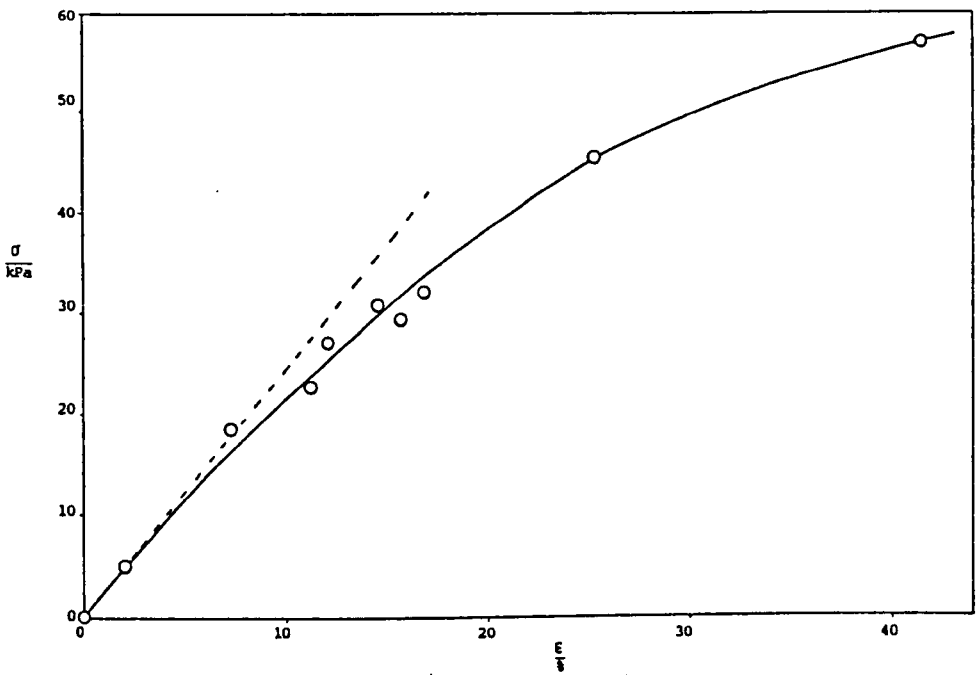
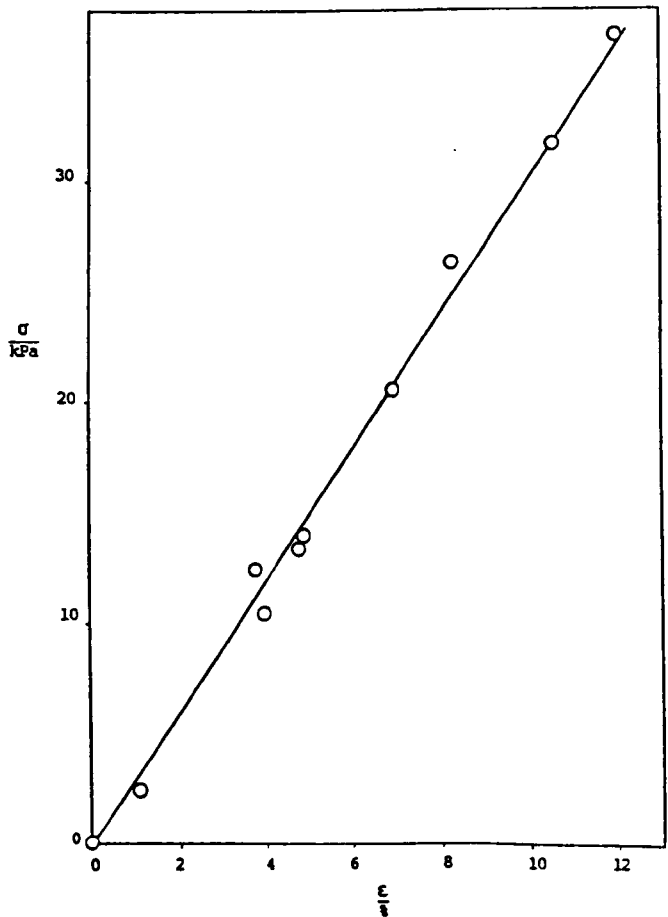


Fig. 4-27: Stress-Strain Curve for a Terpolymer Hydrogel Containing  
30% MMA, Measured by Hanging Weights





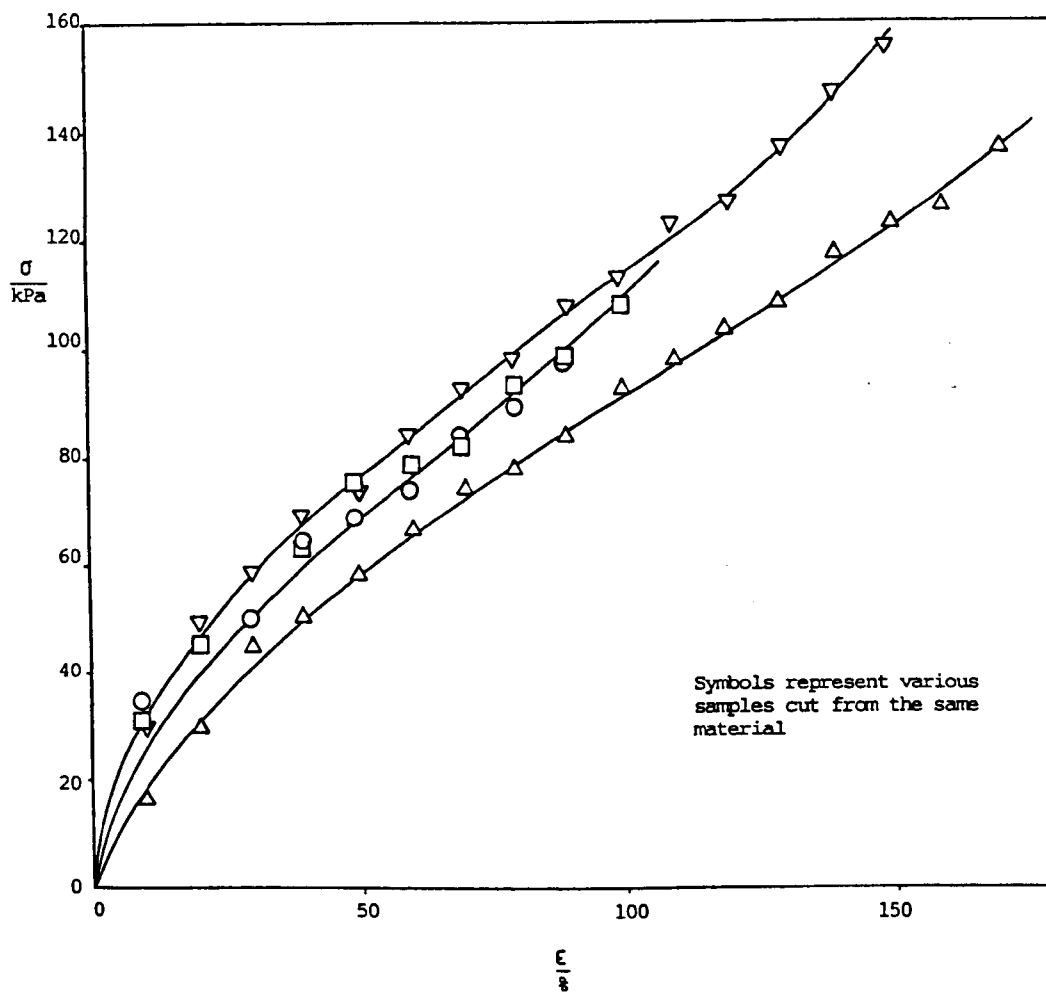
the slope decreased. The low-extension modulus was 245kPa. The stress-strain curve for the 30 mol % sample is shown in Fig. 27. It is linear, the low-extension modulus being 305kPa.

The stress-strain curves up to higher strains for the 20 % MMA sample are shown in Fig. 4-28. The strains were measured with an extensometer attached to the Instron physical testing machine. The slopes of the curves decrease at lower strains, with increasing strain, but, at a strain of approximately 100%, the slopes start to increase. There were differences in the values of stress at given values of strain between each sample. The similarity in shape between the curves and stress-strain curves for vulcanised strain-crystallising rubbers provides some evidence that the terpolymer hydrogels may crystallise on stretching.

The transparency of the hydrogels has been discussed in Section 4.3.1. The swelling ratio  $q$  is shown as a function of  $P$ , the mole fraction of MMA, in Fig. 4-29. Compared with the curve for the HEMA(1)-MAA-MMA terpolymers, the curve appears linear. However, when the point for 100% PMMA is included, a curve similar to that observed for the HEMA(1)-MAA-MMA terpolymers is observed. The implications of the shape of this curve have been discussed above.

Fig. 4-18 shows that, like the previous terpolymers, the tensile strength of the swollen terpolymers increases with increasing proportion of MMA. For a given composition, the tensile strengths are slightly lower than those for the previous terpolymers. One reason for this difference may be an increased level of MAA as an impurity in the HEMA(1), whereas in HEMA(3) much of the MAA has been removed during the purification procedure. This hypothesis is in keeping with the EWC/composition data of Figs. 4-7 and 4-17, which show that for a given composition, the EWC of the hydrogel containing HEMA(3) is lower

Fig. 4-28: Stress-Strain Curve for a Terpolymer Hydrogel Containing  
20% MMA, Measured on the Instron



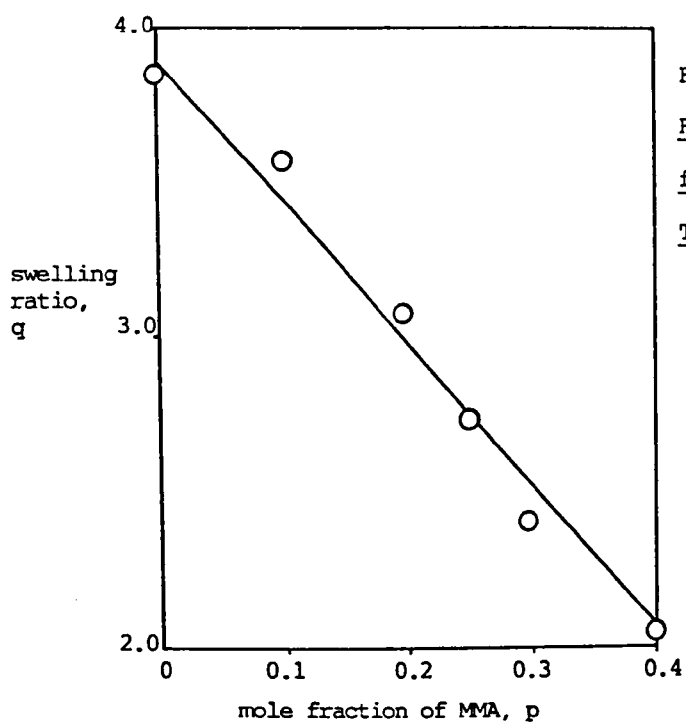


Fig. 4.29: Swelling Ratio vs. Composition  
for HEMA(3)-MAA-MMA  
Terpolymers

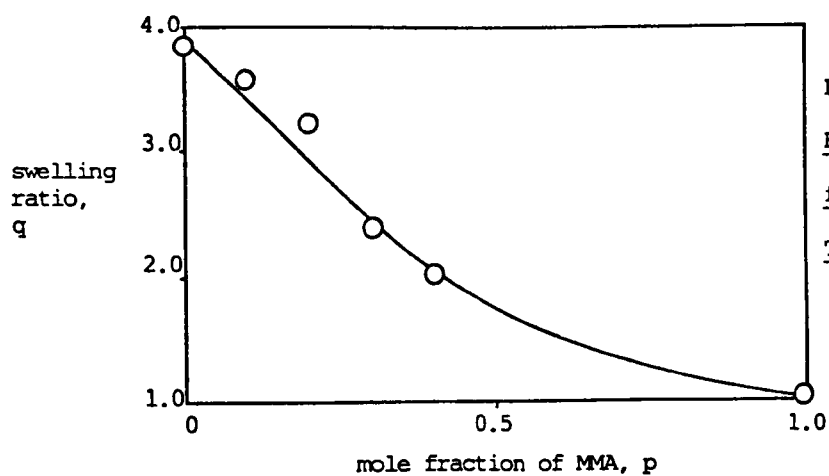


Fig. 4.30: Swelling Ratio vs. Composition  
for HEMA(3)-MAA-MMA  
Terpolymers



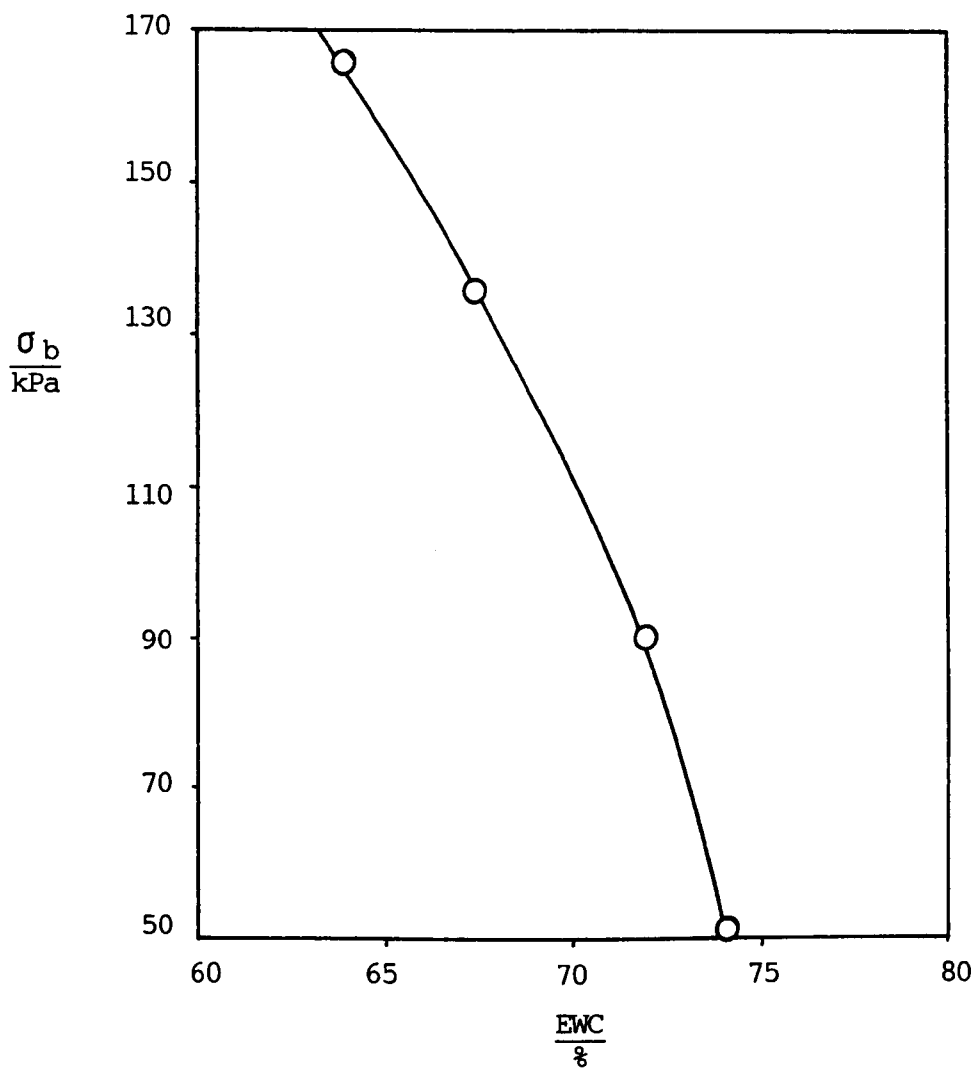
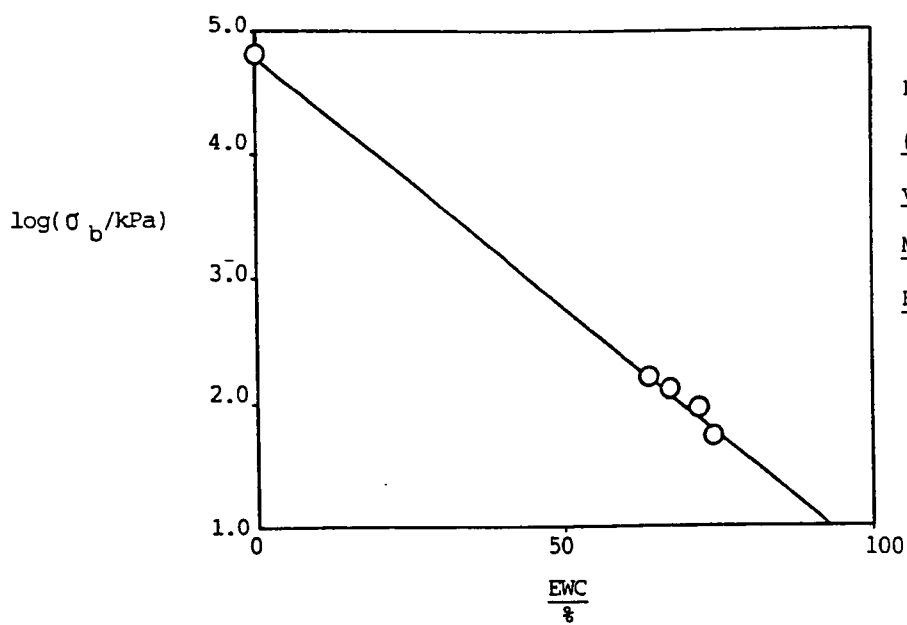
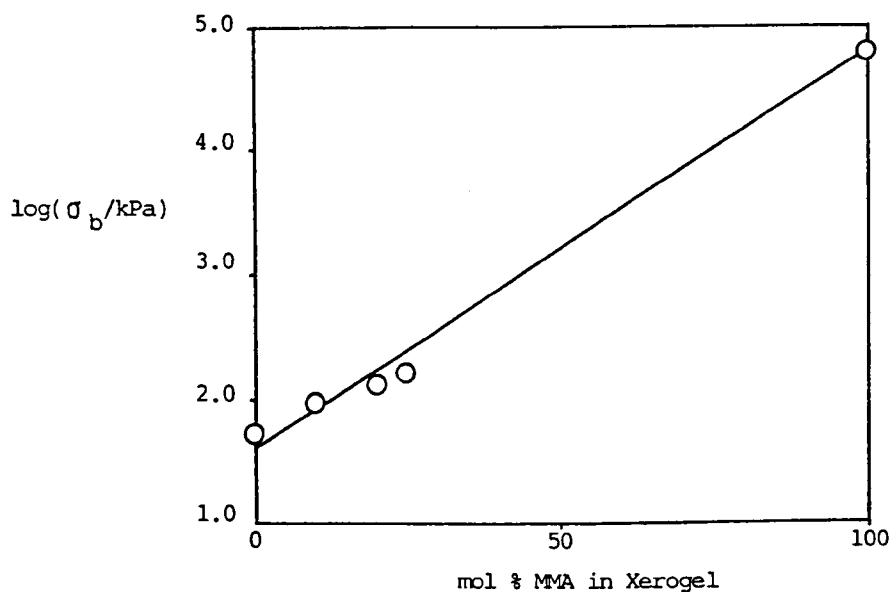


Fig. 4-31: Tensile Strength vs. EWC for HEMA(3)-MAA-MMA Terpolymer Hydrogels extrapolated from Fig. 4-7



two materials, the fracture of the gel being similar to the tearing of an elastomer rather than to the brittle fracture of a glass-like substance.

It may be surmised that the type of rupture at low levels of MMA is similar to that of brittle, glassy materials. Intermediate levels of MMA, giving lower EWCs, produce more rubber-like tearing, while those containing high levels of MMA are again brittle in their behaviour. The materials behave like elastomers in the mid-range of MMA levels.

The tearing results obtained for the 15 mol % MMA material using the Instron can be used to estimate the energy required to tear the material. The procedure of Rivlin and Thomas (1933) was used. The theoretical basis is that the reduction in elastically-stored energy which is produced by cut growth is balanced by the sum of contributions from the increase in surface energy (as in the Griffith theory) and from other energy changes. These other energy changes are assumed to be proportional to the increase in cut length. The rate of change of the free energy of deformation of the sample with cut length,  $(\partial w / \partial c)$ , is given by

$$-(\partial w / \partial c)_1 = Tt \quad \dots(4-14)$$

where  $t$  is the thickness of the sample,  $T$  is the "tearing energy", which is not identical to the surface free energy, but which should be independent of the type of test and of sample size. The suffix 1 indicates that  $(\partial w / \partial c)$  is at constant sample level. The procedure used to calculate  $T$  is as follows:

- (i) Force-length curves are obtained for samples with various cut lengths  $c$  (in this case single edge-notch samples).

- (ii) The length of the sample at which catastrophic tearing occurs is plotted against the initial cut length for each sample.
- (iii) From the force/length curves, the work of deformation  $W_1$ , at a chosen length  $l_1$  is found. This is equal to the area under the curve up to that point.  $W_1$  is then plotted against  $c$ .
- (iv) From the  $l_b/c$  graph, the value of  $c$  at  $l_b = l_1$  is found.
- (v) The slope of the  $W/C$  graph at this value of  $c$  is measured, and is equal to  $(\partial W/\partial c)_{l_1}$ .
- (vi)  $T$  is then found from equation 4-14.

In the case of samples 1 and 2, the initial length was not 31mm, as was the case for the other two samples. The values of  $l_b$  for samples 1 and 2 were adjusted to those expected for samples of length 31mm, using the expression

$$l_b = 31 \times (1 + \epsilon_b) \quad \dots(4-15)$$

where  $l_b$  is the predicted value of  $l_b$  for a sample of initial length 31mm, and  $\epsilon_b$  is the extension ratio at which catastrophic tearing occurred. Fig. 4-34 shows the values of  $l_b$  plotted against the initial crack length  $C$ . A value of  $l_b$  of 35.7mm was chosen; at this length  $\epsilon_b = 0.15$ . The value of  $C$  corresponding to this length was found from Fig. 4-34.

Values of  $W_1$  at  $l_1 = 35.7\text{mm}$  were found from each force/length curve by measuring the area under it by dividing the area into triangles. This could readily be accomplished because each curve was approximately linear. These values of  $W_1$  are plotted against  $c$  in Fig. 4-35. The curve was drawn to have a similar shape to that of Rivlin and Thomas (173). Its slope,  $\partial W_1/\partial c$ , was measured at the value of  $c$  corresponding



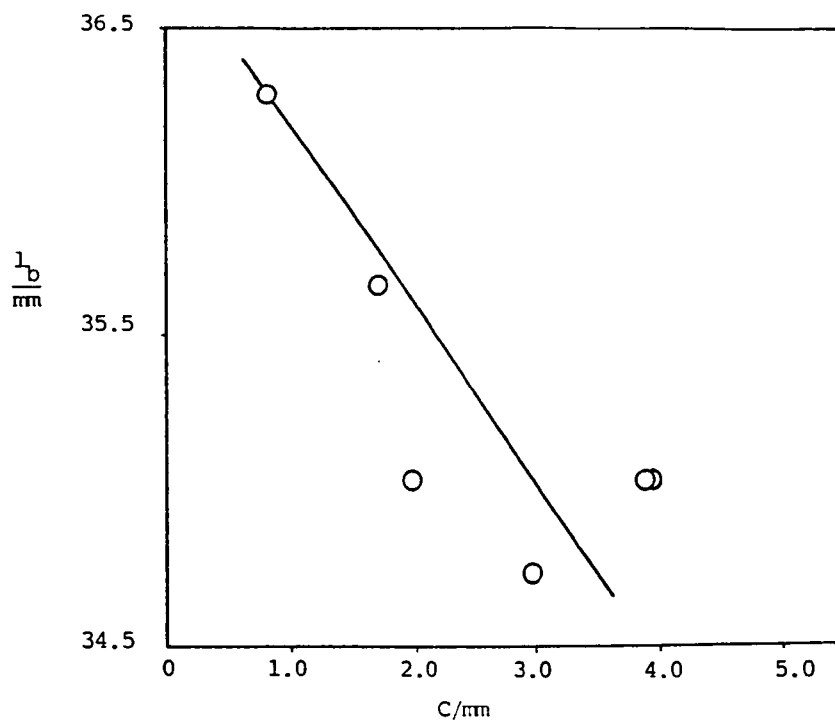


Fig. 4-34: Sample  
Length at Break vs.  
Initial Crack Length

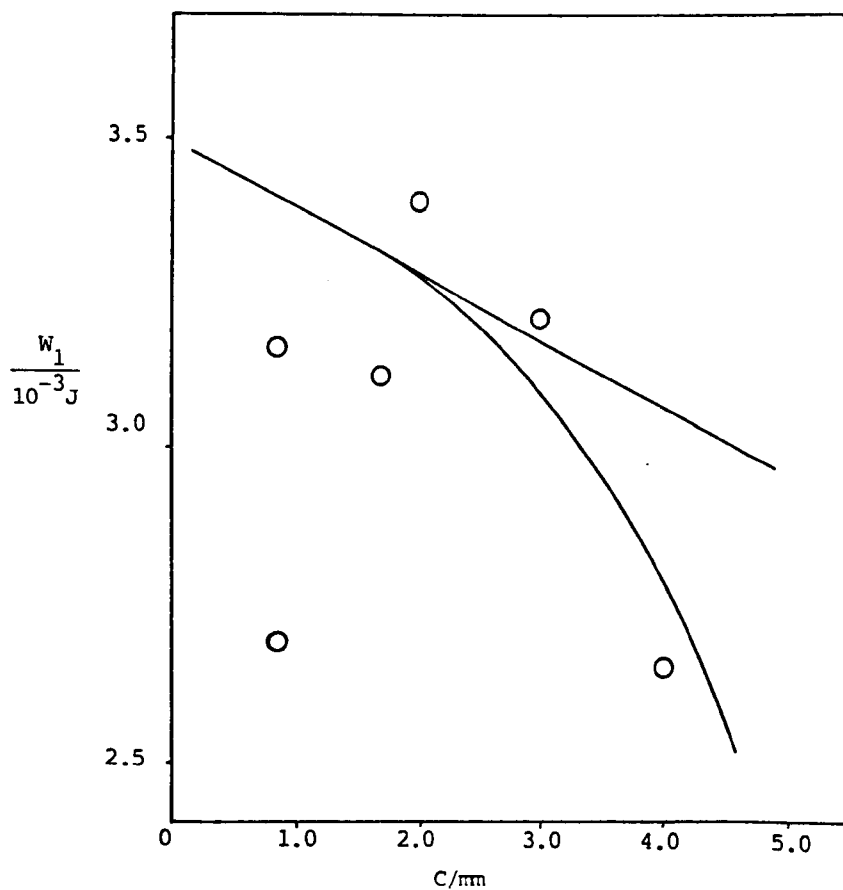


Fig. 4-35: Work of  
Deformation at E =  
0.15 ( $l = 35.7\text{mm}$ ) vs.  
Initial Crack Length

to  $l_b = l_1 = 35.7\text{mm}$ . The slope at this point was found to be  $-0.113\text{Jm}^{-1}$ . The thickness of the samples was  $2.74\text{mm}$ , and hence from equation 4-14 the tearing energy was calculated as  $41\text{Jm}^{-2}$ .

The scattering of the points in both Fig. 4-34 and Fig. 4-35 is large, but although this is the case, the value of  $T$  is of the same order of magnitude as  $T$  obtained for various terpolymer hydrogels using the "trouser" test method and shown in Fig. 4-51.

Rivlin and Thomas (173) found values of  $T$  of approximately  $1.2 \times 10^4$  to  $1.4 \times 10^4\text{Jm}^{-2}$  for vulcanised natural rubber. The difference between the magnitudes of  $T$  for natural rubber and for the terpolymer hydrogels is striking. It suggests that the hydrogels undergo brittle fracture, rather than rubber-like tearing, in agreement with what has been postulated above. In view of both the large degree of experimental error (which Rivlin and Thomas estimated to be  $\pm 30\%$ ), and the time-consuming nature of these experiments, subsequent tearing data were obtained by means of the "trouser" test method. However, the two sets of experimental results tentatively support the hypothesis of Rivlin and Thomas that the tearing energy  $T$  is a material property which is independent of the method of testing. The stress-strain curves for the terpolymers at low strain values, obtained from hanging-weight experiments, show generally good linearity at low strains. Hence at low strains, the gels behave as Hookean materials. There is a small amount of scatter in the experimental data, but on the whole the precision is satisfactory. The two points for 15 mol % MMA terpolymer hydrogels show that there is a problem with irreproducibility. The low-extension modulus as a function of composition is shown in Fig. 4-36. The modulus increases with increasing mol % MMA.

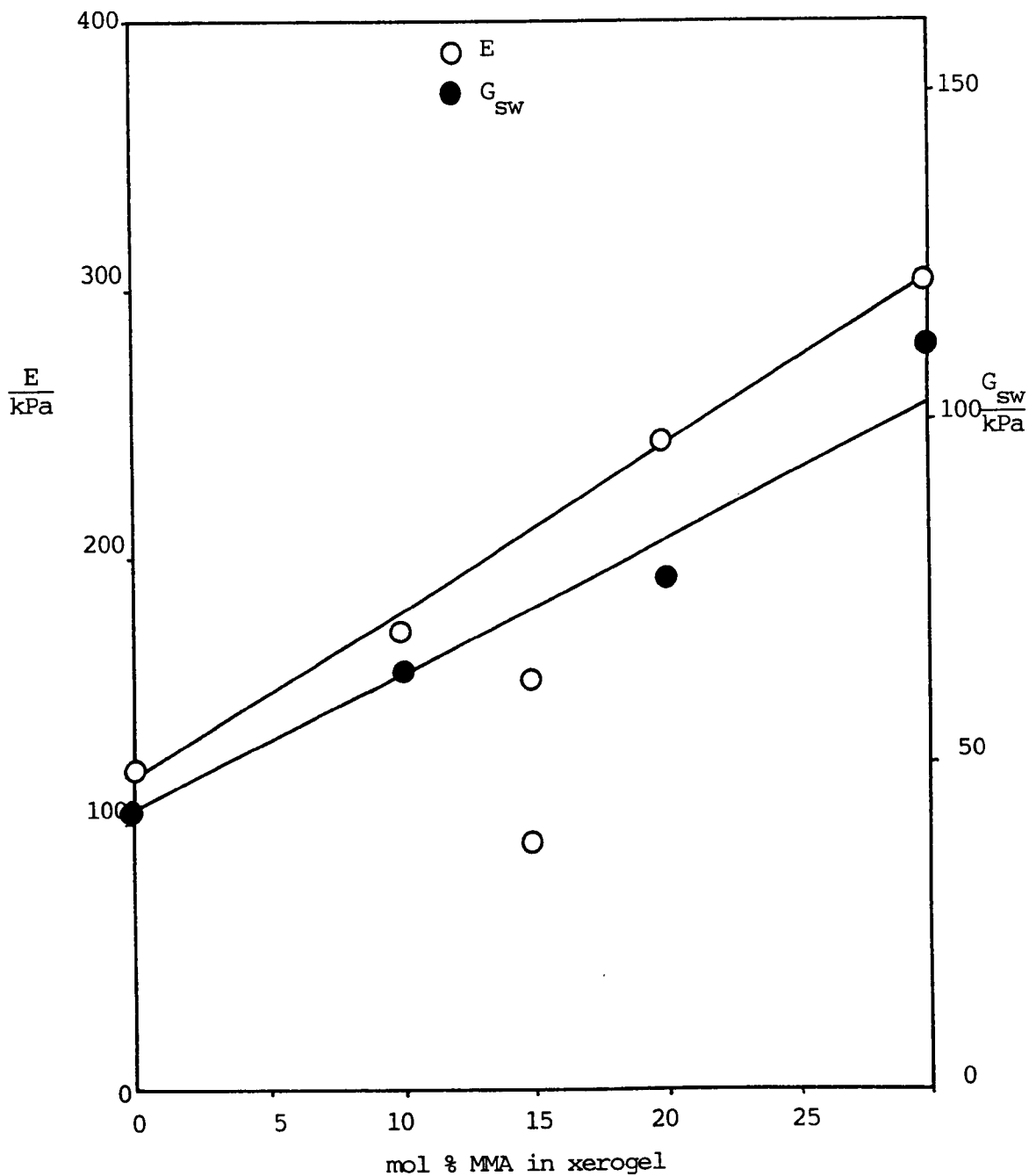


Fig. 4-36: Low-Extension Young's Modulus and Shear Modulus vs. Composition for HEMA-MAA-MMA Terpolymer Hydrogels

This increase may be caused by a combination of at least two factors:

- (i) the decrease in water content of the materials with concomitant increase in the concentration of network chains;
- (ii) an increase in the effective crosslink concentration caused by an increase in the concentration of physical crosslinks, e.g. through hydrophobic bonding;
- (iii) phase-separation of MMA-rich domains.

More information can be obtained from the shear modulus of the terpolymer hydrogels,  $G_{sw}$ . This is obtained as the initial slope of the curve of stress against  $(\lambda - \lambda^{-2})$ , where  $\lambda$  is given by

$$\lambda = 1 + \epsilon \quad \dots(4-16)$$

Such plots for HEMA(3)-MAA-MMA materials are shown in Figs. 4-37 to 4-40. The data were obtained from the hanging-weight experiments. Straight lines can be drawn through all the plots, although the 20% material begins to deviate from linearity at  $(\lambda - \lambda^{-2}) \approx 0.6$ . (Tensile stress-strain data for the 20 mol % MMA material extended to higher strains are plotted as stress vs.  $\lambda - \lambda^{-2}$  in Fig. 4-43. The curve is linear up to strains of about 100%.) The shear moduli obtained from these plots are shown in Fig. 4-36 as a function of composition, and in Fig. 4-41 as a function of EWC. The shear modulus increases as the proportion of MMA in the material increases, which is expected, since for an "ideal" elastomer, the shear modulus is proportional to the concentration of crosslink sites. As the proportion of MMA is increased, the EWC decreases, and therefore the concentration of crosslink sites increases. The shear modulus therefore decreases with increasing water content. The elementary theory of rubber elasticity

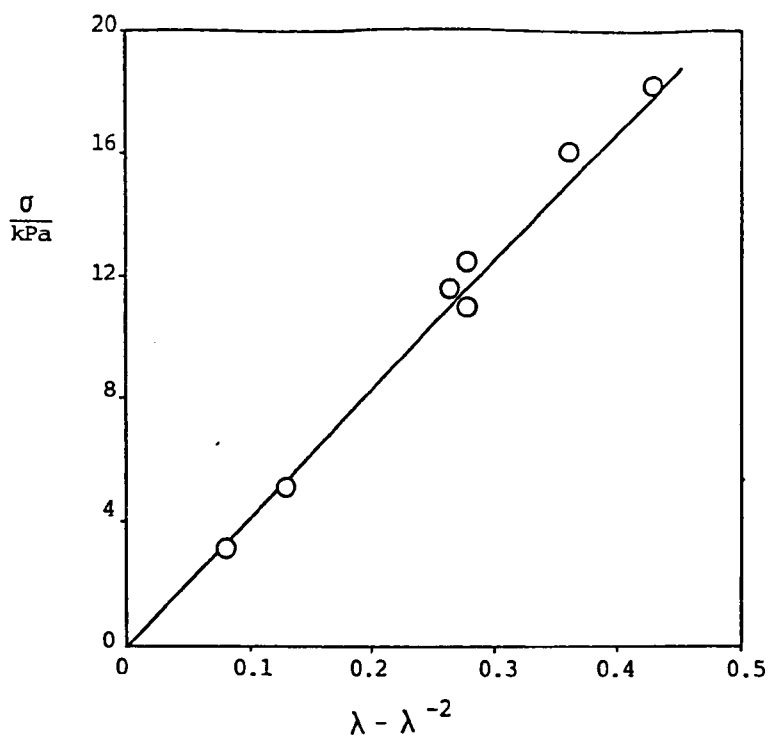


Fig. 4-37:  $\sigma$  vs.  $\lambda - \lambda^{-2}$  for Terpolymer Hydrogel Containing 0% MMA,  
Measured by Hanging Weights

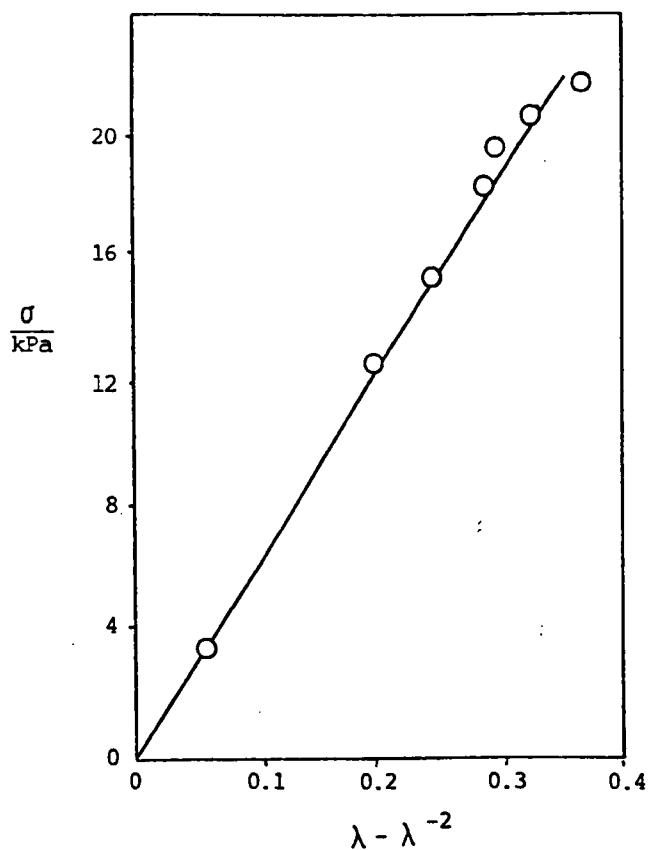


Fig. 4-38:  $\sigma$  vs.  $\lambda - \lambda^{-2}$  for Terpolymer Hydrogel Containing 10% MMA,  
Measured by Hanging Weights

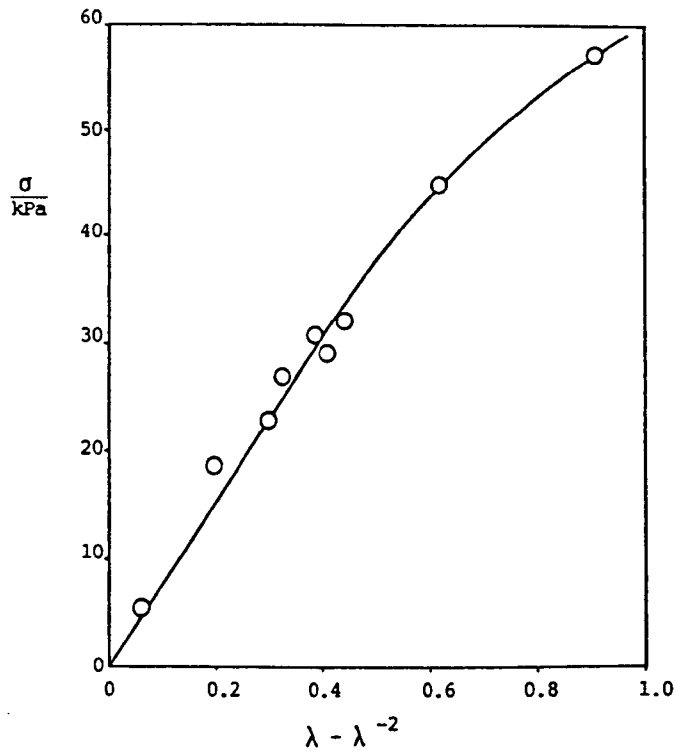


Fig. 4-39:  $\sigma$  vs.  $\lambda - \lambda^{-2}$  for Terpolymer Hydrogel Containing 20% MMA,  
Measured by Hanging Weights

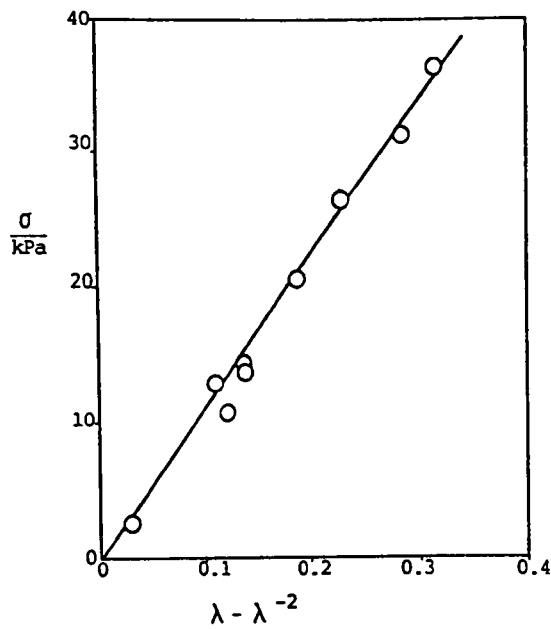


Fig. 4-40:  $\sigma$  vs.  $\lambda - \lambda^{-2}$  for Terpolymer Hydrogel Containing  
30 mol % MMA, Measured by Hanging Weights

Fig. 4-41: Low-Extension Young's Modulus and Shear Modulus vs. EWC  
for HEMA(3)-MAA-MMA Terpolymer Hydrogels

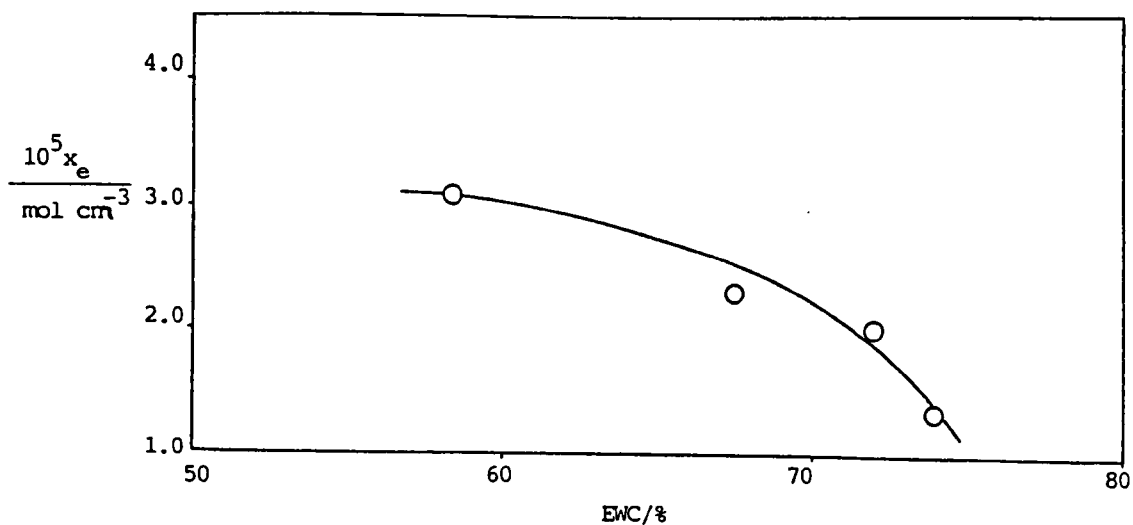
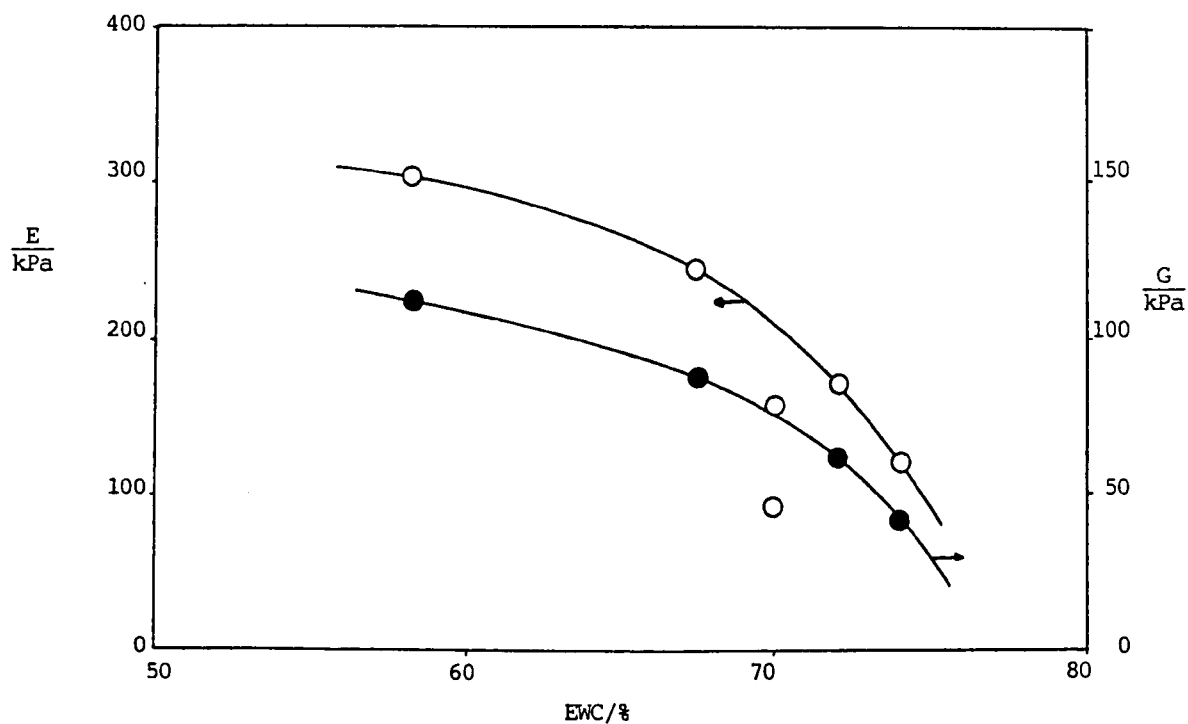


Fig. 4-42: Crosslink Concentration of Polymer Calculated from Shear  
Moduli vs. EWC for HEMA(3)-MAA-MMA Terpolymer Hydrogels

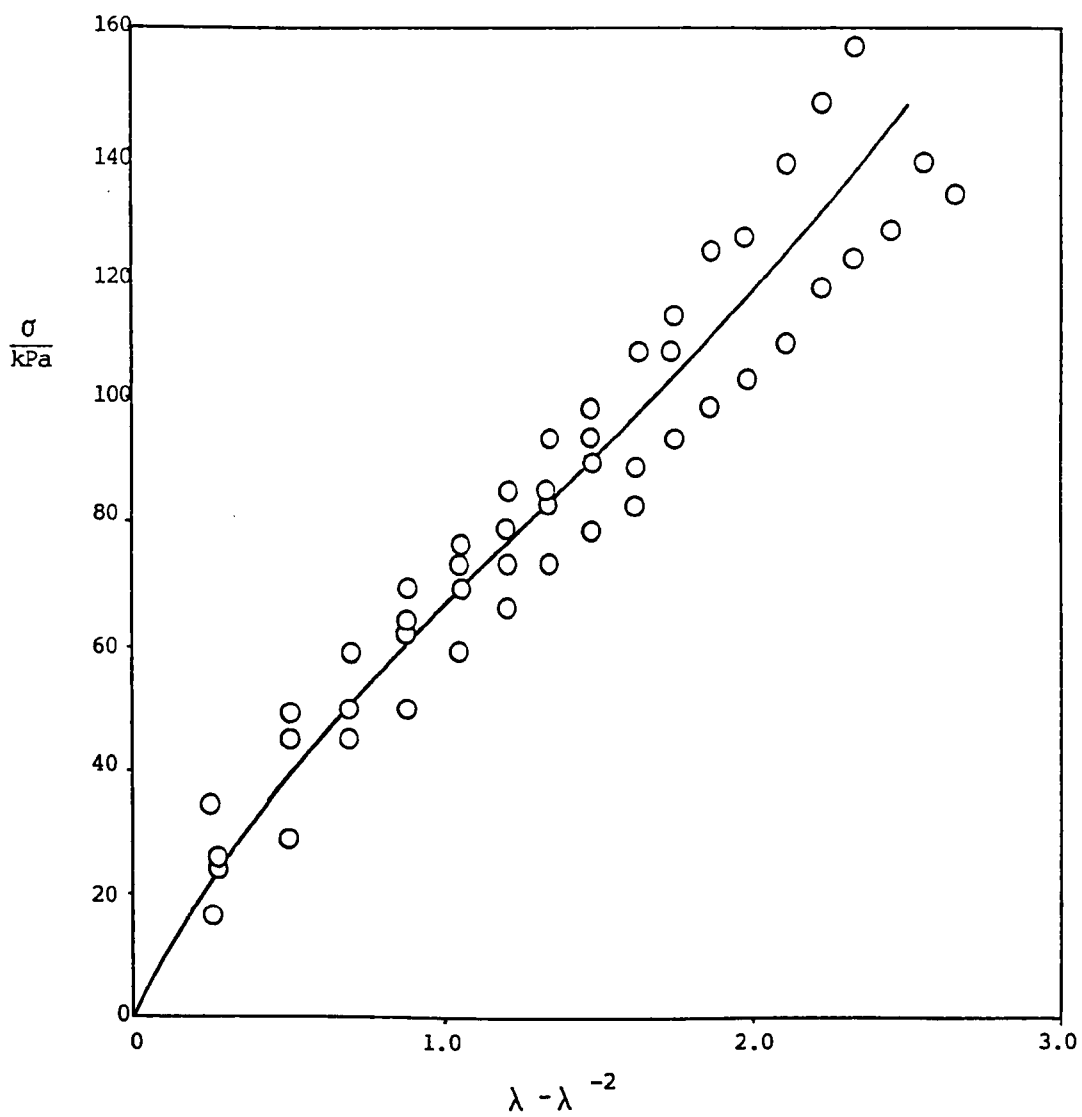


Fig. 4-43:  $\sigma$  vs.  $\lambda - \lambda^{-2}$  for Terpolymer Hydrogel Containing 20 mol % MMA,  
Measured on the Instron



(191) predicts that the shear modulus,  $G$ , of a dry rubber is given by

$$G = 2x_e kT \quad \dots(4-17)$$

where  $x_e$  is the concentration of crosslink sites in the dry rubber, if the crosslinks are tetrafunctional,  $k$  is Boltzmann's constant, and  $T$  is the absolute temperature. For a swollen material, the modulus  $G_{sw}$  is given by

$$G_{sw} = 2x_e kT V_2^{\frac{1}{3}} \quad \dots(4-18)$$

where  $V_2$  is the volume fraction of polymer in the swollen material. Values of  $x_e$  calculated from equation 4-18 are shown in Table 4-6, together with values calculated from the concentration of crosslinker in the polymerisation mixture from which the terpolymers were prepared. The assumptions made were:

- (i) that the volume fraction of polymer is approximately equal to the weight fraction;
- (ii) that the dry polymer density is equal to that of the swelling agent.

Equation 4-18 is applied to materials such as natural rubber, which are rubbery both in the swollen and unswollen states. The hydrogel terpolymers, however, although rubbery in the swollen state, are glassy materials in the unswollen state. The applicability of equation 4-18 to the hydrogel terpolymers may be argued as follows. A "fictional" crosslink concentration may be determined from the equation, which the material would contain if it were rubbery in both the swollen and

unswollen states. This is equal to the real crosslink concentration if it is assumed that passage through the secondary glass-rubber transition does not affect the total number of crosslink sites.

Table 4-6: Values of Concentration of Crosslink Sites Obtained from Shear Moduli Compared with those expected on Basis of Quantity of EGDMA used for Preparation of Terpolymer Hydrogels

mol%MMA	EWC/%	$V_2$	$G_{sw}/\text{kPa}$	$\frac{x_e 10^5}{\text{mol cm}^{-3}}$	$\frac{x_{calc} 10^5}{\text{mol cm}^{-3}}$
0	74.0	0.260	42	1.4	3.1
10	72.0	0.280	63	2.0	3.2
20	67.5	0.325	77	2.3	3.3
30	58.4	0.416	112	3.1	3.3

These results seem to indicate that the increase in effective crosslink density which occurs as the proportion of MMA is increased would be expected on the basis of reduced water content. The values of  $x_e$  are shown graphically as a function of EWC in Fig. 4-42. At very low levels of MMA, the crosslink concentration is smaller than that expected on the basis of the concentration of crosslinker, but as the proportion of MMA increases the effective crosslink concentration approaches the crosslinker concentration, until at 30% MMA  $x_e$  is approximately equal to the crosslinker concentration. If, as Refojo has suggested the chemical crosslinking in poly(HEMA) is augmented by a system of hydrophobic physical crosslinks, it is reasonable to suppose that the total concentration of effective crosslinks increases as the polymer becomes more hydrophobic, thus explaining the observations reported here.

Several conclusions have been drawn from the results reported in this section:

- (i) The effective concentration of crosslinks in the dry terpolymers tends to increase as the MMA content increases and as the EWC of the hydrogel decreases.
- (ii) At low strains, the hydrogels behave as Hookean materials, and in tension over a limited strain range, they show "Gaussian" behaviour.
- (iii) In some cases, the stress-strain curve suggests a process analogous to strain-induced crystallisation, i.e. a similar shape to that of natural rubber was observed, although the modulus was very different.
- (iv) The tensile strengths of the materials increase with decreasing water content, whilst the tendency of the materials to tear in a rubber-like fashion also increases.
- (v) The tearing energy is similar in magnitude to the work of fracture of a glassy or ceramic material (190).

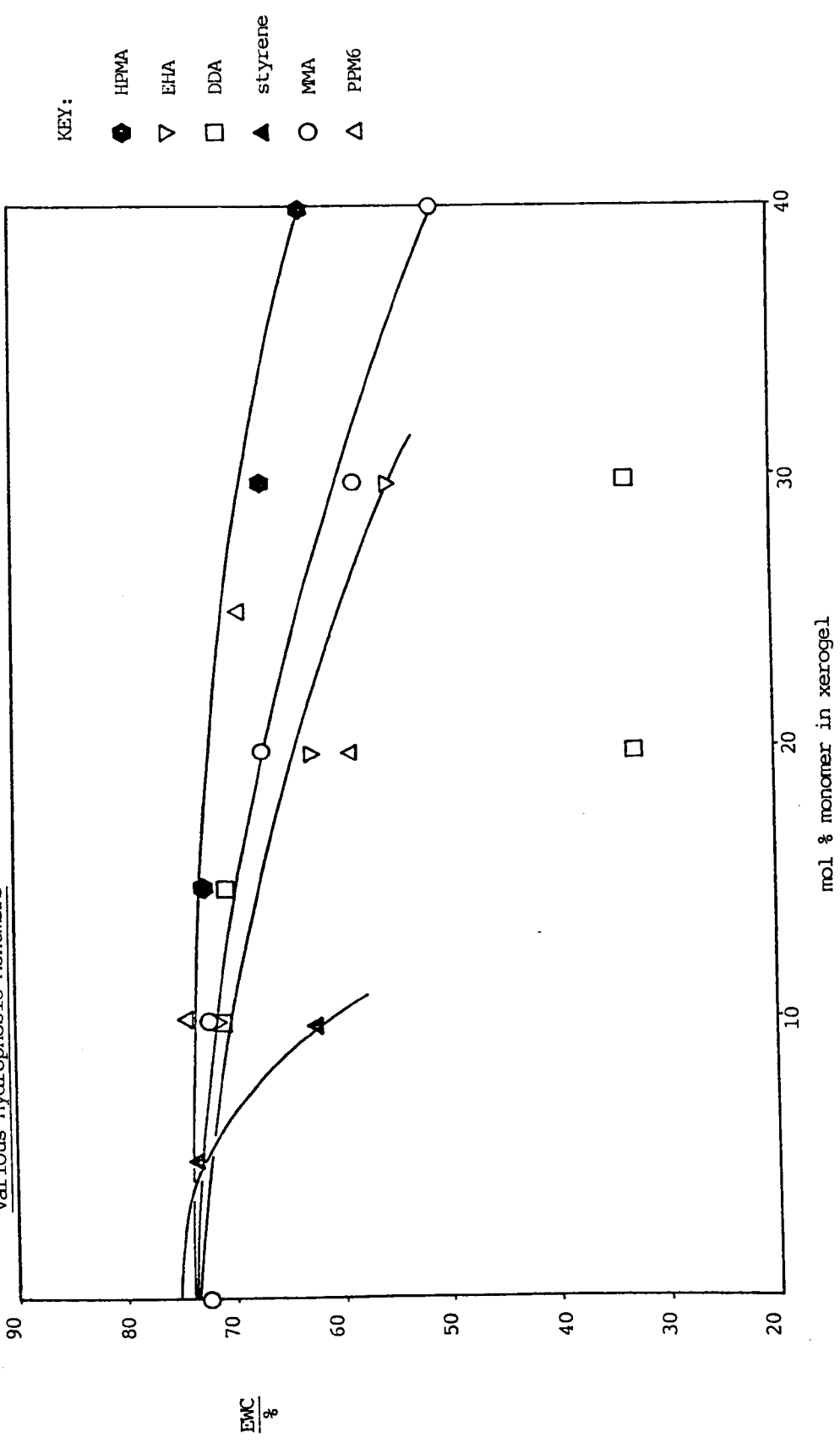
#### 4.4 GELS CONTAINING HEMA(3), MAA AND VARIOUS HYDROPHOBIC MONOMERS

All the terpolymers containing PPM6, MMA and HPMA were transparent in appearance. Those materials containing EHA above a proportion of about 20 mol % were translucent, as were those containing DDA above a proportion of 10 mol %. The purity of the DDA was approximately 60%, and therefore the actual composition was about 6 mol % DDA. Terpolymers containing more than 10 mol % styrene were inhomogeneous when placed in water. The materials were leathery in texture, patchy in appearance, with very little water uptake, and fairly rigid. Physical testing was not carried out because of the inhomogeneity of the materials. As might be expected, the hydrogels containing the more hydrophobic monomers show translucence when swollen, indicating some degree of phase separation. The greater hydrophobicity of styrene is shown not only in the greater reduction in EWC, but also in the inhomogeneity of the styrene-containing materials at higher levels of styrene.

Fig. 4-44 shows the equilibrium water contents of several hydrogels, as a function of the composition of the dry polymer. As the proportion of the hydrophobic monomer was increased, the EWC decreased. The decrease in EWC was most rapid when the hydrophobic monomer was styrene. At a composition of 10 mol % styrene, the EWC had decreased from 74.7% at 0% styrene to 63%. When the hydrophobic monomer was EHA, the EWC decreased to 60% when the composition was 26 mol % EHA. The least rapid reduction in EWC was observed using HPMA as the hydrophobic monomer. At a composition of 30 mol % HPMA, the EWC had decreased to approximately 70%. The EWC as a function of composition reflects the varying hydrophobicities of the monomers which were copolymerised with HEMA and MAA. Hydroxypropyl methacrylate has one more  $\text{CH}_2$  group than HEMA, and therefore its addition reduces the EWC slightly. The water contents of materials containing PPM6 are approximately equal

Fig. 4-44: EW vs. Composition for Terpolymer Hydrogels Containing

Various Hydrophobic Monomers



to those of materials of the same composition containing HPMA. Copolymerising with MMA reduces the EWC to a greater extent than does copolymerisation with HPMA or PPM6. MMA, unlike HPMA and PPM6, has no hydroxyl group. A perhaps surprising result is that the reduction in EWC caused by copolymerisation with EHA is only slightly greater than that caused by MMA, although EHA, comprising a C<sub>8</sub> hydrocarbon moiety attached to the methacrylate group, might be expected to be much more hydrophobic than MMA.

Fig. 4-45 shows the same data plotted as swelling ratio,  $q$ , as a function of composition. Although the points are rather scattered, straight lines can be drawn through the points for the terpolymers containing HPMA and EHA. The EHA line is the steeper of the two. The points for terpolymers containing styrene follow a different type of curve such that the reduction in EWC at compositions below 5 mol % styrene is very small, and the subsequent reduction at higher levels of styrene is much greater. In Section 4.2.2, it has been shown that it is difficult to draw quantitative conclusions concerning the nature of the mechanism of swelling from this type of data. However, what can be seen from Fig. 4-45 is that the reduction in EWC is dependent on the hydrophobic nature of the comonomer. Fig. 4-46 shows this more clearly. The "hydrophobicity" of the comonomer can be simply quantified by its overall ratio of number of oxygen to carbon atoms. This ratio is, of course, an inverse measure of hydrophobicity. Likewise, the hydrophobicity of the terpolymer can be simply quantified by the overall ratio of number of oxygen atoms to carbon atoms in the terpolymer. This ratio can easily be calculated from the composition of the terpolymer. For example, the O:C ratios for DDA, HEMA and MAA are respectively 2:15, 2:4 and 3:6. The molar ratio DDA/HEMA/MAA in a 10/90 DDA

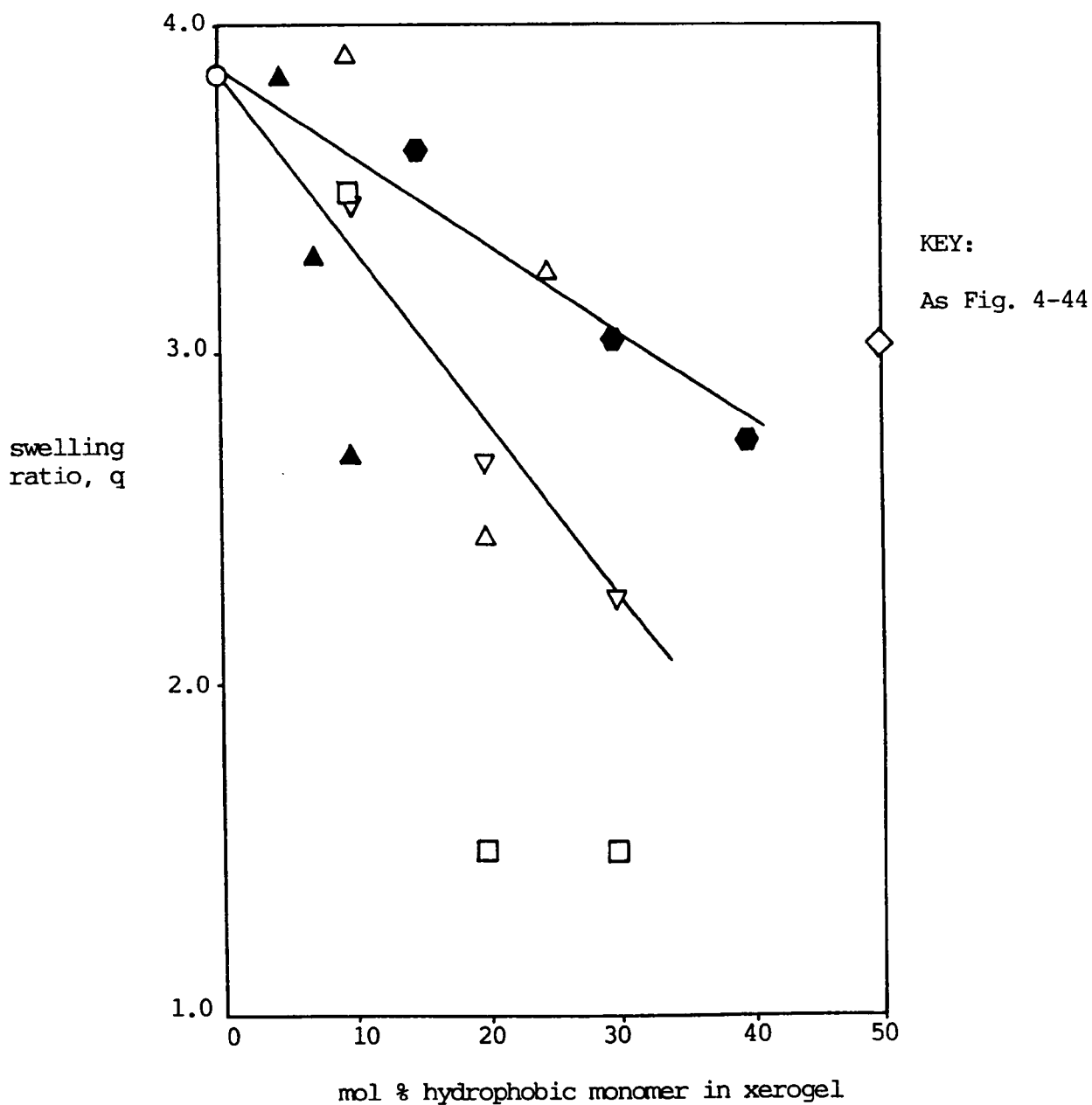


Fig. 4-45: Swelling Ratio vs. Composition for Terpolymers Containing Various Hydrophobic Monomers

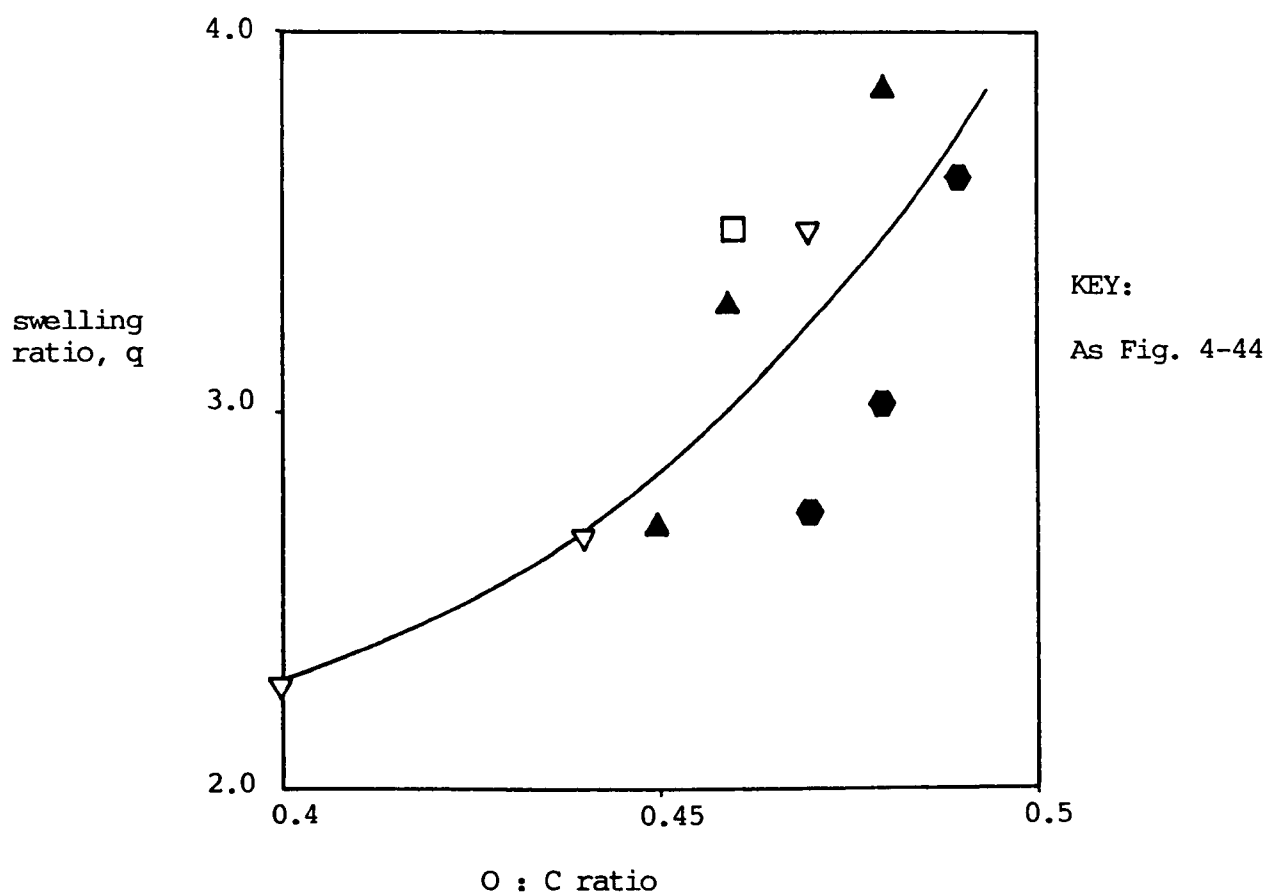


Fig. 4-46: Swelling Ratio vs. Overall Oxygen-Carbon Ratio for Terpolymers Containing Various Hydrophobic Monomers



(90/10 HEMA/MAA) terpolymer is 10/85.5/4.5, from which it follows that the overall O:C ratio is 1:2.54 or 0.394:1. Fig. 4-46 shows that the swelling ratio tends to increase as the O:C ratio increases, and therefore as the hydrophobicity decreases.

Little systematic work has been carried out on copolymers of monomers such as HEMA with hydrophobic comonomers. Kolarik and Migliaresi (47) observed that copolymerisation of ethyl acrylate (EA) with HEMA reduced the EWC to a greater extent for a given composition than did copolymerisation of butyl acrylate (BA) or dodecyl methacrylate (DMA) with HEMA. They postulated that DMA/HEMA copolymers containing 46-62% DMA were nonhomogeneous materials; although being transparent, they did not possess distinct phase boundaries and so could not therefore be classed as truly heterogeneous.

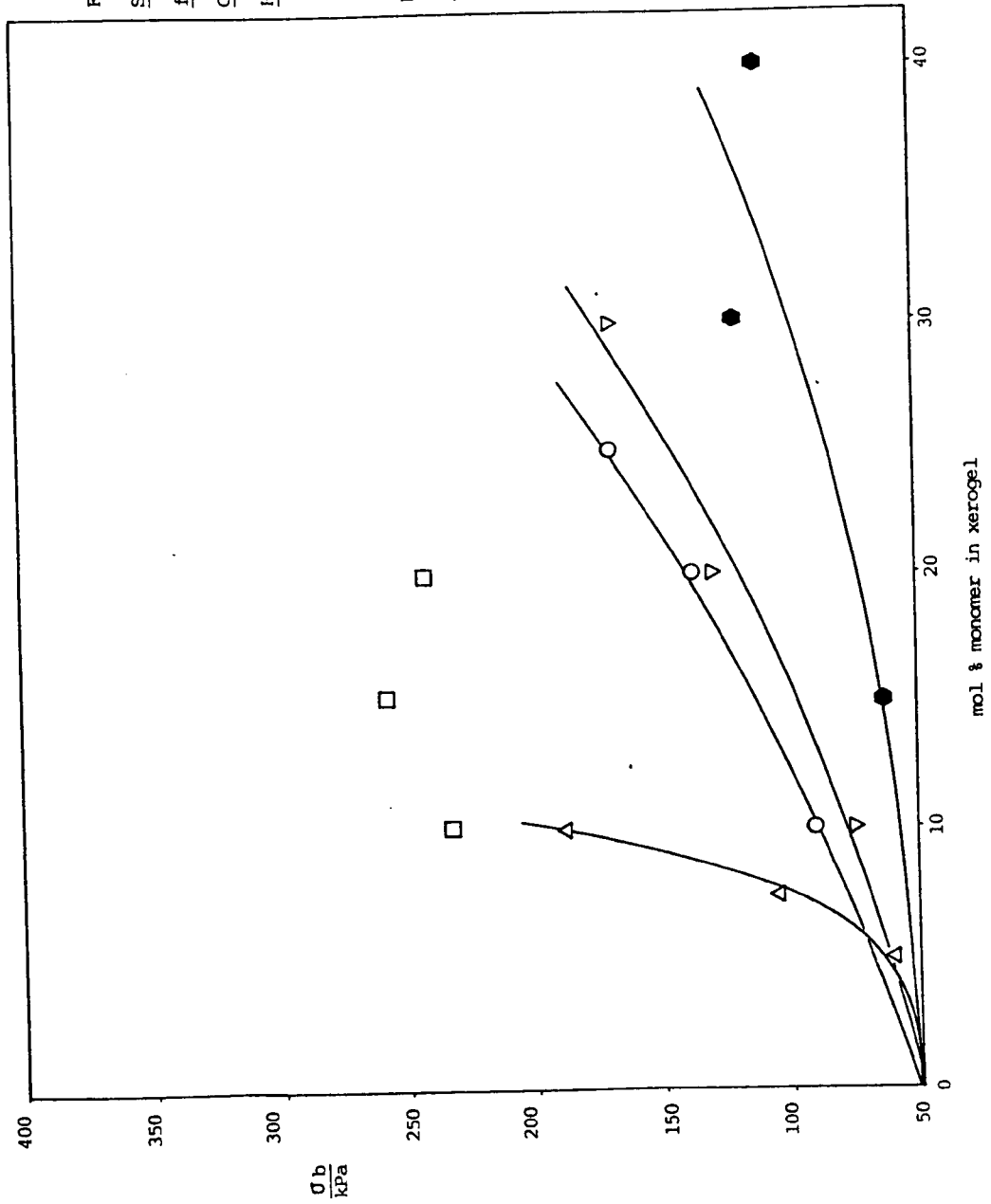
Fig. 4-47 shows the tensile strengths of the various terpolymer hydrogels as a function of composition. The general trend is for the tensile strength to increase with increasing proportion of hydrophobic monomer. The tensile strengths of the terpolymer hydrogels containing styrene increased gradually until the composition reached 5% styrene, when they increased more rapidly. The value at 10 mol % styrene was approximately 186 kPa. The MMA and EHA curves are of similar shape, the slope increasing with increasing content of hydrophobic monomer. The tensile strengths of the MMA terpolymers were slightly higher than those of EHA terpolymers of the same composition. For example, the tensile strength of a 10% EHA terpolymer was 73 kPa while that of a 10 mol % MMA terpolymer was 90 kPa. The interpolated value for a HPMA terpolymer of similar composition was 63 kPa.

The increase of tensile strength with level of hydrophobic monomer can be interpreted using the simple model, as in the last section,

Fig. 4-47: Tensile  
Strength vs. Composition  
for Terpolymer Hydrogels  
Containing Various  
Hydrophobic Monomers

KEY:

AS Fig. 4-44



of an increase in the concentration of active chains in the gel. However, it may be that, as was postulated in the preceding section, an increase in hydrophobic polymer-polymer interactions accompanying the decrease in water content has an effect on the tensile strength, causing the increase in slope as the hydrophobic monomer level increases.

Tensile strength as a function of water content is shown in Fig. 4-48. An interesting feature is that many of the data seem to fall into two groups. The first includes data for terpolymer hydrogels containing MMA and styrene. The tensile strengths of these materials are greater at a given water content than are those of the second set, which consists of the data for terpolymer hydrogels containing HPMA and EHA. The data for the terpolymer hydrogels containing MMA and styrene can be represented by a simple straight line. This was expected, since MMA can be considered to be a "semi-polar" monomer, while styrene is non-polar. Similarly, the data for the terpolymer hydrogels containing HPMA and EHA can be represented by a single straight line. The tensile strengths of the EHA terpolymers were lower than might be expected, considering the hydrophobic nature of EHA. Again, EHA and HPMA differ considerably in polarity, and on this basis would be expected to show rather different behaviour in terpolymer hydrogels.

Fig. 4-49 shows breaking strain as a function of composition for various terpolymer hydrogels. The most striking feature of the graphs is the large increase in breaking strain accompanying copolymerisation of DDA with HEMA and MAA. The breaking strain increased, with the slope decreasing, to a value of 415% for a material containing 30 mol % DDA. For terpolymer hydrogel containing HPMA, the breaking strain increased to a value of 140% for the 50 mol % HPMA material. It was not possible to measure breaking strain for all the gels which were made, because

KEY: As Fig. 4-44

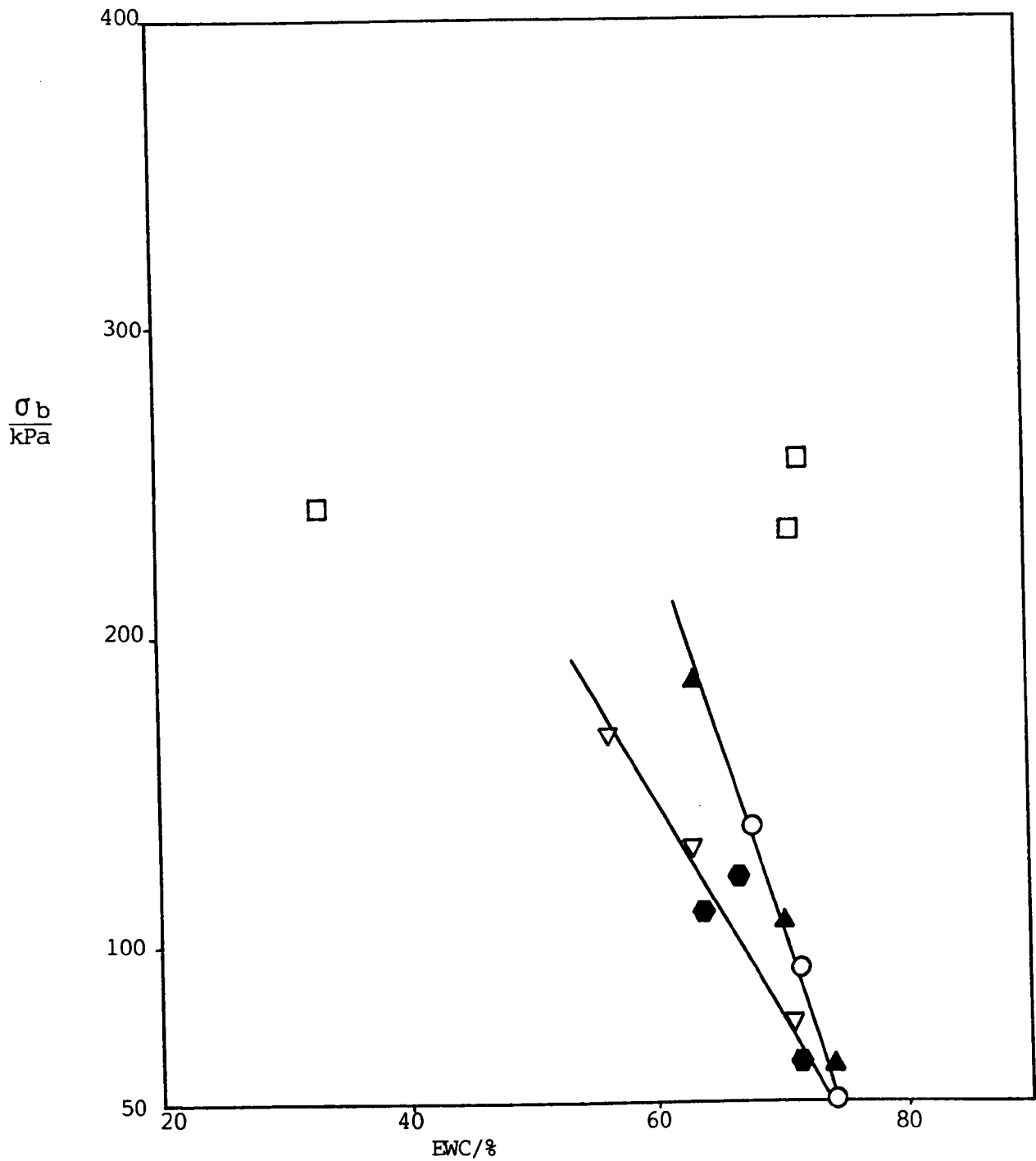
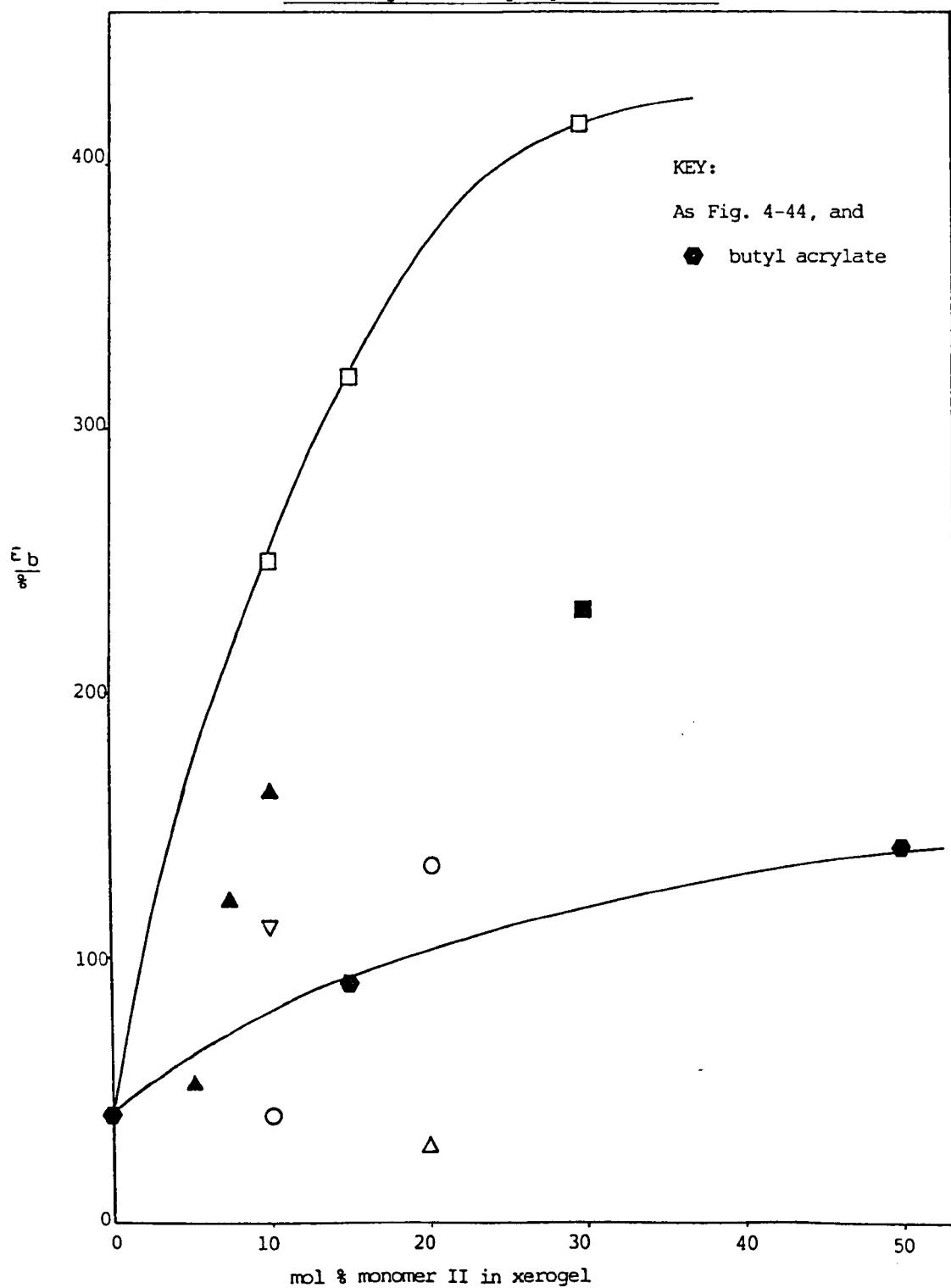


Fig. 4-48: Tensile Strength vs. EWC for Terpolymer Hydrogels Containing Various Hydrophobic Monomers

Fig. 4-49: Breaking Strain vs. Composition for Terpolymer Hydrogels  
Containing Various Hydrophobic Monomers



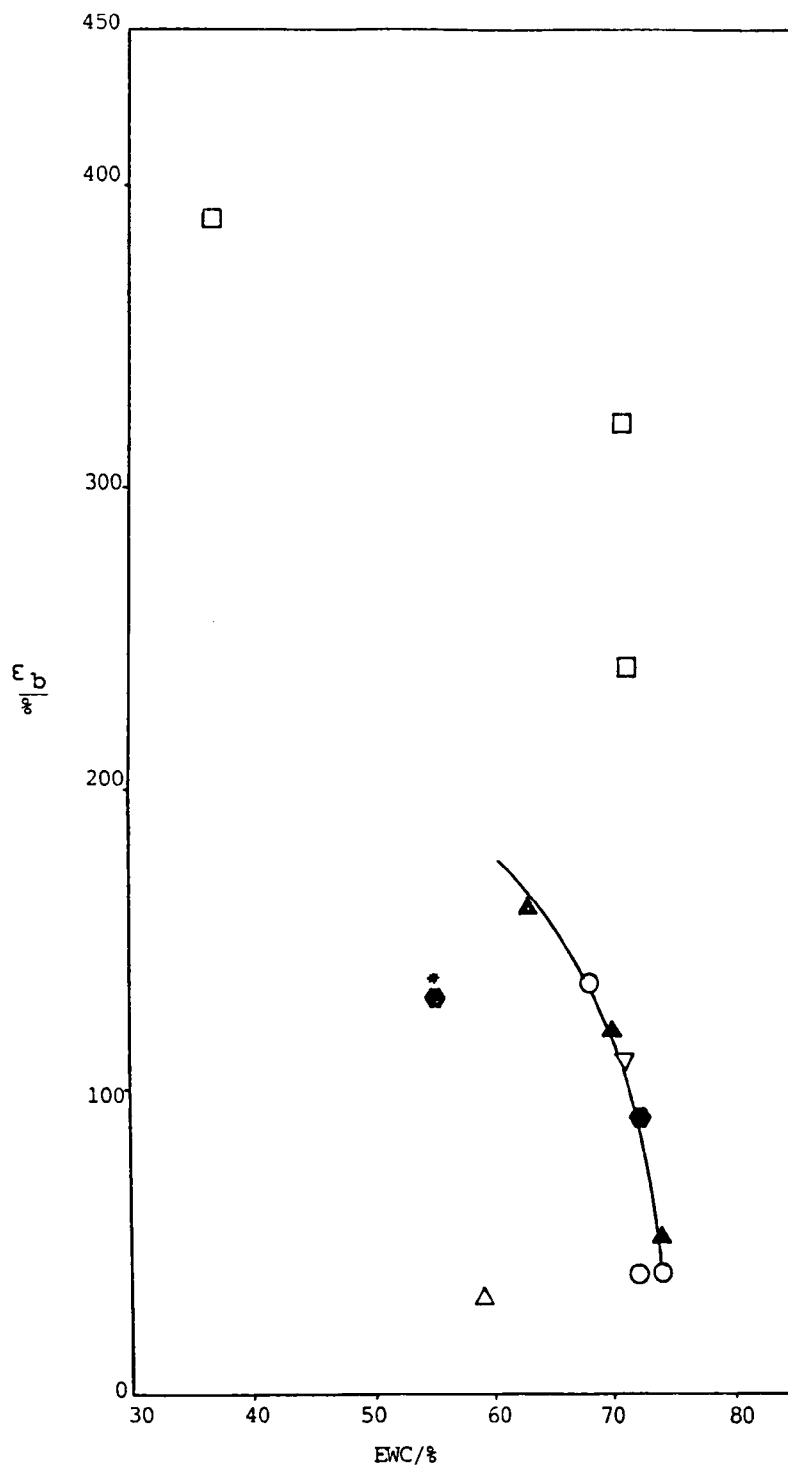
of problems which occurred with the method of measurement using the Instron. The two most common problems were:

- (i) slipping of the sample from the grips at higher strains;
- (ii) breaking of the sample at the edge of the grips, an occurrence which invalidated the test result although stress/strain measurements up to this point were valid.

These problems were to a certain extent alleviated by the use of pieces of polysulphide rubber between the sample and the grips, but still occurred frequently, particularly when testing the more fragile materials of higher water contents.

Both the MMA and styrene-containing materials appear to show a decrease in breaking strain at low levels of added hydrophobic monomer. It is not clear whether this is a result of experimental errors, which are large for this type of measurement, or a true (and certainly unexpected) result. Fig. 4-50 shows breaking strain as a function of water content for these materials. Again, the materials containing styrene and MMA tend to lie on the same curve. For a given water content, the DDA materials show the greatest breaking strain.

Fig. 4-51 shows the results for the tearing energy of these terpolymer hydrogels as a function of composition. It was found that precise results were unobtainable for many of the materials, because the test-pieces tore in a direction perpendicular to that required, as shown in Fig. 4-52. Neither of the modifications of the procedure described in Section 3.2.7.2 solved this problem. For these materials, the tearing energy  $T$  was assumed to be less than  $50\text{Jm}^{-2}$ .



N.B.

\*● EWC extrapolated from  
Fig. 4-44

Fig. 4-50: Breaking Strain  
vs EWC for Terpolymer  
Hydrogels Containing Various  
Hydrophobic Monomers

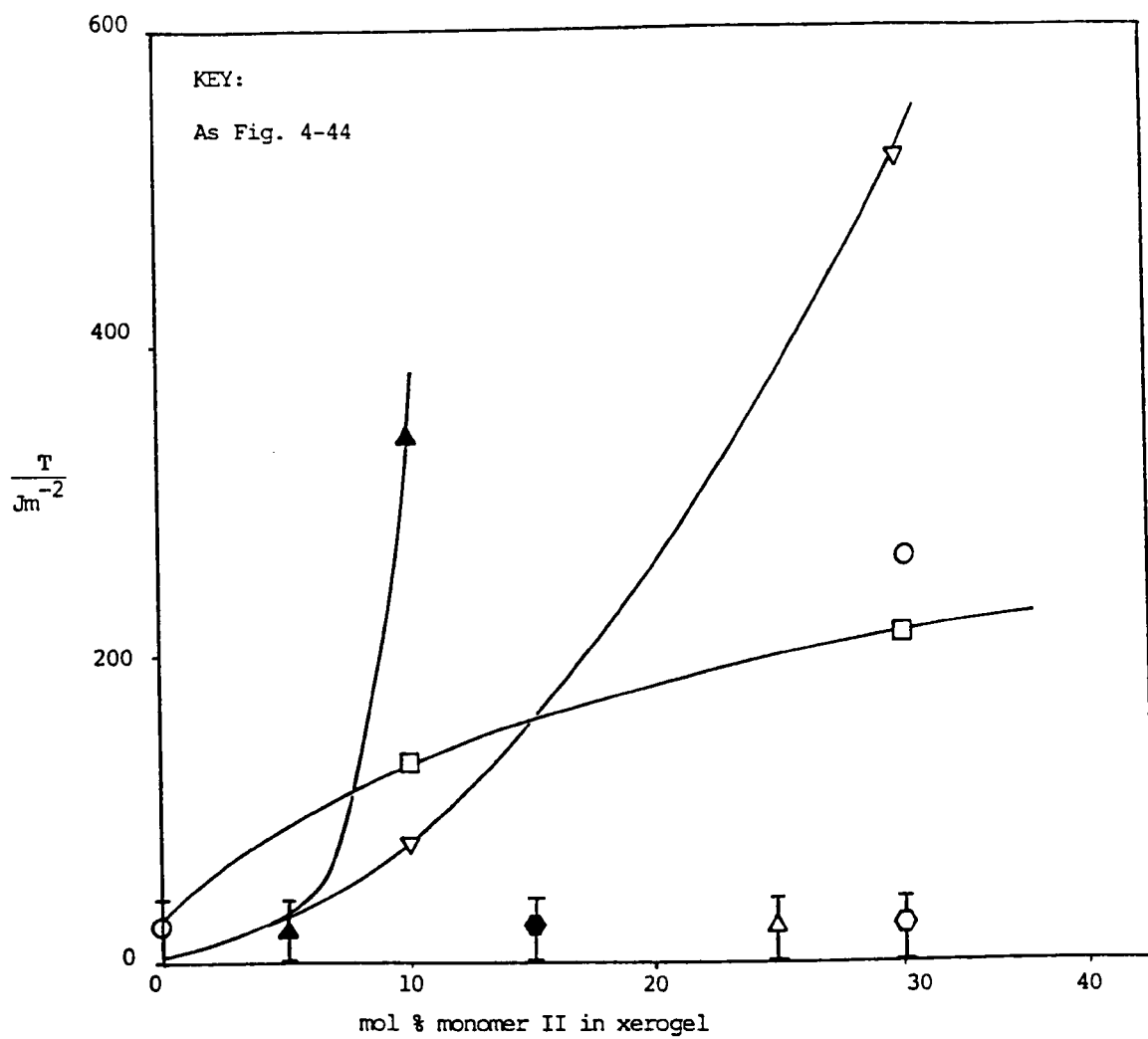


Fig. 4-51: Tearing Energy vs. Composition for Terpolymer Hydrogels  
Containing Various Hydrophobic Monomers



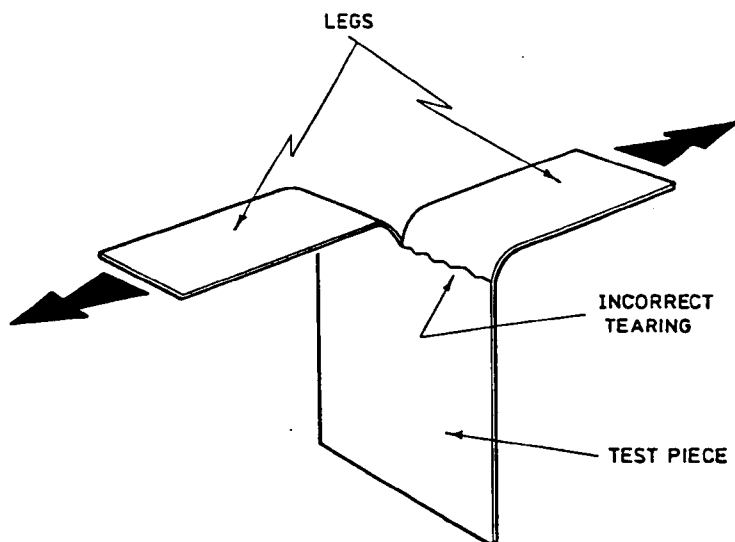


Fig. 4-52: Incorrect Tearing of "Trouser" Test Pieces

The curve of tearing energy as a function of composition for the terpolymer hydrogels containing styrene is similar to that for tensile strength for the same materials. A sharp increase in slope occurs at a composition of about 5 mol % styrene. The tearing energy at 10 mol % styrene was  $346\text{Jm}^{-2}$ . The tearing energy of EHA terpolymers increased with the proportion of EHA, the slope of the curve increasing. The value of  $T$  at 30 mol % EHA was approximately  $520\text{Jm}^{-2}$ . The curve for DDA terpolymers is rather different in shape. The tearing energy increased with the proportion of DDA, but the slope of the curve decreased. At a composition of 30 mol % DDA, the tearing energy was  $260\text{Jm}^{-2}$ .

Fig. 4-53 shows tearing energy as a function of water content for these materials. The results for hydrogels containing styrene and EHA are well represented by a single straight line. These materials would appear to be the most useful of those of this type investigated, since for a given EWC their tearing energies are highest. However, copolymerisation with styrene has the disadvantage that the range of styrene contents which can be used is limited, since materials containing more than 10 mol % styrene are inhomogeneous. The low tearing energy of DDA-containing hydrogels, compared with styrene and EHA-containing

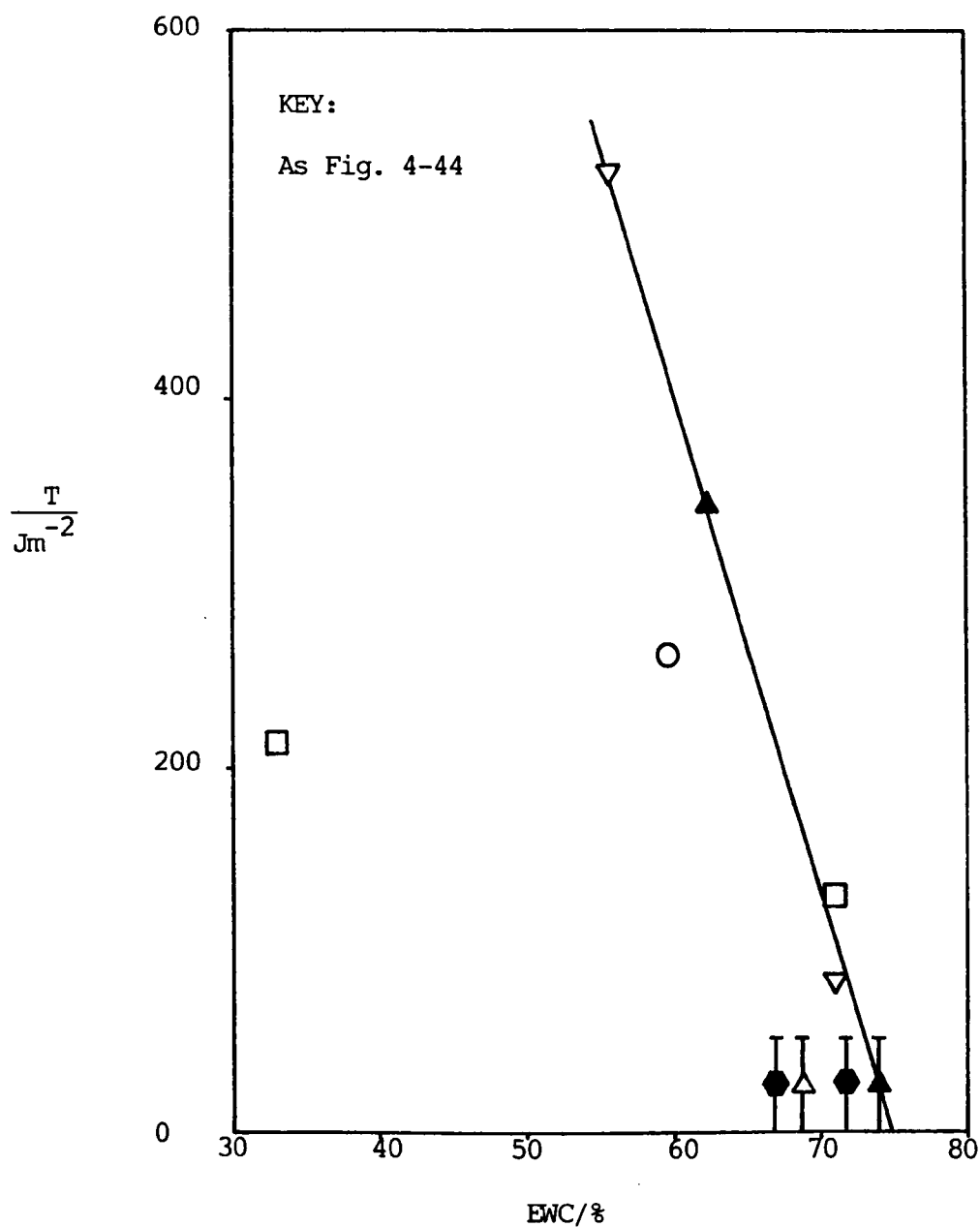


Fig. 4-53: Tearing Energy vs. Water Content for Terpolymers Hydrogels  
Containing Various Hydrophobic Monomers

materials is surprising, particularly in view of the high tensile strength and breaking strain of these gels. It must be borne in mind, however, that the tearing energy as determined by this method is a measure of the energy required to propagate rather than to initiate a crack in the material. The results indicate that, for a given water content, crack propagation takes place more readily in the DDA-HEMA-MAA hydrogels than in the EHA-HEMA-MAA or styrene-HEMA-MAA hydrogels.

Figs. 4-54 to 4-69 show the tensile stress/strain properties of the terpolymer hydrogels plotted in various ways. Fig. 4-54 shows the stress/strain curve for the 10 mol % MMA material. The low-extension modulus obtained from the slope of the curve at the origin is 141 kPa. The modulus at 50% strain is 61 kPa. The stress/strain curve for the 30 mol % butyl acrylate material is shown in Fig. 4-55. The low-extension modulus is 263 kPa, which falls to 31 kPa at 100% strain. At this point the slope begins to increase again. At 300% strain, the modulus is 132 kPa. Figs. 4-56 a and b show the curves obtained for terpolymer hydrogels containing EHA. The 10 mol % EHA terpolymer (Fig. 4-56a) has a low-extension modulus of 215 kPa and a modulus of 69 kPa at 50% strain. The slope steadily decreases until the break-point. The modulus at a strain of 100% is 41 kPa. The 20% EHA material exhibits a curve of a similar shape; the low-extension modulus is 167 kPa, while that at a strain of 50% is 37 kPa.

According to the elementary theory of rubber elasticity (ref. 191, p.64)

$$\sigma = Gv_2^{-\frac{1}{3}} (\lambda - \lambda^{-2}) \quad \dots(4-19)$$

where  $\sigma$  is the stress referred to the unswollen cross-sectional area,  $v_2$  is the volume fraction of polymer in the swollen material, and  $G$  and

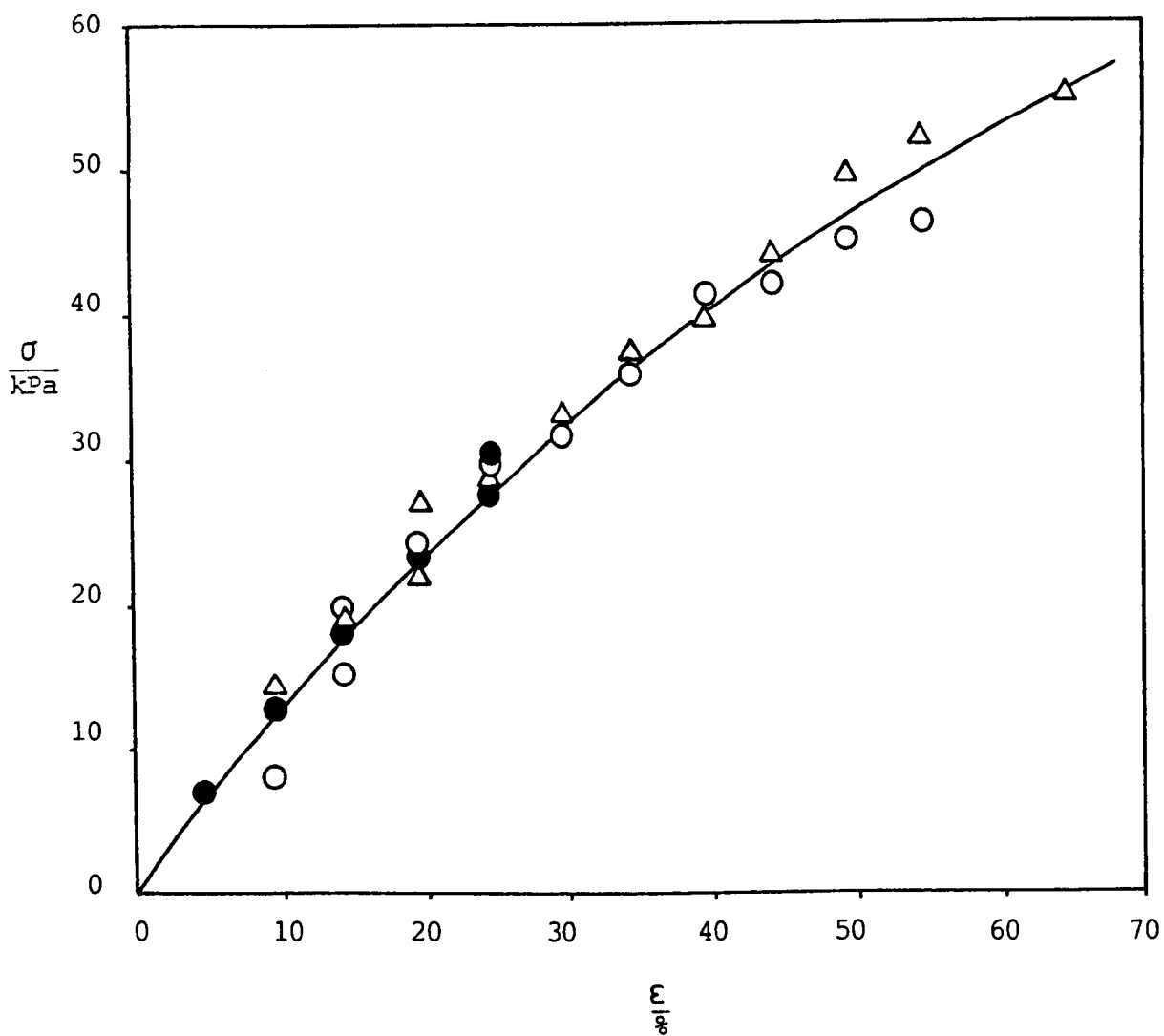


Fig. 4-54: Stress-Strain Curve for Terpolymer Hydrogel Containing 10 mol % MMA

KEY:

○ 1st sample

● 2nd sample

△ 3rd sample

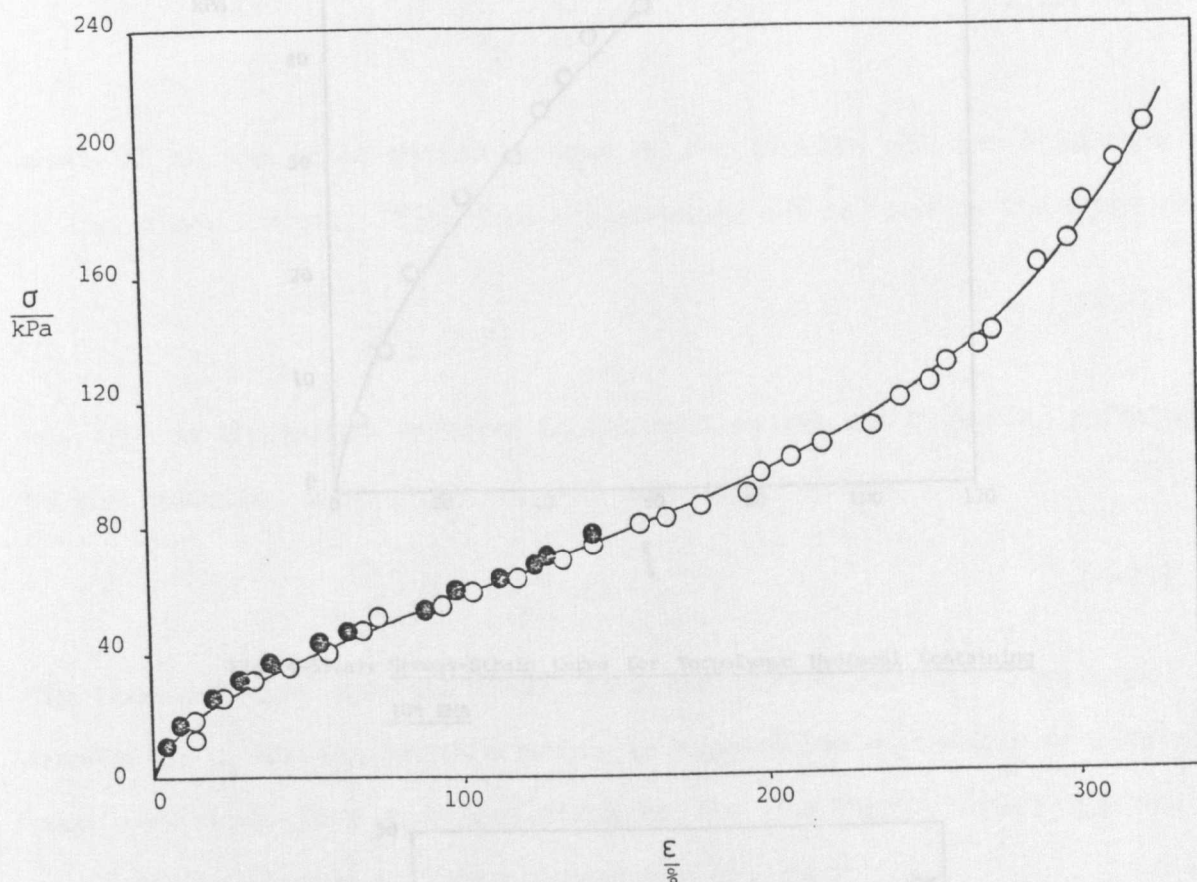


Fig. 4-55: Stress-Strain Curve for Terpolymer Hydrogel Containing 30 mol % Butyl Acrylate

KEY:

○ 1st sample

● 2nd sample

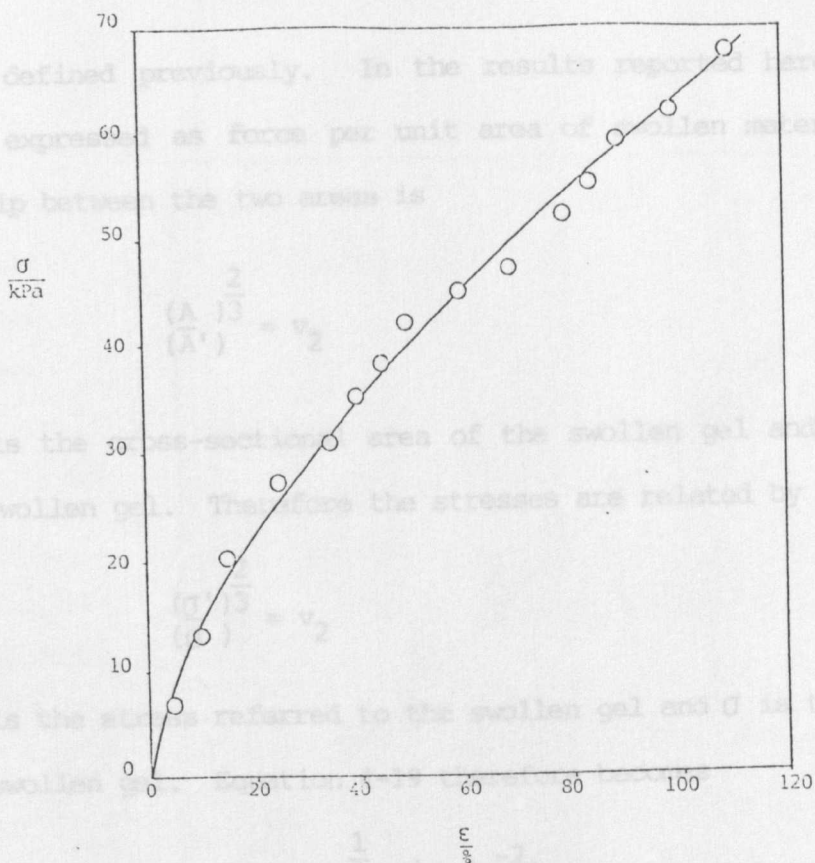


Fig. 4-56(a): Stress-Strain Curve for Terpolymer Hydrogel Containing 10% EHA

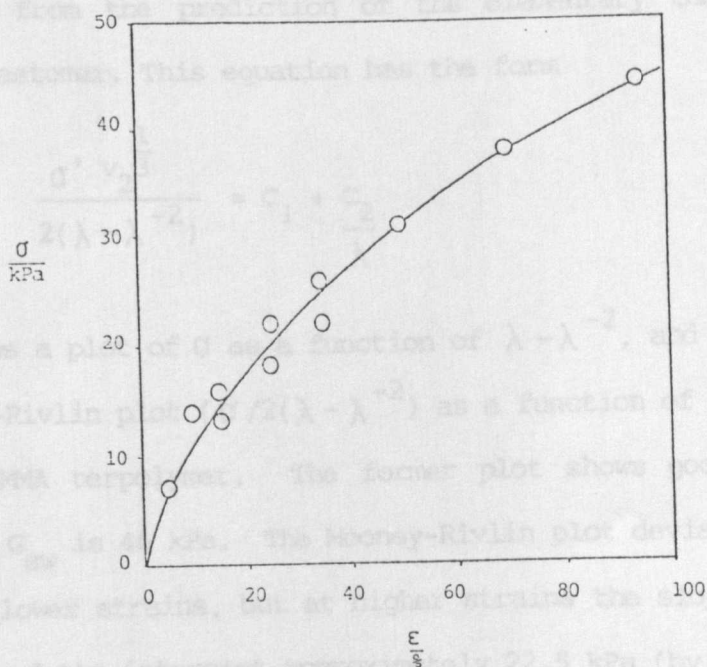


Fig. 4-56(b): Stress-Strain Curve for Terpolymer Hydrogel Containing 20% EHA

$\lambda$  are as defined previously. In the results reported here however, stress is expressed as force per unit area of swollen material. The relationship between the two areas is

$$\frac{(A)^{\frac{2}{3}}}{(A')^{\frac{2}{3}}} = v_2 \quad \dots(4-20)$$

where  $A'$  is the cross-sectional area of the swollen gel and  $A$  is that of the unswollen gel. Therefore the stresses are related by the equation

$$\frac{(\sigma')^{\frac{2}{3}}}{(\sigma)^{\frac{2}{3}}} = v_2 \quad \dots(4-21)$$

where  $\sigma'$  is the stress referred to the swollen gel and  $\sigma$  is that referred to the unswollen gel. Equation 4-19 therefore becomes

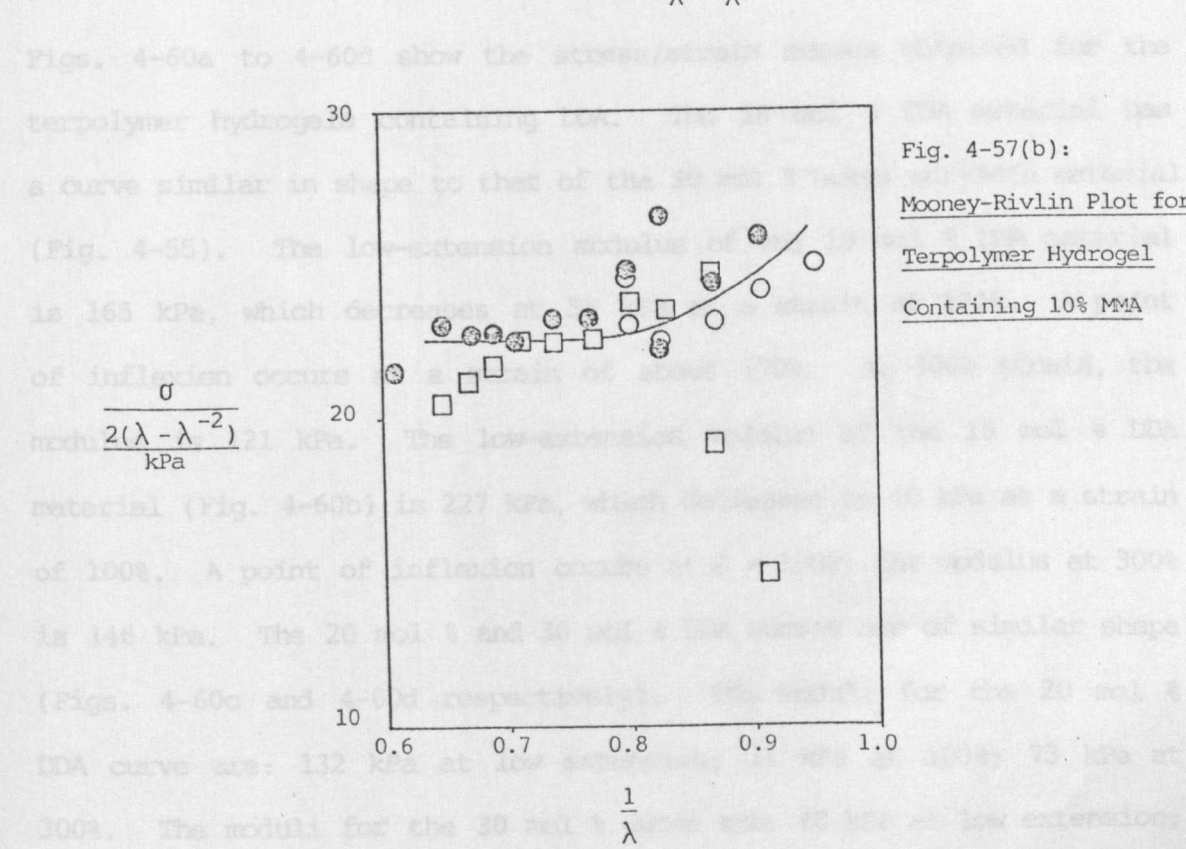
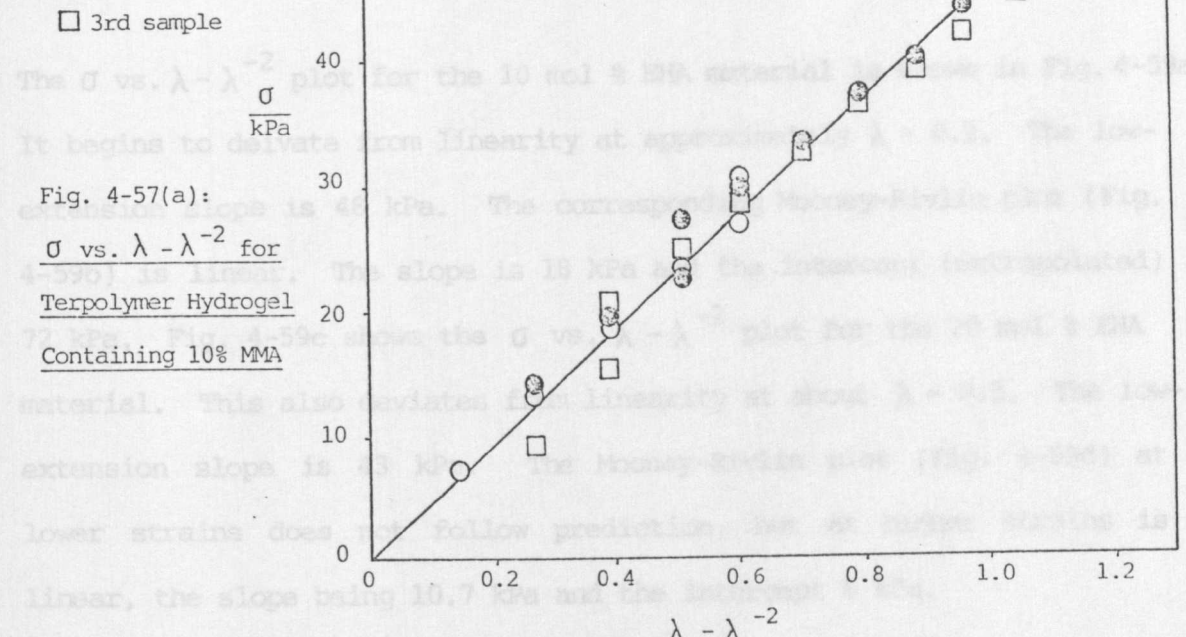
$$\sigma = Gv_2^{\frac{1}{3}} (\lambda - \lambda^{-2}) \quad \dots(4-22)$$

The Mooney-Rivlin equation (4-23) is a formula containing two empirical constants,  $C_1$  and  $C_2$ , which attempts to express the deviations of elastomer behaviour from the prediction of the elementary theory applied to a swollen elastomer. This equation has the form

$$\frac{\sigma' v_2^{\frac{1}{3}}}{2(\lambda - \lambda^{-2})} = C_1 + \frac{C_2}{\lambda} \quad \dots(4-23)$$

Fig. 4-57a shows a plot of  $\sigma$  as a function of  $\lambda - \lambda^{-2}$ , and Fig. 4-57b shows a Mooney-Rivlin plot ( $\sigma / 2(\lambda - \lambda^{-2})$ ) as a function of  $1/\lambda$  for the 10 mol % MMA terpolymer. The former plot shows good linearity, and the slope  $G_{sw}$  is 46 kPa. The Mooney-Rivlin plot deviates from prediction at lower strains, but at higher strains the slope is approximately zero, and the intercept approximately 22.5 kPa (by extrapolation). Curves for the 30 mol % butyl acrylate terpolymer hydrogel are shown

in Figs. 4-58a and 4-58b. The  $\sigma$  vs.  $\lambda - \lambda^{-2}$  curve shows considerable deviation from prediction, although the strains are generally much larger than those imposed on the 10 mol % material. The low-extension Mooney-Rivlin plot (Fig. 4-59a) has large deviations from linearity at both high and low strains.





in Figs. 4-58a and 4-58b. The  $\sigma$  vs.  $\lambda - \lambda^{-2}$  curve shows considerable deviation from prediction, although the strains are generally much higher than those imposed on the 10 mol % material. The low-extension slope is 57 kPa. The Mooney-Rivlin plot (Fig. 4-58a) has large deviations from linearity at both high and low strains.

The  $\sigma$  vs.  $\lambda - \lambda^{-2}$  plot for the 10 mol % EHA material is shown in Fig. 4-59a. It begins to deviate from linearity at approximately  $\lambda = 0.2$ . The low-extension slope is 48 kPa. The corresponding Mooney-Rivlin plot (Fig. 4-59b) is linear. The slope is 18 kPa and the intercept (extrapolated) 72 kPa. Fig. 4-59c shows the  $\sigma$  vs.  $\lambda - \lambda^{-2}$  plot for the 20 mol % EHA material. This also deviates from linearity at about  $\lambda = 0.2$ . The low-extension slope is 43 kPa. The Mooney-Rivlin plot (Fig. 4-59d) at lower strains does not follow prediction, but at higher strains is linear, the slope being 10.7 kPa and the intercept 8 kPa.

Figs. 4-60a to 4-60d show the stress/strain curves obtained for the terpolymer hydrogels containing DDA. The 10 mol % DDA material has a curve similar in shape to that of the 30 mol % butyl acrylate material (Fig. 4-55). The low-extension modulus of the 10 mol % DDA material is 165 kPa, which decreases to 55 kPa at a strain of 100%. A point of inflexion occurs at a strain of about 170%. At 300% strain, the modulus is 121 kPa. The low-extension modulus of the 15 mol % DDA material (Fig. 4-60b) is 227 kPa, which decreases to 40 kPa at a strain of 100%. A point of inflexion occurs at  $\epsilon = 100\%$ ; the modulus at 300% is 146 kPa. The 20 mol % and 30 mol % DDA curves are of similar shape (Figs. 4-60c and 4-60d respectively). The moduli for the 20 mol % DDA curve are: 132 kPa at low extension; 33 kPa at 100%; 73 kPa at 300%. The moduli for the 30 mol % curve are: 48 kPa at low extension;

$$\frac{\sigma}{\frac{2(\lambda - \lambda^{-2})}{\text{kPa}}}$$

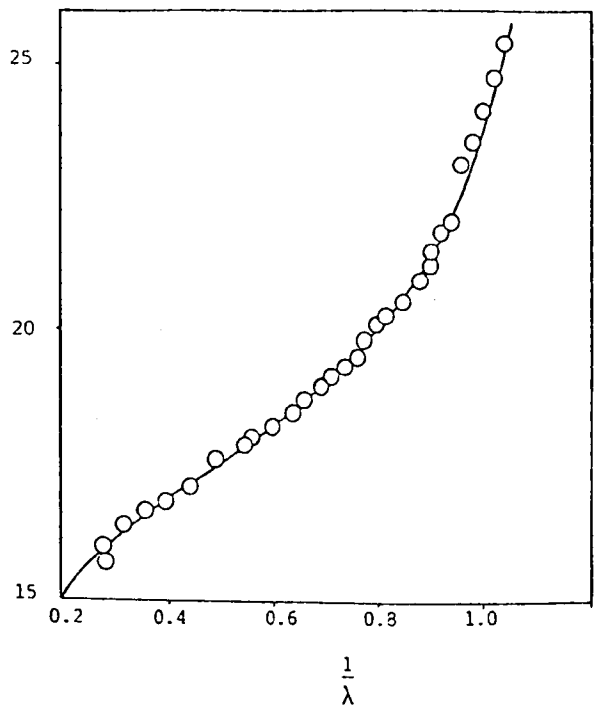


Fig. 4-58(a):  $\sigma$  vs.  $\lambda - \lambda^{-2}$   
for Terpolymer Hydrogel  
Containing 30% Butyl  
Acrylate

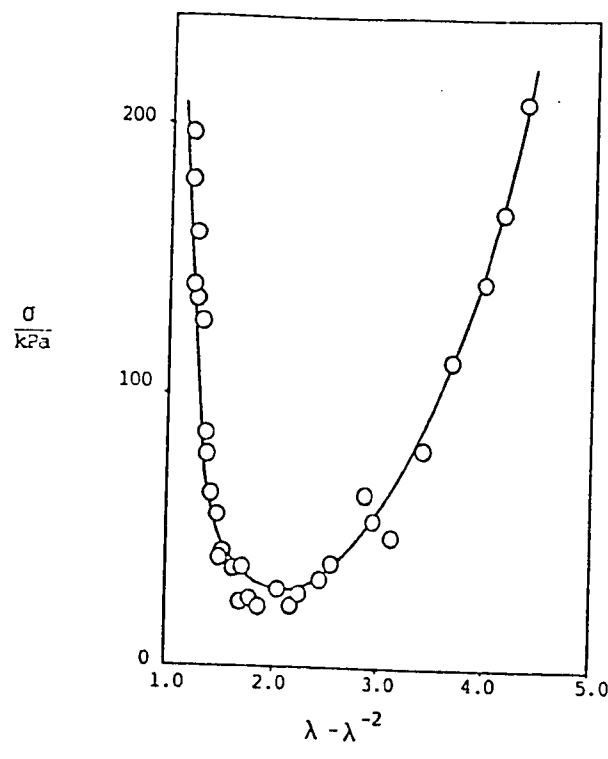


Fig. 4-58(b):  
Mooney-Rivlin  
Curve for Terp-  
olymer Hydrogel  
Containing 30%  
Butyl Acrylate

Fig. 4-59(a):  $\sigma$  vs.  $\lambda - \lambda^{-2}$  for Terpolymer Hydrogel Containing 10% EHA

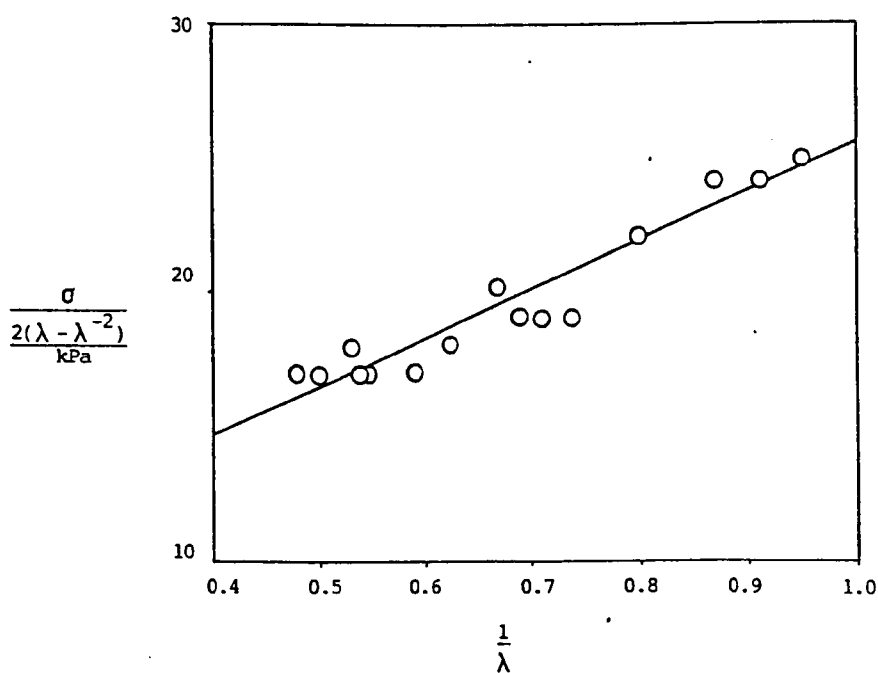
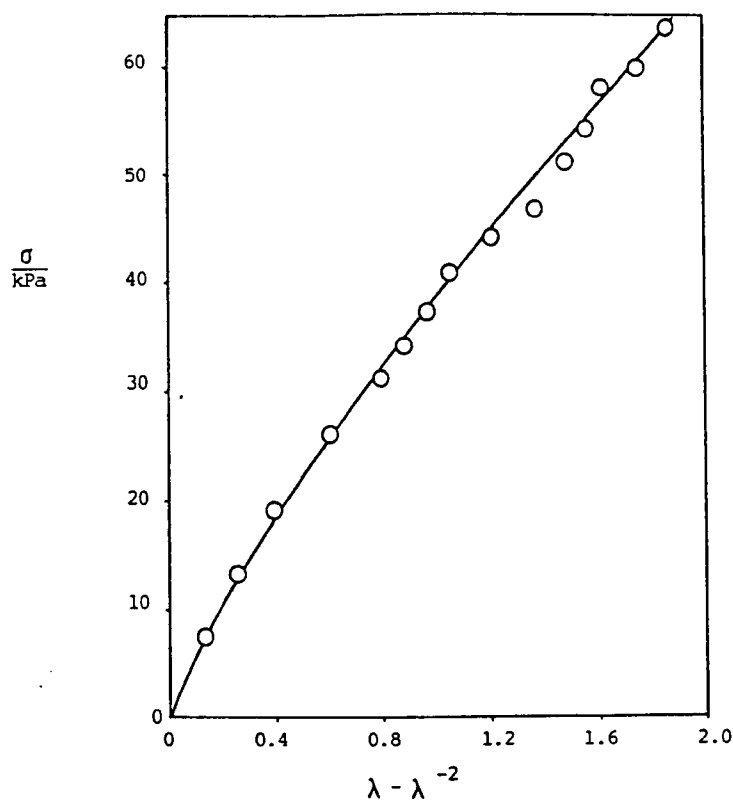


Fig. 4-59(b): Mooney-Rivlin Curve for Terpolymer Hydrogel Containing 10% EHA

Fig. 4-59(c):  $\sigma$  vs.  $\lambda - \lambda^{-2}$  for Terpolymer Hydrogel Containing 20% EHA

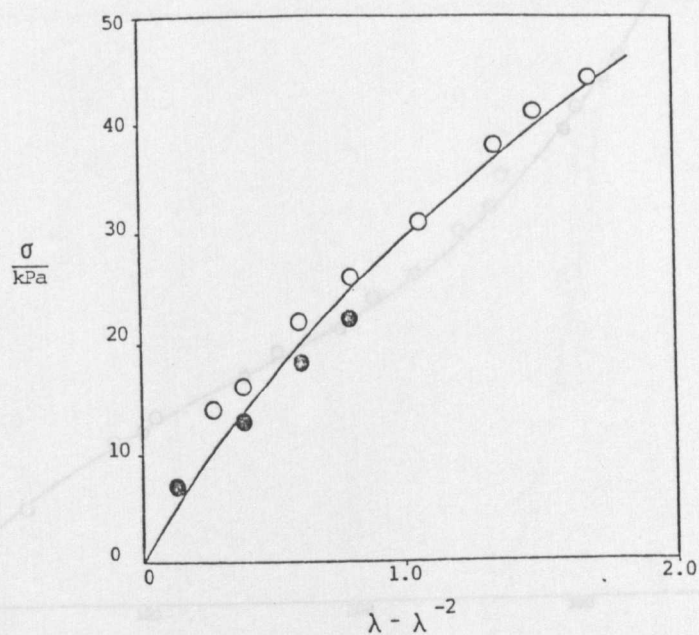


Fig. 4-59(d): Mooney-Rivlin Curve for Terpolymer Hydrogel Containing 20% EHA

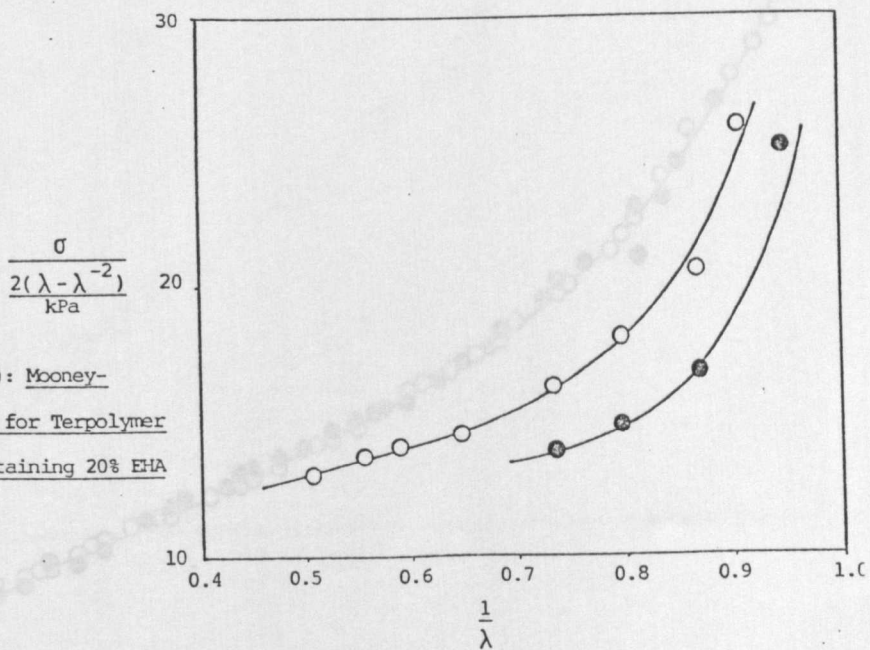


Fig. 4-60(a): Stress-Strain Curve for Terpolymer Hydrogel Containing 10% DDA

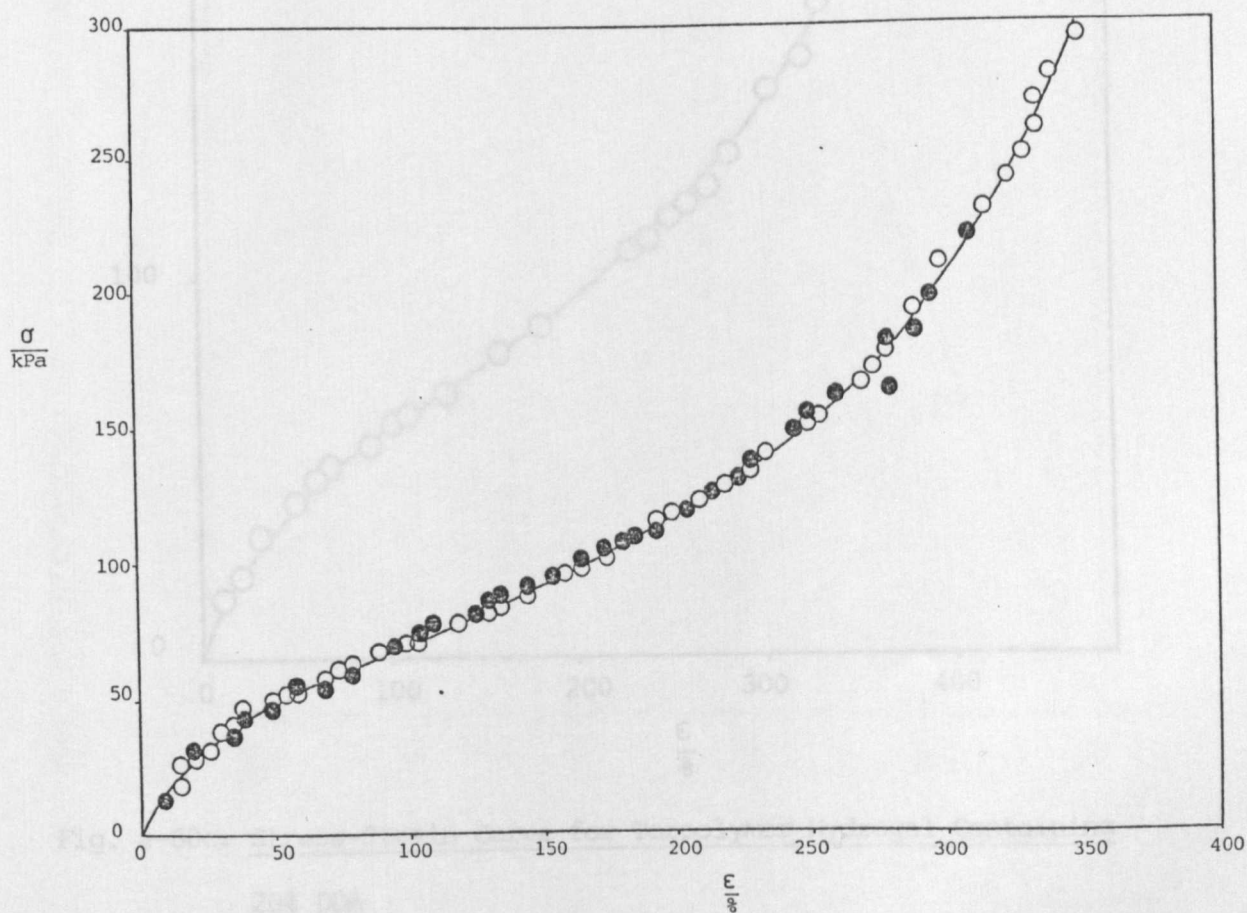
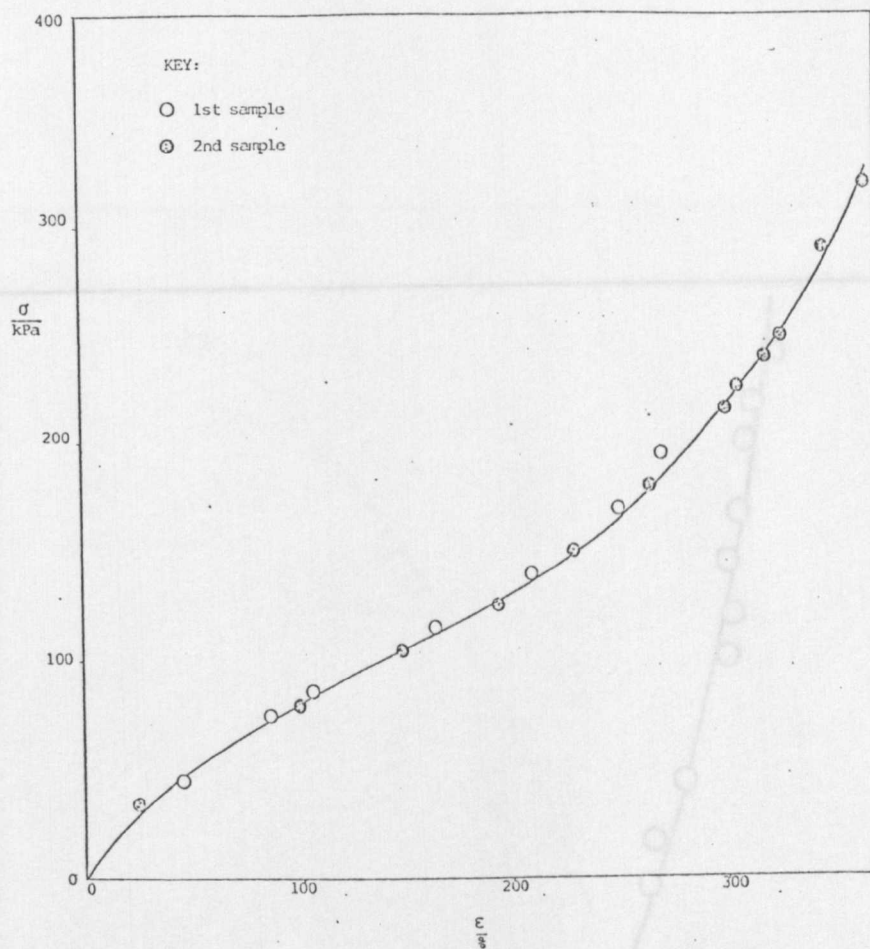


Fig. 4-60(b): Stress-Strain Curve for Terpolymer Hydrogel Containing 15 mol % DDA

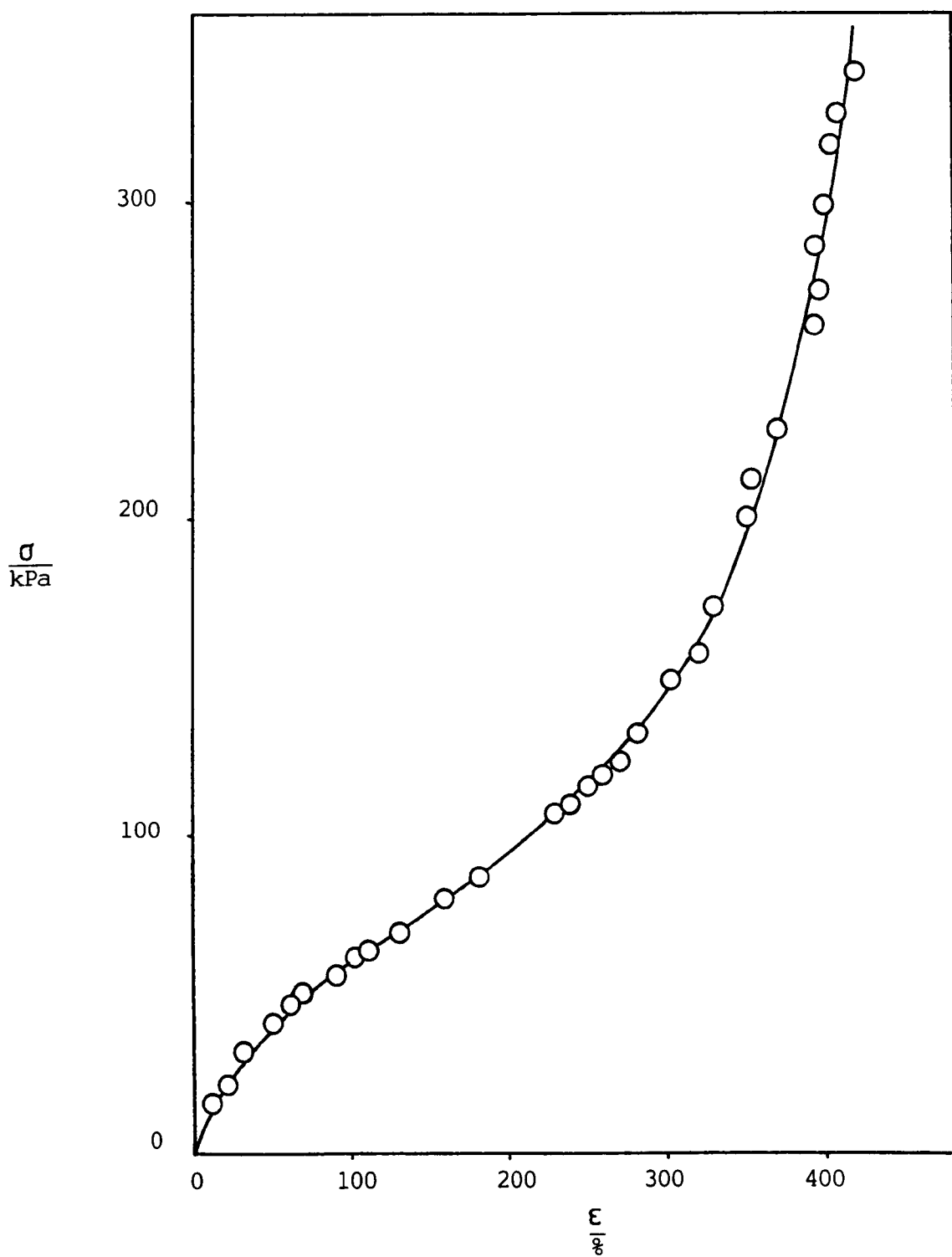
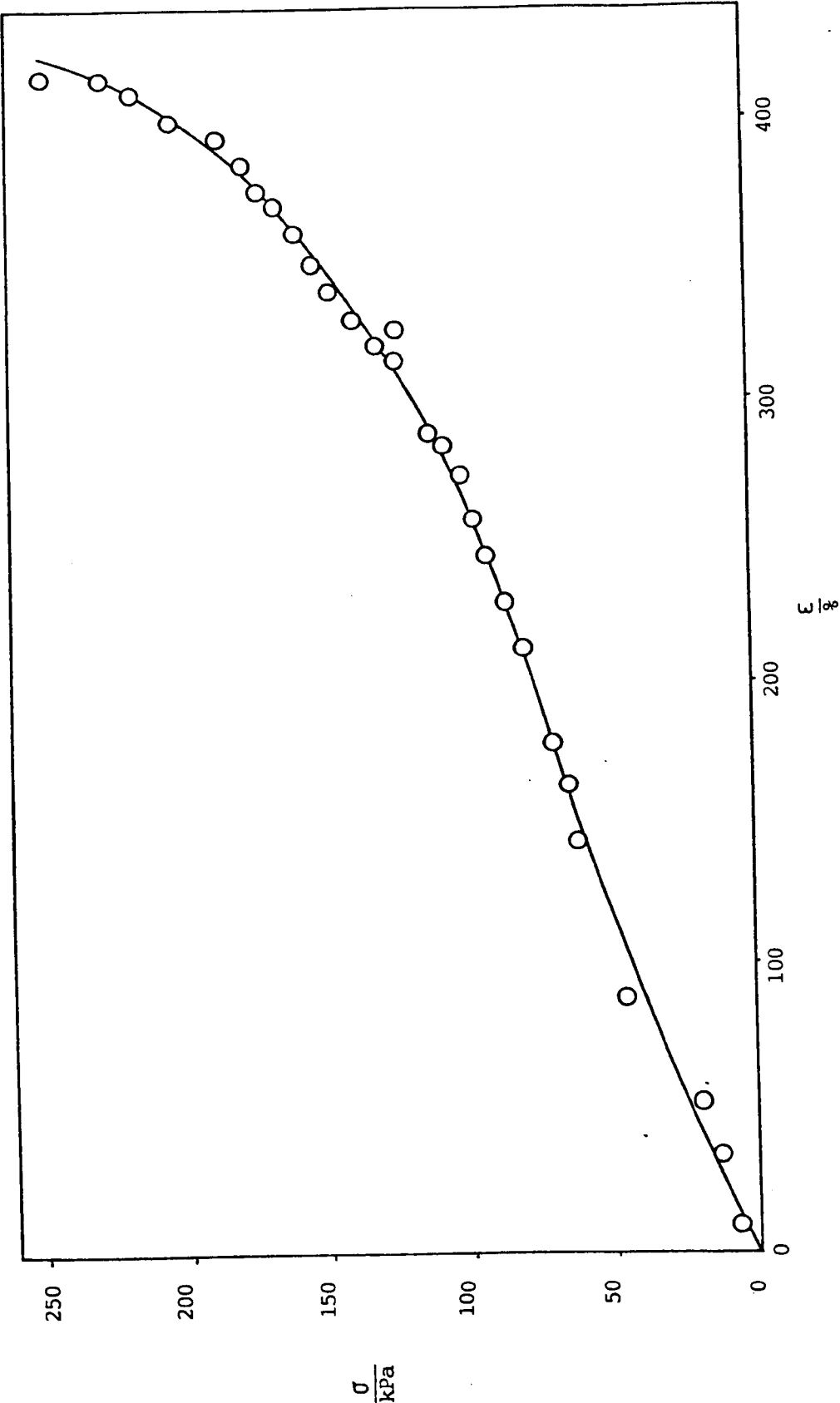


Fig. 4-60c: Stress-Strain Curve for Terpolymer Hydrogel Containing  
20% DDA

Fig. 4-60d: Stress-Strain Curve for Terpolymer Hydrogel Containing 30 mol % DDA



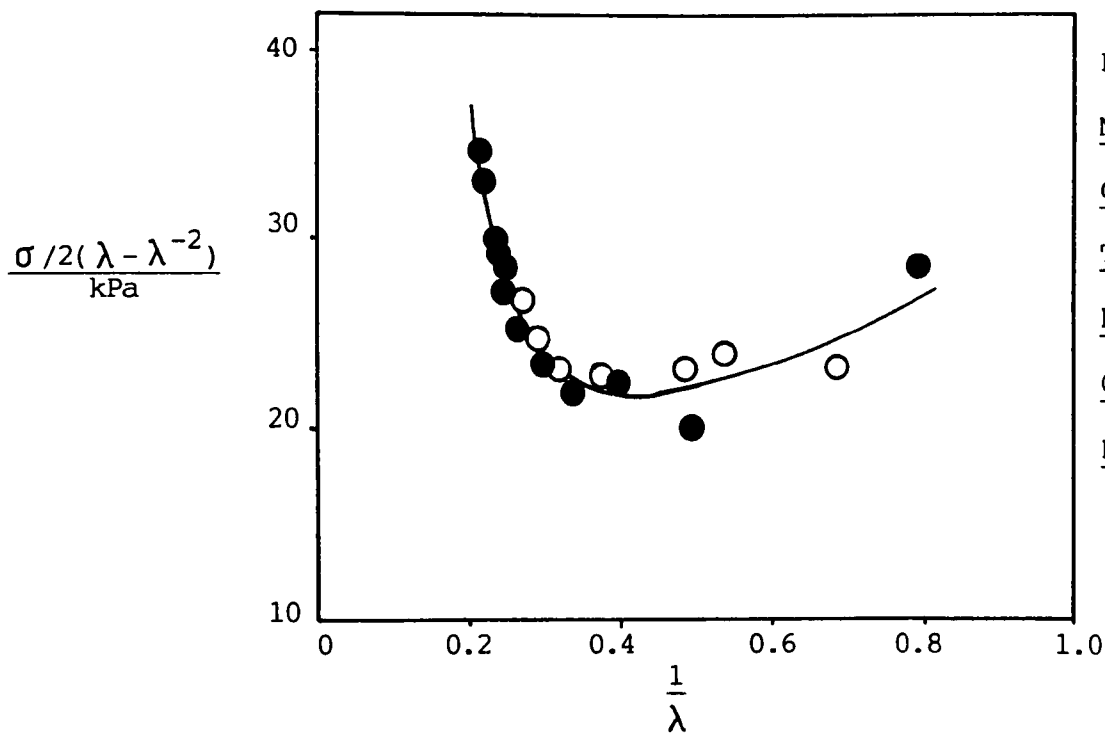
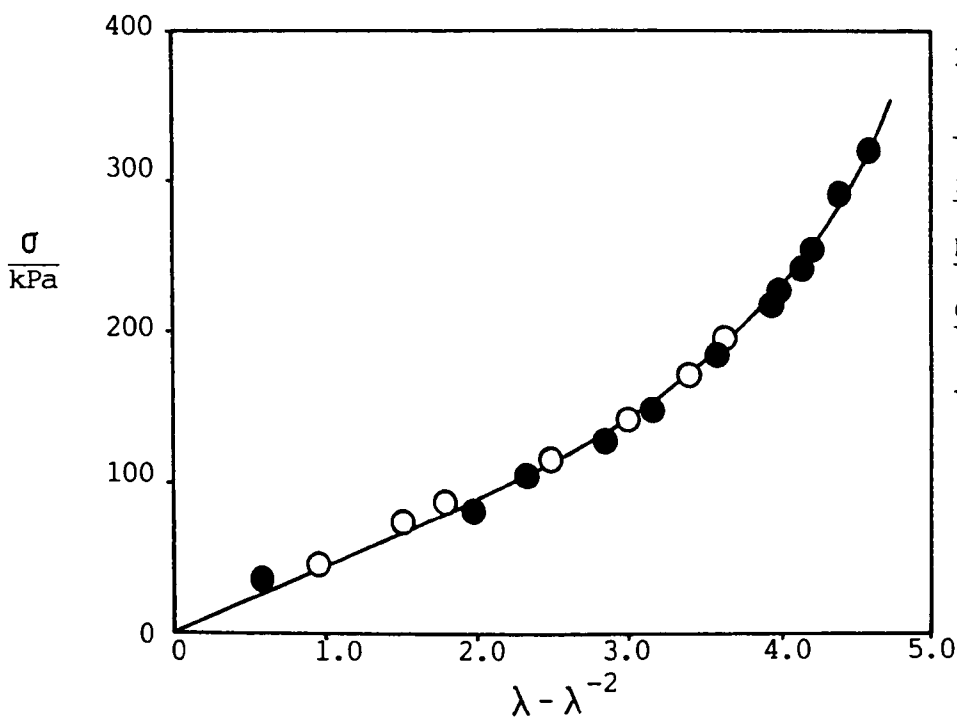
37 kPa at 100%; 51 kPa at 300%.

Fig. 4-61a shows the  $\sigma$  vs.  $\lambda - \lambda^{-2}$  plot for the 10 mol % DDA terpolymer. The shape of the curve is similar to that of the stress/strain curve (Fig. 4-60a). The low-extension slope is 53 kPa. The Mooney-Rivlin plot, shown in Fig. 4-61b, has a minimum at  $1/\lambda = 0.5$ . The curves for the 15 mol % DDA, 20 mol % DDA and 30 mol % DDA, shown in Figs. 4-61c to 4-61h, are of similar shape to those of the 10 mol % DDA material. In each case the Mooney-Rivlin plot follows a smooth curve and shows no signs of linearity. The low-extension slopes of the  $\sigma$  vs.  $\lambda - \lambda^{-2}$  plots are as follows: for the 15 mol % material, 95 kPa; for the 20 mol % material, 48 kPa; for the 30% material, 25 kPa.

Figs. 4-62a to 4-62c show the stress/strain curves obtained for terpolymer hydrogels containing styrene. The 5 mol % styrene material has a low-extension modulus of 250 kPa, the slope decreasing until the material breaks. The curve for the 7.5% styrene material (Fig. 4-62b) is approximately linear between 0% and 40% strain, after which point the slope begins to decrease. The low-extension modulus is 113 kPa; at a strain of 100% the modulus is 75 kPa. At this point, shortly before the material breaks, the slope begins to decrease. The curve for the 10% styrene material (Fig. 4-62c) shows this effect more clearly. The low-extension modulus is 275 kPa, which falls to 96 kPa at a strain of 100%, at which point the slope begins to decrease. At  $\epsilon = 200\%$ , the modulus is 212 kPa.

The  $\sigma$  vs.  $\lambda - \lambda^{-2}$  plot for the 5 mol % styrene material is linear, with a slope of 58 kPa (Fig. 4-63a). The corresponding Mooney-Rivlin plot (Fig. 4-63b) has a positive slope at lower strains, but at higher strains





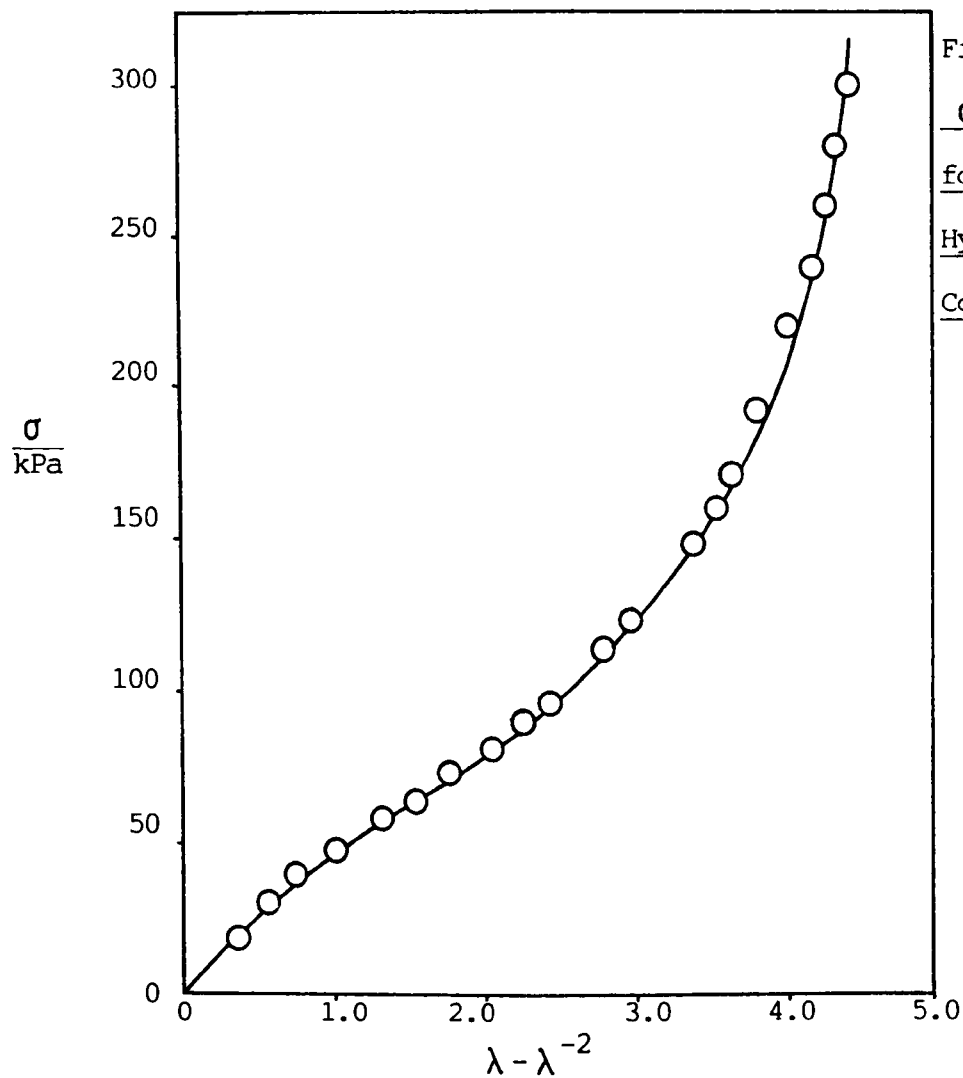


Fig. 4-61c:  
 $\sigma$  vs.  $\lambda - \lambda^{-2}$   
 for Terpolymer  
 Hydrogel  
 Containing 15% DI

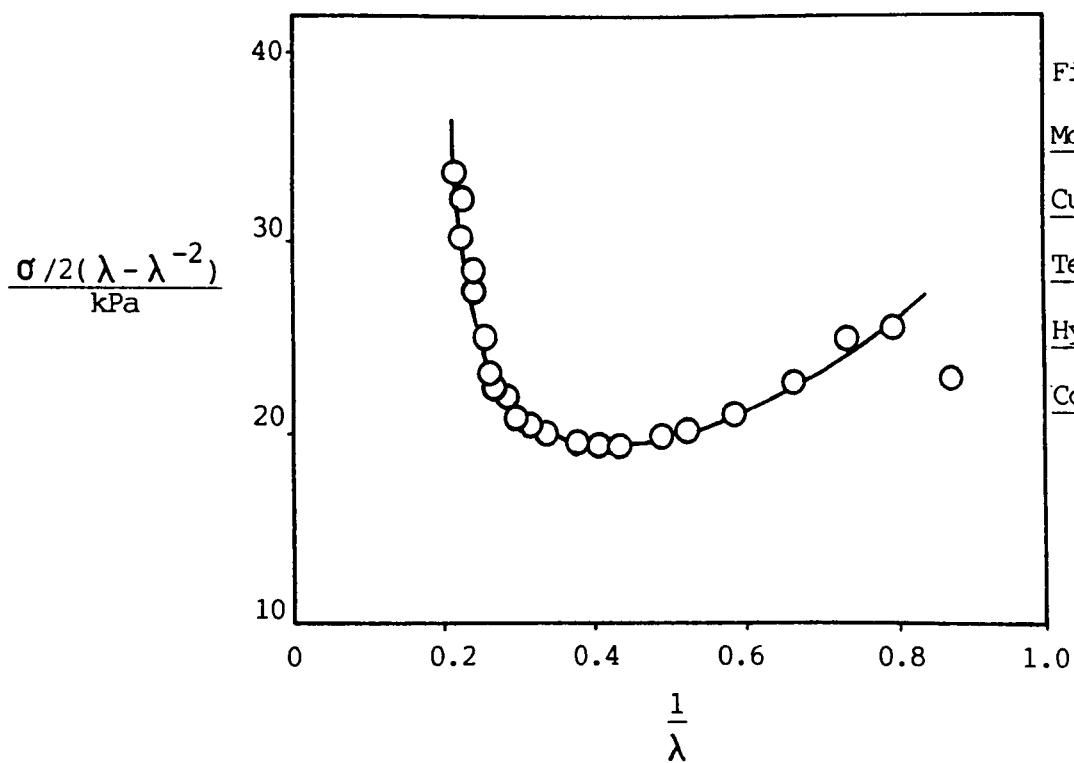


Fig. 4-61d:  
 Mooney-Rivlin  
 Curve for  
 Terpolymer  
 Hydrogel  
 Containing 15% DI

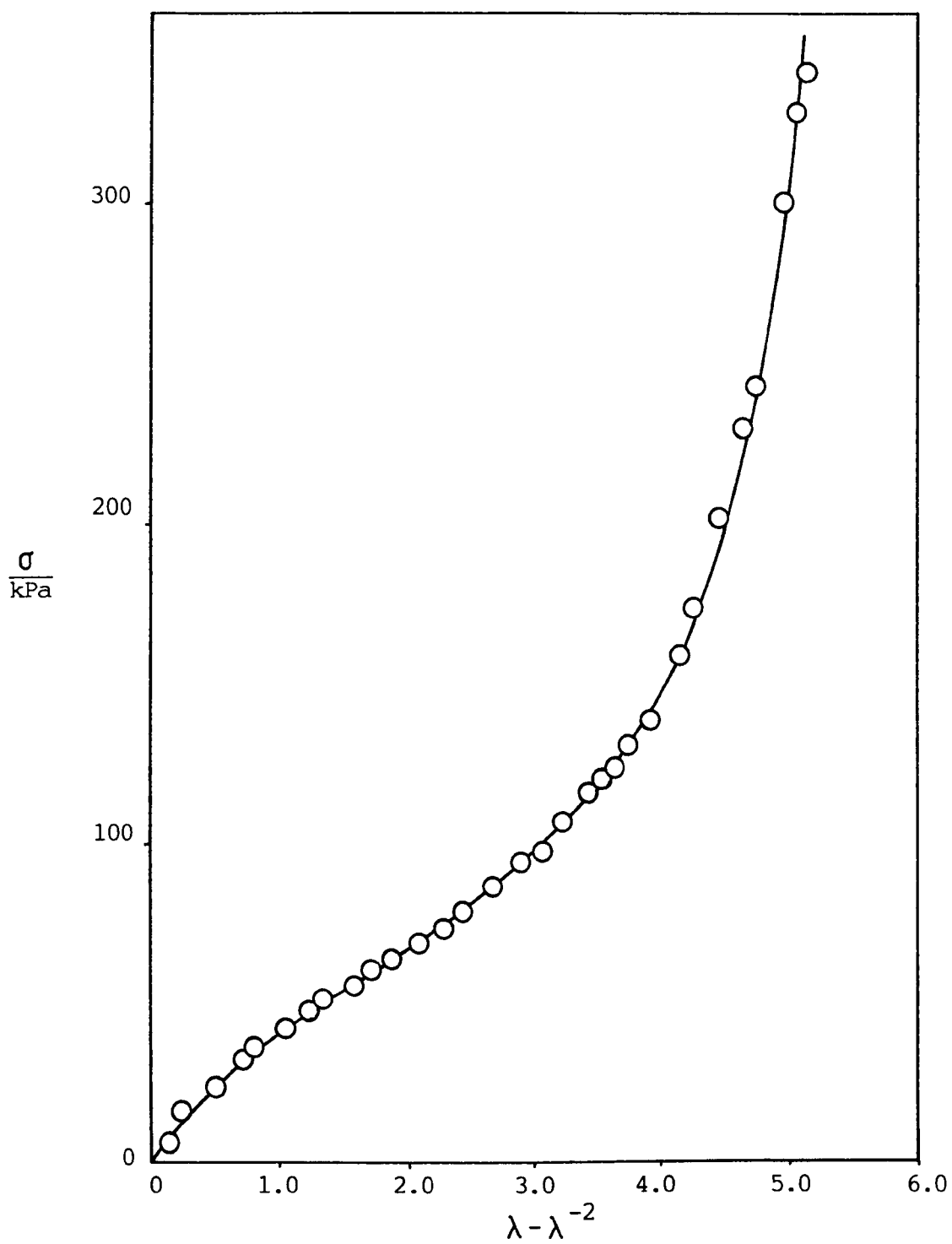


Fig. 4-61e:  $\sigma$  vs.  $\lambda - \lambda^{-2}$  for Terpolymer Hydrogel Containing 20% DDA

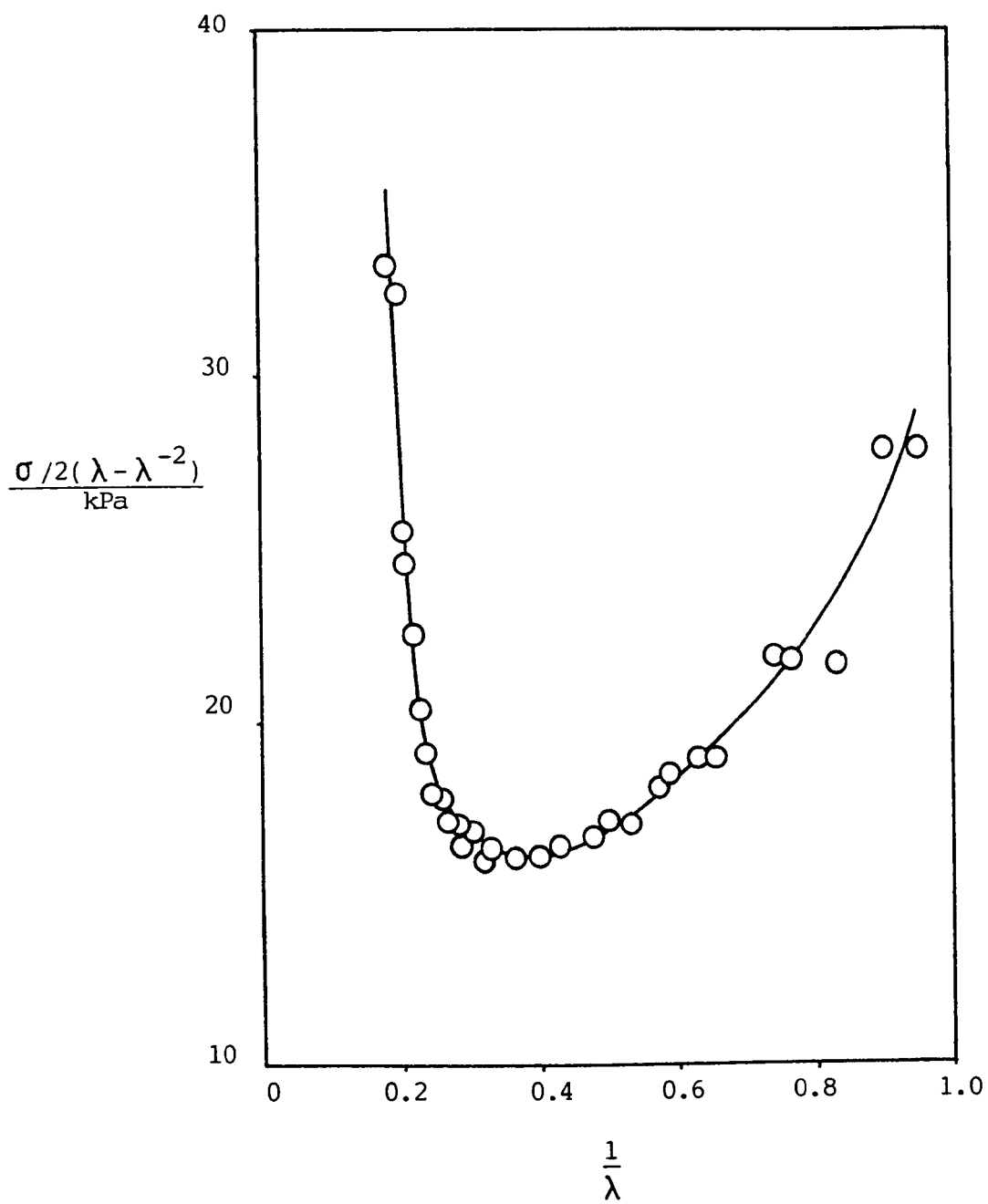


Fig. 4-61f: Mooney-Rivlin Curve for Terpolymer Hydrogel Containing  
20% DDA

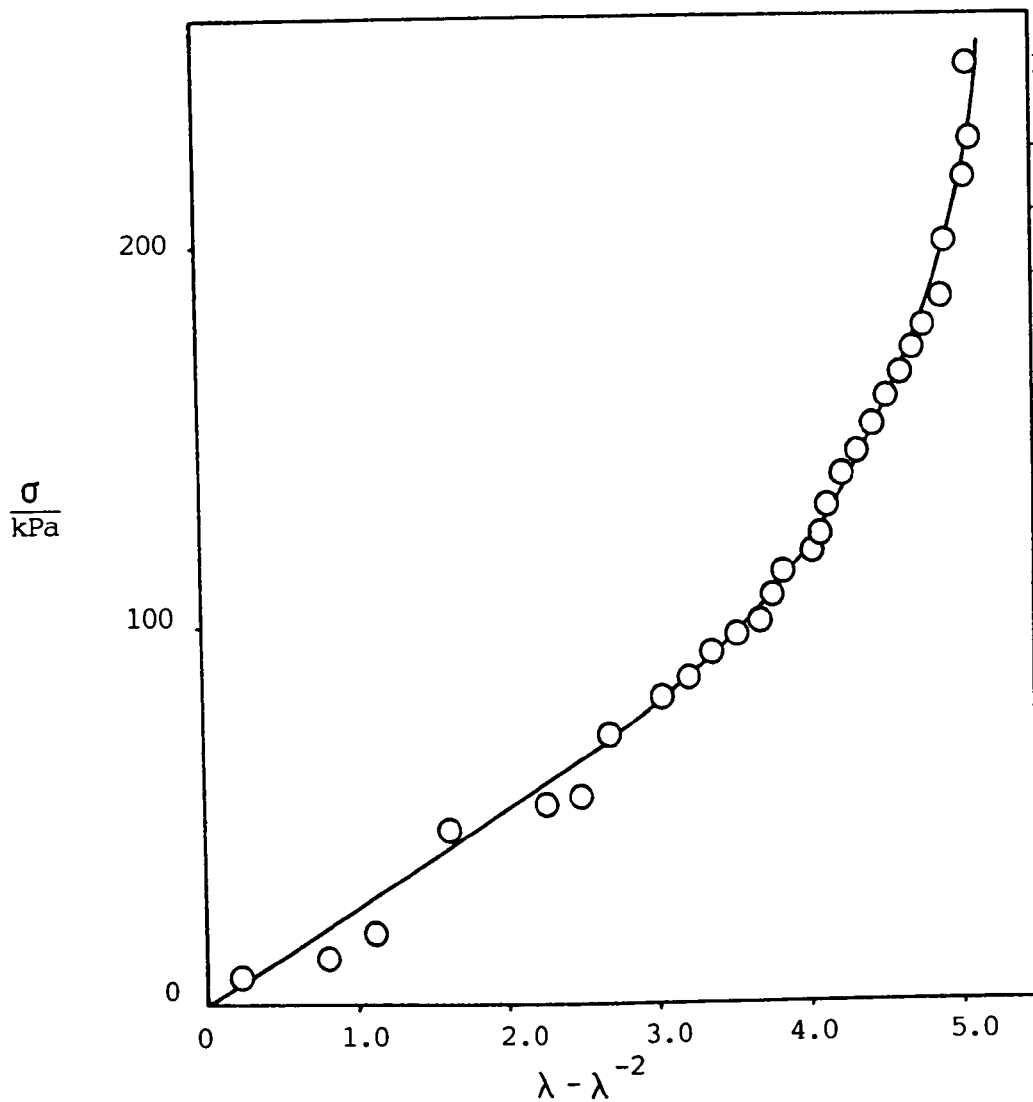


Fig. 4-6lg:  
 $\sigma$  vs.  
 $\lambda - \lambda^{-2}$  for  
 Terpolymer  
 Hydrogel  
 Containing  
 30% DDA

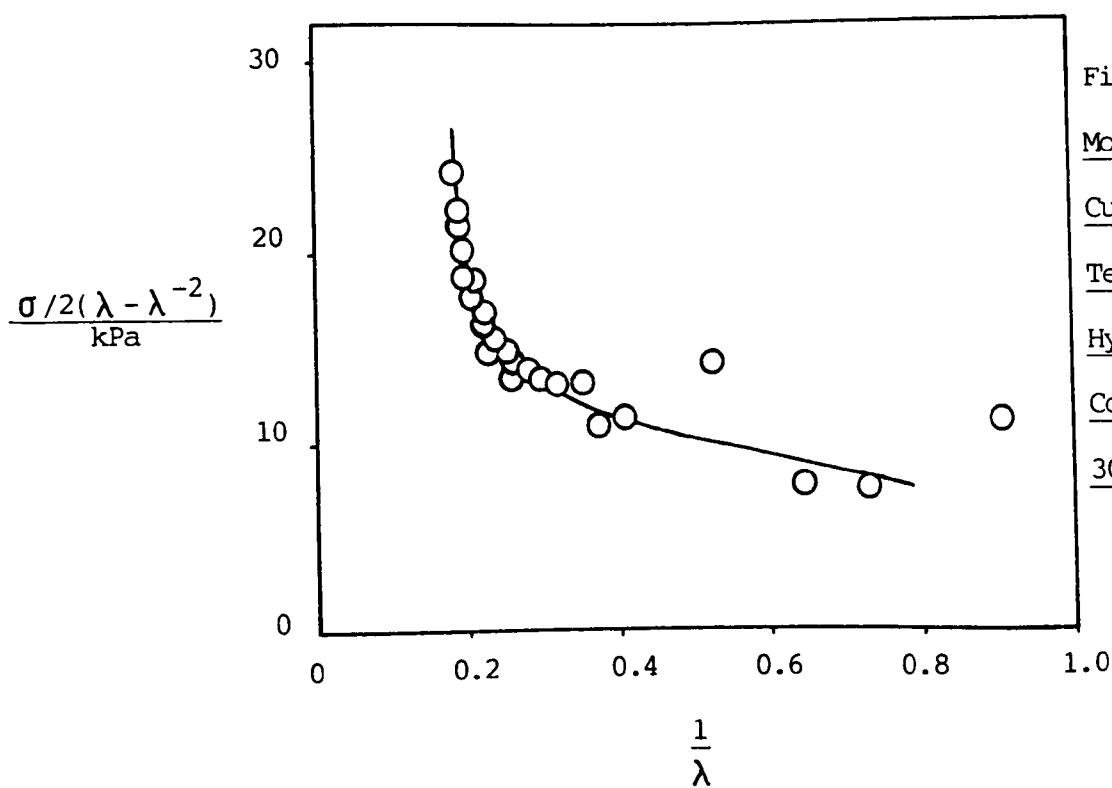


Fig. 4-6lh:  
 Mooney-Rivlin  
 Curve for  
 Terpolymer  
 Hydrogel  
 Containing  
 30% DDA

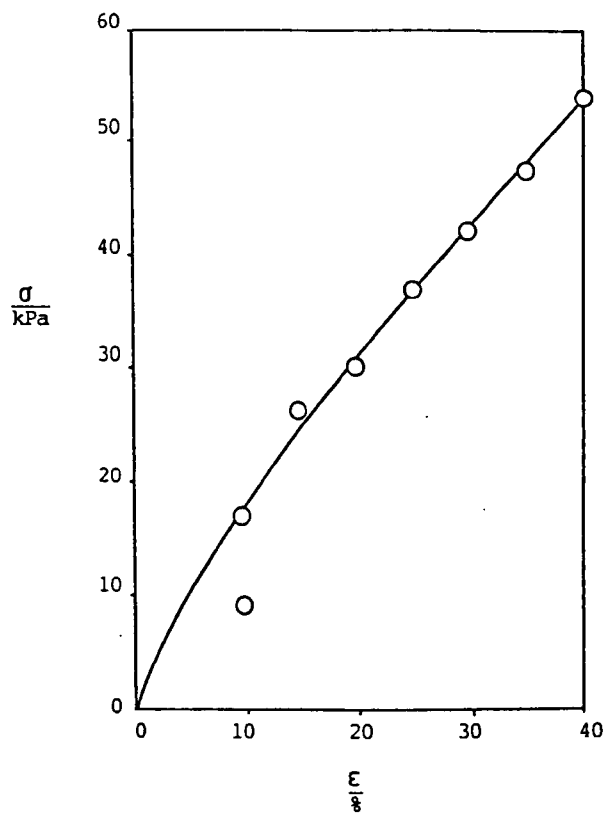


Fig. 4-62a: Stress-Strain Curve for Terpolymer Hydrogel Containing  
5 mol % styrene

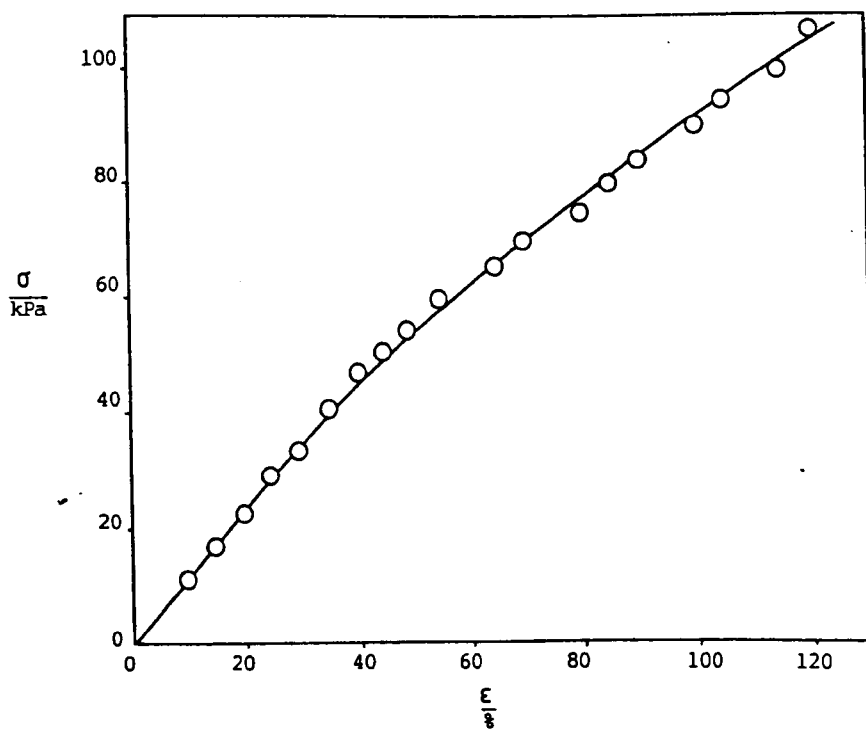


Fig. 4-62b: Stress-Strain Curve for Terpolymer Hydrogel Containing  
7.5% Styrene

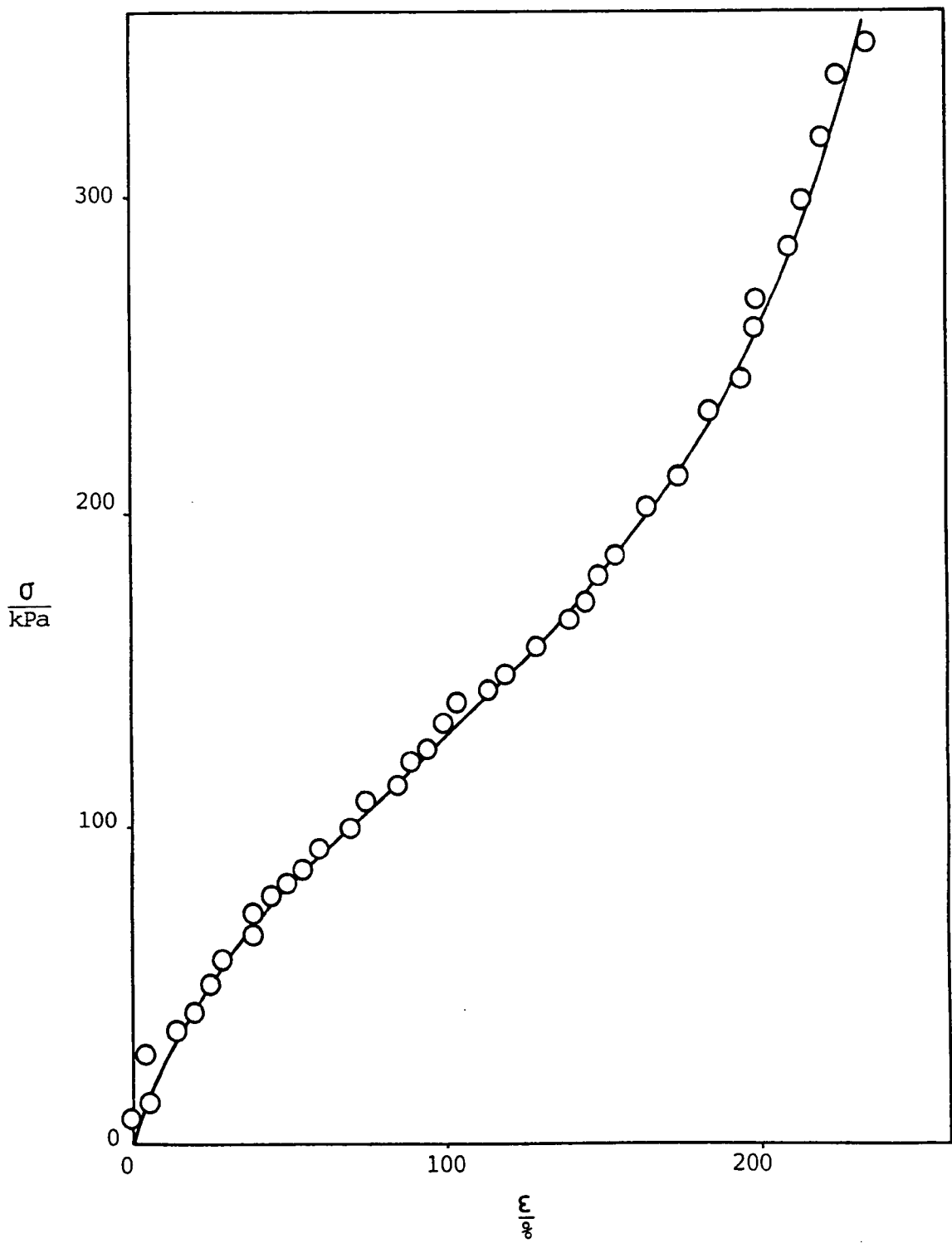


Fig. 4-62c: Stress-Strain Curve for Terpolymer Hydrogel Containing 10% Styrene

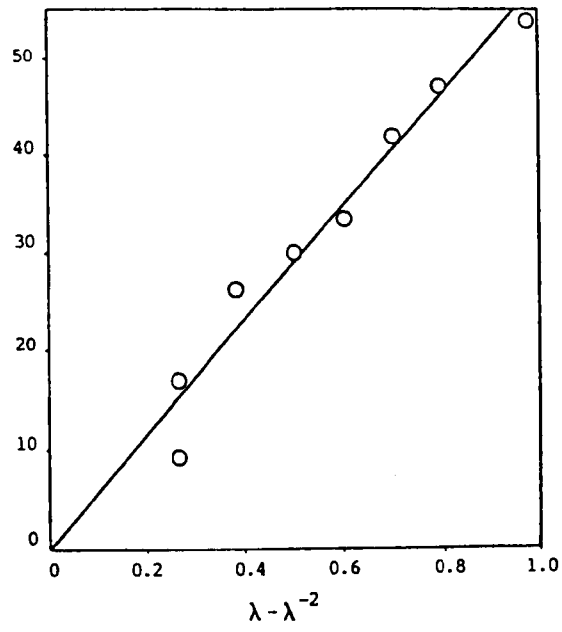


Fig. 4-63a:  $\sigma$  vs.  $\lambda - \lambda^{-2}$  for Terpolymer Hydrogel Containing  
5% Styrene

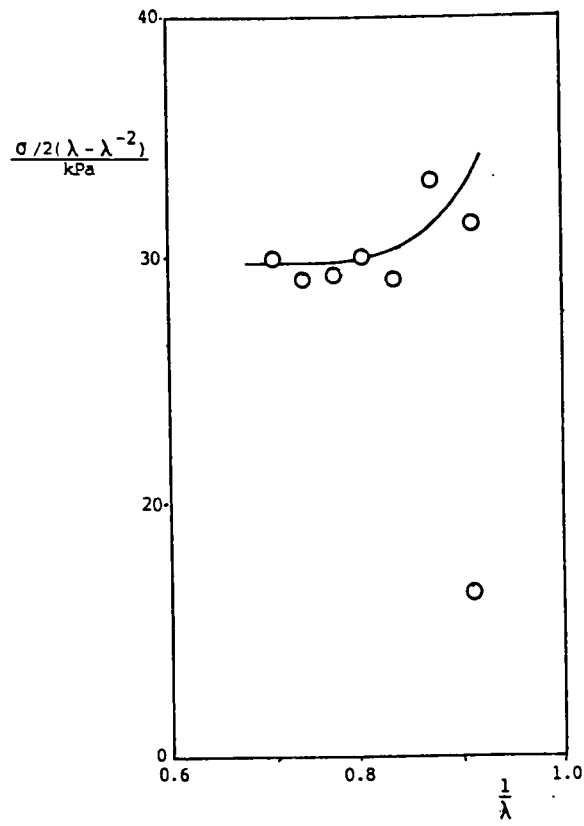


Fig. 4-63b: Mooney-Rivlin Curve for Terpolymer Hydrogel Containing  
5% Styrene



the data can be represented by a straight line of zero slope and intercept (extrapolated) 30 kPa. The  $\sigma$  vs.  $\lambda - \lambda^{-2}$  plots for the 7.5 mol % and 10 mol % styrene materials are shown in Figs. 4-63c and 4-63d respectively. The former is linear, with a slope of 50 kPa, and the latter linear at lower strains, with the slope increasing at higher strains. The slope of the linear portion is 76 kPa. The Mooney-Rivlin plot for the 7.5 mol % styrene material (Fig. 4-63d) is linear at higher strains, with slope zero and intercept (extrapolated) 26 kPa. At lower strains the plot is also linear, but of negative slope. The Mooney-Rivlin plot for the 10 mol % styrene material is linear at intermediate levels of strain, with zero slope and intercept approximately 38 kPa (Fig. 4-63f). At low and high strains the curve deviates from linearity.

Figs. 4-64a to 4-64d show the stress/strain curves obtained for terpolymer hydrogels containing HPMA. The 15% material has a low-extension modulus of 202 kPa. The slope decreases until breakage occurs. The other three HPMA curves all show a point of inflexion at approximately  $\epsilon = 100\%$ . The moduli are given below in Table 4-7.

Table 4-7: Moduli of Terpolymer Hydrogels Containing HPMA

mol % HPMA	modulus/ kPa at		
	0%	50%	100%
15	202	76	-
30	224	74	80
40	254	94	81
50	257	107	92

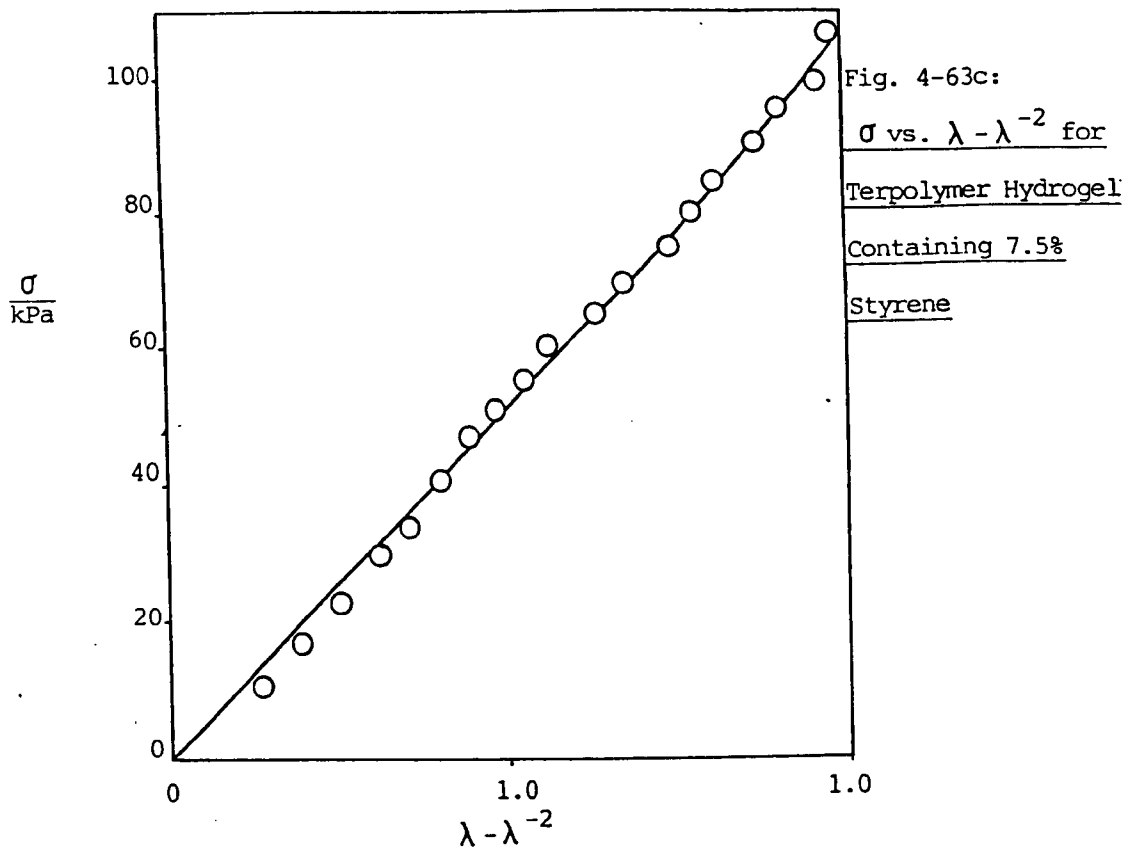
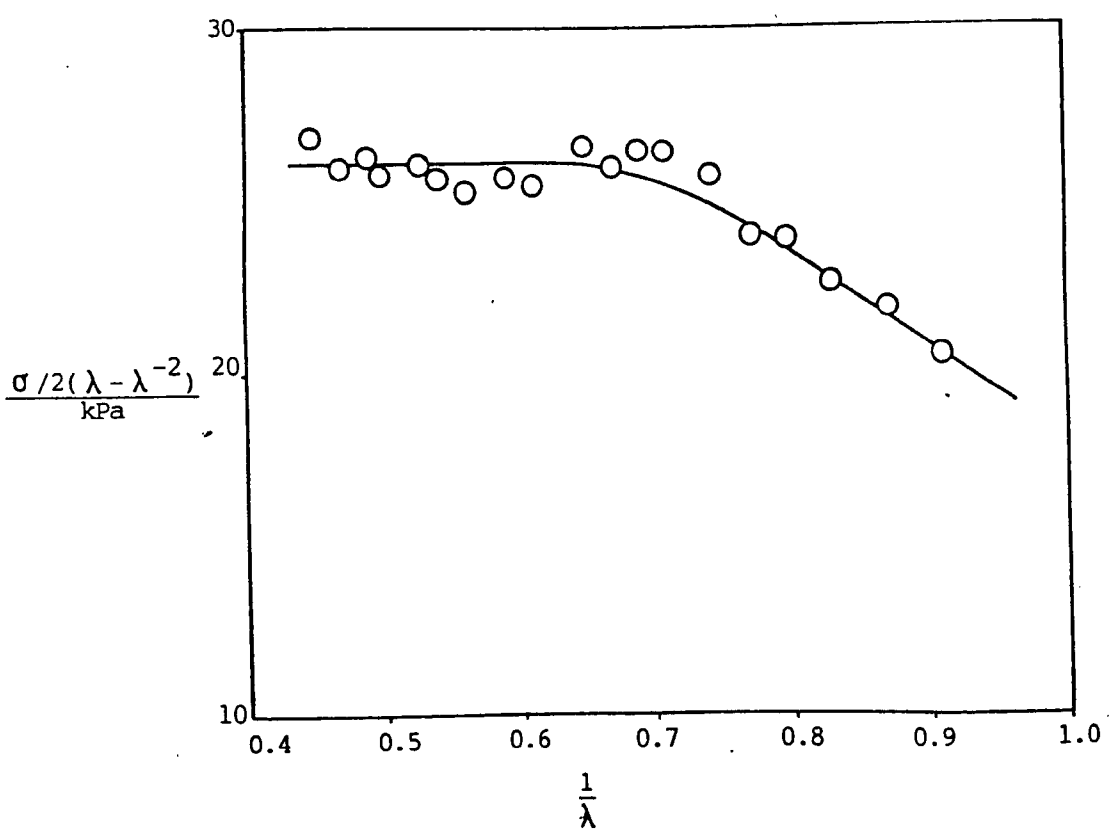


Fig. 4-63d: Mooney-Rivlin Curve for Terpolymer Hydrogel Containing 7.5% Styrene



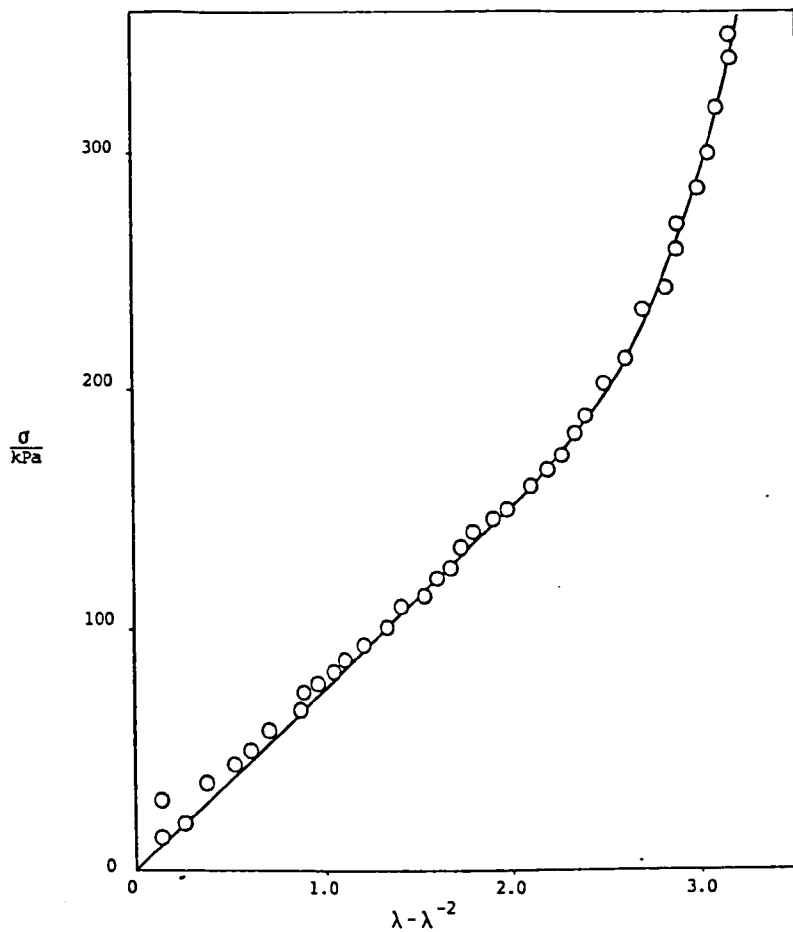


Fig. 4-63e:  $\sigma$  vs.  $\lambda - \lambda^{-2}$  for Terpolymer Hydrogel Containing  
10% Styrene

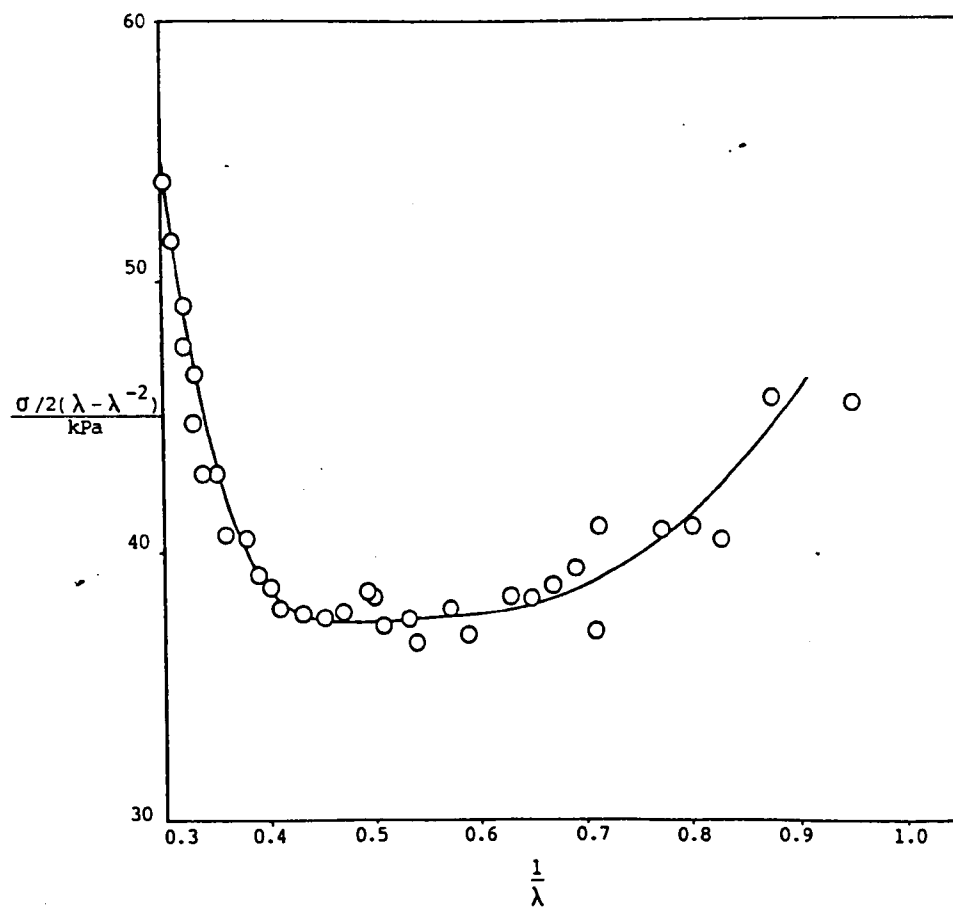


Fig. 4-63f: Mooney-Rivlin Curve for Terpolymer Hydrogel Containing  
10% Styrene

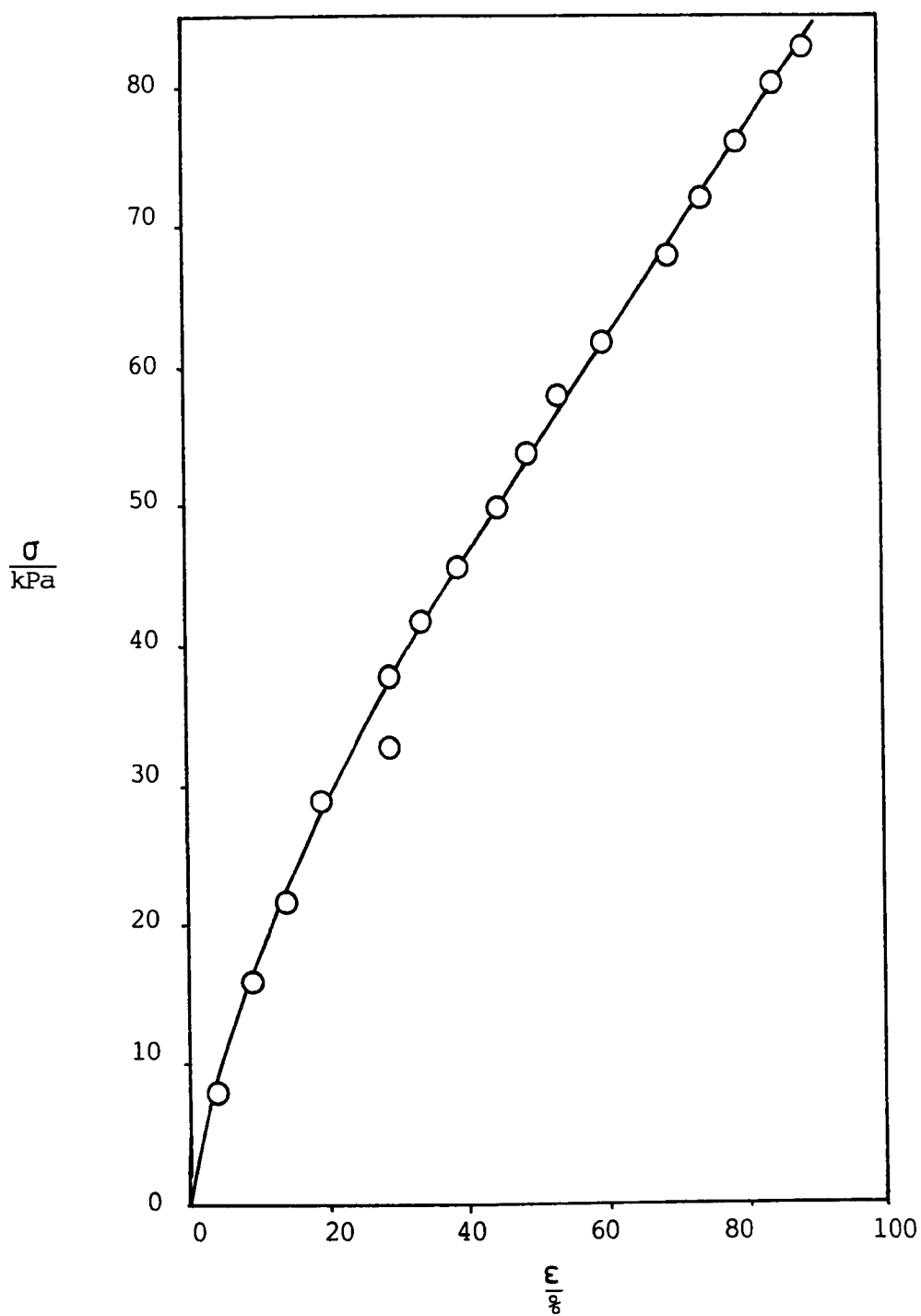


Fig. 4-64a: Stress-Strain Curve for Terpolymer Hydrogel Containing  
15% HPMA

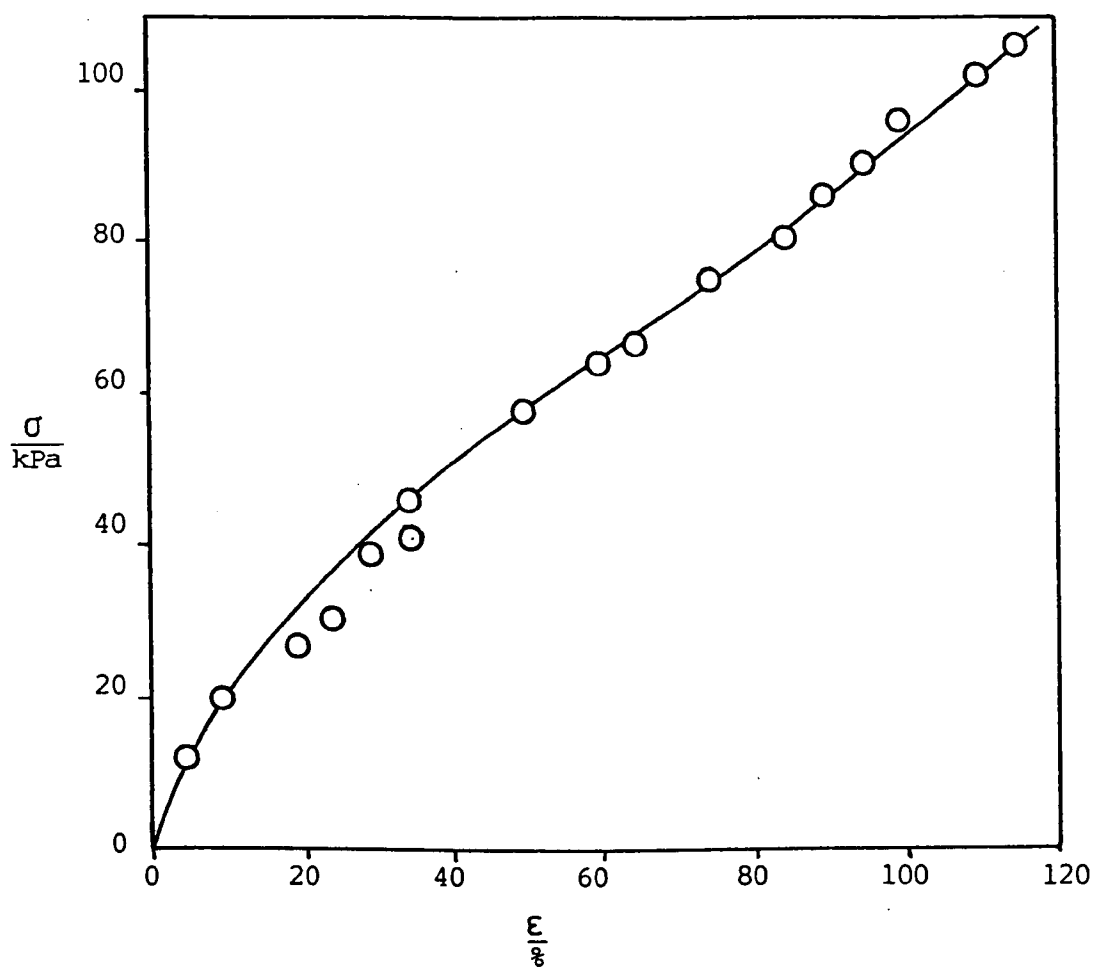


Fig. 4-64b: Stress-Strain Curve for Terpolymer Hydrogel  
Containing 30% HPMA

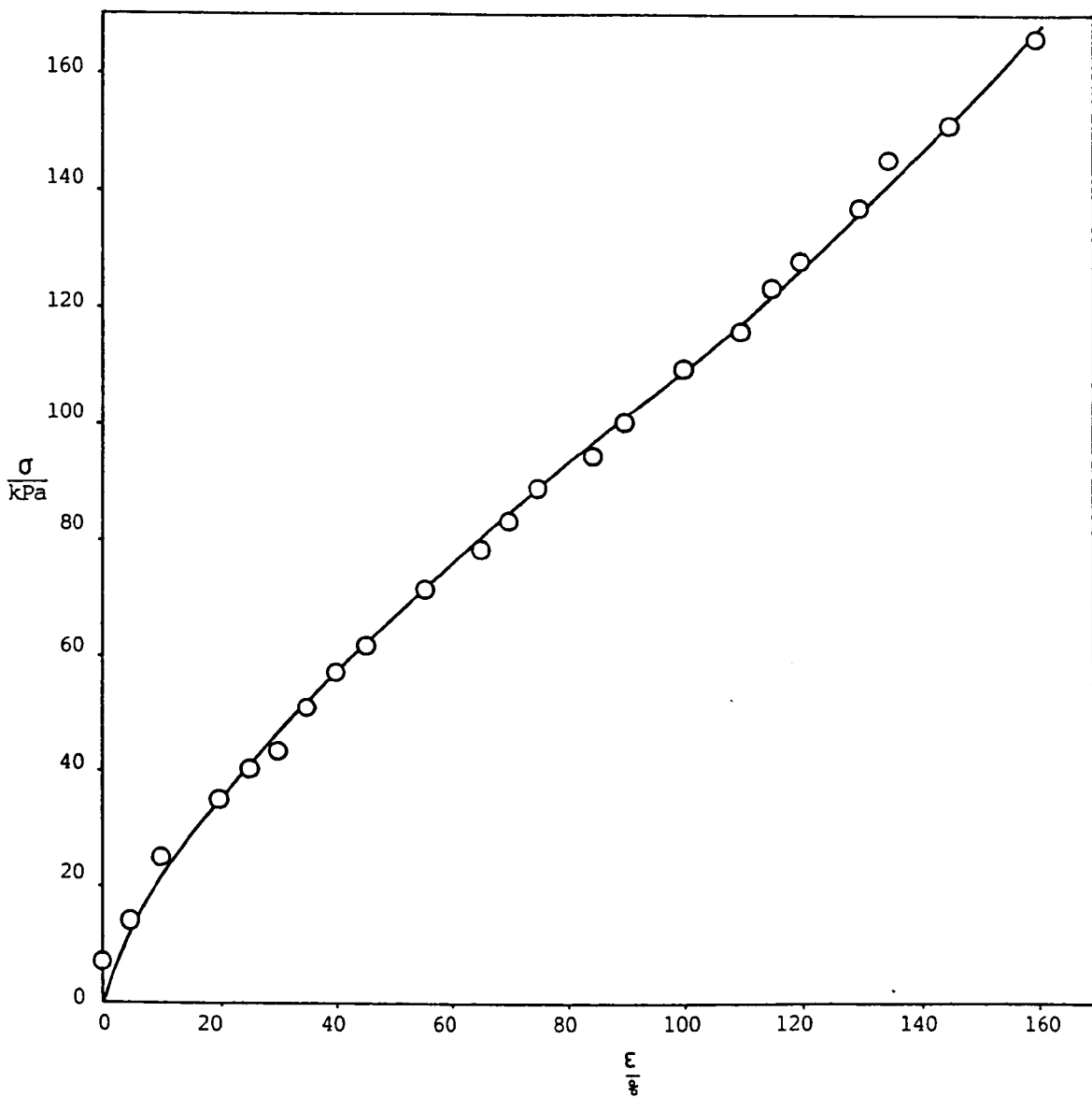


Fig. 4-64c: Stress-Strain Curve for Terpolymer Hydrogel Containing  
40% HPMA

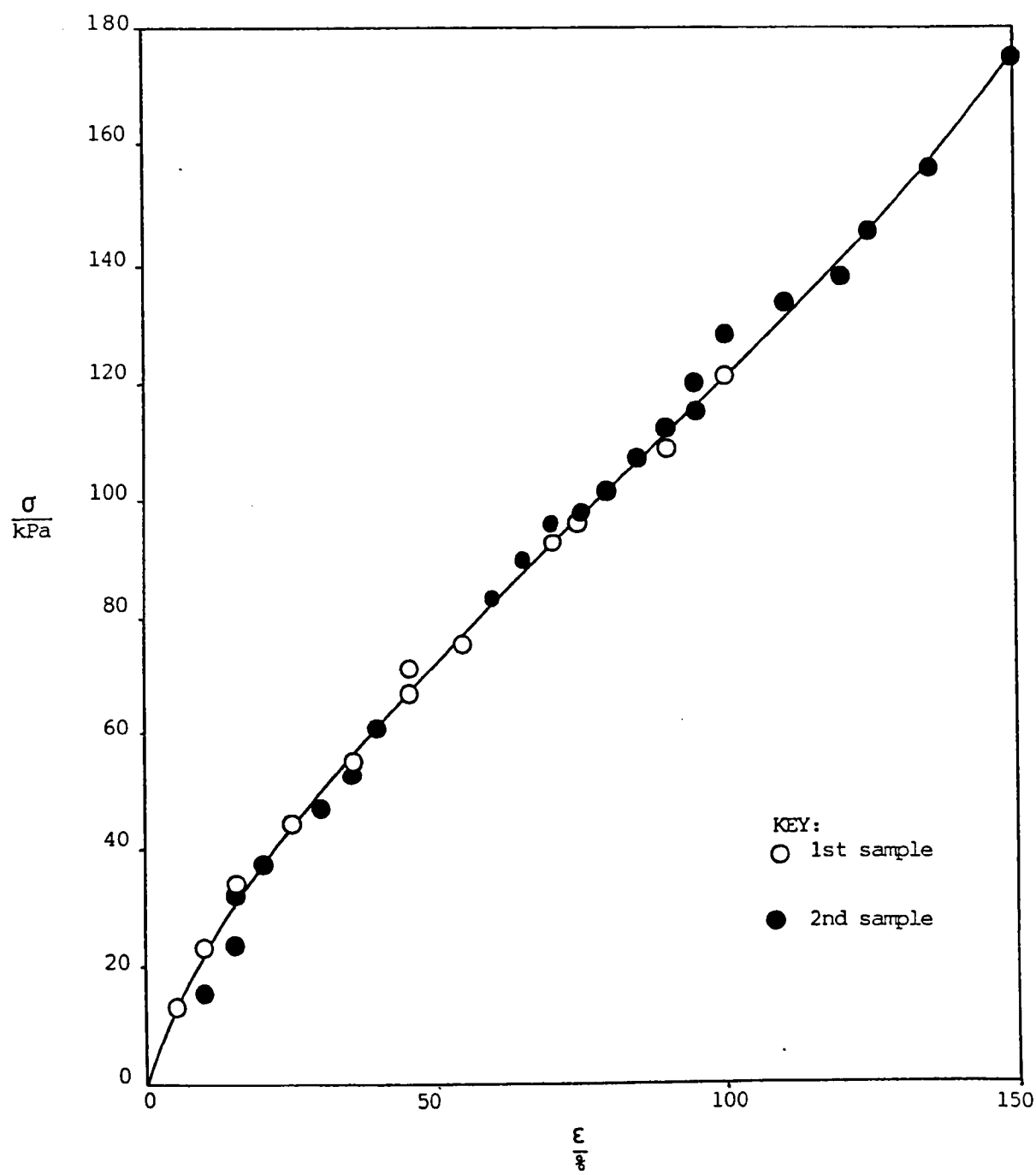


Fig. 4-64d: Stress-Strain Curve for Terpolymer Hydrogel Containing  
50% HPMA

The  $\sigma$  vs.  $\lambda - \lambda^{-2}$  plot for the 15 mol % HPMA material is linear (Fig. 4-65a), the slope being 52 kPa. The Mooney-Rivlin plot (Fig. 4-65b) is linear at high strains, the slope being zero and the intercept 26 kPa (extrapolated). At low strains, the curve deviates from linearity. The  $\sigma$  vs.  $\lambda - \lambda^{-2}$  plots for the 30%, 40% and 50% HPMA materials, shown in Figs. 4-65c, e and g respectively, are linear, although the curves for the 40% and 50% materials show deviations from linearity at higher strains. Their slopes are: for the 30 mol % material, 54 kPa; for the 40 mol % material, 64 kPa; for the 50 mol % material, 70 kPa. The Mooney-Rivlin plot for the 30% gel (Fig. 4-65d) is similar to that for the 15% material. The intercept of the linear portion (extrapolated) is 27 kPa. The Mooney-Rivlin plot for the 40% material retains the linear portion at intermediate strains, but at higher strains deviates from linearity. The intercept of the linear portion is 31 kPa. The linear part of the curve for the 50% material (Fig. 4-65h) is much smaller; its intercept is 34 kPa.

Figs. 4-66a and b show stress/strain curves for terpolymer hydrogels containing PPM6. The curves do not show points of inflexion, the slope in each case decreasing progressively with increasing strain. Table 4-8 gives the various moduli.

Table 4-8: Moduli of Terpolymer Hydrogels Containing PPM6

mol % PPM6	modulus/kPa at	
	0%	50%
10	115	-
15	289	-
20	151	93



Fig. 4-65a:  $\sigma$  vs.  $\lambda - \lambda^{-2}$  for Terpolymer Hydrogel Containing  
15% HPMA

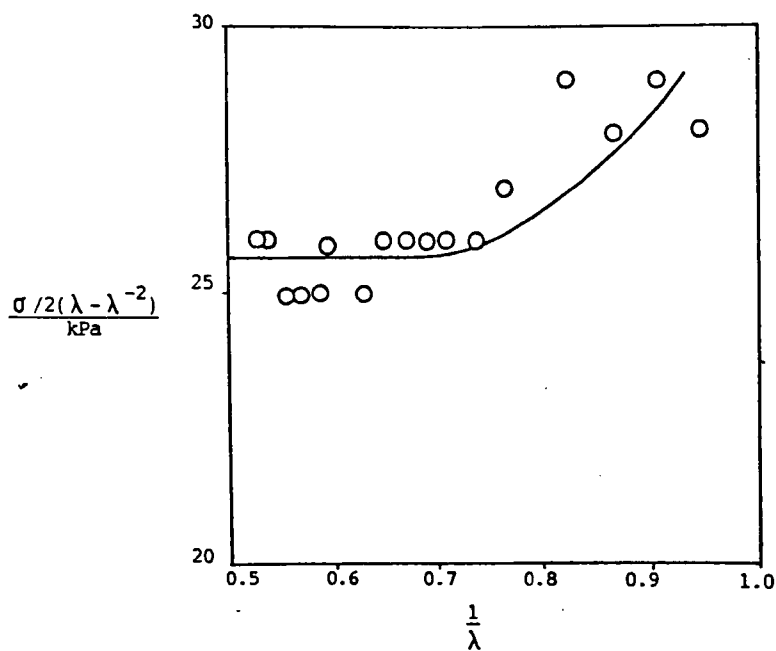
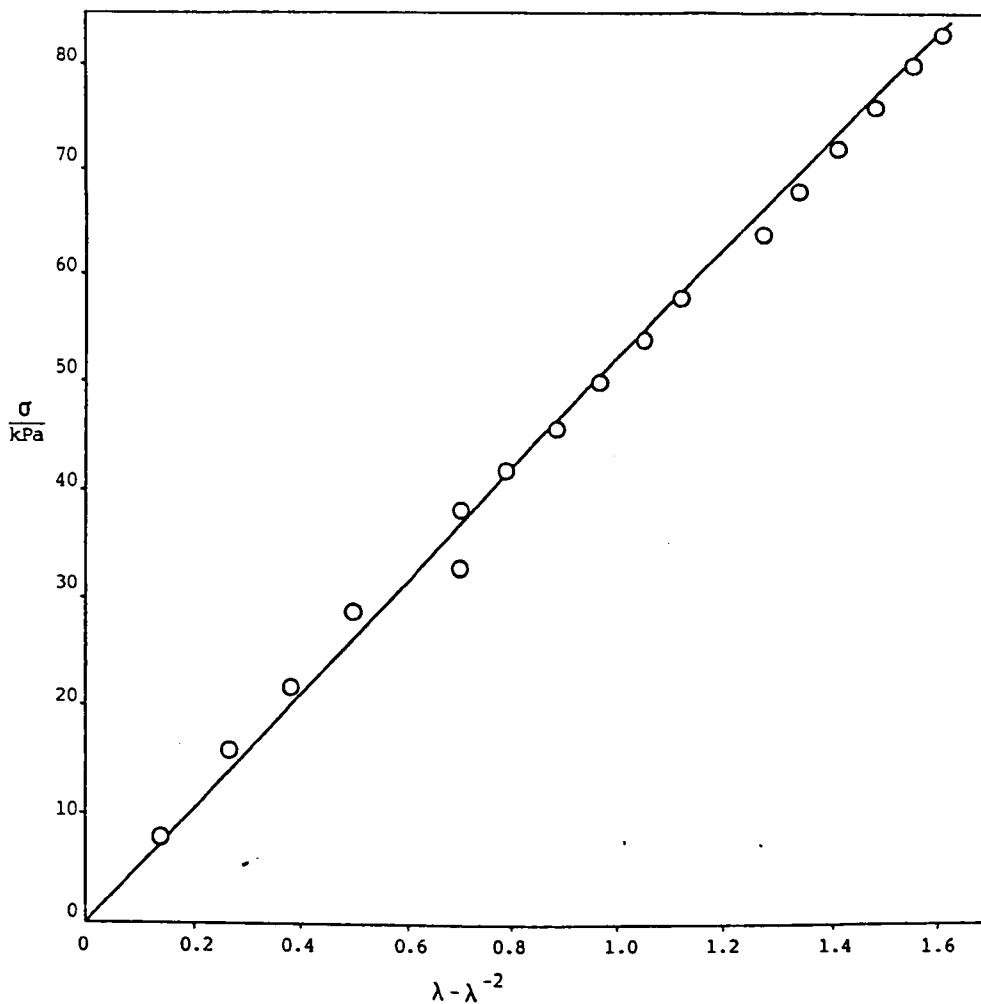


Fig. 4-65b: Mooney-Rivlin Plot for Terpolymer Hydrogel Containing  
15% HPMA

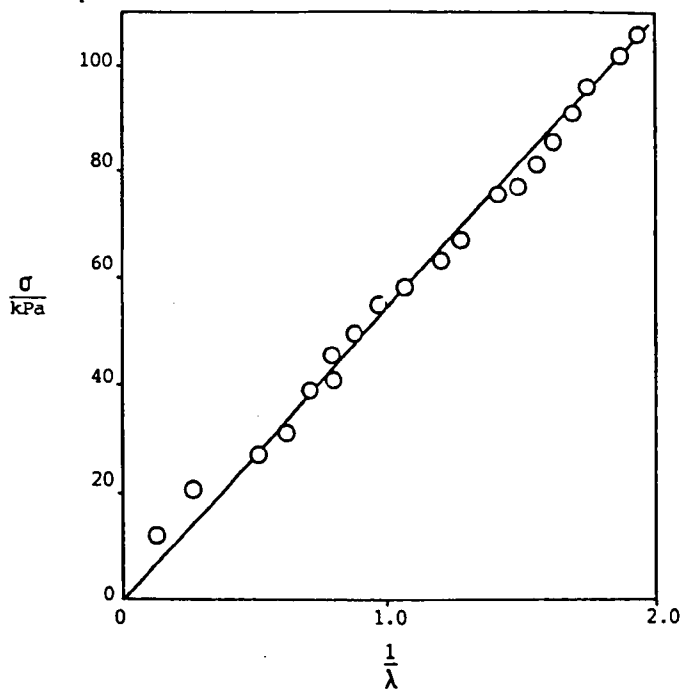


Fig. 4-65c:  $\sigma$  vs.  $\lambda - \lambda^{-2}$  for Terpolymer Hydrogel Containing  
30% HPMA

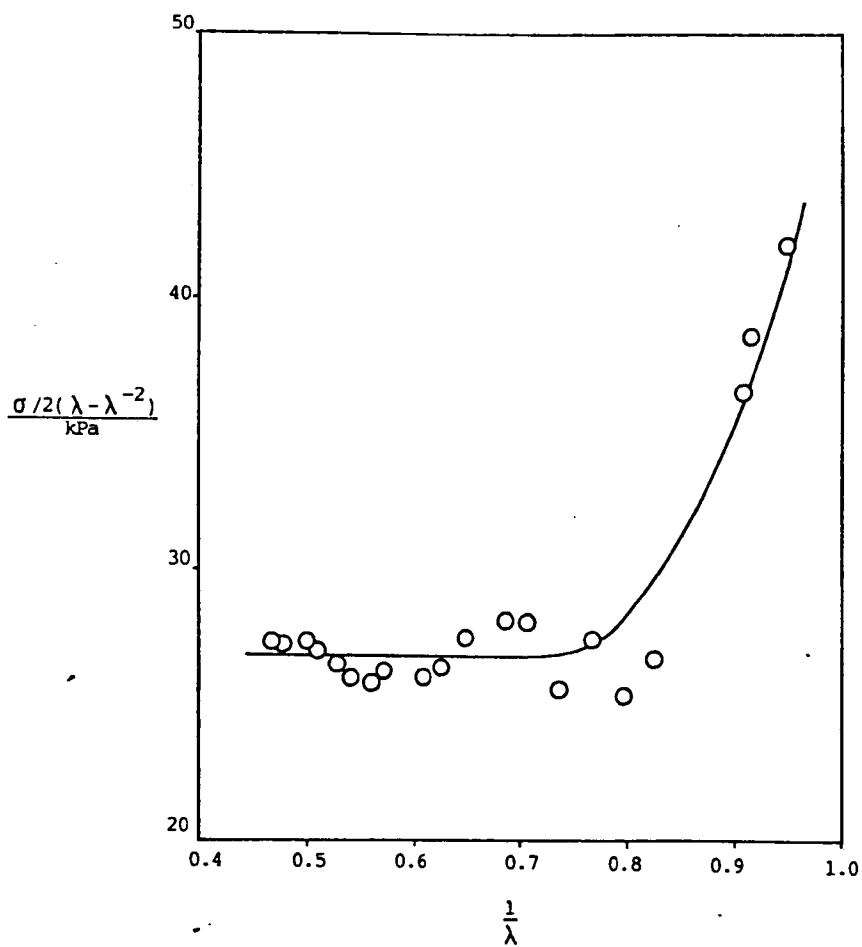


Fig. 4-65d: Mooney-Rivlin Plot for Terpolymer Hydrogel Containing  
30% HPMA

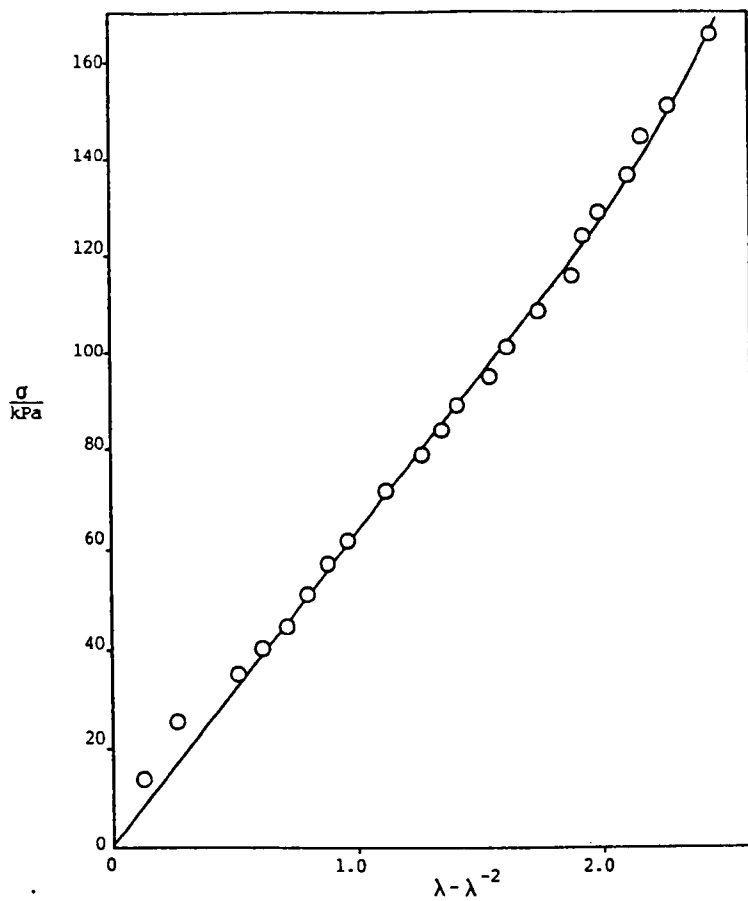


Fig. 4-65e:  $\sigma$  vs.  $\lambda - \lambda^{-2}$  for Terpolymer Hydrogel Containing  
40% HPMA

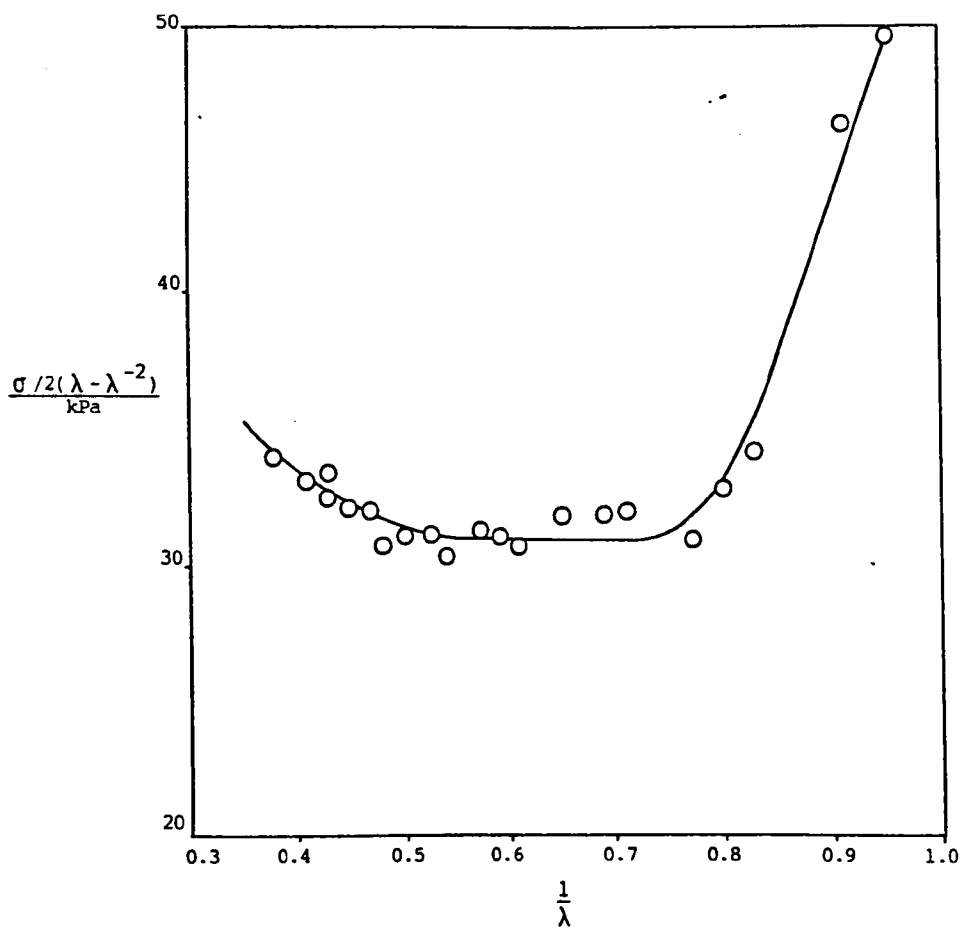


Fig. 4-65f: Mooney-Rivlin Plot for Terpolymer Hydrogel Containing  
40% HPMA

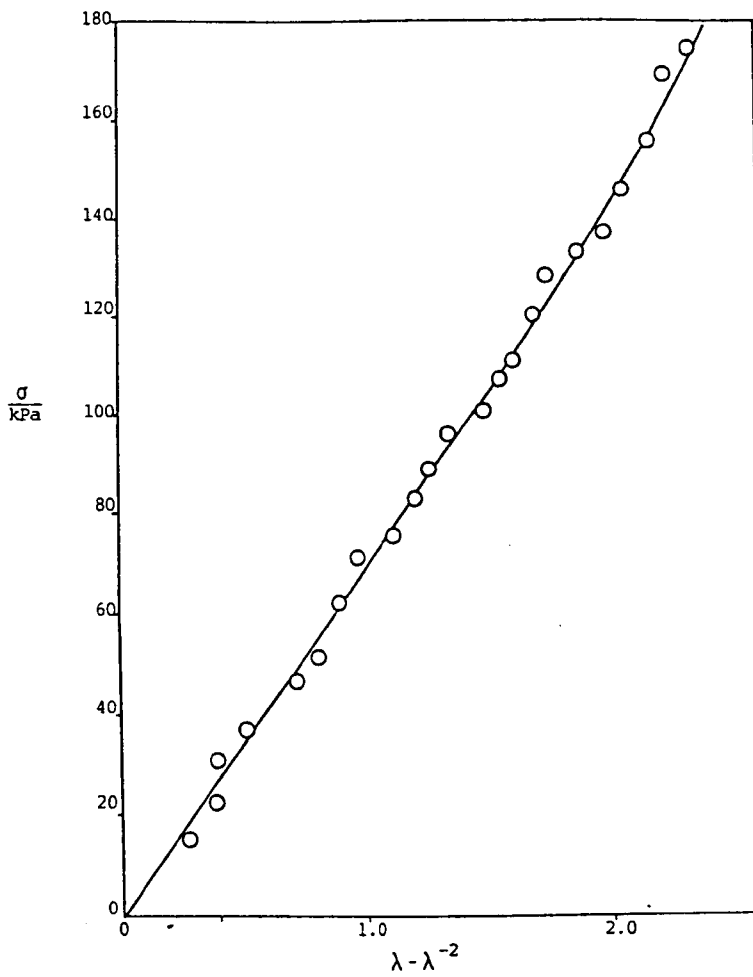


Fig. 4-65g:  $\sigma$  vs.  $\lambda - \lambda^{-2}$  for Terpolymer Hydrogel Containing  
50% HPMA

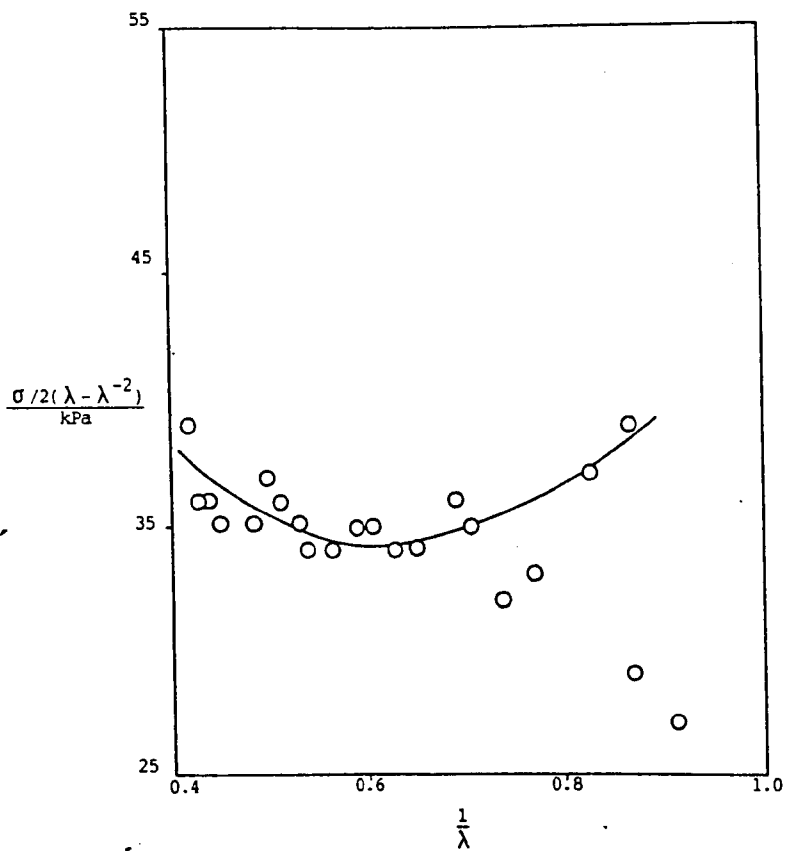


Fig. 4-65h: Mooney-Rivlin Plot for Terpolymer Hydrogel Containing  
50% HPMA

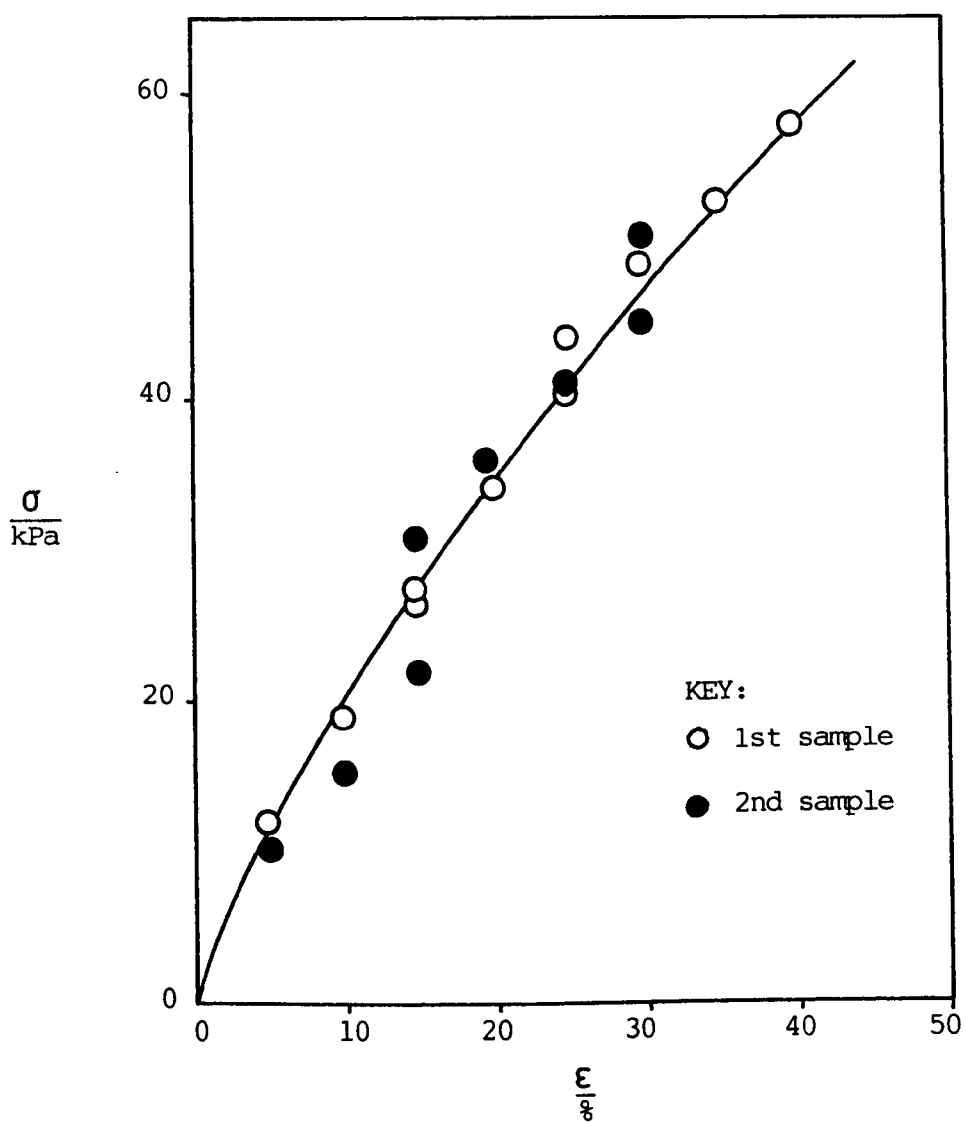


Fig. 4-66a: Stress-Strain Curve for Terpolymer Hydrogel Containing 15% PPM 6

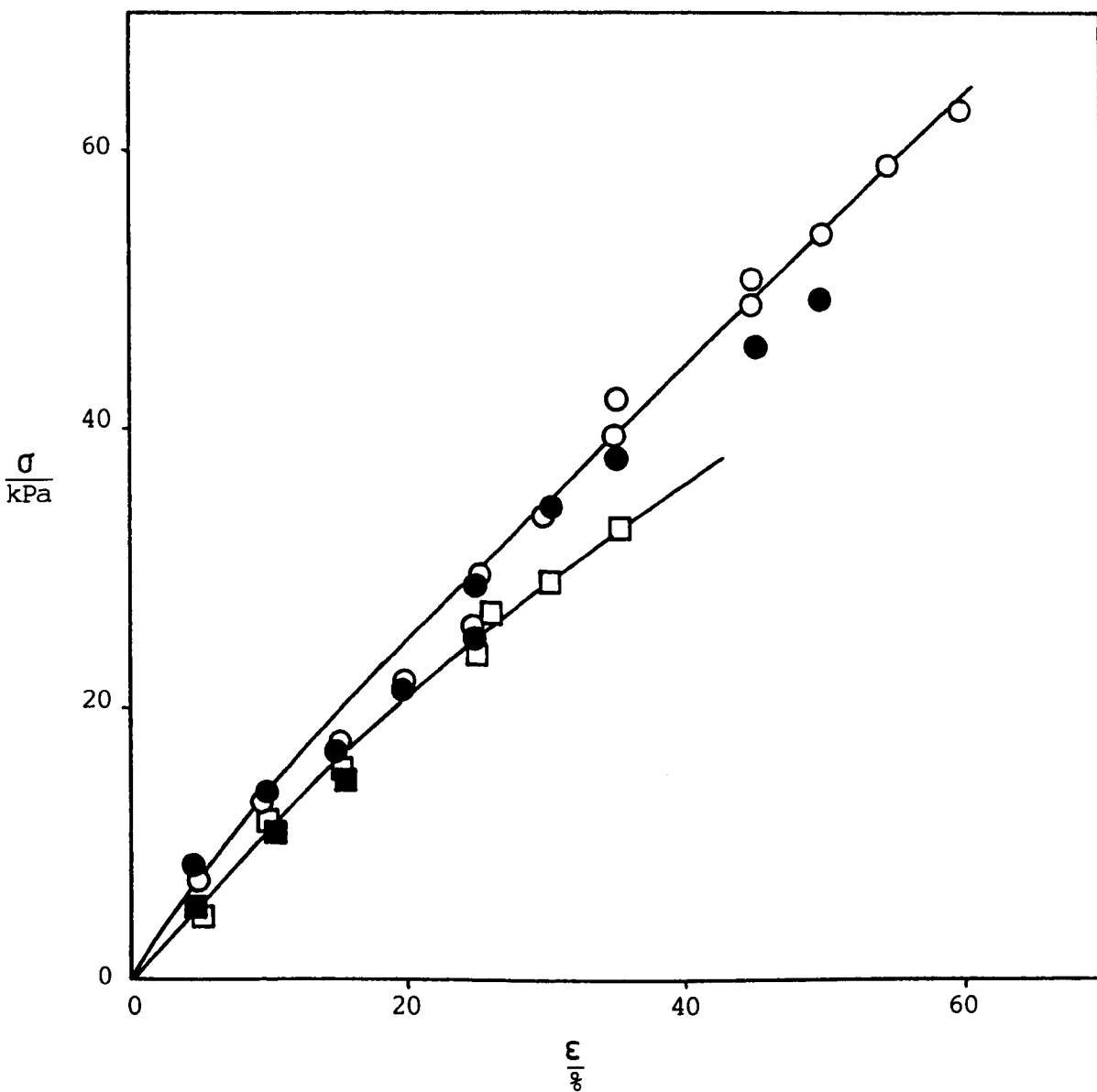


Fig. 4-66b: Stress-Strain Curve for Terpolymer Hydrogels Containing  
10 mol % and 20 mol % PPM 6

KEY:

□ 10% - 1st sample  
 ■ 10% - 2nd sample

○ 20% - 1st sample  
 ● 20% - 2nd sample

The  $\sigma$  vs.  $\lambda - \lambda^{-2}$  plots for the 10 mol % PPM6, 15 mol % PPM6 and 20 mol % PPM6 materials are shown in Figs. 4-67a, c and e respectively. They are all linear. Their slopes are 51 kPa, 69 kPa and 42 kPa respectively. The Mooney-Rivlin plot for the 10% material (Fig. 4-67b) displays a minimum at  $1/\lambda = 0.85$ , and does not show a linear portion. It is also an unusually scattered plot. The Mooney-Rivlin plot for the 15% material (Fig. 4-67d), however, is linear at high strains, the slope being zero and the intercept 33 kPa. At lower strains the curve is non-linear. The Mooney-Rivlin plot for the 20 mol % material (Fig. 4-67f) is linear at low strains, the slope being zero and the intercept 21 kPa but, unusually, at higher strains the deviation from linearity is such that the value of  $\sigma/2(\lambda - \lambda^{-2})$  decreases with decreasing strain.

Fig. 4-68 shows the stress-strain curve for a terpolymer hydrogel containing 50% HEMA(3)/50% HEMA/MAA. The shape is similar to those for the PPM6 terpolymers. The low-extension modulus is 179 kPa. The  $\sigma$  vs.  $\lambda - \lambda^{-2}$  plot (Fig. 4-69a) is linear, the slope being 51 kPa. Fig. 4-69b shows the Mooney-Rivlin plot, which is linear at higher strains with slope zero and intercept 50 kPa and deviates from linearity at lower strains.

The shapes of the foregoing stress/strain curves fall into two categories: (i) those in which the slope steadily decreases with strain before the material breaks; (ii) those in which at higher strains a point of inflexion is observed, where the slope begins to increase with increasing strain. Table 4-9 shows the distribution of these materials between these categories. It is clear that terpolymers containing higher levels of hydrophobic monomer tend to fall into category (ii),

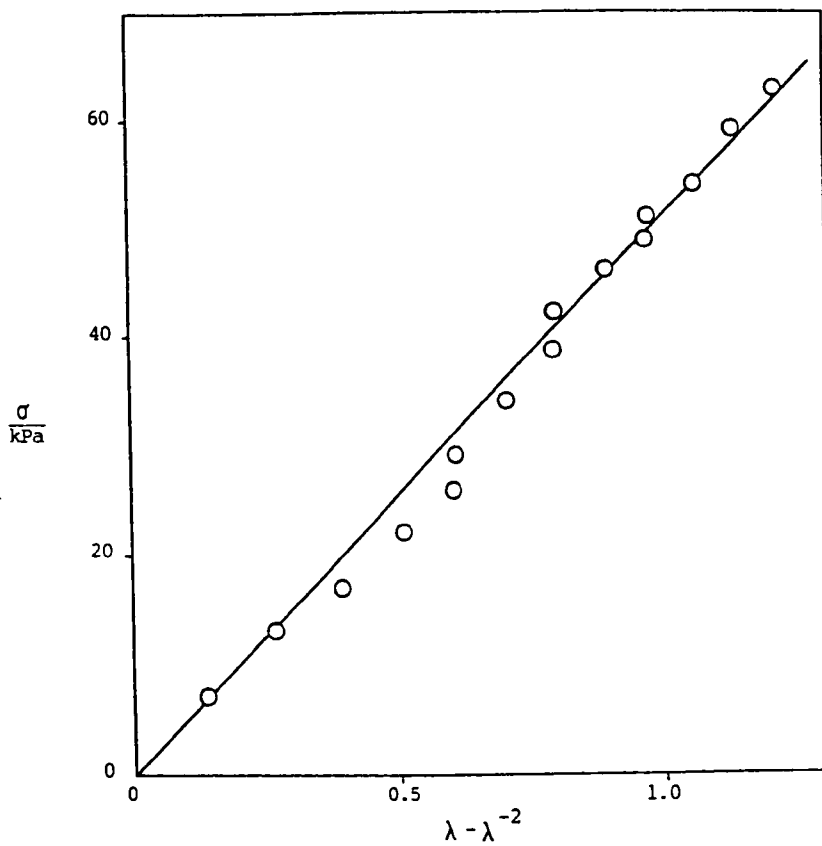


Fig. 4-67a:  $\sigma$  vs.  $\lambda - \lambda^{-2}$  for Terpolymer Hydrogel Containing  
10% PPM 6

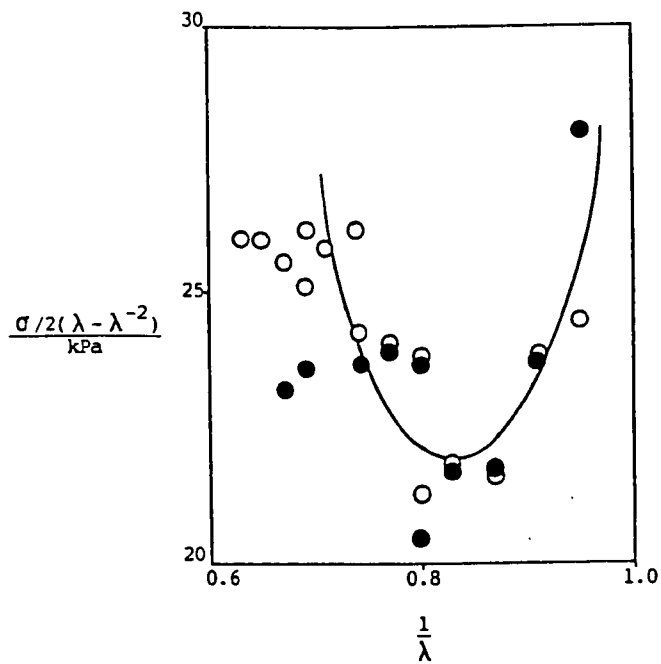


Fig. 4-67b: Mooney-Rivlin Plot for Terpolymer Hydrogel Containing  
10% PPM 6

KEY:  
○ 1st sample  
● 2nd sample



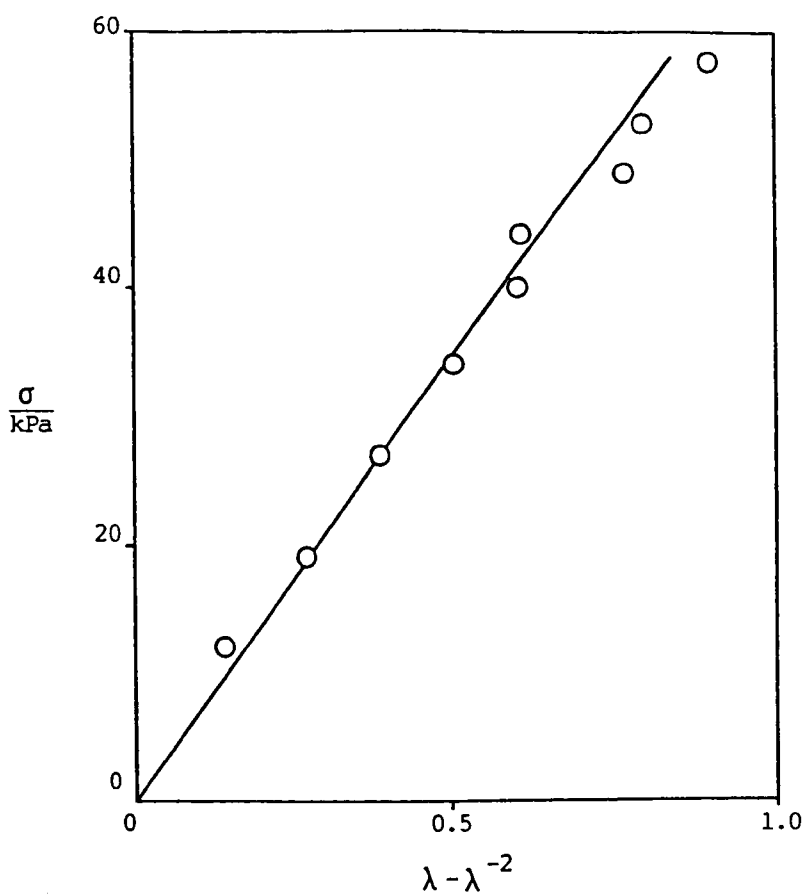


Fig. 4-67c:  $\sigma$  vs.  $\lambda - \lambda^{-2}$  for Terpolymer Hydrogel Containing  
15% PPM 6

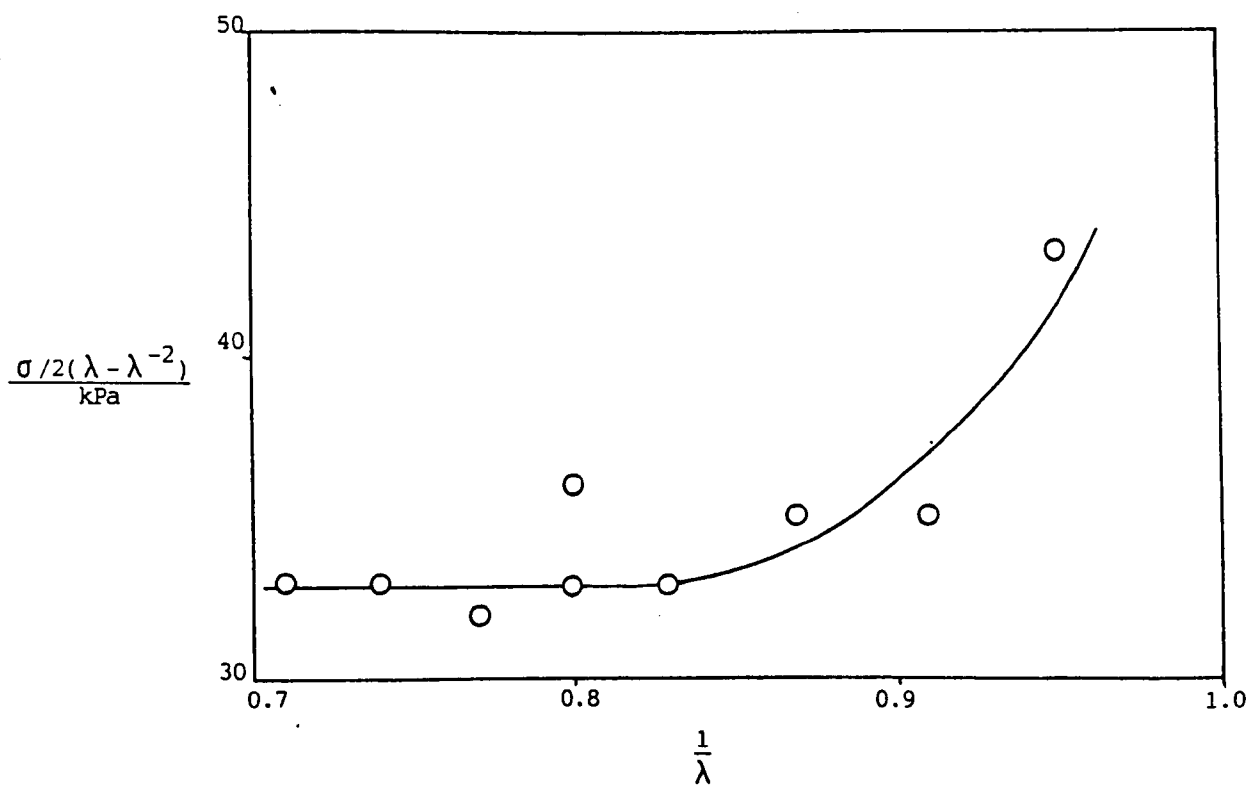


Fig. 4-67d: Mooney-Rivlin Plot for Terpolymer Hydrogel Containing 15% PPM 6

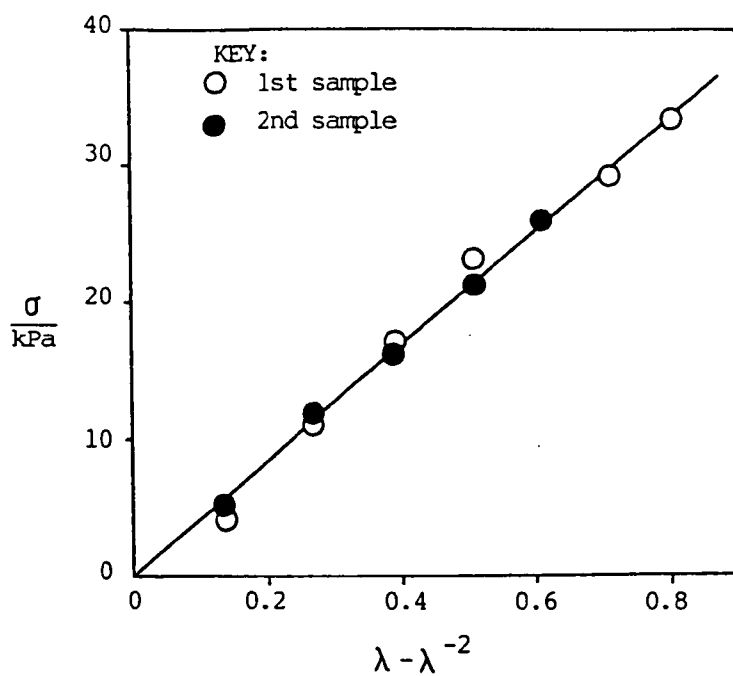


Fig. 4-67e:  $\sigma$  vs.  $\lambda - \lambda^{-2}$  for Terpolymer Hydrogel Containing  
20% PPM 6

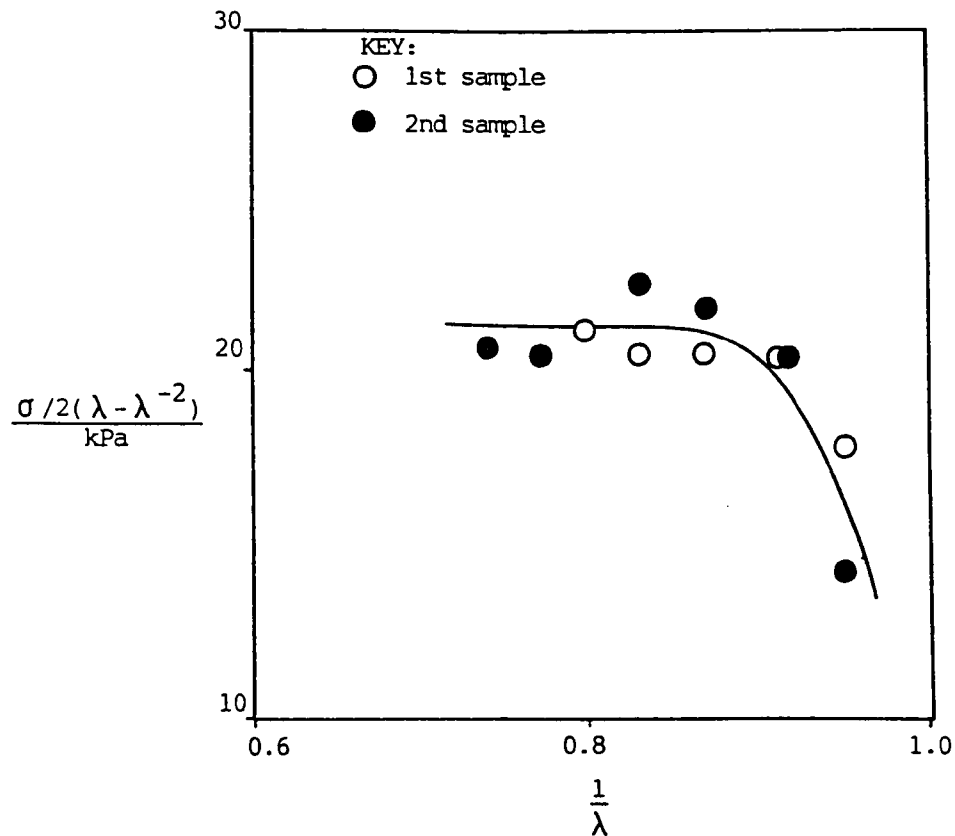


Fig. 4-67f: Mooney-Rivlin Plot for Terpolymer Hydrogel Containing  
20% PPM 6

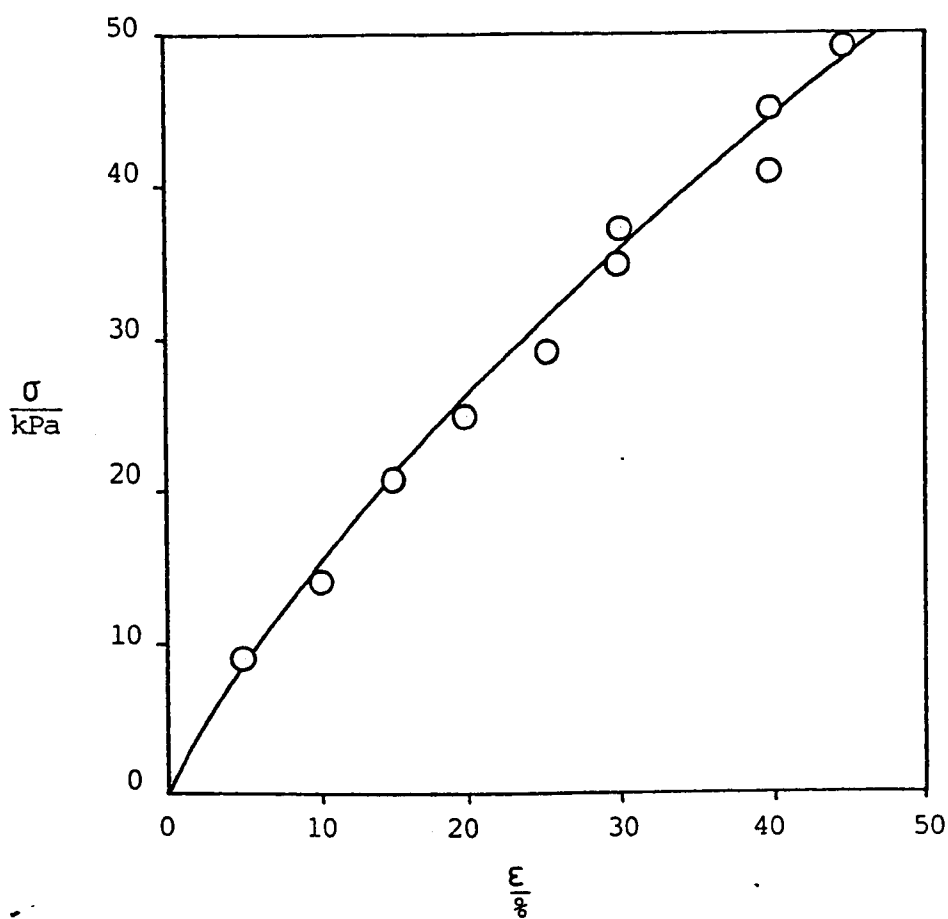


Fig. 4-68: Stress-Strain Curve for Terpolymer Hydrogel Containing  
50% HEMA as "Third Monomer"

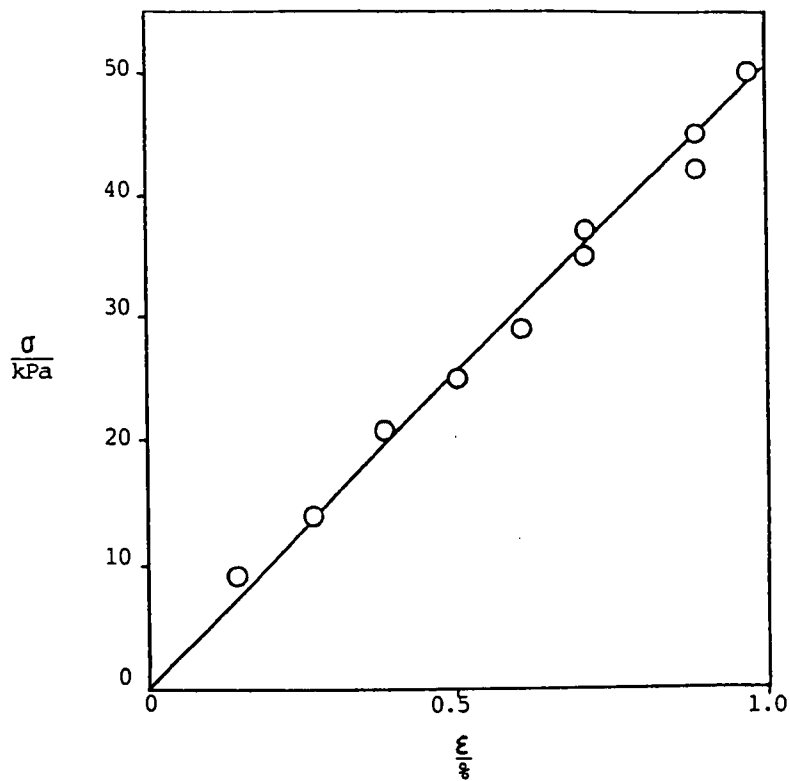


Fig. 4-69a:  $\sigma$  vs.  $\lambda - \lambda^{-2}$  for Terpolymer Hydrogel Containing  
50% HEMA

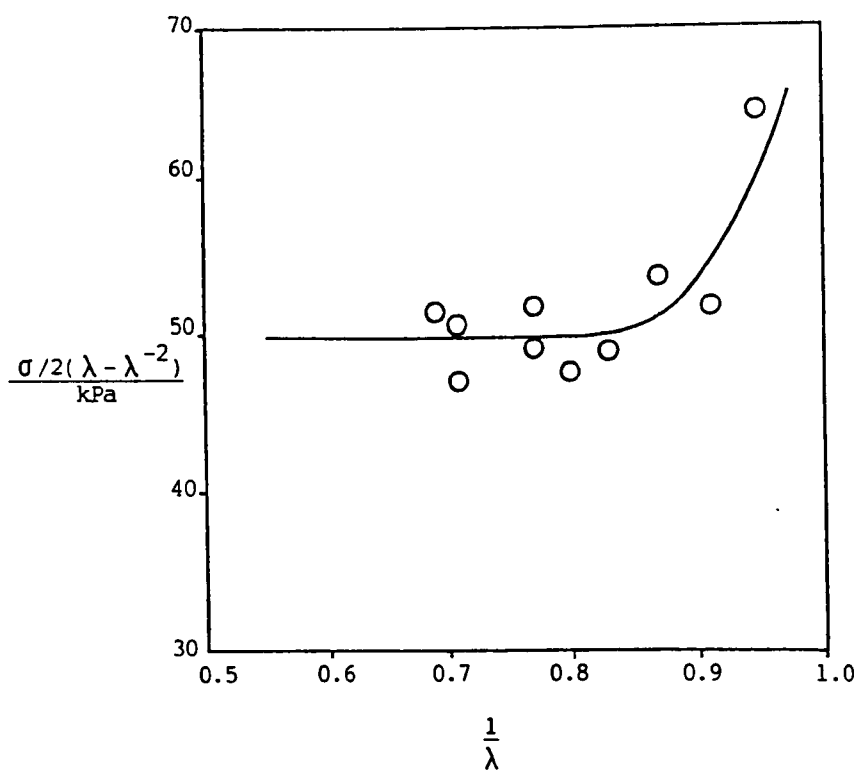


Fig. 4-69b: Mooney-Rivlin Plot for Terpolymer Hydrogel Containing  
50% HEMA

Table 4-9: Classification of Shapes of Stress/Strain Curves for Terpolymer Hydrogels

Category (i)	Category (ii)
10% MMA	30% BA
20% MMA*	10% DDA
10% EHA	15% DDA
5% styrene	20% DDA
7.5% styrene	30% DDA
15% HPMA	10% styrene
30% HPMA	40% HPMA
10% PPM6	50% HPMA
15% PPM6	
20% PPM6	
50% HEMA	

\* data from Section 4.3.1

whereas those containing lower levels tend to fall into category (i). The level at which the category changes seems to depend on the hydrophobicity of the added monomer. For example, the curves for materials containing up to 30% HPMA fall into category (i), whereas all the curves for materials containing DDA fall into category (ii). Kolarik and Migliaresi (47) observed that the stress-strain curves for copolymers of HEMA with EA and with BA, swollen to equilibrium in water, were of category (ii), although these authors did not distinguish between the two categories. They stated that this shape was "typical of rubbers". However, this should be corrected to "typical of some rubbers". Strain-crystallising rubbers do indeed display this type of behaviour,

but materials such as SBR do not (ref. 191, p.280) unless reinforced by a filler such as carbon black, which is capable of fulfilling the function of the crystallites in natural rubber. This strongly suggests that in the case of terpolymer hydrogels which have stress-strain curves in category (ii), a change occurs on deformation which is analogous to crystallisation in a strain-crystallising rubber. A possible change is phase-separation causing the production of phase domains which act in the same way as crystallites or filler particles. It is reasonable to suppose that, as the proportion of hydrophobic groups in the material is increased by increasing the level of hydrophobic monomer, so the tendency to phase-separation increases. Hence at higher hydrophobic monomer contents, this effect occurs. It would be expected that the more highly hydrophobic monomers, such as styrene and dodecyl acrylate, would display the effect at lower levels of hydrophobic monomer, since the extent of phase-separation would be higher for a given composition than that of the equivalent material containing, for example, HPMA. The observations are consistent with this hypothesis.

The 10% styrene, 40% and 50% HPMA and 30% BA materials, all of whose stress-strain curves fall into category (ii), were transparent in the unstretched state. If the phase-separation were extensive, some degree of turbidity might be expected. However, it may be, as Kolarik and Migliaresi suggested for their copolymers (47), that "these systems cannot be designated as heterogeneous with a distinctly perceptible interphase boundary."

Young's moduli for the swollen materials are shown in Fig. 4-70 as a function of composition. Although the data are rather scattered, several trends are possibly discernible. The moduli of the materials

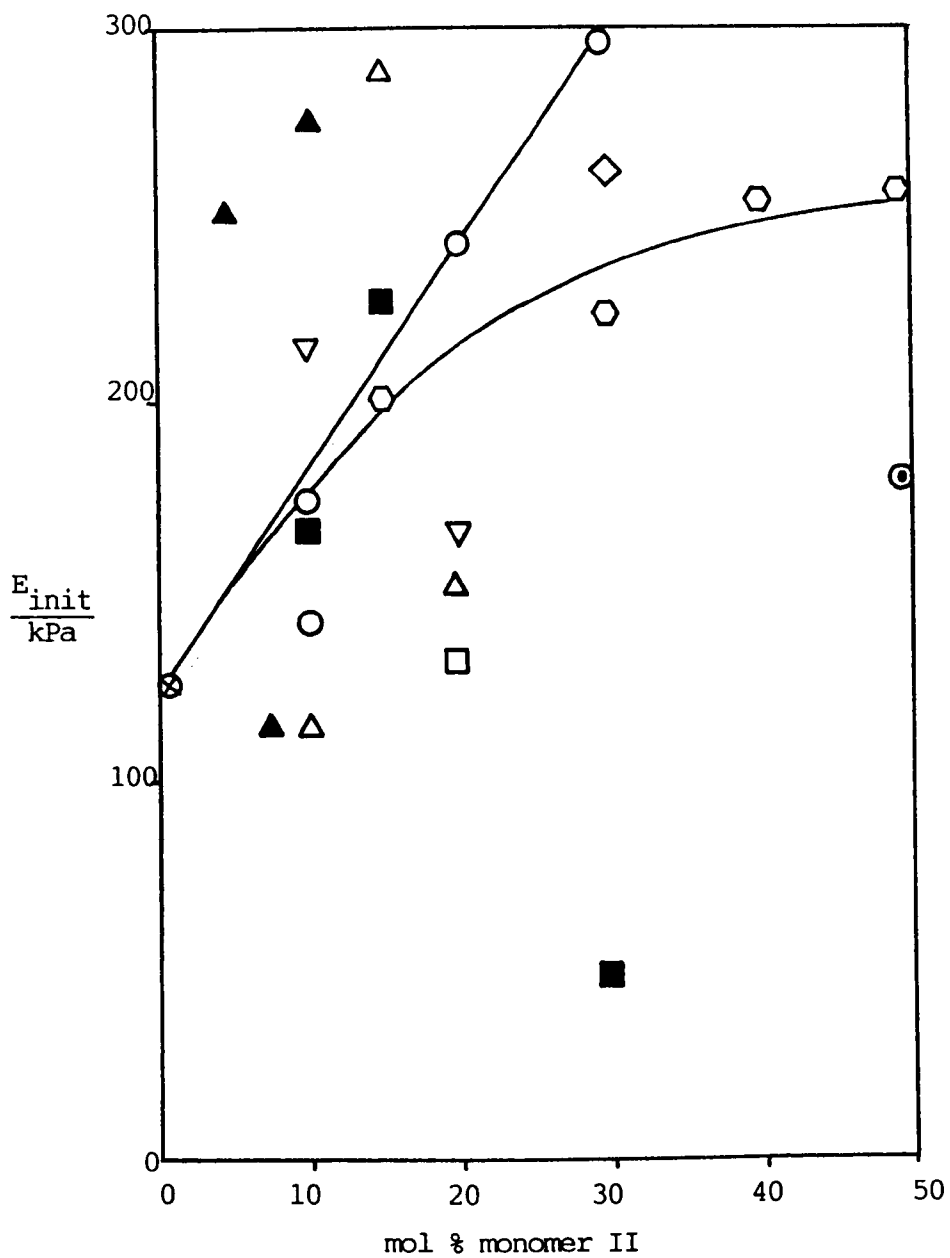


Fig. 4-70: Low-Extension Modulus vs. Composition for Terpolymer Hydrogels

KEY:

- |                 |           |       |
|-----------------|-----------|-------|
| ○ MMA           | ▲ Styrene | ◇ BA  |
| ⬡ HPMA          | ■ DDA     | ▽ EHA |
| △ PPM 6         | ⊙ HEMA    |       |
| ⊗ 0% monomer II |           |       |

containing DDA appear to increase with increasing level of DDA to a maximum, and then decrease. The HPMA materials increase in modulus as the level of hydrophobic monomer is increased, as do those containing styrene, if the 7.5% result is regarded as anomalous. Confirmation of the trends might be obtained using a more precise method, such as the method of hanging weights (Section 3.2.5).

Young's modulus as a function of equilibrium water content is shown in Fig. 4-71. the majority of the moduli lie on one of two curves. This suggests that a major factor influencing the low-extension modulus is the water content. The materials which show most deviation from the curves are those containing monomers with longer side-chains, such as DDA, EHA and PPM6. The DDA terpolymer hydrogels of lower water content in particular show large deviations from the curves.

There are three main influences on the moduli:

- (i) the water content;
- (ii) the extent of physical crosslinking;
- (iii) the  $T_g$  of the terpolymer.

The effect of (i) is to decrease the moduli of the swollen materials as the water content increases. If, as postulated in the preceding section, hydrophobic interactions are involved in these materials, then (ii) would result in an increase of modulus. It may be, therefore, that the  $T_g$  of the terpolymer, which is dependent on its viscoelastic properties, exerts a greater influence than either the EWC or the extent of crosslinking, at low water contents.

Fig. 4-72 shows shear modulus of the swollen materials as a function of composition, and Fig. 4-73 shear modulus as a function of equilibrium water content. The shear modulus of the swollen material is related



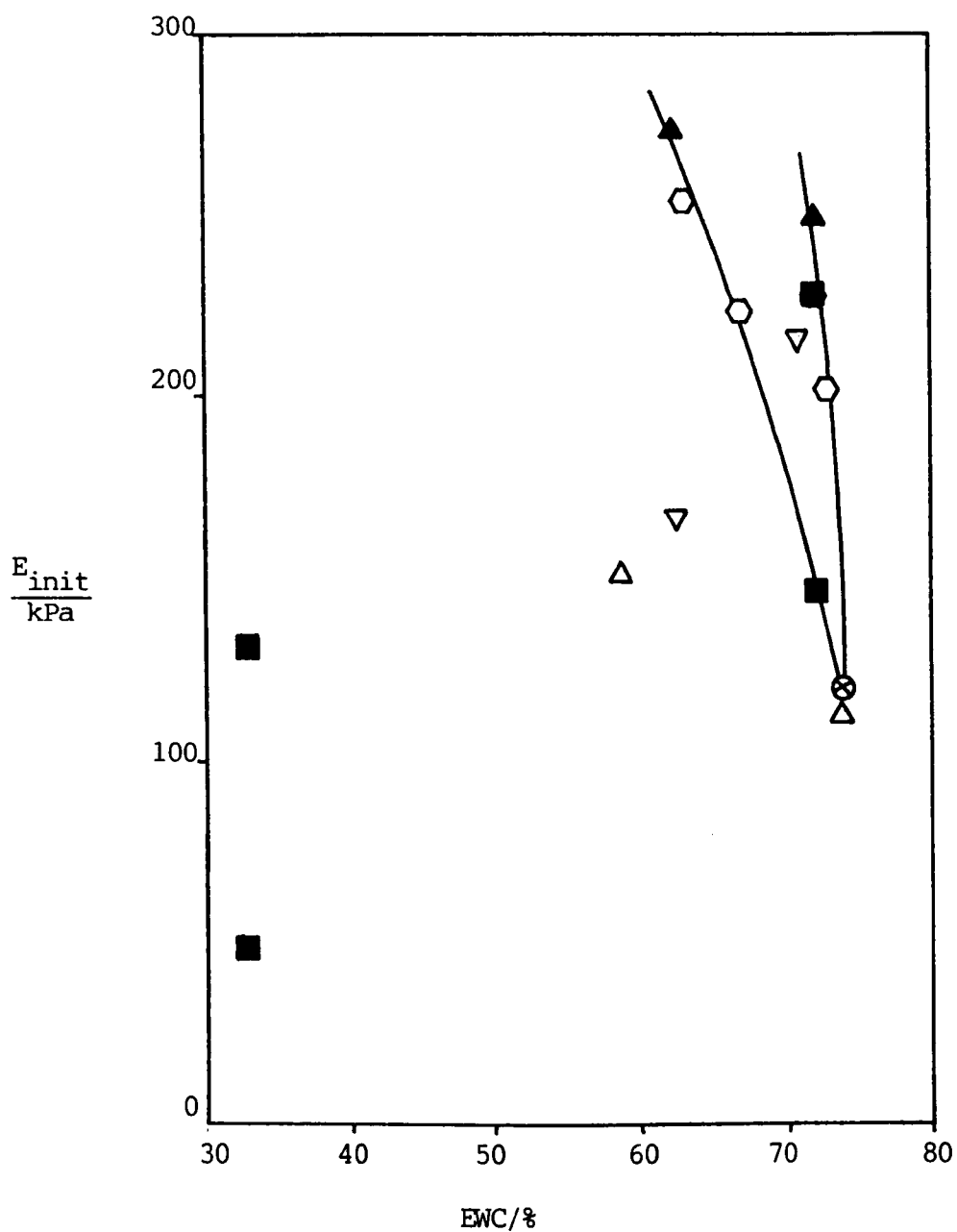


Fig. 4-71: Low-Extension Modulus vs. EWC for Terpolymer Hydrogels

KEY:

As Fig. 4-70

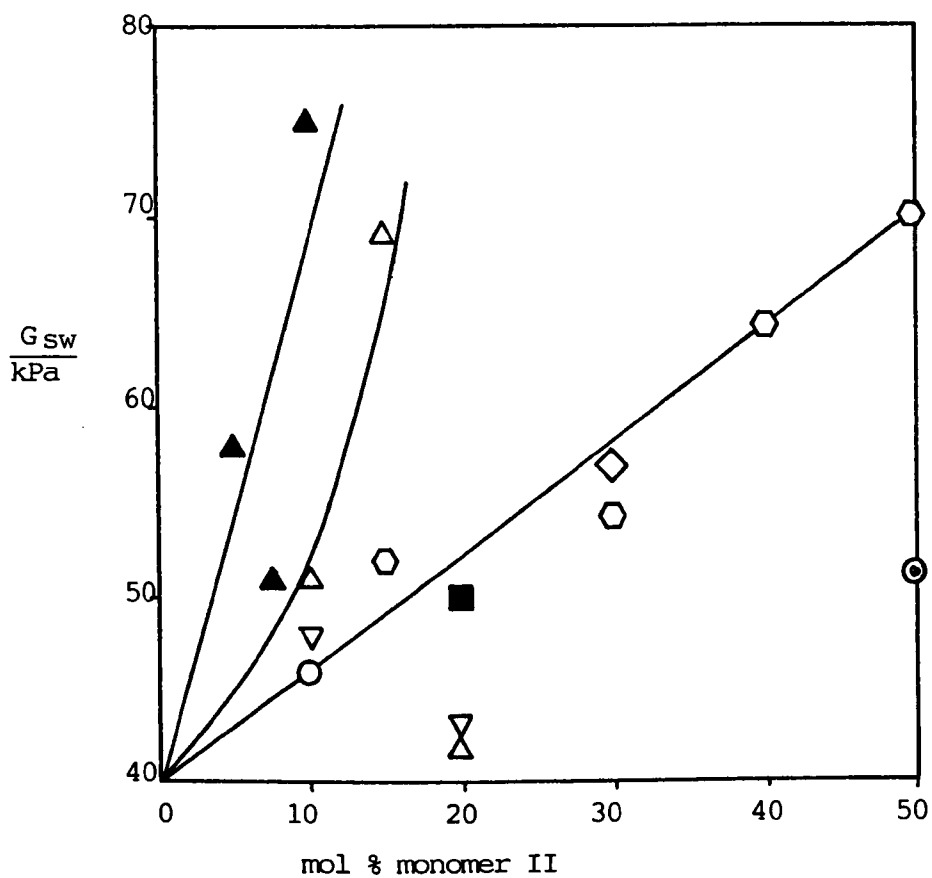


Fig. 4-72: Shear Moduli vs. Composition for Terpolymer Hydrogels

KEY:

As Fig. 4-70

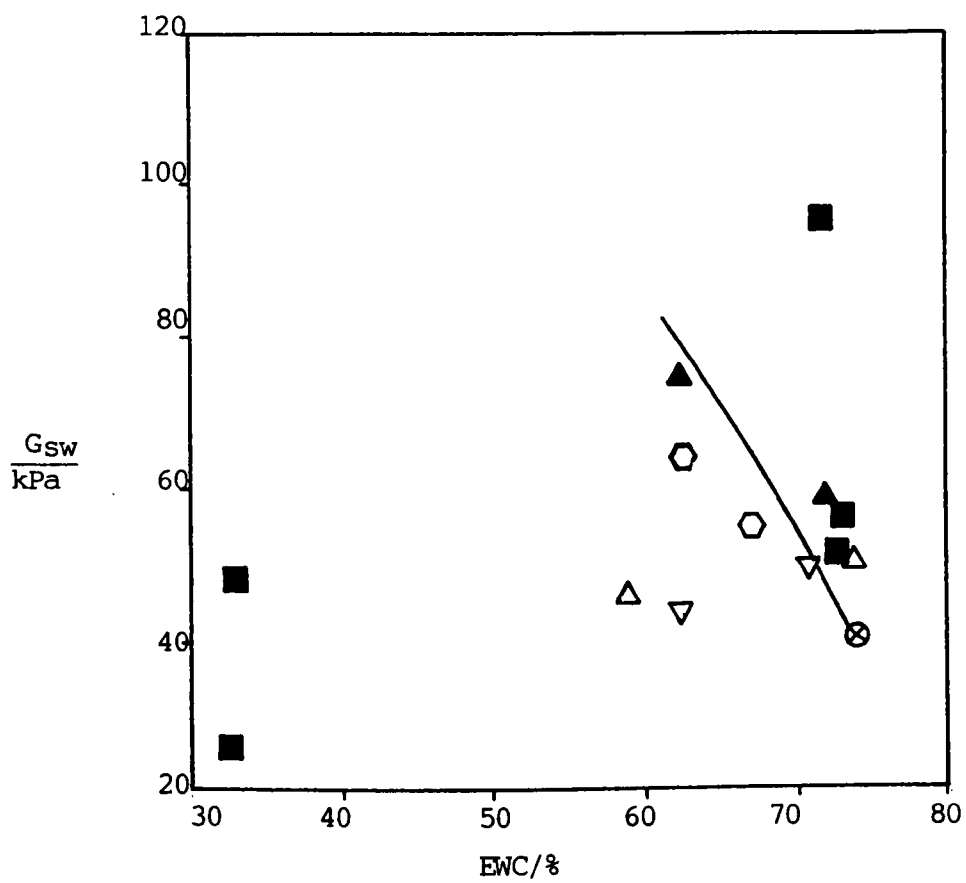


Fig. 4-73: Shear Moduli vs. EWC for Terpolymer Hydrogels

KEY:

As Fig. 4-70

to the effective crosslink concentration  $x_e$ , and the volume fraction of polymer,  $v_2$ , by equation 4-18:

$$G_{sw} = 2v_2^{\frac{1}{3}} x_e RT \quad \dots(4-18)$$

Table 4-10 shows the values of  $G_{sw}$  obtained for the terpolymers, together with the values of  $x_e$  calculated from equation 4-18, and cross-link concentrations calculated on the basis of the amounts of cross-linker used,  $x_{calc}$ . The latter were calculated in the same way as those in Section 4.3.2. In addition, Table 4-10 shows strain energy densities at break,  $W_b$ , for several terpolymers. These were obtained as the area under the stress/strain curve up to the break point. They were measured using a planimeter. It should be noted that the break points were those of the particular samples used for stress/strain measurements, and not the average tensile strengths and strains at break. These values of strain energy density at break therefore give merely an indication of trends, and cannot be regarded as providing definitive values for the properties of the materials. The coefficients  $C_1$  and  $C_2$  obtained from the Mooney-Rivlin plots, are given in the table where appropriate.

The strain energy density at break is a measure of the energy input per unit volume of material which is required to initiate a crack, and hence cause rupture. This energy would be expected to increase with decreasing water content of the hydrogel, and hence with increasing level of added hydrophobic monomer. This is indeed found to be the case, as the data for the styrene-containing materials shows. The materials which exhibit stress/strain curves in category (ii) have much higher values of  $W_b$  than those which exhibit stress/strain curves

in category (i). The presence of a crack-deflection mechanism, such as a type of particulate reinforcement caused by strain-induced phase separation, as was postulated above, would account for these observations.

Table 4-10: Various Quantities Obtained from Stress/Strain Data for Several Terpolymer Hydrogels

Hydrophobic monomer (M)	mol % M	$\frac{G_{sw}}{kPa}$	$\frac{x_e \cdot 10^5}{mol\ cm^{-3}}$	$\frac{x_{calc.} \cdot 10^5}{mol\ cm^{-3}}$	$\frac{W_b}{kJm^{-3}}$	$\frac{C_1}{kPa}$	$\frac{C_2}{kPa}$
MMA	10	46	2.9	3.2		22.5	0
BA	30	57			289	16.3	0
EHA	10	48	3.0	3.0	45	7.2	18
EHA	20	43	2.5	2.9		8	10.7
DDA	10	53	3.3	2.9	482	22	0
DDA	15	95	5.9	2.8	412	-	-
DDA	20	48	2.2	2.7	509	-	-
DDA	30	25	1.2	2.5	374	-	-
styrene	5	58	3.7	3.2	12	30	0
styrene	7.5	50	-	3.2	70	26	0
styrene	10	76	4.3	3.2	351	38	0
HPMA	15	52	3.2	3.1	44	26	0
HPMA	30	54	3.2	3.0	70	27	0
HPMA	40	64	3.6	3.0	145	31	0
HPMA	50	70	-	3.0	142	34	0
PPM6	10	51	3.3	2.5		-	-
PPM6	15	69	-	2.3	13	33	0
PPM6	20	42	2.3	2.1		21	0

N.B.     $W_b$  denotes the strain energy density at break

The values of  $x_e$  calculated from equation 4-18 are of the same order as the concentrations calculated on the basis of the amounts of crosslinker added. They do not suggest that the level of physical crosslinking increases as the proportion of hydrophobic monomer increases. The coefficients of the Mooney-Rivlin equation should be multiplied by  $\frac{1}{V_2^3}$  because the materials are swollen, as equation 4-26 indicates. In the majority of cases, the value of  $C_2$  is zero. Gumbrell et al (192) observed that, for natural rubber swollen in benzene,  $C_2$  decreased with increasing swelling ratio. Values of  $C_2$  of zero are reasonable, because most of the terpolymers are highly swollen. In general, as the proportion of hydrophobic monomer was increased, the linear portion of the Mooney-Rivlin curve decreased in extent. Various interpretations of  $C_2$  have been given (193). In order to compare the stress-strain functions for the terpolymer hydrogels with that for natural rubber, in Fig. 4-74 "reduced" stress is shown as a function of strain for two of the terpolymer hydrogels and for a gum rubber (194). "Reduced" stress is defined here as the actual stress divided by the stress at a strain of 100%. The curves show a striking similarity in shape, particularly considering the chemical dissimilarity of the hydrogels to natural rubber. At low strains, the points all lie on one curve, as the expanded-scale graph of Fig. 4-74 shows. Strain-induced "reinforcement" in the hydrogels appears to occur at lower strains than in natural gum rubber. It is postulated that, as the hydrogels are elongated, attraction between water molecules brings together, in the case of the DDA terpolymer, hydrocarbon chains. Crystallites are formed, which are responsible for the reinforcement effect, in a similar way to natural rubber. In the case of the styrene terpolymer hydrogel, crystallites may be formed in a similar way to those formed

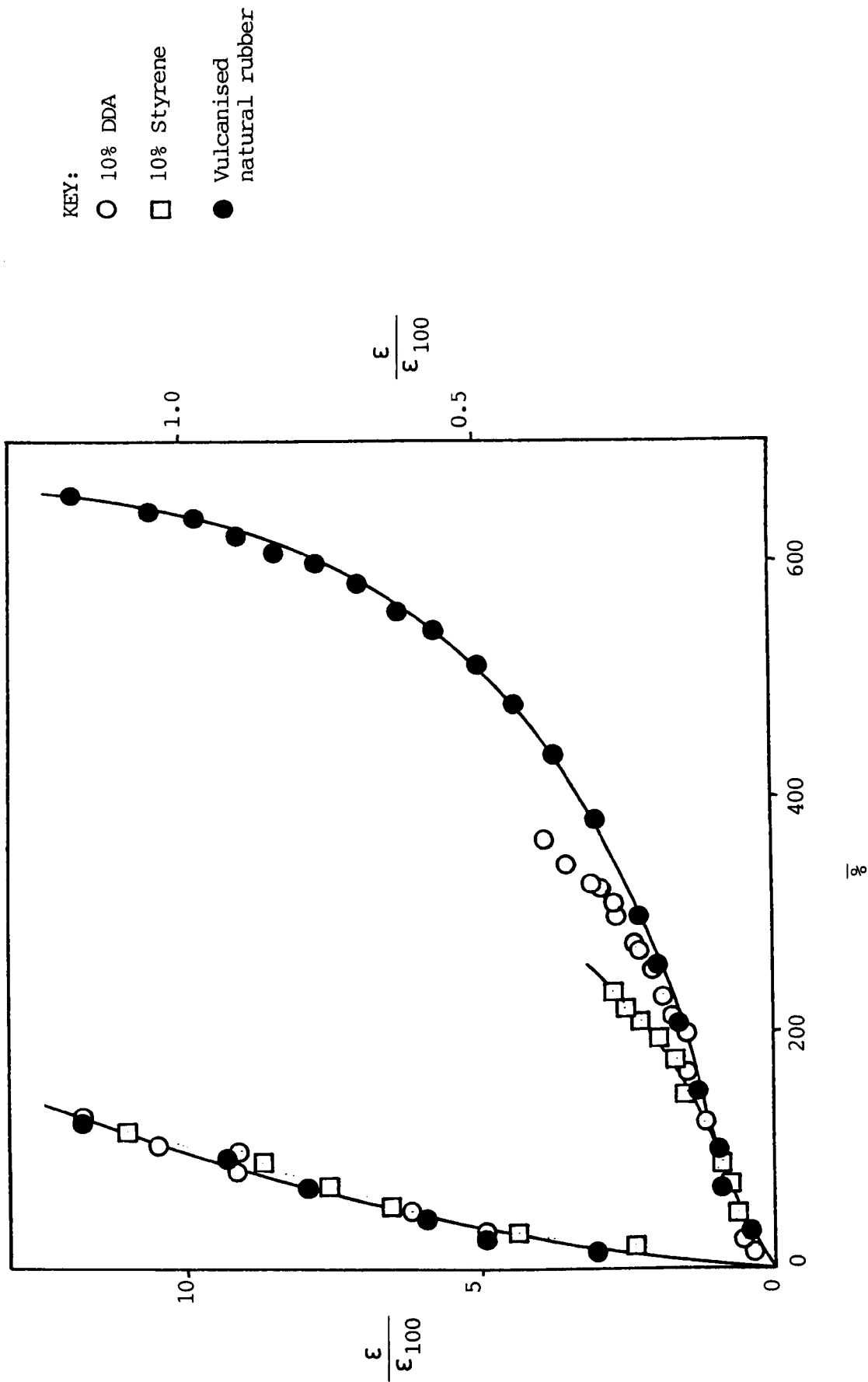


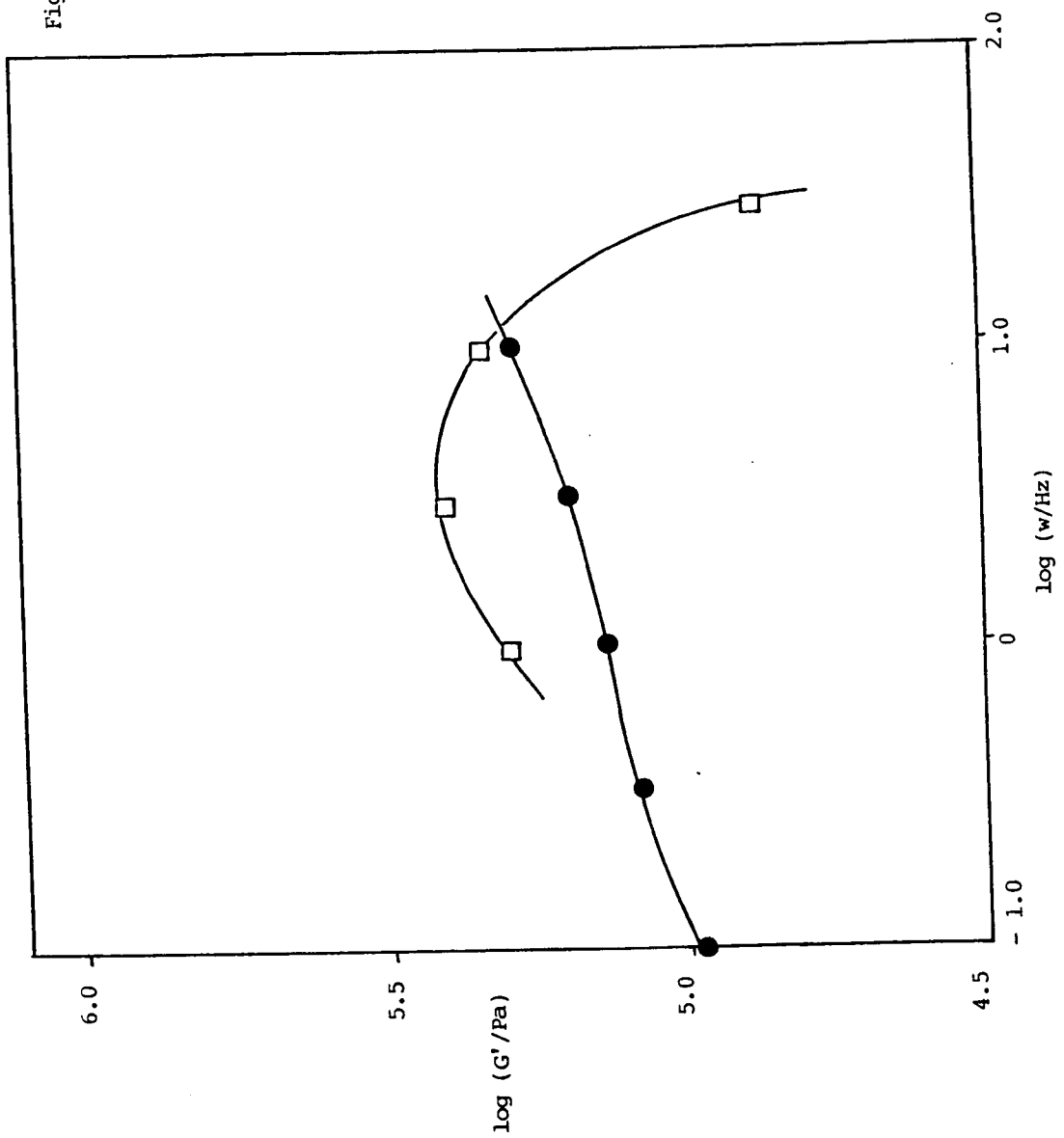
Fig. 4-74: Reduced Stress as a Function of Strain for Various Terpolymer Hydrogels Compared with Data for Natural Rubber (194)

in the DDA terpolymer hydrogel. However, in this case, interactions are between  $\pi$ -electrons of neighbouring benzene rings. This occurs with the formation of a layered crystallite structure at lower strains than are required for the formation of crystallites in the DDA terpolymer.

Some of the viscoelastic properties of terpolymer hydrogels are shown in Figs. 4-75 to 4-78. For reasons of clarity and also to enable comparisons to be made, the results for the hydrogel containing no added hydrophobic monomer are included on each graph. The properties of the terpolymer hydrogels containing DDA are shown in Figs. 4-75a to 4-75c. The storage modulus of the material containing no added hydrophobic monomer increases with frequency,  $\omega$ . At lower frequencies ( $\log \omega/\text{Hz} = -1.0$  to  $0$ ), the slope of the curve appears to decrease slightly with increasing  $\omega$ , whereas at higher frequencies ( $\log \omega/\text{Hz} = 0$  to  $1.0$ ) it increases slightly. The graph for the material containing 30% DDA, in marked contrast, exhibits a pronounced maximum at 3.8Hz, where the storage modulus is 250kPa. At frequencies below 11.7Hz, within the range of measurements, the value of  $G'$  is greater than that of the unreinforced material. Fig. 4-75b shows the loss modulus  $G''$  as a function of frequency for the same materials. The modulus of the hydrogel not containing a hydrophobic monomer has a shallow minimum at  $\omega = 0.18\text{Hz}$ , where  $G'' = 44\text{kPa}$ . At frequencies higher than this,  $G''$  increases with  $\omega$ . The loss moduli are lower than those of the hydrogel not containing a hydrophobic monomer. The loss tangents  $\tan \delta$  for the same materials are shown in Fig. 4-75c. The material containing no hydrophobic monomer has a shallow minimum at a frequency of 0.26Hz, where the value of  $\tan \delta$  is 0.26. At frequencies higher than this, the slope decreases with increasing frequency; a point of inflexion occurs at approximately 3Hz. At higher frequencies,



Fig. 4-75a: Log Storage Modulus vs.  
Log Frequency for Terpolymer  
Hydrogels Containing DDA



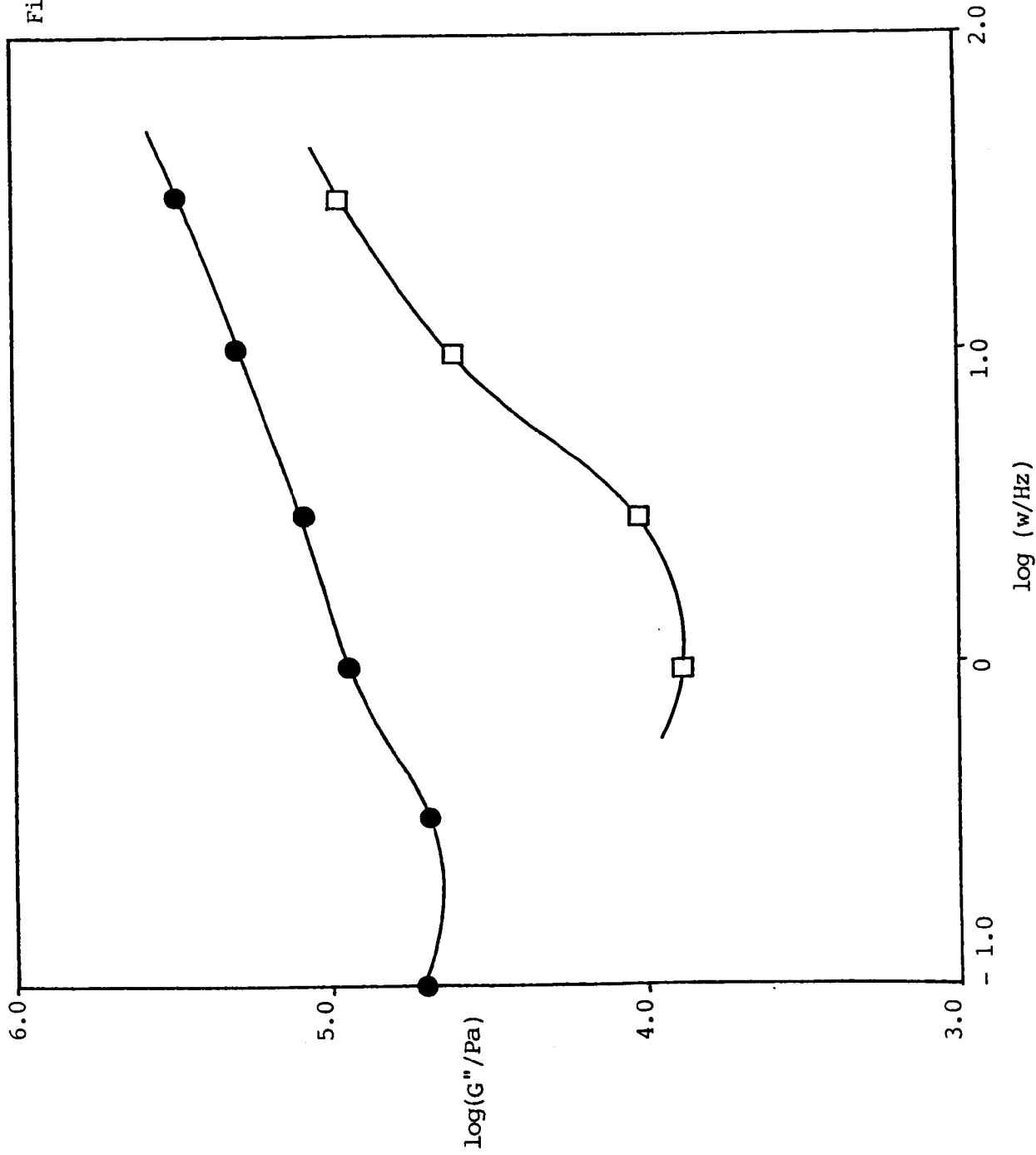
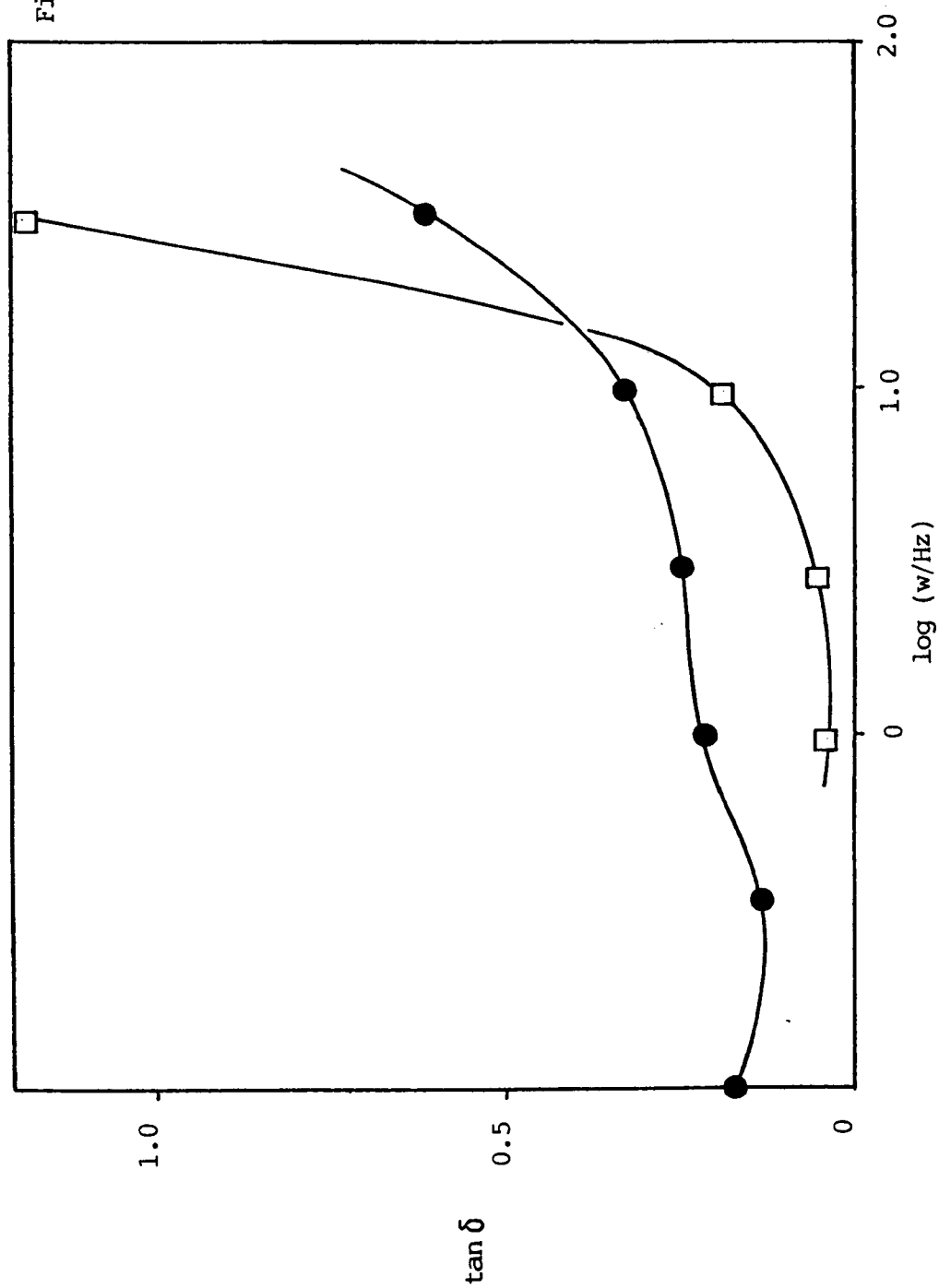


Fig. 4-75c:  $\tan \delta$  vs. Log  
Frequency for  
Terpolymer Hydrogels  
Containing DDA



the slope increases with frequency. At  $\omega = 15.1\text{Hz}$ , the  $\tan \delta$  values for the two materials are identical, being 0.42.

The results for the storage moduli for terpolymer hydrogels containing styrene and MMA are shown in Fig. 4-76a. The moduli of the 30% MMA hydrogel are greater than those of the hydrogel not containing a hydrophobic monomer, and the slope of the 30% MMA material curve is greater than that of the other two curves. Fig. 4-76b illustrates the loss moduli as a function of frequency for the same materials. The curve for the 30% MMA gel is approximately the same shape as that for the hydrogel not containing a hydrophobic monomer, but both the slope and the magnitude of the moduli are greater than those for the latter hydrogel. The 7.5% styrene curve, however, exhibits markedly different behaviour. A shallow maximum occurs at a frequency of 0.33Hz, the loss modulus being 4800kPa. A shallow minimum occurs at 1.58Hz, where  $G'' = 2100\text{kPa}$ , and a second shallow maximum at  $\omega = 4.07\text{Hz}$ , where  $G'' = 2600\text{kPa}$ . At a frequency of 7.94Hz, the loss moduli of both the 7.5% styrene and 30% MMA materials are 2300kPa. The results for  $\tan \delta$  are shown in Fig. 4-76c. The curve for the 7.5% styrene gel is very similar to that of the hydrogel not containing a hydrophobic monomer. The 30% MMA curve is of similar shape, although the values of  $\tan \delta$  are higher. The 30% MMA curve has a shallow minimum at a frequency of 0.20Hz, where the loss tangent is 0.33.

The storage moduli as a function of frequency for materials containing EHA are shown in Fig. 4-77a. Moduli for the 20% EHA terpolymer hydrogel at frequencies below 10Hz show the same trend as those for the hydrogel not containing hydrophobic monomer, although the values of  $G'$  for the 20% EHA gel are somewhat lower than those for the latter hydrogel. A maximum occurs at  $\omega = 10\text{Hz}$ , where the storage modulus is 4800kPa.

Fig. 4-76a:  $G'$  vs. Log Frequency  
for Terpolymer Hydrogels  
Containing Styrene and MMA

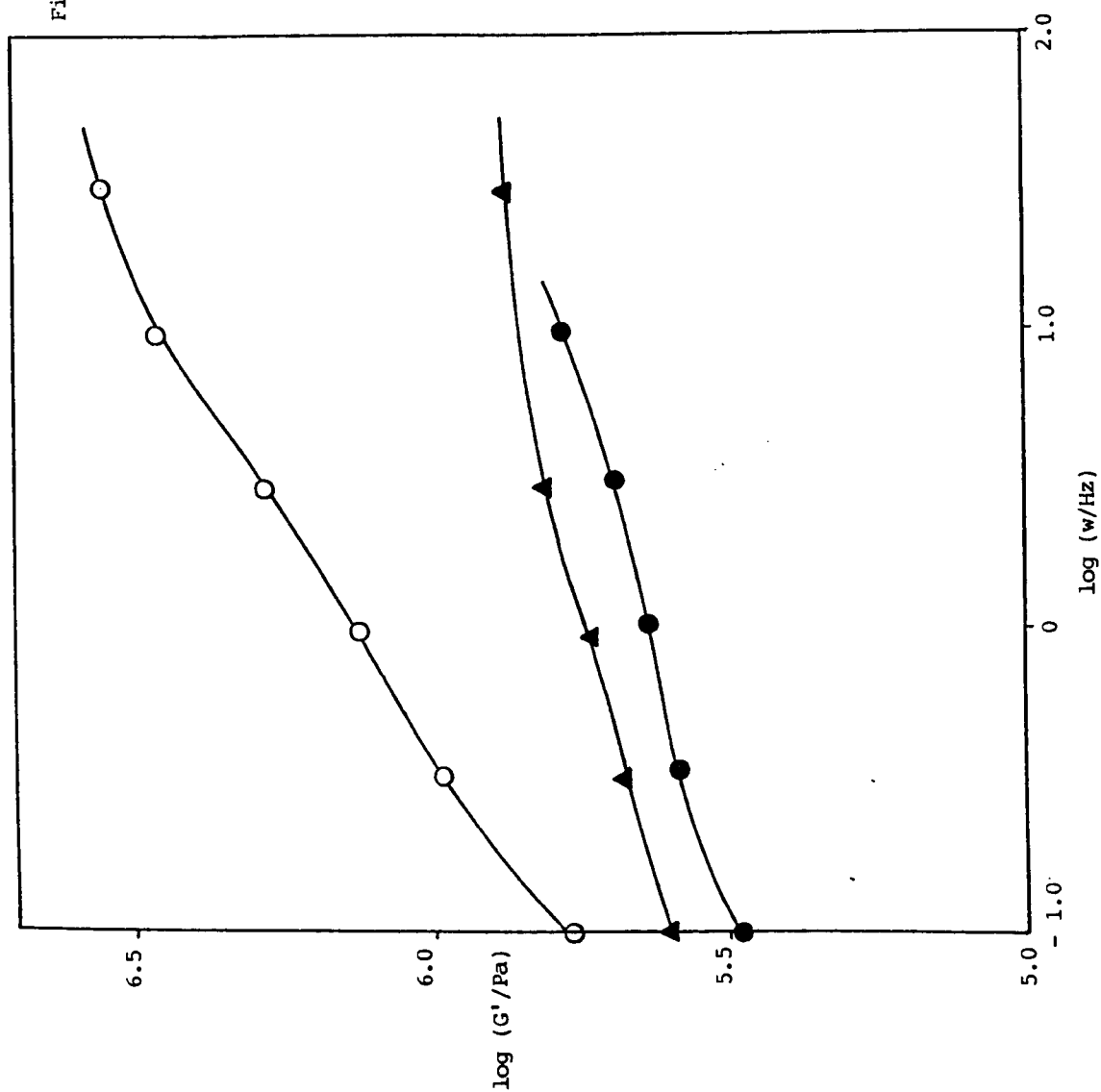


Fig. 4-76b:  $\log G''$  vs.

Log Frequency for  
Terpolymer Hydrogels  
Containing Styrene  
and MMA

KEY:  
 ● 0% MMA  
 ○ 30% MMA  
 ▲ 7.5% S

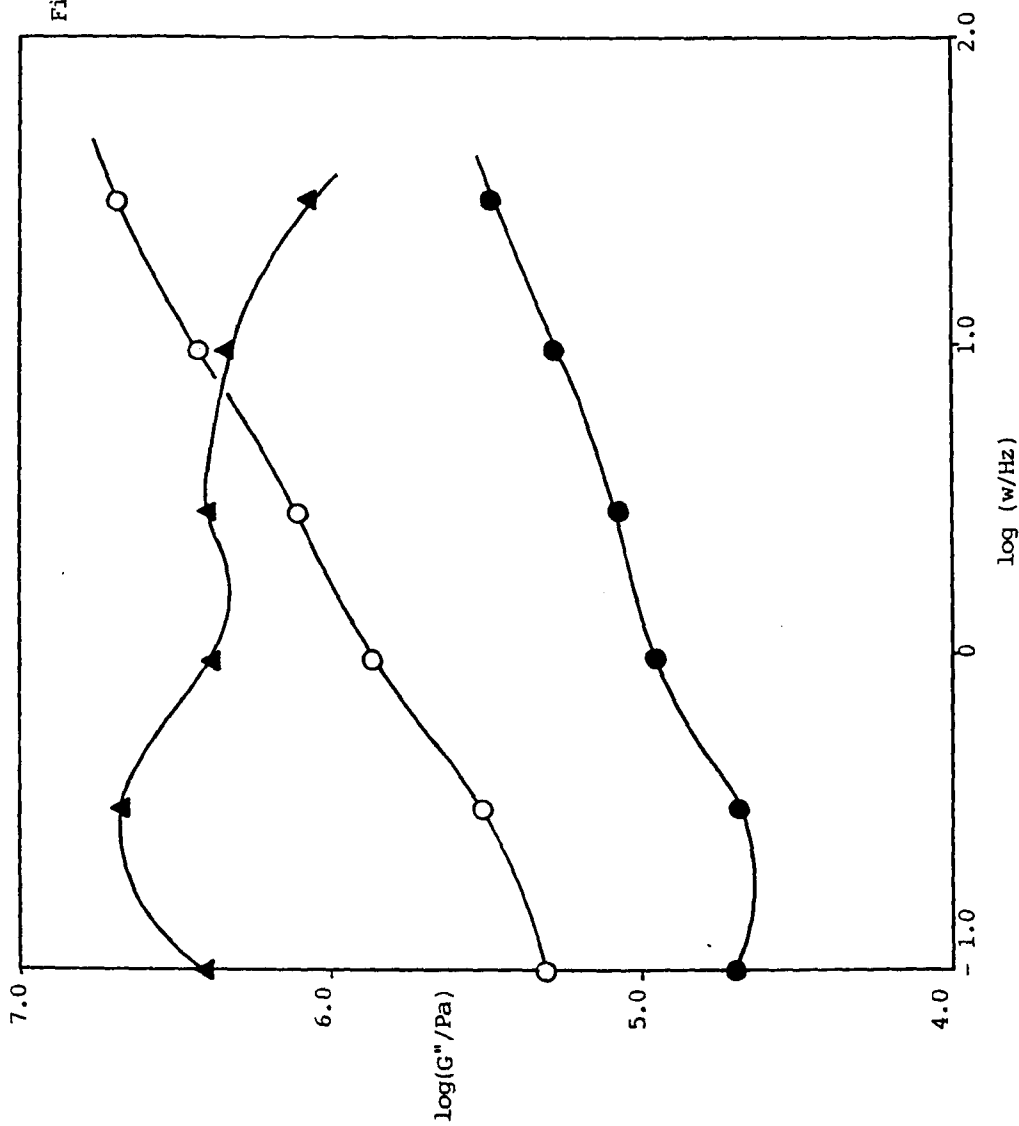


Fig. 4-76c:  $\tan \delta$  vs.

Log Frequency for

Terpolymer Hydrogels

Containing Styrene and

MMA

KEY:

● 0% MMA

○ 30% MMA

▲ 7.5% S

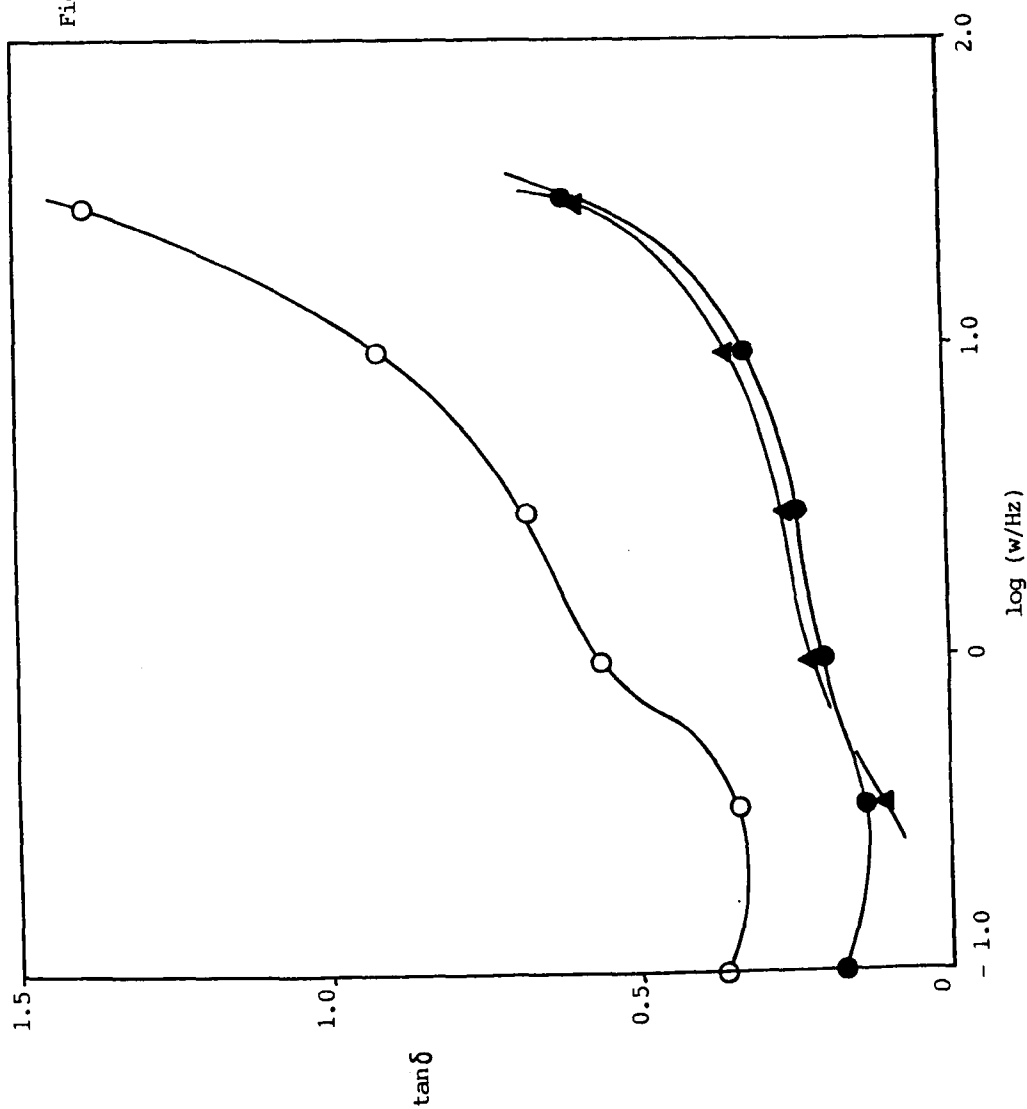
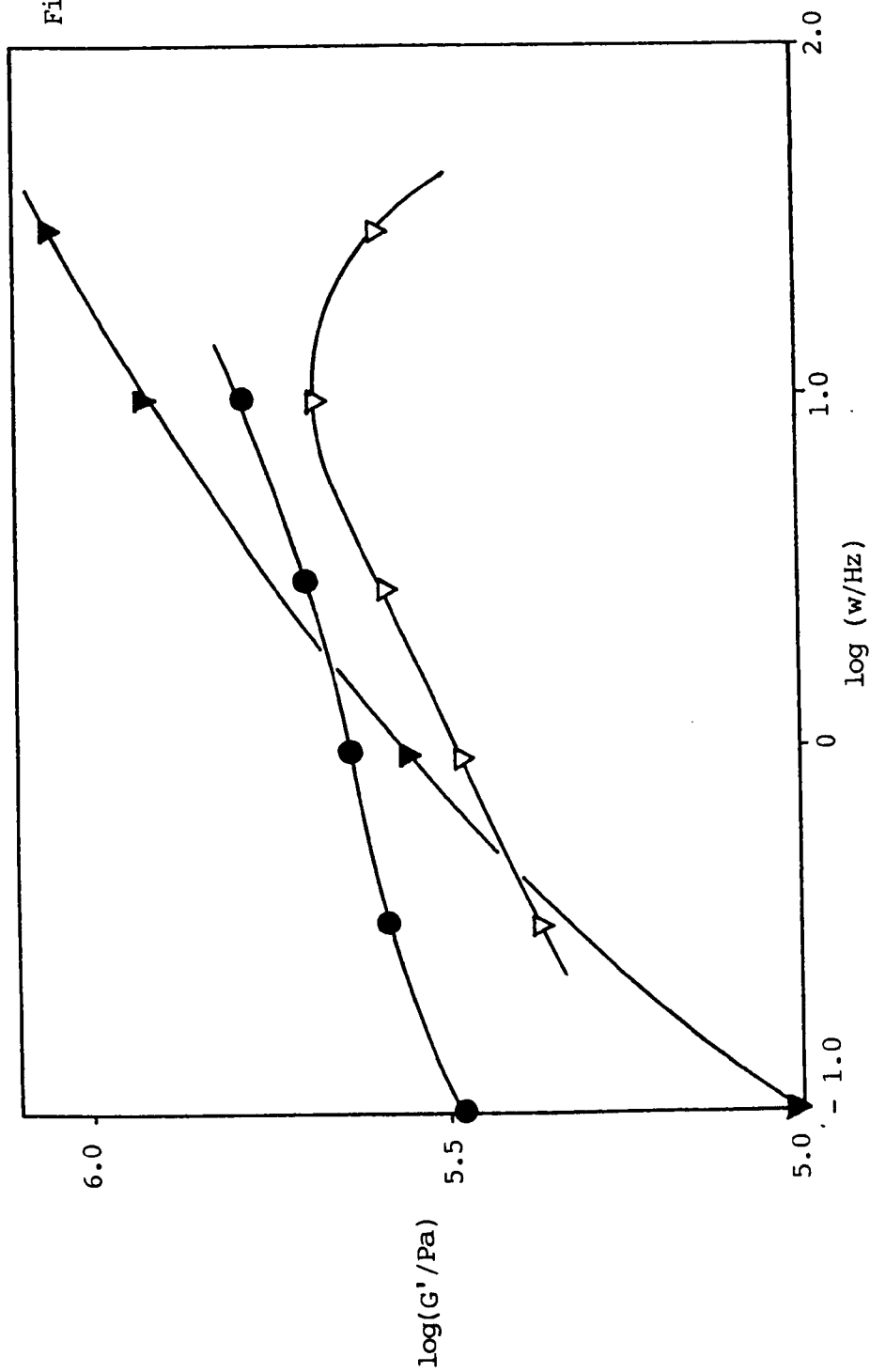


Fig. 4-77a: Log G' vs.

Log Frequency for  
Terpolymer  
Hydrogels  
Containing EHA

KEY:

- 0% EHA
- ▽ 20% EHA
- ▼ 30% EHA





The values of  $G'$  for the 30% EHA gel increase with increasing frequency. At a frequency of 0.55Hz ( $G' = 260\text{kPa}$ ), the moduli of the 20% and 30% EHA materials are equal. At 1.82Hz ( $G' = 460\text{kPa}$ ), the moduli of the 0% and 30% EHA gels are equal. The loss moduli of the same materials as a function of frequency are shown in Fig. 4-77b. The moduli for the hydrogel not containing a hydrophobic monomer and the 20% EHA gel are similar, but the moduli for the 30% EHA terpolymer are markedly higher. Fig. 4-77c shows the loss tangent results for these materials. At a frequency of 0.33Hz, the values of  $\tan \delta$  for the 0% and 20% EHA gels are equal, being 0.14. At frequencies higher than this, the loss tangents are higher for the 20% EHA gel, the shapes of the curves being similar. At a frequency of 33Hz, the loss tangents for the 20% and 30% materials both equal 1.0, while below this frequency  $\tan \delta$  is higher for the 30% gel.

Fig. 4-78a shows the results for the storage moduli for the terpolymer hydrogels containing HPMA. For frequencies below 2.95Hz, the 15% HPMA curve is approximately parallel to that of the hydrogel not containing a hydrophobic monomer. At 4.36Hz, the 15% HPMA curve shows a pronounced maximum, the value of  $G'$  being 260kPa. The results for the loss moduli for the same materials are shown in Fig. 4-78b. At frequencies above 1Hz, the curves are slightly convergent, both sets of moduli increasing with frequency. Below 1Hz, the slope of the 15% HPMA curve is greater than that above 1Hz.  $\tan \delta$  as a function of frequency for these materials is shown in Fig. 4-78c. The shapes of the 0% and 15% HPMA curves are similar, although the 15% HPMA curve shows a shallow maximum at 0.79Hz, where  $\tan \delta$  is 0.07, and a shallow minimum at 3.31Hz, where  $\tan \delta$  is 0.01. At a frequency of 15.5Hz, the  $\tan \delta$  values of the two materials both equal 0.40.

Fig. 4-77b: Log G'' vs. Log  
Frequency for Terpolymer  
Hydrogels Containing EHA

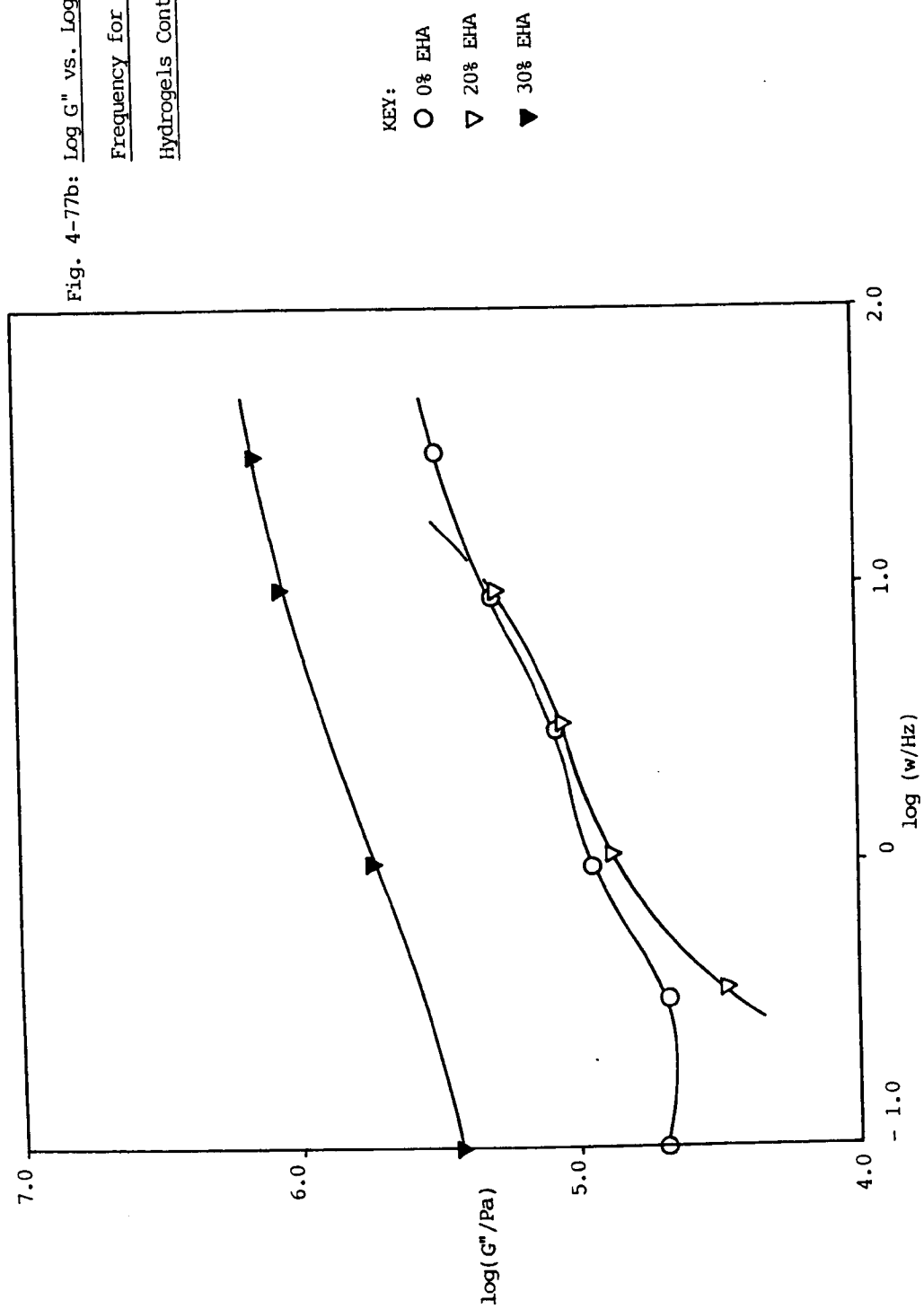
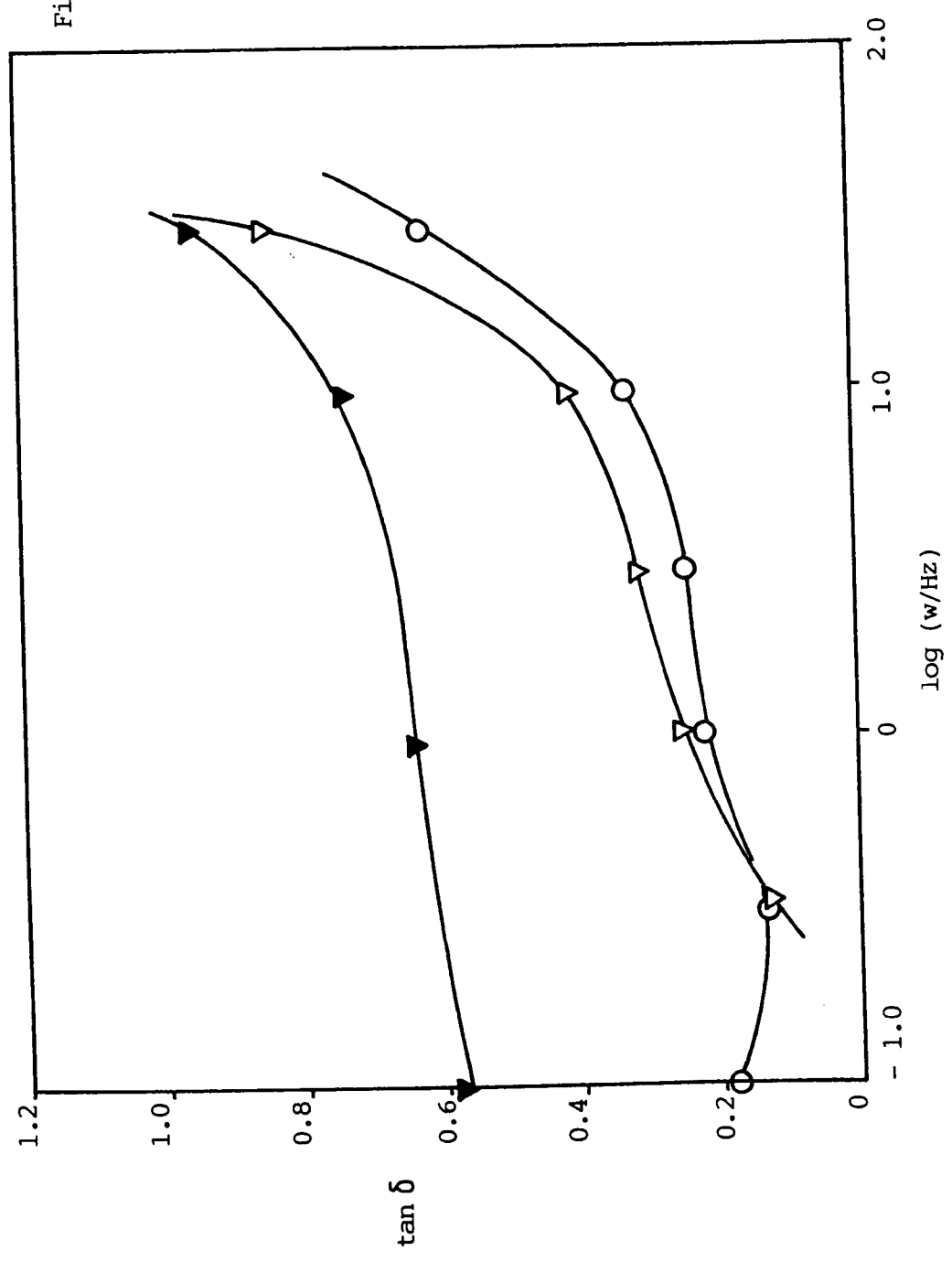


Fig. 4-77c:  $\tan \delta$  vs.

Log Frequency for  
Terpolymer Hydrogels  
Containing EHA

- KEY:
- 0% EHA
  - ▽ 20% EHA
  - ▼ 30% EHA



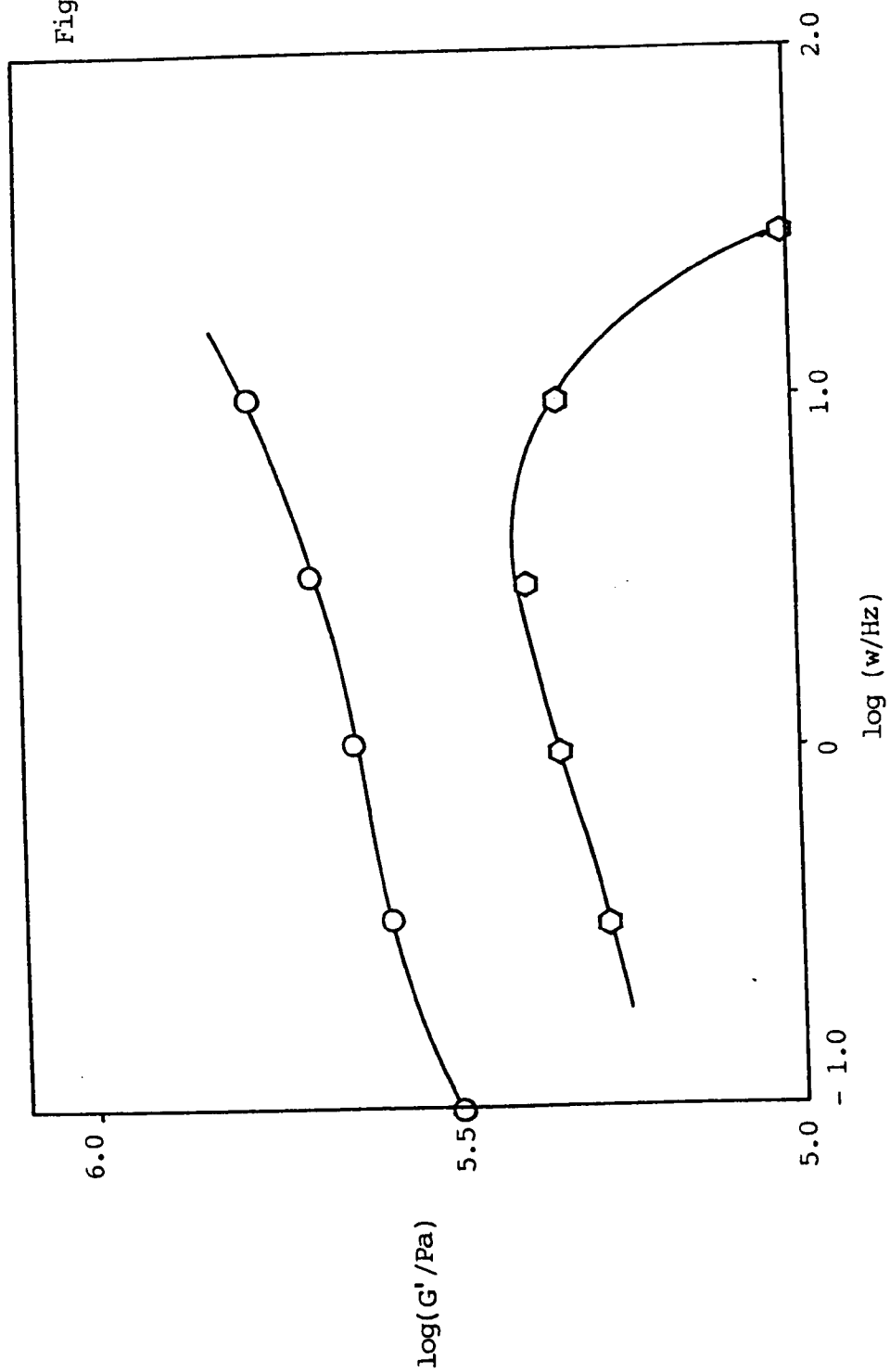


Fig. 4-78a: Log G' vs.  
Log Frequency for  
Terpolymer Hydrogel  
Containing HPMA

KEY:  
 ○ 0% HPMA  
 ⬡ 15% HPMA

Fig. 4-78b: Log G'' vs.

Log Frequency for

Terpolymer Hydrogels

Containing HPMA

KEY:

As Fig. 4-78a

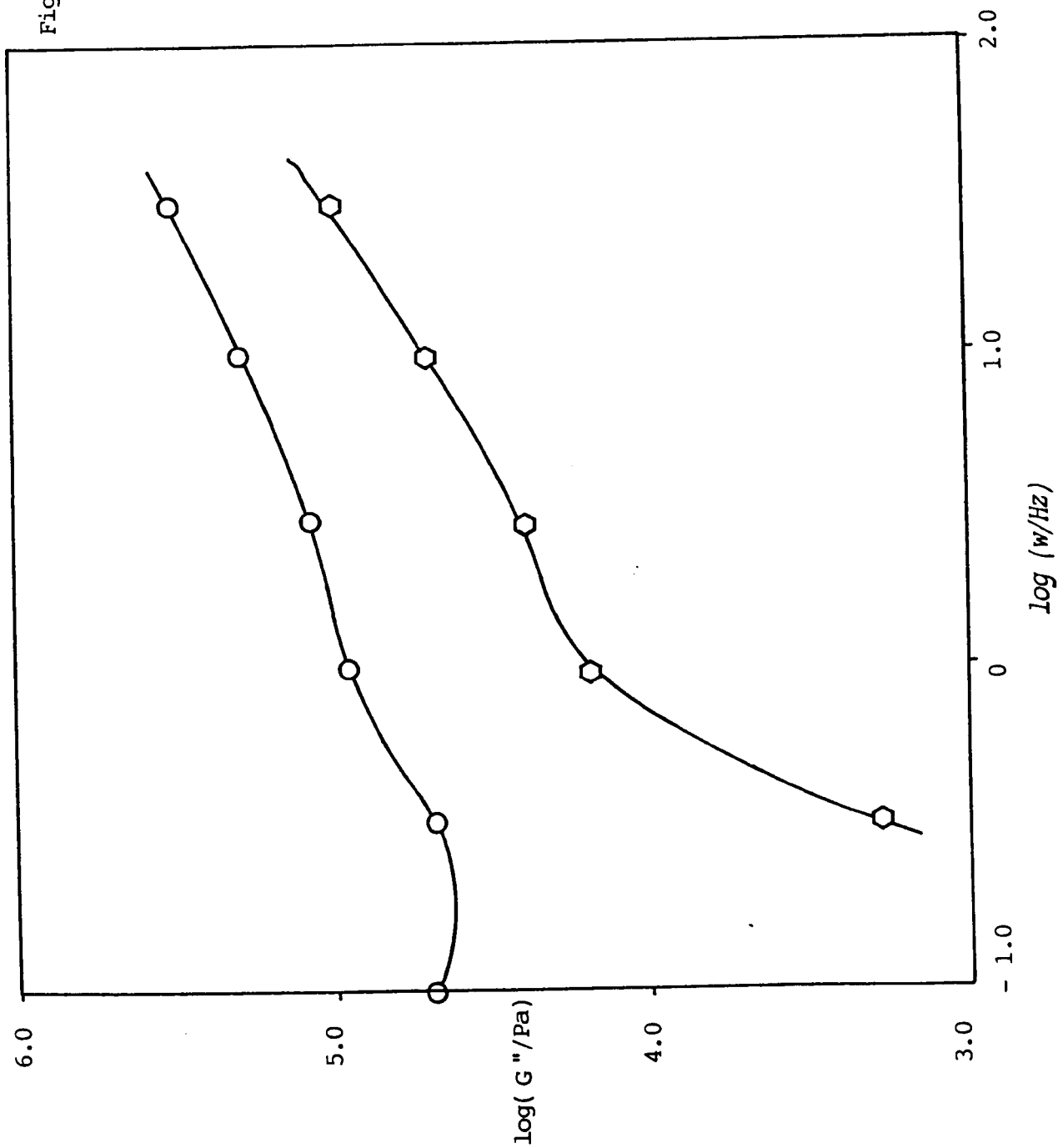
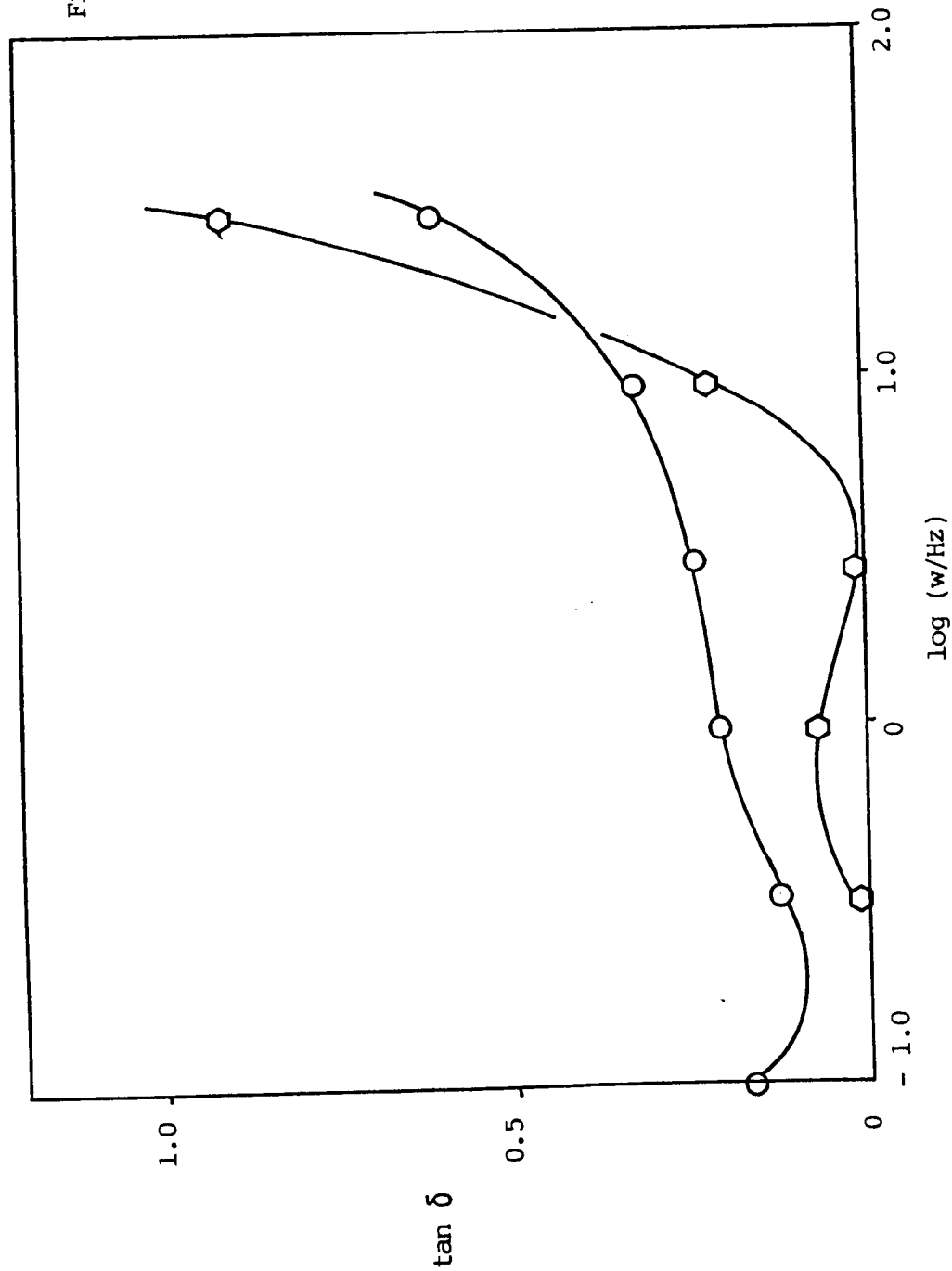


Fig. 4-78c:  $\tan \delta$  vs.

Log Frequency for

Terpolymer Hydrogels

Containing HPMA



KEY:

As Fig. 4-78a

The storage modulus curve for the 30% DDA terpolymer bears a closer resemblance to that of the Voigt model, than that of the Maxwell model, although Ward (ref. 193, p.100) pointed out that the simple models do not describe the behaviour of most materials.  $\tan \delta$  particularly, for viscoelastic materials does not conform to that predicted by the viscoelastic models, and often the relaxation spectrum approach is used. However, at a qualitative level, the hydrogel is acting as a viscoelastic material at higher frequencies, as is shown by the large increase in  $\tan \delta$  with frequency above about 1Hz. At low frequencies,  $\tan \delta$  is relatively small, and the material is rubbery. The copolymerisation of monomers whose homopolymers are plastic materials produces curves such as those shown in Figs. 4-76a to c. The storage modulus curves are similar to that for the hydrogel not containing a hydrophobic monomer, following the shape typical of a Maxwell model, and at higher frequencies than those used would be expected to reach a plateau. The loss modulus data for the 7.5% styrene material (Fig. 4-76b) are consistent with there being two relaxation times, at approximately 3 and 0.3 seconds. Although the form of this curve differs significantly from that of the hydrogel not containing a hydrophobic monomer, the  $\tan \delta$  curves for the two materials are almost identical. The materials are viscoelastic at high frequencies. The copolymerisation of MMA changes the magnitude of  $\tan \delta$  at a given frequency, but the shape of the curve remains the same. This might be expected, since the monomers are similar, but differing in hydrophilicity.

Copolymerisation with EHA brings about smaller changes in the dynamic viscoelastic properties than might be expected, since EHA is significantly more hydrophobic than either HEMA or MAA. The storage modulus data (Fig. 4-77a) are consistent with the Maxwell model, although

the modulus of the 20% material falls off at higher frequencies. The copolymerisation of 20% EHA with HEMA/MAA changes the values of  $\log G''$  and  $\tan \delta$  little. However, the 30% EHA materials show significantly different values of  $G''$  and  $\tan \delta$  as a function of frequency. At high frequencies, the viscoelastic nature of the materials increases, as shown by the sharp increase in  $\tan \delta$ .

The data for the HPMA-containing materials are interesting, since the monomers HEMA and HPMA are very similar. Therefore it would not be expected that the viscoelastic properties would change significantly on copolymerisation with HPMA. At low frequencies, the loss moduli of the 15% HPMA material are low compared to that of the hydrogel not containing a hydrophobic monomer. At high frequencies, the materials are viscoelastic.

In concluding this section, it may be noted that this investigation, although exploratory in nature, raises questions regarding the morphology of these materials. Copolymerisation of HEMA and MAA with hydrophobic monomers is accompanied by an increase in tensile strength and tearing energy at equivalent water content. From the point of view of tearing energy, which is one of the most important physical properties in relation to the applications of hydrogels, the materials containing styrene and EHA appear to show the greatest improvement over the hydrogel not containing a hydrophobic monomer.



## CHAPTER FIVE

### INTERPENETRATING POLYMER NETWORKS:

#### RESULTS AND DISCUSSION

## 5.1 INITIAL EXPERIMENTS ON IPNS

The initial work which was carried out on hydrogel IPNs took the form of an investigation into the feasibility of using sequential IPN synthesis as a means of effecting hydrogel reinforcement. The method of synthesis is described in Section 2.3.2.1. It comprises the swelling of network polymer I in monomer mixture II, followed by the polymerisation of monomer II with simultaneous crosslinking to form the IPN. The monomers chosen for monomer II in the early stages of the project were MMA and styrene, the homopolymers of which are non-rubbery at room temperature. Results of experiments (a) to (i) in Section 3.3.1 are shown in Table 5-1. In Table 5-1, "no polymerisation" indicates that no visible or tactile evidence for polymerisation was found, i.e. no change in modulus or hardness, and no colour change, translucence or opacity was observed. An IPN was produced in only one case, viz that of experiment (i).

The observations made in the course of experiment (a) indicate that, if thermal polymerisation of monomer II were to be used, then evaporation of monomer had to be prevented. The absence of apparent polymerisation was thought to be caused by a combination of the following:

- (i) excessive dilution of monomer II by IMS;
- (ii) presence of inhibitors in the styrene;
- (iii) the possibility that AZDN is not absorbed by the gel.

Experiment (b) gave similar results, as did an attempted UV photopolymerisation (experiment (c)). Unsuccessful attempts at the polymerisation of undiluted unwashed styrene by both thermal and photoinitiated methods (experiment (d)) supported the hypothesis that the presence of inhibitors in the styrene was responsible. Hence, washed styrene, styrene (2), was used in experiment (e). This experiment was also unsuccessful.

Table 5-1: Results of Initial Experiments on IPNs

Experiment	Type of Experiment	Result
(a)	IMS/styrene swollen, oven/water bath	No polymerisation
(b)	As (a), but greater EGDMA concentration	No polymerisation
(c)	UV polymerisation between glass plates	No polymerisation
(d)	Polymerisation of styrene-control experiment	No polymerisation
(e)	(a) UV-styrene/IMS, "Quantacure" photoinitiator	No polymerisation
	(b) Control	No polymerisation
(f)	UV polymerisation-IMS/styrene/AZDN and MMA/AZDN	No polymerisation
(g)	UV polymerisation-MMA/IMS/"Quantacure" and control	MMA-swollen sheet colourless, while IMS-swollen control sheet yellow
(h)	UV polymerisation-MMA/IMS	No polymerisation
(i)	A UV polymerisation-MMA/AZDN	Resulting material was 34% PMMA. Its water content was 33%.
	B, C, D. See Section 3.3.1	No polymerisation

It is possible that, in the case of experiment (a), oxygen may have permeated through the gel, entering the system through the edges, since a rubber gasket was not used. Oxygen inhibits the polymerisation reaction. In the same way, oxygen may have inhibited polymerisation in experiment (b), being present in the small air gap above the monomer mixture. In experiment (f), polymerisation did not occur to any appreciable extent, although a rubber gasket was used to surround the gel strips during polymerisation. It is thought that the reason for this is the excessive dilution of monomer II. However, using undiluted MMA as monomer II, an IPN was formed (experiment (i)A).

Several conclusions were drawn from the observations described above:

- (i) When using styrene as monomer II, the monomer should be de-inhibited by washing with alkali.
- (ii) Monomer II should not be excessively diluted.
- (iii) It may be necessary to use initiator concentrations as high as 1 - 2% w/w to ensure that polymerisation occurs at a reasonable rate.
- (iv) Reactions should be carried out between glass plates, in a similar manner to the method used for producing the 95/5 molar HEMA/MAA copolymers (Section 3.2.1).
- (v) Air should be excluded from the system.
- (vi) Experiment A shows that it is possible to produce IPNs of this type. The water content of the resulting material is only approximately 6% lower than that of poly(HEMA), although the material is 34% PMMA. Clearly these materials are worthy of further study.

## 5.2 FURTHER EXPERIMENTS ON SEMI-IPNS

Table 5-2 summarises some of the physical properties of these materials. They were all transparent when removed from the mould. On swelling in water, they became translucent and noticeably stiffer than the standard poly(HEMA) hydrogel.

Table 5-2: Results for IPNs 1 - 10

sample	swelling mixture	w/w % MMA in mixture	w/w % AZDN	w/w % water in IPN	$\sigma_b$ kPa	$\epsilon_b$ %
IPN1	MMA/IMS	28	1.0	-	1800	125
IPN2	MMA/IMS	50	1.0	37.0	3100	45
IPN3	MMA/IMS	80	1.0	↑	↑	
IPN4	MMA/IMS	75	1.0	Patchy		
IPN5	MMA/IMS	44	1.0	↓		
IPN6	MMA/IMS	75	1.0	↓		
IPN7	MMA/butan-2-ol	50	0.5	41.1		
IPN8	MMA/IMS	30	1.0	↓		
IPN9	MMA/IMS	30	2.0	Patchy		
IPN10	MMA/IMS	22	2.0	↓		

Although a preparative procedure for IPNs had been developed, there remained the problem of visual non-uniformity. This was thought to be caused by:

- (i) the absence of a good seal around the gel strips when enclosed in the glass mould. This enabled evaporation of the swelling mixture to occur;

(ii) heat of the UV lamp causing the vapour pressure of the swelling mixture to increase. This resulted in the formation of bubbles between the gel and the glass plate of the mould.

It was thought that the latter cause might be eliminated by diluting monomer II with a diluent which was less volatile than IMS. Hence an experiment was carried out using butan-2-ol in the swelling mixture (IPN7). This IPN, although of similar water content to poly(HEMA), was noticeably stiffer and harder.

IPNs 1 - 10 all showed non-uniformity, albeit to different degrees. The parts of the gels which became stiffer after exposure to UV light were translucent on swelling in water, the rest of the material retaining its transparency. IPNs 1, 2 and 7 were non-uniform, but to a lesser extent - the transparent region was restricted to a strip approximately 2 - 3mm wide around the edge of the gel strip.

Sperling (140) commented that polymer I is usually an elastomer, while polymer II is a plastic material. Stress cracking may occur during the swelling of network polymer I if this polymer is plastic at room temperature. Such cracking was not observed in experiments IPN 1 - 10, nor in the experiments described in Section 5.1. It is thought that diffusion was sufficiently slow to enable uniform swelling to occur.

The presence of a diluent such as IMS in the mixture facilitates the variation of the polymer II content of the IPN. In order that the effects of compositional variations can be systematically investigated, it is essential that the composition can be varied. This may be accomplished in a number of ways:

- (i) as described above, by changing the proportion of monomer II to diluent - this varies the amount of monomer II per unit weight of polymer I;
- (ii) by curtailing the absorption of the swelling mixture before equilibrium has been attained - by this means degrees of swelling other than that corresponding to equilibrium can be achieved;
- (iii) by changing the conditions of polymerisation of polymer II, such as intensity of the UV irradiation and time of polymerisation - this can in principle be used as a means of varying the conversion of monomer II to polymer II.

The calculation of the content of polymer II (Section 3.3.2.2) can be modified so that the composition of the IPN regions of non-uniform materials can be found. Fig. 5-1 illustrates such a material. The assumption is made that no polymerisation of monomer II has occurred in the transparent regions of the strip. The weight percentage of polymer II in the translucent part of the material is given by

$$P_{II} = \frac{W_{IPN} - (W_{INIT} - W_E)}{W_{IPN}} \times 100\% \quad \dots(5-1)$$

$$= \frac{W_{IPN} + W_E - W_{INIT}}{W_{IPN}} \times 100\% \quad \dots(5-2)$$

where  $W_{IPN}$  is the dry weight of the translucent, IPN region,  $W_{INIT}$  is the dry weight of the standard poly(HEMA/MAA) material prior to swelling in the monomer II mixture, and  $W_E$  is the dry weight of the transparent region around the edge of the material.

It should be noted that, according to Sperling's nomenclature (140),

the gels described above are semi-IPNs, since no crosslinker was used in the monomer II mixture.

Fig. 5-1: Illustrating Calculation of IPN Composition for Non-uniform Materials

Table 5-3: Results for IPN 11-21 Hydrogels

Material	Composition	Results
$W_E$ TRANSPARENT NON-IPN REGION	$W_{IPN}$ TRANSLUCENT IPN REGION	
IPN 12	50 HEMA/2 PS/50.4% acetone	soft gel which became white in water, turned over off as droplets.
IPN 13	50 HEMA/0.5 PS/49.5% acetone	translucent, greyish-white, violet tinted off to the light.
IPN 14	50 HEMA/0.1 PS/49.9% acetone	very soft, white, clear-like material.
IPN 15	50 HEMA/0.05 PS/49.95% acetone	very soft, white, clear-like material.
IPN 16	50 HEMA/0.3 PS/49.7% acetone/ 10 cyclohexane	very soft, white, clear-like material.
IPN 17	50 HEMA/0.5 PS/49.5% acetone/ 25 cyclohexane	PS did not dissolve.
IPN 18	50 HEMA/0.5 PVAL/ 25 H <sub>2</sub> O/25 H <sub>2</sub> O	PVAL did not dissolve.
IPN 19	50 HEMA/0.5 PVAL/5% acetone/5% H <sub>2</sub> O	PVAL did not dissolve.
IPN 20	20 HEMA/1.0 PS/79% H <sub>2</sub> O	big opaque thick gel.
IPN 21	30 HEMA/0.2 PS/79.8% H <sub>2</sub> O	translucent-yellow soft opaque gel.

These experiments were attempts to produce semi-IPNs using a different method to that used in section 5.1 and 5.2. The monomers were



### 5.3 FURTHER EXPLORATORY WORK ON SEMI-IPNS

In these experiments, hydrogel monomers were mixed with other polymers and then polymerised, in an attempt to prepare semi-IPNs. Compositional details were given in Table 3-8, and are summarised below, together with the results, in Table 5-3. Ratios used in this table are on a weight basis.

Table 5-3: Results for IPN 11-21 Hydrogels

Material	Composition	Results
IPN 11	50 HEMA/1 PS/50 toluene	Soft gel which became white in water; toluene came off as droplets.
IPN 12	50 HEMA/2 PS/50 ethyl acetate	Greenish-grey gel - violet when held up to the light.
IPN 13	50 HEMA/0.5 PS/50 toluene/50 acetone	Very soft, white, cheese-like material.
IPN 14	50 HEMA/0.5 PS/12 toluene/12 acetone	Very soft, white, cheese-like material.
IPN 15	50 HEMA/0.5 PS/12 acetone	Very soft, white, cheese-like material.
IPN 16	50 HEMA/0.5 PS/10 acetone/10 cyclohexane	Very soft, white, cheese-like material.
IPN 17	50 HEMA/0.5 PS/25 acetone/25 cyclohexane	PS did not dissolve.
IPN 18	50 HEMA/0.5 PVAL/25 IMS/25 EG	PVAL did not dissolve.
IPN 19	50 HEMA/0.5 PVAL/5 water	PVAL did not dissolve.
IPN 20	20 HEMA/0.1 PS/20 THF	Soft pinkish opaque gel.
IPN 21	30 HEMA/0.2 PS/20 THF	Greenish-yellow soft opaque gel.

These experiments were attempts to produce semi-IPNs using a different method to that used in Sections 5.1 and 5.2. Uncrosslinked polymers

were dissolved in the hydrogel polymerisation mixture.

The opacity of IPN 11 is thought to be caused not only by the presence of the polystyrene, but also by that of the toluene. Toluene was included in the hydrogel polymerisation mixture as a co-solvent for the hydrogel monomers and the polystyrene. The material showed a reduction in stiffness and hardness compared to the standard gels. IPN 12, prepared with ethyl acetate as the solvent, showed what might be the Tyndall effect (195). The gel, when swollen in water, was greenish-grey when viewed by reflected light, and violet when viewed under transmitted light. This suggests that small phase domains are present. It is thought that these domains were formed by the presence of hydrophobic polystyrene molecules in a hydrophilic environment.

More highly polar diluents were used for IPNs 13 - 16. These materials were markedly different in appearance to the 95/5 HEMA/MAA copolymer gel, and were opaque and very soft. Hence, physical testing could not be carried out. IPNs 20 and 21 had similar properties. This set of experiments has resulted in some new materials. However, the materials did not possess improved physical properties compared with the 95/5 HEMA/MAA copolymer hydrogels. It was decided therefore, that attention should be concentrated on sequential IPNs of the types described in Sections 5.1 and 5.2.

#### 5.4 FURTHER WORK ON IPNs

Attempts were made to prepare poly(HEMA-MAA)/PMMA IPNs, with various ratios of poly(HEMA-MAA) to PMMA, as described in Section 3.3.4. These ratios were varied by varying the proportions of MMA, polar solvent and saturated monomer analogue in the swelling mixture. Table 5-4 shows the results which were obtained.

Table 5-4: Results for IPN Hydrogels Containing Poly(HEMA/MAA) and PMMA

Material	Composition of swelling mixture	Remarks	$\sigma_b$ /kPa	ENC/%	$P_{II}$ /%(w/w)
IPN 22	5 MMA/0.05 AZDN/95 butan-2-ol	No swelling			
IPN 23	1 MMA/0.01 AZDN/99 butan-2-ol	No swelling			
IPN 24	20 MMA/0.2 AZDN/80 butan-2-ol	No swelling			
IPN 26	60 MMA/20 DMF/40 ethyl acetate	Patchy			
IPN 27	100 MMA/100 DMF/0.5 AZDN/100 ethyl acetate	Slightly patchy	120	61.7	23.0
IPN 28	100 MMA/40 DMF/0.5 AZDN/100 ethyl acetate	Uniform	130	64.1	18.0
IPN 29	100 MMA/20 DMF/0.5 AZDN	Patchy	Not sufficient material		15.2
IPN 30	100 MMA/20 DMF/1 AZDN	Patchy	Not sufficient material		23.0
IPN 31	50 MMA/20 DMF/1 AZDN/50 ethyl acetate	Patchy	Not sufficient material		26.9

IPN 7, for which butan-2-ol was included in the monomer II mixture, was a uniform material. However, this solvent could not be used for the gels described in this section, because the 5% MMA/95% HEMA material used as polymer I would not swell appreciably in butan-2-ol/MMA mixtures (IPNs 22 - 24). Thus, IPNs 26 - 31 used DMF and ethyl acetate as solvents. These two materials fulfil different roles in the monomer II mixture:

- (i) DMF is a highly polar molecule which therefore increases the amount of monomer II mixture absorbed into the hydrophilic poly(HEMA/MAA) gel. Hence only small amounts of DMF are required for the mixture to swell the polymer to a large extent;
- (ii) ethyl acetate is a saturated, non-polymerisable analogue of methyl methacrylate. The two molecules are similar, and therefore expected to swell the polymer I to approximately the same degree. Ethyl acetate may therefore be substituted for a portion of the MMA in the swelling mixture, as a method of controlling the polymer II content of the IPN, in addition to those listed in Section 5.2.

The uniformity of IPNs 27 and 28 shows that the problem of non-uniformity is not one which is inherent in this type of synthesis. Rather, it is a consequence of the preparative procedure. Clearly, modifications to the procedure were necessary to prepare consistently uniform materials. It was thought that the main cause of non-uniformity was the evaporation of swelling mixture caused by the heat of the UV lamp. This was modified in the two ways described in Sections 3.3.5.1 and 3.3.5.2, viz. by surrounding the samples with oil and cooling the mould during photopolymerisation. Further comments on these procedures are given in Section 5.5.

IPNs 27 and 28 both showed marked improvement in tensile strength compared

with the 95/5 HEMA/MAA copolymer hydrogel. This was accompanied by a decrease in EWC, which is expected, since hydrophobic material has been introduced into the gel structure.

## 5.5 FURTHER DEVELOPMENTS IN THE IPN PREPARATION PROCEDURE

### 5.5.1 Surrounding Samples with Oil

This modification to the procedure was intended to have two functions:

- (i) to prevent the formation of bubbles between the glass plate and the sample;
- (ii) to reduce diffusion of the swelling mixture into the surrounding medium, since the viscosity of the oil is relatively high.

This modification improved the uniformity of the product.

### 5.5.2 Cooling of Samples under UV Light (i)

This modification supplemented that described in Section 5.5.1. A reduction in the temperature of the reaction was thought necessary in order to improve the uniformity of the IPNs. IPNs 47 to 58, prepared using this method, showed improved uniformity (see Table 5-6). However, the inherent problem of this cooling method is that the temperature of the polymerisation is dependent upon the temperature of the water supply. This is evident from Table 5-6. The experiments summarised there fall into two groups, carried out during two different periods. It is noticeable that the PMMA contents of IPNs prepared at about 6°C are smaller than those of IPNs prepared at about 20°C.

### 5.5.3 Cooling of Samples (ii) and Pre-swelling

The second method of cooling, described in Section 3.3.5.3, gave rise to reaction temperatures which were almost independent of the ambient temperature. Over four hours, the temperature increased by 1°C from 25°C, the temperature at which the thermostat was set, to 26°C. This method, together with pre-swelling in DMF described in Section 3.3.5.5, was used for IPNs 59 onwards. The results are described in subsequent sections.

The object of the DMF pre-swelling was to prepare a material which was above its glass transition temperature when swelling commenced. Sperling (Ref. 140, p.71) recognised that it was necessary to take extreme care when swelling samples whose  $T_g$  was above ambient temperature. Pre-swelling provides an elastomeric material, and therefore eliminates stress-cracking. It was found that the xerogels swelled evenly in the DMF vapour. Hence this method was a successful modification to the IPN preparation procedure.

#### 5.5.4 Interpenetrating Networks

Table 5-5 shows results for IPNs 32 - 46. IPNs 32 - 34 cracked while swelling in the monomer II mixture, and broke into highly-swollen pieces. This phenomenon is caused by the high proportion of the IMS in the swelling mixture. As the highly hydrophilic swelling mixture is absorbed by the xerogel, the surface of the polymer is in contact with the swelling mixture. It therefore achieves a high degree of swelling at an early stage in the process, whilst the inner region of the polymer remains unswollen. Thus, stresses are set up in the material, and cracking occurs. Hence, in subsequent experiments, the hydrophilicity of the monomer II mixture was reduced.

Table 5-5 illustrates another problem which was encountered, particularly in the case of swelling mixtures containing high proportions of monomer II. This was polymerisation of monomer II during the swelling process. This was eliminated by storing the bottles containing the gels and swelling mixtures in dark cupboards. This eliminated photopolymerisation through exposure to the fluorescent lighting in the laboratory.

The consistency of the IPN compositions in IPNs 32 - 46 was poor. This may be caused by fluctuations in the temperature during polymerisation

Table 5-5: Results for IPN 32 - 46 Hydrogels





wt.

Material	Composition of Swelling Mixture	Remarks	Cooling	Pre-Swelling	$\sigma_b$ /kPa	EMC/%	P <sub>II</sub> /%
IPN 32	40 MMA/160 IMS/0.4 AZDN	Broke up on swelling	None	None			
IPN 33	40 MMA/160 IMS/0.4 AZDN	Broke up on swelling	None	None			
IPN 34	40 MMA/160 IMS/0.4 AZDN	Broke up on swelling	None	None			
IPN 35	100 MMA/100 IMS/1 AZDN		None	None	515	59.5	36.5
IPN 36	100 MMA/100 IMS/1 AZDN		None	None			40.1
IPN 37	100 MMA/100 IMS/1 AZDN		None	None	351		43.6
IPN 38	100 MMA/100 IMS/1 AZDN	Slightly non-uniform	None	None		54.6	
IPN 39	140 MMA/60 IMS/1.4 AZDN	Polymerised in bottle	None	None			
IPN 40	160 MMA/40 IMS/1.6 AZDN	Polymerised in bottle	None	None			
IPN 41	160 MMA/40 IMS/1.6 AZDN	Polymerised in bottle	None	None			
IPN 42	140 MMA/60 DMF/1.4 AZDN		None	None	3212		48.0
IPN 43	140 MMA/60 DMF/1.4 AZDN		None	None			48.8
IPN 44	160 MMA/40 DMF/1.6 AZDN	Polymerised in bottle	None	None			
IPN 45	160 MMA/40 DMF/1.6 AZDN		None	None	160		23.1
IPN 46	160 MMA/40 DMF/1.6 AZDN		Method (i)				26.0



of monomer II. Table 5-6 shows results for IPNs 47 - 58.

Table 5-6: Results for IPN 47 - 58 Hydrogels

Material	Wt. % Swelling mixture Composition	Appearance	P <sub>II</sub> /%	Temperature of polymerisation
IPN 47	154 MMA/46 DMF/ 1.54 AZDN	Translucent	35.5	 Approx. 20°C 
IPN 48	154 MMA/46 DMF/ 1.54 AZDN	Translucent	35.7	
IPN 49	154 MMA/46 DMF/ 1.54 AZDN	Non-uniform		
IPN 50	144 MMA/56 DMF/ 1.44 AZDN	Translucent	35.7	
IPN 51	144 MMA/56 DMF/ 1.44 AZDN	Non-uniform		
IPN 52	154 MMA/46 DMF/ 1.54 AZDN	Translucent	32.5	
IPN 53	160 MMA/40 DMF/ 0.80 AZDN	Non-uniform		 Approx. 6°C 
IPN 54	160 MMA/40 DMF/ 0.80 AZDN	Non-uniform		
IPN 55	160 MMA/40 DMF/ 0.80 AZDN	Non-uniform		
IPN 56	160 MMA/40 DMF/ 0.80 AZDN	Non-uniform		
IPN 57	160 MMA/40 DMF/ 0.80 AZDN	Translucent	17.7	
IPN 58	160 MMA/40 DMF/ 0.80 AZDN	Translucent	20.9	

The materials shown in Table 5-6 were mentioned above (Section 5.5.2) with regard to the method of cooling which was used. The rates of conversion were reduced by the reduction in temperature from 20°C to 6°C, resulting in lower polymer II contents, since the reaction times were equal.

## 5.6 EXTENT OF PHOTOPOLYMERISATION VS. TIME OF REACTION

Figures 5-2 and 5-3 show the extent of polymerisation as a function of time,  $t$ , for the two experiments described in Sections 3.3.6.1 and 3.3.6.2 respectively. Fig. 5-2 is sigmoidal. In this experiment,  $P_{II}$  was approximately constant at 27% after approximately 3.5 hours. In the second experiment (Fig. 5-3),  $P_{II}$  increased rapidly with time and reached a plateau value of 34% after 1.5 hours.

The shape of Fig. 5-3 is similar to that expected for a solution polymerisation (Ref. 2, p. 124). That of Fig. 5-2 however, is rather different. This may be a consequence of experimental error in the point at 1.5 hours on Fig. 5-2. The rates of reaction, shown by the slopes of the curves, are higher at short times for Fig. 5-3 than for Fig. 5-2. The following equation describes the rate of reaction,  $R_p$ , for photopolymerisation in solution, the kinetics of which are similar to a thermally initiated reaction (196):

$$R_p = \frac{-d[M]}{dt} = k_p \left\{ \frac{fEI_0}{kt} \right\}^{1/2} [M]^{3/2} \quad \dots(5-3)$$

where  $[M]$  is the monomer concentration at time  $t$ ,  $k_p$  is the rate coefficient for propagation,  $k_t$  is the rate coefficient for termination,  $f$  is the number of pairs of chain radicals generated by each quantum of light absorbed, and  $I_0$  is the incident light intensity.  $E$  is defined below.

If no photosensitiser is used,

$$\frac{I_{abs}}{I_0} = E[M] \quad \dots(5-4)$$

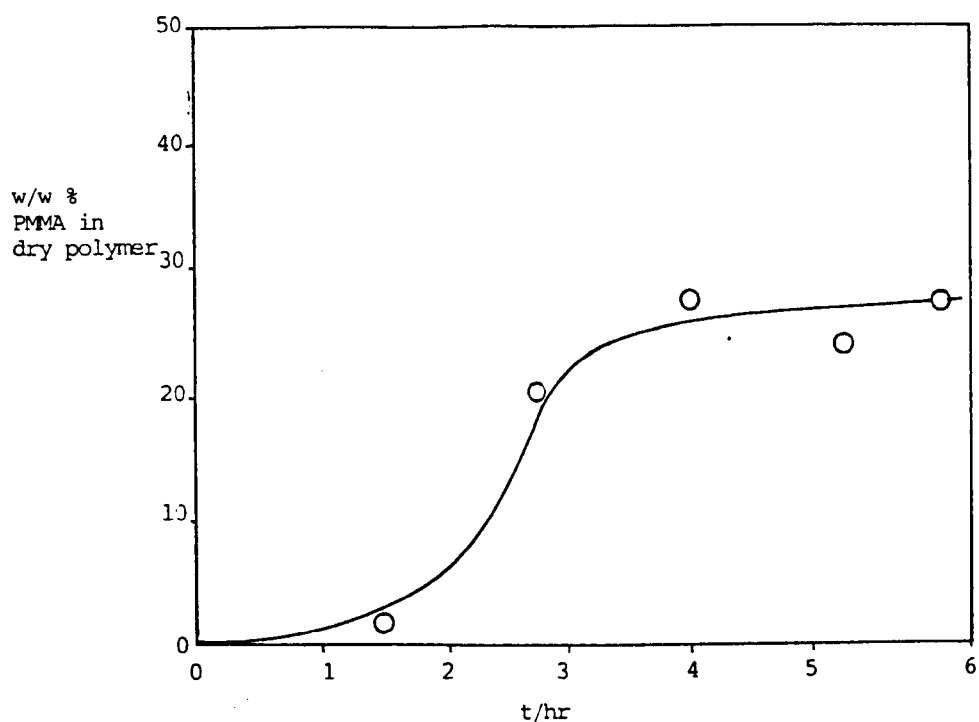


Fig. 5-2: Extent of Polymerisation vs. Time:  
First Experiment

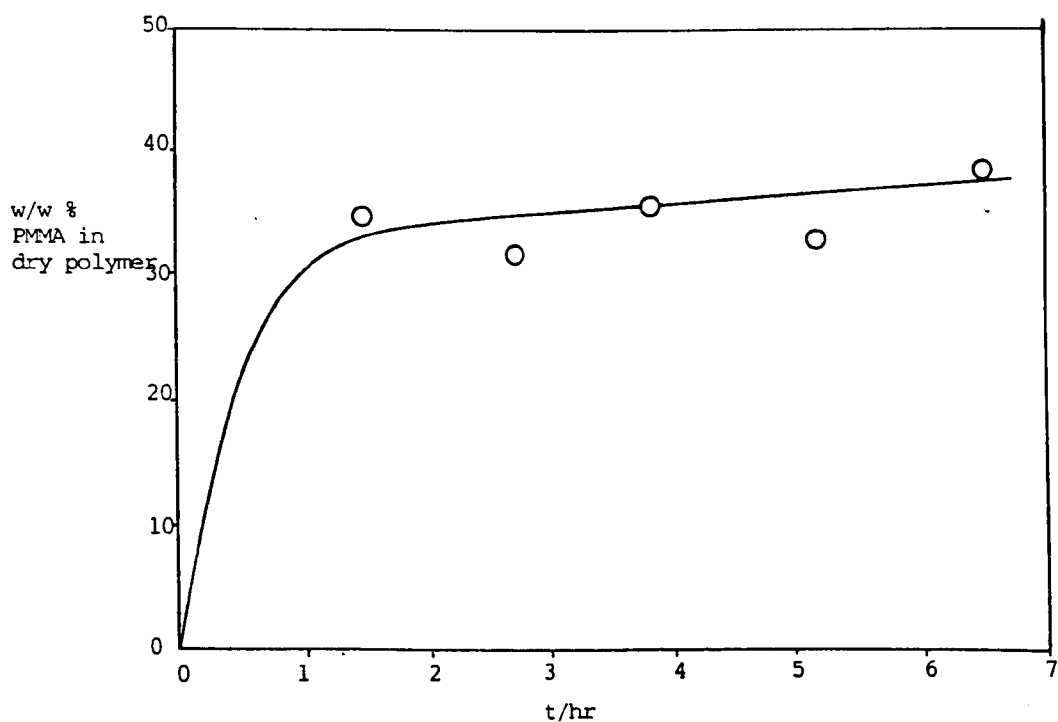


Fig. 5-3: Second experiment

If a photosensitiser is used,

$$\frac{I_{\text{abs}}}{I_0} = EC_s \quad \dots(5-5)$$

where in both cases  $I_{\text{abs}}$  is the intensity of the light absorbed,  $E$  is in the first case the molar absorption coefficient of the monomer, and in the second case that of the photosensitiser, and  $C_s$  is the concentration of photosensitiser.

Hence where a photosensitiser is used,

$$\frac{-d[M]}{dt} = k[M] \quad \dots(5-6)$$

$$\text{where } k = k_p \frac{fEI_0 C_s}{kt}^{\frac{1}{2}} \quad \dots(5-7)$$

The integrated form of equation 5-6 is

$$\ln \frac{[M]_0}{M} = kt \quad \dots(5-8)$$

where  $[M]_0$  is the concentration of monomer at  $t = 0$ .

Where no photosensitiser is used, the corresponding integrated form is

$$[M]^{-\frac{1}{2}} - [M]_0^{-\frac{1}{2}} = \frac{kt}{2} \quad \dots(5-9)$$

The results for  $P_{II}$ , shown in Figs. 5-2 and 5-3, can be converted to monomer concentrations  $[M]$  in the following way. If the initial weight of the dry polymer before swelling in the monomer mixture is denoted by  $m_d$ , the total weight of swelling mixture absorbed at equilibrium by  $m_{\text{abs}}$ , and the weight fraction of monomer in the swelling mixture

by  $f_m$ , then  $[M]_O$  is given by

$$[M]_O = \frac{m_{abs} f_m P_s}{m_d + m_{abs}} \quad \text{....(5-10)}$$

where  $P_s$  is the density of the swollen material.

$[M]_O$  is expressed as mass per unit volume. If, at a time  $t$ , the weight of monomer which has polymerised is  $m_p$ , and the weight of that remaining unpolymerised is  $m_m$ , then

$$m_{abs} f_m = m_p + m_m \quad \text{....(5-11)}$$

and

$$[M] = \frac{m_m P_s}{m_d + m_{abs}} \quad \text{....(5-12)}$$

Combining equations 5-10 and 5-12:

$$[M]_O = \frac{m_{abs} f_m}{m_m} \quad \text{....(5-13)}$$

From equation 5-11 this becomes

$$\frac{[M]_O}{[M]} = \frac{m_{abs} f_m}{m_{abs} f_m - m_p} \quad \text{....(5-14)}$$

The proportion of polymer in the final material is given by

$$P_{II} = \frac{m_p}{m_p + m_d} \times 100\% \quad \text{....(5-15)}$$

Hence

$$m_p = \frac{m_d P_{II}}{100 - P_{II}} \quad \text{....(5-16)}$$

Substituting in equation 5-14:

$$\frac{[M]_O}{[M]} = \frac{(m_{abs}/m_d) f_m (100 - P_{II})}{(m_{abs}/m_d) f_m (100 - P_{II}) - P_{II}} \quad \text{....(5-17)}$$

Therefore, using the data shown in Figs. 5-2 and 5-3, a first order rate plot can be constructed, using equation 5-8. The ratio  $m_{abs}/m_d$  which appears in equation 5-17 is related to the swelling at equilibrium  $s$ , given by

$$s = \frac{m_{abs}}{m_d + m_{abs}} \times 100\% \qquad \text{....(5-18)}$$

Therefore  $\frac{m_{abs}}{m_d} = \frac{s}{100 - s} \qquad \text{....(5-19)}$

In Fig. 5-13, the value of  $s$  is given for the standard gels swollen in DMF/MMA mixtures of various compositions. For the first rate experiment (Fig. 5-2),  $s$  was 55%, and  $m_{abs}/m_d$  was therefore 1.22, from equation 5-19; for the second experiment (Fig. 5-3),  $s$  was 46%, and  $m_{abs}/m_d$  was therefore 0.85. The values of  $f_m$  were 0.75 and 0.80 respectively.

The quantity  $\ln [M]_0/[M]$  , calculated from equation 5-17, is shown for both experiments as a function of time of polymerisation,  $t$ , in Fig. 5-4. The second set of data is consistent with a linear plot. For the first set, linearity is far more open to question. The first-order rate coefficients,  $k$ , obtained from the slopes of the straight lines drawn through the sets of points, are shown in Table 5-7.

Table 5-7: First-Order Rate Coefficients for Photopolymerisations

experiment	$\frac{10^5 k}{s^{-1}}$
first (Section 3.3.6.1)	2.8
second (Section 3.3.6.2)	11.7

From equation 5-7, it would be expected that the overall rate constant  $k$  would depend on  $I_0^{1/2}$ . Therefore the ratio of the rate coefficients for the two experiments should depend upon the ratios of the square roots of their incident light intensities. This ratio will also be proportional to the square roots of the respective sensitiser concentrations.

$$\text{Hence} \quad \frac{k_1}{k_2} \propto \frac{I_{o1} \cdot C_{s1}^{1/2}}{I_{o2} \cdot C_{s2}^{1/2}} \quad \dots(5-20)$$

where the subscripts 1 and 2 indicate the first and second experiment respectively.

$$\text{Therefore} \quad \frac{k_1}{k_2} \propto \frac{d_2}{d_1} \left\{ \frac{C_{s1}}{C_{s2}} \right\}^{1/2} \quad \dots(5-21)$$

where  $d$  is the distance of the lamp from the sample. Furthermore, since  $C_s$  is proportional to the swelling  $s$ ,

$$\frac{k_1}{k_2} \propto \frac{d_2}{d_1} \left\{ \frac{s_1}{s_2} \right\}^{1/2} \quad \dots(5-22)$$

Using the appropriate values for  $d$  and  $s$ , the expected ratio  $k_1/k_2$  is 0.86. The observed ratio was 0.24. Therefore the difference between the rate coefficients obtained from the two experiments cannot be entirely explained by the differences in light intensity and concentration of photosensitiser.

The model which was used as a theoretical basis for the analysis above was that of polymerisation in solution. Polymerisation in the presence of monomer, solvent and also of polymer network I may require a modified model, although Fig. 5-4 shows that first order kinetics may apply to the system. It might be thought that the increase in  $k$  for the



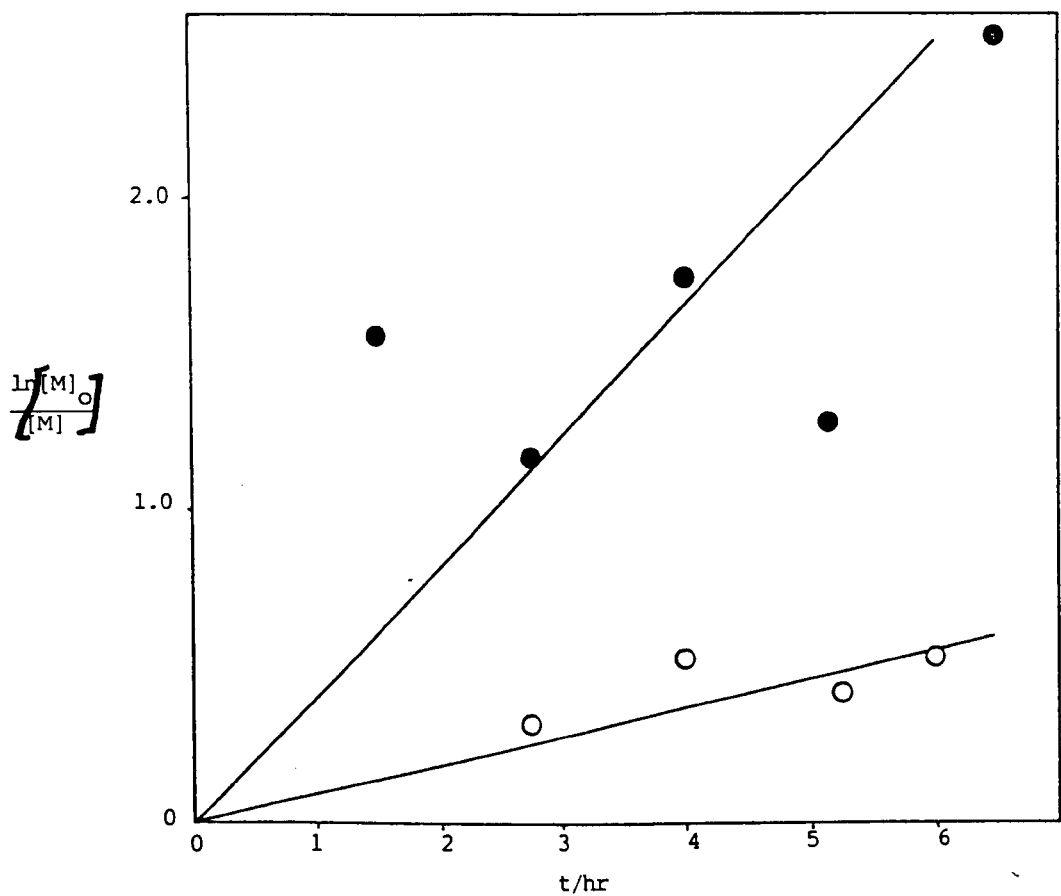


Fig. 5-4: First-Order Rate Plots for Photopolymerisation

KEY:

○ First experiment

● Second experiment

second experiment was partly caused by an increase in temperature. However, this is unlikely, since the reactions were carried out in a thermostatically-controlled water-bath.

## 5.7 SWELLING OF CROSSLINKED POLY(HEMA-MAA) HYDROGELS IN MMA-DMF-ETHYL ACETATE MIXTURES

In order to ascertain the most suitable swelling mixtures for the sequential IPN polymerisations, swelling measurements of 95/5/0.4 molar HEMA/MAA/EGDMA in MMA/IMS, MMA/DMF and MMA/ethyl acetate/DMF were made.

### 5.7.1 Swelling in MMA-IMS and MMA-DMF Mixtures

HEMA(1) was used for these experiments (Section 3.3.7.1). In order that the 95/5/0.4 molar HEMA/MAA/EGDMA copolymer might swell appreciably in the monomer II swelling mixture, as described in the preceding sections, a polar solvent was included in the mixture. DMF was thought to be suitable, since it is less volatile than IMS and therefore evaporation of swelling mixture during polymerisation would be minimised. The optimum swelling  $s$  for the materials swollen in the monomer II swelling mixture was about 70%. At this level, the gels are strong enough to be handled, yet thick enough to fit tightly between the glass plates, when using the silicone rubber tubing gasket. At higher swellings, problems may be caused by the exudation of swelling mixture from gels, caused by pressure on the gels exerted by the glass plates. Therefore the polar solvent must be such that, at a degree of swelling of approximately 70%, the level of monomer in the mixture must be high, i.e. the gels should swell extensively even though the concentration of polar solvent in the swelling mixture is low.

Fig. 5-5a shows the swelling in MMA-IMS mixtures as a function of mixture composition. The swelling  $s$  is defined in the same way as in Section 5.6. At high IMS concentrations,  $s$  is approximately constant, but as the MMA content is increased above 40%, the swelling decreases with increasing MMA content. A point of inflexion occurs at about

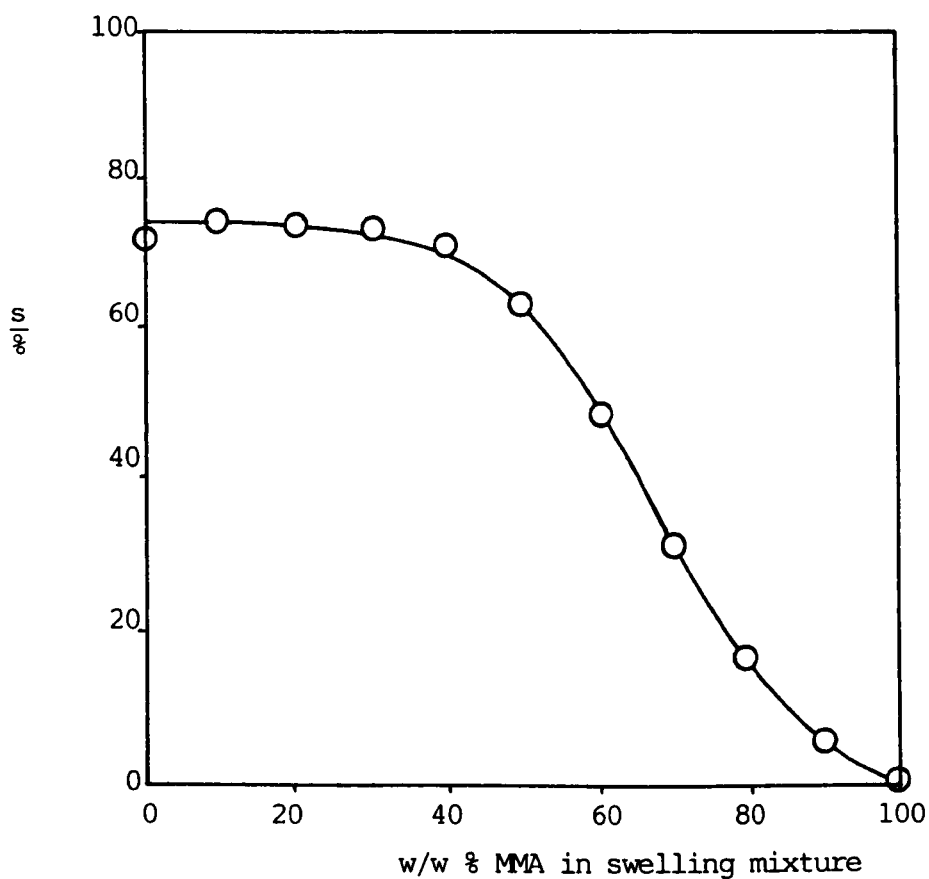


Fig. 5-5a: Swelling  
of 95/5 HEMA/MAA  
Hydrogels in IMS/MMA  
Mixtures

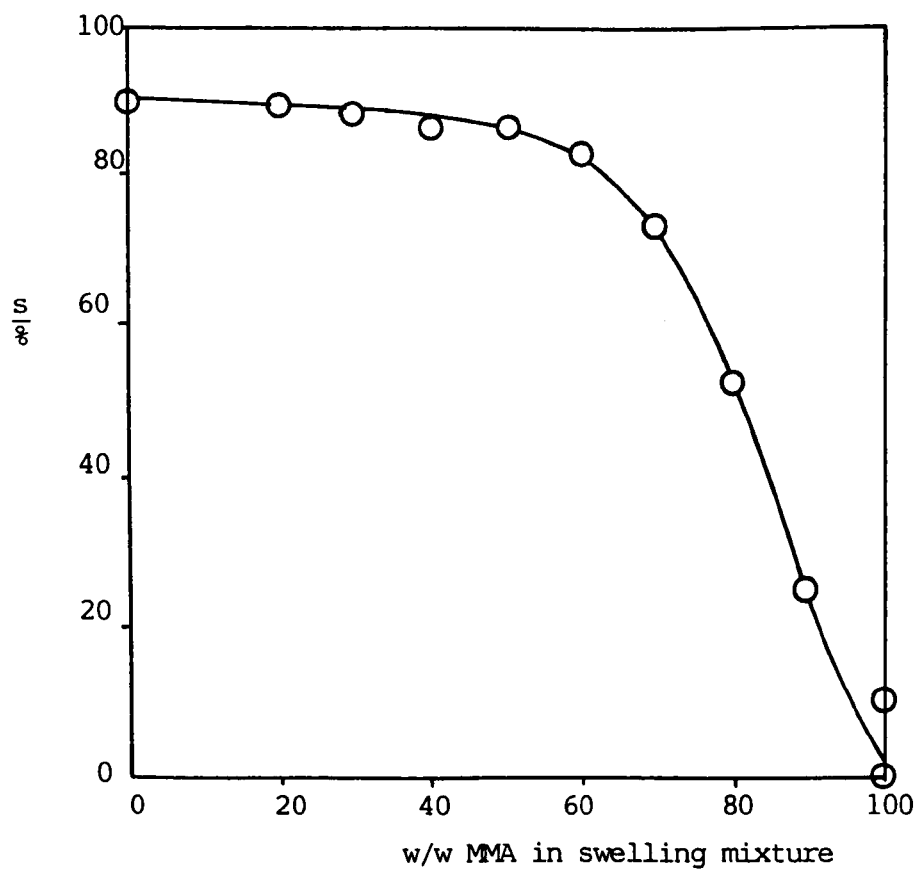


Fig. 5-5b: Swelling  
of 95/5 HEMA/MAA  
Hydrogels in DMF-MMA  
Mixtures

70 - 80% MMA. A similar curve for copolymers swollen in DMF-MMA mixtures is shown in Fig. 5-5b. The shape of the curve is similar to that of Fig. 5-5a, but in Fig. 5-5b swelling values at a given composition were higher. At a swelling of 70%, the proportion of DMF in the DMF-MMA mixture was 27%; at the same swelling value the proportion of IMS in the IMS-MMA mixture was about 60%. Hence it was concluded that DMF is a suitable polar solvent for the monomer II mixture.

At a given swelling mixture composition, the amount of polymer II in the resulting IPN is controlled by both the swelling and the proportion of monomer in the swelling mixture. If all the monomer contained in the swollen polymer I gel is converted to polymer II, then the composition of the resulting IPN can be calculated in the following way. The swelling  $s$  is given by equation 5-18 (Section 5.6):

$$s = \frac{m_{abs}}{m_d + m_{abs}} \times 100\% \quad \dots(5-18)$$

where  $m_{abs}$  is the weight of mixture absorbed, and  $m_d$  is the weight of the basic gel before swelling. The weight of monomer absorbed by polymer I, which is equal to the weight of polymer II, is therefore  $m_{abs} \cdot f_m$  where  $f_m$  is the weight fraction of monomer II in the swelling mixture.

The weight of polymer II,  $m_{PII}$ , is therefore given by

$$m_{PII} = \frac{m_d \cdot s \cdot f_m}{100 - s} \quad \dots(5-23)$$

The weight fraction of polymer II in the resulting IPN,  $P_{II}$ , is therefore

$$P_{II} = \frac{m_{PII}}{m_{PII} + m_d} \quad \dots(5-24)$$

which from equation 5-23, expressed as a percentage is

$$P_{II} = \frac{f_m}{f_m - 1 + 100/s} \times 100\% \quad \dots(5-25)$$

Values of  $P_{II}$ , calculated from the data shown in Figs. 5-5a and 5-5b using equation 5-25 are shown as a function of composition of swelling mixture in Figs. 5-6a and 5-6b respectively. For gels swollen in IMS-MMA mixtures (Fi. 5-6a), the maximum possible content of polymer II is expected to occur when a 60% IMS mixture was used. For a swelling of 70%,  $P_{II}$  ranges from 0 - 45%. For gels swollen in DMF-MMA mixtures (Fig. 5-6b), the maximum possible value of  $P_{II}$  is expected to occur when an approximately 40% DMF mixture is used. For a swelling of 70%,  $P_{II}$  is approximately 65%.

From such graphs, it is possible to calculate the degree of conversion of monomer II to polymer II, since  $P_{II}$  in equation 5-25 represents the maximum weight fraction which can be achieved for a particular swelling and swelling mixture composition if the monomer is completely converted to polymer.

Flory (ref. 2, p.579) has given expressions for the swelling ratio,  $q$ , of a lightly crosslinked polymer as a function of the degree of crosslinking, from which the interaction parameter for the polymer and swelling agent can be calculated as follows:

$$\text{approximate : } \chi_1 = \frac{1}{2} - 2xV_1q^{5/3} \quad \dots(5-26a)$$

$$\text{exact : } \chi_1 = -q^2 \ln(1 - \frac{1}{q}) + \frac{1}{q} + 2xV_1(q^{-1/3} - \frac{1}{2}q) \quad \dots(5-26b)$$

where  $x$  is the crosslink concentration, expressed as the number of moles of active chains per unit volume of dry polymer,  $\chi_1$  is the polymer-solvent interaction parameter, and  $V_1$  is the molar volume of the solvent.

Hence, if the crosslink concentration is known, it is possible to estimate the polymer-solvent interaction parameter, and vice-versa.

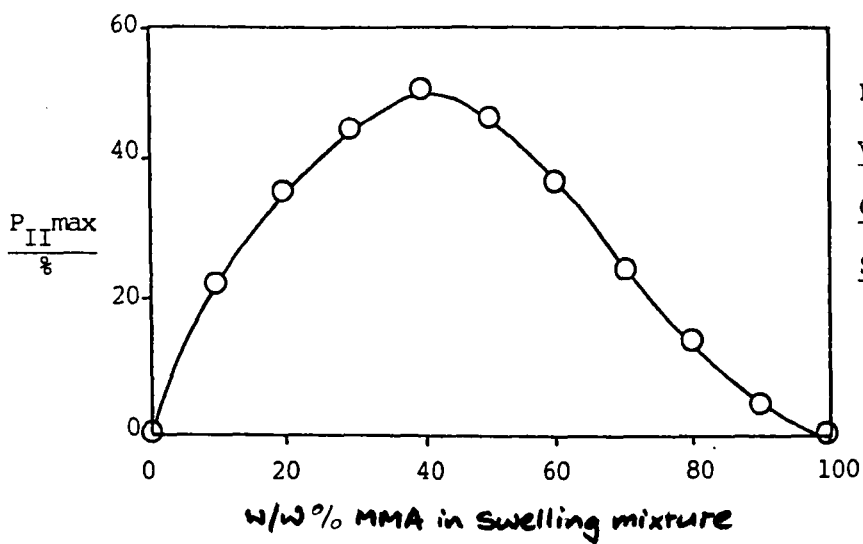


Fig. 5-6a: Maximum  
Value of  $P_{II}$  vs.  
Composition of IMS/MMA  
Swelling Mixture

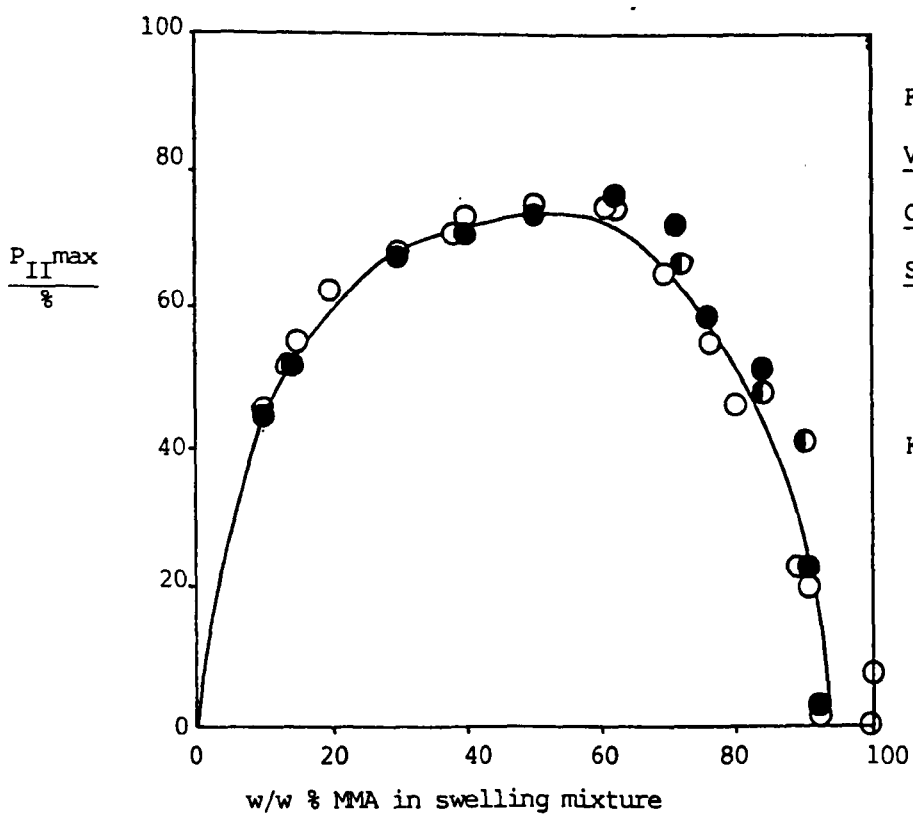


Fig. 5-6b: Maximum  
Value of  $P_{II}$  vs.  
Composition of DMF/MMA  
Swelling Mixture

KEY:  
 ○ After 2 days swelling  
 ◐ After 5 days  
 ● After 56 days

$V_1$  can be calculated if it is assumed that no volume change occurs on mixing together the components of the swelling mixture.  $V_1$  is then given by

$$V_1 = \frac{\text{volume of mixture}}{\text{number of moles of mixture}} \quad \dots(5-27)$$

$$= \frac{f_m \bar{V}_m + (1 - f_m) \bar{V}_{pd}}{\frac{f_m}{M_m} + (1 - f_m) \frac{1}{M_{pd}}} \quad \dots(5-28)$$

where  $\bar{V}_m$  and  $\bar{V}_{pd}$  are the specific volumes of the monomer and polar diluent respectively, and  $M_m$  and  $M_{pd}$  are the relative molecular masses of the monomer and polar diluent respectively. The specific volumes are reciprocals of the densities of the liquids and are, at 20°C (197): for IMS  $1.23 \text{ cm}^3 \text{ g}^{-1}$ ; for DMF  $1.05 \text{ cm}^3 \text{ g}^{-1}$ ; for MMA  $1.06 \text{ cm}^3 \text{ g}^{-1}$ . The theoretical crosslink density, calculated from the mole fraction of EGDMA, was  $3.13 \times 10^{-5} \text{ mol cm}^{-3}$ .

The swelling factor  $q$  in equations 5-26a and 5-26b is defined by

$$q = \frac{v_s}{v_d} = \frac{m_s / \rho_s}{m_d / \rho_d} \quad \dots(5-29)$$

where the subscripts  $s$  and  $d$  refer to the swollen and dry materials respectively,  $v$  is the volume,  $m$  is the weight, and  $\rho$  is the density. If it is assumed that the volume of the swollen material is equal to the sum of the volumes of dry polymer and swelling agent, then

$$\rho_s = f_{vs} \rho_{sm} + (1 - f_{vs}) \rho_d \quad \dots(5-30)$$

where  $f_{vs}$  is the volume fraction of swelling mixture in the swollen gel, and  $\rho_{sm}$  is the density of the swelling mixture. Substitution of equation 5-30 into equation 5-29 gives



$$q = \frac{m_s}{m_d} \cdot \frac{\rho_d}{f_{vs} \rho_{sm} + (1 - f_{vs}) \rho_d} \quad \dots(5-31)$$

and, since  $f_{vs} = 1 - 1/q$  ....(5-32)

q is obtained as  $q = \left\{ \frac{s}{1-s} \right\} \frac{\rho_d}{\rho_{sm}} + 1$  ....(5-33)

The value of  $\rho_{sm}$  is given by

$$\rho_{sm} = \rho_{MMA} f_{vm} + (1 - f_{vm}) \rho_{pd} \quad \dots(5-34)$$

where  $\rho_{MMA}$  and  $\rho_{pd}$  are the densities of MMA and the polar diluent respectively, and  $f_{vm}$  is the volume fraction of the MMA in the swelling mixture. The volume fraction of MMA in the swelling mixture,  $f_{vm}$ , is related to the weight fraction,  $f_m$ , by the equation

$$f_{vm} = \frac{f_m}{f_m + (1 - f_m) \rho_{MMA} / \rho_{pd}} \quad \dots(5-35)$$

The procedure for calculating  $\chi_1$  is therefore as follows:

- (i)  $v_1$  is found from equation 5-28;
- (ii)  $f_{vm}$  is calculated from equation 5-35, and this value used to find  $\rho_{sm}$  from equation 5-34;
- (iii) using the value of  $\rho_{sm}$ , q is calculated from equation 5-33;
- (iv) using the values of  $v_1$  and q,  $\chi_1$  is calculated from equations 5-26a or 5-26b.

Fig. 5-7 shows the values of  $\chi_1$  calculated for gels swollen in both IMS-MMA and DMF-MMA swelling mixtures, using both the approximate and exact expressions for  $\chi_1$ . At low MMA contents, where the swelling ratio is high, the values of  $\chi_1$  are similar. However, where  $f_m > 0.4$ , discrepancies between values of  $\chi_1$  given by the two equations are greater, and increase with increasing  $f_m$ . This is consistent with the fact that the approximate expression only holds where the crosslink

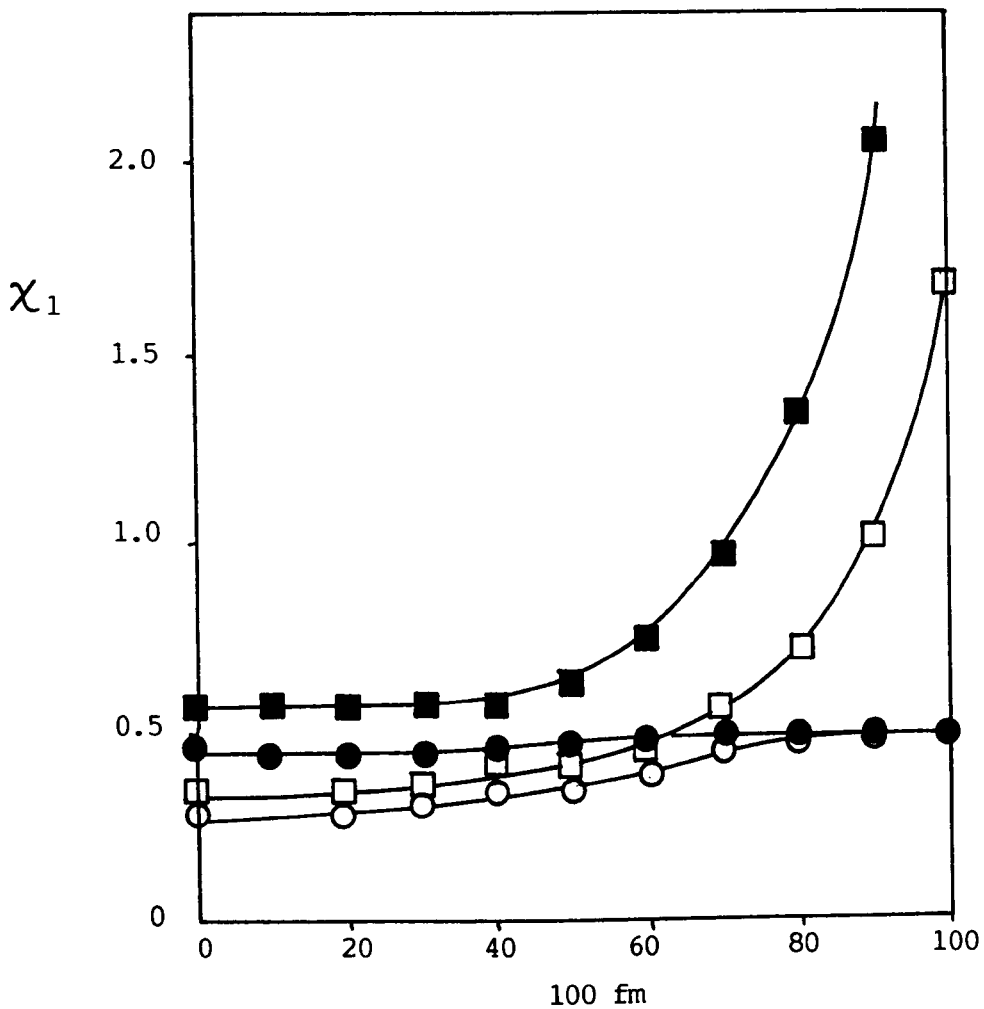


Fig. 5-7: Calculated Values of the Flory-Huggins Interaction Parameter as a Function of Composition of Swelling Mixture, for IMS/MMA and DMF/MMA Mixtures

KEY:      ■ IMS/MMA ) Using equation  
           □ DMF/MMA ) 5-28b  
           ● IMS/MMA ) Using equation  
           ○ DMF/MMA ) 5.28a

density is small and the swelling ratio is large.

In general the values of  $\chi_1$  for the IMS-MMA mixture are higher than those for the DMF-MMA mixture. This reflects the higher hydrophilicity of DMF compared with MMA. The slight decrease in  $\chi_1$  with increasing  $f_m$  at low values of  $f_m$  is a result of the change in  $v_1$ , the molar volume of the solvent, whilst the swelling ratio remains approximately constant over a range of compositions. At higher MMA contents, the molar volume effect is dwarfed by the effect of the decrease of the swelling ratio as  $f_m$  increases. Hence  $\chi_1$  increases with increasing  $f_m$ . Minima in  $\chi_1$  as a function of swelling mixture composition were observed for both IMS-MMA and DMF-MMA mixtures. As  $f_m$  increases, and the swelling mixture polarity therefore decreases,  $\chi_1$  increases. However, it should be noted that the value of  $\chi_1$  at  $f_m = 1.0$  is undefined, since  $q$  is 1.0.

#### 5.7.2 Swelling in MMA-DMF-Ethyl Acetate Mixtures

Mixtures of MMA, DMF and ethyl acetate were intended for use, with initiator and in some cases crosslinking agent, as monomer II mixtures in the preparation of sequential IPNs. The roles of these components are summarised below:

- (i) MMA is monomer II, which is converted to polymer II;
- (ii) DMF is a polar diluent which enables the network polymer I to swell in mixtures containing the monomer II;
- (iii) ethyl acetate is a saturated analogue of monomer II, which enables the composition of the IPN to be varied by substituting part of the MMA by ethyl acetate, whilst maintaining a constant degree of swelling of network polymer I.

Figs. 5-8a to 5-8j show the swelling of the 95/5/0.4 molar HEMA/MAA/EGDMA copolymers in DMF-MMA-ethyl acetate mixtures. These experiments, A to L, were described in Section 3.3.7.2. The ratio of ethyl acetate to MMA was varied in experiments A to L. Within each experiment, the ratio DMF/(MMA + ethyl acetate) was varied. Figs. 5-8a to 5-8e illustrate experiments carried out over the full range of compositions; Figs. 5-8f to 5-8i show data in more detail, over the range  $60 \leq 100f_m \leq 90$ . For those mixtures which contained ethyl acetate,  $f_m$  denotes the weight fraction of (ethyl acetate + MMA) in mixture.

In each case, as the value of  $100f_m$ , the weight percentage of (ethyl acetate + MMA), approached 90, a steep decrease in swelling with increasing  $f_m$  was observed. It is expected that as the polarity of the swelling medium is decreased, the swelling decreases. It is possible that this decrease in swelling is enhanced by the presence of an increasing number of polymer-polymer interactions as the solvent polarity decreases, augmenting the number of chemical crosslinks. Therefore the effective crosslink concentration is increased. The swelling was zero at a value of  $100f_m$  of approximately 90. Hence although DMF was present in the swelling mixture, the gels did not swell in mixtures for which the DMF content was less than 10%.

When describing the properties of ternary mixtures such as these, the triangular diagram is a useful tool. Fig. 5-9 shows the swelling data of Figs. 5-8a to 5-8j plotted on such a diagram. The vertices represent pure MMA, DMF and ethyl acetate respectively. The compositions at which the swelling was 50%, 60%, 70% and 80% were interpolated from each swelling/composition curve. They are joined by contour lines on the triangular diagram. Fig. 5-9 shows that, as

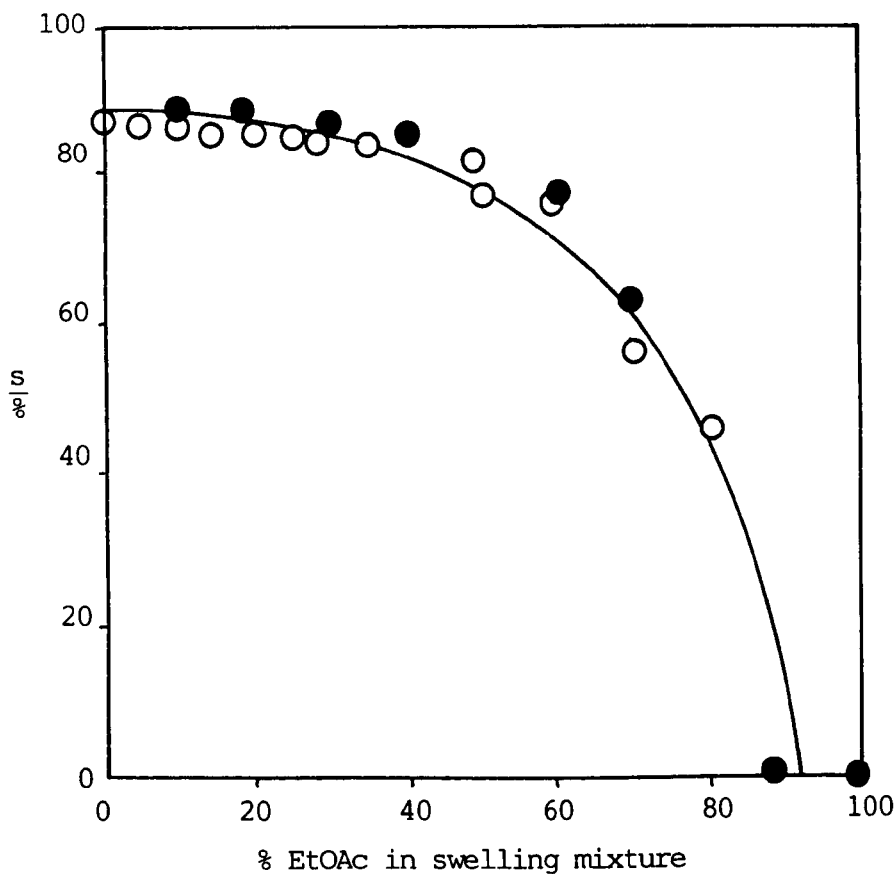


Fig. 5-8a: Swelling  
of 95/5 HEMA/MAA  
Copolymer in DMF/  
Ethyl Acetate  
Mixtures

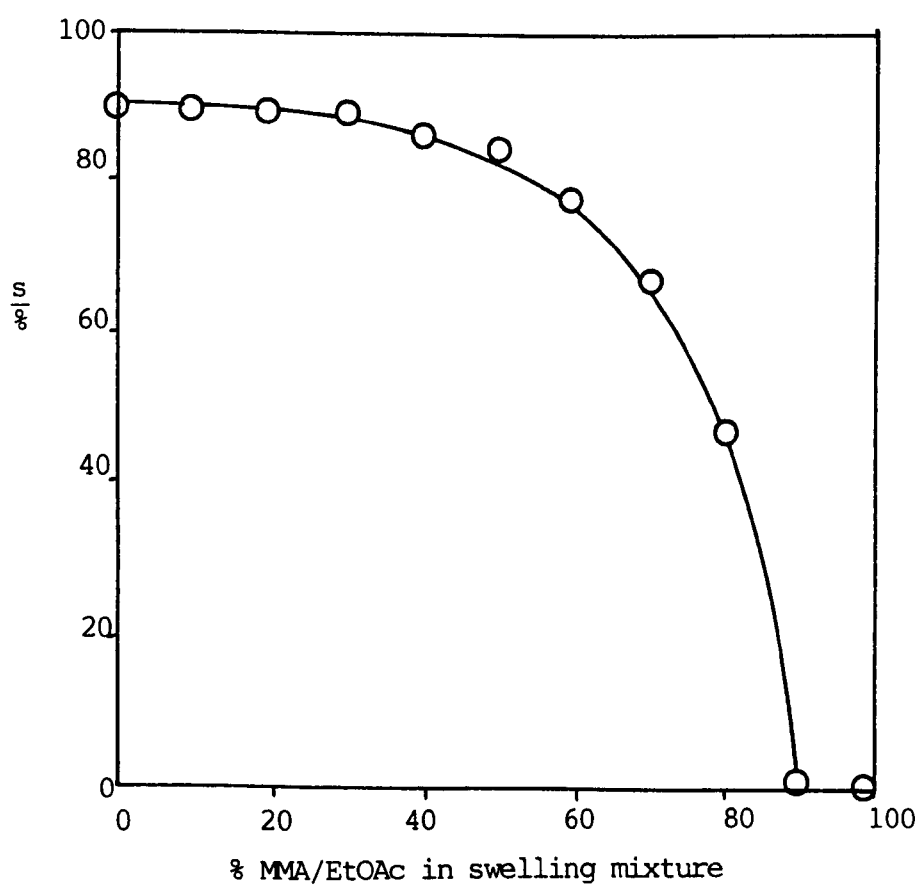


Fig. 5-8b: Swelling  
of 95/5 HEMA/MAA  
Copolymer in DMF/  
MMA/Ethyl Acetate  
Mixtures where MMA:  
Ethyl Acetate = 1:1

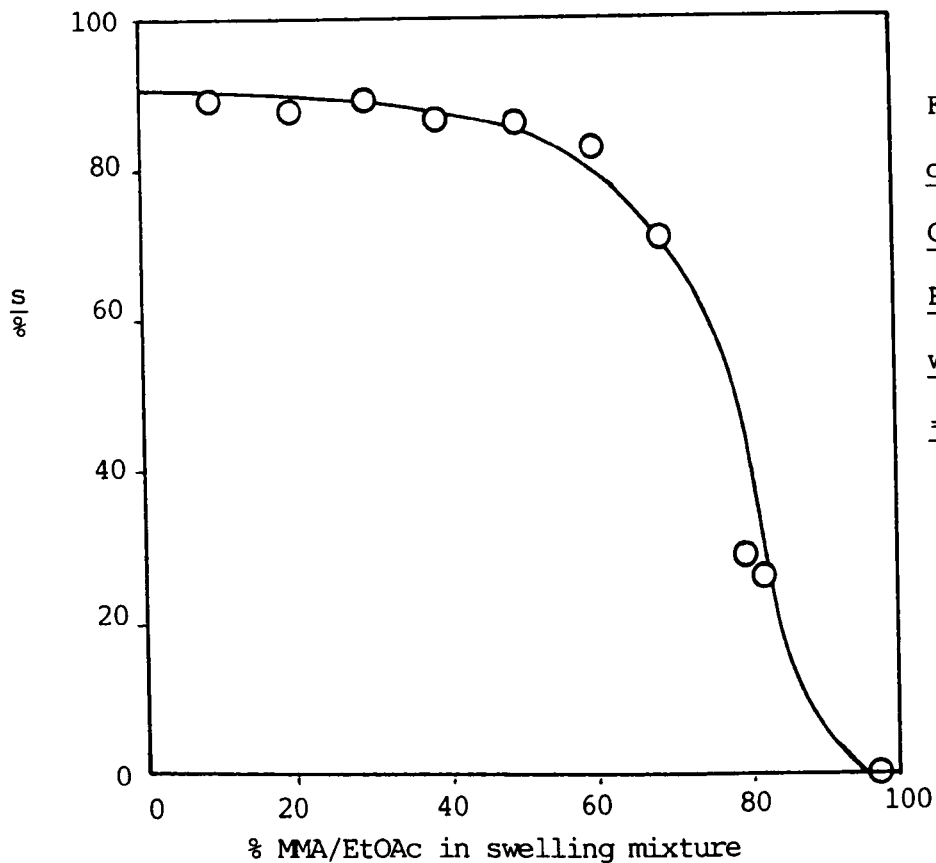


Fig. 5-8c: Swelling  
of 95/5 HEMA/MAA  
Copolymer in DMF/MMA/  
Ethyl Acetate Mixtures  
where MMA/Ethyl Acetate  
= 3:1

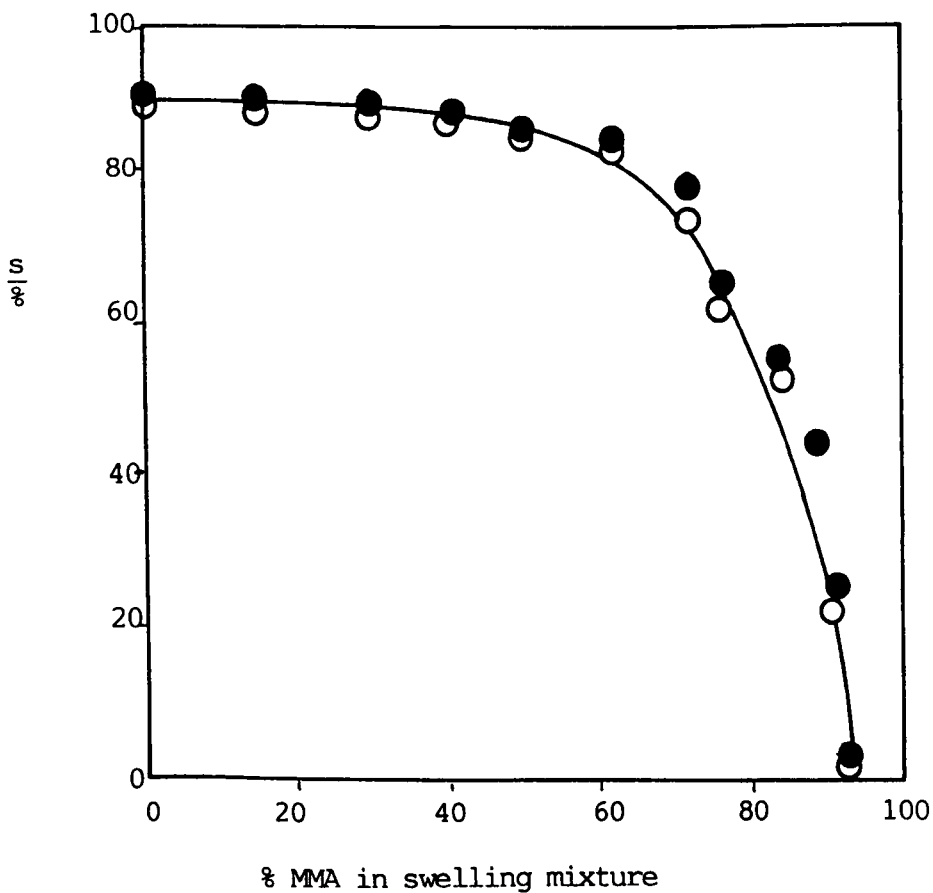


Fig. 5-8d: Swelling  
of 95/5 HEMA/MAA  
Copolymer in DMF/MMA  
Mixtures

KEY:

● After 56 days

○ After 3 days

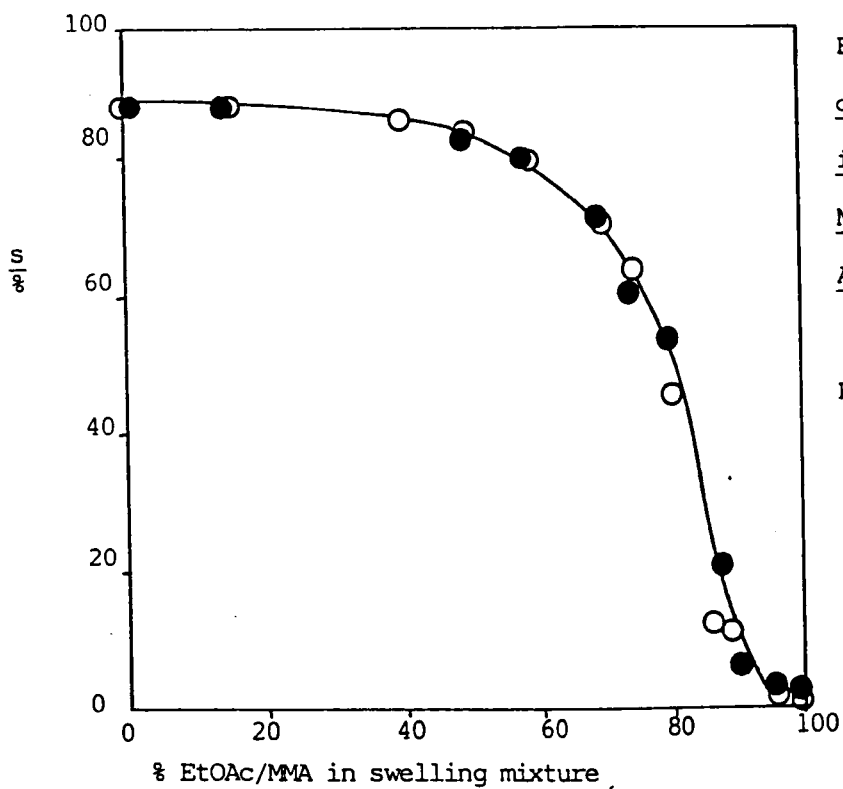


Fig. 5-8e: Swelling  
of 95/5 HEMA/MAA Copolymer  
in DMF/MMA/Ethyl Acetate  
Mixtures where MMA/Ethyl  
Acetate = 1:3

KEY:

○ After 5 days

● After 11 days

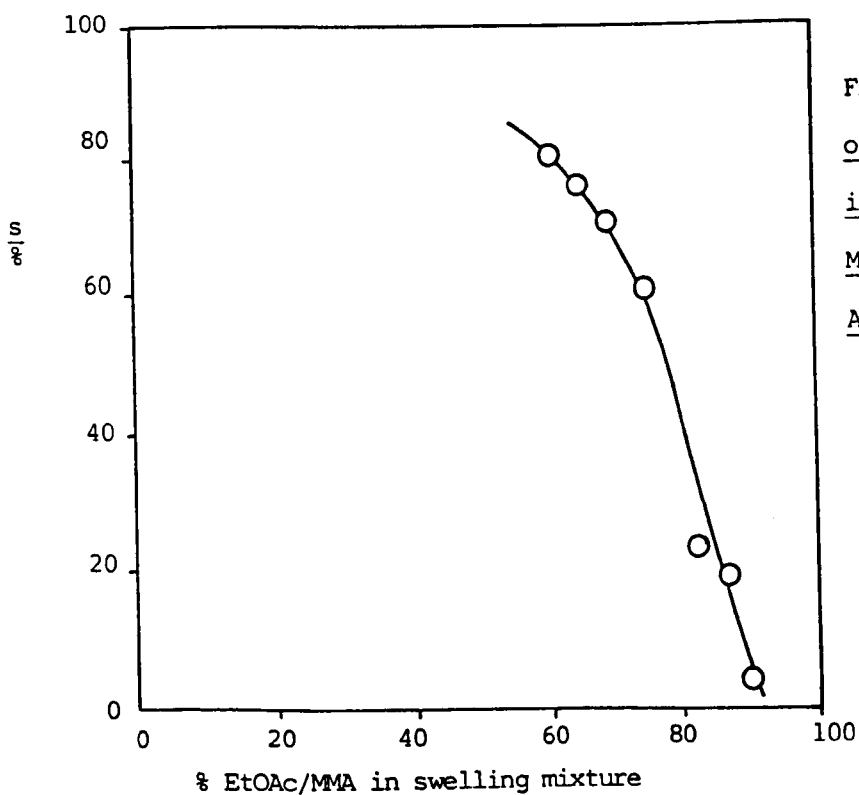


Fig. 5-8f: Swelling  
of 95/5 HEMA/MAA Copolymer  
in DMF/MMA/Ethyl Acetate  
Mixtures where MMA/Ethyl  
Acetate = 1:3

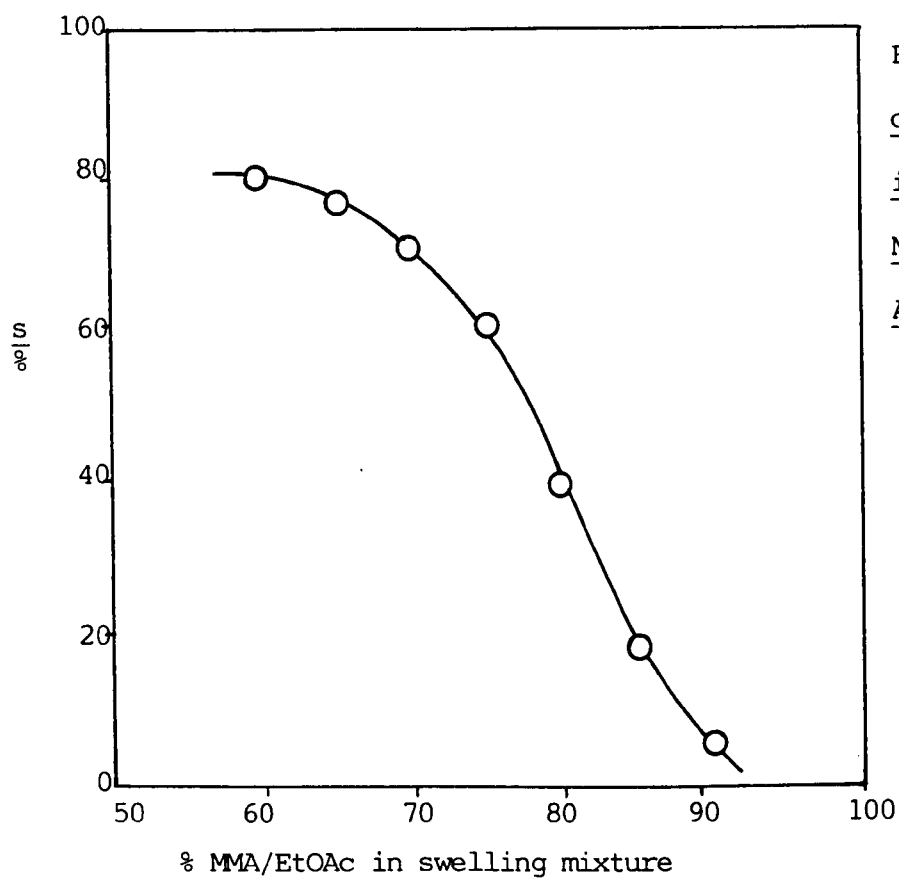


Fig. 5-8g: Swelling  
of 95/5 HEMA/MAA Copolymer  
in DMF/MMA/Ethyl Acetate  
Mixtures where MMA:Ethyl  
Acetate = 1:1

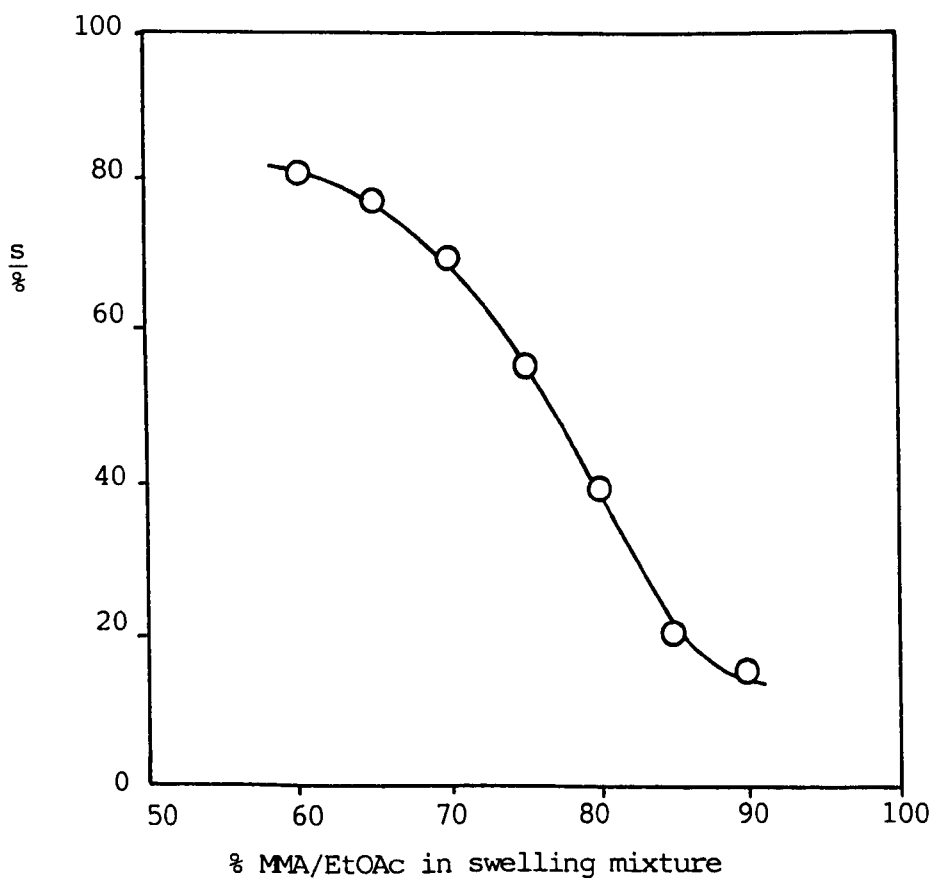


Fig. 5-8h: Swelling  
of 95/5 HEMA/MAA Copolymer  
in DMF/MMA/Ethyl Acetate  
Mixtures where MMA:  
Ethyl Acetate = 3:1



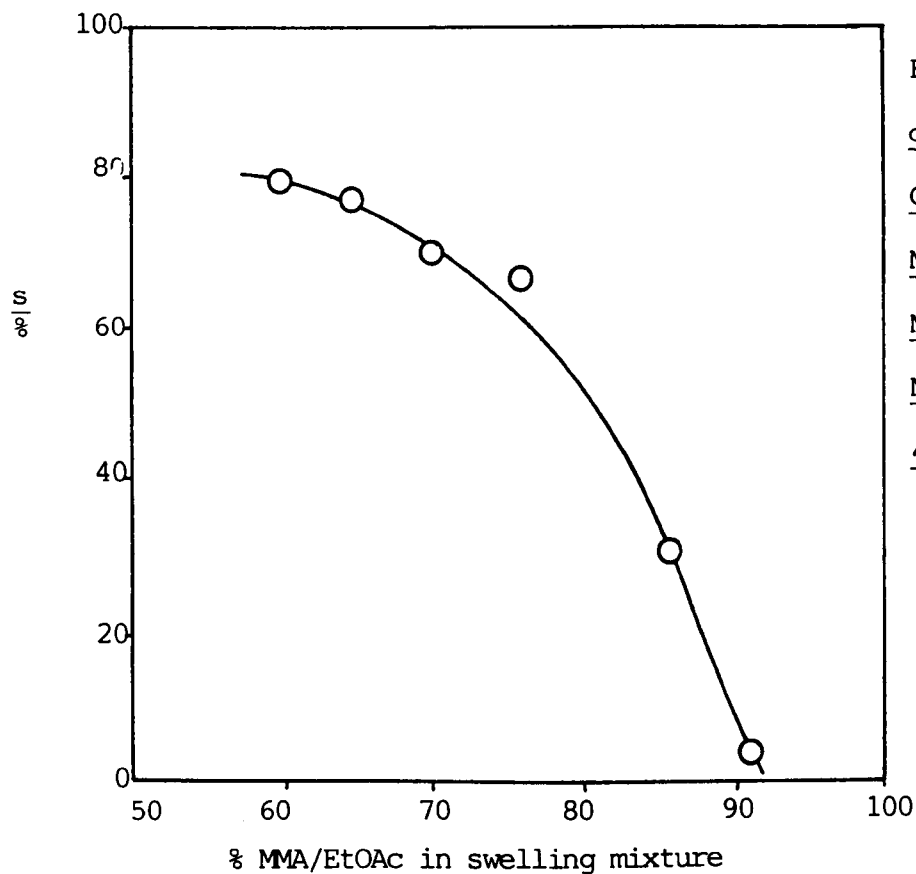


Fig. 5-8i: Swelling  
of 95/5 HEMA/MAA  
Copolymer in DMF/  
MMA/Ethyl Acetate  
Mixtures where  
MMA:Ethyl Acetate =  
4:1

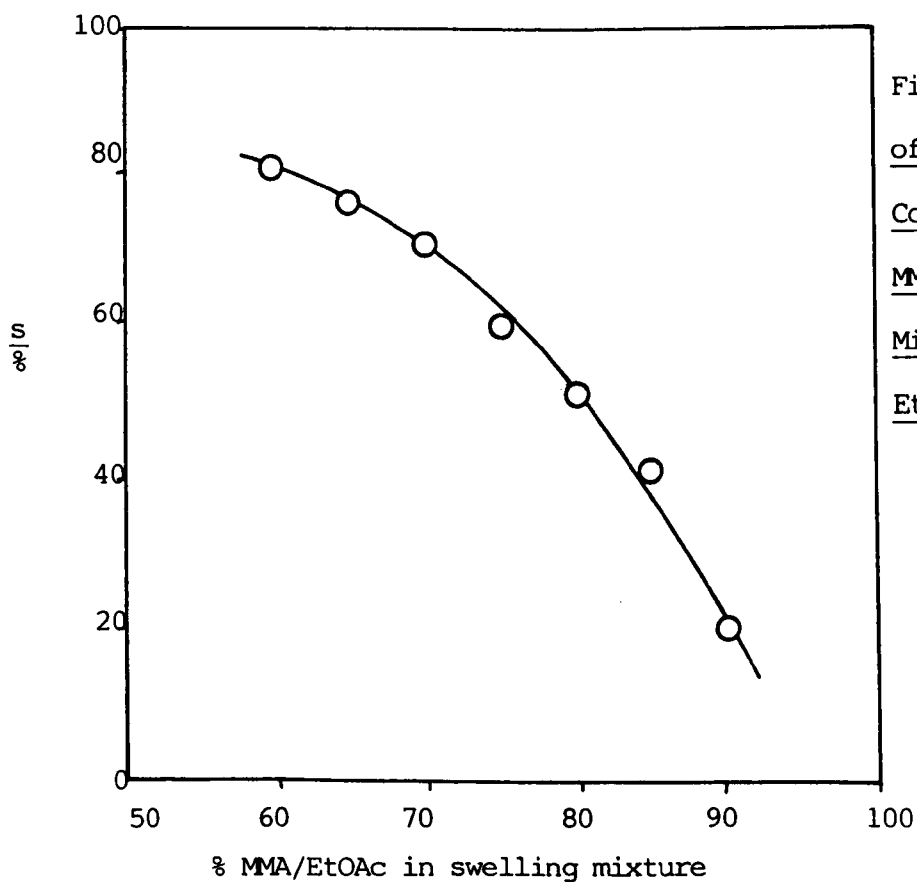
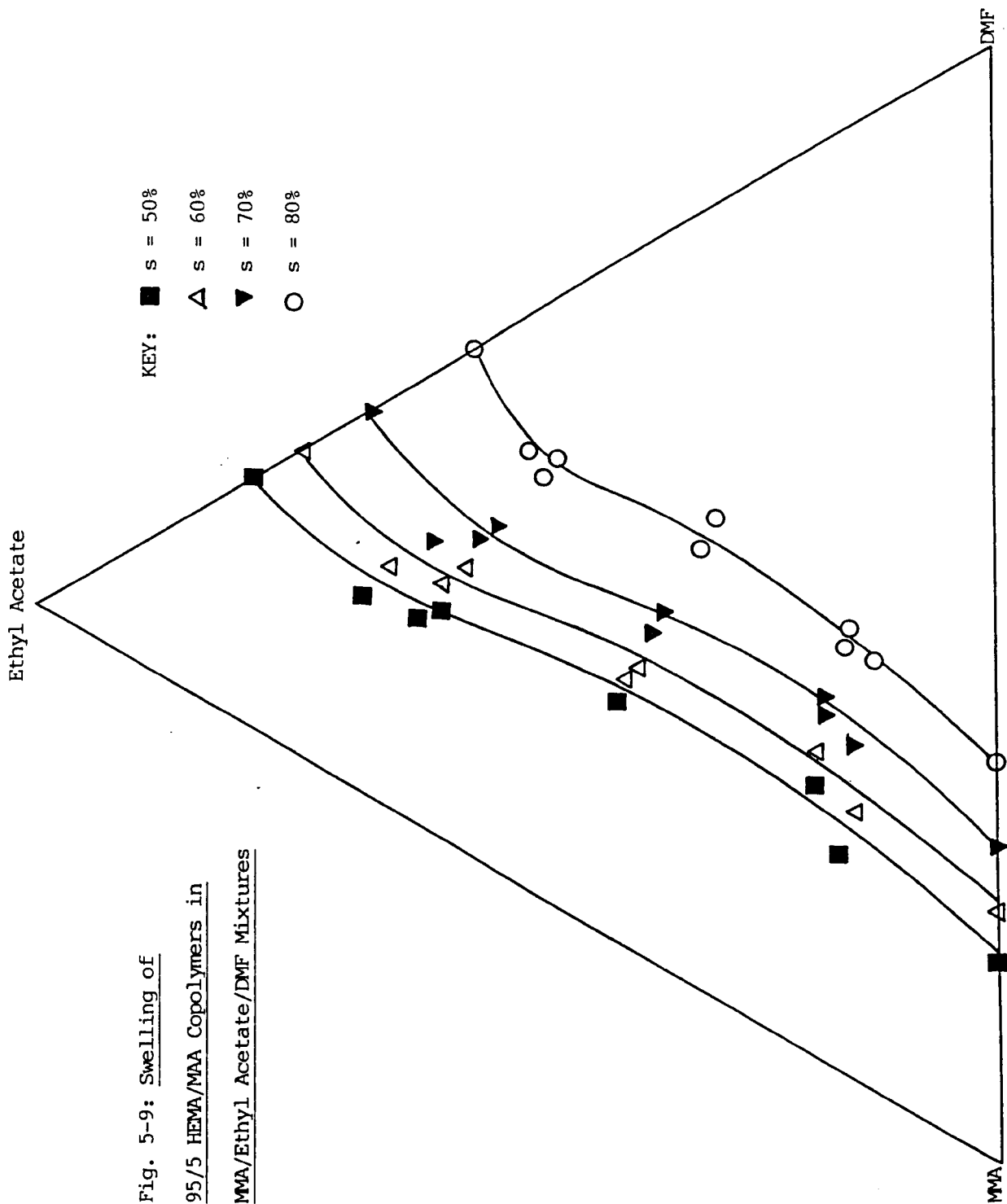


Fig. 5-8j: Swelling  
of 95/5 HEMA/MAA  
Copolymer in DMF/  
MMA/Ethyl Acetate  
Mixtures where MMA:  
Ethyl Acetate = 4:1



the ratio ethyl acetate/MMA increases, the fraction of DMF at which a given value of swelling is achieved increases. This trend may be explained by the similarity of the MMA molecule to the structural unit of the network polymer. The trend is small, however, and the suitability of ethyl acetate as a non-polymerisable analogue for MMA is apparent.

Figs. 5-10a to 5-10h illustrate  $P_{II \text{ max}}$ , the maximum polymer II content, as a function of the composition of the swelling mixture, for the DMF-MMA-ethyl acetate mixtures. The curves show maxima in  $P_{II}$  at approximately  $100f_m = 50$ . They are similar in shape to Fig. 5-6b, which was discussed in Section 5.7.1. The data of Figs. 5-10a to 5-10h are shown plotted on a triangular diagram in Fig. 5-11. This figure shows that the largest values of  $P_{II \text{ max}}$  occur when the ethyl acetate/MMA ratio is low, at intermediate levels of DMF. It also shows that, at constant swelling, a range of IPN compositions can be achieved. For example, the line which connects the compositions which give 70% swelling is superimposed on the diagram. It can be seen that, using these compositions, a range of IPNs can be obtained having PMMA contents from 0 - 60% w/w.

Using the procedure described in Section 5.7.1, the Flory-Huggins polymer-solvent interaction parameters were calculated for the 95/5 HEMA/MAA copolymer swollen in various MMA-ethyl acetate-DMF mixtures. If no change in total volume occurred on mixing MMA and ethyl acetate, the density of the hydrophobic component of the mixture, i.e. ethyl acetate + MMA, is given by

$$\rho_H = \frac{1}{f(\bar{V}_{\text{MMA}} - \bar{V}_{\text{EA}}) + \bar{V}_{\text{EA}}} \quad \dots(5-36)$$

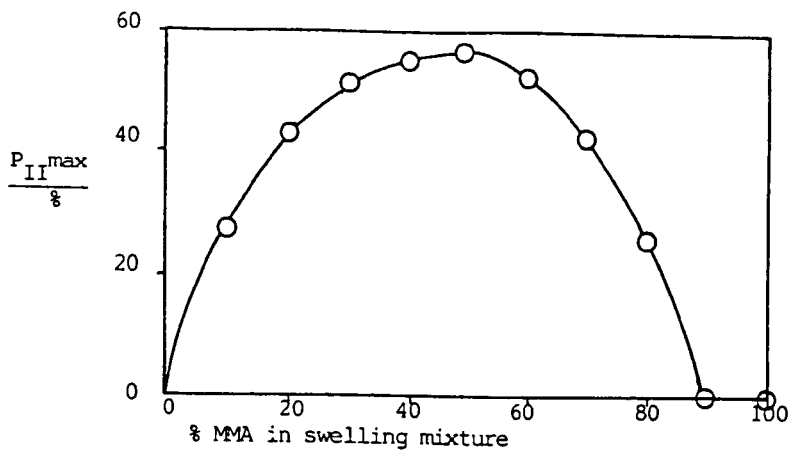


Fig. 5-10a: Maximum Value  
of  $P_{II}$  vs. Composition of  
Swelling Mixture for 1:1  
MMA/Ethyl Acetate Mixtures

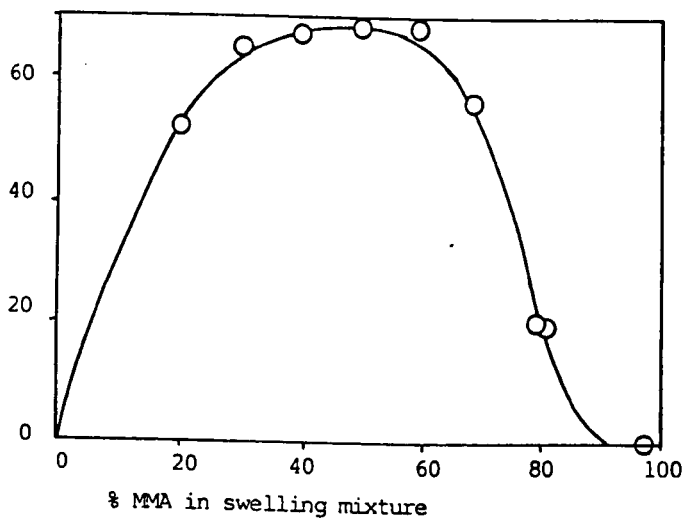


Fig. 5-10b: Maximum Value  
of  $P_{II}$  vs. Composition of  
Swelling Mixture for 3:1  
MMA/Ethyl Acetate Mixtures

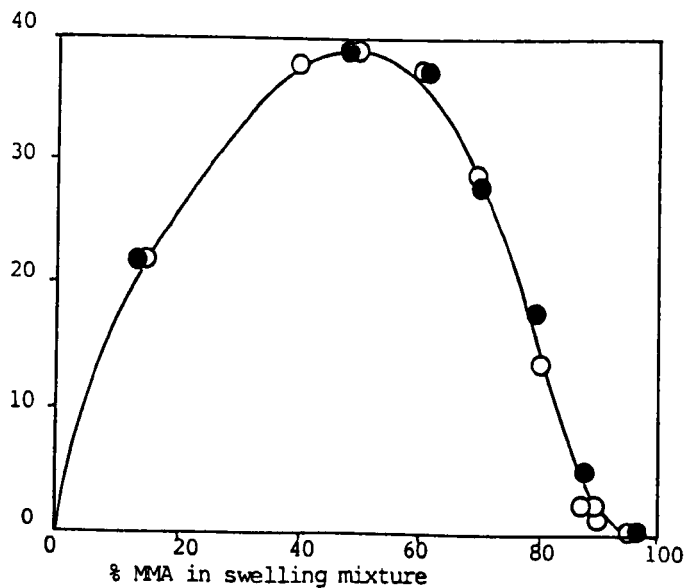


Fig. 5-10c: Maximum Value  
of  $P_{II}$  vs. Composition of  
Swelling Mixture for 1:3  
MMA/Ethyl Acetate Mixtures

KEY:  
○ 5 days  
● 11 days  
Swelling

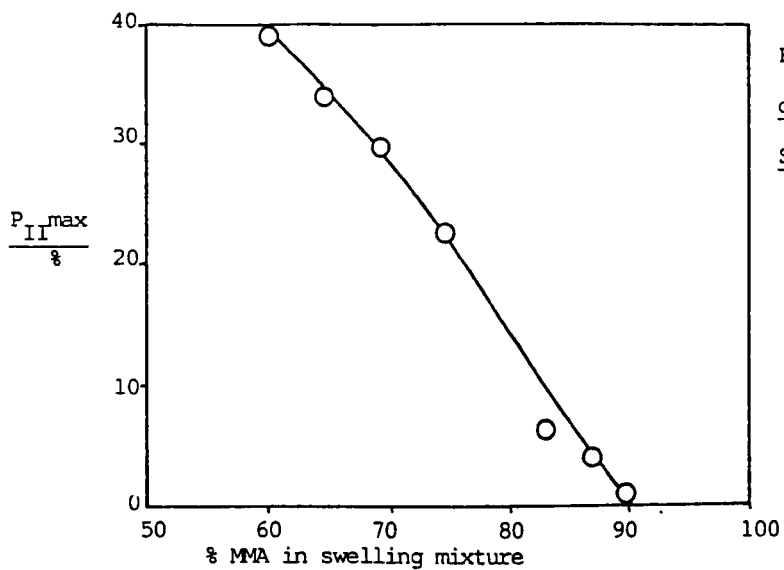


Fig. 5-10d: Maximum Value  
of  $P_{II}$  vs. Composition of  
Swelling Mixture for 1:3

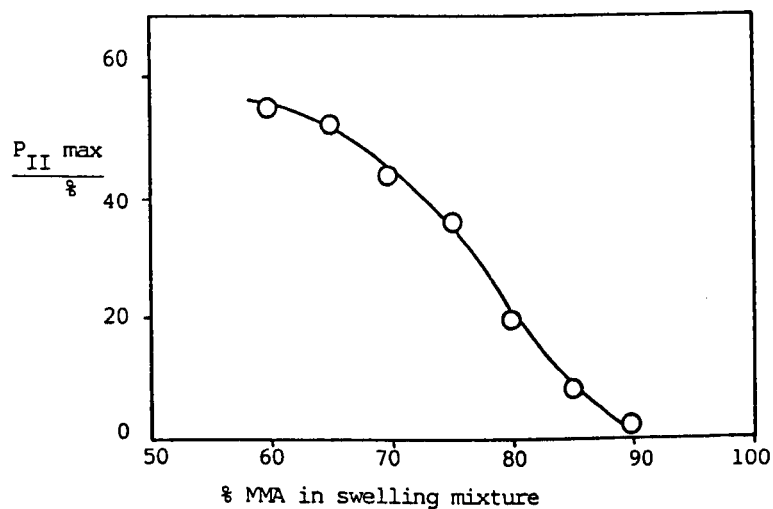


Fig. 5-10c: Maximum Value  
of  $P_{II}$  vs. Composition of  
Swelling Mixture for 1:1  
MMA/Ethyl Acetate Mixtures

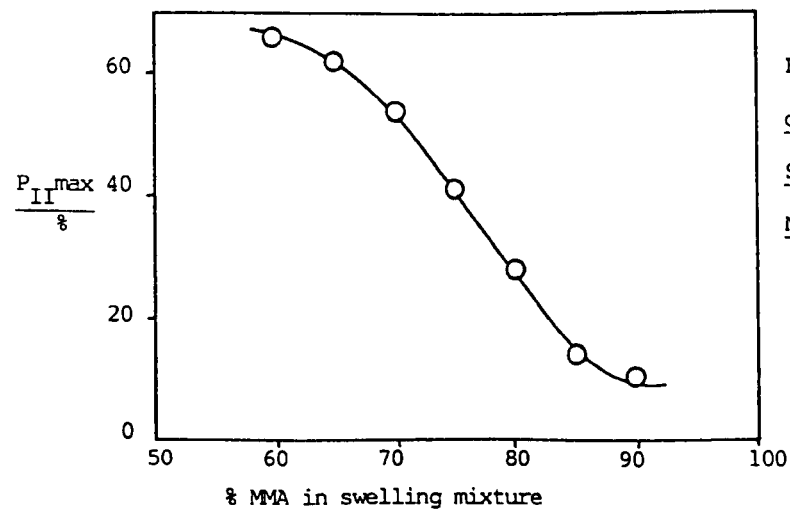


Fig. 5-10f: Maximum Value  
of  $P_{II}$  vs. Composition of  
Swelling Mixture for 3:1  
MMA/Ethyl Acetate Mixtures

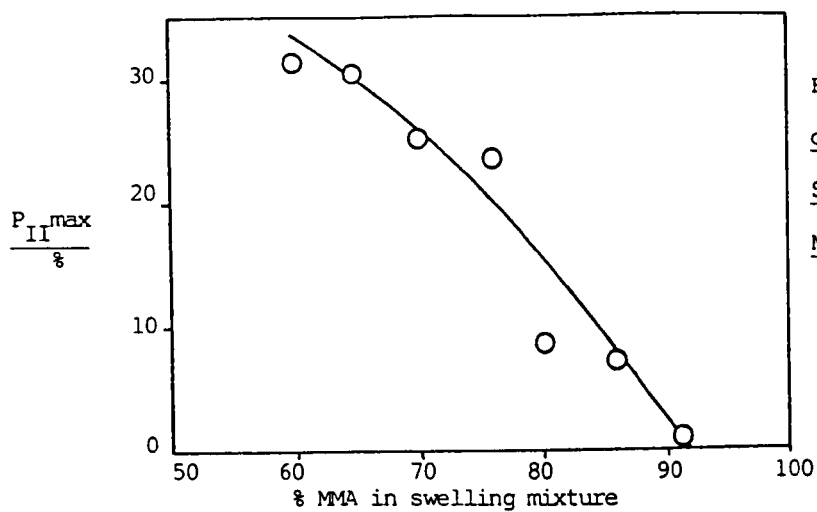


Fig. 5-10g: Maximum Value  
of  $P_{II}$  vs. Composition of  
Swelling Mixture for 1:4  
MMA/Ethyl Acetate Mixtures

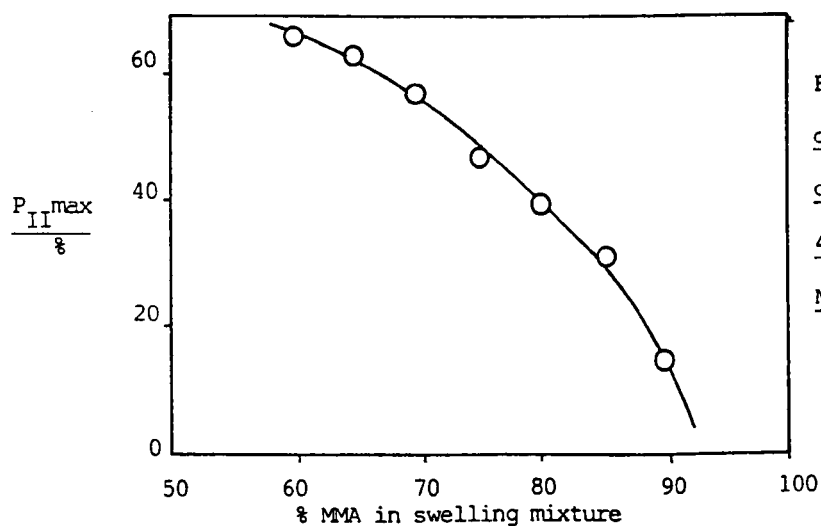


Fig. 5-10h: Maximum Value  
of  $P_{II}$  vs. Composition  
of Swelling Mixture for  
4:1 MMA/Ethyl Acetate  
Mixtures

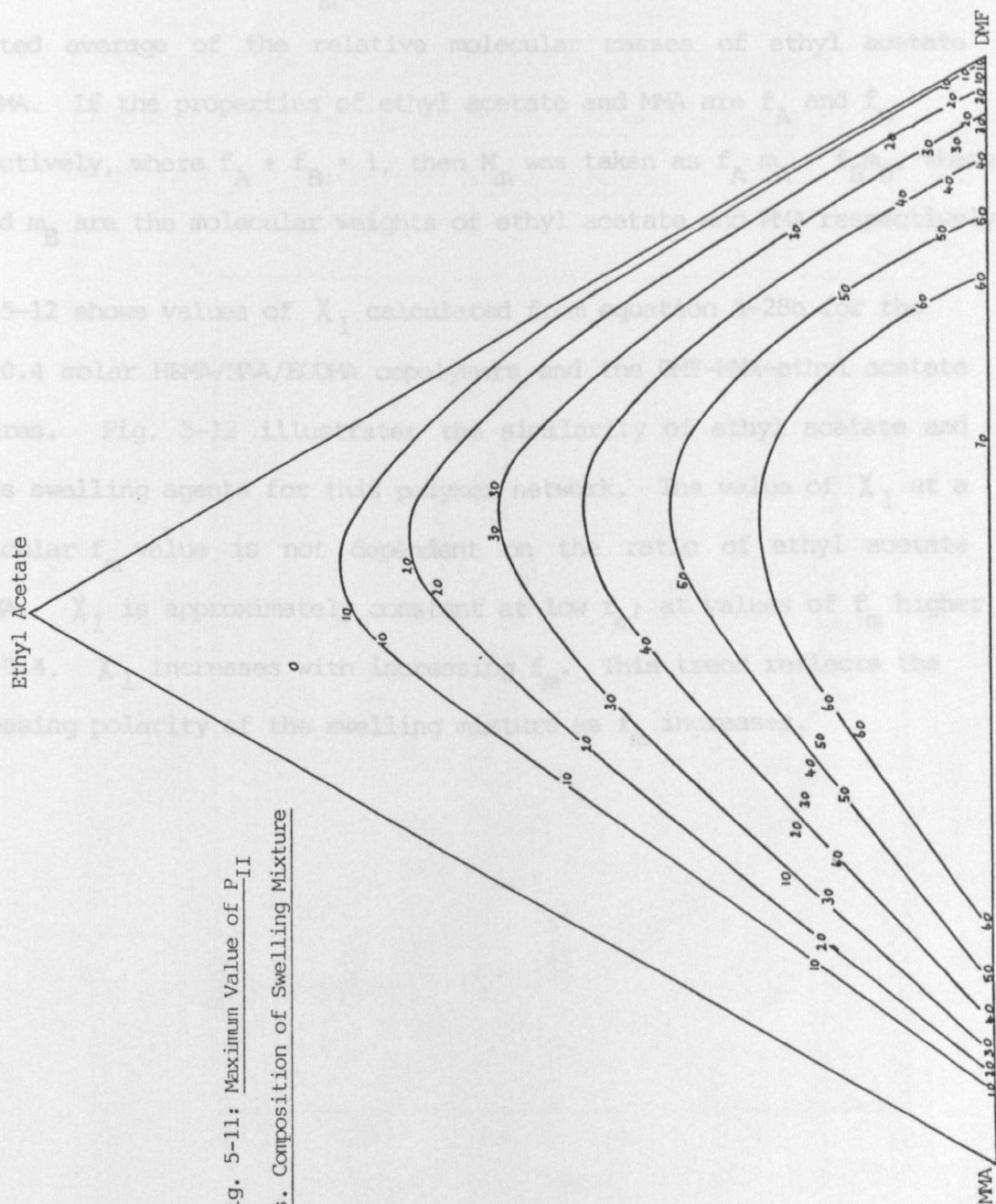


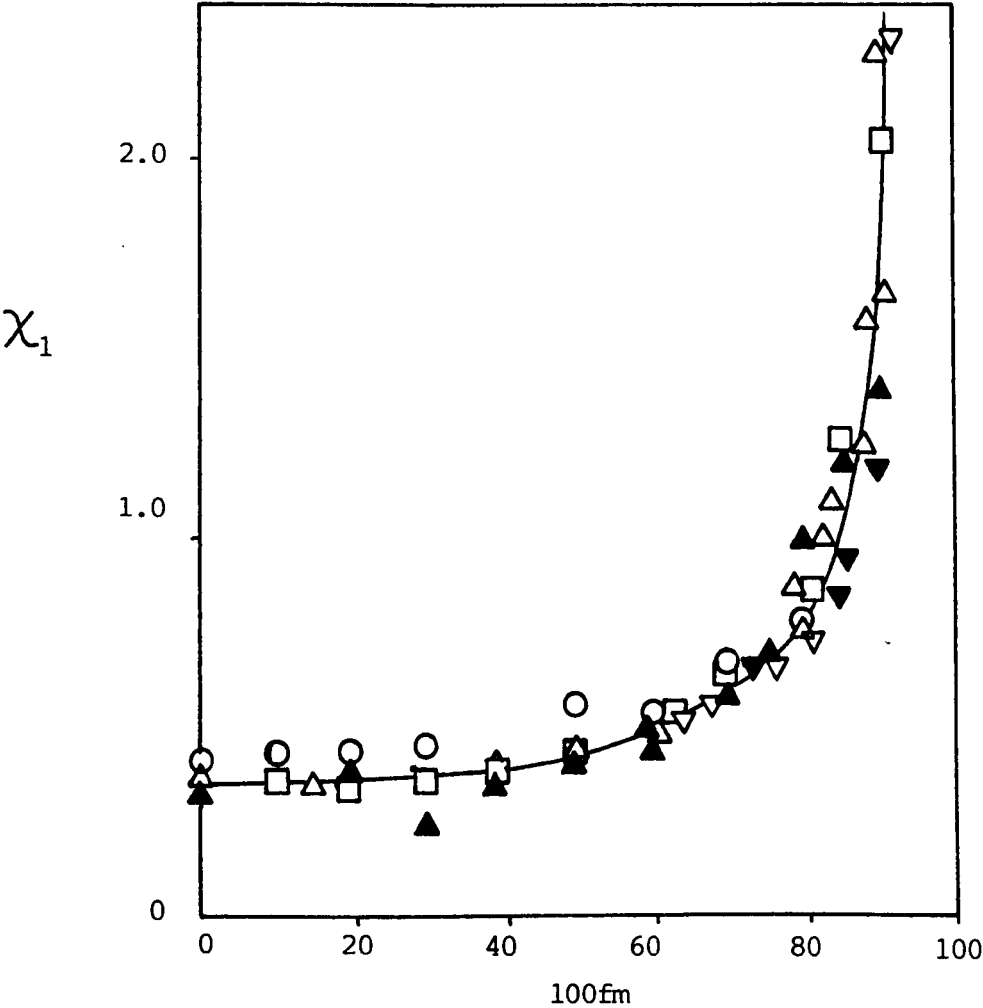
Fig. 5-11: Maximum Value of  $P_{II}$   
vs. Composition of Swelling Mixture

where  $\bar{V}_{\text{MMA}}$  and  $\bar{V}_{\text{EA}}$  are the specific volumes of MMA and ethyl acetate respectively,  $f$  is the weight fraction of MMA in the mixture of MMA + ethyl acetate (EA). In these calculations,  $\rho_H$  replaces  $\rho_{\text{MMA}}$  in equations 5-34 and 5-35.  $M_m$  in equation 5-28 was replaced by the weighted average of the relative molecular masses of ethyl acetate and MMA. If the properties of ethyl acetate and MMA are  $f_A$  and  $f_B$  respectively, where  $f_A + f_B = 1$ , then  $M_m$  was taken as  $f_A m_A + f_B m_B$ , where  $m_A$  and  $m_B$  are the molecular weights of ethyl acetate and MMA respectively.

Fig. 5-12 shows values of  $\chi_1$  calculated from equation 5-28b for the 95/5/0.4 molar HEMA/MAA/EGDMA copolymers and the DMF-MMA-ethyl acetate mixtures. Fig. 5-12 illustrates the similarity of ethyl acetate and MMA as swelling agents for this polymer network. The value of  $\chi_1$  at a particular  $f_m$  value is not dependent on the ratio of ethyl acetate to MMA.  $\chi_1$  is approximately constant at low  $f_m$ ; at values of  $f_m$  higher than 0.4,  $\chi_1$  increases with increasing  $f_m$ . This trend reflects the decreasing polarity of the swelling mixture as  $f_m$  increases.



Fig. 5-12: Calculated Values of the Floyr-Huggins Interaction  
Parameter vs. Swelling Mixture for Swelling of 95/5  
HEMA/MAA Gels in DMF/MMA/EtOAc Mixtures



KEY:

- |                 |                 |
|-----------------|-----------------|
| ○ EtOAc         | ▽ 1:4 MMA/EtOAc |
| ● MMA           | ▼ 4:1 MMA/EtOAc |
| △ 1:3 MMA/EtOAc | □ 1:1 MMA/EtOAc |
| ▲ 3:1 MMA/EtOAc |                 |

## 5.8 MORE SYSTEMATIC STUDY OF IPN HYDROGELS

### 5.8.1 First Series : IPN Hydrogels of Poly(HEMA-MAA) with PMMA

Two main problems were encountered with the preparation of these materials:

- (i) mould growth was found in several of the hydrogels (Section 3.3.8.1)
  - this problem was overcome by the procedure described in Section 3.3.8.1;
- (ii) some of the hydrogels showed visual non-uniformity. Although the modifications to the synthesis procedure such as pre-swelling and surrounding samples with oil reduced the occurrence of non-uniform hydrogels, this problem was not completely overcome.

Fig. 5-13 shows tensile strength as a function of composition for uniform materials. Table 5-8 shows the equilibrium water contents at pH 8.5 for some of the IPNs. Two observations on Fig. 5-13 may be made:

- (i) The tensile strength at a given composition is not dependent on the EGDMA content of polymer II. It is possible that the crosslink density is largely due to polymer-polymer interactions and entanglements. Therefore adding EGDMA makes little difference to the overall crosslink density.
- (ii) A sharp increase in tensile strength with increasing  $P_{II}$  occurs at  $P_{II} = 0.35$ . A possible explanation for this phenomenon is that when  $P_{II} > 0.35$ , phase separation is present, whereas when  $P_{II} < 0.35$ , it is not. Phase separation results in reinforcement similar to that observed in many filled rubbers, the rigid PMMA-rich domains acting as filler particles. An argument against this hypothesis is that all the materials show translucence, which may indicate phase separation to some degree in all the materials. However, a mechanism may exist whereby the degree of phase

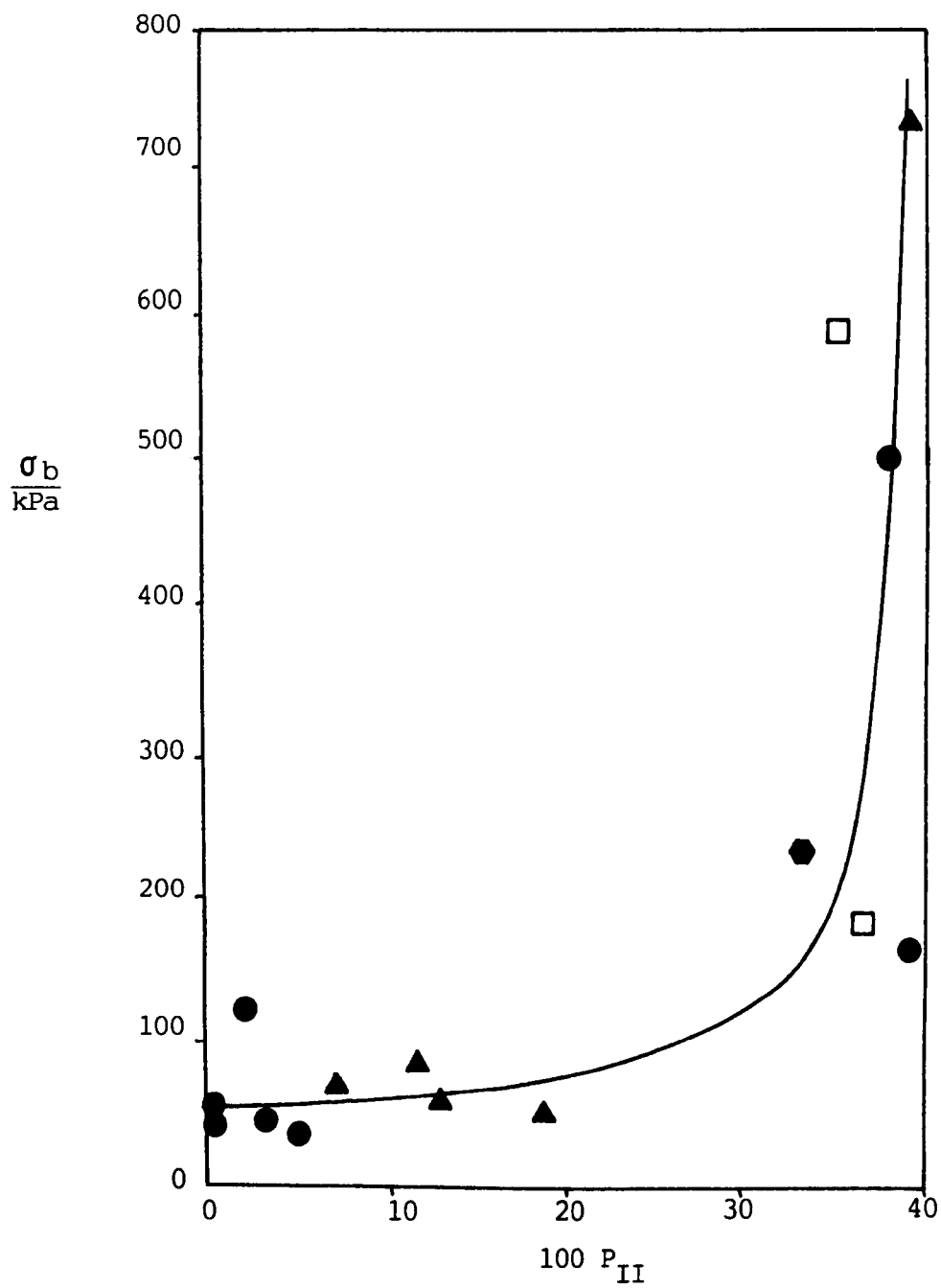


Fig. 5-13: Tensile Strength vs. Composition for IPN Hydrogels

KEY:

- ▲ 0% EGDMA in polymer II
- ⬢ 0.5% EGDMA in polymer II
- 2% EGDMA in polymer II
- 5% EGDMA in polymer II

separation sharply increases above  $P_{II} = 0.30$ .

Table 5-8: Equilibrium Water Contents of Various Poly(HEMA-MAA)/  
PMMA IPNs

material	swelling mixture		EWC %	$P_{II}$ % w/w
	w/w ratio EtOAc:MMA	w/w % DMF      EGDMA		
IPN 59	0:1	30      0	73.3	33.3
60	0:1	30      0	71.6	35.1
61	0:1	30      0	73.2	31.0
62	0:1	30      0	72.4	36.6
63	0:1	30      0	72.2	39.0
64	0:1	30      0	61.1	17.9
65	0:1	30      0	80.1	7.6
67	0:1	30      0.5	67.1	33.0
75	1:4	34      2.0	64.0	36.2
76	1:4	34      2.0	66.5	35.3
77	1:4	34      2.0	54.5	35.9

Fig. 5-13 shows that a wide range of tensile strengths was observed over a small range of water contents. The following conclusions may be drawn:

- (i) if the tensile strength is used as an indication of the quality of the materials which have been produced, then the implication is that irreproducibility is occurring in the preparation procedure. The wide range of tensile strengths, as a function of water content, show no apparent trend. In some cases, only one tensile strength

measurement could be made, because of the small quantity of material available.

- (ii) the water contents are very high, considering the proportion of hydrophobic material which the IPNs contain. Most of the IPNs contain more than 30% PMMA, and yet their water contents are only a few percent below that of the 95/5 molar HEMA/MAA copolymer hydrogel. This observation, if corroborated by subsequent work, might imply that, using this type of material, increased strength may be achieved whilst retaining a high equilibrium water content.

At this stage of the work, no further conclusions with regard to the tensile strength as a function of water content could be drawn, until (a) the synthesis procedure was improved; (b) the quantity of material available was increased.

In order to evaluate both the reproducibility of the preceding experiments, and the extent of polymerisation of monomer II, several sets of IPNs were prepared, the materials in each set being prepared in an identical manner. Table 5-9 gives the results for  $P_{II}$ , and Table 5-10 shows the percentage conversions of monomer II to polymer II for the same materials, calculated as

$$c = \frac{P_{II}}{P_{II \text{ max}}} \times 100 \quad \dots(5-37)$$

where  $c$  is the conversion, expressed as a percentage, and  $P_{II \text{ max}}$ , the weight fraction of polymer II at 100% conversion, is found for the particular swelling mixture concerned, from Figs. 5-10a to 5-10h.

Table 5-9: Reproducibility of Procedure for Synthesis of IPN Hydrogels

materials	swelling mixture			$P_{II}/w/w\%$
	w/w ratio	w/w %		
	EtOAc:MMA	DMF	EGDMA	
IPN59-65	0:1	30	0	33.3, 35.1, 31.0, 36.6, 39.0, 17.9*, 7.6*
IPN71-74	1:4	34	0	38.7, 49.6, 44.0, 32.5
IPN75-77	1:4	34	2.0	36.2, 35.3, 35.9
IPN82-86	3:1	30	0	18.6, 14.4, 11.7, 13.5, 24.9
IPN87-88	3:1	30	5.0	5.7, 3.7, 2.5, 7.3, 0.0

NOTES

1. Polymer II in IPNs 75-77 contained 2.0 w/w%EGDMA, and in IPNs 87-92 contained 5.0%EGDMA; all other materials contained 0% EGDMA.
2. IPNs 72(49.6%PMMA) and 74(32.5%PMMA) were prepared using method 2 (Section 3.3.8.1).
3. IPNs marked \* were not immersed in the swelling mixture for sufficient time to allow equilibrium swelling to be reached.

Table 5-10: Percentage Conversions from Data of Table 5-9

materials	c/%
IPN59-65	50.0, 51.6, 45.6, 53.8, 57.4, 26.3, 11.2
IPN71-74	66.7, 85.5, 75.9, 56.0
IPN75-77	62.4, 60.0, 61.9
IPN82-86	66.4, 51.4, 41.8, 48.2, 88.9
IPN87-88 ) ) 90-92 )	20.4, 13.2, 8.9, 26.1, 0

As Table 5-9 shows, the reproducibility for these experiments was generally poor. For example,  $P_{II}$  for IPNs 59-65 varied from 0.310 to 0.390 about a mean of 0.423, a variation of approximately  $\pm 12\%$ .  $P_{II}$  for IPNs 82-86 varied from 0.117 to 0.249 about a mean of 0.593, a variation of approximately  $+73\%$  and  $-19\%$ . It is possible that the position of the gel strips in relation to the UV lamp whilst undergoing polymerisation of monomer II, was partly responsible. However, in these sets of experiments, the polymerisation for each material was carried out separately, the samples being in an identical position during each experiment. In addition, there is no evidence that the displacement of a sample by a few millimetres caused significant variation in incident UV light intensity at the sample. The central part of the light beam was always directed on to the gel strip.

However, the experimental data show that it is possible to control the compositions of the IPNs by varying the ratio ethyl acetate to MMA. A series of materials has been produced, with compositions ranging from zero to 49.6% PMMA. The uniformity of the materials was not good however. It was thought that, with further modifications to the experimental procedure, this might be improved in subsequent work. Table 5-9 also shows, from the error made in giving two of the samples insufficient time for equilibrium swelling in the monomer II mixture, that the composition of the IPN can also be controlled in this way.

The compositions of the materials in the first three series shown in Table 5-9 were similar, although two different swelling mixtures were used. This suggests that a limiting value of  $P_{II}$  exists, higher values than which cannot be achieved. It is possible that the opacity of the materials increases with the degree of conversion, and therefore

the incident intensity of the light at the sample decreases with time, curtailing the reaction. This hypothesis is rejected for two reasons:

- (i) On removal of the samples from the mould after polymerisation, opacity was not observed. Clouding of the gel strips occurred only when swollen in aqueous media.
- (ii) If the hypothesis is correct, a gradient of composition between the front face of the sample and the back face would result. This was not observed.

The hypothesis that a limiting level of  $P_{II}$  exists requires further experimental work to examine its validity.

Table 5-10 shows that the conversions of monomer II to polymer II were low. The decrease in conversion from the first to the final series is a consequence of the decrease in monomer concentration, since the polymerisation times were identical (6 hours). Therefore in subsequent experiments it would be advantageous to increase the polymerisation time. However, times above 10 hours would necessitate further modification of the apparatus, since the consequent rise in temperature of the water-bath would be unacceptable.

The conversions in the last series in Table 5-10 are particularly low. It is possible that this is a consequence of the presence of 5% EGDMA in the monomer II mixture. This is thought unlikely, however, since IPNs 75-77, where polymer II contained 2% EGDMA, did not show a similar reduction in conversion.

The materials prepared using method 2 (Section 3.3.8.1), in which the mould was slightly modified, showed slight visual non-uniformity, i.e. differences in opacity throughout the IPN when swollen in aqueous



media. This was caused by wrinkling of the polypropylene sheet which covered the face of the gel (see Fig. 3-9 in Section 3.3.8.1). This modification was therefore not adopted, and method 1 was used for all further IPN preparations.

#### 5.8.2 Second Series: IPN Hydrogels of Poly(HEMA-MAA) with Various Polymers and Copolymers

It was intended that the degree of hydrophobicity of polymer II should be varied, so that the effects on the properties of the IPNs might be studied. All the IPNs which were produced were translucent or opaque when swollen in water (pH8.5). In general, as the polymer II content increased for a given polymer II, the opacity of the IPNs increased. However, the degree of opacity was also dependent on the hydrophobicity of polymer II. For example, a hydrogel containing 60.6% of a 70/30 molar HEMA/MAA(HEMA:MAA = 95:5 molar) copolymer was much more opaque than a hydrogel containing 75.6% of a 95/5 molar HEMA/MAA copolymer. It is thought that the hydrophobic nature of polymer II in the former case results in larger phase domains.

An interesting observation is that the homo-IPNs, where polymer II is identical to polymer I, show translucence. This indicates a degree of immiscibility which results in phase separation, which was unexpected for identical materials. However, two points are noted which might, in part, account for these observations:

- (i) The average molecular weights of the two polymers were different, since different initiators and methods of polymerisation were used.
- (ii) Polymer I is likely to exist in a condition where the average end-to-end displacements of the polymer molecules are greater

than those of polymer II. This situation arises because, at the time of polymerisation of polymer II, the polymer I molecules are extended as a result of swelling in the swelling mixture. The weight percentage of solvent in the mixture during polymerisation of polymer I was approximately 50%, while that of the swelling mixture during polymerisation of polymer II was approximately 70%.

Table 5-11 shows the IPN compositions which were obtained, using the numbering system of Section 3.3.8.2.

Table 5-11: Compositions of Hydrogel IPNs

materials	swelling mixture			polymer II	P <sub>II</sub> /mol %
	mol % monomer II	w/w %			
		SAM	DMF		
IPN99-104 <sup>a</sup>	MMA	0	30	PMMA	37.6, 34.2, 37.7, 41.4, 37.8, 39.0
105-107 <sup>a</sup>	S	0	30	PS	translucent while swelling
108-109 <sup>a</sup>	S	0	40	PS	broke up while swelling
110-112 <sup>a</sup>	50MMA/50 MAA	0	30	poly(50 MMA/50 MAA)	49.2, 33.8,38.5
113-114 <sup>a</sup>	70MMA/30 MAA	0	30	poly (70 MMA/30 MAA)	36.6, 29.6
115-120 <sup>a</sup>	95HEMA/ 5MAA	0	10	poly(95 HEMA/5 MAA)	74.6, 75.1, 75.6, 77.5, 77.3, 77.8
121-123 <sup>a</sup>	50MMA/ 50HEMA-MAA*	0	10	poly(50 MMA/50 HEMA-MAA)	2.8, 2.8, 5.7
124-127 <sup>a</sup>	50MMA/50 HEMA-MAA*	0	17	poly50 MMA/50 HEMAMAA)	42.3, 58.3, 58.7, 62.5

materials	swelling mixture			polymer II	P <sub>II</sub> /mol %
	mol % monomer II	w/w %			
		SAM	DMF		
IPN128-131 <sup>b</sup>	95HEMA/ 5MAA	0	10	poly(95 HEMA/5 MAA)	68.0, 76.4, 72.9, 72.2
132-135 <sup>a</sup>	70MMA/30 HEMA-MAA*	0	20	poly(70 MMA/30 HEMA-MAA)	60.1, 58.7, 59.2, 60.6
136-139 <sup>a</sup>	5 195HEMA- MAA*	0	10	poly(5 S/ 95HEMA-MAA)	77.7, 69.3, 69.7, 64.2
140-143 <sup>a</sup>	50MMA/50 HEMA-MAA*	50	17	poly(50MMA/ 50HEMA-MAA)	20.2, 44.6, 21.2
144-147 <sup>a</sup>	50MMA/50 HEMA-MAA*	80	17	poly(50 MMA/50HEMA- MAA)	11.6, 13.2, 12.9, 13.5
148-151 <sup>a</sup>	95HEMA/ 5MAA	50	10	poly(95 HEMA/5MAA)	64.9, 64.7, 53.8, 56.5
152-155 <sup>a</sup>	95HEMA/ 5MAA	20	10	poly(95HEMA/ 5MAA)	76.3, 75.6, 76.4, 73.8
156-159 <sup>a</sup>	70MMA/ 30HEMA-MAA*	20	25	poly(70 MMA/30 HEMA-MAA)	43.0, 38.3, 42.8, 39.3
160-162 <sup>a</sup>	70MMA/30 HEMA-MAA	50	25	poly(70 MMA/30HEMA- MAA)	23.1, 45.7, 32.7

NB

PS = polystyrene

S = styrene

\* denotes a HEMA/MAA ratio of 95mol:5mol

a denotes 0% EGDMA in polymer II

b denotes 0.4mol%EGDMA in polymer II

The reproducibility of the above experiments was poor, although better than for the experiments reported in Section 5.8.1. The best reproducibility occurred for IPNs 115-120 (mean value  $P_{II} = 76.3\%$ , deviation  $\pm 2\%$  of this value), IPNs 152-155 (mean  $P_{II} = 75.5\%$ , deviation  $\pm 3\%$  of this value) and IPNs 156-159 (mean  $P_{II} = 40.9\%$ , deviation  $\pm 9\%$  of this value). The causes of the non-reproducibility are unknown, since each set of IPNs was prepared under identical conditions.

In Section 5.8.1, the results of a detailed study of the swelling of polymer I networks in monomer mixtures containing MMA are reported. However, it was not possible to carry out a similar investigation for the monomer mixtures used for the experiments described in this section, because of the number of different copolymers used for polymer II. Therefore estimates were made of the DMF content required in the swelling mixture. This is dependent on the hydrophilicity of the other components of the mixture. Where saturated analogues of the monomer were used, they were assumed to have the same effect on the swelling of polymer network I as the monomer itself. Table 5-11 shows that, for IPNs 105-107, where the DMF content of the swelling mixture was 30% w/w, the samples became translucent while swelling. The monomer mixture was excessively hydrophobic and phase separation occurred within the gel, although the mixture was not so hydrophobic as to prevent swelling. Increasing the DMF content in an attempt to overcome this problem increased both the swelling and the rate of swelling, resulting in cracking of the very fragile strips of gel.

Table 5-11 shows that the use of saturated monomer analogues is an effective method of controlling the composition of the IPNs. For example, for IPNs containing a 50/50 molar MMA/(HEMA/MAA) copolymer (HEMA/MAA = 95/5 molar), increasing the saturated analogue content

from zero to 50% w/w decreased the mean value of  $P_{II}$  from 55.5 mol % to 28.7 mol %. Increasing it further to 80% w/w decreased the mean  $P_{II}$  to 12.8 mol %. For IPNs containing a 70/30 molar MMA/(HEMA/MAA) copolymer (HEMA/MAA = 95/5 molar), increasing the proportion of the saturated analogue from zero to 20% w/w decreased the mean  $P_{II}$  from 59.7 mol % to 40.9 mol %. Increasing it further to 50% w/w decreased the mean  $P_{II}$  to 33.8 mol %. However, the method was less effective in the case where polymer II was a 95/5 molar HEMA/MAA copolymer. On increasing the saturated monomer analogue content from zero to 20% w/w, the mean  $P_{II}$  changed from 72.4 mol % to 75.5 mol %. Increasing it further to 50% w/w caused a decrease in the mean  $P_{II}$  to 60.0 mol %.

Fig. 5-14 shows the equilibrium water contents of several of the IPNs as a function of composition. In general, the water contents at a given value of  $P_{II}$  reflect the hydrophobicity of polymer II. Those materials where polymer II contained 30 or 50 mol % MAA contained a higher proportion of water than the 95/5/0.4 molar HEMA/MAA/EGDMA copolymer gel. For materials where polymer II was a HEMA/MAA/MMA copolymer, the water content decreased, for a given  $P_{II}$ , as the MMA content of polymer II increased. This result was expected, since as the proportion of MMA was increased, polymer II became more hydrophobic. The proportion of MMA-rich, low water content phase domains increased, and hence the overall water content was reduced. Fig. 5-14 shows that the water contents of the homo-IPNs were lower than that of the basic polymer I network. This is thought to be the result of an increase in the effective crosslink density caused by an increase in polymer chain entanglements. Lightly crosslinking polymer II had the effect of reducing the EWC still further for a given  $P_{II}$ , possibly for the same reason.

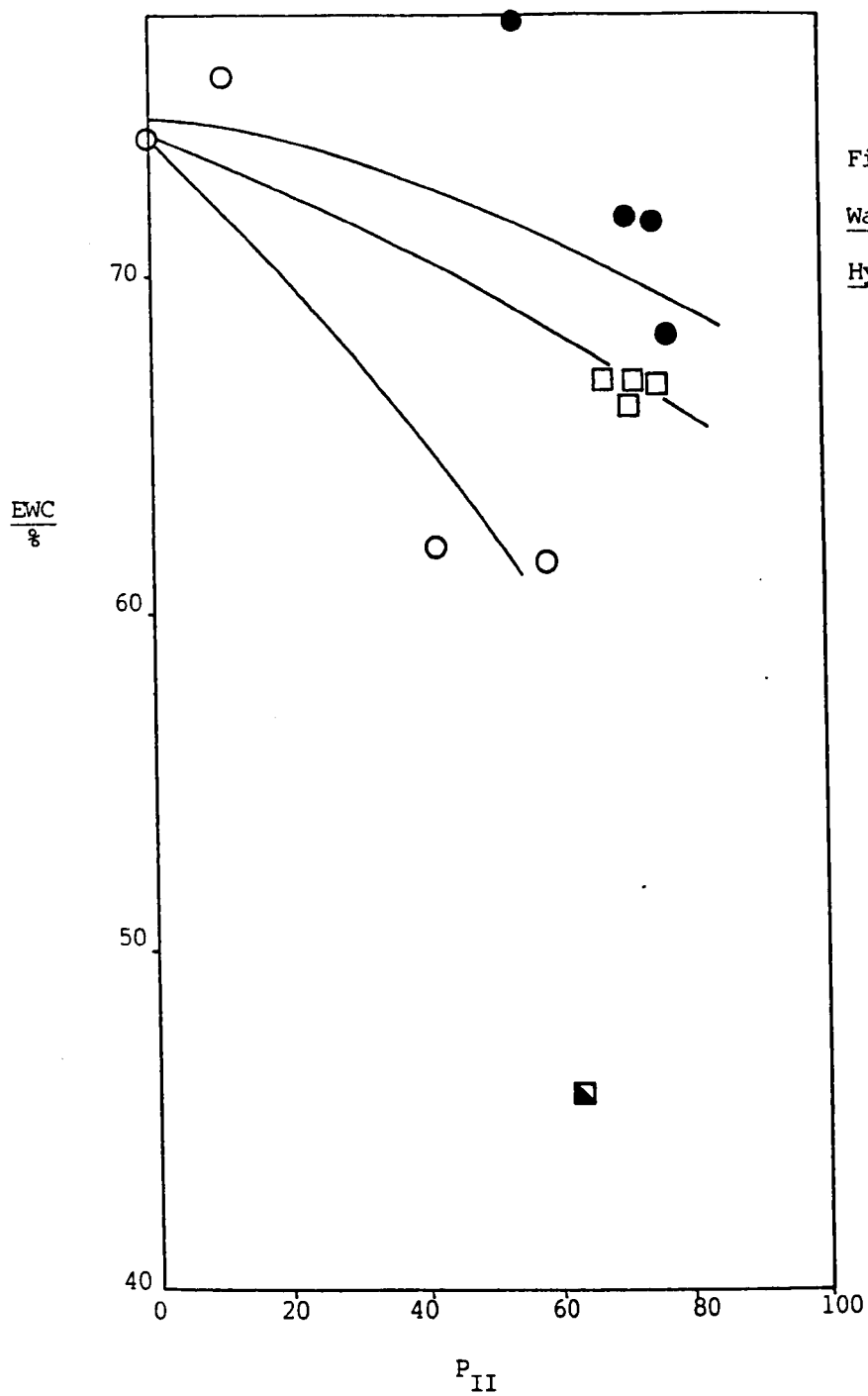


Fig. 5-14: Equilibrium  
Water Contents of IPN  
Hydrogels vs. Composition

Composition of Polymer II:

- 50 mol % MMA/50 mol % HEMA/MAA
- 95 mol % HEMA/5 mol % MAA
- 95 mol % HEMA/5 mol % MAA with 0.4% EGDMA
- 70 mol % MMA/30 mol % HEMA/MAA
- △ 70 mol % MMA/30 mol % MAA

Figs. 5-15a and 5-15b show the tensile strengths of several of the materials as a function of composition and of EWC respectively. The tensile strength at a given composition (Fig. 5-15a) increases as the hydrophobicity of polymer II increases. Hence the slope of the graph was greater for materials where polymer II was 50 mol MMA - 50 mol HEMA/MAA than for those where polymer II was 95mol HEMA - 5mol MAA. The incorporation of a small proportion of EGDMA crosslinker into polymer II had no effect on the tensile strength at a given  $P_{II}$ . These facts are consistent with the hypothesis that the tensile strength is principally a function of the volume fraction of polymer, since

- (i) as the hydrophobicity of polymer II increases, the volume fraction of polymer in the swollen material increases;
- (ii) low levels of EGDMA have little effect on the volume fraction of polymer in the swollen gel.

A more important graph is that of Fig. 5-15b, since one of the aims of this work was to prepare gels of increased strength and high water content. Fig. 5-15b shows that points for several IPNs, of various  $P_{II}$  values and polymer II compositions, fall on a common curve. The tensile strength decreases as the EWC is increased and the magnitude of the slope decreases. Therefore for these materials the EWC seems to be the major factor controlling the tensile strength. Hence it is possible to increase the tensile strength by using the IPN method, with an accompanying decrease in EWC. In Chapter 7 a comparison between the three methods of modification will be made, showing the relationship between tensile strength and water content for each method.

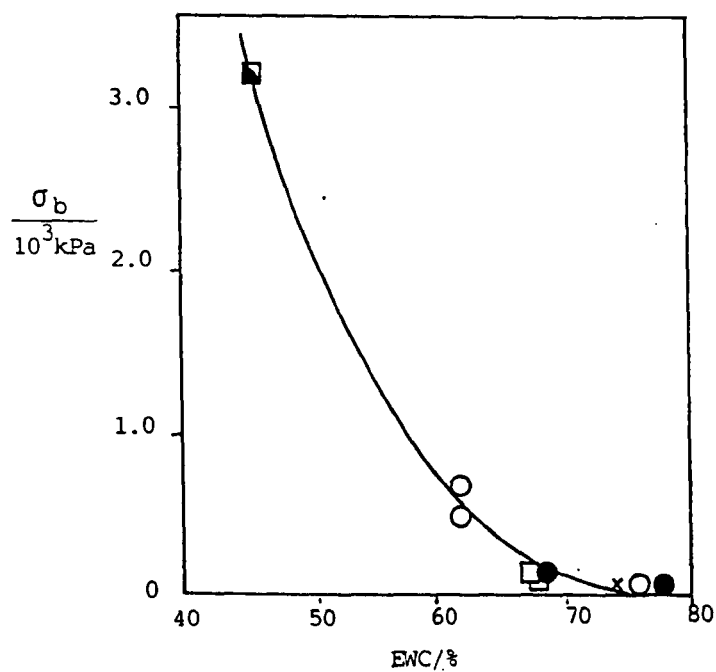
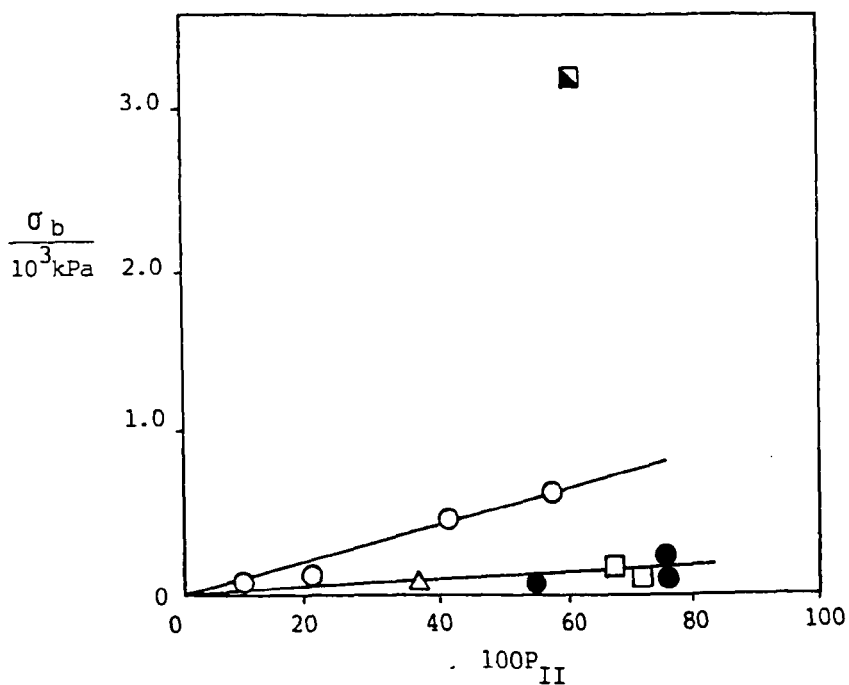
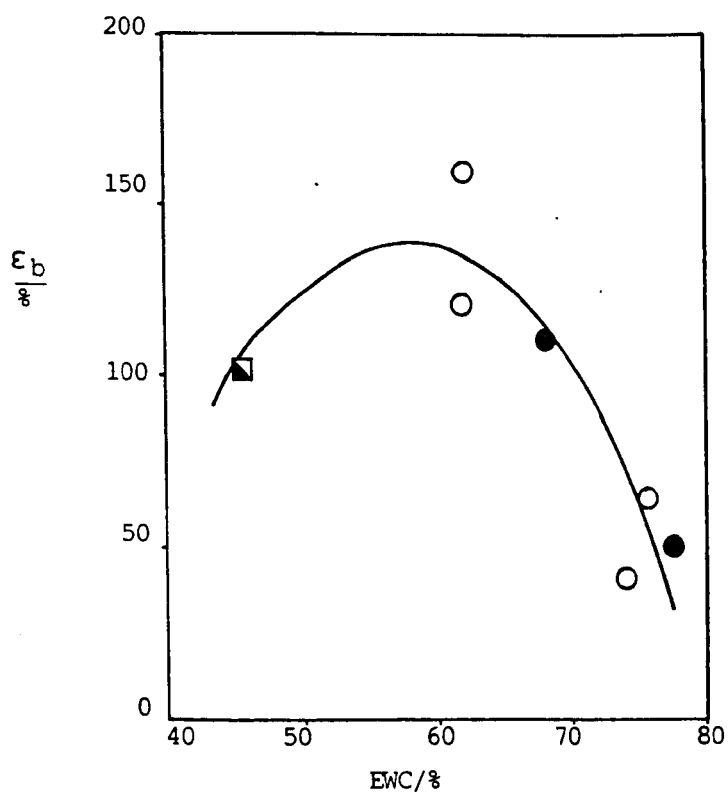
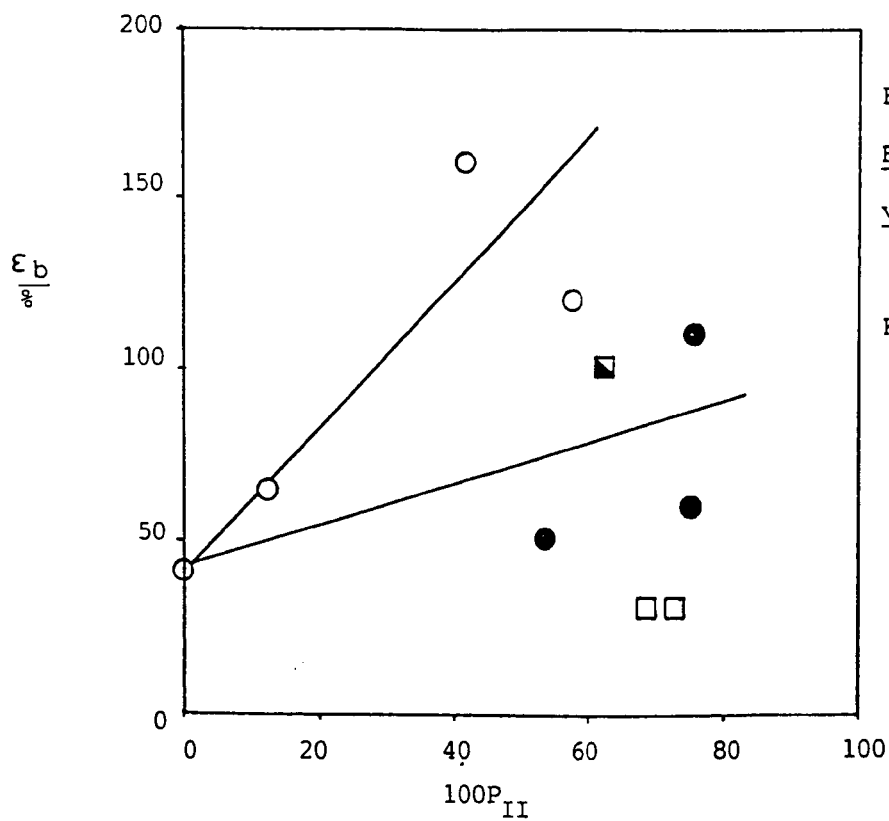




Fig. 5-16a and 5-16b show values of strain at break for several IPNs as a function of composition and of water content respectively. In Fig. 5-16a, the points are very scattered as a result of both the inherent nature of the rupture process and the imprecise method of measuring strain. In general, however, the materials where polymer II is more hydrophobic (i.e. the MMA content of polymer II is greater) have higher  $\epsilon_b$  values. The exception is IPN 135, containing 60.6 mol % of the 70/30 molar MMA/(HEMA/MAA) copolymer (HEMA/MAA = 95/5 molar). It is possible that, as the hydrophobicity of polymer II increases, the value of  $\epsilon_b$  at a given  $P_{II}$  increases to a maximum, and then decreases with increasing  $P_{II}$  at higher hydrophobicity. As the degree of hydrophobicity increases, the strain at break increases as a result of the reduced water content of the IPN. However, at higher degrees of hydrophobicity, the strain at break decreases as a result of the increasingly plastic nature of the material. In order to confirm this hypothesis, further experimental work is required.

The strain at break as a function of EWC is shown in Fig. 5-16b for several of the IPNs. The points for the IPNs where polymer II was a 95/5 HEMA/MAA copolymer, and where it was a 50/50 MMA/(HEMA/MAA) terpolymer, lie on the same curve. This confirms that, where polymer II is of low or intermediate hydrophobicity, the equilibrium water content is the factor which controls the strain at break. A maximum in  $\epsilon_b$  occurs at a value of EWC of 57%. Further investigation is necessary in order to confirm the shape of this curve. However, its general shape can be explained in the manner described above.

Figs. 5-17a to 5-17c show stress/strain, Gaussian and Mooney-Rivlin plots for various IPNs in this series. Fig. 5-17a shows the stress-



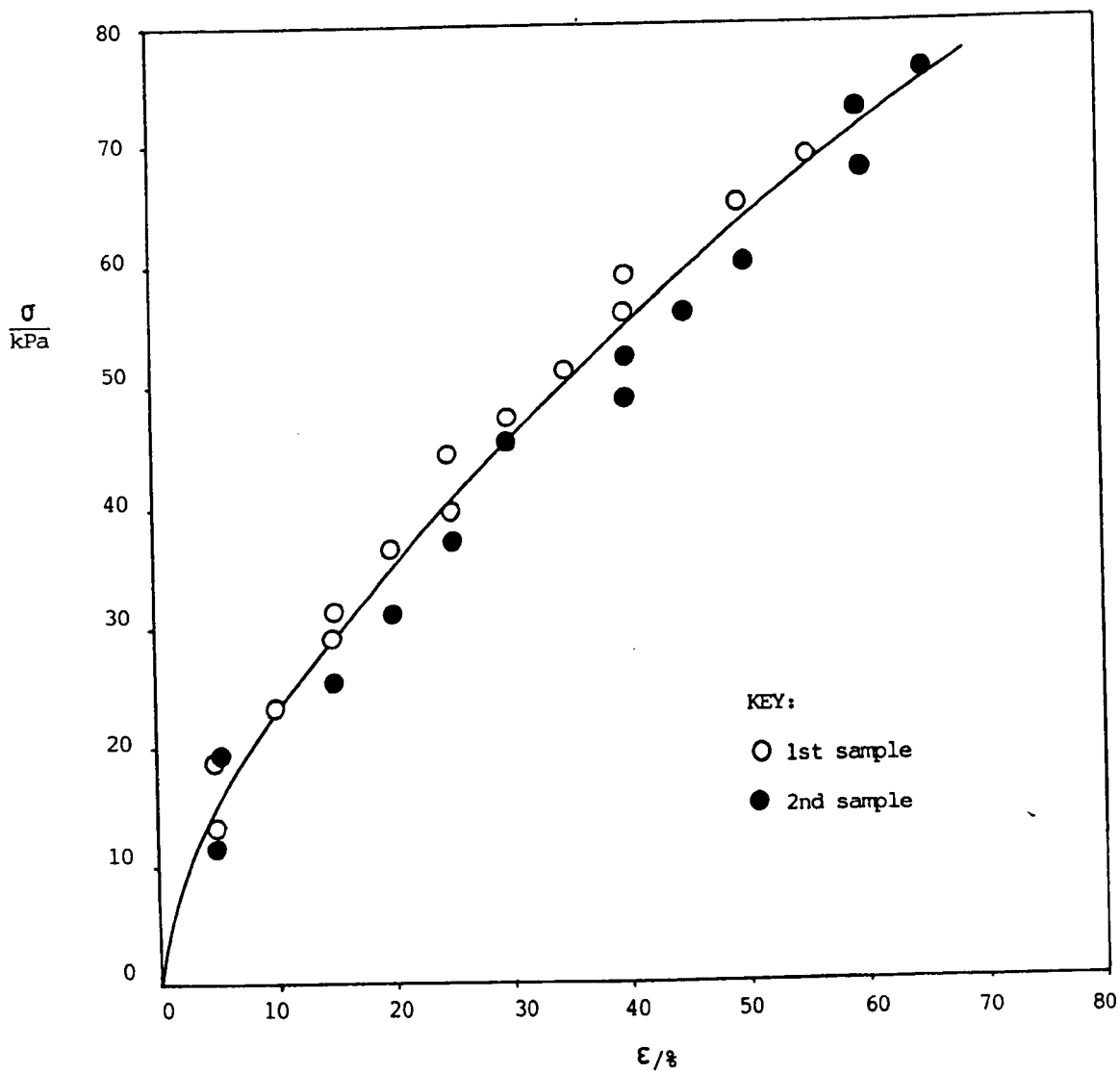


Fig. 5-17a: Stress vs. Strain for IPN 150 Hydrogel, Containing 53.8 mol % of a 95/5 HEMA/MAA Copolymer

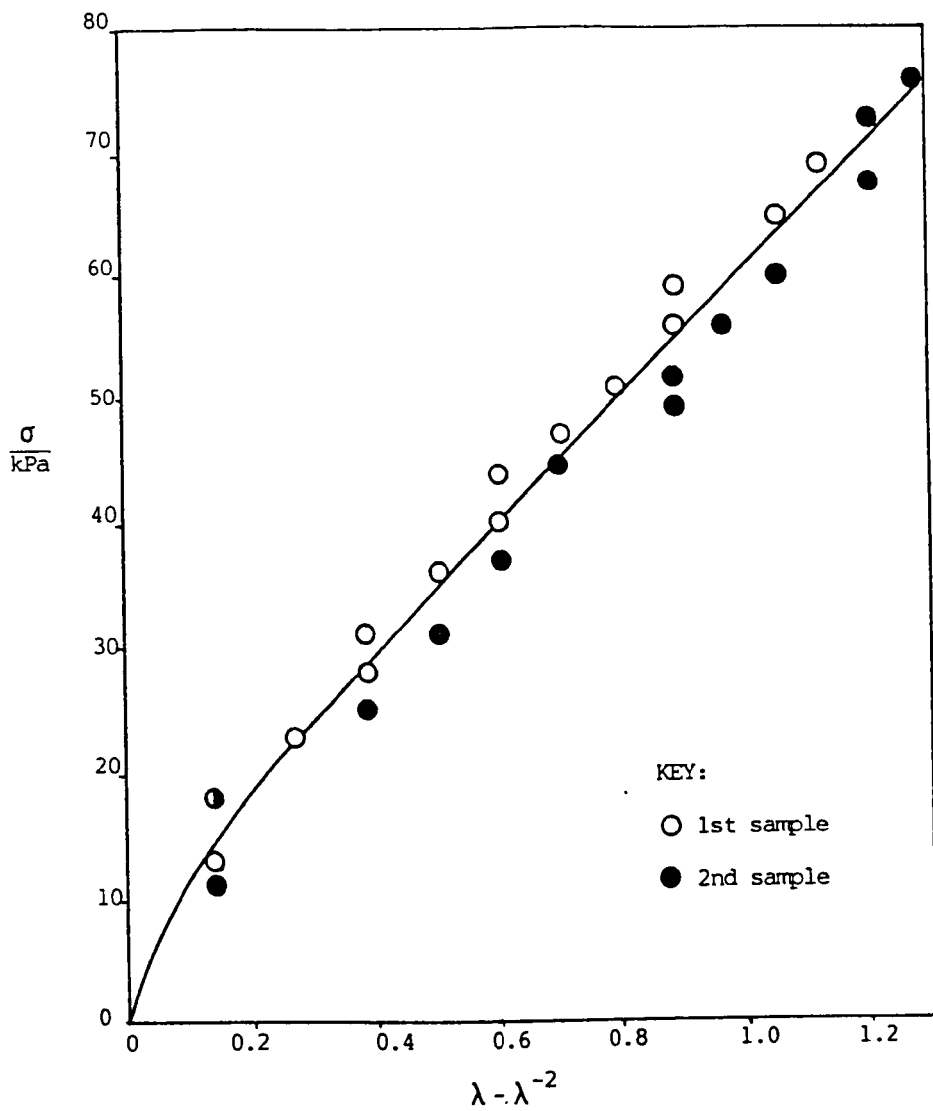


Fig. 5-17b: Gaussian Curve for IPN 150 Hydrogel

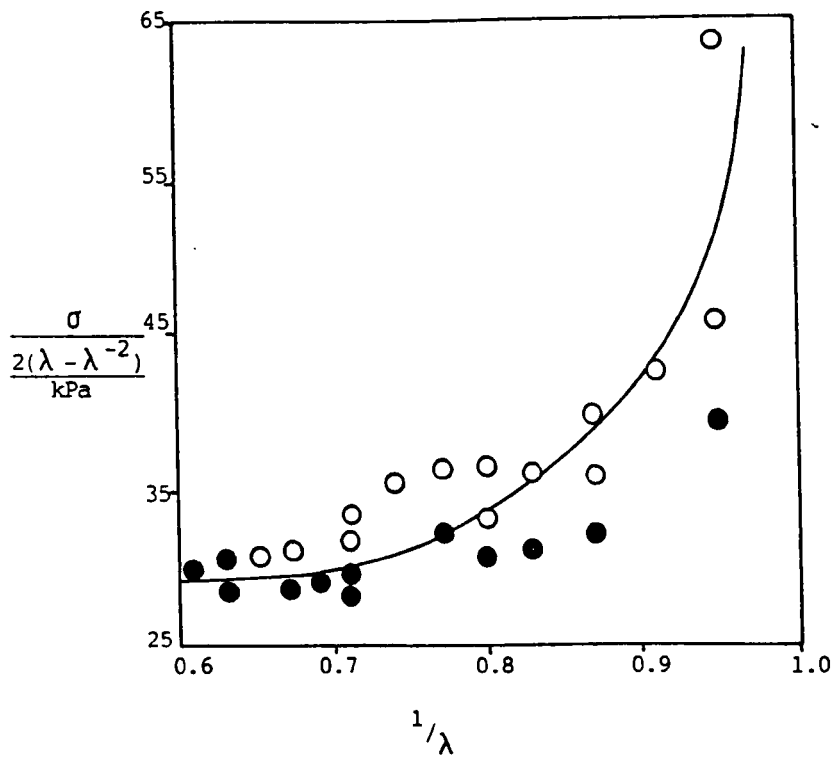


Fig. 5-17c: Mooney-Rivlin Curve for IPN 150 Hydrogel

strain curve for IPN 150. The initial modulus is 417 kPa, and the slope decreases with increasing strain. The Gaussian curve for the same material is shown in Fig. 5-17b. The shear modulus, given by the slope at zero strain, is 120 kPa. As the strain increases, the slope decreases at low strains but at values of  $\lambda - \lambda^{-2}$  higher than 0.4 the slope is approximately constant at 61 kPa. The Mooney-Rivlin curve for the same material (Fig. 5-17c) shows that, at high strains,  $\sigma/2(\lambda - \lambda^{-2})$  is approximately constant, the value being 29.5 kPa. Hence  $C_2$  is zero and  $C_1$  29.5 kPa. However, at small strains, there is a large deviation from the Mooney-Rivlin prediction. The stress-strain curve for a similar material, but containing 77.5% polymer II is shown in Fig. 5-17d. The stress increases with strain and the slope decreases as the strain increases. The initial modulus is 667 kPa. The shape of the curve is similar to that of Fig. 5-17a, although the modulus is much higher; the latter is probably a consequence of the increased concentration of polymer II. The shear modulus  $G$  for this material is also higher than that of IPN 150, at 160 kPa. The Gaussian plot (Fig. 5-17e) for this material is linear, showing no evidence of deviation from the statistical theory. The Mooney-Rivlin plot (Fig. 5-17f) shows a minimum value of  $\sigma/2(\lambda - \lambda^{-2})$  of approximately 75 kPa at  $1/\lambda = 0.64$ . However, the points are scattered, and it is possible that a linear portion exists at intermediate strains, where the slope ( $C_2$ ) is zero and the intercept on the  $\sigma/2(\lambda - \lambda^{-2})$  axis ( $C_1$ ) is 77 kPa.

Figs. 5-17g to 5-17l show data for materials where polymer II was similar to that of the above materials but contained 0.4 mol % EGDMA as the crosslinking agent. The stress-strain curve for the material containing 68.0 mol % polymer II, IPN 128, is shown in Fig. 5-17g.

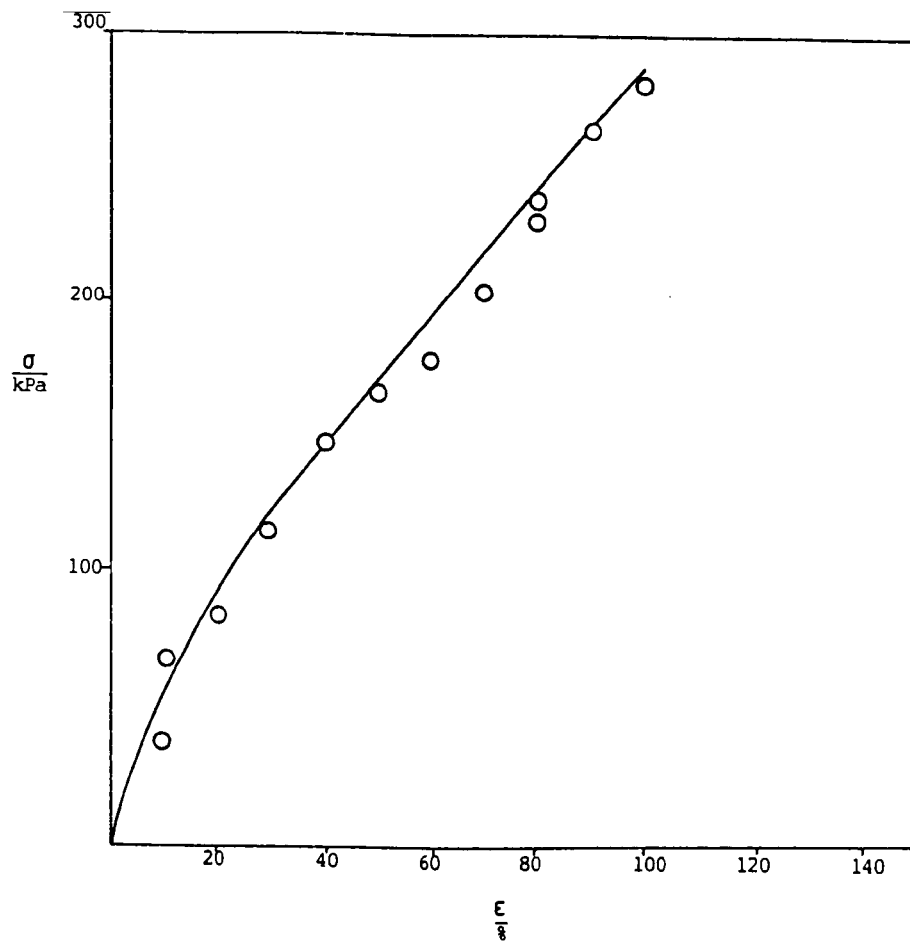


Fig. 5-17d: Stress vs. Strain for IPN 118 Hydrogel, Containing 77.5  
mol % of a 95/5 HEMA/MAA Copolymer

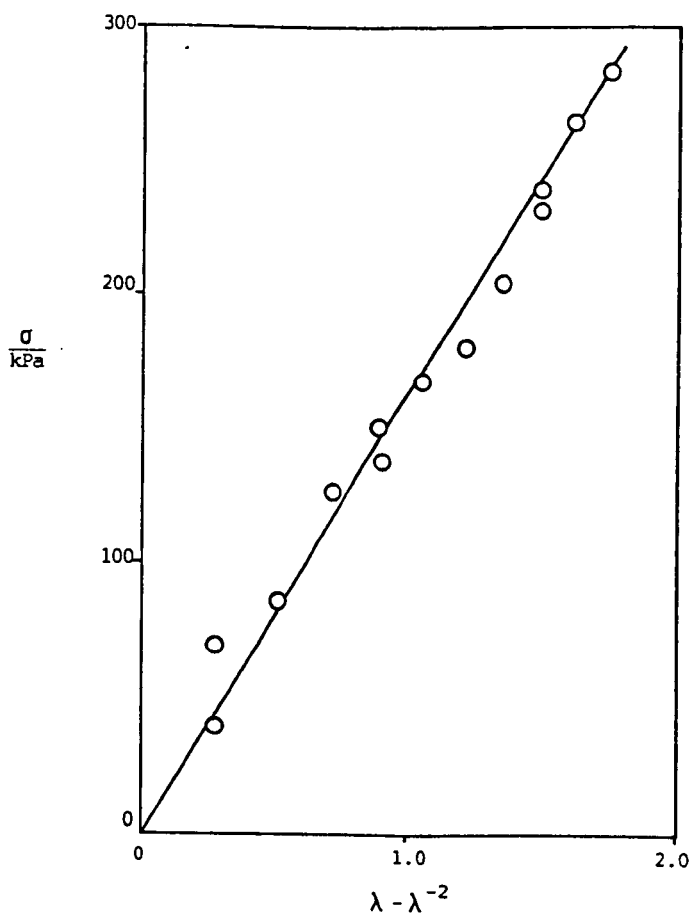


Fig. 5-17e: Gaussian Curve for IPN 118 Hydrogel

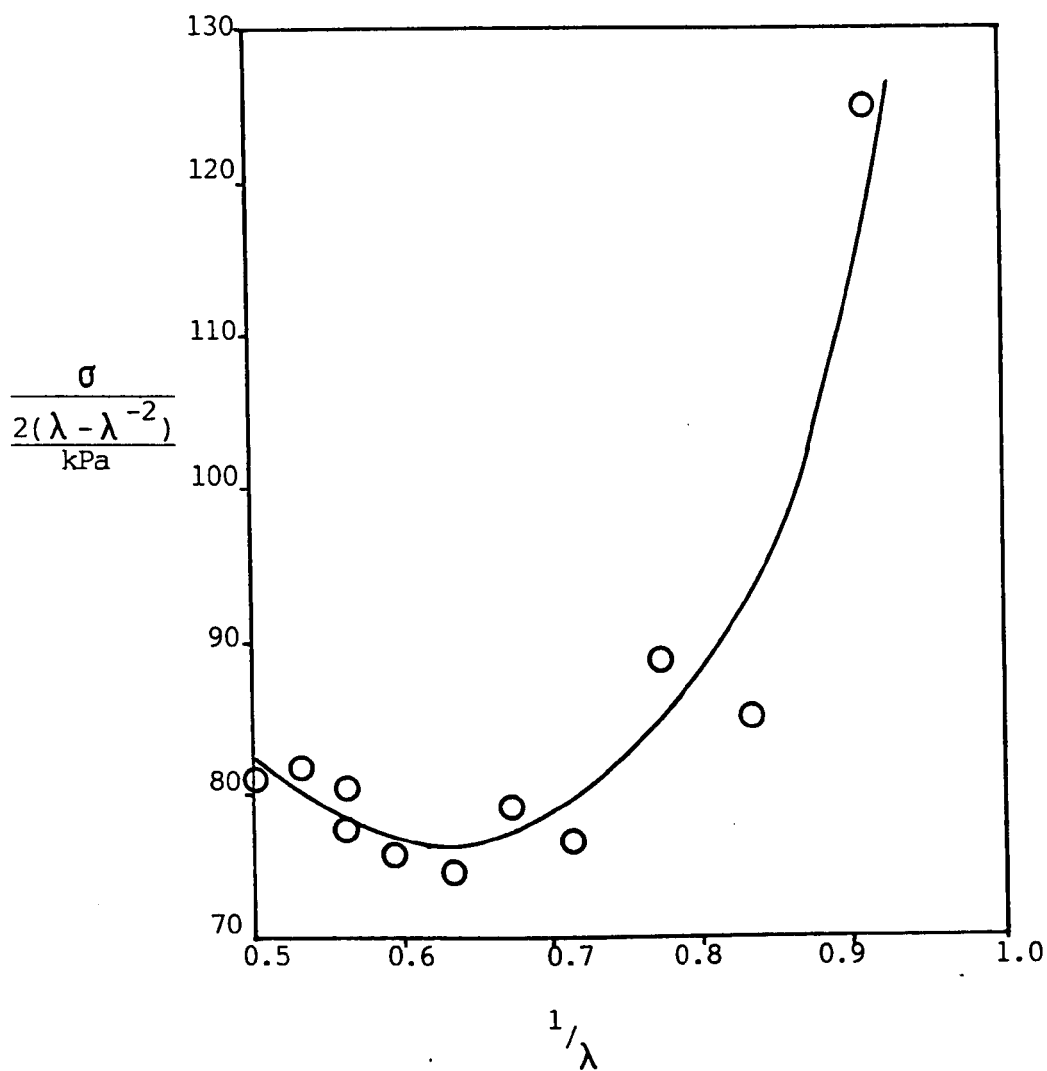
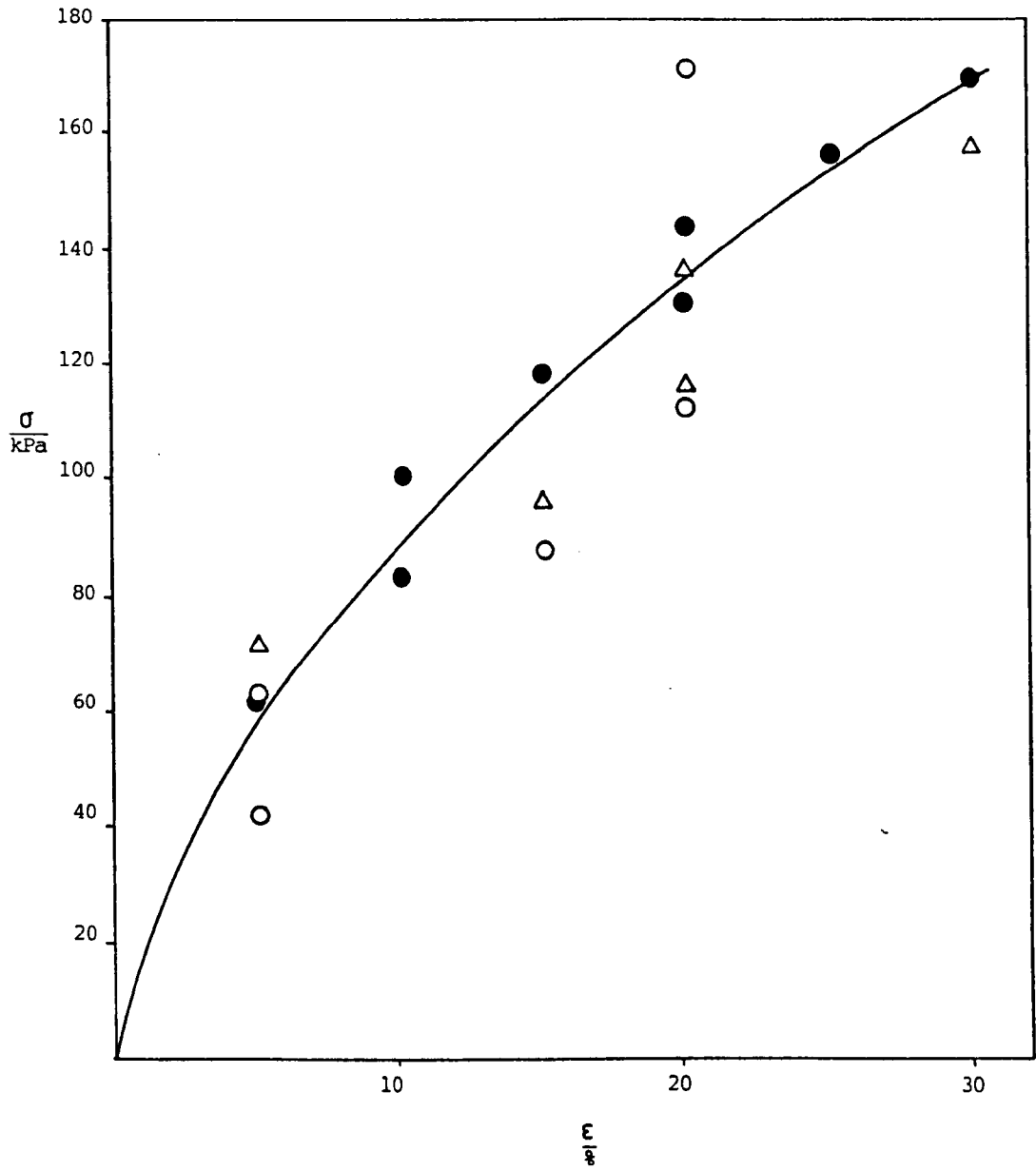


Fig. 5-17f: Mooney-Rivlin Curve for IPN 118 Hydrogel

Fig. 5-17g: Stress vs. Strain for IPN 128 Hydrogel Containing 68.0  
mol % of a 95/5/0.4 HEMA/MAA/EGDMA Copolymer





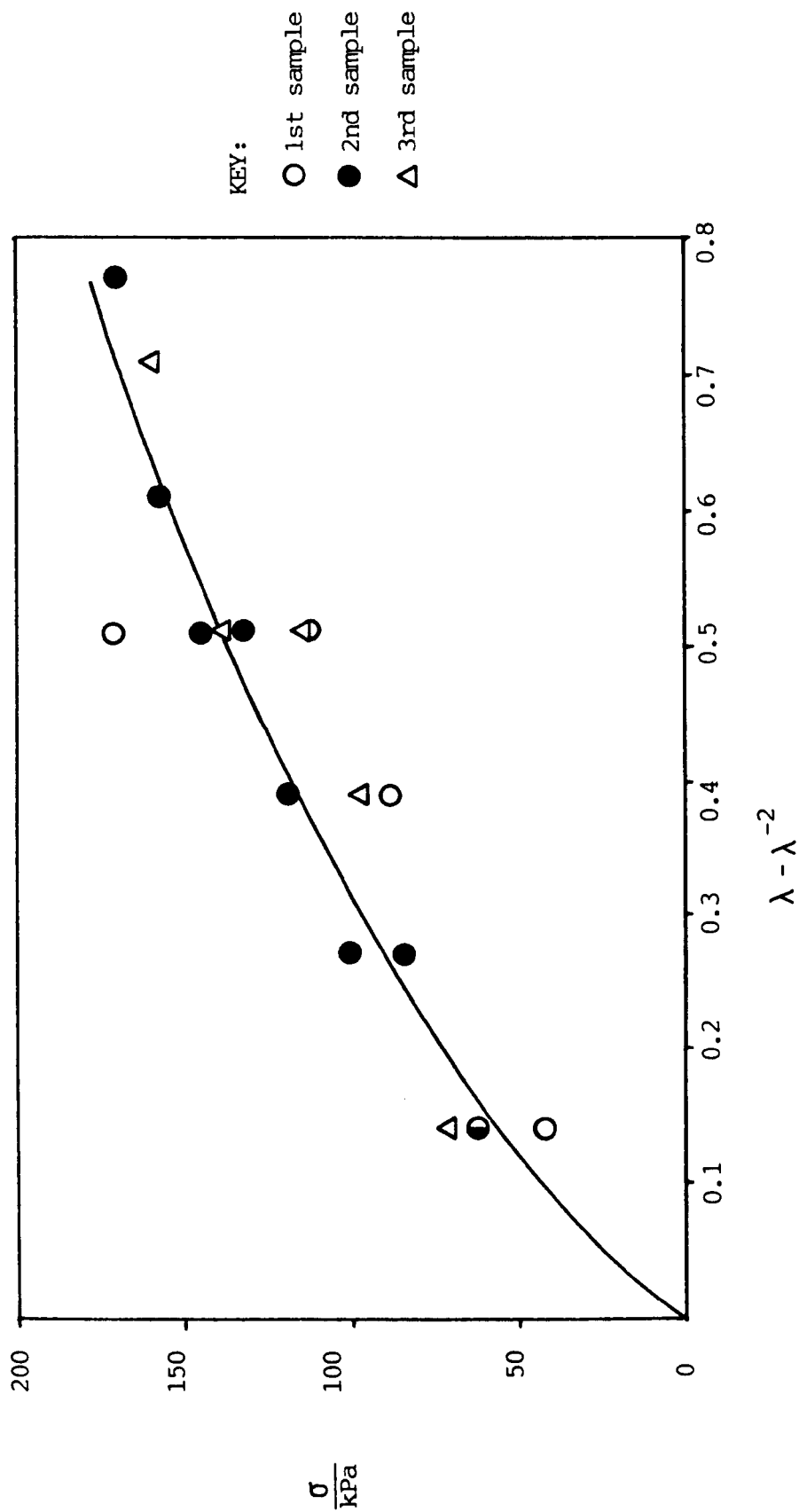


Fig. 5-17h: Gaussian Curve for IPN .128 Hydrogel

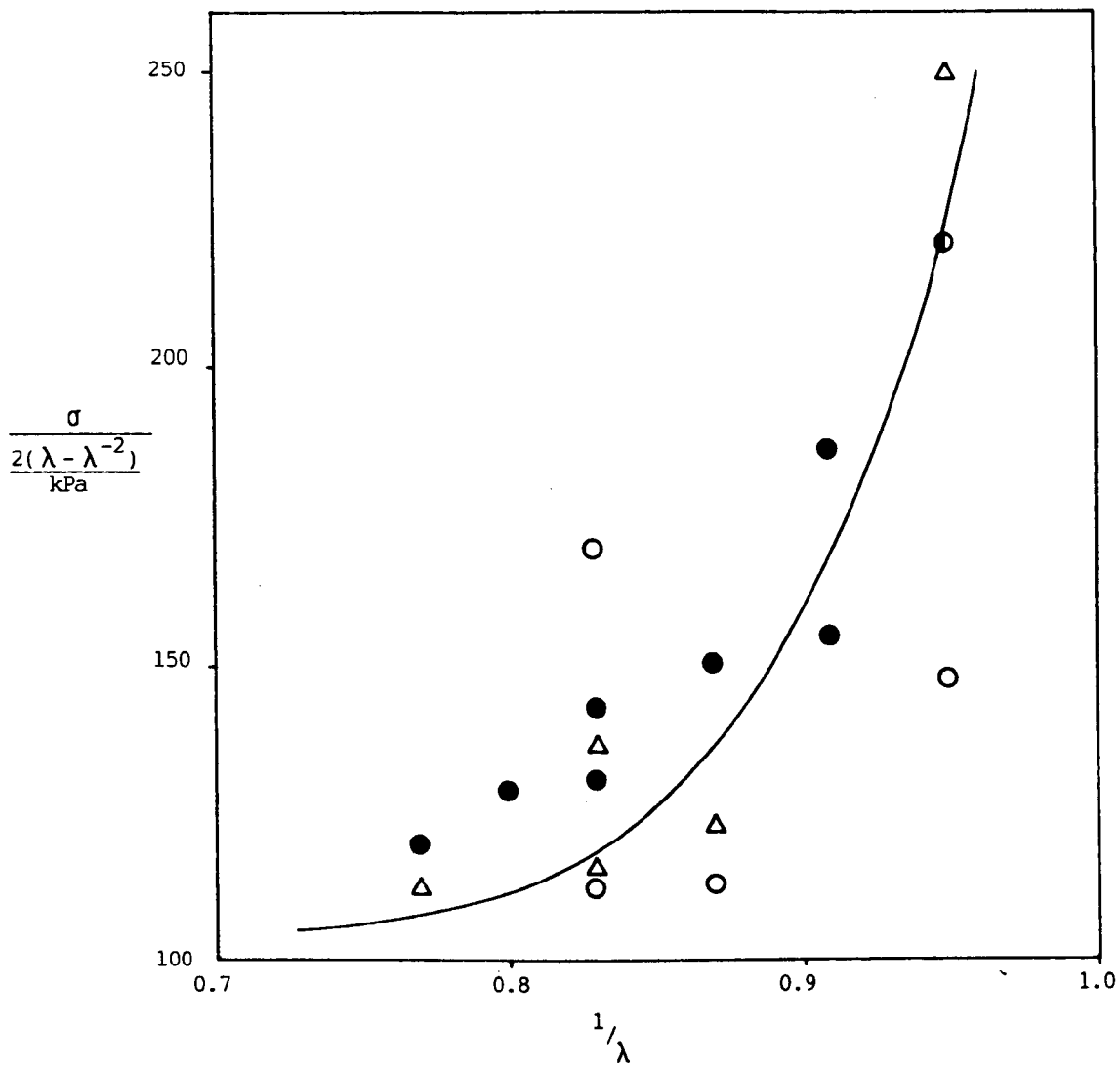


Fig. 5-17i: Mooney-Rivlin Curve for IPN 128 Hydrogel

Fig. 5-17j: Stress vs. Strain for IPN 131 Hydrogel, Containing 72.2  
mol % of a 95/5/0.4 HEMA/MAA/EGDMA Copolymer

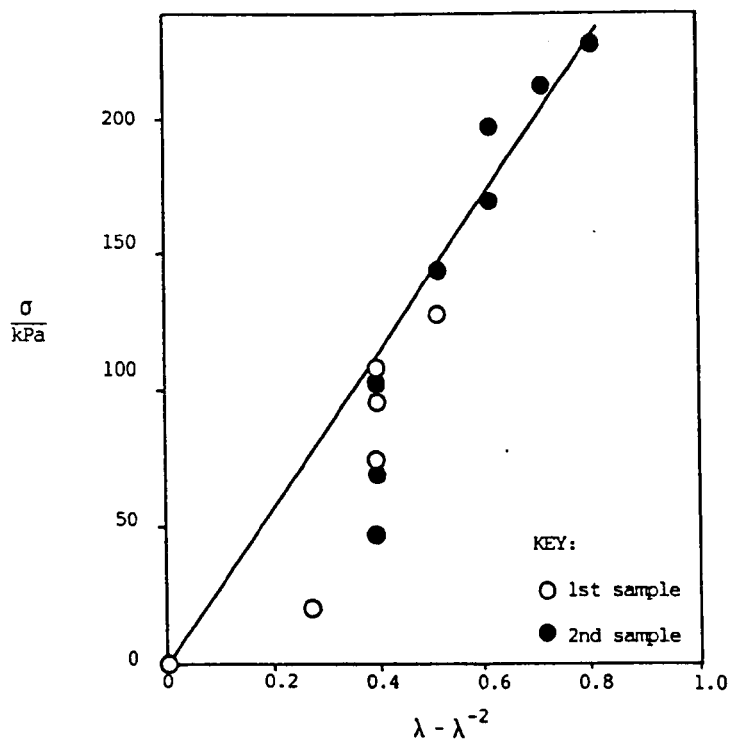
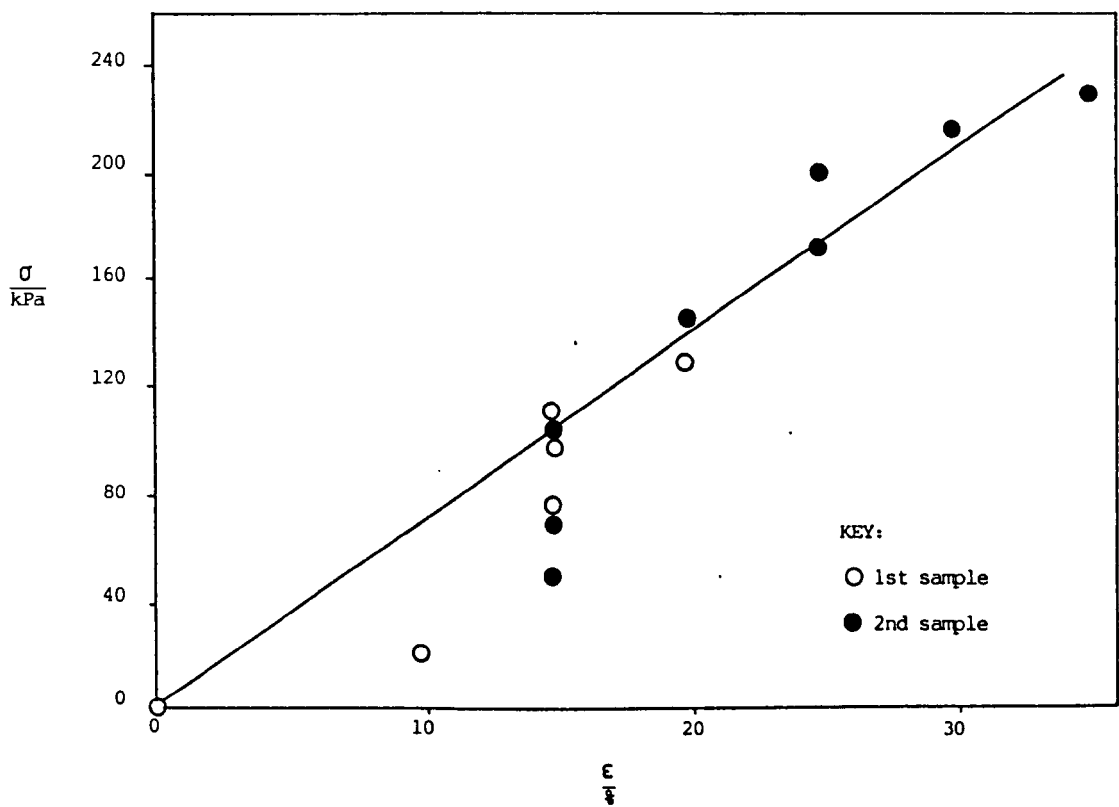
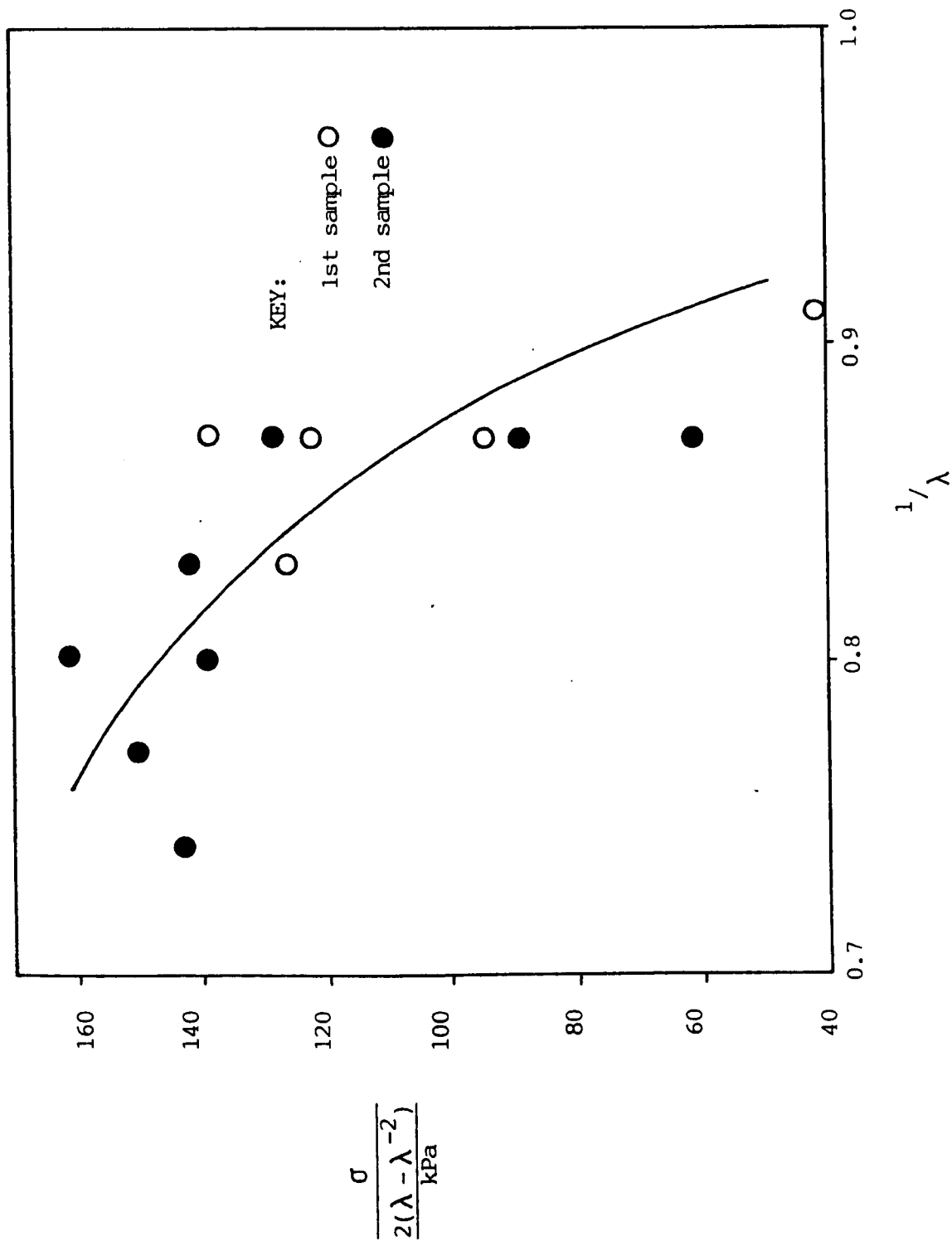


Fig. 5-17k: Gaussian Curve for IPN 131 Hydrogel

Fig. 5-171: Mooney-  
Rivlin Curve for IPN  
131 Hydrogel



The shape of the curve is similar to those of the IPNs described above. The initial modulus is rather larger at 1700 kPa. Fig. 5-17h shows the Gaussian curve for the same IPN, which deviates from the prediction of classical rubber elasticity theory. The initial shear modulus  $G$  is 480 kPa. The Mooney-Rivlin plot (Fig. 5-17i) is difficult to analyse, since the data are widely scattered. Whether the graph has a linear portion cannot be ascertained from these data. The stress-strain curve for IPN 131, a similar material but containing 72.2 mol % polymer II, is shown in Fig. 5-17j. The scatter of the data at low strains is a consequence of the errors involved in estimating the strain at lower values. The graph is approximately linear, the modulus being 693 kPa. These errors are also evident in the Gaussian curve (Fig. 5-17k). Allowing for these errors, the graph is linear, with a slope of 284 kPa. As in the case of Fig. 5-17i, no quantitative analysis of the Mooney-Rivlin curve could be carried out, as a result of the wide variation in values of  $\sigma/2(\lambda - \lambda^{-2})$ .

Figs. 5-17m to 5-17t show data for IPNs where polymer II was a 50/50 molar MMA/(HEMA/MAA) copolymer (HEMA/MAA = 95/5 molar). The stress-strain curve for the material containing 13.2 mol % polymer II is shown in Fig. 5-17m. The curve is similar in shape to those in Figs. 5-17a, 5-17d and 5-17g, not showing the increase in slope with strain at higher strains, which is characteristic of reinforced rubbers and for some of the terpolymer hydrogels described in Chapter 4. The initial modulus is 350 kPa. The Gaussian curve (Fig. 5-17n) deviates from the statistical theory; the slope decreases with increasing strain. The initial shear modulus is 113 kPa. The slope of the linear part of the Mooney-Rivlin curve (Fig. 5-17o) is zero, the intercept on the  $\sigma/2(\lambda - \lambda^{-2})$  axis ( $C_1$ ) being 28.5 kPa. At lower strains, a

Fig. 5-17m: Stress vs. Strain for IPN 145 Hydrogel Containing 13.2

mol % of a 50/50 MMA/(HEMA/MAA) Copolymer (HEMA/MAA =  
95/5)

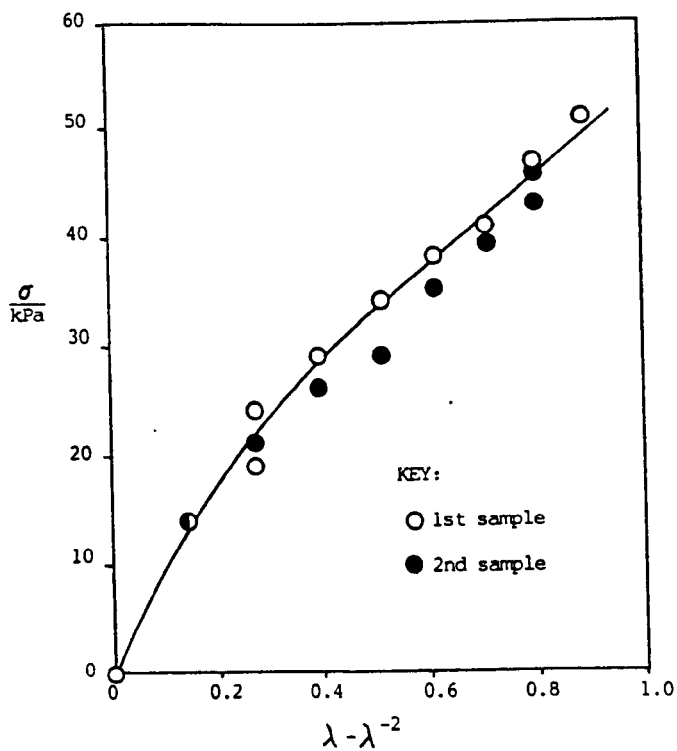
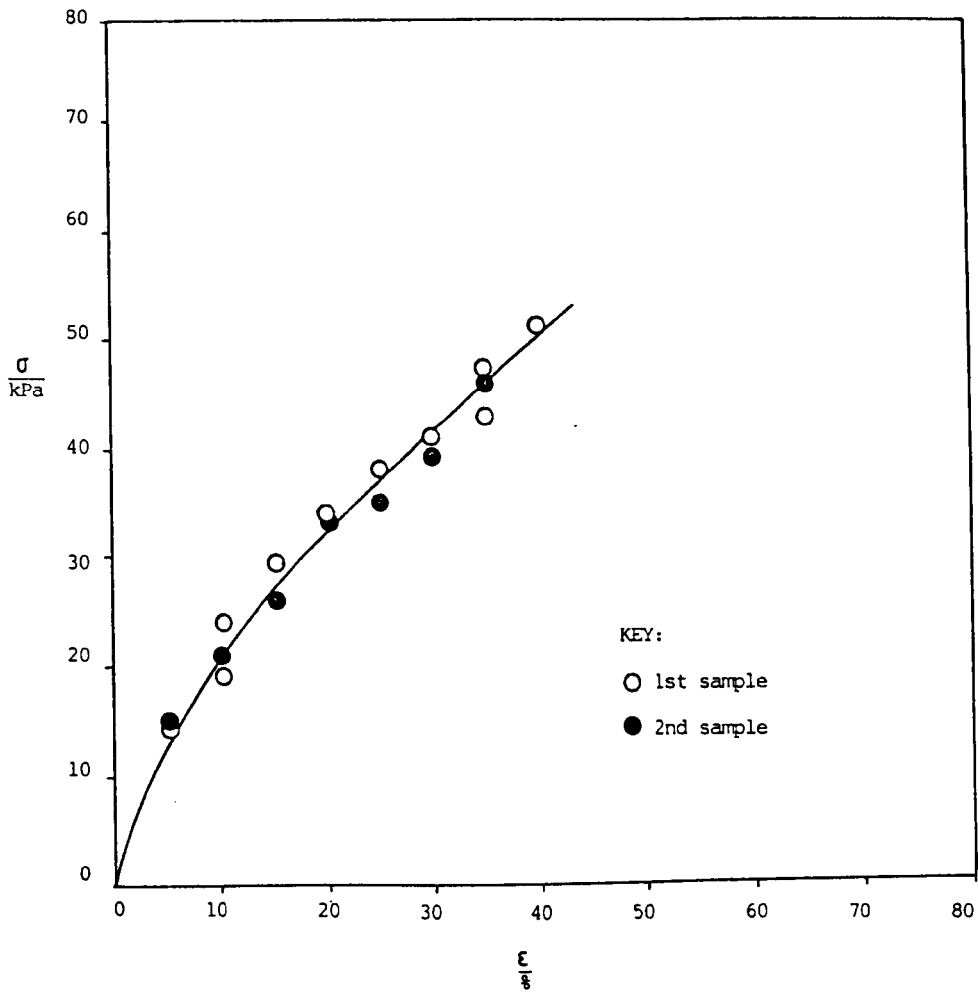
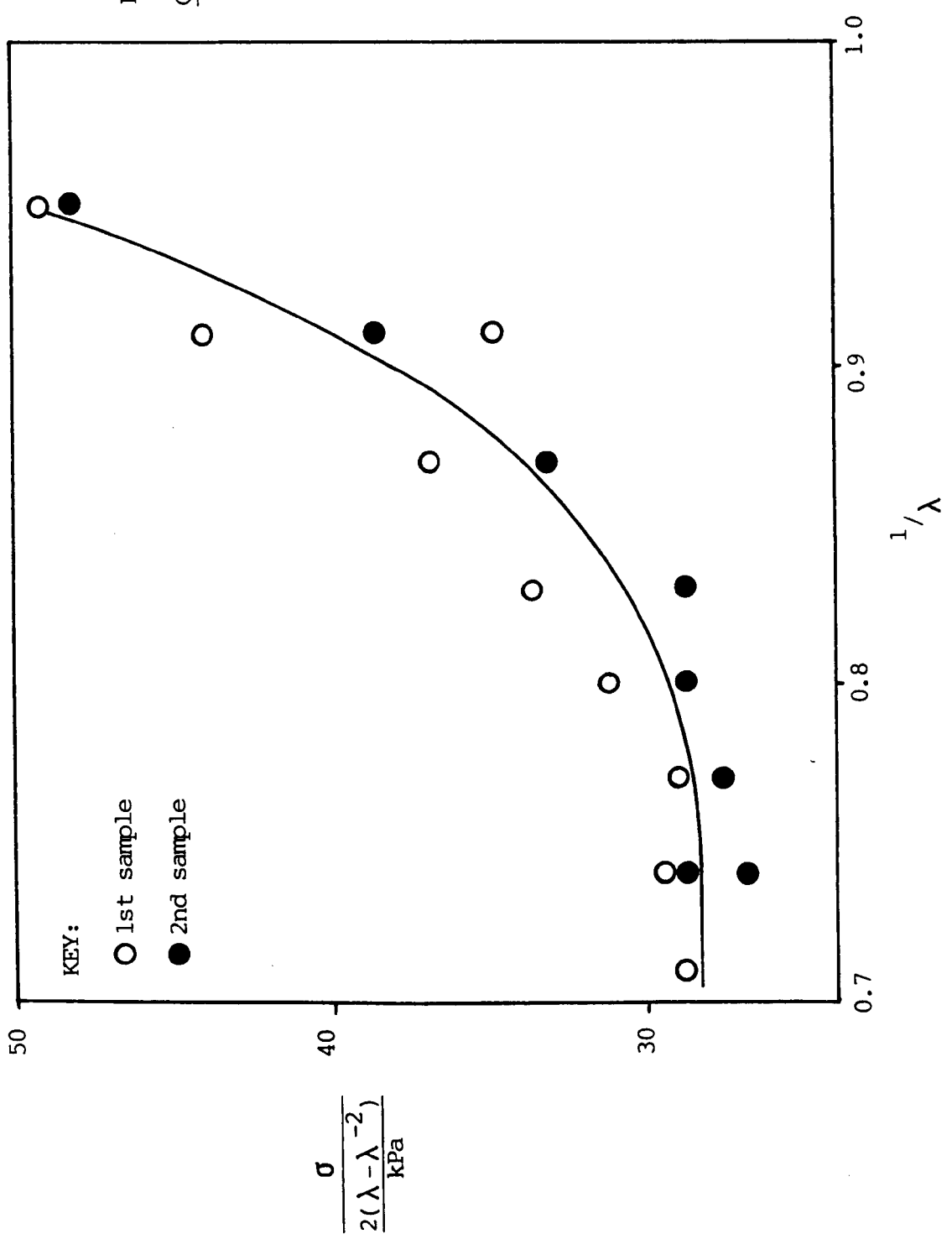


Fig. 5-17n: Gaussian Curve for IPN 145 Hydrogel

Fig. 5-17o: Mooney-Rivlin  
Curve for IPN 145 Hydrogel

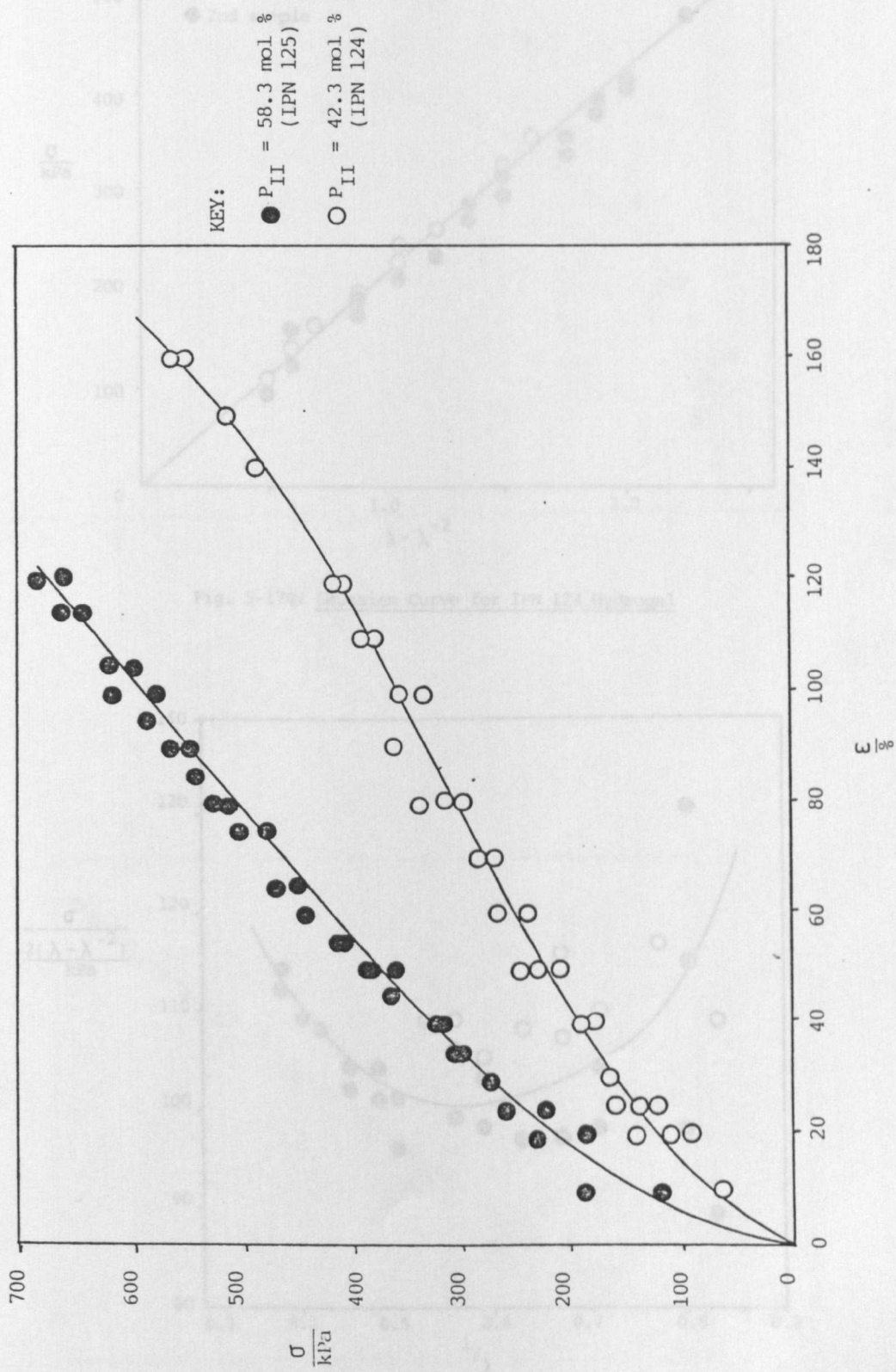


sharp increase in slope with  $1/\lambda$  is observed. Fig. 5-17p shows stress-strain curves for both IPN 124 and IPN 125, containing 42.3 and 58.3 mol % of polymer II respectively. The curve for IPN 124 is similar to that of a reinforced rubber. The slope increases with strain at high values of strain. The initial modulus is 725 kPa. The curve for IPN 125 does not have this feature. The initial modulus is 1667 kPa. The Gaussian curve for IPN 124 (Fig. 5-17q) is linear, and the initial shear modulus is 213 kPa. The Mooney-Rivlin curve (Fig. 5-17r) has a minimum in  $\sigma/2(\lambda - \lambda^{-2})$  at the point  $\sigma/2(\lambda - \lambda^{-2}) = 100$  kPa,  $1/\lambda = 0.55$ . It is not clear whether the curve has a linear region, since the points are widely scattered. The Gaussian curve for IPN 125 (Fig. 5-17s) is linear, and therefore the material conforms to the prediction of the statistical theory of rubber elasticity. The initial shear modulus is 350 kPa. The Mooney-Rivlin curve (Fig. 5-17t) is linear at high values of strain. The slope ( $C_2$ ) is zero and the intercept on the  $\sigma/2(\lambda - \lambda^{-2})$  axis is 140 kPa.

Fig. 5-17u shows the stress-strain curves for three samples of IPN 135, which contained 60.6 mol % of a 70/30 molar MMA/(HEMA/MAA) copolymer (HEMA/MAA = 95/5 molar). Two curves were drawn. Data obtained for the first sample follow one curve, and those obtained for the second and third follow the other. The low-extension moduli are 11,000 and 17,500 kPa. The data, when plotted as a Gaussian curve (Fig. 5-17v), are rather scattered. However, a single straight line can be drawn through the points. The low-extension shear modulus is 1760 kPa. The Mooney-Rivlin curve (Fig. 5-17w) is similar in shape to that of Fig. 5-17t. The slope of the linear part is zero at high strains, and the intercept on the  $\sigma/2(\lambda - \lambda^{-2})$  axis ( $C_1$ ) is 840 kPa.



Fig. 5-17p: Stress vs. Strain for IPN Hydrogels Containing a 50/50  
MMA/(HEMA/MAA) Copolymer (HEMA/MAA = 95/5)



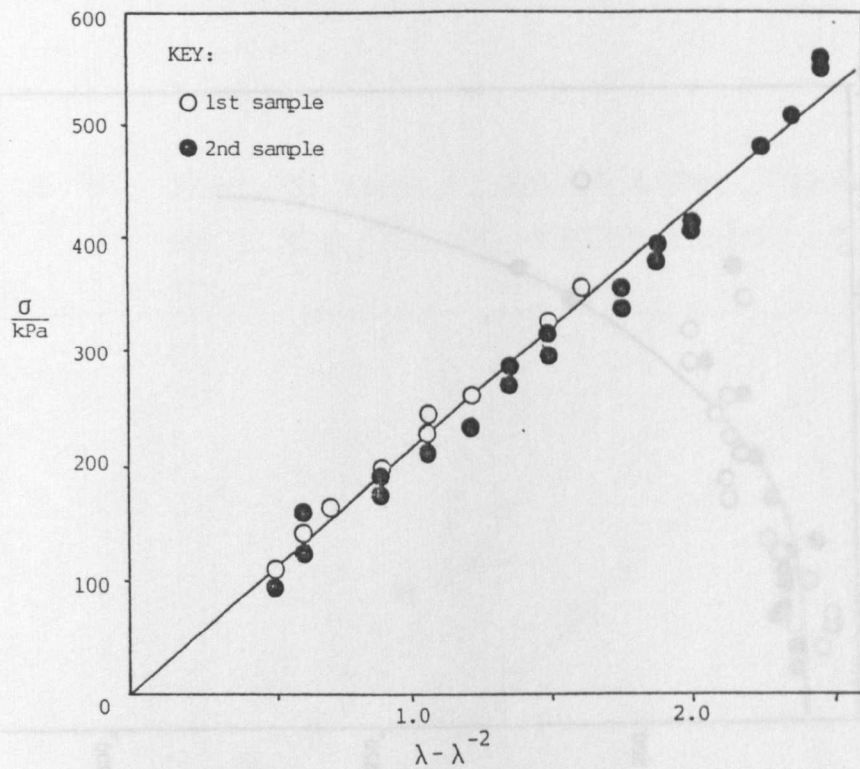


Fig. 5-17q: Gaussian Curve for IPN 124 Hydrogel

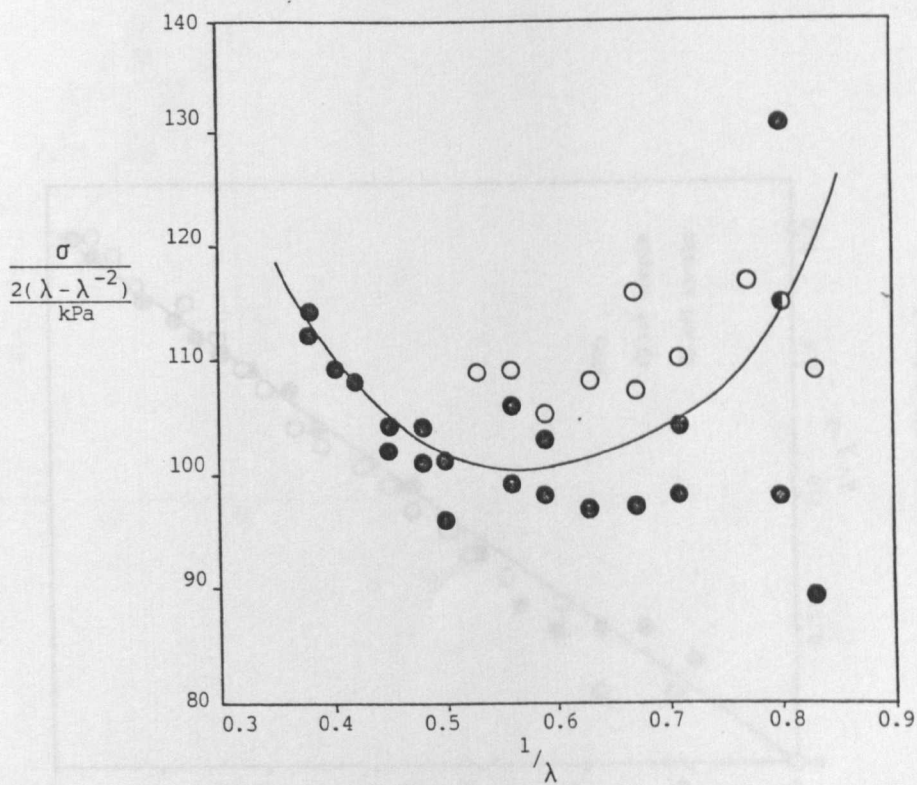


Fig. 5-17r: Mooney-Rivlin Curve for IPN 124 Hydrogel

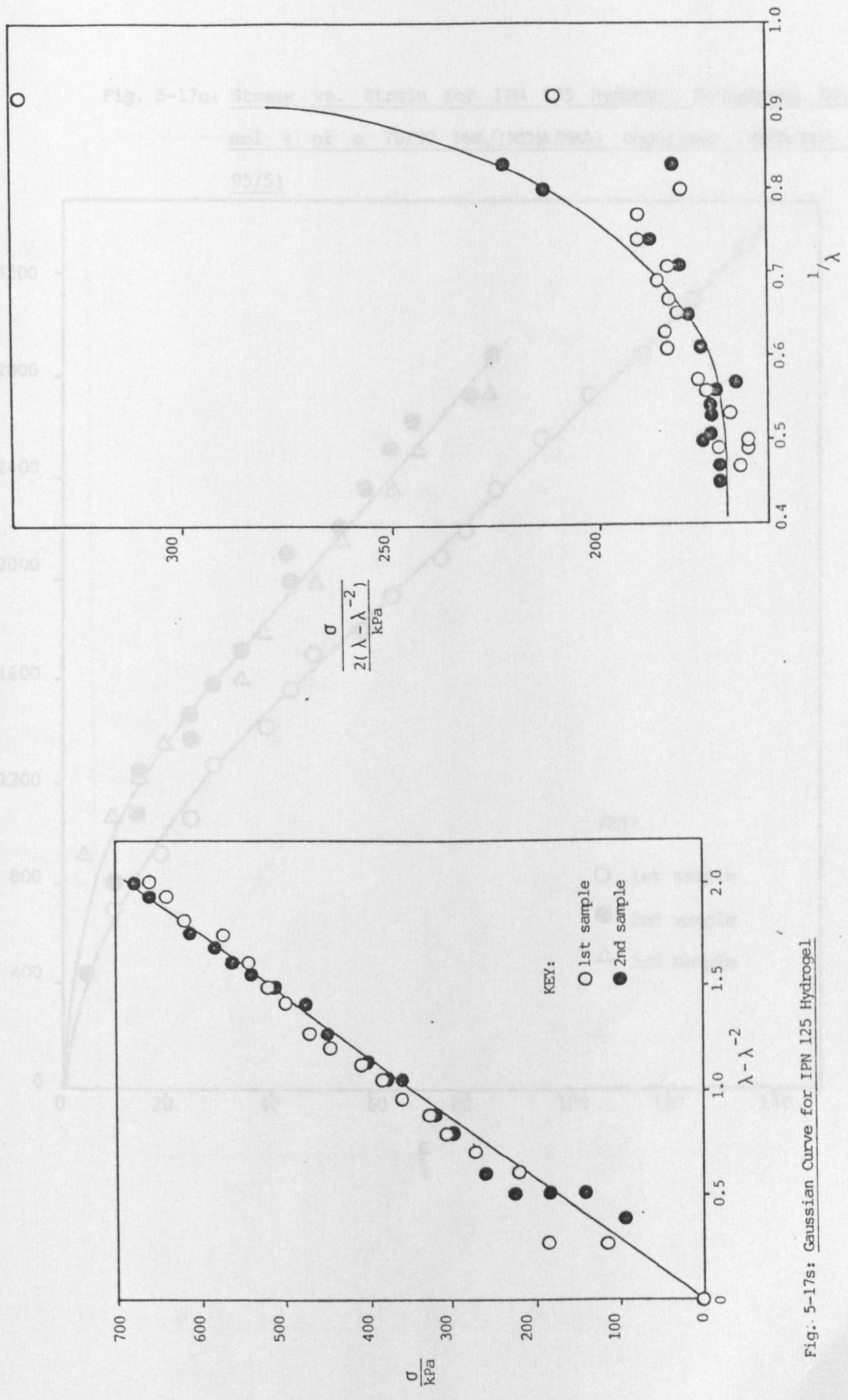
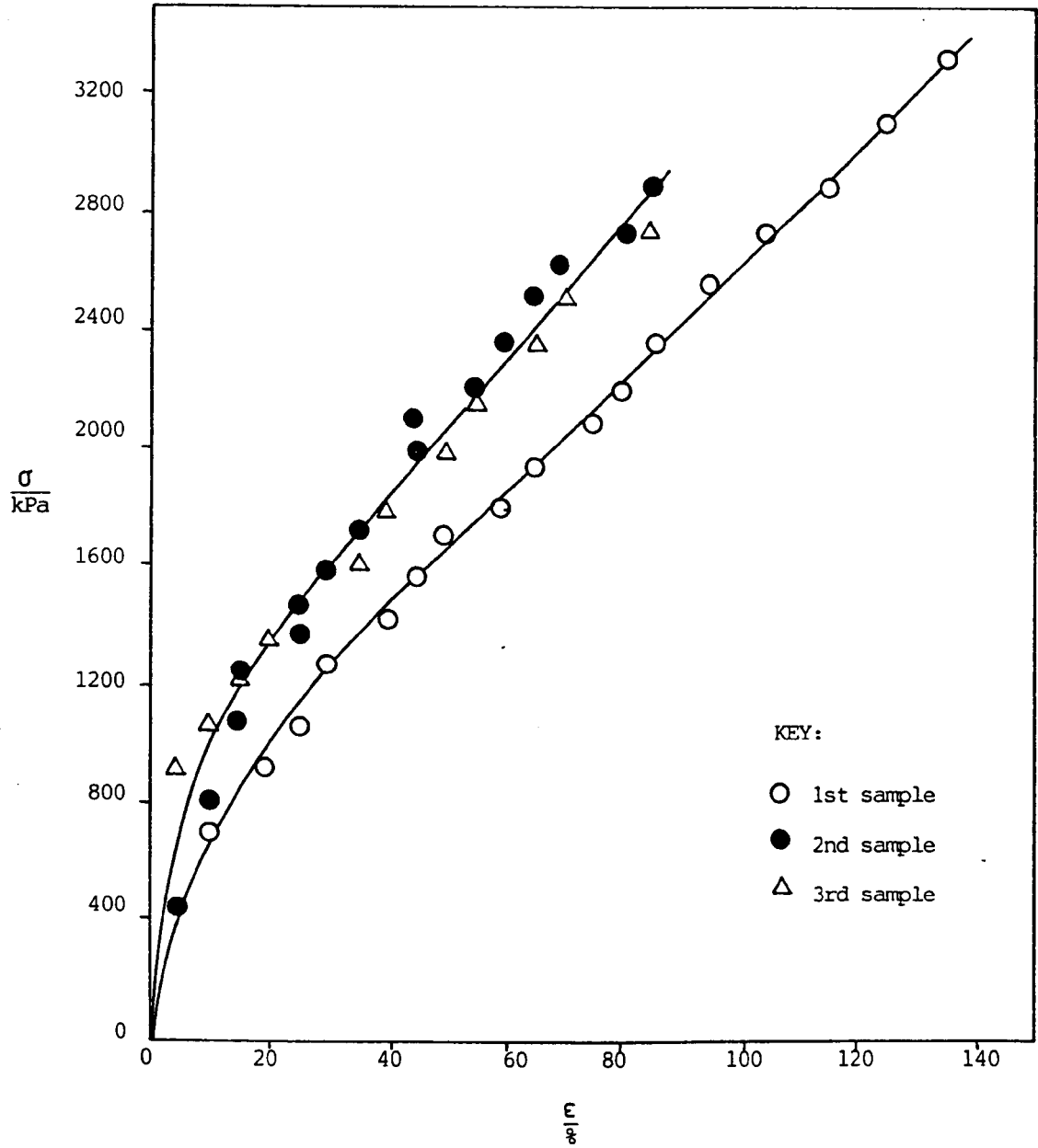


Fig. 5-17s: Gaussian Curve for IPN 125 Hydrogel

Fig. 5-17t: Mooney-Rivlin Curve for IPN 125 Hydrogel

Fig. 5-17u: Stress vs. Strain for IPN 135 Hydrogel Containing 60.6  
mol % of a 70/30 MMA/(HEMA/MAA) Copolymer (HEMA/MAA =  
95/5)



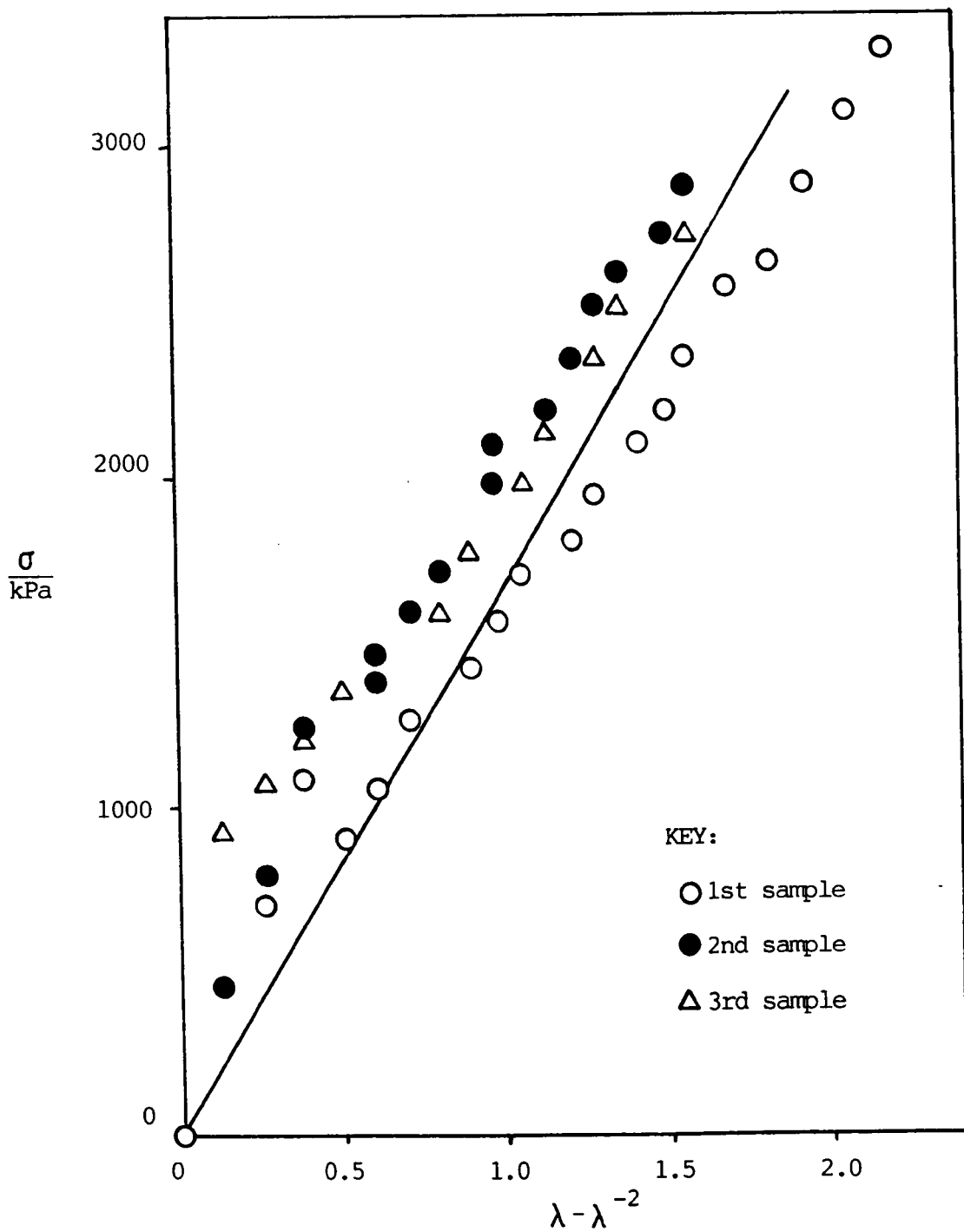


Fig. 5-17v:  $\sigma$  vs.  $\lambda - \lambda^{-2}$  for IPN 135 Hydrogel

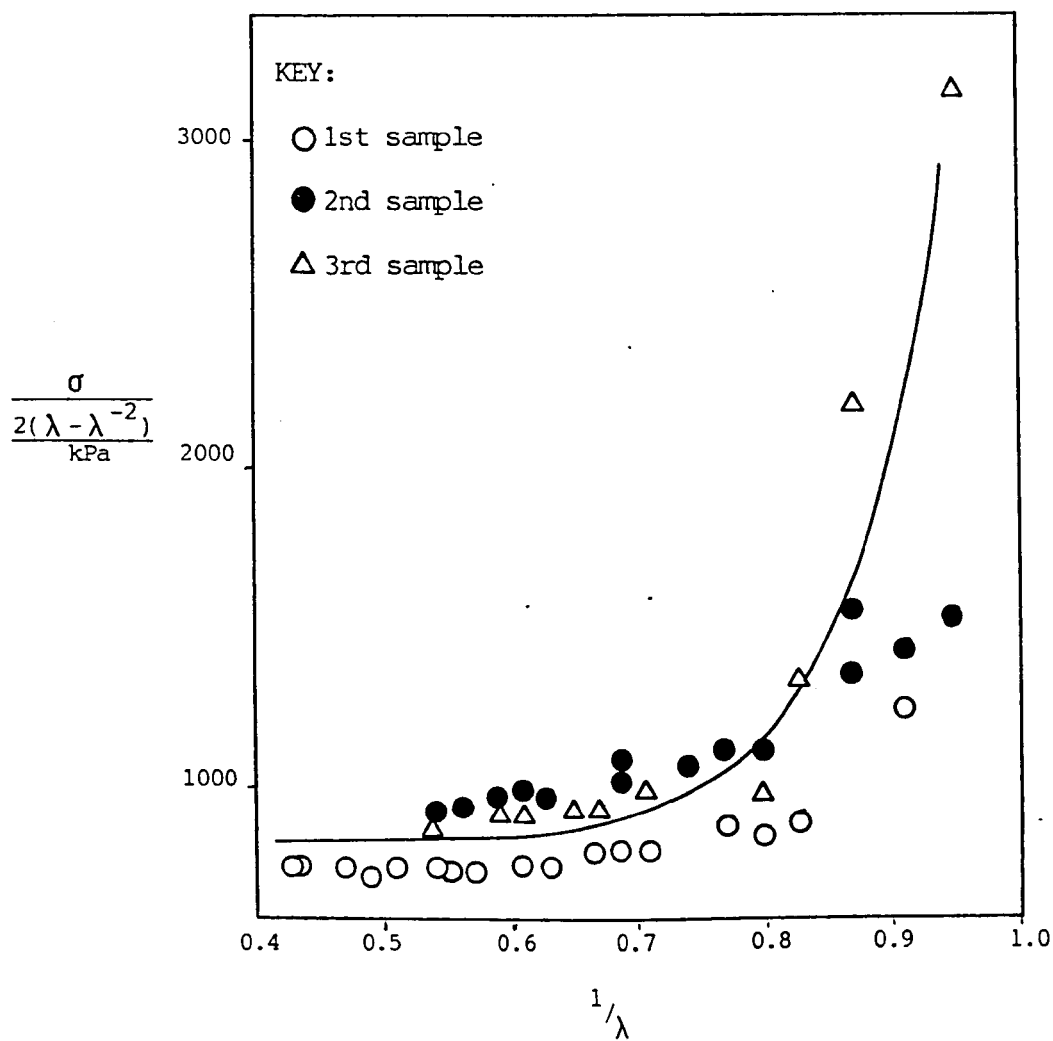


Fig. 5-17w: Mooney-Rivlin Curve for IPN 135 Hydrogel

Figs. 5-17x to 5-17cc show data obtained for IPNs where polymer II was a 95/5 (HEMA/MAA)/styrene copolymer (HEMA/MAA = 95/5 molar). Fig. 5-17x shows the stress-strain curve for IPN 139, which contained 64.2 mol % of polymer II. The graph is linear, showing no signs of increased modulus at higher strains. The initial modulus is 350 kPa. The Gaussian curve (Fig. 5-17u) is also linear, the shear modulus, given by the slope, being 140 kPa. The Mooney-Rivlin curve, illustrated in Fig. 5-17z, has a linear portion at high strains, the slope of which is zero. The intercept on the  $\sigma/2(\lambda - \lambda^{-2})$  axis is approximately 70 kPa. However, as in the case of most of the Mooney-Rivlin plots, the data are widely scattered. The deviations from the Mooney-Rivlin equation at lower strains are in different directions for the two different samples. Small variations in strain may cause large variations in  $\sigma/2(\lambda - \lambda^{-2})$ , particularly at low strains. The stress-strain curve for a similar material containing 77.7 mol % of polymer II, is shown in Fig. 5-17aa. In this case a slight increase in slope with strain occurs at high strains. The initial modulus is 400 kPa. The Gaussian plot (Fig. 5-17bb) is linear, although at high strains ( $\lambda - \lambda^{-2} = 1.7$ ) the slope increases slightly with strain. The low-extension modulus is 140 kPa. The Mooney-Rivlin curve, illustrated in Fig. 5-17cc, shows deviations from linearity at high and low strains, with a central linear portion, the slope of which is zero. The intercept on the  $\sigma/2(\lambda - \lambda^{-2})$  axis is 70 kPa.

Table 5-12 summarises the moduli of the various IPN hydrogels. Several comments may be made regarding the results summarised in Table 5-12:

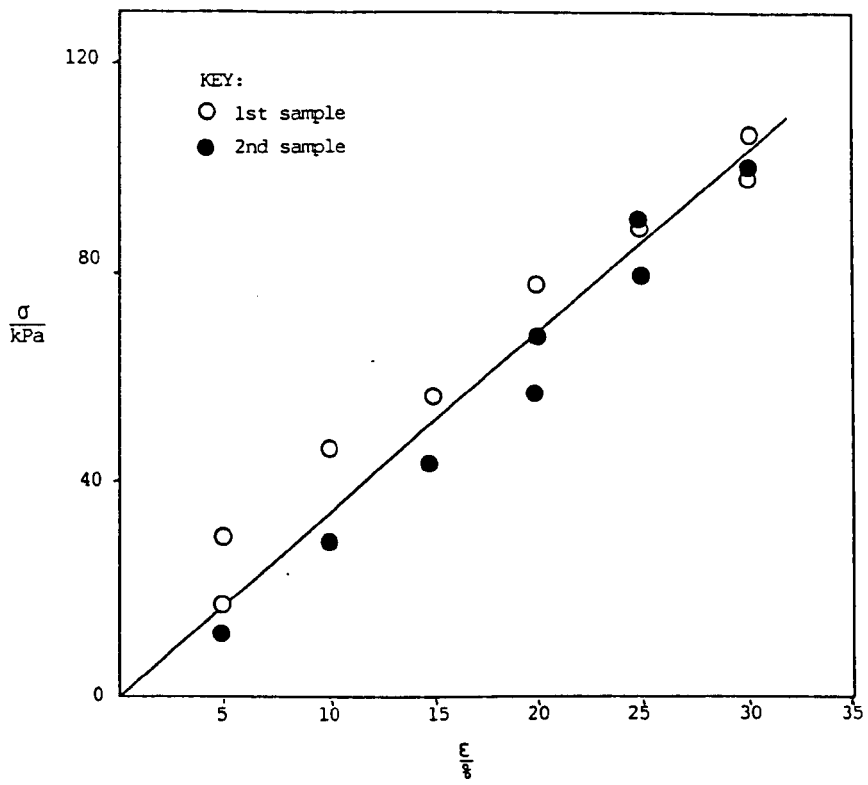


Fig. 5-17x: Stress vs. Strain for IPN 139 Hydrogel, Containing 64.2 mol of a 95/5 (HEMA/MAA) Styrene Terpolymer (HEMA/MAA = 95/5)

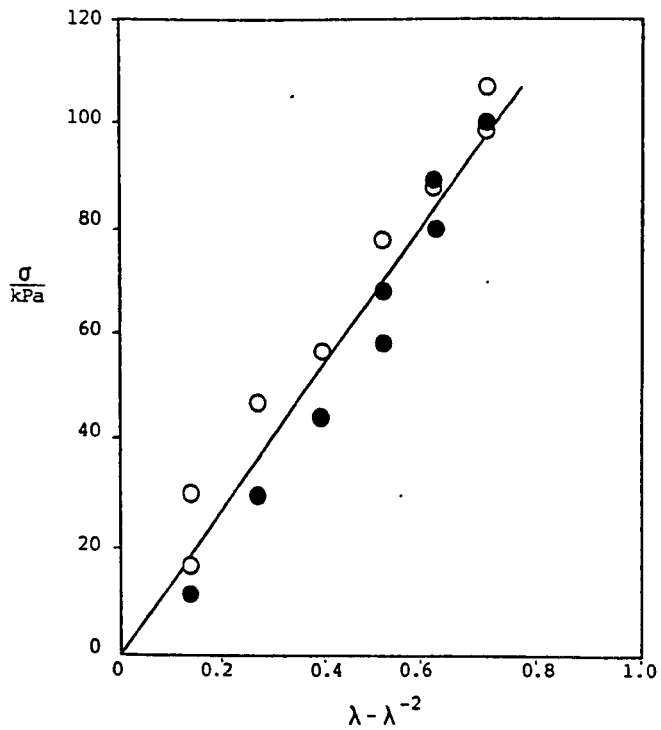


Fig. 5-17y:  $\sigma$  vs.  $\lambda - \lambda^{-2}$  for IPN 139 Hydrogel

KEY:

- 1st sample
- 2nd sample



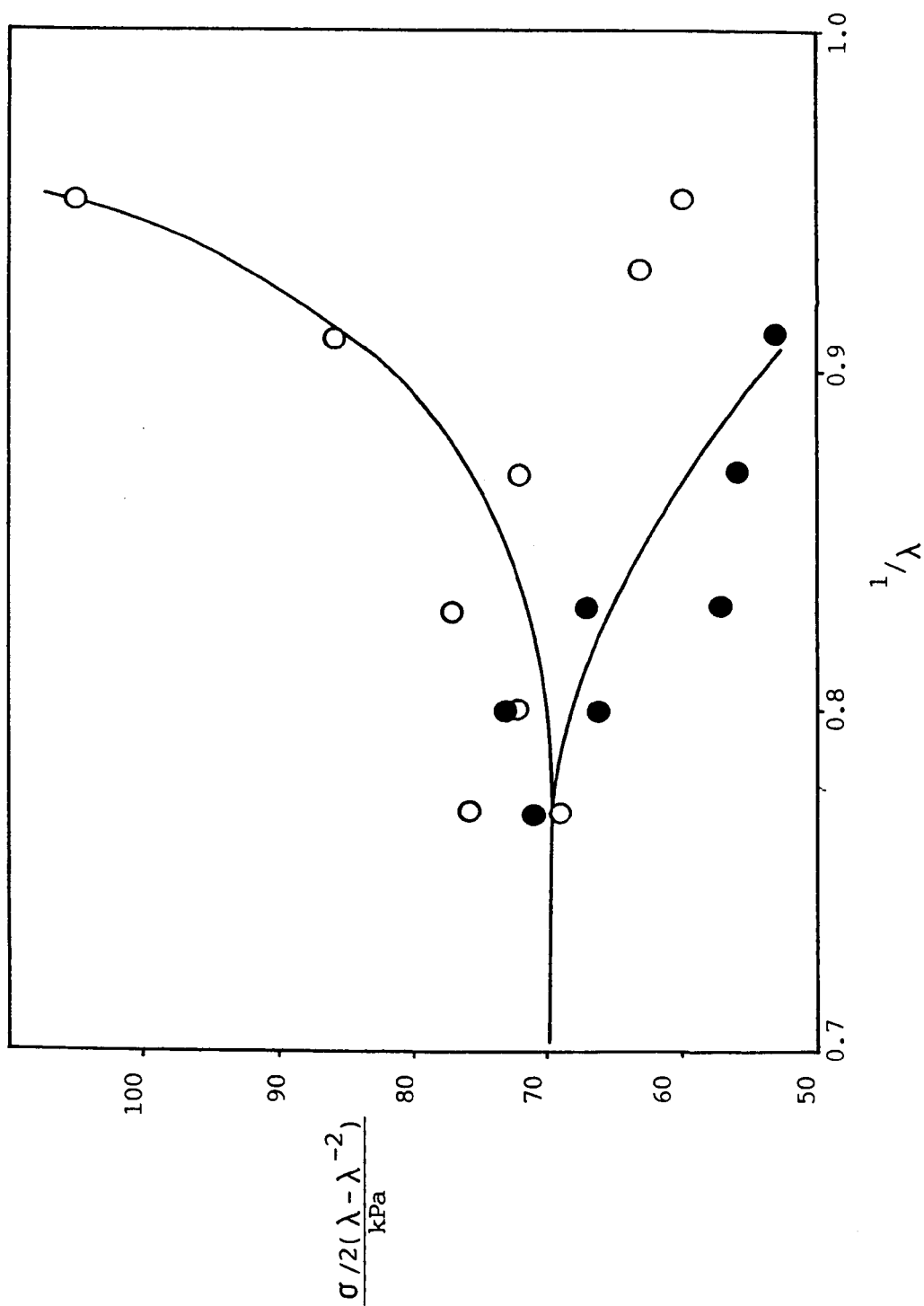


Fig. 5-17z: Mooney-Rivlin Curve for IPN139 Hydrogel

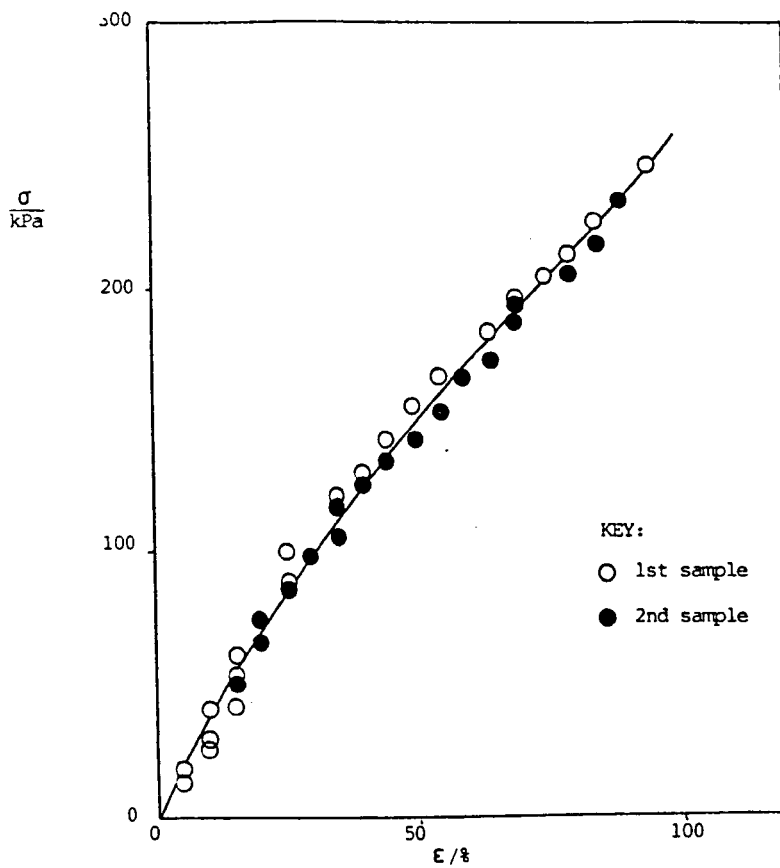


Fig. 5-17aa: Stress vs. Strain for IPN Hydrogel 136, Containing  
77.7 mol % of a 95/5 (HEMA/MAA)/Styrene Terpolymer

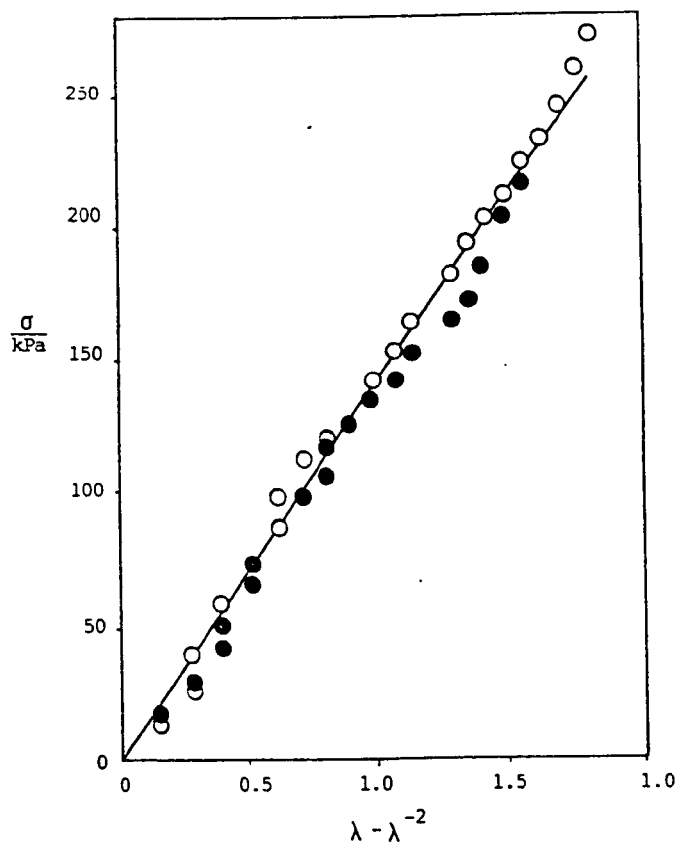


Fig. 5-17bb:  $\sigma$  vs.  $\lambda - \lambda^{-2}$  for IPN 136 Hydrogel

KEY:  
○ 1st sample  
● 2nd sample

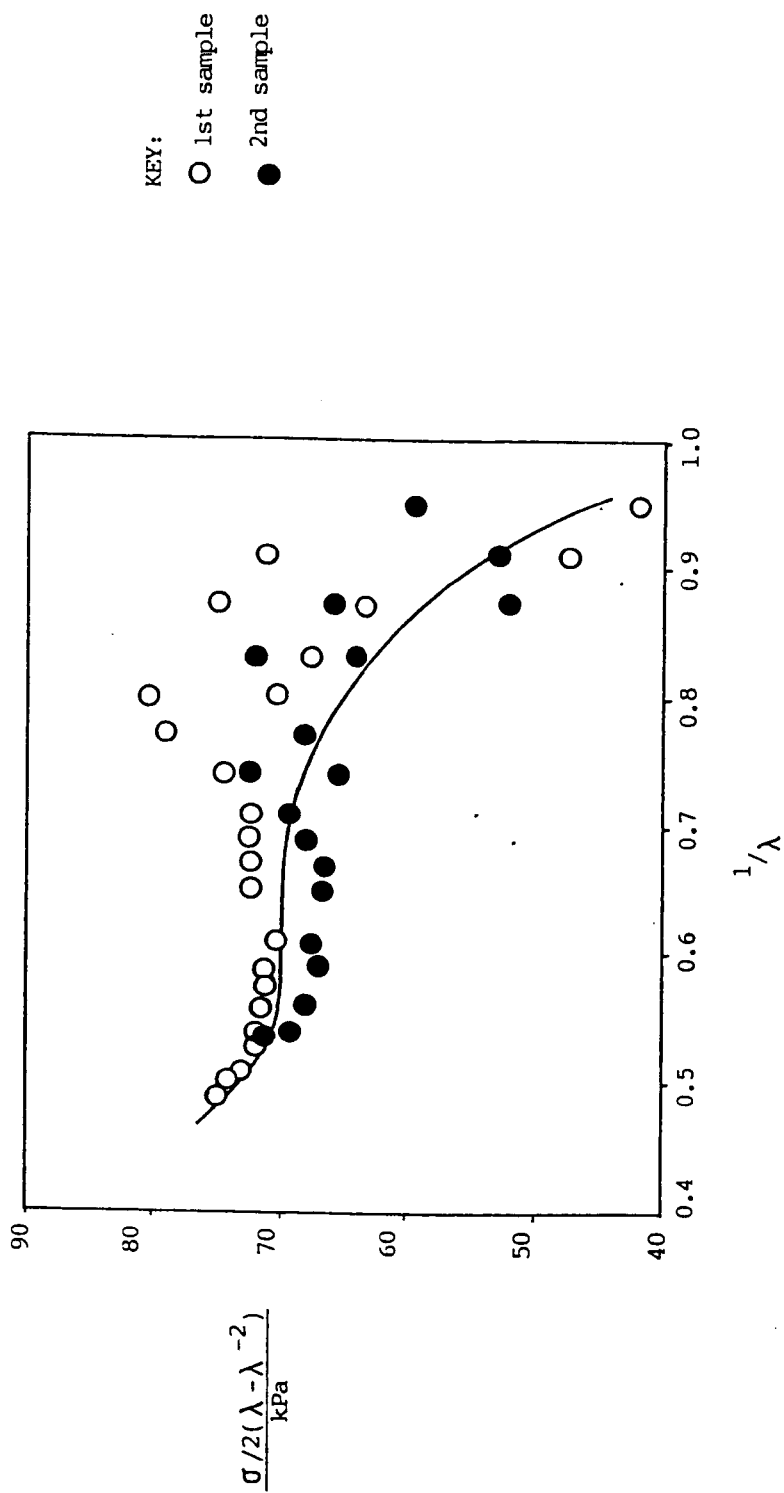


Fig. 5-17cc: Mooney-Rivlin Curve for IPN 136 Hydrogel

Table 5-12: Moduli of IPN Hydrogels

material	polymer II	P <sub>II</sub> /%	E <sub>init</sub> /kPa	G/kPa
IPN150	95 HEMA/5 MAA	53.8	417	120
IPN118	95 HEMA/5 MAA	77.5	667	160
IPN128	95 HEMA/5 MAA (x)	68.0	1700	480
IPN131	95 HEMA/5 MAA (x)	72.2	693	284
IPN145	50 MMA/50 HEMA-MAA	13.2	350	113
IPN124	50 MMA/50 HEMA-MAA	42.3	725	213
IPN125	50 MMA/50 HEMA-MAA	58.3	1667	350
IPN135	70 MMA/30 HEMA-MAA	60.6	11,000 - 17,500	1760
IPN139	5S/95 HEMA- MAA	64.2	350	140
IPN136	5S/95 HEMA- MAA	77.7	400	140

Note: "(x)" denotes that the swelling mixture contained  
0.4 mol % EGDMA.

- (i) Trends in E should be regarded as indicative of general trends, rather than of absolute quantitative values. The data were obtained from slopes at small strains, where the experimental precision is low.
- (ii) For IPN hydrogels containing the 50/50 molar MMA/(HEMA/MAA) copolymer (HEMA:MAA = 95:5 molar), G increases as P<sub>II</sub> increases. This is a consequence both of the reduced water content of the material,

and of the increase in polymer chain interactions which increases the effective crosslink concentration.

(iii) However, the IPN hydrogels containing the 95/5 molar HEMA/MAA copolymer as polymer II show a similar trend, although there is no increase in hydrophobicity. Hence, in this case, the decrease in water content and consequent increase in modulus with increasing  $P_{II}$  must arise from factors such as an increase in effective crosslink concentration.

(iv) The incorporation of EGDMA into polymer II increases the modulus of the IPN hydrogel, although the figure of 1700 kPa for the initial modulus of IPN128 requires confirmation by further experimental work.

(v) A striking effect is shown by hydrogel IPN135. This material, together with IPNs 150 and 125, which contain similar proportions of polymer II, clearly shows the effect of increasing the hydrophobicity of polymer II. As the mole fraction of MMA in polymer II increases from zero to 0.5, the modulus increases by a factor of approximately 4. As the mole fraction further increases to 0.7, the modulus increases by a further factor of approximately 10.

Most of the Mooney-Rivlin curves shown a linear portion of slope approximately zero. This is consistent with the high water contents of the materials (198). In contrast to materials such as natural rubber swollen in benzene (198) however, large deviations from the Mooney-Rivlin expression occur at both high and low strains. It should be noted that the quantities  $C_1$  and  $C_2$  are given by the intercept and slope respectively of the  $v_2^{1/3}/2(\lambda - \lambda^{-2})$  against  $1/\lambda$  graph, where  $v_2$  is the volume fraction of polymer in the swollen material. Hence if quantit-

ative results are required, the intercepts and slopes for materials should be multiplied by the factor  $v_2^{1/3}$

Shear moduli found from the Gaussian curves are estimates of the quantity  $G_{sw}$  in equation 4-18. The effective crosslink concentration of the materials,  $x_e$ , may then be estimated using the equation:

$$G_{sw} = 2v_2^{1/3} x_e RT \quad (....4-18)$$

where R is the gas constant, and T is the absolute temperature. Values of crosslink concentration calculated by this method are shown in Table 5-13. They may be compared with values calculated from the EGDMA concentrations used in the polymerisations.

The volume of dry polymer is increased by the incorporation of polymer II into the material. Assuming that the volumes are additive, it is given by the expression:

$$V_{TOT} = V_I + V_{II} \quad (....5-38)$$

Table 5-13: Values of Effective Crosslink Density Calculated from Equation 4-18

material	polymer II	P <sub>II</sub> /%	$v_2$	$G_{sw}$ /kPa	$10^5 x_e / \text{molcm}^{-3}$
IPN150	95 HEMA/5 MAA	53.8	0.222	120	3.98
IPN128	95 HEMA/5 MAA (x)	68.0	0.331	480	13.96
IPN131	95 HEMA/5 MAA (x)	72.2	0.325	284	8.31
IPN124	50 MMA/50 HEMA- MAA	42.3	0.379	213	5.93
IPN125	50 MMA/50 HEMA- MAA	58.3	0.383	350	9.70
IPN135	70 MMA/30 HEMA- MAA	60.6	0.540	1760	43.55

where  $V_{TOT}$  is the total volume of dry polymer,  $V_I$  is the volume of polymer I, and  $V_{II}$  is the volume of polymer II. The mole fraction of polymer repeat units of polymer II,  $P_{II}$ , is defined as

$$P_{II} = \frac{m_{II}/M_{II}}{m_{II}/M_{II} + m_I/M_I} \quad (...5-39)$$

where  $m_I$  and  $m_{II}$  are the weights of polymers I and II respectively, and  $M_I$  and  $M_{II}$  are the weighted averages of the molecular weights of the monomer units comprising polymers I and II respectively, weighted in the following way. If polymer I has two different repeat units, A and B, in the proportions  $f_A$  and  $f_B$ , where  $f_A + f_B = 1$ , then  $M_I$  is equal to  $f_A m_A + f_B m_B$ , where  $m_A$  and  $m_B$  are the molecular weights of the repeat units A and B respectively.

Equation 5-38 may be expressed as follows:

$$V_{TOT} = \frac{m_I}{I} + \frac{m_{II}}{II} \quad (....5-40)$$

For the semi-IPNs, if no crosslinking occurs as a result of the incorporation of polymer II, by means of entanglements, polymer-polymer interactions, grafting or by any other means, then the new crosslink concentration  $x'$  after incorporation of polymer II is given by

$$x' = x \frac{V_I}{V_{TOT}} \quad (....5-41)$$

where  $x$  is the crosslink concentration of the dry polymer I prior to incorporation of polymer II.

For IPNs (i.e. where polymer II is crosslinked) the new crosslink concentration is given by

$$x' = x \frac{V_I}{V_{TOT}} + \frac{C m_{II}/M_{II}}{V_{TOT}} \quad (....5-42)$$

where C is the crosslink concentration of polymer II.

Combining these various equations, the new crosslink densities become:

$$\text{for semi-IPNs, } x' = x \left( 1 + \frac{M_I}{M_{II}} \frac{I}{II} \left( \frac{1}{P_{II}} - 1 \right) \right)^{-1} \quad (...5-43)$$

$$\text{for IPNs, } x' = x \left( 1 + \frac{M_I}{M_{II}} \frac{I}{II} \left( \frac{1}{P_{II}} - 1 \right) \right)^{-1}$$

$$+ \frac{C}{\frac{M_I}{I} \left( \frac{1}{P_{II}} - 1 \right) + \frac{M_{II}}{II}}$$

Using these equations, theoretical crosslink concentrations for the IPNs were calculated. They are shown in Table 5-14, together with the experimental values derived from the shear moduli. Table 5-14 shows that the observed crosslink densities are higher than the calculated

Table 5-14: Comparison of Experimental and Theoretical Crosslink Densities

material	(a) $10^5 x_e / \text{mol cm}^{-3}$	(b) $10^5 x' / \text{mol cm}^{-3}$
IPN150	3.98	1.45
IPN128	13.96	3.13
IPN131	8.31	3.13
IPN124	5.93	1.87
IPN125	9.70	1.37
IPN135	43.55	1.33

Notes: (a) calculated from shear moduli

(b) calculated from equations 5-45 and 5-46



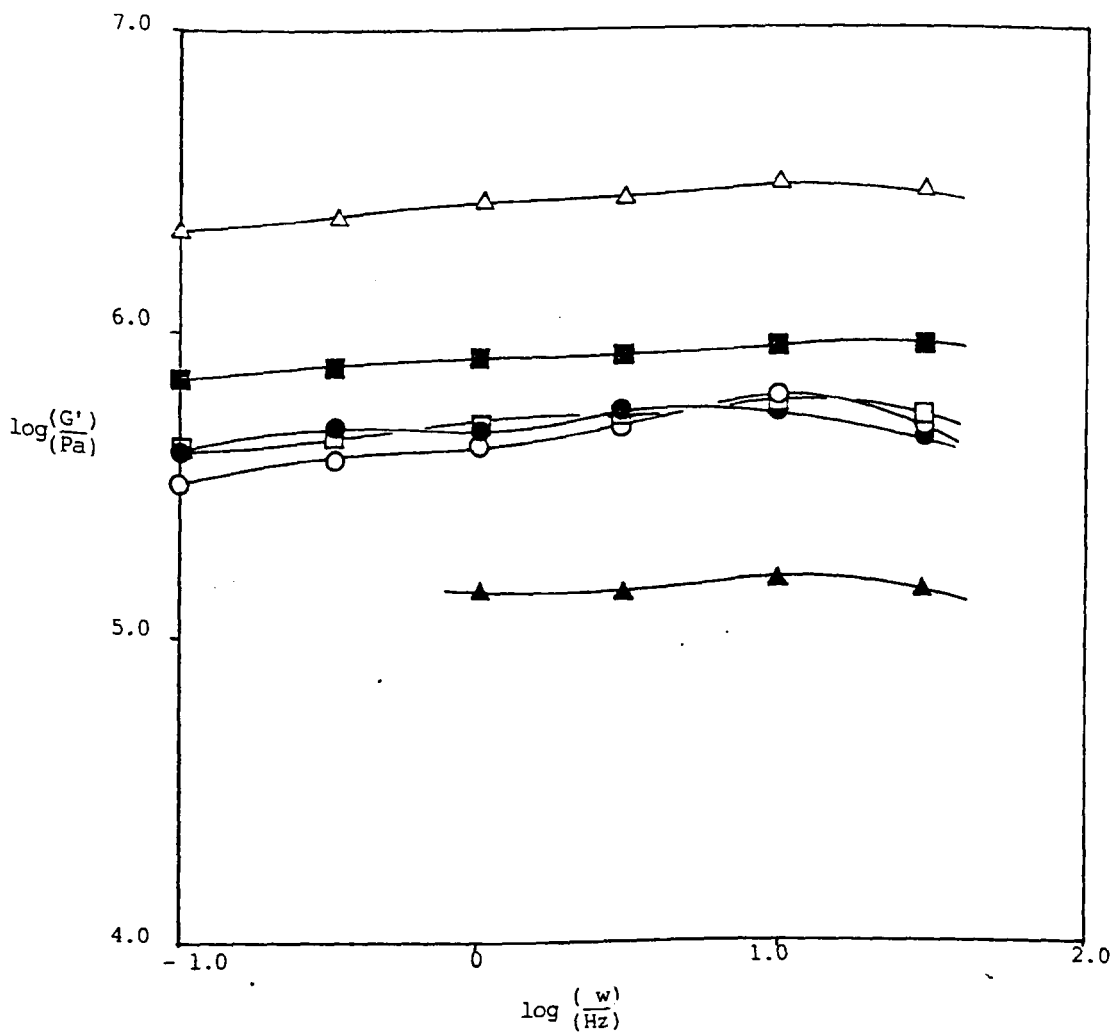
values based on the proportion of EGDMA introduced into the material. The largest difference in the two values occurs for IPN135, where  $x_e/x'$  is 32.7. Hence for IPN135, the observed modulus of the material predicts a crosslink density far higher than that which is expected. This difference is thought to arise from a variety of causes:

- (i) polymer-polymer physical interactions - the number of these interactions is expected to increase as the hydrophobicity of polymer II increases, in the form of a network of hydrophobic physical bonds;
- (ii) polymer chain entanglements - such entanglements increase the effective crosslink concentration, and their number increases with factors such as the proportion of polymer II, its molecular weight and the polymer II content;
- (iii) grafting of polymer II on to polymer I - such chemical bonding increases the concentration of chemical crosslinks.

The high observed crosslink concentration of IPN135 may be explained by the high hydrophobicity and high proportion of polymer II. This causes an increase in both polymer-polymer interactions and polymer chain entanglements.

Figs. 5-18a to 5-18i show the results of viscoelastic measurements on several IPN hydrogels. Figs. 5-18a to 5-18c show results for IPN hydrogels where polymer II was a copolymer of 95 mol HEMA: 5 mol MAA, i.e. homo-IPNs, and where polymer II was 95 mol HEMA/MAA: 5 mol styrene. The curves of  $\log G'$  as a function of frequency (Fig. 5-18a) are all similar in shape.  $\log G'$  increases slightly with  $\log w$  to a shallow maximum at approximately 16 Hz. The incorporation of styrene into

Fig. 5-18a: Storage Modulus vs. Frequency for IPN Hydrogels Containing  
a 95/5 molar HEMA/MAA Copolymer or a 95/5 molar (HEMA/MAA)/  
Styrene Terpolymer (HEAM/MAA = 95/5 molar)



KEY:

- P<sub>II</sub> = 0
- IPN 120: P<sub>II</sub> = 77.8% HEMA/MAA
- △ IPN 136: P<sub>II</sub> = 77.7% HEMA/MAA/S
- ▲ IPN 149: P<sub>II</sub> = 64.7% HEMA/MAA
- IPN 153: P<sub>II</sub> = 75.6% HEAM/MAA
- IPN 130: P<sub>II</sub> = 72.9% HEMA/MAA/EGDMA

polymer II (IPN136) increases the moduli by a factor of approximately 3.5 when compared with the basic gel (polymer network I alone). The moduli of the basic gel are also increased, by a factor of about 2, by the incorporation of 0.4 mol % EGDMA into polymer II (IPN130). IPN149, which contained 64.7% HEMA/MAA as polymer II showed moduli below those of the basic gel. This raises doubts concerning the validity of the absolute values of moduli obtained by this method. The reliability of data obtained using this apparatus has not yet been ascertained. The loss modulus values as a function of frequency are shown in Fig. 5-18b. The general trend of the curves is that  $G''$  increases with increasing frequency, and that at a given frequency, incorporation of polymer II and thus formation of IPNs, results in a decrease in loss modulus. This feature indicates that the material becomes more elastic and less viscoelastic as polymer II is incorporated. This conclusion is confirmed by the curves of  $\tan \delta$  as a function of frequency (Fig. 5-18c). The shapes of the  $\tan \delta$  curves are similar: in each case, as the frequency increases,  $\tan \delta$  decreases to a minimum. At higher frequencies, a sharp increase in  $\tan \delta$  with frequency occurs, a feature characteristic of polymers in the rubbery and viscoelastic states.

The storage moduli as a function of frequency for IPN hydrogels where polymer II was a copolymer of 50 mol HEMA/MAA: 50 mol MMA are shown in Fig. 5-18d. The curves for IPN hydrogels containing 11.6% (IPN144) and 20.2% (IPN140) of polymer II differ by a factor of 1.3, the values of  $G'$  for the 20.2% material being higher. In both cases, the maximum in  $G'$  is less sharp than that of the basic gel, and the increase in  $G'$  with frequency at lower frequencies less steep. The values of  $G'$  for the material containing 44.6% polymer II are higher than those

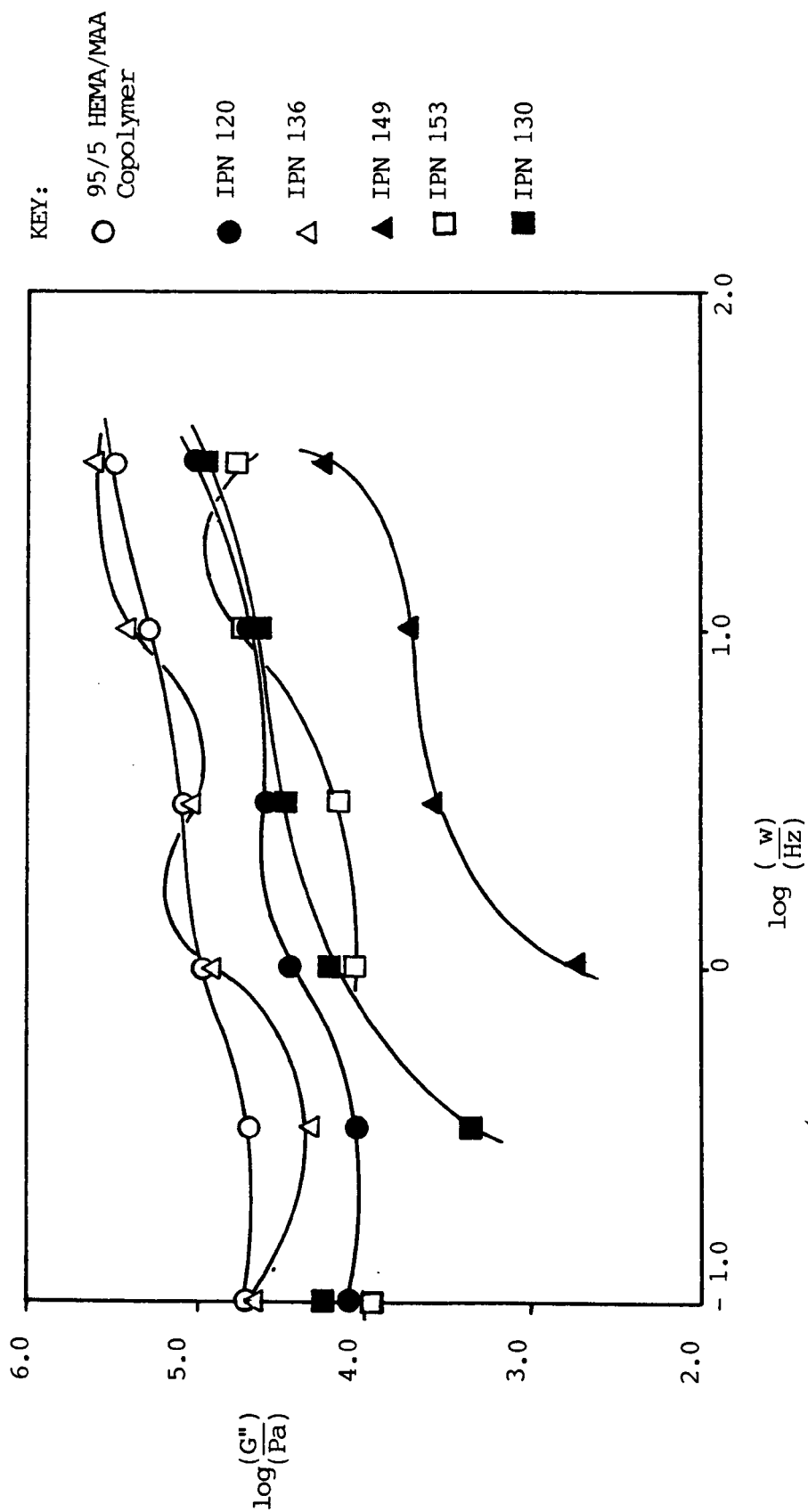
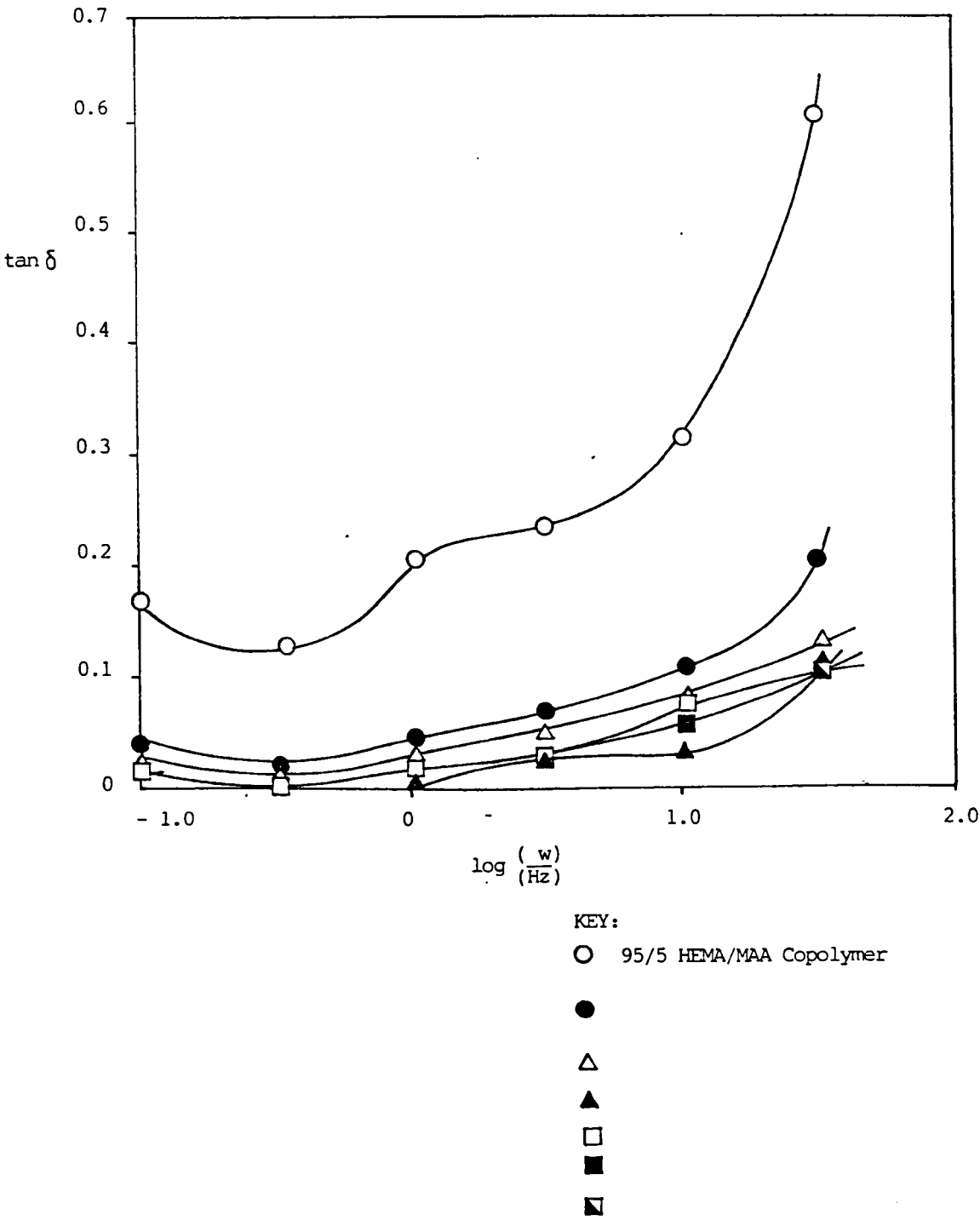


Fig. 5-18b: Loss Modulus vs. Frequency for IPN Hydrogels Containing a 95/5 molar HEMA/MAA Copolymer or a 95/5 molar (HEMA/MAA)/Styrene Terpolymer (HEMA/MAA = 95/5 molar)

Fig. 5-18c:  $\tan \delta$  vs. Frequency for IPN Hydrogels Containing a  
 95/5 molar HEMA/MAA Copolymer or a 95/5 (HEMA/MAA)/  
 Styrene Terpolymer (HEMA/MAA = 95/5 molar)



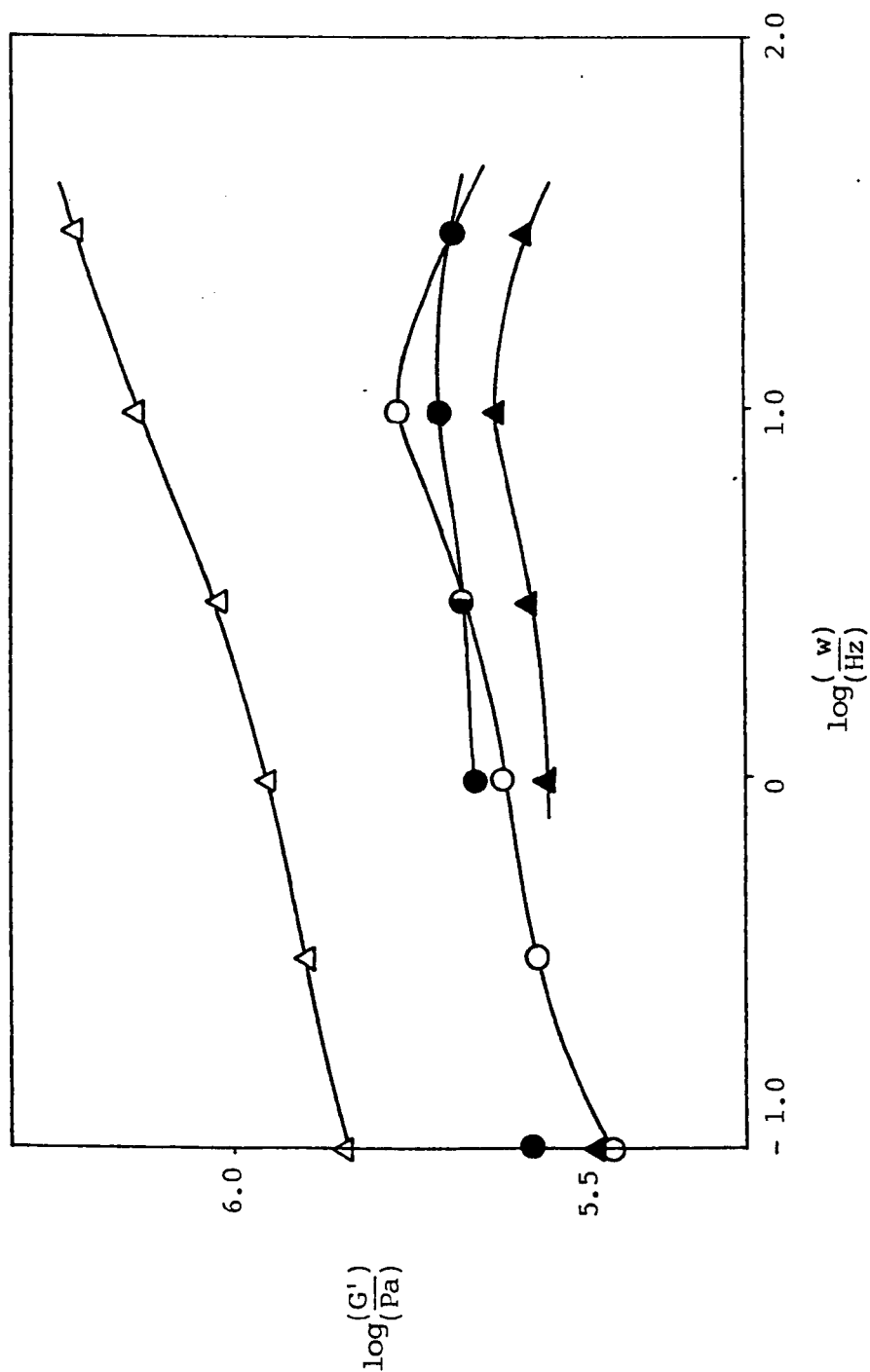


Fig. 5-18d: Storage Modulus vs. Frequency for IPN Hydrogels Containing a 50/50 MMA/(HEMA/MAA) Terpolymer

of the basic gel, and no maximum is observed: the slope of the curve increases with frequency over the full range of frequencies which were used. The loss moduli for the same materials are shown as a function of frequency in Fig. 5-18e. The IPN containing the greatest proportion of polymer II bears most resemblance to the basic gel. The two curves show a minimum in  $G'$  at a frequency of 0.2Hz, but the values of  $G''$  are higher by a factor of 2 for the IPN than  $G''$  for the basic network polymer. In the case of the IPN containing 20.2% polymer II, the minimum is shifted to a frequency of 2Hz and the values of  $G''$  are much lower than those for the basic gel. In the case of the IPN containing 11.6% polymer II, the minimum is shifted to a frequency of 0.6Hz, where  $G''$  is 3.2 kPa. The  $\tan \delta$  curves (Fig. 5-18f) for these materials show that the curves for the 11.6 and 20.2% polymer II IPNs are very similar, as are the curves for the basic gel and the 44.6% polymer II IPN. In all cases, the curves show a sharp increase in  $G''$  with frequency at high frequencies, and a minimum in  $G''$  at low frequencies, although for IPNs 140 and 144 this minimum almost disappears. At low frequencies,  $\tan \delta$  for these two IPNs is very small, indicating that in this frequency region, the materials are mainly elastic, whereas IPN141 and the basic hydrogel are still appreciably viscoelastic over the lower range of frequencies.

Figs. 5-18g to 5-18i show viscoelastic data for one of the IPN hydrogels containing a copolymer of 70 mol MMA: 30 mol HEMA/MAA. The material illustrated (IPN132) contained 60.1 mol % polymer II. Fig. 5-18g shows that considerable modification of  $G'$  may be achieved by the formation of IPNs such as this. At a given frequency, the value of  $G'$  for the IPN is approximately 100 times that for the basic gel. The shape of the curve is also modified: the IPN curve is approximately linear, suggesting the relationship

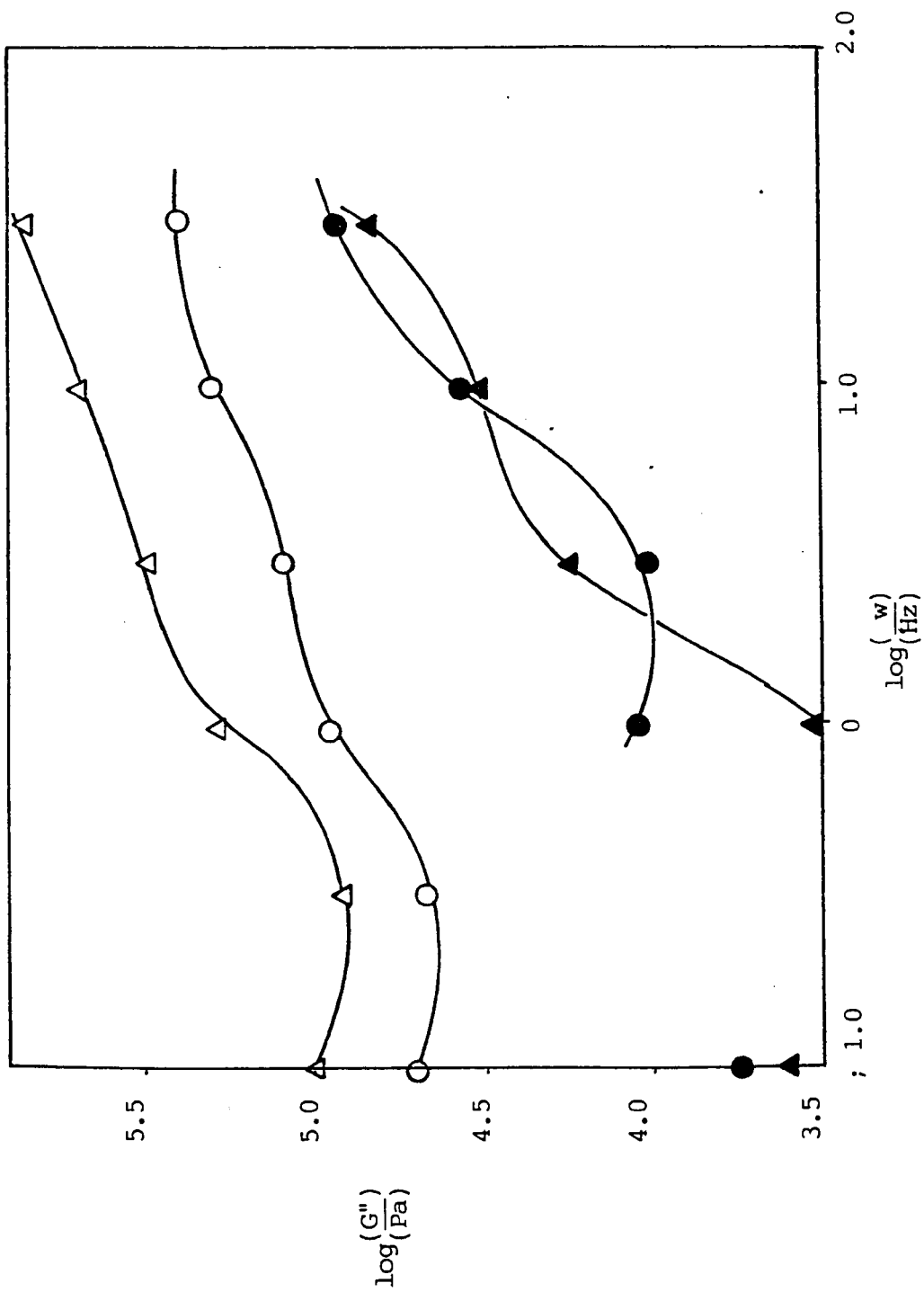


Fig. 5-18e: Loss Modulus vs. Frequency for IPN Hydrogels Containing a 50/50 Molar MMA/(HEMA/MAA) Terpolymer



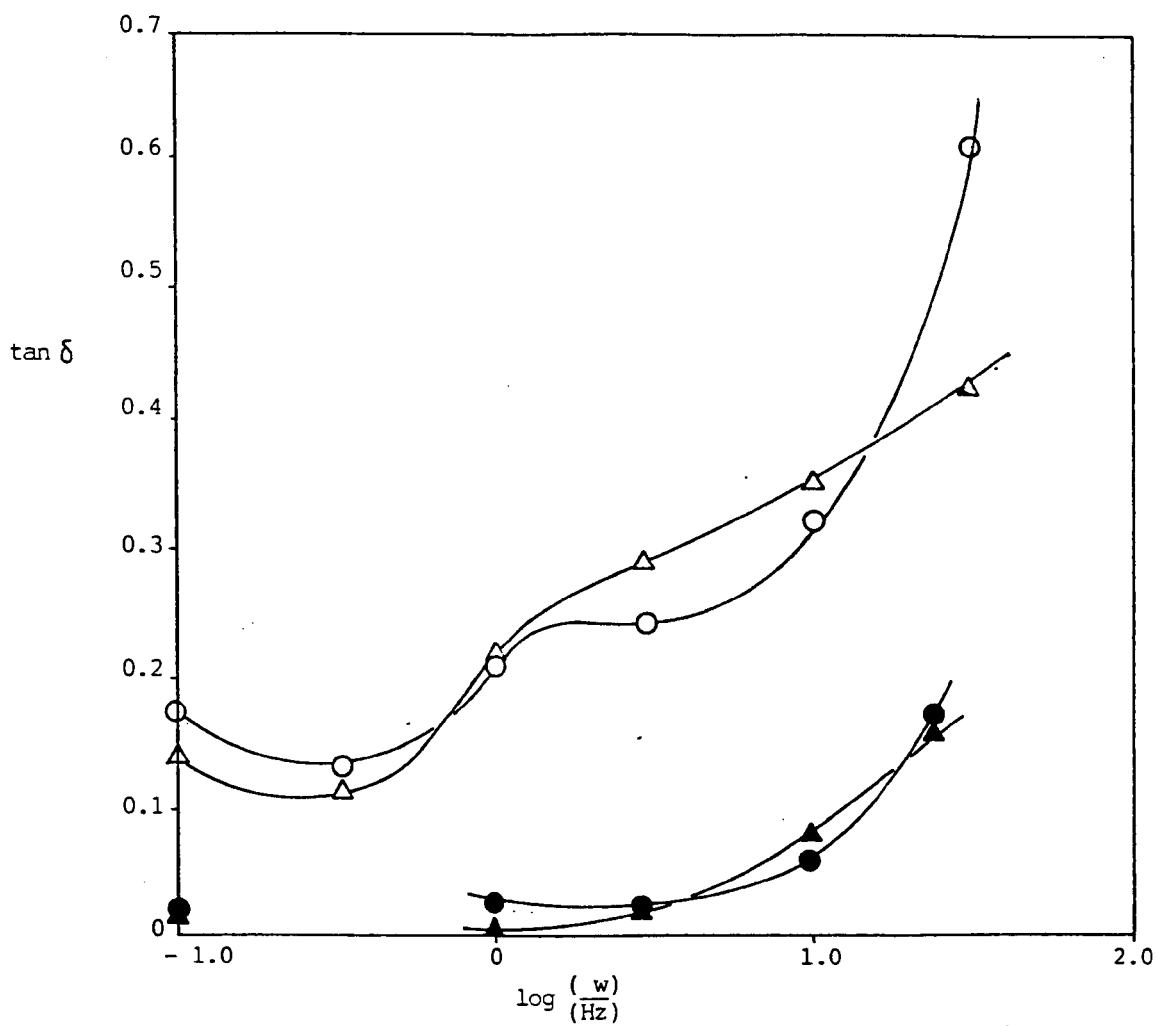


Fig. 5-18f:  $\tan \delta$  vs. Frequency for IPN Hydrogels Containing a  
50/50 MMA/(HEMA/MAA) Terpolymer

KEY:

○ 95/5 HEMA/MAA Copolymer

● IPN 140

△ IPN 141

▲ IPN 144

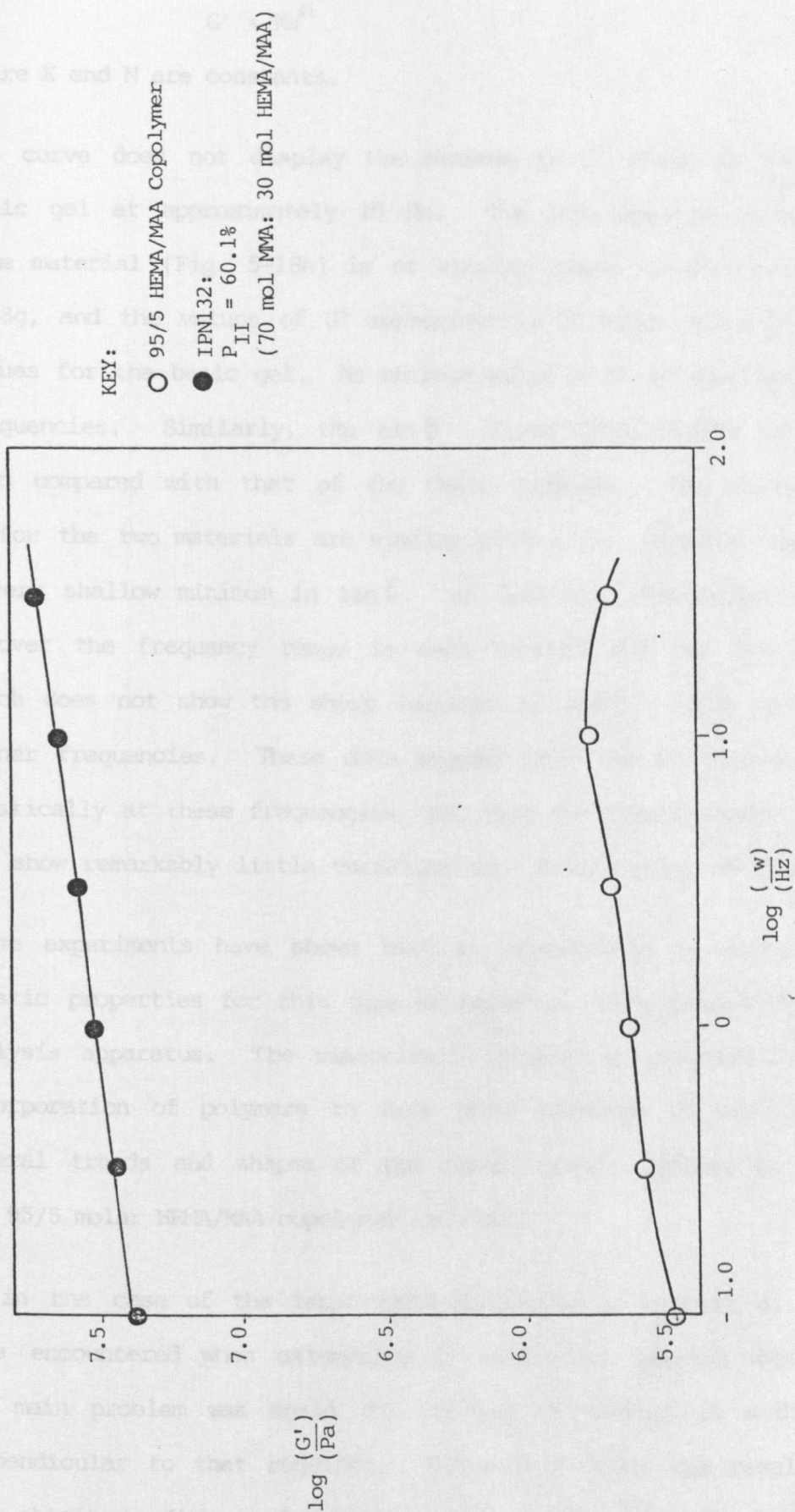


Fig. 5-18g: Storage Modulus vs. Frequency for IPN Hydrogels Containing a 70/30 MMA/(HEMA/MAA) Terpolymer

$$G' = KW^N \quad (....5-45)$$

where K and N are constants.

The curve does not display the maximum in  $G'$  shown by that of the basic gel at approximately 10 Hz. The loss modulus curve for the same material (Fig. 5-18h) is of similar shape to the curve in Fig. 5-18g, and the values of  $G''$  approximately 50 times the corresponding values for the basic gel. No minimum value of  $G''$  is observed at lower frequencies. Similarly, the  $\tan \delta$  curve (Fig. 5-18i) is modified when compared with that of the basic hydrogel. The values of  $\tan \delta$  for the two materials are similar at 0.1 Hz. However the IPN has a very shallow minimum in  $\tan \delta$  at 0.25 Hz. The variation in  $\tan \delta$  over the frequency range is much smaller for the IPN hydrogel, which does not show the sharp increase in  $\tan \delta$  with frequency at higher frequencies. These data suggest that the IPN responds visco-elastically at these frequencies, but that the loss tangents are small and show remarkably little variation over a wide range of frequencies.

These experiments have shown that it is possible to measure visco-elastic properties for this type of material using dynamic mechanical analysis apparatus. The viscoelastic properties are modified by the incorporation of polymers to form IPNs, although in most cases the general trends and shapes of the curves remain similar to those of the 95/5 molar HEMA/MAA copolymer hydrogel.

As in the case of the terpolymers described in Chapter 4, problems were encountered when attempting to carry out tearing experiments. The main problem was again the tearing of samples in a direction perpendicular to that required. Table 5-15 shows the results which were obtained. Values of tearing energy,  $T$ , were calculated as described

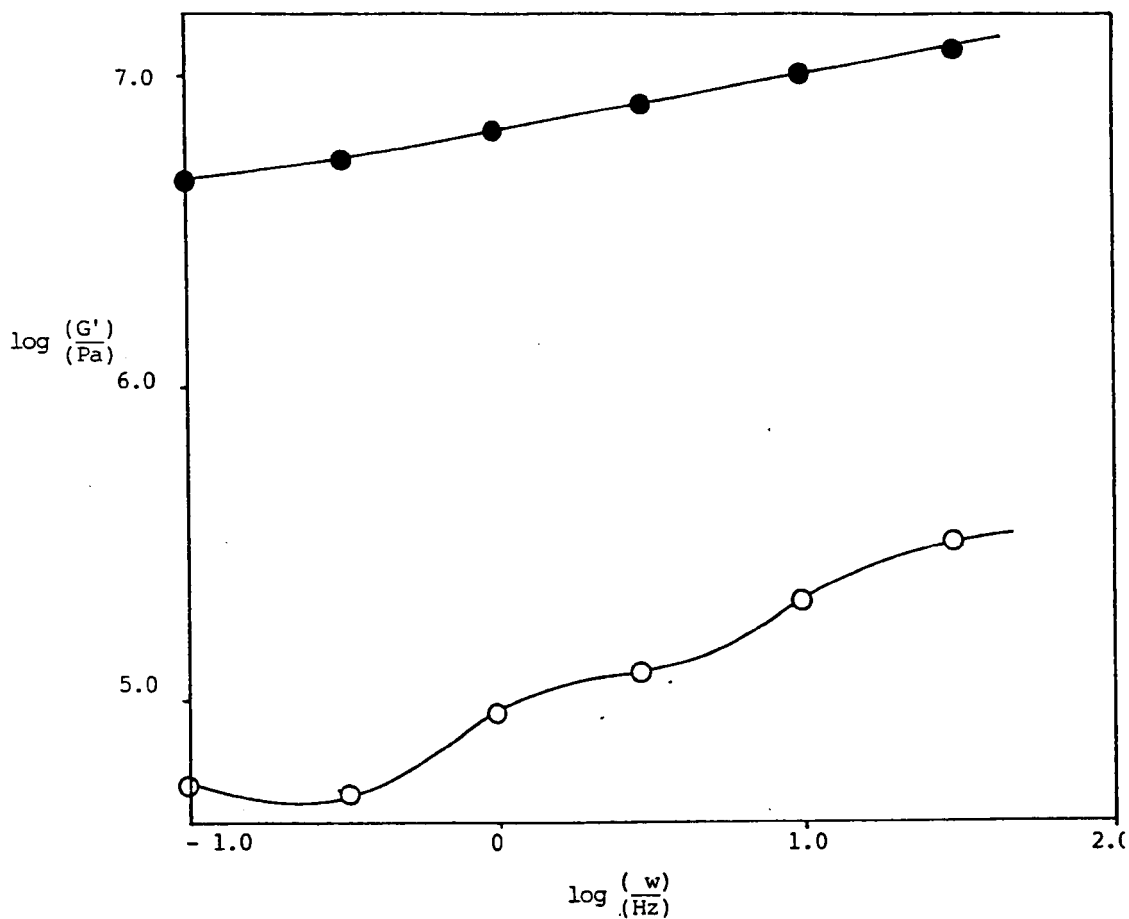


Fig. 5-18h: Loss Modulus vs. Frequency for IPN Hydrogels Containing a 70/30 Molar MMA/(HEMA/MAA) Terpolymer

KEY:

○ 95/5 HEMA/MAA Copolymer

● IPN 132

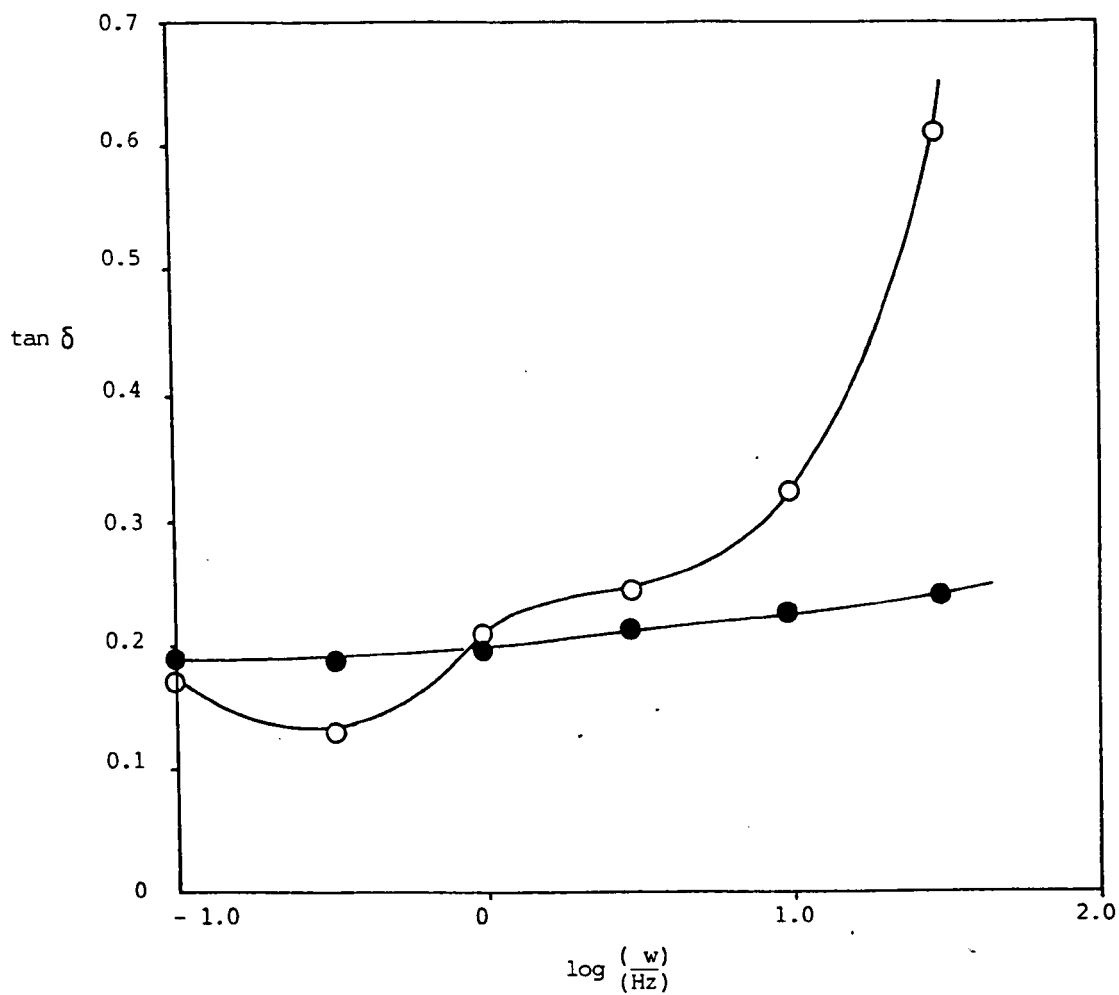


Fig. 5-18i: Tan  $\delta$  vs. Frequency for IPN Hydrogels Containing a 70/30 Molar MMA/(HEMA/MAA) Terpolymer

KEY:

○ 95/5 HEMA/MAA Copolymer

● IPN 132

in Chapter 4. Table 5-15 shows that for the IPN hydrogels containing the 50/50 molar MMA/(HEMA/MAA) copolymer (HEMA/MAA = 95 molar),  $T$  increases with increasing  $P_{II}$ . Qualitatively, the tearing energy is expected to increase with increasing  $P_{II}$  and therefore with decreasing water content, since as  $P_{II}$  is increased, both the surface free energy and the low-extension modulus of the material increase.

Table 5-15: Tearing Results for IPN Hydrogel

material	polymer II	$P_{II}/\%$	tearing energy/ $Jm^{-2}$
IPN132	70 MMA/30 HEMA- MAA	60.1	324
IPN141	50 MMA/50 HEMA- MAA	44.6	237
IPN126	50 MMA/50 HEMA- MAA	58.7	487
IPN127	50 MMA/50 HEMA- MAA	62.5	591

However, the value of  $T$  for IPN132 hydrogel is smaller than  $T$  for IPN126 and 127 hydrogels, although it is greater than that of the 95/5 HEMA/MAA copolymer hydrogel. Hence, although the 70/30 molar MMA/(HEMA-MAA) copolymer produces an increase in tensile strength and modulus, better reinforcement from the point of view of tearing energy is provided by the 50/50 copolymer. In addition, the water contents of the 50/50 materials at a given  $P_{II}$  are higher.

## 5.9 USE OF METHYLENE BLUE AS A PHOTSENSITISER

It was found in this work that heating of samples exposed to UV light caused problems of sample inhomogeneity. Therefore the possibility of using a visible light source which causes minimal heating was investigated. These experiments used methylene blue as the photosensitiser together with dibenzoyl peroxide as the polymerisation initiator. The results are shown in Table 5-16.

The results of MB1 show that methylene blue may be used as a photosensitiser, since a sheet of PMMA was produced. This precipitated from the IMS used as the solvent during the polymerisation. However, since the intensity of sunlight is inconsistent and therefore unreliable, a 40-W fluorescent lamp was used for further experiments. It was thought that a lamp of this power would cause minimal heating of the samples.

Using this lamp, experiment MB2 was carried out to explore the possibility of producing an IPN. A photochemical reaction occurred, which was apparent by the loss of blue coloration. However, no polymer II was produced. Similar results were obtained for experiments MB3 and MB4. For MB5, the distance between the lamp and the gel strip was reduced, thereby increasing the incident light intensity at the sample. No change in the gel strip was observed.

For experiments MB6 - MB9, the samples were surrounded with the swelling solution, in an attempt to reduce evaporation. This method also provided a means of subjecting the swelling mixture to the same conditions as the swollen polymer network I. The swelling mixture increased in viscosity, but no evidence of polymerisation within the gel was found.

Table 5-16: Results of the Experiments Using Methylene Blue

experiment	results
MB1	Sheet of yellowish polymer produced.
MB2	Centre part of sheet lost blue colour, became yellow, but no apparent change in physical properties.
MB3	Sheet became colourless, but no other apparent change.
MB4	Sheet became colourless, but no other apparent change.
MB5	After 2 hours, sheet was still blue, and apparently unchanged.
MB6	Sheet still blue and apparently unchanged, but solution around it polymerised.
MB9	No apparent polymerisation.
MB10	No apparent polymerisation.
MB11	One side of the gel became slightly stiffer. Blue colour was lost.
MB12	Edges of sheet became hard polymer - but the centre remained soft.
MB13	No change to the gel, but the solution around it became more viscous.

On exposure of the swollen gels to UV light, an increase in stiffness was observed (MB11 - MB13). However, it was concluded that no advantage would be gained by using methylene blue as an alternative to AZDN as a photosensitiser.



## 5.10 LATEX IPNs

Dispersions of polymers such as PMMA in hydro-carbon dispersion media have been investigated by other workers, and an extensive review is available on the general subject of dispersion polymerisation in organic media (199). Latex IPNs, comprising core-shell latices, have also been reviewed (140). The possibility of combining the two ideas was investigated, the envisaged product being a dispersion containing particles, the core of which was PMMA and the shell poly(HEMA).

Evaporation of the solvent or coagulation of the dispersion might then produce a matrix of poly(HEMA) filled with small PMMA phase domains.

Initially, a dispersion of PMMA in heptane was prepared, as described in Section 3.3.10.1 (i) and (ii). Similar experiments were described in ref. 199, p. 120. The dispersant which was formed was in the form of a solution in heptane, the solution being slightly more viscous than water.

During the seed stage of the polymerisation, when a large number of small particles was produced, the reaction mixture became white and opaque. On adding the main monomer feed mixture, the dispersion showed no signs of coagulation until approximately 20 ml had been added. The dispersion then coagulated.

In experiment (b) of Section 3.3.10.1 (ii), the seed process alone was carried out. This resulted in a dispersion, the particle size of which was 446 nm (Nanosizer, averaged over 4 min.). The polydispersity reading was 4. Hence the polydispersity was quite high, and the particles were large, which may explain the coagulation described above, since it is thought that the particles attained a size too great to form a stable dispersion. The solids content of the dispersion

was 4.9% w/w, which indicates a conversion of monomer to polymer of 33%.

An investigation was made into the possibility of forming a similar dispersion of poly(HEMA), instead of PMMA, and subsequently co-coagulating the two dispersions. This would result in a material similar to Sperling's "Interpenetrating Elastomeric Networks (IENs)" (140). Hence an experiment was carried out (Section 3.3.10.1 (ii) (c)) in which MMA was replaced by HEMA in the dispersion polymerisation. A dispersion was formed, but a large amount of solid polymer was also present. The average particle size of the dispersion was 1786 nm, and the polydispersity reading 9. Further experimental work is required in order to find a more suitable dispersant for this type of dispersion.

In order to reduce the large size of the PMMA particles, the concentration of dispersant solution in the dispersion polymerisation mixture was increased (Section 3.3.10.1 (ii) (d)). This produced a dispersion of particle size 252 nm and the polydispersity reading was 2. Reducing the dispersant concentration (Section 3.3.10.1 (ii) (e)) resulted in an average particle size of over 3000 nm (the upper limit of the Nanosizer being 3000 nm).

The attempt to produce a core-shell dispersion (Section 3.3.10.2) resulted in a dispersion with an average particle size of 408 nm, and a polydispersity reading of 3 - 6. The particle size therefore increased. This is not thought to be caused by the swelling of PMMA particles by HEMA, since the hydrophilicities of HEMA and MMA are dissimilar. Therefore the tentative conclusion is that a core-shell material was produced. However, it was not considered that subsequent investigation on this topic would be a useful contribution to this

project, and therefore no further work was carried out. It is possible that further exploration of this subject by other workers might yield reinforced, water swellable IENs.

## CHAPTER SIX

### FILLED HYDROGELS:

### RESULTS AND DISCUSSION

## 6.1 INTRODUCTION

The third method for modification of the physical properties of hydrogels which was investigated was the incorporation of polymeric particles into the hydrogel matrix. The chosen polymer was poly(methylmethacrylate) (PMMA). It is glassy at room temperature, with a Young's modulus of 3000 MPa and a tensile strength of 56 - 70 MPa (201). Initially it was proposed that the method of reinforcement should be by the addition of IMS - dispersed PMMA particles to the monomer mixture, in place of a portion of the IMS. Subsequently the incorporation of dried PMMA latex into hydrogels was attempted.

## 6.2 PREPARATION OF PMMA DISPERSIONS IN IMS (See Section 3.4.1)

### 6.2.1 DISP 1

On cooling the mixture, the polymer precipitated, coacervating to form a solid mass. During the polymerisation the mixture did not show turbidity or opacity. At room temperature, PMMA is negligibly soluble in IMS, but this experiment shows that the polymer is soluble at elevated temperatures. Haynes (202) confirmed this. Barrett and Thomas (195) gave values of the solubility parameter,  $\delta$ , shown in Table 6-1 for MMA, PMMA and ethanol. Since the coefficient of thermal expansion is greater for ethanol than for PMMA, the difference between the solubility parameters decreases with increasing temperature. Hence it is expected that the solubility of PMMA increases as the temperature is increased, a trend similar to that of polystyrene in alcohols (ref. 195, p. 123).

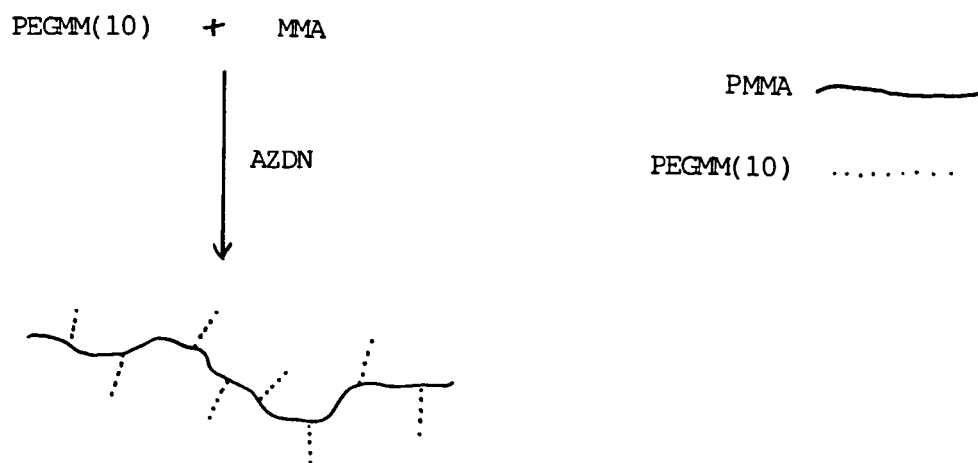
Table 6-1: Solubility Parameters of Various Materials  
(From Ref. 195)

material	$\frac{\delta}{[\text{cal cm}^{-3}]^{\frac{1}{2}}}$
MMA	8.8
PMMA	9.3
ethanol	12.7

As a result of the solubility of PMMA in IMS at elevated temperatures, the reaction is solution rather than dispersion polymerisation. Consequently large particles are formed, which quickly agglomerate. It was found however (Section 6.2.3) that by using a modified dispersant, a suspension of smaller, more monodisperse particles could be obtained.

### 6.2.2 Pre-formed Dispersants

In reactions (a) and (b) a flaky white polymer was precipitated. Reaction (c) resulted in a cloudy solution at room temperature, with a slightly pinkish coloration. The composition of the polymers resulting from reactions (a) and (b) was 50% w/w MMA (84 mol % MMA assuming high conversion and similar reactivity ratios). The turbidity produced in reaction (c) was similar to the opalescence observed in the initial stages of dispersion polymerisation. The pink coloration might be a manifestation of the Tyndall effect, which is caused by the presence of small monodisperse particles (ref. 195, p. 116). These might be micellar, consisting either of one polymer molecule per micelle, or groups of aggregated polymer molecules. The polymerisation is shown diagrammatically below:



### 6.2.3 DISP 2

A clear solution was formed. On cooling, a very fine precipitate was observed. Sedimentation of the precipitate was slow. The particle size was measured, and found to be 200 - 500 nm; the polydispersity reading (Coulter Nanosizer) was 0 to 3. The similar reaction DISP 1 produced larger particles, which agglomerated. However, DISP 2 was

carried out in more dilute solution, and the dispersant was more hydrophilic, i.e. the ratio of the "soluble" component to the "anchor" component was higher (ref. 195, ch. 3). The particle size, although small enough to ensure that sedimentation occurred in a matter of days rather than minutes, was larger than examples given in Chapter 5 of ref. 195 for various dispersions, which were generally of the order of 100 nm.

#### 6.2.4 DISP 3

On cooling, an orange solution resulted. No precipitation of polymer occurred. It is thought that an oxidation reaction involving atmospheric oxygen and the tertiary amine had occurred. This prevented the amine from participating in the redox initiation reaction. The reaction was carried out at room temperature to facilitate dispersion polymerisation rather than solution polymerisation, since the polymer is soluble in IMS at higher temperatures.

#### 6.2.5 DISP 4

Purging with nitrogen was used to minimise the effect of atmospheric oxygen, assuming that atmospheric oxygen prevents polymerisation (Section 6.2.4). A turbid dispersion was formed, with an orange coloration, which indicates that some oxidation had occurred. The average particle size was 520 nm, and the polydispersity reading was 1. The solids content was 4.2g per 100g of dispersion, corresponding to a conversion of 41.3%. Dispersions of PMMA in IMS can therefore be prepared, but the particle size is large, although the polydispersity is low. The polymer particles sedimented in approximately 1 day, leaving a clear pinkish serum.



#### 6.2.6 DISP 5

In order to prepare dispersions of higher solids content, the ratio monomer/IMS in the polymerisation mixture was increased. The resulting dispersion was turbid with a slight pink coloration. The average particle size was 303 nm, the polydispersity reading being 4. The solids content was 2.0g per 100g of dispersion, indicating a conversion of 18.3%.

#### 6.2.7 Use of a Comb-Type Graft Copolymer Dispersant

Poly(vinyl pyrrolidone) (PVP) was the "soluble" component and PMMA the "anchor" component. The resulting polymer was not soluble in IMS. By varying the PMMA/PVP ratio it might be possible to produce an IMS - soluble polymer. Methods for using and synthesising this type of dispersant have been given by Waite and Thompson (200). Methods of synthesis for several types of dispersant are outlined in Chapter 3 of ref. 195.

### 6.3 FILLED HYDROGELS

#### 6.3.1 FIL 1 to FIL 7

##### 6.3.1.1 FIL 1 and FIL 2

The two hydrogels filled with dispersion DISP 1 were opaque gels. Coagulation was evident, i.e. flocs could be seen in the gels. It appears that the stability of the particles is destroyed by the addition of monomers, causing flocculation.

##### 6.3.1.2 FIL 3 to FIL 7

The dispersion used in these composite materials was of smaller particle size than that used for gels FIL 1 and FIL 2. The gels appeared similar to those in 6.3.1.1 above, and some data are shown in Figs. 6-1 and 6-2 as a function of composition. The equilibrium water content (Fig. 6-1) decreased almost in proportion to the percentage of added PMMA, although the EWC was slightly higher than might be expected from additivity. On reducing the proportion of hydrogel from 100% to 90%, the water content decreases to 93% of its original value.

The tensile strength (Fig. 6-2) increased with increasing filler content. This is similar to the effect of adding reinforcing fillers to rubbers, as described in Section 2.2. The reinforcement effect indicates that good adhesion is obtained between the hydrogel and the PMMA particles, a criterion which is necessary for reinforcement, as Oberth (203) showed. A question which may deserve investigation in future work is whether the flocculation of the PMMA particles produces agglomerates which act in the same way as "structured" carbon black particles, the "structure" of the latter increasing the degree of reinforcement imparted by the filler.

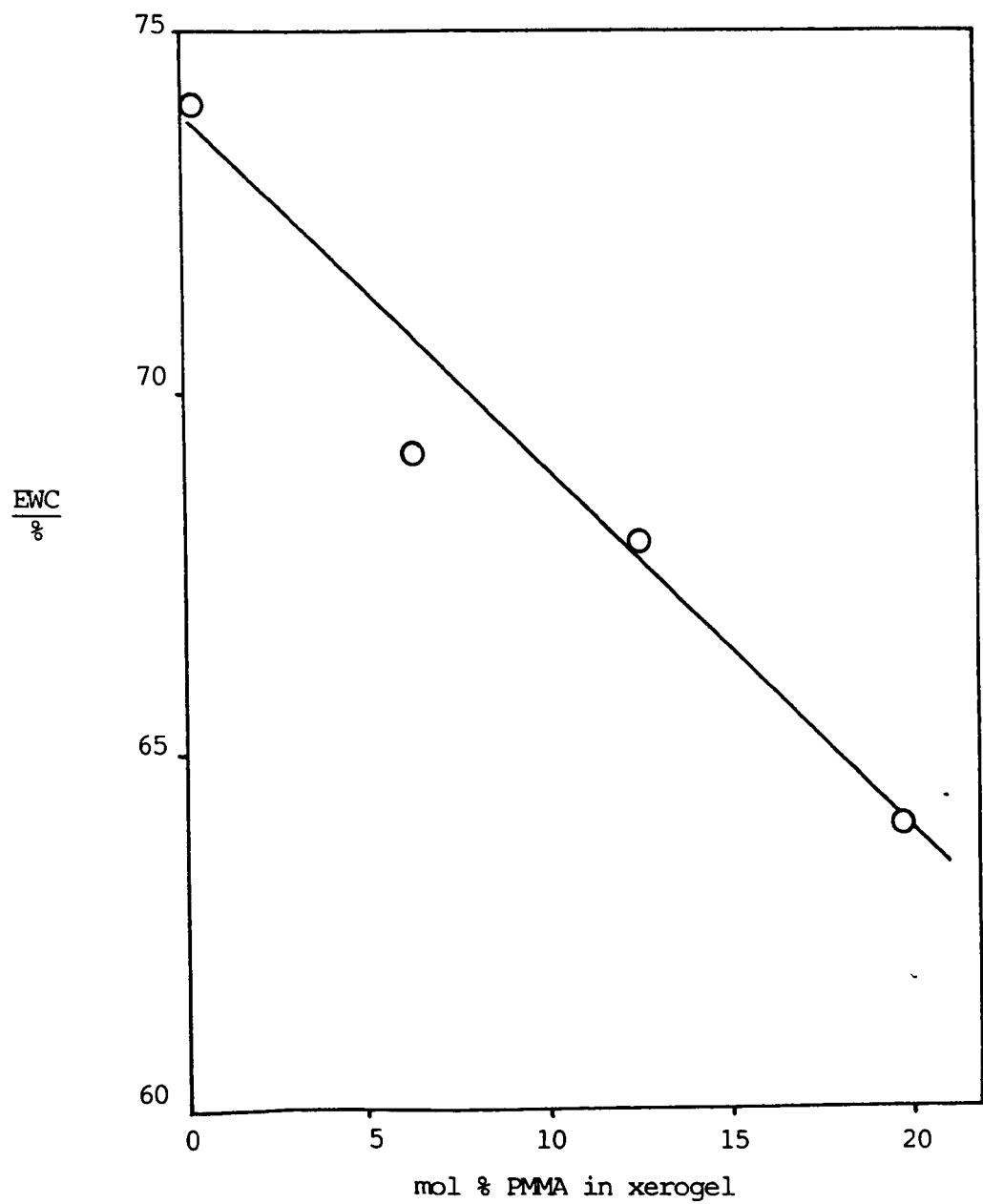
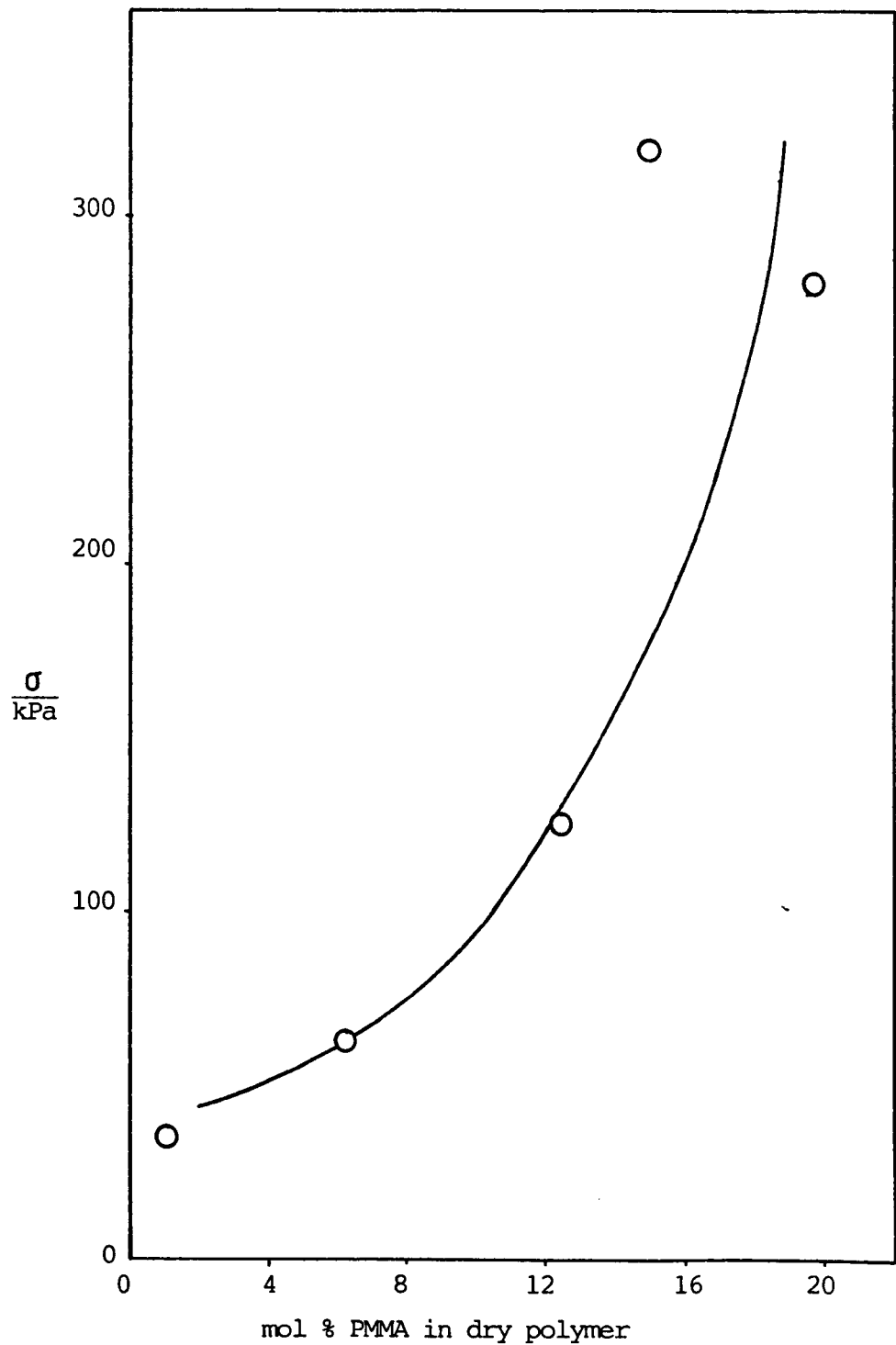


Fig. 6-1: EWC vs. Composition for Filled Hydrogels

Fig. 6-2: Tensile Strength vs. Composition for Filled Hydrogels



Janacek et al (126) prepared filled poly(HEMA) hydrogels containing 10% by volume of various poly(HEMA) fillers having different crosslink concentrations. The particle size was 1  $\mu\text{m}$ . They observed a reinforcing effect which increased with increasing crosslink concentration of filler. This was explained as follows: during polymerisation, HEMA monomer swells the poly(HEMA) particles, and hence interpenetrating networks are formed. This mechanism is unlikely to operate during the formation of PMMA-filled materials, since HEMA is significantly more hydrophilic than PMMA, and would therefore be unlikely to swell the PMMA particles.

Ilavsky et al studied similar materials (127), and observed that the reinforcing effect increases with increasing volume fraction of filler for most materials. The filler particle size was in this case 2.5  $\mu\text{m}$ . Fig. 6-3 shows results for materials prepared in this work. As the water content of the materials decreases, the tensile strength increases. The results are compared with those of both the terpolymers and the interpenetrating polymer networks in Chapter 7.

### 6.3.2 Incorporation of Dried Latex into Hydrogels

#### 6.3.2.1 Dried Latices

The average particle size of latex L1 was 70 nm; the polydispersity reading was 1 - 2. Both latices, after drying and attempting to re-disperse in IMS, showed average particle sizes greater than 3000 nm (the upper limit of the Coulter Nanosizer). After treatment in an ultrasonic bath, the particle size remained greater than 3000 nm.

#### 6.3.2.2 Filled Hydrogels

(a) The gel which was formed was opaque when swollen in water. It showed signs of aggregation of the dried latex powder. On immersion

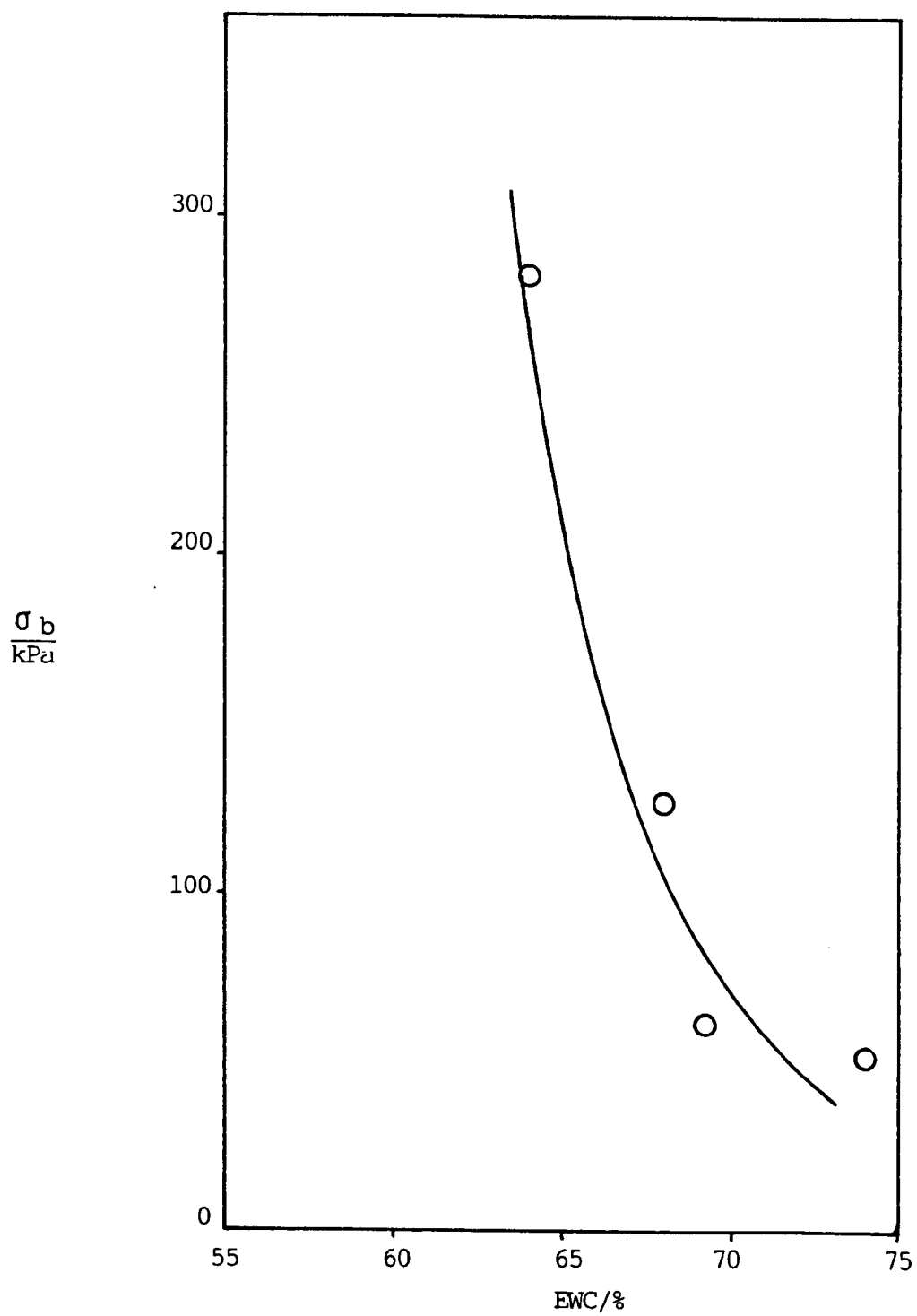


Fig. 6-3: Tensile Strength vs. EWC for Filled Hydrogels

in water, cracking accompanied the swelling of the material. This cracking is thought to have been caused by the presence of large volumes of non-swellable material. Such inhomogeneity, with the resultant cracking, clearly preclude tensile testing.

(b) The gel was opaque. Very fine cracks appeared when it was swollen in water. Its EWC (0.1M sodium bicarbonate solution) was 62.7% by weight. The tensile strength of the swollen material was 240 kPa. The absence of cracking when swelling in aqueous solution is thought to be the result of the smaller proportion of PMMA, compared with (a) above.

(c) The gel was similar in appearance to (a) and (b) above. Its tensile strength was 141 kPa.

#### 6.4 SUMMARY

It has been shown in previous work (126, 127) that reinforcement of hydrogels by the incorporation of polymer particles may be effected. This work has shown that it is possible to improve the tensile strength of high-water content hydrogels by the addition of particles of a glassy, non-water-absorbing polymer. However, there are two main difficulties involved with this type of reinforcement:

- (i) the difficulty of producing a monodisperse PMMA dispersion of small particle size in IMS or a similar dispersion medium;
- (ii) the fact that coagulation of the polymer particles occurs when the disperison is added to the hydrogel polymerisation mixture.

The solution of the former problem is outside the scope of this project, and hence this section of the work has been left at the exploratory stage. It is hoped, however, that further work on this topic might be stimulated. It might be possible that by using much smaller particles and eliminating flocculation, much greater increases in tensile strength could be obtained.



## CHAPTER SEVEN

### COMPARISON OF THE VARIOUS METHODS OF

### HYDROGEL MODIFICATION

### 7.1 EQUILIBRIUM WATER CONTENT (EWC)

Fig. 7-1 shows values of EWC for terpolymer, IPN and filled hydrogels. Increasing the hydrophobicity of the reinforcing agent reduces the EWC of the resulting material, both for IPN and terpolymer hydrogels. The EWCs of the filled materials were similar to those of MMA terpolymers of similar overall composition. Comparing IPN hydrogels containing PMMA with terpolymer hydrogels containing MMA, the EWC values for the IPN hydrogels were generally higher than those for the terpolymer hydrogels. It can be tentatively postulated that the effective cross-link concentration of the dry polymer is increased to a greater extent by terpolymerisation than by IPN formation.

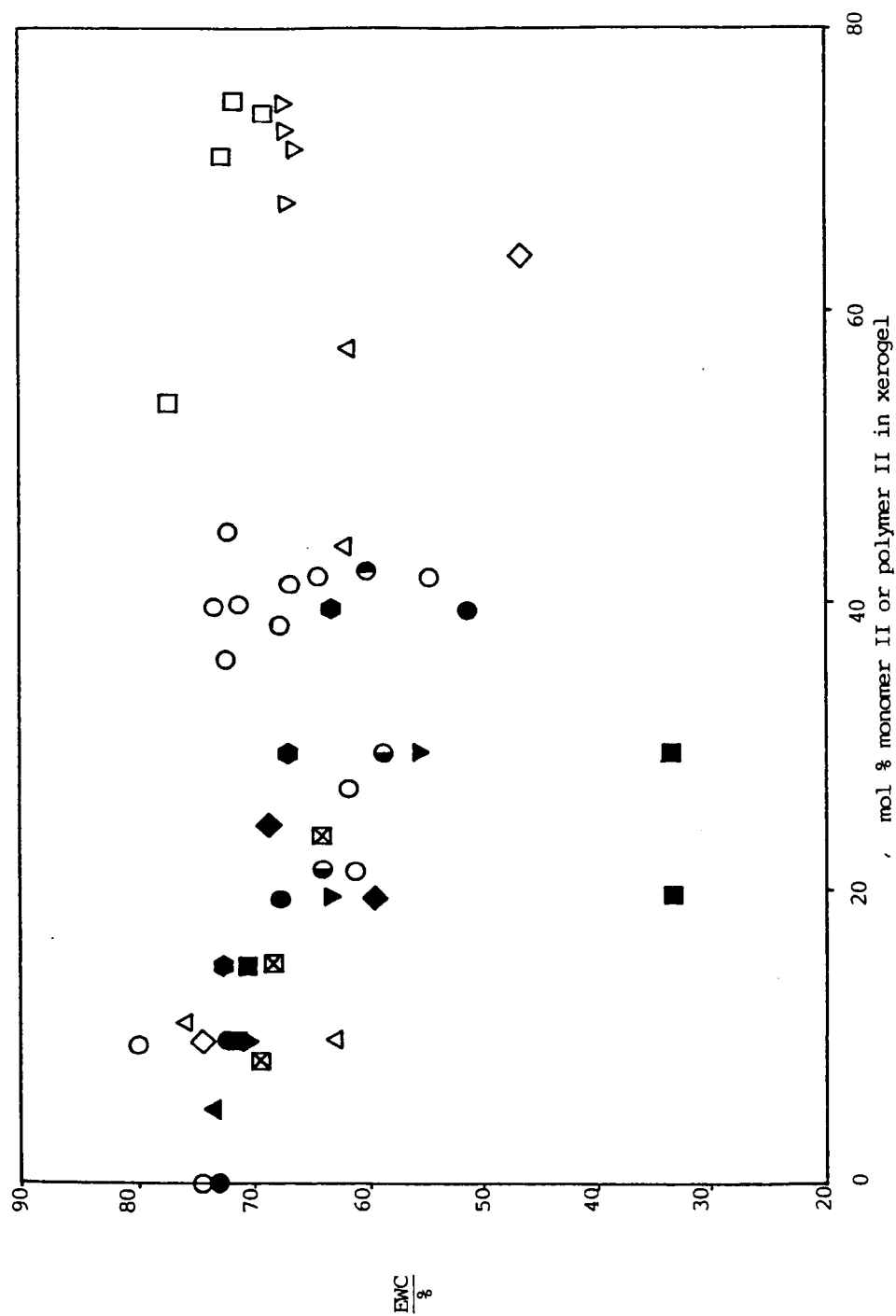


Fig. 7-1: EMC vs. Composition for Terpolymers, IPNs and Filled Hydrogels

KEY: Terpolymers : Monomer II

- MMA
- ▲ Styrene
- ⬡ HPMA
- DDA
- ◆ PPM 6
- ▼ EHA

IPNs : Polymer II

- PMMA (Section 5.8.1)
- PMMA (Section 5.4)
- ⊙ PMMA (Section 5.5.3)
- △ 50 mol MMA:  
50 mol HEMA/MAA
- ▽ 95 mol HEMA:  
5 mol MAA
- 95 mol HEMA:  
5 mol MAA: 0.4% EGDMA
- ◇ 70 mol HEMA:  
30 mol MAA

Filled Hydrogels

- ☒ PMMA

## 7.2 TENSILE STRENGTH ( $\sigma_b$ )

Fig. 7-2 shows tensile strengths of the three types of modified hydrogels vs. composition. Fig. 7-3 shows some of the data on a different tensile strength scale. Fig. 7-2 shows that, at a given composition, the IPN hydrogels containing either PMMA or the 70/30 molar MMA/(HEMA/MAA) terpolymer display greater tensile strengths than any other material which was studied. The data may be divided into two groups (Fig. 7-2):

- (i) hydrogels based upon more hydrophilic materials, such as the HPMA terpolymers and homo-IPNs, where the tensile strength does not rise steeply with increasing mol % polymer II;
- (ii) hydrogels based upon more hydrophobic materials, such as the DDA terpolymers and the IPNs containing the 50/50 MMA/(HEMA/MAA) copolymer. The IPN hydrogel containing the 70/30 MMA/(HEMA/MAA) copolymer had a very high tensile strength. This group of IPN hydrogels appears to merit further investigation.

Figs. 7-4 and 7-5 show the tensile strengths of materials vs. water content. The data of Fig. 7-4 may be divided into two sets, as above. However, this diagram shows that the IPNs are stronger at a given water content. The two sets of data are for (i) hydrophobic IPN hydrogels, and (ii) hydrophilic IPN and terpolymer hydrogels respectively.

Fig. 7-5 shows that at higher water contents the data are rather scattered. Perhaps the only significant trend at these water contents is that, in general, the tensile strengths of the IPN hydrogels are higher than those of the terpolymer hydrogels at a given EWC.

Kolarik and Migliaresi (47) obtained results for tensile strengths vs. EWC for various copolymers of HEMA with butyl acrylate, ethyl

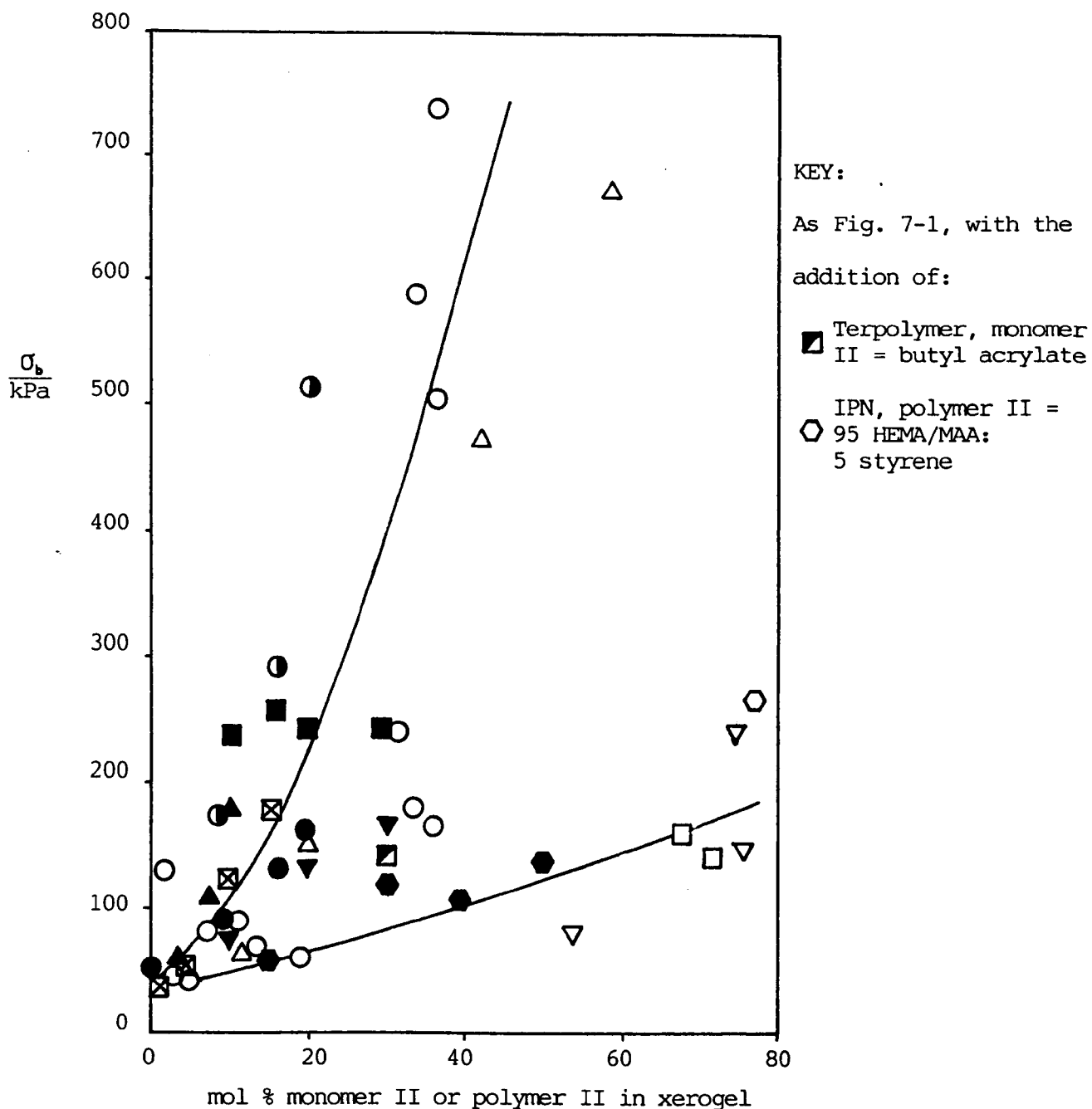


Fig. 7-2: Tensile Strength vs. Composition for Terpolymer, IPN and Filled Hydrogels

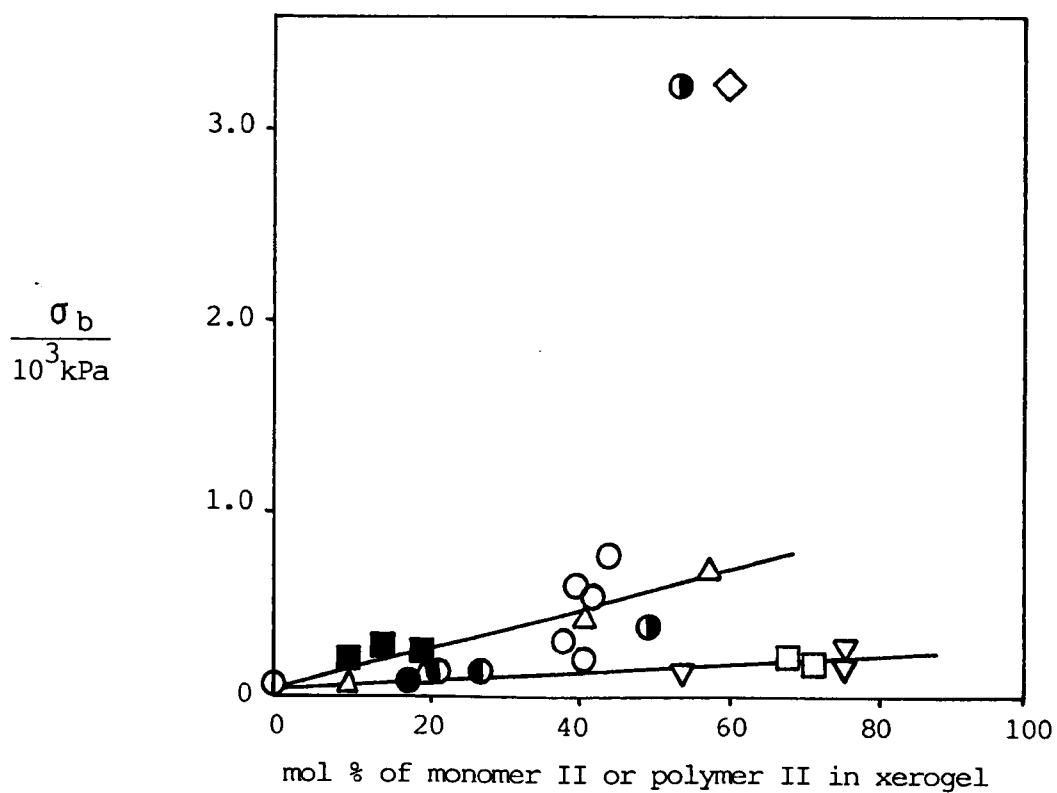


Fig. 7-3: Tensile Strength vs. Composition for Tepolymer, IPN and Filled Hydrogels

KEY:

As Fig. 7-1

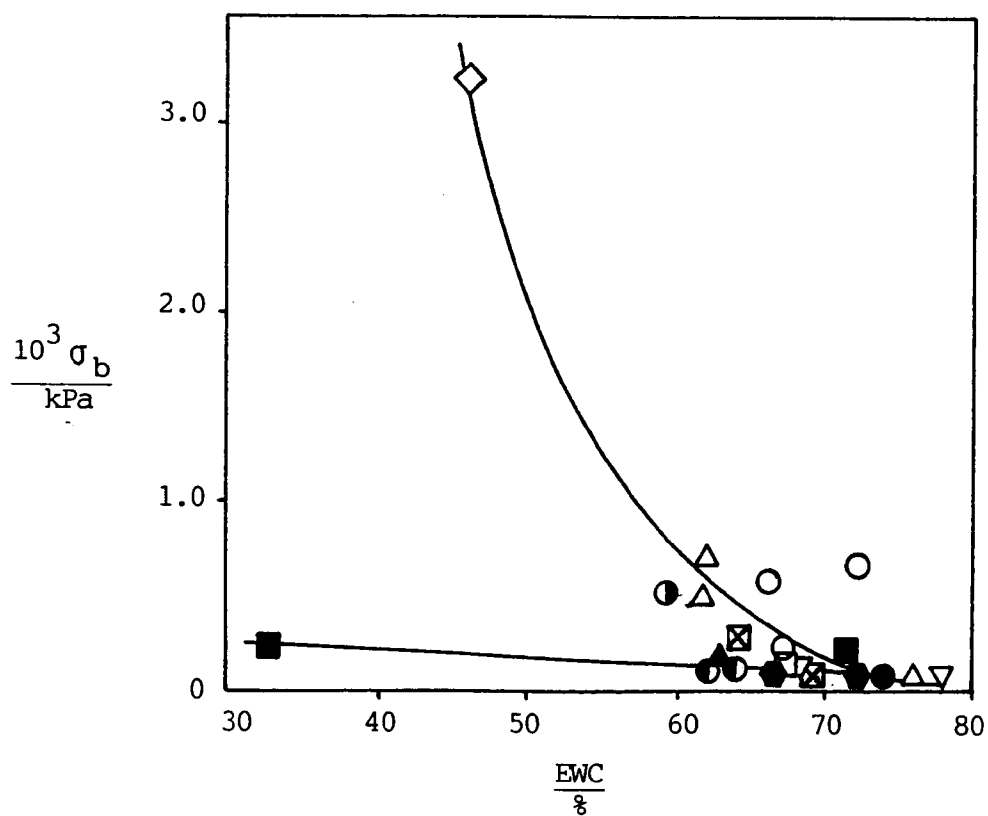


Fig. 7-4: Tensile Strength vs. EWC for Terpolymer, IPN and Filled Hydrogels

KEY:

As Fig. 7-1



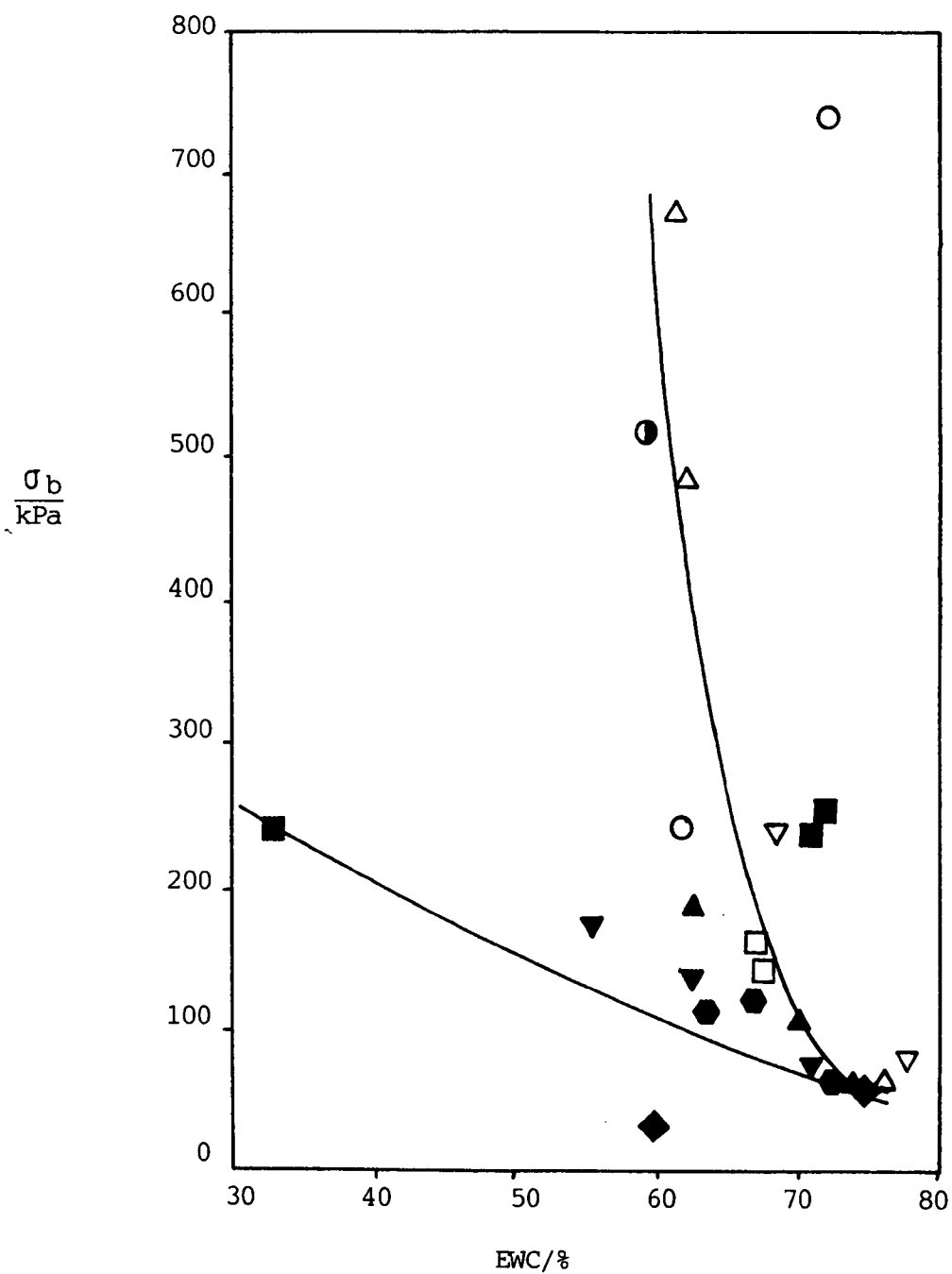


Fig. 7-5: Tensile Strength vs. EWC for Terpolymer IPN and Filled Hydrogels

KEY:

As Fig. 7-1

acrylate and dodecyl methacrylate. If materials are required which combine high water content with high tensile strength, however, then materials such as the IPN containing the 70/30 MMA/(HEMA/MAA) copolymer are superior to the copolymers of Kolarik and Migliaresi. For example, they prepared a 46/54 dodecyl methacrylate/HEMA copolymer which had a tensile strength of 4020 kPa. However, its EWC was only 12%. A 14/86 dodecyl methacrylate/HEMA copolymer had a tensile strength of 2060 kPa and an EWC of 26%. The highest water content exhibited by the materials was that of poly(HEMA) (approximately 40%).

Janacek, Stoy and Stoy (103) produced materials whose water contents and tensile strengths exceeded those reported by Kolarik and Migliaresi and obtained in this work. These materials were partially-hydrolysed polyacrylonitrile networks. For example, one hydrogel had an equilibrium water content of 53.9% and a tensile strength of 4160 kPa.

### 7.3 STRAIN AT BREAK ( $\epsilon_b$ )

The strain at break is shown for both terpolymer and IPN hydrogels vs. composition in Fig. 7-6. DDA terpolymer hydrogels have the largest values of  $\epsilon_b$  at a given composition. Values for IPN hydrogels are generally lower than those for terpolymers. HPMA terpolymer hydrogels have intermediate breaking strains between those of the homo-IPN hydrogels and those of the more hydrophobic materials such as DDA terpolymer hydrogels.

Fig. 7-7 shows strain at break vs. water content. Most of the IPN and terpolymer hydrogels fall on a curve. A maximum value of  $\epsilon_b$  of 140% occurs when the EWC is 61%. This suggests that for these hydrogels, the EWC controls the strain at break, and that  $\epsilon_b$  is unaffected by changes in morphology. An attempt was made to explain the cause of this maximum in Chapter 5. The second feature of Fig. 7-7 is the curve for the DDA terpolymers. At a given water content, the strains at break were significantly greater than those of any other hydrogel which was studied. Hence, in applications where a high strain at break is required, the DDA terpolymers would be preferred. Janacek, Stoy and Stoy (103), however, prepared materials with higher values of  $\epsilon_b$  at high water contents. For example, a partially-hydrolysed acrylonitrile polymer hydrogel of 68.4% EWC had a strain at break of 1000%.

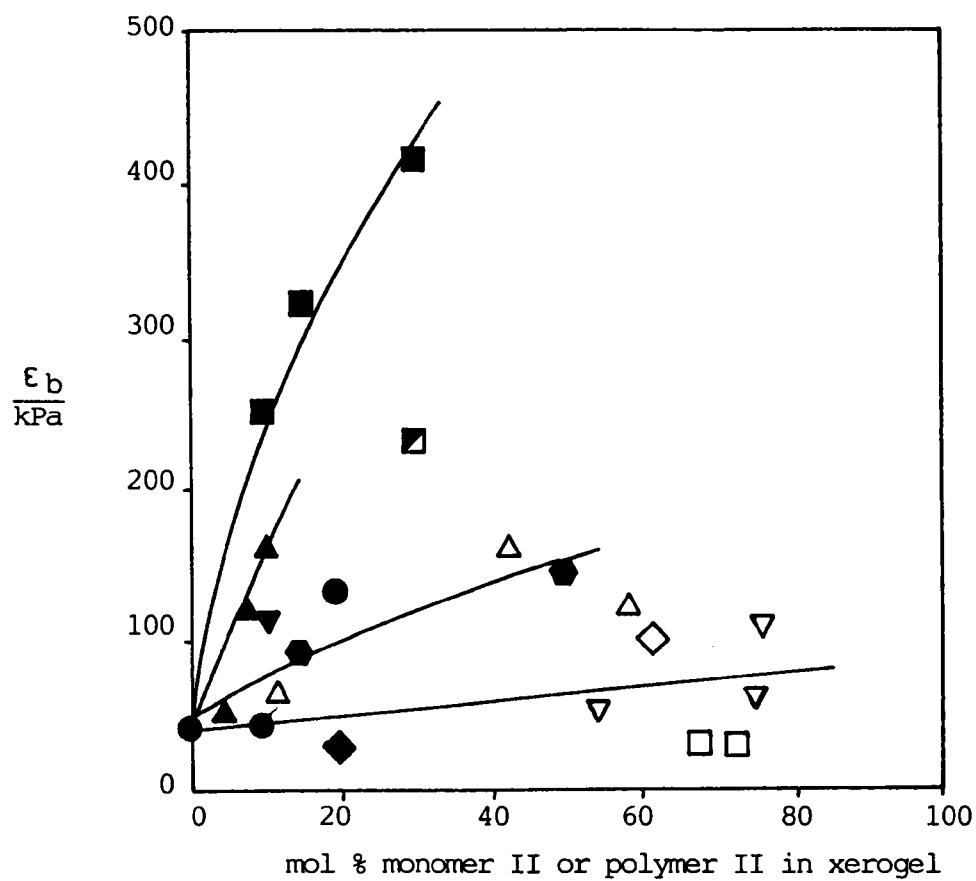


Fig. 7-6: Strain at Break vs. Composition for Terpolymer, IPN and Filled Hydrogels

KEY:

As Fig. 7-1

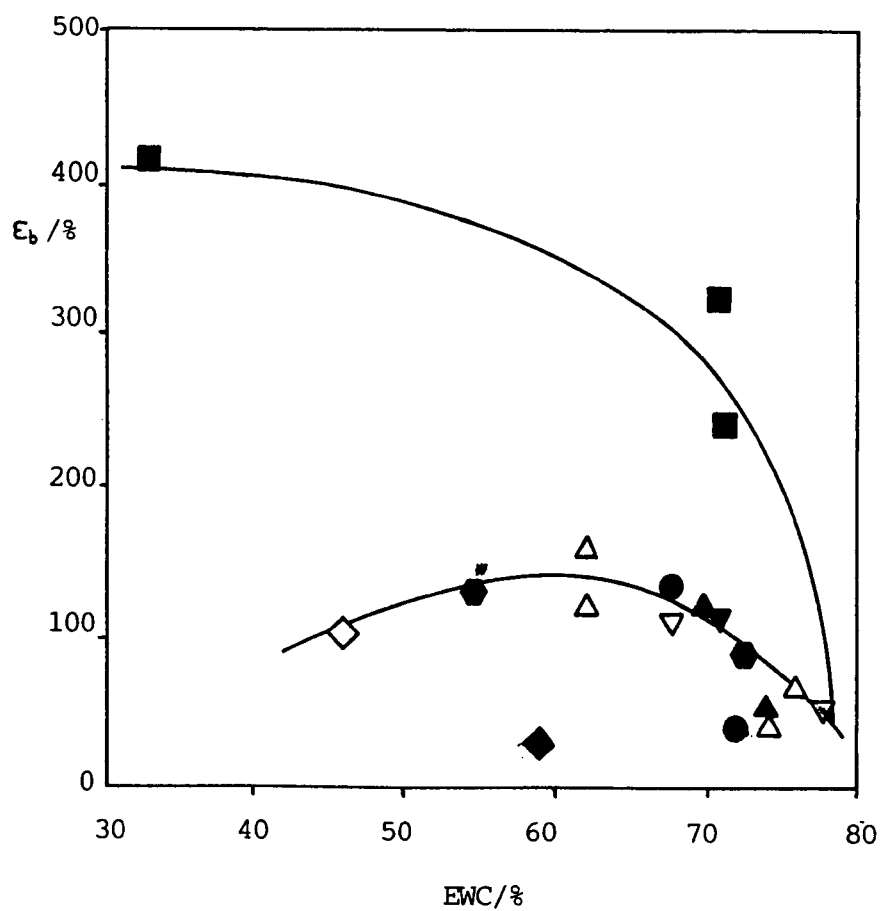


Fig. 7-7: Strain at Break vs. EWC for Terpolymer and IPN Hydrogels

KEY:

As Fig. 7-1

● EWC extrapolated from Fig. 4-44

#### 7.4 TEARING ENERGY (T)

Fig. 7-8 shows the tearing energy,  $T$ , of various terpolymer and IPN hydrogels was smaller than  $T$  for terpolymer hydrogels. Exceptions were the PPM6 and HPMA terpolymers. The curves for the 50/50 MMA/(HEMA/MAA) IPN hydrogels are generally of similar shape to those of the terpolymers. The exception is the DDA terpolymer curve. The 70/30 MMA/(HEMA/MAA) IPN hydrogel has a tearing energy similar to that of the 10% styrene terpolymer. The tearing energies of two of the 50/50 MMA/(HEMA/MAA) IPN hydrogels, however, are higher than that of the 10% styrene terpolymer, even though the EWCs are similar (58.8% for the 58.7% IPN hydrogel, 61.7% for the 62.5% IPN hydrogel and 63.0% for the terpolymer hydrogel).  $T$  for the 62.5% IPN hydrogel is greater than that of the 30% DDA terpolymer hydrogel, and the water content of the IPN hydrogel almost twice that of the terpolymer hydrogel: the EWC of the 30% DDA terpolymer hydrogel was 33.1%. Thus, the data indicate that the formation of IPNs results in a greater improvement of hydrogel tear resistance at a given water content than copolymerisation with hydrophobic monomers. No systematic study of tearing energies of hydrogels has been published previously. It is suggested that such a study should be made, since this work has shown that, as higher values of  $T$ ,  $T$  can be measured by the "trouser" test method, previously applied to conventional rubbers.

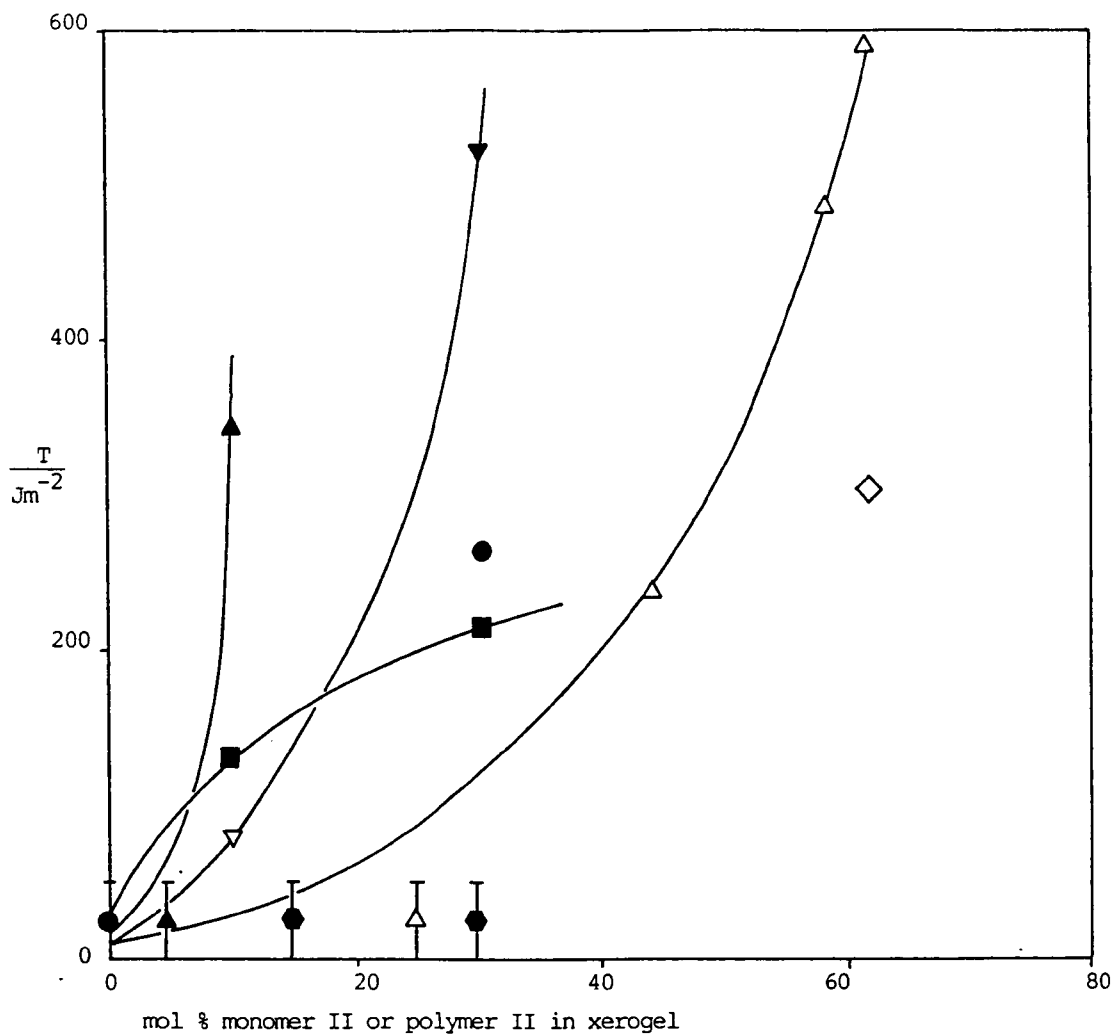


Fig. 7-8: Tearing Energy vs. Composition for IPN and Terpolymer Hydrogels

KEY:

As Fig. 7-1

## 7.5 SHEAR MODULUS (G)

Fig. 7-9 shows shear moduli of both terpolymer and IPN hydrogels vs. composition. The graph indicates that values of G for IPN hydrogels are greater than those for terpolymers at a given composition. The value which is particularly remarkable is that for the 70/30 MMA/(HEMA/MAA) IPN hydrogel. At a given water content, the shear moduli of IPN hydrogel are far greater than those for any of the terpolymer hydrogels (Fig. 7-10). Although the modulus is not a criterion used in the definition of the mechanical strength of a material, it may be used to indicate the nature and morphology of the material. It is possible that phase domains within the IPNs are larger and more rigid than those within the terpolymers. The fact that all the IPN hydrogels are turbid is evidence for the existence of large phase domains.



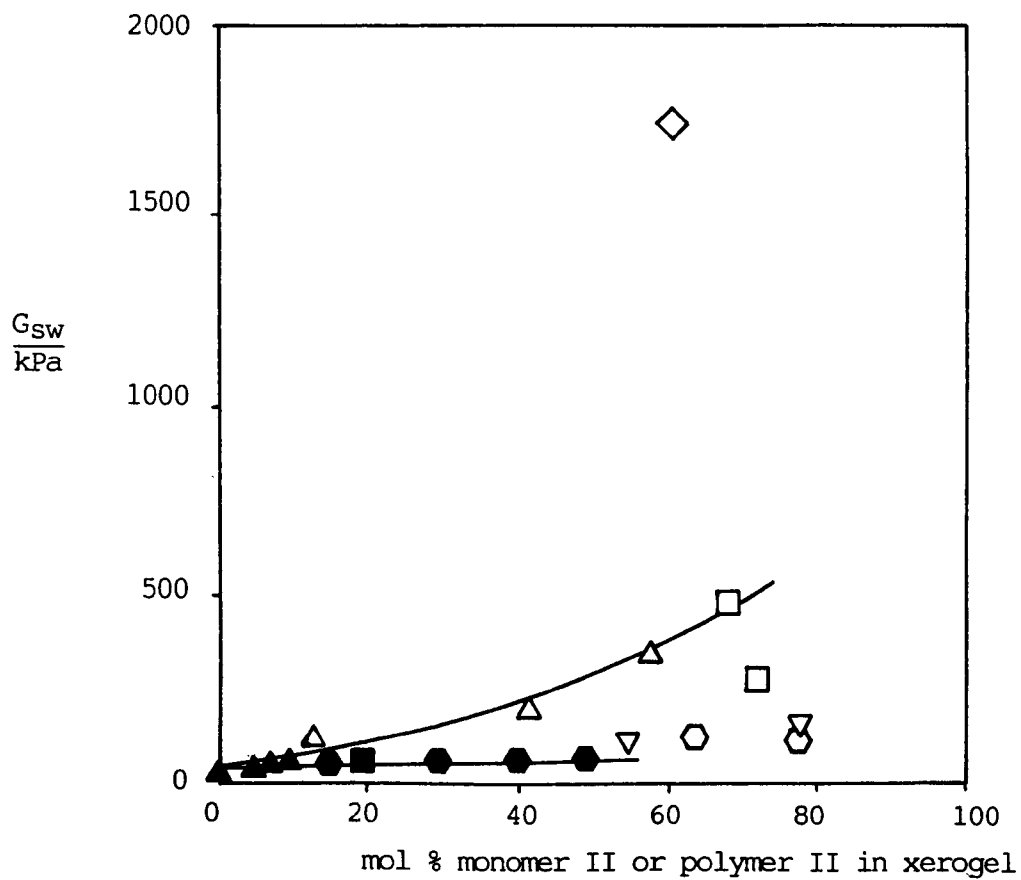


Fig. 7-9: Shear Moduli of Swollen Terpolymer and IPN Hydrogels  
vs. Composition

KEY:

As Fig. 7-1

◻ IPN: 95 mol HEMA/MAA  
5 mol Styrene

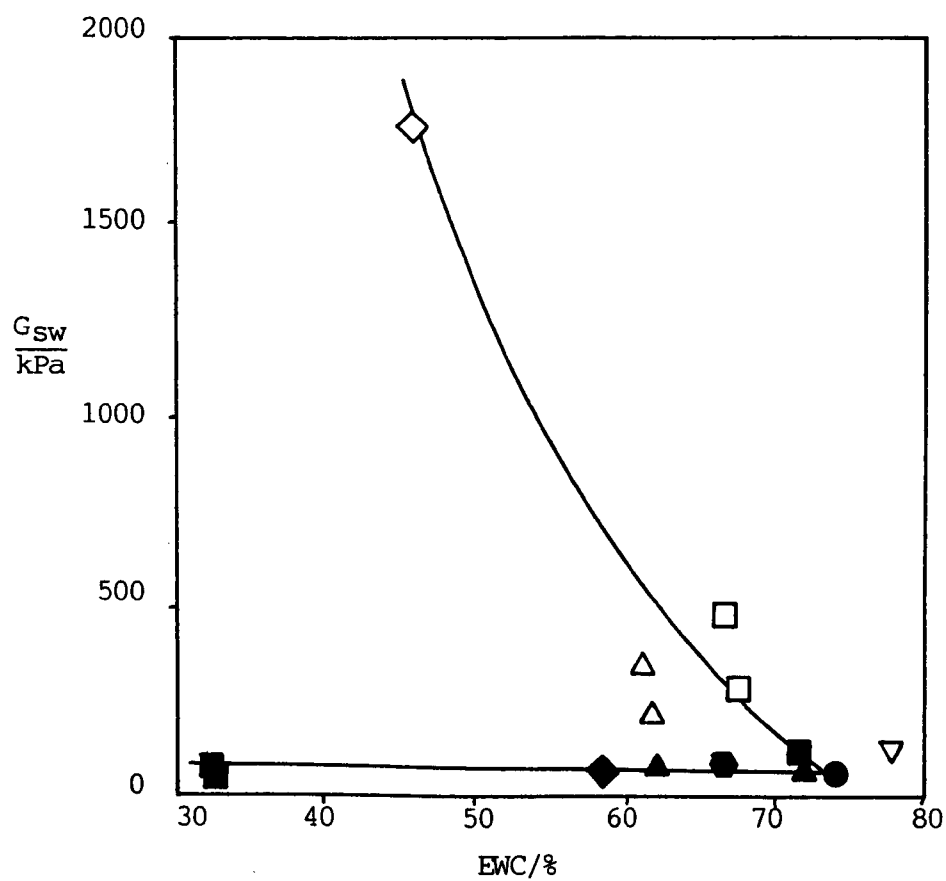


Fig. 7-10: Shear Moduli of Terpolymer and IPN Hydrogels vs. EWC

KEY:

As Fig. 7-1

## 7.6 STRESS-STRAIN CURVES

Fig. 7-11 shows several stress-strain curves for IPN and terpolymer hydrogels, to illustrate the comparisons which can be made. The IPN hydrogels do not show an increase in slope with increasing mol % polymer II at high strains, as do terpolymer hydrogels such as the 30% DDA material. An explanation, which is consistent with the presence of large hydrophobic phase domains within the IPN hydrogels, may be postulated as follows. The hydrophobic domains in the case of the IPNs form a continuous network throughout the material, whereas in the case of the terpolymers, the domains are discrete. Hence the terpolymers tend to show reinforcement characteristic of an elastomer filled with particulate material, while the IPN hydrogels respond as a combination of a hydrogel elastomer and a plastic material.

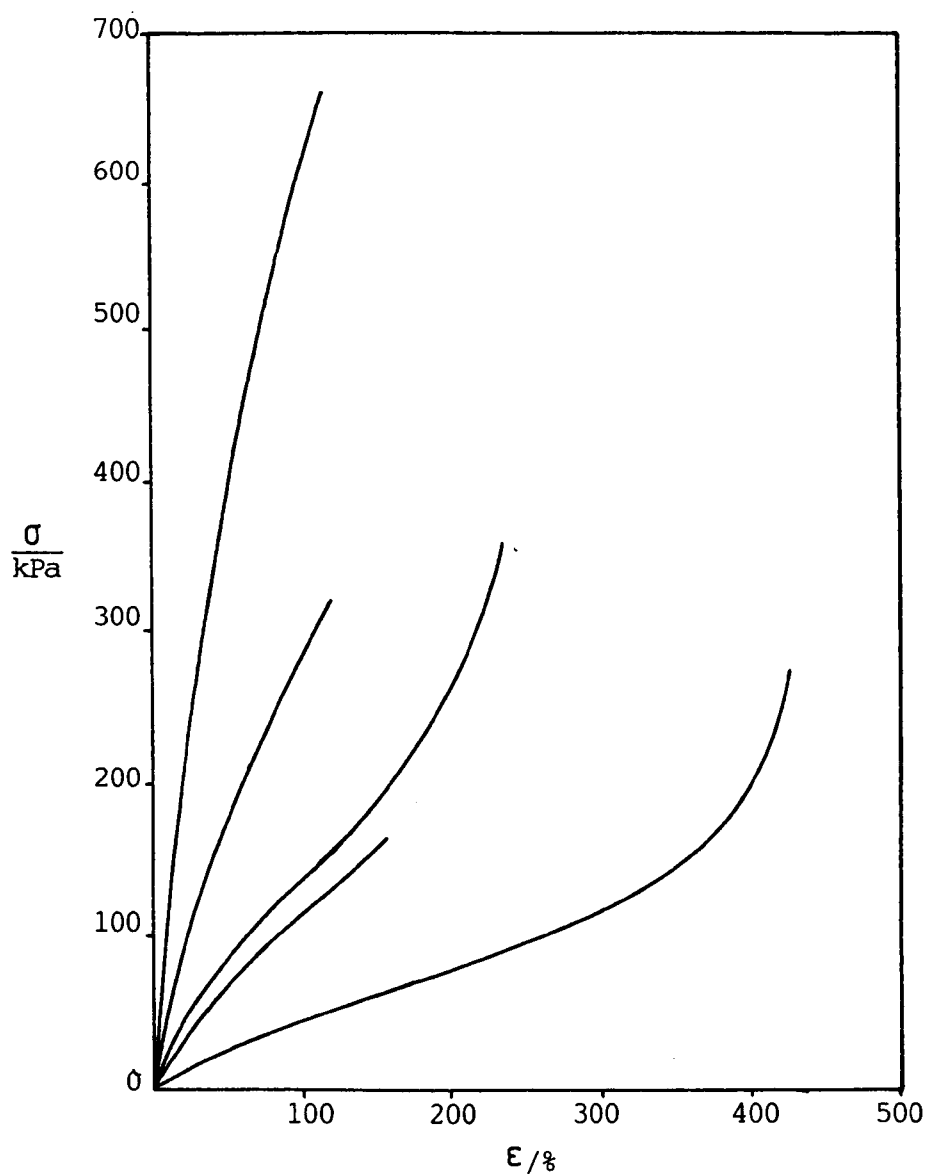


Fig. 7-11: Stress-Strain Curves for Various Terpolymer and IPN Hydrogels

KEY:

- a IPN: 58.3% (50 MMA/50 HEMA-MAA)
- b IPN: 77.5% (95 HEMA/5 MAA)
- c Terpolymer: 10% Styrene
- d Terpolymer: 40% HPMA
- e Terpolymer: 30% DDA

## 7.7 VISCOELASTIC PROPERTIES ( $G'$ , $G''$ , $\tan \delta$ )

Fig. 7-12 to 7-14 show viscoelastic properties of several terpolymer and IPN hydrogels vs. frequency of vibration. A characteristic of the storage modulus curves for the IPN hydrogels is that they show little variation over the range of frequencies studied (Fig. 7-12). The curves for the terpolymer hydrogels, however, are the same shape as that of the basic gel, but the decrease in  $G'$  with increasing frequency at high frequencies is more pronounced. The 70/30 MMA/(HEMA/MAA) IPN hydrogel has values of loss modulus  $G''$  greater than those of any of the other hydrogels (Fig. 7-13). The  $\tan \delta$  curves (Fig. 7-14) show that  $\tan \delta$  for the IPN hydrogels increases only slightly with  $w$  at high frequencies. This is in contrast with the terpolymer hydrogels, which show a sharp increase. The curve for the IPN hydrogel containing a 70/30 MMA(HEMA/MAA) copolymer is almost parallel to the  $\log w$  axis. Little dissipation occurs even at high frequencies. At these higher frequencies, the IPN hydrogels are less viscoelastic than the terpolymers.

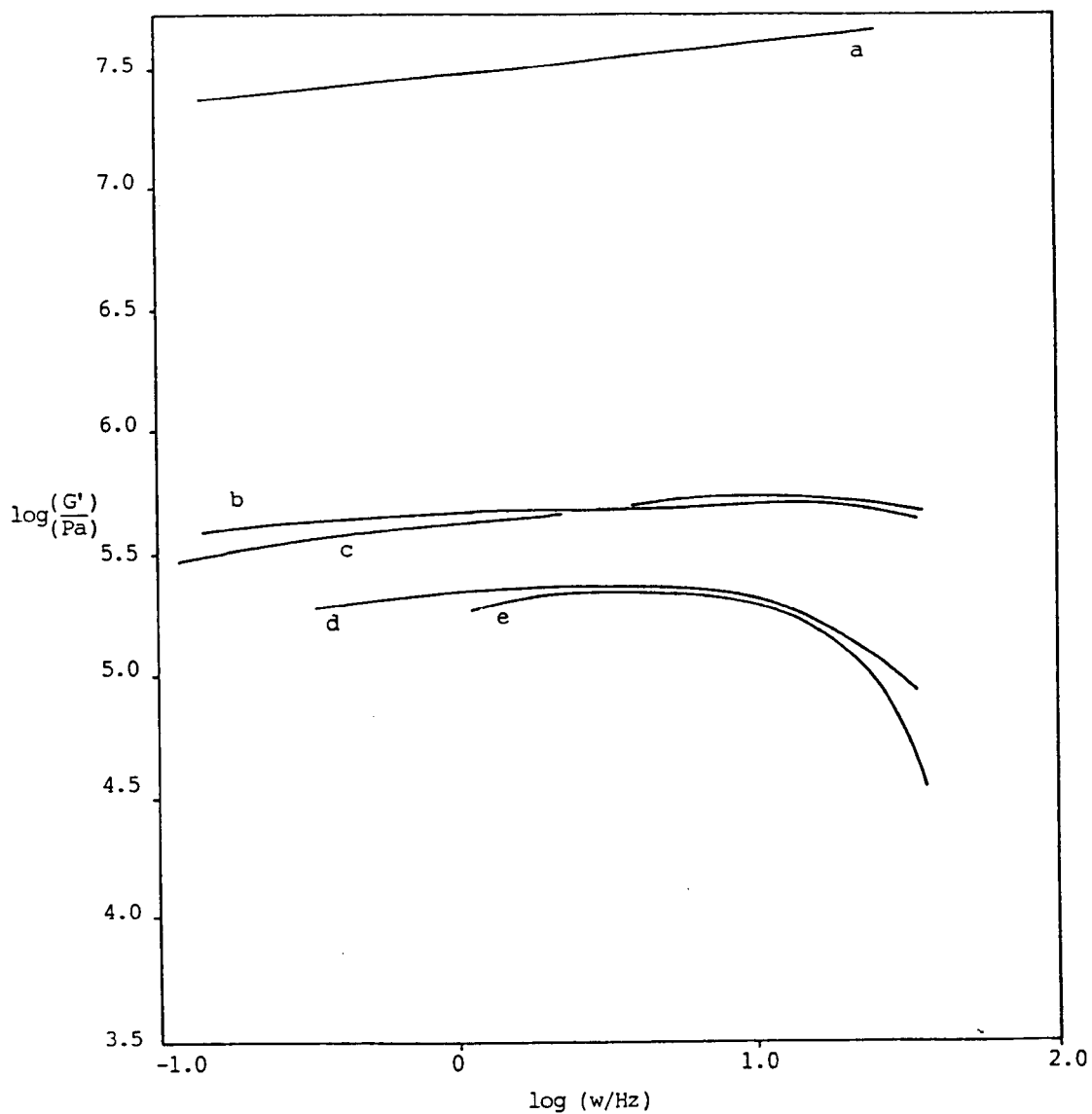


Fig. 7-12: Storage Modulus vs. Frequency for Several Terpolymer and IPN Hydrogels

KEY:

- a IPN: 60.1% (70 MMA/30 HEMA-MAA)
- b IPN: 20.2% (50 MMA/50 HEMA-MAA)
- c 95/5 HEMA/MAA Copolymer
- d 15% HPMA Terpolymer
- e 30% DDA Terpolymer

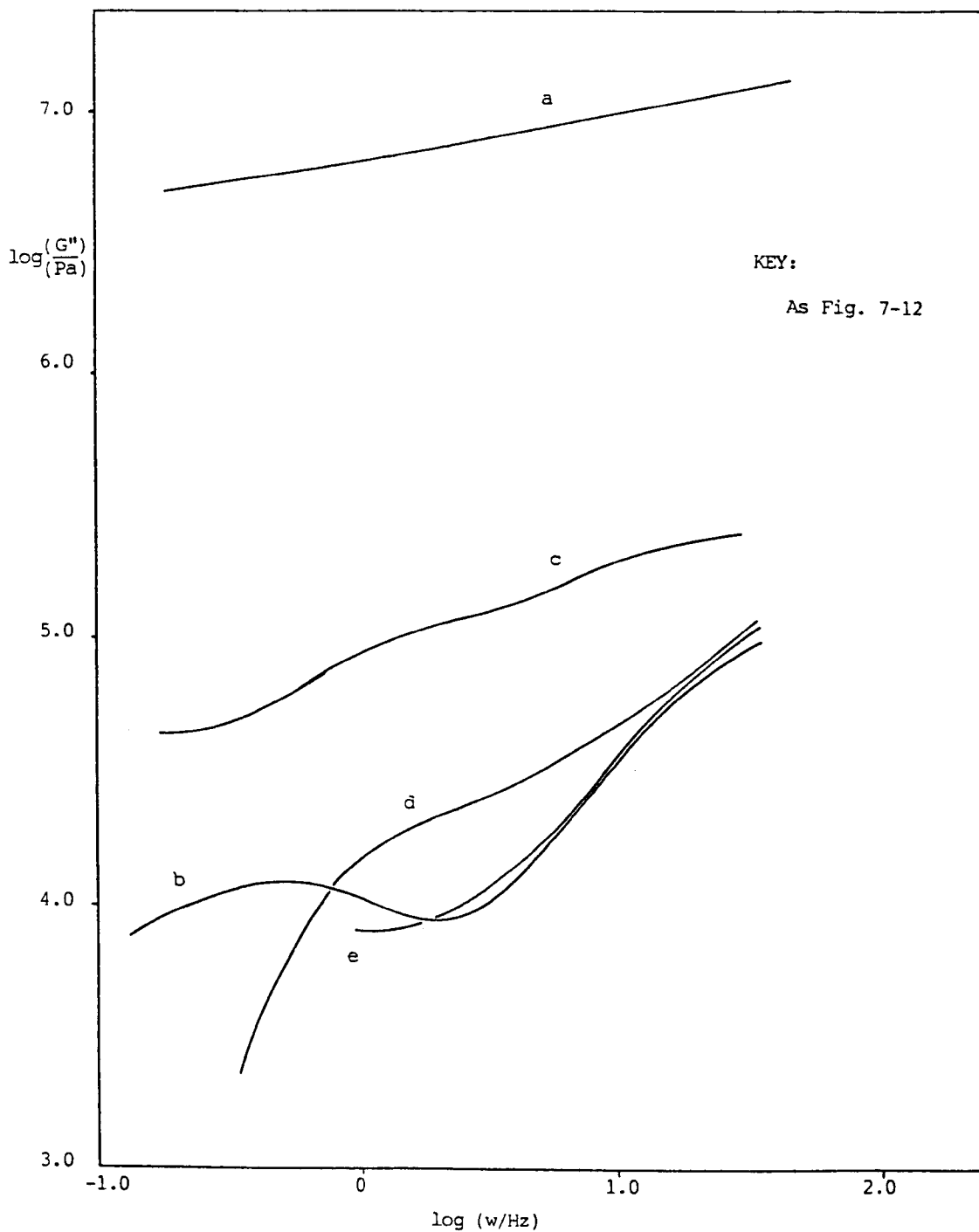
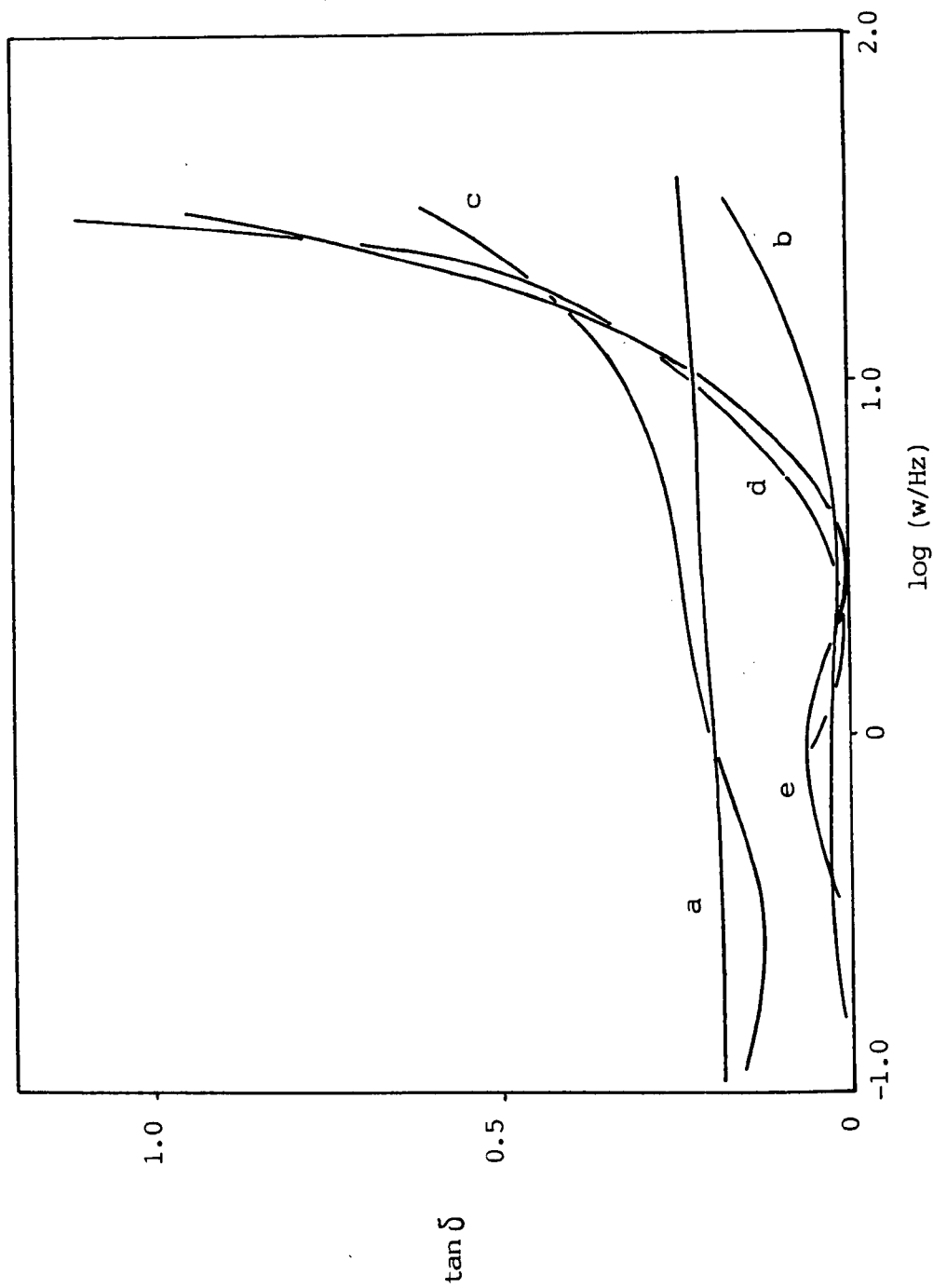


Fig. 7-13: Loss Modulus vs. Frequency for Several Terpolymer and IPN Hydrogels



KEY:

As Fig. 7-12

Fig. 7-14:  $\tan \delta$  vs. Frequency for Several Terpolymer and IPN Hydrogels



CHAPTER EIGHT

CONCLUSIONS AND SUGGESTIONS

FOR FURTHER WORK

## 8.1 GENERAL CONCLUSIONS

Several general conclusions can be drawn from the work described in this thesis.

- (i) The mechanical properties of hydrogels can be modified by all three methods. In all cases, reinforcement is accompanied by a decrease in equilibrium water content.
- (ii) Of the three types of reinforced hydrogel studied, those based upon terpolymers are the simplest to prepare. The preparation of IPNs is complex.
- (iii) Detailed investigation of filled hydrogels was found to be beyond the scope of this project, since consistently monodisperse dispersions of small particle size are required. Attempts to fill hydrogels with low levels of aqueous dispersions of polymer particles were successful, but the reinforcement achieved was no greater than that achieved by terpolymerisation.
- (iv) Some of the IPN hydrogels showed an improvement in mechanical strength as a function of water content, when compared with the terpolymer hydrogels. However, from a commercial point of view, the terpolymers are simple to make, and show significant reinforcement.
- (v) From an academic point of view, several of the materials are interesting, notably the homo-IPN hydrogels, which are translucent.

Hence, an exploratory study has been carried out, which may serve to stimulate further investigation. Several particular conclusions can be drawn, and these lead to some suggestions for further work.

## 8.2 PARTICULAR CONCLUSIONS

- (i) IPNs of hydrogels with thermoplastic polymers can be prepared, using the procedure developed in Chapter 5.
- (ii) The IPNs are probably phase-separated, and reinforced in comparison with the 95/5 HEMA/MAA copolymer hydrogel. In general, at a given water content, the reinforcement is greater in the case of IPN hydrogels than in the case of terpolymer hydrogels.
- (iii) The photopolymerisation reaction used to produce the IPNs probably follows first-order kinetics.
- (iv) The swelling characteristics of the 95/5 HEAM/MAA copolymer hydrogel in ethyl acetate were similar to those in MMA, and therefore ethyl acetate can be used as a saturated analogue of MMA.
- (v) Stress-strain curves of several terpolymer hydrogels showed an increase in slope at high strains, thought to be caused by the presence of hydrophobic phase domains.
- (vi) Tearing energies of hydrogels may be measured by the "trouser" method, which has been previously applied to "dry" rubbers. Terpolymers containing EHA or styrene show particularly high tearing energies at a given mol % hydrophobic monomer.
- (vii) The strain at break/EWC curve for IPN and terpolymer hydrogels seems to have a maximum, most of the materials falling on the curve.
- (viii) Observations of hydrogels filled with aqueous polymeric dispersions suggest that commercially this would not be a successful method of reinforcement.

### 8.3 SUGGESTIONS FOR FURTHER WORK

- (i) The formation of IPNs of hydrophilic crosslinked polymers with a wider range of hydrophobic polymers should be investigated.
- (ii) The effects of crosslink concentration and the molecular weight of polymer II on the physical properties of the IPNs could be studied.
- (iii) Transmission electron micrographs of microtomed sections of IPNs, perhaps in conjunction with freeze-drying, might give an insight into their morphology.
- (iv) Methods of simplifying the IPN preparation procedure should be sought.
- (v) The effects of varying degrees of grafting of polymer II onto polymer I in the IPNs might be investigated, since this grafting might significantly affect the mechanical properties of the IPN. For example, a "grafting" comonomer such as allyl methacrylate could be incorporated in polymer I.
- (vi) The formation of core-shell particles in hydrocarbons might provide a simpler method for preparing water-swellaable IPN-type materials.
- (vii) It would be very interesting to make a more detailed study of the homo-IPN hydrogels.

## REFERENCES

1. O. Wichterle and D. Lim, Brit. Pat. 814, 009 (1959).
2. P.J. Flory, "Principles of Polymer Chemistry", Cornell U.P., Ithaca, New York (1953).
3. S.B. Ross-Murphy and H. McEvoy, Brit. Polym. J. 18(1), 2 (1986).
4. M.F. Refojo, J. Polym. Sci. A-1 5, 3103 (1967).
5. E.R. Morris, Brit. Polym. J. 18(1), 14 (1986).
6. G.M. Yenwo et al, J. Appl. Polymer Sci. 21, 153 (1977).
7. D.K. Carpenter, "Encyclopaedia of Polymer Science and Technology" 4, 63, Interscience (1966).
8. H.H. Young, "Encyclopaedia of Polymer Science and Technology" 1, 446, Interscience (1966).
9. O. Wichterle, "Encyclopaedia of Polymer Science and Technology" 15 (Supp.), 273, Interscience (1966).
10. B.D. Ratner and A.S. Hoffman, ACS Symp. Ser. 31, 1 (1976).
11. M.F. Refojo, Polymer Sci. Technol. 8, 313 (1975).
12. W. Timmer, CHEMTECH 9(3), 175-9 (1979).
13. P.L. Keough, Biomater. Med. Devices Artif. Organs 7, 307 (1979).
14. R.M. Rubin and J.L. Marshall, J. Biomed. Mater. Res. 9, 375 (1975).
15. J. Kolarik et al, J. Biomed. Mater. Res. 15(2), 147 - 157 (1981).
16. N.B. Graham, D.A. Wood, Polym. News 8, 230 (1982).
17. Nippon Carbide Industries Co., Jpn. Kok. 80, 104, 876 (1980).
18. O. Wichterle and D. Lim, Nature 185, 117 - 8 (1960).
19. B.J. Tighe, Brit. Polymer J. 18(1), 8 (1986).
20. O.R. Tarwater, D.R. Cowsar and A.C. Tanquary, Polym. Prepr., ACS Div. Polym. Chem. 16(2), 382 - 6 (1975).
21. S.I. Gordon, Ger. Offen. 2, 751, 453 (1978).
22. J.K. Fink, Makromol. Chem. 182(7), 2105 - 7 (1981).
23. C. Migliaresi et al, J. Biomed. Mater. Res. 18(2), 137 - 46 (1984).
24. N.M. Franson and N.A. Peppas, Polym. Prepr., ACS Div. Polym. Chem. 24(1), 53 - 4 (1983).

25. Kuraray Co. Ltd. Jap. 58, 44, 685 Appl. 1974.
26. M. Kuriaki and T. Harata, Maku 8(1), 39 - 45 (1983).
27. Ng Chiong O and B.J. Tighe, Brit. Polymer J. 8(4), 118 (1976).
28. J. Larke, D.G. Pedley and B.J. Tighe, Brit. Pat. 1, 478, 455 (1977).
29. I.B. Atkinson and B.C. Holdstock, Brit. Pat. Appl. 2, 036, 765 (1980).
30. W.M. Foley, U.S. Pat. 4, 243, 790 (1981).
31. I.B. Atkinson, D.C. Blackley, B.C. Holdstock and J.L. Knowlton, Eur. Pat. Appl. 32, 443 (1981).
32. B.J. Grucza, U.S. Pat. 4, 042, 552 (1977).
33. A.R. Le Boeuf and W.R. Grovesteen, U.S. Pat. 4, 045, 547 (1977).
34. TRE Corporation, Jap. Pat. 78 30, 685 (1978).
35. M. Ilavsky, K. Dusek, J. Vacik and J. Kopecek, J. Appl. Polymer Sci. 23(7), 2073 (1979).
36. L. Pinchuk, E.C. Eckstein and M.R. Van de Mark, J. Appl. Polymer Sci. 29, 1749 - 60 (1984).
37. K. Tanaka, Jap. Pat. 77 84, 273 (1977).
38. American Optical Corporation, Jap. Pat. 78 35, 764 (1978).
39. K. Dusek, Brit. Pat. 1, 405, 056 (1975).
40. M.F. Refojo and H. Yasuda, J. Appl. Polymer Sci, 9, 2425 (1965).
41. M.S. Choudhary, I.K. Varma, Eur. Polymer J. 15(10), 957 (1979).
42. K.F. Mueller, S.J. Heiber and W.L. Plank. U.S. Pat. 4, 224, 427 (1977).
43. K. Tanaka, Jap. Pat. 80 02, 605 (1980).
44. L. Plambeck, U.S. Pat. 4, 130, 706 (1978).
45. F.O. Holcombe, U.S. Pat. 4, 113, 686 (1978).
46. M.V. Rostoker and L. Levine, Can. Pat. 1, 034, 698 (1978).
47. J. Kolarik and C. Migliaresi, J. Biomed. Mater. Res. 17(5), 757 (1983).
48. I. Shinohara et al, Jap. Pat. 76 109, 093 (1976).
49. I. Kaetsu et al, Jap. Pat. 77 39, 783 (1977).

50. C.L. Sieglaff, C.J. Hora and J.P. Tiefenback, Ger. Offen. 2, 715, 514 (1977).
51. R.A. Abrahams, Ger. Offen. 2, 623, 056 (1977).
52. C.P. Creighton and C.R. Teschemacher, U.S. Pat. 4, 109, 074 (1978).
53. M. Stol et al, J. Polym. Sci., Polym. Symp. 66, 221 (1979).
54. I.B. Atkinson, B.C. Holdstock and J.L. Knowlton, Eur. Pat. Appl. 24, 164 (1981).
55. J. Palacky et al, Czech Pat. 188, 620 (1981).
56. M. Ilavsky and W. Prins, Macromolecules 3, 145 (1970).
57. M. Ilavsky and W. Prins, Macromolecules 3, 425 (1970).
58. J. Janacek and J.D. Ferry, Rheol. Acta 9, 208 (1970).
59. J.M. Wood et al, Inst. J. Pharm. 7(3), 189 (1981).
60. D.E. Gregonis et al, Polymer 19(11), 1279 (1978).
61. J.W. Lee, E.H. Kim and M.S. Jhon, Bull. Korean Chem. Soc. 4(4), 162 (1983).
62. R.J. Fort and T.M. Polyzoidis, Eur. Polym. J. 12(9), 685 (1976).
63. S.J. Wisniewski et al, ACS Symp. Ser. 31, 80 (1976).
64. K.L. Dorrington, N.G. McCrum and W.R. Watson, Polymer 18(7), 712 (1977).
65. K. DeGroot and A.A. Driessen, J. Appl. Polym. Sci. 22, 859 (1978).
66. B.S. Plaut, D.J.G. Davies and B.J. Meakin, J. Pharm. Pharmacol. 29, 79 (1977).
67. P. van den Hoek and K. Polzhofer, GIT Fachz. Lab. 22(9), 778 (1978).
68. Y.K. Sung et al, Polymer 19(11), 1362 (1978).
69. J. Janacek, J. Macromol. Sci. - Rev. Macromol. Chem. C9, 1 (1973).
70. C. Migliaresi et al, J. Biomed. Mater. Res. 15(3), 307 (1981).
71. E.H. Kim et al, Bull. Korean Chem. Soc. 2(2), 60 (1981).
72. J.M. Wood, D. Attwood and J.H. Collett, Drug Dev. Ind. Pharm. 9, 93 (1983).
73. S.H. Ronel et al, J. Biomed. Mater. Res. 17(5), 855 (1983).

74. R.Y.S. Chen, Poly. Prepr. 15(2), 387 (1974).
75. D.E. Gregonis, C.M. Chen and J.D. Andrade, ACS Symp. Ser. 31, 88 (1976).
76. Y. Iwakura et al, J. Polym. Sci. C4, 673 (1963).
77. M.F. Refojo, J. Appl. Polym. Sci. 9, 3161 (1965).
78. H. Yasuda, M. Gochin and W. Stone, J. Polym. Sci. A-1 4, 2913 (1966).
79. W.L. Mancini et al, Ger. Offen. 2, 349, 528 (1974).
80. M. Macret and G. Hild, Polymer 23, 81 (1982).
81. Y.K. Sung et al, Pollimo 8(2), 123 (1985).
82. J. Kopecek, J. Jokl and D. Lim, J. Polym. Sci. C16, 3877 (1968).
83. Fluka Chemicals Catalogue, p.484, Fluka AG, Switzerland (1986).
84. Nippon Shokubai Kagaku Kogyo Co. Ltd., Jap. Pat. 81, 166, 148 (1981).
85. V. Rattay et al, Czech. Pats. 186, 582; 186, 581 (1978).
86. R. Frater, Stain Technol. 54, 241 (1979).
87. M.B. Huglin and M.B. Zakaria, Polymer 25, 797 (1984).
88. M. Luttinger and C.W. Cooper, J. Biomed. Mater. Res. 1, 67 (1967).
89. B.K. Davis, Proc. Nat. Acad. Sci. USA 71, 3120 (1974).
90. K. Yokota et al, Macromolecules 11, 95 (1978).
91. S.G. Starodubtsev et al, Vysokomol. Soedin Ser.A 23, 830 (1981).
92. J.G.B. Howes, Braz. Pat. PI 75 00, 544 (1976).
93. S. Hosaka et al, J. Biomed. Mater. Res. 14, 557 (1980).
94. S. Hosaka, Ger. Pat. 2, 748, 898 (1978).
95. F. Kenjo and S. Osumi, Jap. Pat. 79 43, 284 (1979).
96. G.W. Schwach, Ber. Oesterr. Stud. Atomenerg. (1978).
97. O.P. Boiko et al, Vysokomol. Soedin. B 25, 904 (1983).
98. N.A. Peppas and E.W. Merrill, J. Biomed. Mater. Res. 11, 423 (1977).
99. M. Nagura, M. Nagura and H. Ishikawa, Polym. Commun. 25, 313 (1984).



100. G. Jokyu and Y. Ikada, Jap. Pat. 60 177, 066 (1985).
101. M. Watase and K. Nishinari, J. Polym. Sci. - Polym. Commun. 24, 270 (1983).
102. M.F. Refojo, J. Appl. Polym. Sci. 9, 3161 (1965).
103. J. Janacek, A. Stoy and V. Stoy, J. Polym. Sci. Symp. 53, 299 (1975).
104. A. Silberberg, ACS Symp. Ser. 31, 198 (1976).
105. G.M. Brauer, Org. Coat. Plast. Chem. 42, 321 (1980).
106. M.F. Refojo, J. Polym. Sci. A-1 5, 3103 (1967).
107. B.D. Ratner and I.F. Miller, J. Polym. Sci. A-1, 10, 2425 (1972).
108. E. Ahad, J. Appl. Polym. Sci. 22, 1665 (1978).
109. H.B. Lee, M.S. Jhon and J.D. Andrade, J. Coll. Int. Sci. 51, 225 (1975).
110. M.S. Jhon and J.D. Andrade, J. Biomed. Mater. Res. 7, 509 (1973).
111. D.G. Pedley and B.J. Tighe, Brit. Polym. J. 11, 130 (1979).
112. M.F. Refojo, ACS Symp. Ser. 31, 37 (1976).
113. B.J. Tighe, Brit. Polym. J. 18, 8 (1986).
114. M.F. Refojo, F.J. Holly and F.L. Leong, Contact Intraocul. Lens Med. J. 3, 27 (1977).
115. G.M. Zentner et al, J. Pharm. Sci. 68, 794 (1979).
116. J. Hasa and J. Janacek, J. Polym. Sci. C16, 317 (1967).
117. J. Janacek and M. Raab, J. Polym. Sci. - Polym. Phys. 11, 2311 (1973).
118. M. Kumakura and I. Kaetsu. J. Mater. Sci. 18, 2430 (1983).
119. J. Janacek and J.D. Ferry, Macromolecules 2, 370 (1969).
120. J. Janacek and J.D. Ferry, J. Macromol. Sci.-Phys. B5, 245 (1971).
121. J. Kolarik and J. Janacek, J. Polym. Sci. A-2, 10, 11 (1972).
122. M. Ilavsky and W. Prins, Macromolecules 3, 425 (1970).
123. M. Raab and J. Janacek, Proc. Conf. "Polymers 71", Bulgaria (1971).
124. J. Janacek et al, Czech. Pat. 131, 188 (1969).
125. B.V. Rejda et al, Polym. Prepr. ACS 16, 365 (1975).
126. J. Janacek et al, J. Polym. Sci.-Polym. Phys. 13, 1591 (1975).
127. M. Macret and G. Hild, Polymer 23, 81 (1982).

128. C. Migliaresi, S. Piccarolo and L. Nicolais, *Polymer* 23, 1242 (1982).
129. P. Predecki, *J. Biomed. Mater. Res.* 8, 487 (1974).
130. M. Dror, M.Z. Elsabee and G.C. Berry, *J. Appl. Polym. Sci.* 26, 1741 (1981).
131. D.J. Highgate, *Brit. Pat.* 1, 463, 301 (1979).
132. C. Migliaresi *et al*, *Chim. Ind. (Milan)* 67, 114 (1985).
133. K.R. Shah, *Polym. Mater. Sci. Eng.* 52, 149 (1985).
134. I. Iwai *et al*, *Jap. Pat.* 79 72, 288 (1979).
135. C. Hepburn, *Plast. Rub. Int.* 9, 15 (1984).
136. B.B. Boonstra, "Rubber Technology and Manufacture", p. 230, Butterworths, London (1971),
137. W.B. Wiegand, *India Rub. J.* 60, 379, 423, 453 (1920).
138. G. Kraus, *Adv. Polym. Sci.* 8, 155 (1971).
139. G. Kraus, ed., "Reinforcement of Elastomers", Wiley, New York (1971).
140. L.H. Sperling, "Interpenetrating Polymer Networks and Related Materials", Plenum, New York (1981).
141. V. Huelck, D.A. Thomas and L.H. Sperling, *Macromolecules* 5, 340, 348 (1972).
142. A.A. Donatelli, L.H. Sperling and D.A. Thomas, *Macromolecules* 9, 671, 676 (1976).
143. J.M. Widmaier and L.H. Sperling, *Macromolecules* 15, 625 (1982).
144. J.M. Widmaier, J.K. Yeo and L.H. Sperling, *Coll. and Polymer Sci.* 260, 678 (1982).
145. G.M. Yenwo *et al*, *J. Appl. Polym. Sci.* 21, 153 (1977).
146. H. Adashi and T. Kotaka, *Polym. J.* 14, 3791 (1982).
147. H. Adashi, S. Nishi and T. Kotaka, *Polym. J.* 15, 985 (1983).
148. L.H. Sperling, *NATO ASI SER., SER.E*, 89, 267 (1985).
149. R.E. Touhsaent, D.A. Thomas and L.H. Sperling, *J. Polym. Sci.* C46, 175 (1974).
150. Y. Suzuki *et al*, *J. Macromol. Sci.-Phys.* B17, 787 (1980).
151. K.C. Frisch *et al*, *J. Polym. Sci-Polym. Chem. Ed.* 12, 885 (1974).

152. J. Sionakidis, L.H. Sperling and D.A. Thomas, J. Appl. Polym. Sci. 24, 1179 (1979).
153. D.J. Hourston and R. Satgurunathan, J. Appl. Polym. Sci 29, 2969 (1984).
154. L.H. Sperling, J. Polym. Sci. - Macromol. Revs. 12, 141 (1977).
155. A.A. Donatelli, L.H. Sperling, D.A. Thomas, J. Appl. Polym. Sci. 21, 1189 (1977).
156. D. Klemperer et al, Macromolecules 9, 258 (1976).
157. N. Devia et al, Macromolecules 12, 360 (1979).
158. M. Matsuo et al, Polym. Eng. Sci. 10, 327 (1970).
159. A.J. Curtius et al, Polym. Eng. Sci. 12, 101 (1972).
160. J.A. Manson and L.H. Sperling, "Polymer Blends and Composites", Plenum, New York (1976).
161. R.E. Touhsaent, D.A. Thomas and L.H. Sperling, in "Toughness and Brittleness of Plastics", eds. R.D. Deanin and A.M. Crugnola, p.206, ACS, Washington D.C. (1976).
162. S.C. Kim et al, J. Appl. Polym. Sci. 21, 1289 (1977).
163. N. Devia et al, Polym. Eng. Sci. 19, 878 (1979).
164. G.M. Yenwo et al, Polym. Eng. Sci. 17, 251 (1977).
165. D. Klemperer, H.L. Frisch and K.C. Frisch. J. Polym. Sci. A-2 8, 921 (1970).
166. A.J. Kinloch and R.J. Young, "Fracture Behaviour of Polymers", Applied Science Publishers, London (1983).
167. E.H. Andrews, "Fracture in Polymers", Oliver and Boyd, London (1968).
168. A.A. Griffith, Phil. Trans. Roy. Soc. A221, 163 (1920).
169. R.J. Young, "Introduction to Polymers", chapter 5, Chapman and Hall (1981).
170. G.J. Lake and P.B. Lindley, J. Appl. Polym. Sci. 9, 1233 (1965).
171. E.H. Andrews, "Developments in Polymer Fracture - 1", chapter 1, Applied Science Publishers, London (1979).
172. A.N. Gent, in "Fracture - An Advanced Treatise, Vol. III", ed. H. Liebowitz, chapter 6, Academic Press, New York (1971).
173. R.S. Rivlin and A.G. Thomas, J. Polym. Sci. 10, 291 (1953).

174. A.N. Gent, J. Mater. Sci. 15, 2884 (1980).
175. A.G. Thomas, J. Polym. Sci. 18, 177 (1955).
176. H.W. Greensmith, J. Appl. Polym. Sci. 3, 183 (1960).
177. "Polymer Handbook", 2nd Edition, Wiley (New York), p.VII-11 (1975).
178. T. Tanaka, S.-T. Sun and I. Nishio, in "Scattering Techniques Applied to Supramolecular and Nonequilibrium Systems", ed. Chen. Chu and Nossal, p.321, Plenum, New York (1981).
179. T. Tanaka, Sci. Amer. 244, 124 (1981).
180. J. Ricka and T. Tanaka, Macromolecules 18, 83 (1985).
181. K. Kudela, A. Stoy and R. Urbanova, Eur. Polym. J. 10, 905 (1974).
182. V. Stoy et al, Czech. Pat. 164, 437 (1976).
183. V. Stoy, O. Wichterle and A. Stoy, Fr. Pat. 2, 292, 991; Brit. Pat. 1, 486, 045 (1976).
184. J.A. Ward, Ger. Pat. 2, 737, 994 (1978).
185. Nippon Oil Co. Ltd., Jap. Pat. 58 92, 359 (1983).
186. J.C. Bray and E.W. Merrill, J. Biomed. Mater. Res. 7, 431 (1973).
187. H. Becker, ed., "Organicum - Practical Handbook of Organic Chemistry", trans. B. Hazzard, Pergamon Press, Oxford, p.421, 422 (1973).
188. O. Wichterle and R. Chromacek, J. Polym. Sci. C16, 4677 (1965).
189. A. Lyskowski, Private Communication.
190. J.E. Gordon, "The New Science of Strong Materials", 2nd Ed., Penguin p.108 (1976).
191. L.R.G. Treloar, "The Physics of Rubber Elasticity", 2nd Ed., Oxford University Press, p.70 (1958).
192. S.M. Gumbrell et al, Trans. Faraday Soc. 49, 1495 (1953).
193. I.M. Ward, "Mechanical Properties of Solid Polymers", Wiley, London, p.75 (1971).
194. L.R.G. Treloar, "The Physics of Rubber Elasticity", 3rd Ed., Oxford University Press, p. 122 (1973).
195. K.E.J. Barrett and H.R. Thomas, in "Dispersion Polymerisation in Organic Media", Ed. K.E.J. Barrett, Wiley (London), p. 122 (1975).
196. G.M. Burnett and H.W. Melville, Proc. Roy. Soc. (London) A189, 456 (1947).

197. R.C. Weast, Ed., "Handbook of Chemistry and Physics", Chemical Rubber Co. (Cleveland, Ohio), Section C (1970).
198. S.M. Gumbrell et al, Trans. Faraday Soc. 49, 1495 (1953).
199. K.E.J. Barrett, Ed., "Dispersion Polymerisation in Organic Media", Wiley (London) (1975).
200. F.A. Waite and M.W. Thompson, G.B. Pat. 1, 096, 912 (1967).
201. H. Saechtling, "International Plastics Handbook", Hanser Verlag, Munich, p.255 (1983).
202. A.C. Haynes, <sup>(LSP)</sup>Private Communication.
203. J.V. Dawkins, in "Block Copolymers", ed. D.C. Allport and W.H. Jones, Applied Science, London, p. 363 (1973).
204. A.E. Oberth, Rub. Chem. Technol. 40, 1355 (1967).